ROBOT-AIDED NEURO-REHABILITATION AND FUNCTIONAL IMAGING

by

Hermano Igo Krebs

B.S. in Naval Architecture and Marine Engineering
Escola Politecnica da Universidade de Sao Paulo - Brazil (1980)

M.S. in Naval Engineering
Escola Politecnica da Universidade de Sao Paulo - Brazil (1987)

M.S. in Ocean Engineering
Yokohama National University - Japan (1989)

SUBMITTED IN PARTIAL FULFILLMENT
OF THE REQUIREMENTS FOR THE DEGREE OF

DOCTOR OF PHILOSOPHY IN OCEAN ENGINEERING

at the

MASSACHUSETTS INSTITUTE OF TECHNOLOGY
February, 1997

© Massachusetts Institute of Technology 1997. All rights reserved.

Signature of Author: _____
Department of Ocean Engineering
October 07, 1996

Certified by: _____
Neville Hogan
Professor of Mechanical Engineering
Professor of Brain and Cognitive Sciences
Thesis Supervisor

Approved by: _____
J. Kim Vandiver
Chairman, Department Committee on Graduate Students

APR 29 1997 ARCHIVES

ROBOT-AIDED NEURO-REHABILITATION AND FUNCTIONAL IMAGING

by

Hermano Igo Krebs

Submitted to the Department of Ocean Engineering
in partial fulfillment of the requirements for the
degree of Doctor of Philosophy in Engineering at the
Massachusetts Institute of Technology
October 7, 1996

ABSTRACT

This thesis summarizes the development of two novel applications of robotics in the biomedical field: robot-aided neuro-rehabilitation and robot-aided functional imaging. It also describes MIT-MANUS (MIT Patent U.S. # 5,466,213) and a novel biologically-based decomposition and encoding of human upper limb movement.

The goal of robot-aided neuro-rehabilitation was to assess the application of robotic technology to assist, enhance, quantify, and document the neuro-rehabilitation of patients with different neurological disorders. The efforts in this thesis concentrated primarily on stroke patients, although some examples will be presented involving patients with myoclonus, and Parkinson's disease. This document summarizes some results of this multi-disciplinary effort during a one-and-a-half year pilot clinical trial at the Burke Rehabilitation Hospital in White Plains, NY.

The goal of robot-aided functional imaging was twofold: (a) to integrate robotic technology with functional brain imaging, thus providing a facility to manipulate, as well as measure, motor consequences of neural activity measured by imaging technologies, and influenced by pharmacological interventions, and (b) to investigate motor control and learning, in particular the different levels of organization of the putative higher level controller. This document summarizes this novel biomedical engineering application via experiments in motor learning by using the PET (Positron Emission Tomography) facility of the Massachusetts General Hospital.

Functional imaging devices register regional cerebral blood flow (rCBF), glucose metabolism, or blood oxygenation. Those measurements are presumed to correlate with cellular activity in the brain. Functional activation is obtained by subtracting scans obtained during two different conditions. It assumes that differential brain activity is due solely to the different requirements of each condition. In practice, the experiment cannot be totally controlled, leading researchers in the area to question several significant activations that cannot be accounted for by prior models of brain activity. Here, a technique for cross-validation of the observed activations in motor tasks will be presented.

This line of research required the development of a novel robot designed and built for clinical neurological applications. The robot MIT-MANUS was configured for safe, stable, and compliant

operation in close contact with humans. It can move, guide, or perturb the movement of a human upper limb, as well as record motions and mechanical quantities such as position, velocity, and forces applied.

Likewise, this research required the development of a robot-aided assessment procedure. The assessment procedure is based on observations of upper limb movement. The efforts focused on incorporating experimental evidence of segmentation and primitives of arm movement into a decomposition and encoding algorithm, summoning attention to the episodic interventions and asynchronous character of the symbolic level or high-level controller. The episodic intervention character of the decoding-encoding algorithm has important engineering consequences. It constitutes a biologically-based scheme for data-compression, human-machine interface, and communication in telerobotics.

Thesis Committee:

Prof. Neville Hogan (Chairman)
Professor of Mechanical Engineering
Professor of Brain & Cognitive Sciences
Massachusetts Institute of Technology

Prof. Michael Triantafyllou
Professor of Ocean Engineering
Massachusetts Institute of Technology

Dr. Dana Yoerger
Principal Research Scientist
Woods Hole Oceanographic Institutions

ACKNOWLEDGMENTS

I was reading similar pages of my master dissertations in engineering in Brazil and in Japan, and realized that though it is a different country, a different culture, different values, and different protagonists, there is a common thread of elements: family, friends, special friends, and mentors. Likewise in those occasions, I prefer to talk about the people with whom I interacted during the last seven years of my life. They are the fabric of the institutions, which have value only with them.

I was fortunate to have the best insight into the U.S. through small talk and observation of three leaders in their respective environments: Professor Francis T. Ogilvie, Dr. Fletcher McDowell, and William Casper. Fifteen minutes of conversation with Professor Ogilvie (then head of the Ocean Engineering Department) was the best "eye-opener" anybody can have. Most memorable was his comment that at MIT, I could count on all the support required to be the "number one". But to keep in mind that nobody at MIT cares who is the "number two". Dr. Fletcher McDowell from the Burke Rehabilitation Hospital and Cornell Medical School enabled me to focus on what really matters. His vision also allowed me the luxury of not worrying during the last two and half years about financial support. I first met Bill Casper (Casper, Phillips & Associates) in 1984 in the very south of Brazil during a "minuano" (freezing wind occasionally blowing from Antartica during winter time). The British crew of riggers interrupted their "tea-time" on the containercrane that was being installed in Rio Grande shouting to each other: "Ringo is coming". It was easy to identify him with his "poncho". I was amazed by these men's total belief in the power of one individual and his influence over the system. I guess I had the best available crash course on the American way. Thank you !

As the saying goes, graduate life at MIT is extremely intense and overwhelming, but it can be exciting or miserable depending on the advisor. My life at MIT was intense, overwhelming, and exciting. I learned a great deal of what I know from Neville Hogan. Neville shines not only in the versatility of his knowledge & know-how, but also in the depth of his discussions with you. He has inexaustable energy and patience for searching and for extracting knowledge. He showed an admirable open-mindedness, and capacity to "realpolitik" in the face of my fiascos, and made me understand the meaning of the word "re-search". Not less important, I came to MIT without any financial support. Neville took the time to talk to me when everybody else was so busy, and I was counting how many pennies I had left. I look forward to continue to work with you. Thank you !

I would like to thank the other members of my thesis committee: Prof. Michael Triantafyllou (Ocean Engineering Department) and Dr. Dana Yoerger (Woods Hole Oceanographic Institutions). I really appreciate the time, suggestions, and unconditional support. Thank you !

At the Burke Rehabilitation Hospital, I had daily conversations with Dr. Mindy Aisen and Dr. Bruce T. Volpe (both from Cornell Medical School). I was overwhelmed at how much there was to learn about neurological diseases when I set foot in White Plains, and I don't have words to express my gratitude for your patience. Bruce made complicated things look so simple, and Mindy was always ready to listen and explain my "discoveries". I think we make a hell of a good team, and I look forward to continue to work with the two of you. Thank you !

I would not consider MIT a university without the superb classes that the Institute offer, neither without Prof. A. Douglas Carmichael company during uncountable lunches, or Prof. Aaron Fleisher's cold beers and jewish empathy. Aaron offered me a sound board to think aloud and challenged me continuously to think over discussions on how to determine the distance between two colors or how architects do what they do. I had a great time. Thank you !

I acknowledge the specific technical contributions throughout the thesis, and I will wait to mention my labmates or individuals from different laboratories who contribute in one sort or another to different facets of this work. But I wanted to register a line for my labmates. Being from an older generation and spending half of the time out of MIT, I did not spend too much time with my labmates. Nonetheless I admire you all deeply. I am still trying to figure out what Justin Won and Joe Doeringer don't know. Jain Charnnarong (presently University of Bangkok) is an amazing mechanical designer, Srikrishna always carries a smile, and the only reason old folks such as Dennis Rancourt (presently University of Laval), Anthony Hodgson (presently University of British Columbia), Michel Lemay and Ernest Fasse (presently University of Arizona) can't learn new tricks is because they know them all. I also feel compel to register a line for the three undergraduates (UROPS) that worked extensively, over a year each, under my "supervision": Christopher Minekime, Amy Gorin, and Donna Louise Scott. They proved at least to me, that MIT undergraduates are awesome. Good Luck !

Sergio and Eliane Kostek and their children Natasha and Vladimir are my family in this country. They put perspective, magnificent dinners and good Brazilian laughs throughout the last 20 years. My good friends in the last seven years supported me with friendship or pheromones: Robert(o) Parlow, Christiaan (Mauritz) Van Schalkwyk, David Goldwater, Ilana Fogelman, June Komisar, Caroline Schwartz, Kathryn Flynn, Natasha Sabath, Nomadic, and Mary Jane Boyd. Robert Parlow, Stacy Spivack, and Mary Jane Boyd also put uncountable hours making you able to read this thesis. Thank you !

I could not conclude without expressing my appreciation and wishes of good luck to thirty six previous patients at the Burke Rehabilitation Hospital (so far). Nor without expressing my admiration and confidence in the ingenuity of *"those magnificent men and their flying machines"* (tools) that allow me to go, to predict, and to do things that my father would only dream of. I can't wait for the next century, the new tools, and wonders that wait for us. May we all live in interesting times!

And special thanks to my parents,

Katarzyna Krebs

and

Abraham Krebs ז"ל

Hermano Igo Krebs
Cambridge, 07 October 1996

TABLE OF CONTENTS

Abstract 3

Acknowledgments 5

Table of Contents 7

List of Figures 11

List of Tables 19

1. Introduction 21

1.1. Motion Language 21

1.2. Class of Applications of a Motion Language 25

1.3. Thesis Overview 33

2. From the Symbolic Level to the Energy-Dominated Level via a "Submovement"

2.1. Literature Overview 35

2.2. Example of Arm Movement 42

2.2.1. Experimental Setup and Procedure 42

2.2.2. Drawing Circles at Constant Speeds 43

2.2.3. Drawing Circles at Increasing Speeds 64

2.3. Movement Segmentation 65

2.4. Movement Curvature 72

2.5. Working Model: Motor Control Hierarchy 74

2.6. Working Hypothesis: Segments and Primitives of Arm Movement 75

2.7. Working Hypothesis: Minimum Action Unit Conjecture and Learning 75

2.8. March of Progress - Chapter II 76

Apéritif 77

3. A Task-Encoding Scheme for Human Motion 79

3.1. Competent Description of Arm Movement 79

3.2. Best Basis Function 80

3.3. Radial Basis Function Networks 102

3.3.1. Generalized Radial Basis Function (RBF) 103

3.3.2. Generalized Radial Basis Function (GRBF) 105

3.3.3. Shannon's Radial Basis Function (SRBF) 106

3.3.4. Hyper Radial Basis Function (HRBF) 107

3.3.5. Irregular Sampling Radial Basis Function (ISRBF) 110

3.3.5.1. Gaussian and Minimum-Jerk Compiler Engines 110

3.3.5.2 Upperbound on the Number of Bases 111

3.3.5.3. Gradient-Descent Refinemet 112

3.4. March of Progress - Chapter III 113

Apéritif 119

4. MIT-MANUS: A Workstation for Manual Therapy and Training 123

4.1. Overview of Design Concept 124

4.2. Overview of Mechanical Design 126

4.3. Carpentry Overview 131

4.4. Overview of Electrical Design 135

4.5. Overview of Software Design 140

4.6. Overview of Hand-Holders 143

4.7. Overview of Video-Games 146

5. Robot-Aided Neuro-Rehabilitation 151

5.1. Background on Cerebral Vascular Accident (CVA) 151

5.1.1. ABC of Brain Attack 151

5.1.2. Health Care Cost and Potential Cost Savings 153

5.1.3. Overview - Does Peripheral Manipulation Influences Brain Recovery ? 159

5.2. Patients 160
5.3. Experimental Setup and Procedure 164
5.4. Primary Research Results 165
5.4.1. Patient's Tolerance for the Procedure 166
5.4.2. Standard Assessment 167
5.4.3. Robot-Aided Assessment 169
5.4.4. Working Hypothesis: Peripheral Manipulation Influences Brain Recovery 169
5.4.5. Automatization of Standard Assessment Procedures 178
5.4.6. Working Hypothesis: Post-stroke sensorimotor behavior is more segmented than normal limb movements 180
5.4.7. Working Hypothesis: Peripheral Manipulation and Training Influences Movement Recovery of Stroke Victims in the Stable Phase 190
5.5. Miscellaneous 197
5.5.1. Parkinson's Disease: Procedure for Evaluation of Pharmacological Effect on Motor Performance 197
5.5.2. Myoclonus: Capturing a Shock-Like Movement 202

6. Robot-Aided Functional Imaging: Learning a Dynamic Task 211
6.1. Background 212
6.1.1. Functional Imaging 213
6.1.2. Learning 213
6.2. Subjects 214
6.3. Experimental Setup and Procedure 214
6.4. Results 221
6.4.1. Changes in Neural Activity 221
6.4.2. Kinematics Analysis via a Simple Motor Performance Index 227
6.4.3. Kinematics Analysis via the Submovement Motor Performance Index 246

7. Technique to Investigate Ipsilateral Functional Activation in Motor Task 271

7.1. Background 271

7.2. Patients 272

7.3. Experimental Setup and Procedure 272

7.4. A Handful of Results 274

7.4.1. Motor Performance Improvement 274

7.4.2. Kinematics Analysis 276

8. Conclusions and Future Research 301

Appendices:

A. Robot-Aided Neuro-Rehabilitation: Consent Forms 309

B. Robot-Aided Neuro-Rehabilitation: Clinical Scales 315

C. Robot-Aided Neuro-Rehabilitation: Patent 333

D. Robot-Aided Functional Imaging: Tables of Significant Activation 361

E. Robot-Aided Functional Imaging: Trace, Speed, and Jerk Records 373

Bibliography 399

LIST OF FIGURES

1.1. Body Elements, Direction & Vigor of Motion in Labanotation. 23

1.2. Body Parts in Relation to Stances. 24

1.3. First Stances of Beethoven, Prometheus, N#9. 24

1.4. Prosthesis Emulator and Power Output During a Crank Task. 28

1.5. Anti-Sway Devices. 30

1.6. Underwater Vehicles will Install Drilling Tables in Very Deep Waters (>1000 meters). 31

1.7. Example of Telemedicine. 32

2.1. Drawing Circles. 43

2.2. Subject A Drawing Four Circles at Constant Target Speed. 45

2.3. Subject B Drawing Four Circles at Constant Target Speed. 46

2.4. Subject C (Violinist) Drawing Three Circles at Constant Target Speed. 47

2.5. Subject A Drawing a Circle at Constant Target Speed(12 o'clock). 48

2.6. Subject A Drawing a Circle at Constant Target Speed(3 o'clock). 49

2.7. Subject A Drawing a Circle at Constant Target Speed(6 o'clock). 50

2.8. Subject A Drawing a Circle at Constant Target Speed(9 o'clock). 51

2.9. Subject B Drawing a Circle at Constant Target Speed(12 o'clock). 52

2.10. Subject B Drawing a Circle at Constant Target Speed(3 o'clock). 53

2.11. Subject B Drawing a Circle at Constant Target Speed(6 o'clock). 54

2.12. Subject B Drawing a Circle at Constant Target Speed(9 o'clock). 55

2.13. Subject C (Violinist) Drawing a Circle at Constant Target Speed (12o'clock). 56

2.14. Subject C (Violinist) Drawing a Circle at Constant Target Speed(3 o'clock). 57

2.15. Subject C (Violinist) Drawing a Circle at Constant Target Speed(6 o'clock). 58

2.16. Subject C (Violinist) Drawing a Circle at Constant Target Speed(9 o'clock). 59

2.17. Subject B Drawing a Straight Line at Constant Target Speed from Left to Right. 60

2.18. Subject B Drawing a Straight Line at Constant Target Speed from Right to Left. 61

2.19. Subject C Drawing a Straight Line at Constant Target Speed from Right to Left. 62

2.20. Subject B Drawing a Circle at Constant Target Speed(12 o'clock) - Counterclockwise from Subject's View Point. 63

2.21. Subject C (Violinist) Drawing Circles at Increasing Target Speeds. 64

2.22. Subject A Drawing a Circle at Constant Target Speed (6 o'clock). 66

2.23. Example of Velocity Profile Normalization. 66

2.24. Polar Plots of Subject A Drawing Four Circles at Different Constant Target Speeds. 68

2.25. Polar Plots of Subject B Drawing Four Circles at Different Constant Target Speeds. 69

2.26. Polar Plots of Subject C (Violinist) Drawing Three Circles at Different Constant Target Speeds. 70

2.27. Polar Plots of Subject C (Violinist) Drawing Circles at Increasing Target Speeds. 71

2.28. Curvature Correlates with Speed. 73

2.29. A Mass-Spring-Damping Mechanical System Speed vs Curvature. 73

3.1.1&2. Kinematic Data of Subject A in a Point-to-Point Movement without Time Constraint. 84 & 85

3.2.1&2. Kinematic Data of Subject A in a Point-to-Point Movement without Time Constraint. 86 & 87

3.3.1.to 10. Two Samples of the Initial Post-Stroke Recovery Phase for Each of the 20 Patients Enrolled in the Clinical Trial. 88 to 97

3.4. Kinematic Data of Subject D in a Point-to-Point Task without Time Constraint. 98

3.5. Examples of Normalized Beta Density Function for Different Values of ρ and σ. 100

3.6. Beta Density Function Parameters Determination. 100

3.7. Normalized Beta Density Function with υ of 6.28, ρ of 2.96 and σ of 3.32. 101

3.8. Multilayer Neural Network Structure. 105

3.9. Sketches of Radial Basis Function, Generalized Radial Basis Function, Shannon's Basis Function, and Hyper Radial Basis Function. 108

3.10. Hyper Radial Basis Function (HRBF) Multigrid Approximation. 109

3.11. Irregular Sampling Radial Basis Function (ISRBF). 111

3.12. Patient (A) Drawing Clockwise Single Circles Starting and Ending at Position P2 (9o'clock). 115

3.13. Application of the Irregular Sampling Radial Basis Function Algorithm (ISRBF) to the Circles of Fig.3.12. 116 to 118

3.14. Filter Bank, Wavelet, and Scaling Function. 122

4.1. Mechanical Configurations. 128

4.2. Estimated Dimensions and Forces During Design. 129

4.3. MIT-MANUS: Translational 2-dof Package (Degrees of Freedom). 130

4.4. Wrist Device: 3-dof Package (Degrees of Freedom). 132

4.5. Overview of Design Selections. 133

4.6. Carpentry Overview. 134

4.7. System Integration. 137

4.8. Power Circuit Logic. 138

4.9. Safety Logic. 139

4.10. C++ Classes in a Video-Game Executable File. 142

4.11. Hand-Holder Design. 143

4.12. Hand-Holders Manufacture Process and Materials. 145

4.13. Basic Set for Elbow & Shoulder Exercise. 147

4.14. Video-Games. 148

4.15. Video-Games for Elbow, Shoulder and Wrist. 149

5.1. Robot-Aided Neuro-Rehabilitation: Classroom or Group Session. 155

5.2. Robot-Aided Neuro-Rehabilitation: Self Care Therapy at Home. 156

5.3. Robot-Aided Neuro-Rehabilitation: Self Instruction or Mirror Exercise. 157

5.4. Time-Evolution of Shoulder/Elbow Motor Status Score of Trial's Groups. 171

5.5. Robot-Aided Assessment Rose (1) Procedure versus Timeline of Motor Status Score. 179

5.6.a.to h. Robot-Aided Assessment Rose (1) Procedure. 182 to 189

5.7. Time-Evolution of Shoulder/Elbow Motor Status Score on Selected Subjects After Hospital Discharge. 192

5.8. Visual and Spatial Exercise and Target Range During Training. 193

5.9. Mean Lateral Deviation form a Straight Line for Subject M. 194

5.10. Mean Lateral Deviation form a Straight Line for Subject A. 195

5.11. Mean Lateral Deviation form a Straight Line for Subject S. 196

5.12. Holding Task for Parkinson Patient without Tremor. 199

5.13.a. Parkinson Patient Holding Task Before Administration of Medication. 200

5.13.b. Parkinson Patient Holding Task 30 Minutes After Administration of Medication. 200

5.13.c. Parkinson Patient Holding Task 60 Minutes After Administration of Medication. 201

5.13.d. Normal Subject Holding Task with Dexterous Arm. 201

5.14. Target Range to Evoke Myoclonus. 204

5.15.a. Kinematic Data of Myoclonus Subject in Task 5 without Time Constraint. 207

5.15.b. Kinematic Data of Myoclonus Subject in Task 5 without Time Constraint. 208

5.16. Kinematic Data of Myoclonus Subject in Task 6 without Time Constraint. 208

5.17. Beta Density Function Parameters Determination for Myoclonus Shock-Like Movements. 209

5.18. Normalized Beta Density Function for Myoclonus Shock-Like Movements. 209

6.1 Robot-Aided Functional Imaging Apparatus Setup. 216

6.2. Robot-Aided Functional Imaging Setup with Subject. 217

6.3. Visual and Spatial Target Range. 219

6.4. General Arrangement and Force Fields in Different Conditions. 220

6.5. Early vs Baseline rCBF Activations. 224

6.6. Late vs Baseline rCBF Activations. 225

6.7. Negative Transfer vs Baseline rCBF Activations. 226

6.8. Example of Relative Increase in the Regional Cerebral Blood Flow During the Early Learning Phase (vs Baseline Motor Performance). 227

6.9. Mean Lateral Deviation from a Straight Line Averaged Across Eight Normal Subjects. 228

6.10.a.&b. Mean Lateral Deviation from a Straight Line for Subject CR. 230 & 231

6.11.a.&b. Mean Lateral Deviation from a Straight Line for Subject DB. 232 & 233

6.12.a.&b. Mean Lateral Deviation from a Straight Line for Subject DG. 234 & 235

6.13.a.&b. Mean Lateral Deviation from a Straight Line for Subject DS. 236 & 237

6.14.a.&b. Mean Lateral Deviation from a Straight Line for Subject DD. 238 & 239

6.15.a.&b. Mean Lateral Deviation from a Straight Line for Subject ES. 240 & 241

6.16.a.&b. Mean Lateral Deviation from a Straight Line for Subject MU. 242 & 243

6.17.a.&b. Mean Lateral Deviation from a Straight Line for Subject TH. 244 & 245

6.18.a.to d. Trace Record for Subject CR. 247 to 250

6.19.a.to d. Speed Record for Subject CR. 251 to 254

6.20. Mean Jerk Magnitude Across Eight Normal Subjects. 256

6.21. Example of Velocity Record for Subject DS. 258

6.22. Mean Number of Basis Functions Across Eight Normal Subjects. 259

6.23. A Point Mass-Spring Mechanical System in the Force Field. 261

6.24. Basal Submovement Mean Values for Subject CR. 265

6.25. Basal Submovement Mean Values for Subject DB. 265

6.26. Basal Submovement Mean Values for Subject DG. 266

6.27. Basal Submovement Mean Values for Subject DS. 266

6.28. Basal Submovement Mean Values for Subject DD. 267

6.29. Basal Submovement Mean Values for Subject ES. 267

6.30. Basal Submovement Mean Values for Subject MU. 268

6.31. Basal Submovement Mean Values for Subject TH. 268

6.32.a.&b. Mean Number of Basis for all Subjects. 269 & 270

7.1. Visual and Spatial Exercise and Target Range. 273

7.2. Mean Lateral Deviation from a Straight Line for the Unimpaired Arm of Three Hemiparetic Stroke Victims. 276

7.3. Mean Jerk for the Unimpaired Arm of Three Hemiparetic Stroke Survivors. 277

7.4.a. to c. Trace Record for Subject A. 281 to 283

7.5.a. to c. Trace Record for Subject G. 284 to 286

7.6.a. to c. Trace Record for Subject O. 287 to 289

7.7.a. to c. Speed Record for Subject A. 290 to 292

7.8.a. to c. Speed Record for Subject G. 293 to 295

7.9.a. to c. Speed Record for Subject O. 296 to 298

7.10. Basal Submovement Mean Values for Subject A. 299

7.11. Basal Submovement Mean Values for Subject G. 299

7.12. Basal Submovement Mean Values for Subject O. 300

Trace.1. Trace Record for Subject CR - Batch 7 & 8. 374

Trace.2. Trace Record for Subject DB - Batch 7 & 8. 375

Trace.3. Trace Record for Subject DG - Batch 7 & 8. 376

Trace.4. Trace Record for Subject DS - Batch 7 & 8. 377

Trace.5. Trace Record for Subject DD - Batch 7 & 8. 378

Trace.6. Trace Record for Subject ES - Batch 7 & 8. 379

Trace.7. Trace Record for Subject MU - Batch 7 & 8. 380

Trace.8. Trace Record for Subject TH - Batch 7 & 8. 381

Speed.1. Speed Record for Subject CR - Batch 7 & 8. 382

Speed.2. Speed Record for Subject DB - Batch 7 & 8. 383

Speed.3. Speed Record for Subject DG - Batch 7 & 8. 384

Speed.4. Speed Record for Subject DS - Batch 7 & 8. 385

Speed.5. Speed Record for Subject DD - Batch 7 & 8. 386

Speed.6. Speed Record for Subject ES - Batch 7 & 8. 387

Speed.7. Speed Record for Subject MU - Batch 7 & 8. 388

Speed.8. Speed Record for Subject TH - Batch 7 & 8. 389

Jerk_Index.1. Mean Jerk Magnitude for Subject CR. 390

Jerk_Index.2. Mean Jerk Magnitude for Subject DB. 391

Jerk_Index.3. Mean Jerk Magnitude for Subject DG. 392

Jerk_Index.4. Mean Jerk Magnitude for Subject DS. 393

Jerk_Index.5. Mean Jerk Magnitude for Subject DD. 394

Jerk_Index.6. Mean Jerk Magnitude for Subject ES. 395

Jerk_Index.7. Mean Jerk Magnitude for Subject MU. 396

Jerk_Index.8. Mean Jerk Magnitude for Subject TH. 397

LIST OF TABLES

5.1. Age, Sex, and Time Pieces of Information about the Trial's Groups. 161

5.2.a. Experimental Group Descriptive Data. 162

5.2.b. Control Group Descriptive Data. 163

5.3. Patients' Tolerance for the Procedure. 167

5.4.a. Experimental Group FIM, Fugl-Meyer, and Pain Data. 174

5.4.b. Control Group FIM, Fugl-Meyer, and Pain Data. 174

5.5.a. Experimental Group Motor Power, and Motor Status Score for Shoulder/Elbow. 175

5.5.b. Control Group Motor Power, and Motor Status Score for Shoulder/Elbow. 175

5.6.a. Experimental Group Motor Status Score for Wrist and Hand. 176

5.6.b. Control Group Motor Status Score for Wrist and Hand. 176

5.7. Admission Scores: Mean, Standard Deviation, P-Value for the Trial's Groups with Standard Assessment Scales. 177

5.8. Discharge Scores: Mean, Standard Deviation, P-Value for the Trial's Groups with Standard Assessment Scales. 177

5.9. Change During Acute Rehabilitation: Mean, Standard Deviation, P-Value for the Trial's Groups with Standard Assessment Scales. 177

5.10. Rose Drawing Scores: Mean, Standard Deviation, P-Value for the Patient's 181

6.1. Example of Motor Consolidation. 229

Activation.1.a. Early Motor Learning Minus Motor Performance Pet Activation (batches 3 & 4 minus batches 1 & 2). 362

Activation.1.b. Motor Performance Minus Early Motor Learning Pet Activation (batches 1 & 2 minus batches 3 & 4). 363

Activation.2.a.. Late Motor Learning Minus Motor Performance Pet Activation (batches 5 & 6 minus batches 1 & 2). 364

Activation.2.b. Motor Performance Minus Late Motor Learning Pet Activation (batches 1 & 2 minus batches 5 & 6). 365

Activation.3.a. Negative Transfer Minus Motor Performance Pet Activation (batches 7 & 8 minus batches 1 & 2). 366

Activation.3.b. Motor Performance Minus Negative Transfer Pet Activation (batches 1 & 2 minus batches 7 & 8). 367

Activation.4.a. Late Motor Learning Minus Early Motor Learning Pet Activation (batches 5 & 6 minus batches 3 & 4). 368

Activation.4.b. Early Motor Learning Minus Late Motor Learning Pet Activation (batches 3 & 4 minus batches 5 & 6). 369

Activation.5.a. Negative Transfer Minus Early Motor Learning Pet Activation (batches 7 & 8 minus batches 3 & 4). 370

Activation.5.b. Early Motor Learning Minus Negative Transfer Pet Activation (batches 3 & 4 minus batches 7 & 8). 371

CHAPTER 1. INTRODUCTION

"What has been will be again, what has been done will be done again; there is nothing new under the sun."

Kohelet 1:9 (Ecclesiastes)

1.1. Motion Language

Lan-guage - 1 a: the words, their pronunciation, and the methods of combining them used and understood by considerable community b (1): audible, articulate, meaningful sound as produced by the action of the vocal organs (2): a systematic means of communicating ideas or feelings by the use of conventionalized signs, sounds, gestures, or marks having understood meanings (3): the suggestion by objects, actions, or conditions of associated ideas or feelings < body ~ > (4): the means by which animals communicate (5): a formal system of signs and symbols (as FORTRAN or calculus in logic) including rules for the formation and transformation of admissible expressions (6): MACHINE LANGUAGE 2 a: form or manner of verbal expression; specif: style b: the vocabulary and phraseology belonging to an art or a department of knowledge c: PROFANITY 3: the study of language esp. as a school subject.

[Webster Dictionary]

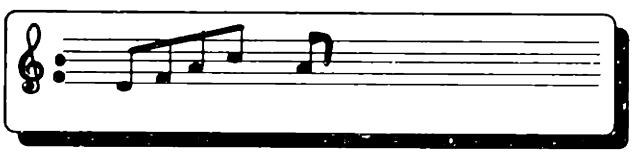

Musical notation is impressive. It took eight centuries to formalize (10th to 18th centuries). Five lines or staves and a few symbols proved to be an efficient language for encoding and decoding music. This is evidenced by a solid track record of more than five hundred years. It brings the music of Beethoven and Chopin to us. One might ask, could a similar coding for human motion be built?

A language for human movement is part of a large class of ill-posed problems with endless alternatives. For example, consider the case of dance. Several years ago, I went to see a performance of my aikido partner, dancer and ballerina. Sitting next to me was a painter who with fast pencil strokes tried to capture the dancer's body motion. It was feasible to visualize in that static drawing: motion. The painter could not explain her technique. But what were those strokes that so well captured Eve's spin ? There are other alternatives to encode dance movements such as the Labanotation -- Rudolf von Laban (1879-1958) [Von Laban, 1956][Brown and Parker, 1984] or the Benesh Movement Notation -- Joan and Rudolf Benesh (1955) [Brown and Parker, 1984]. As an illustration, Labanotation was developed to record the motion of parading soldiers and of folk dancers in Germany and in the Austro-Hungarian Empire, and later factory workers in the post-World War II England. Labanotation subdivides the body, the movement direction, the speed and the muscular characteristics into a set of components: space, shape, body and effort life (Labanotation terminology). The latter is further subdivided into smaller components: intent, body weight, flow, and time.

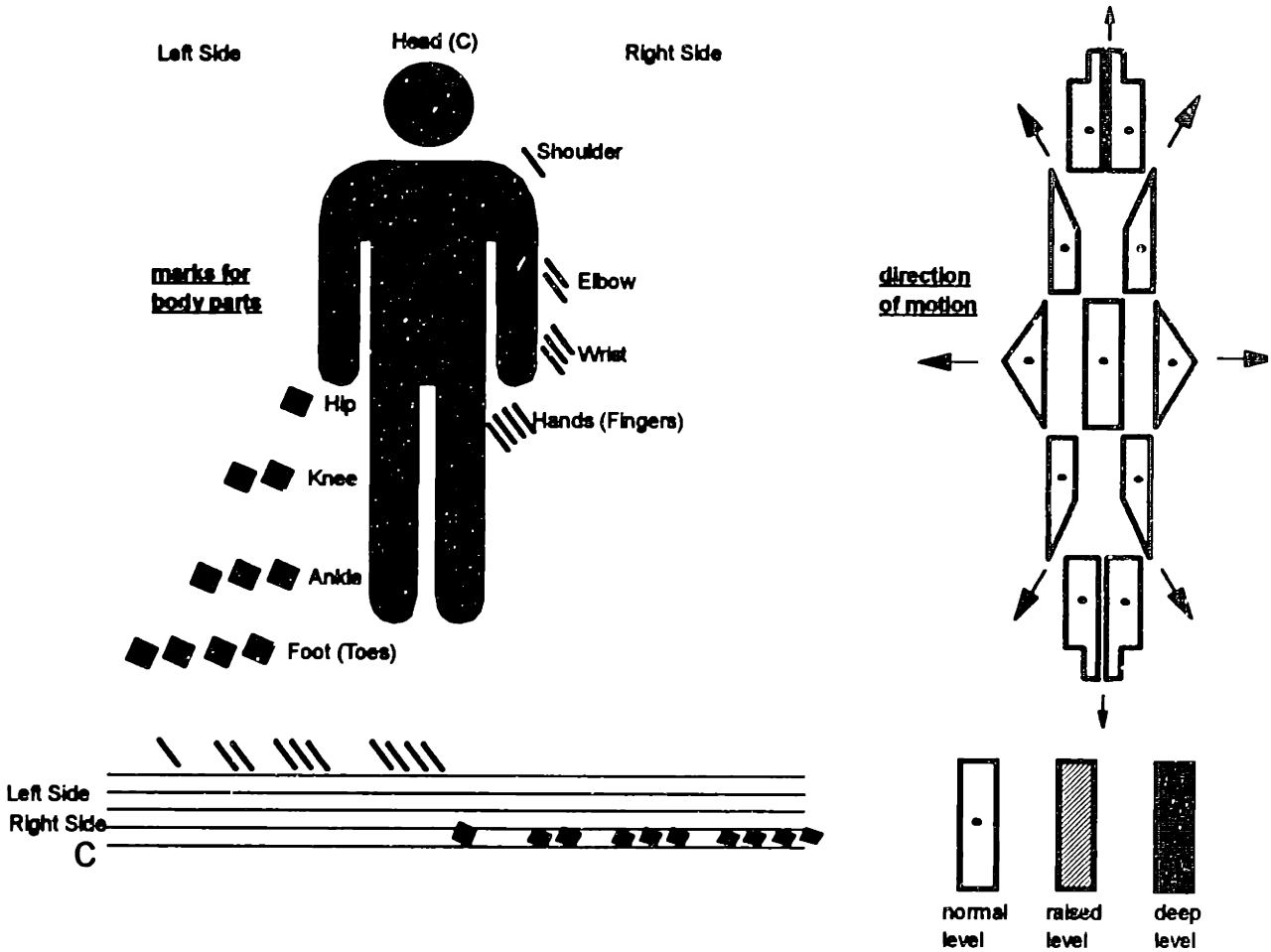

FIG.1.1. Body Elements, Direction & Vigor of Motion in Labanotation.
Labanotation encodes the dance's motion in five stances as musical notation. The right side of the body is represented in the lower half and the left side in the upper half of the stances (lower left quadrant of the figure). Body elements are identified by (a) bullets – hip, knee, ankle, and foot; (b) backslashes – shoulder, elbow, wrist, and hands; and (c) letters – head (upper left quadrant). Direction of motion is indicated by geometric shapes (upper right quadrant). The muscular characteristic, i.e. vigor or intensity, is indicated by the geometric shape filling pattern (lower right quadrant).

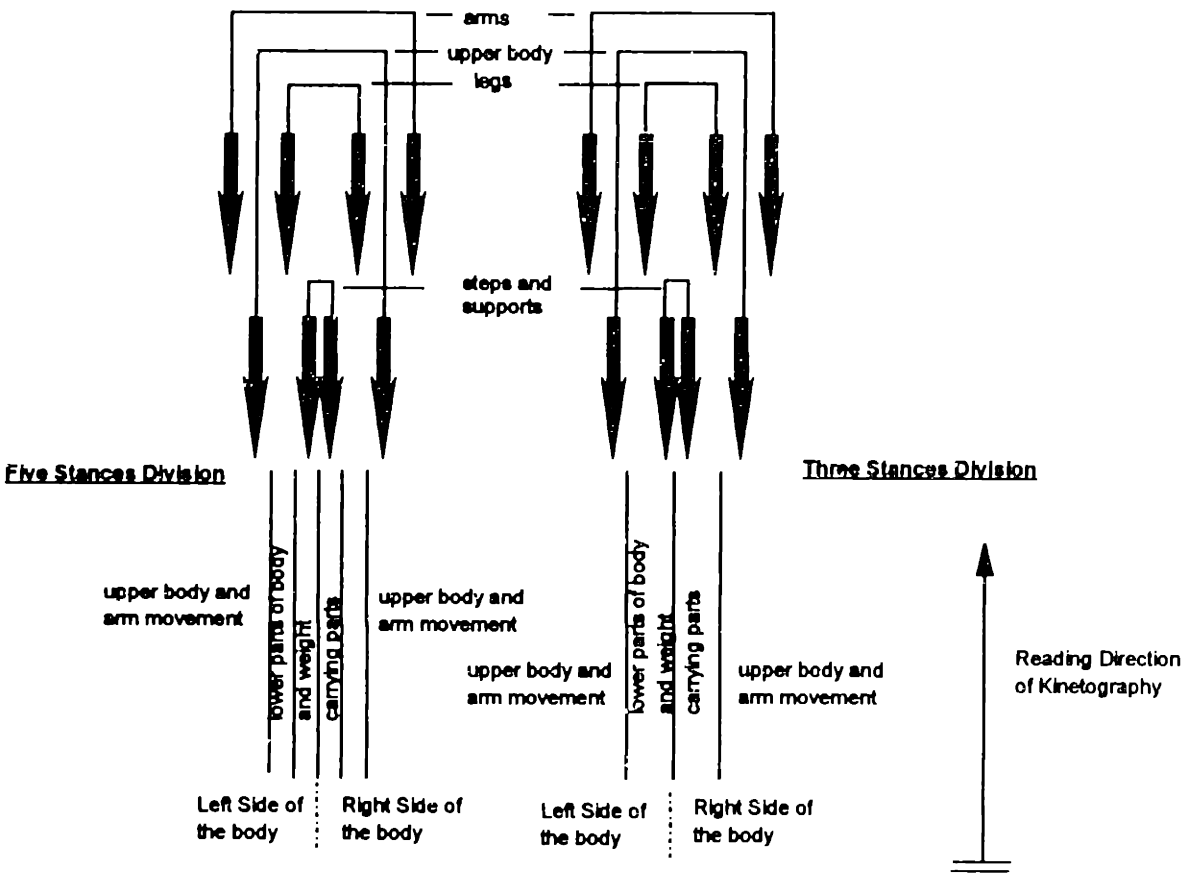

FIG.1.2. Body Parts in Relation to Stances.
Labanotation uses five or three horizontal stances, with the lower half representing the right side of the body and the upper half representing the left side. Notation from the centerline outward indicates leg, upper body, and arm movement.

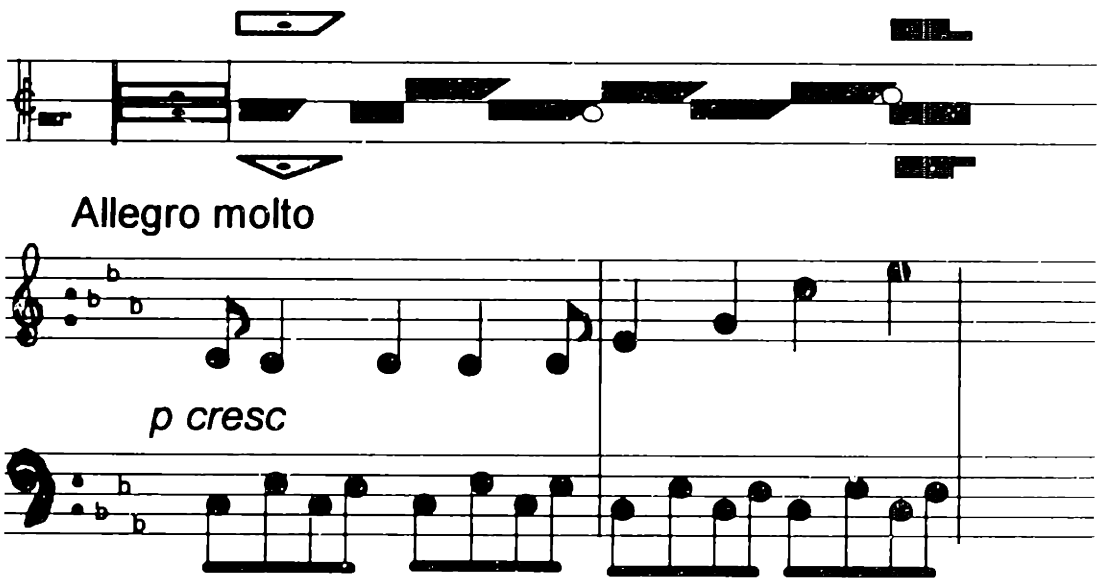

FIG.1.3. First Stances of Beethoven, Prometheus, N#9.
Free-hand illustration of music and dance notation.

Within the multitude of possibilities for human motion language, a biologically-based candidate would have an unquestionable advantage in engineering and the biomedical field. This represents the main thrust of this work:

> *To explore the central theme of studies in human motor control, which is to understand how intentions are translated into actions and build a biologically-based language derived from present consensus in the field.*

Consider the original motivator and funding source of this project: robot-aided neuro-rehabilitation. A biologically-based language for human motion is an ideal tool for assessment of post-traumatic sensorimotor behavior and recovery. It has also important engineering consequences. As explored in the following section, it constitutes a biologically-based scheme for data-compression, for human-machine interface, and for communication in telerobotics.

1.2. Class of Applications of a Motion Language

Keep in perspective the comment by IBM's Tom Watson about the personal computer market:

> *" I think there is a world market for about five computers."*
>
> -- Thomas J. Watson, 1943 -- Chairman of the Board of IBM

Rather than creating ideological boundaries, this research is limited to the class of upper-limb human-machine interactions and human motor control. The generality of the movement language problem is exemplified via the cases of the motorized arm prosthesis, of anti-sway devices in containercranes, of deep sea oil exploration, and of surgery telementoring.

Motorized arm prostheses are a mature technology with its major development efforts occurring during the Vietnam War decades of the 1960's and 1970's. The end result is a solid engineering design in which the elbow prosthesis sits on the subject's stump and his/her contraction of the

biceps or of the triceps, commands the prosthesis to flex or extend. The contraction of the biceps or triceps is sensed via electromyographic signals. Batteries power a geared electrical motor with a normally "on" locking mechanism, "off" during activation. In some designs, the velocity of the movement is proportional to the differential electromyographic activation of the biceps and triceps, resulting in a high output impedance controller. Though a well-engineered device has been available for over 25 years, its market share is below 5 percent. In practice, most amputees prefer Northrop Aircraft's World War II (WWII) body-powered arm prosthesis. This remarkable difference in people's preference cannot be solely explained by cost, since in general, either alternative is covered by the insurance carrier.

In order to understand the causes of such results, an elbow powered arm prosthesis emulator was built in the MIT-Newman Laboratory allowing several different controller strategies to be simulated. Figure 1.4. illustrates the prosthesis emulator and some results during a task that required the amputee to turn a crank up and down. The plots on this figure show on the top row results using the velocity controller (NYU) implemented in the commercially available prosthesis [Mansfield, 1992]. The first column shows a plot of the elbow angle versus crank angle. The second column shows the power output with the vertical line representing the boundary between positive power output from the prosthesis (to the right), and negative power output (to the left). Positive power output indicates that the prosthesis is delivering power to the task, while negative power output indicates power consumption by the prosthesis. It indicates that between the range of 150 to 200 degrees of the crank task, the prosthesis is a hindrance to the movement, consuming power. For comparison purposes, the lower row shows the passive case, i.e. the prosthesis has not been powered in which the amputee completes the task using inertial forces and motions of other (intact) body segments. The impedance controller is shown in the center row. It uses the differential and additive electromyographic activation of the biceps and triceps. The additive component controls the prosthesis impedance in a similar fashion to the intact arm impedance control via activation and coactivation of the biceps-triceps during flexion of the elbow, or triceps-biceps during the extension of the elbow, respectively. The differential component estimates the differences between actual and desired angular positions and velocities. The end-product is a low output impedance controller. Note that the impedance controller did not

absorb power and was unanimously preferred by subjects unaware of the implemented controller strategy. Mansfield suggested that power consumption indicates the reason for the small market share of the motorized elbow prosthesis: its control strategy makes it unnatural and difficult for amputees to learn to operate. Human movement speed is not proportional to the myoelectrical activity in muscles, and during part of the task the prosthesis hinders the movement. This is a good example of a sound engineering solution that did not take into consideration how the brain encodes movement. Therefore, this unnatural solution was rejected by the market. Mansfield suggested that the impedance controller is a natural controller. Thereby suggesting that a biologically-based controller could change the market selection.

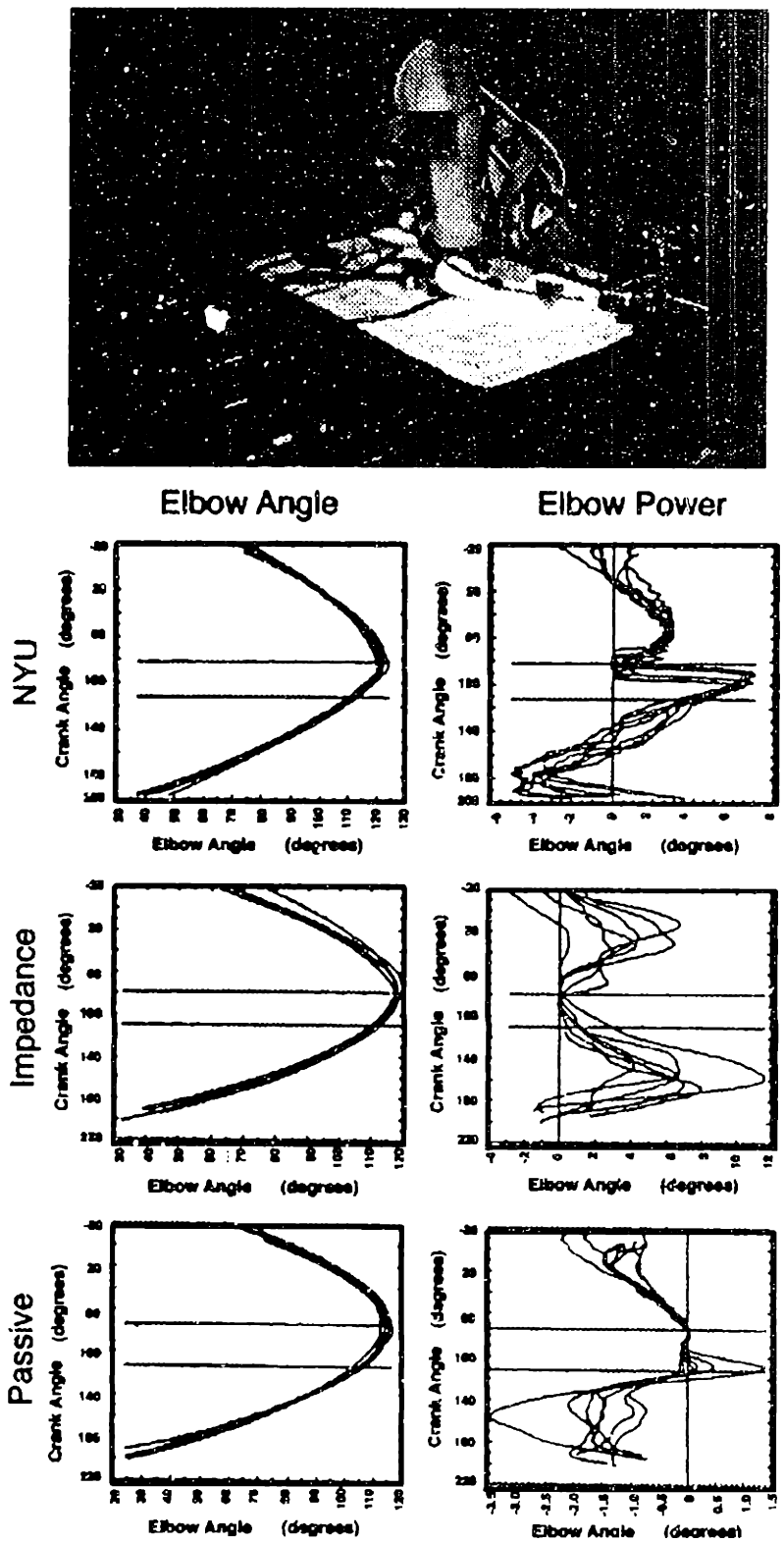

Fig. 1.4. Prosthesis Emulator and Power Output During a Crank Task.
The left column shows the elbow angle versus crank angle, and on the right column shows the power output for the crank task with the emulator implementing different control strategies. To the right of the vertical line indicates that the prosthesis isdelivering power to the task, while to the left of the vertical line indicates power consumption by the prosthesis.

Another example of a sound engineering design that requires a new approach is anti-sway devices for containercranes. Market forces dictate that a basic feature of a good product or service is its cost. In the maritime transport service, the concept of standardized packaging is associated with the objective of minimizing time spent in port while increasing the overall transported cargo by an increase in the number of a ships' round-trips per year. Since the 1950's, container transport has proven to be the most efficient mode for break-bulk cargo with a trend in the last fifteen years toward "round-the-world" services, in which shipments are routed through two main ports with smaller ports being served by feeder lines. The capacity and size of containerships increased dramatically from 500 to more than 3,000 boxes for the Post-Panamax. Consequently, the height of the containercranes, as well as the trolley and the hoist speeds increased. Likewise, the sway of the pendulum carrying the box increased. Skilled crane operators manage to stop the box without any delay due to sway. This skill is crane specific and is acquired over years of operating the same set of machines. To generalize this trait and minimize the average time per cycle, several anti-sway devices are presently being introduced into the market. These devices are typically being installed in new, higher, and faster containercranes. Although the manufacturers do not clearly specify the control algorithm, I believe that the fact that the operator's cab is under the trolley was not taken into consideration. The trolley is jerked back-and-forth, and my personal observation is that the unskilled operator turns off the anti-sway device after his first encounter with the system (skill is crane specific and these are new cranes). This is another example of sound engineering design that did not take the user into consideration. A controller that considers the approach of good crane operators in existing facilities has a significantly better chance of becoming a useful tool.

FIG.1.5. Anti-Sway Devices.
The capacity and size of containerships increased dramatically from 500 to over 3,000 boxes. Therefore, the height of the container cranes, trolley and hoist speeds did increas Several anti-sway devices are being introduced into the market to minimize the sway of th box, generalize operator's skill, and minimize the average time per cycle.

Consider the case of extracting oil from deep waters. Presently the cost prohibits the extraction of oil at sea depths below 300 meters, although vast oil reservoirs have been found in deep waters. For example, the largest oil field on the Brazilian continental shelf is below 1,000 meters of water. This depth is below the acceptable level for divers, but the drilling table must be properly installed. Underwater vehicles are the logical tools to install this table, but the task of the operator of the manipulator of either manned or unmanned vehicles requires enormous dexterity and training. A biologically-based movement encoder would help reducing the installation time, the cost, and the inherit difficulty of the operation.

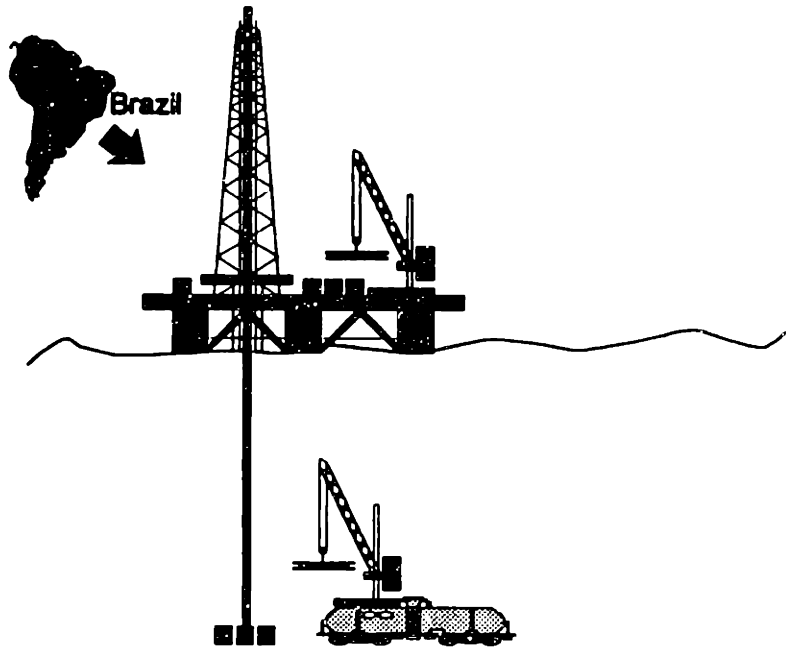

FIG.1.6. Underwater Vehicles will Install Drilling Tables in Very Deep Waters (>1000 meters).

The final example corresponds to a whole new form of on-line services that are evolving from fast means of electronic communication. In fact, I have argued that we are on the verge of a new loop in the industrial revolution, namely: telepresence [H.I.Krebs - Ph.D. Thesis Proposal]. One of the best examples of this new technology is the videophone and the on-line video in computers, which will shortly be commercially available on the market. In my opinion, these advances will revolutionize society. While we are making rapid progress in visual and auditory telepresence, the pace is several orders of magnitude slower in haptic telepresence. Haptic sense refers to the feeling of touch and proprioception, i.e. sense of position in the static limb and of limb movement (kinesthesia). Consider the practical example of the U.S.S. Abraham Lincoln Battle Group somewhere in the Indian Ocean, during a six month seaborne mission with its 7,000 crew members. A female crew member had an emergency that required immediate surgery. The surgery was successfully performed, although the battle group's head surgeon had never performed a

similar operation. An experienced gynecological surgeon at Johns Hopkins Medical School "telementored" the battle group surgeon via images transmitted by satellite (IMARSAT) over a 14,400 baud communication line of the carrier (9,600 baud for auxiliary vessels). Telementoring is a neologism meaning that an expert utilizes on-line visual and auditory information to discuss and explain the indicated procedure to a non-expert. While telementoring is a present option, telerobotics is not. Several universities, research facilities, and companies are working in making telerobotics reality. In this case, a biologically-based movement encoder would help in data-compression, in human-machine interface, and in communication.

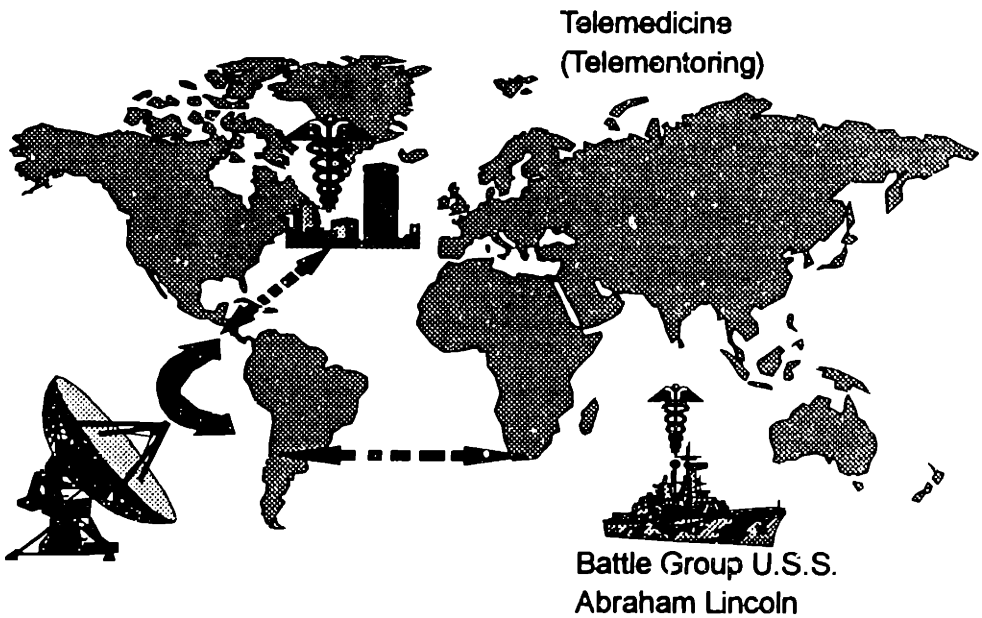

FIG.1.7. Example of Telemedicine.
Expert uses visual and auditory information to view and explain to non-experts the indicated procedure and steps.

These examples have illustrated the generality and engineering consequences of a biologically-based movement encoder. I would like to conclude this section repeating and extending an early statement regarding the main thrust of this research:

To explore the central theme of studies in human motor control, which is to understand how intentions are translated into actions and build a biologically-based language derived from present conjecture in the field. In particular, to explore the concept that arm movement is segmented with identifiable invariant movement characteristics. These segments or submovements constitute the primitives or building blocks of more complex movements.

1.3. Thesis Overview

Chapter 2 presents a bibliographic overview on submovements and examples of arm movement. These examples show raw data from three normal, unimpaired subjects performing simple tasks, such as drawing straight lines, circles, squares, and diamonds. These examples are explored in different manners to reveal the concepts and the working models underlying this work, as well as the difficulties of the task encoding scheme. Once the working models are presented, Chapter 3 explains how the basis function was chosen, the limitations of this representation, and the details of the algorithm engines used for encoding the movement mimicking the human. The robot design philosophy, mechanical, electrical, software, and manufacturing aspects are described in Chapter 4. Chapters 5 through 7 describe several applications such as: (a) the original motivator and funding source of this research: robot-aided neuro-rehabilitation, assessing the application of robotic technology to assist, enhance, quantify, and document the neuro-rehabilitation of patients with different neurological disorders (Chapter 5); (b) robot-aided functional imaging, which describes the integration of robotics with functional imaging, thus providing a facility to manipulate as well as measure motor consequences of neural activity measured by imaging technologies and influenced by pharmacological interventions. This chapter also describes experimental results in motor control and learning theory, in particular suggesting different levels of organization of the higher level controller (Chapter 6); (c) technique for validation of functional imaging results is described in Chapter 7. Future directions, a "wish-list", and conclusions are presented in Chapters 8.

CHAPTER 2. FROM THE SYMBOLIC LEVEL TO THE ENERGY-DOMINATED LEVEL VIA A "SUBMOVEMENT"

"Original ideas are exceedingly rare and the most that philosophers have done in the course of time is to erect a new combination of them."

– G. Sarton

"We master archers say: one shot - one life! What this means, you cannot yet understand. But perhaps another image will help you, which expresses the same experience. We master archers say: with the upper end of the bow the archer pierces the sky; on the lower end, as though attached by a thread, hangs the earth. If the shot is loosed with a jerk there is a danger of the thread snapping."

"Only now, when expressly watching out for it, did I observe that though the right hand of the Master, suddenly opened and released by the tension, flew back with a jerk, it did not cause the least shaking of the body. The right arm, which before the shot had formed an acute angle, was jerked open, but ran gently back into full extension. The unavoidable jerk had been cushioned and neutralized."

– Eugen Herrigel – 1953 –

– Zen in der Kunst des Bogenschiessens

2.1. Literature Overview

To write a bibliographic review of any subject is quite a dangerous enterprise. It deals with egos and national interests. I learned this as an undergraduate engineering student in Brazil. Many excellent translated Russian textbooks were sold in Sao Paulo at bargain price for public relations at the time of the defunct Soviet Union. It was quite an experience to learn that many of the major

scientific discoveries and engineering advances were first developed by Soviet scientists and engineers, and not by Americans, Germans, British and French copycats, as claimed in other textbooks. It was not too different during my years in Japan. Japanese and Western news agencies routinely reported an event, and I often wondered if they were really talking about the same event. Therefore, this review is an overview biased and limited fundamentally to early British (during the era when the sun did not dare set over the empire) and American sources. The objective is to provide a survey of the subject.

The earliest work that identifies submovements, also called movement segments or movement primitives, and referred to in several articles on the subject, is Woodworth's Ph.D. Thesis at Columbia [Woodworth, 1899]. He argued that movement was composed of two submovement components: the initial impulse and the current control. The current control consisted of a sequence of finer adjustments added to the initial impulse as the hand approaches the target. He argued that current control could be eliminated by either having the person close his eyes or by requiring very fast movements. The literature on submovements remained dormant for the following half a century.

During WWII, it became very important to study the process of aiming at a target. The scientific result of that effort turned into the well known Fitts' Law [Fitts, 1954]:

$$Ip = -\frac{1}{T}\log_2\left(\frac{W}{2A}\right) \qquad \text{(eq. 2.1.)}$$

Fitts applied an information-theoretical approach to characterize the task in terms of information transmission rates. In the above equation, Ip is bits/sec, T is the movement time, W is the target width, and A is the movement amplitude. The term $-\log_2\left(\frac{W}{2A}\right)$ is the index of task difficulty. This empirical law was followed by different variations on the theme, such as underwater studies [Kerr, 1973], which is not discussed in this overview.

Several researchers formulated different models proposing variations of the submovement concept in an attempt to explain the microstructure of Fitts' Law. Crossman & Goodeve (conference 1963

- published in 1983) considered two different models: a continuous velocity control of a dynamic model (linear system) and an intermittently sampled submovement model. Their experiments suggested that the continuous velocity control model could not explain some of their results, while the submovement model could. They considered periodic submovements with displacement in the shape of error function (erf) [Crossman & Goodeve, 1983]. Jagacinski showed that the periodicity in the Crossman & Goodeve submovement model was unacceptable. His results reject both the second-order linear system and the periodic segmentation. He showed that the first segment is quite different from the subsequent segments. However, Jagacinski and other researchers could not provide enough experimental evidences to support the common hypothesis, first hypothesized by Woodworth, that the first submovement is performed open-loop, while the subsequent ones are under feedback control [Jagacinski, 1978][Jagacinski, 1980].

Crossman & Goodeve's suggestion of a single shape scaled and dilated to describe the submovement is one of the earliest suggestions of a single basis function to describe movement segments. Their suggestion of the integral of a Gaussian to describe the segment displacement was followed by others such as minimum jerk (first derivative of acceleration), minimum snap (second derivative of acceleration), minimum crackle (third derivative of acceleration), minimum time, minimum energy, minimum acceleration, and Gaussian velocity profile [Nelson, 1983][Hogan, 1984][Hollerbach, 1987]. There is a remarkable space-time invariance in handwriting [Viviani & Terzuolo, 1980]. There is good evidence that this invariance is expressed in terms of kinematics world-coordinates (i.e., trajectory of the hand in space) and not in joint-space coordinates or dynamics [Morasso, 1981]. Morasso and Mussa-Ivaldi suggested a model similar to Crossman & Goodeve to analyze trajectory formation and handwriting. They considered submovements, which they called "strokes" to occur periodically, and used B-Splines and S-Splines to fit the arm trajectory or handwriting. They brought to light the potential for data compression of a scheme such as the above [Morasso & Mussa-Ivaldi, 1982]. Viviani & Terzuolo showed the correlation between tangential velocity (V) and radius of curvature (R) [Viviani & Terzuolo, 1982], and Lacquaniti described it as the one-third power law [Lacquaniti, Terzuolo & Viviani, 1983]:

$$V(t) = K.R(t)^{1/3} \qquad \text{with} \qquad R < \infty \qquad \text{(eq. 2.2.)}$$

Flash and Hogan observing that natural unconstrained movements are characteristically smooth and graceful, formulated a mathematically concise model of motor coordination by postulating that voluntary unconstrained movement minimizes a quadratic jerk type cost function (C). Experimental results for a point-to-point movement in one and two dimensions confirmed this hypothesis. From optimization techniques, the velocity can be reconstructed from the knowledge of the initial and final position and time interval [Flash & Hogan, 1985].

$$C = \min \int_0^d \left| \frac{d^3 r}{dt^3} \right|^2 dt \qquad \text{with r the hand position coordinates.} \qquad \text{(eq. 2.3.)}$$

Flash and Henis' experimental results suggested how segments could blend together. In their experiment, the arm trajectory modification in response to an unexpected target displacement was given by superposing to the existing plan, a new plan for moving between the first and second target. The initial arm movement is not aborted, but added to the movement resulting from the new plan [Flash & Henis, 1994]. Milner suggested that the intermittent sampling feedback proposed by Woodworth holds for three-dimensional movement. His experiment consisted of a series of peg-insertion tasks. The hole sizes were changed and the hand path in space showed the "initial impulse and current control" structures of Woodworth, or in Crossman & Goodeve's words the "intermittent sampling feedback". He considered the minimum-jerk basis function, reasoning that the initial ascending part of the subject's movement velocity profiles was very consistent and fit the minimum-jerk bell-shaped profile very well. In separate papers, he presented two different approaches to extract the strokes: zero-crossing of the velocity in the Y-Z plane or manually adjusting the scaling, dilation, and translation of the minimum-jerk basis [Milner, 1992]. It would be hard to segregate Milner's experimental results from Ojakangas' experimental results with monkeys, showing that Woodworth's observation of an "initial impulse and current control" is ubiquitous. He also suggested the role of visual feedback in the submovement phenomenon [Ojakangas & Ebner, 1991]. Bahill & Stark presented an interesting review of their results on the trajectory of saccadic and vergence eye movement. Saccades happens at speeds up to 900 degrees/sec, and there is no time for visual feedback to modify the course of a saccade.

Corrections are made by smaller saccades after the primary one in a similar fashion to Woodworth's model of arm movement [Bahill & Stark, 1979]. The latency between saccadic movements and hand movements is approximately 100 msec [Prablanc, 1979]. There are suggestions of evidence of correlation between saccadic movement and hand movement (Flash - personal conversation - 1995), although no convincing results were available.

In hindsight, it is easy to observe the natural evolution of these ideas: motor learning. Hollerbach suggested that it is conceivable that motor learning might take place by learning the basic torque profiles and then scaling them to movement requirements [Hollerbach, 1982]. Although the concept was correct, the views of this thesis are more inline with Milner's closing comment in his conclusions that an appropriate strategy for motor learning consists of blending the discrete series of segments or submovements observed in the first approximation of the desired movement [Milner, 1992].

In the distinct field of child psychology and development, similar observations may be found both in terms of movement segmentation, as well as in motor learning. Hofsten ran a series of experiments among infant subjects 12 to 24 weeks old until they become "mature" babies at 36 weeks old. The task consisted of reaching a moving multicolor wobbler. The results supported that movement is composed of segments with a macro-micro structure (initial impulse and current control), and that with practice (age) these submovements blended into a single segment that resembled adult movements [Von Hofsten & Lindhagen, 1979] [Von Hofsten,1980].

The underlying premise on all the research previously mentioned is to explore the motor system limitations and understand it via input-output relations. Though one may explore the motor system limitations and preferred operational modes to infer the system control structure, one may also explore the structure of the black-box (biological system). Polit & Bizzi showed in an experiment involving deafferented monkeys that limbs exhibit strong stability properties during movement, and proposed that movement is executed by commanding an "equilibrium-point" [Polit & Bizzi, 1979]. The equilibrium-point hypothesis was extended to include a reference trajectory which consists of a sequence of postures along the path of the extended motion [Feldman, 1966]

[Bizzi, 1982]. This sequence of postures was termed "virtual trajectory". These results suggest that a higher level in the motor control hierarchy appears to be exploiting the limb's strong stability property and computing only the task kinematics, i.e. virtual trajectory. This approach represents a remarkable simplification of the computational effort required to attempt to fully control the system dynamics. Recent experimental results have categorically proven the existence of this trajectory [Hodgson, 1994]. Yet while proving that an attractor trajectory can be identified, he also proved that the concept that the virtual trajectory is more invariant than the actual trajectory does not hold for unconstrained movements, implying that more than kinematics is needed.

Another powerful insight on the black-box came with experimental results pointing to the direct cortical representation of movement [Georgopolous, 1982]. Georgopolous showed that the discharge of populations of cells in the motor and parietal cortex of primates is correlated to the direction of the movement in a two-dimensional task. This result supports the world-coordinate's hypothesis. Kalaska showed that the discharge of these populations of cells was in general invariant to load, but correlated to the arm trajectory [Kalaska, 1989]. This result supports the hypothesis of kinematics coding and computational simplification, but it raises a very important question: Does it mean that the population of cells is continuously controlling movement? The answer is likely no. The population cells firing might be a predictor mechanism for the movement or the virtual trajectory. Recently, Schwartz showed that in primates this direct cortical representation of arm movement in spiral drawing only preceded the movement in predictive manner for a radius of curvature above 6 cm. He concludes that the population vector method is only relevant to discrete parts of the movement [Schwartz, 1994].

Another important insight in the nervous system chain of command comes from recent results in frogs. These results suggest that the composition of limb movement might have a similar control architecture as previously suggested for the eye. It has been shown that the innervation of a single interneuron and/or axon pool moves the eye to the same equilibrium position. By activating two of these pools, the equilibrium position will be located between the two initial equilibrium positions. By modulating the innervation of each of the single pools, different equilibrium points

may be achieved. The results on frogs showed that innervation of pools of interneurons and/or axons at the same location in the spinal-cord generates multidimensional movement of the limb towards the same equilibrium point. By stimulating two of those pools, the frog leg rests at an equilibrium position that could be modelled as a vectorial superposition of two fields identified from the innervation of each pool separately [Giszter, Mussa-Ivaldi & Bizzi, 1993]. This result also supports the hypothesis of kinematics coding and computational simplification due to the exploration of the intrinsic strong limb stability properties. It can be speculated that the higher level computes or predicts kinematic behavior, and recruits and modulates the proper sequence of motor primitives resident at the lower level, in particular, in the spinal cord.

Summarizing this survey:

1) Submovement is an old concept.

2) Woodworth suggested the "initial impulse and current control".

3) Kerr showed that Fitts' Law is also valid underwater.

4) Crossman & Goodeve's suggested a plausible intermittently sampled submovement model.

5) Jagacinski showed the need to relax the periodicity in Crossman & Goodeve's model.

6) Morasso & Mussa-Ivaldi applied a variation of Crossman & Goodeve with periodic splines, and showed the potential of data-compression.

7) Saccadic eye movements also fits Woodworth suggestion of an "initial impulse and current control".

8) Milner considered Jagacinski's remark and Flash & Hogan's concise model and applied it to a peg insertion task. He also suggested my preferred method of motor learning.

9) Hofsten showed similar results in the field of chid psychology.

10) Georgopolous, Kalaska, and Schwartz showed that the discharge of populations of cells in the motor and parietal brain areas are correlated with the direction of the movement (kinematics).

11) Giszter, Mussa-Ivaldi, and Bizzi showed that coordinated multidimensional limb movement may be achieved in a predictable fashion from the combination of stimuli at different locations of the frog spinal cord.

2.2. Examples of Arm Movement

The objective of this section is to summon attention to the evidence for submovement and models underlying this work. The proverb stating that a picture is worth a thousand words has never been so valid, and I will resort to examples. There are several potential techniques used to evoke submovements: a) alter the task goal location after its initiation, e.g. Flash & Henis displaced the target after movement initiation; b) perturb the arm movement, e.g. Mussa-Ivaldi introduced a force perturbation perpendicular to the movement; c) increase the complexity of task, e.g. Milner reduced the size of the hole during the peg-insertion task; and d) explore the different time-scales of movement compared to the natural response of system. The raw data of different normal subjects drawing simple geometrical forms will be shown to expose and clarify these points.

2.2.1. Experimental Setup and Procedure

This study used the 2-dof module of a novel portable robot designed for clinical neurological applications: MIT-MANUS. The robot will be described in more detail in Chapter 4. Three neurologically normal young subjects with no previous experience in manipulating the robot volunteered for this comparative study. They are right handed with average age of 27 years. Two subjects were male and the female was an amateur violinist recruited from MIT's Symphony Orchestra. Written consent was obtained from the subjects in accordance with the guidelines of the MIT-Committee on the Use of Humans as Experimental Subjects (Protocol # 2187). They sat facing the robot and were instructed to move the robot end-effector drawing clockwise circles, squares, diamonds, and lines, starting and ending at pre-specified positions in the workspace, as illustrated in Fig.2.1. Their hand was within view, but no explicit feedback was provided.

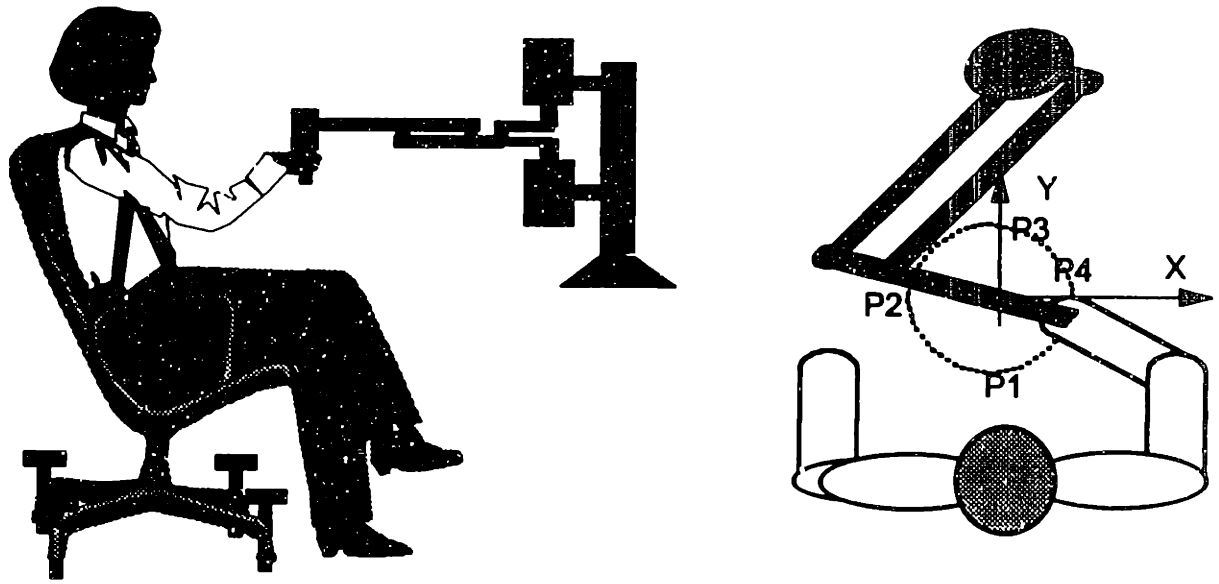

FIG.2.1. Drawing Circles.
Subjects sit facing the robot and grasped the handle of the robot with the palm of the hand. The task required the subject to draw circles or lines at pre-determined positions, e.g., draw a circle starting and ending at P1.

2.2.2. Drawing at Constant Speeds

The subjects were asked to draw at constant speeds. They were first instructed to draw the geometric form at very low constant speed. In the subsequent trials, they were asked to redraw the geometric shape with a higher constant speed. Trials continued until the subject considered himself/herself unable to maintain a constant speed. Figures 2.2. and 2.3. show the displacement and tangential velocity of the two male subjects drawing four consecutive circles.

Note that the subjects were unable to maintain a constant speed. At low speeds, any inertial effects of the mechanism are expected to be small. Yet, a speed oscillation in the range of 30 percent of the mean may be observed. Figure 2.4. shows the results of a similar experiment with an amateur violinist from the MIT Symphony Orchestra who has years of training and the ability to maintain constant bow speed, drawing three consecutive circles. As with all subjects, her hand

was in view, but she had no other form of feedback such as the audio feedback a violin provides. Subjects had to perform the task with visual and proprioceptive information only. Her results differ from the other subjects regarding the interpretation of the experimental instructions. First, her chosen initial constant target speed was substantially lower than the other subjects. Second, the results suggests that she chose to double the average speed between trials with remarkable accuracy. These results will be revisited in Section 2.3. For now, note that her movement retains the oscillatory characteristic at target speeds comparable to the other subjects (lower row). The next batch of figures show the results for each subject drawing a single circle with target constant speed, starting and ending in the same region of the circle. Figures 2.5. to 2.16. present sets with initial and final points at P1 (6 o'clock), P2 (9 o'clock), P3 (12 o'clock), P4 (3 o'clock). This section concludes by presenting straight lines (Fig. 2.17. to 2.19.) and counterclockwise circle (Fig.2.20.) for different subjects with a target constant speeds. Note that in the case of straight lines, the speed profile presents an oscillatory characteristic at low speed values. It blends together with increasing target speed and starts to resemble the stereotypical minimum-jerk profile of an unconstrained point-to-point movement.

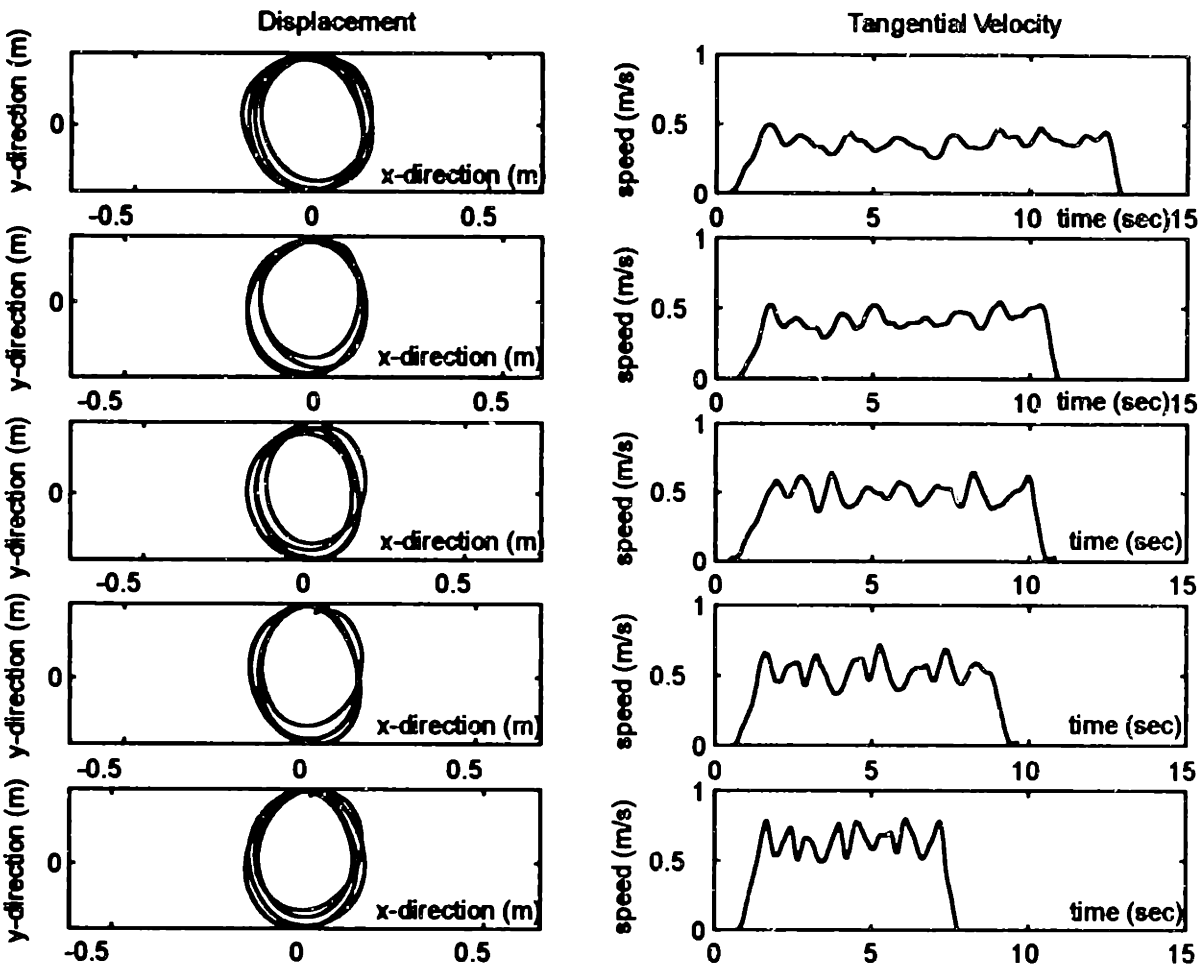

FIG.2.2. Subject A Drawing Four Circles at Constant Target Speed. Subject grasped the robot handle with the palm and was instructed to draw circles at constant speed. The trial was repeated until the subject considere himself/herself unable to maintain constant speed. The left column shows the circle traces and the right column shows the speed profiles at different target constant speeds. Note the oscillatory characteristic of the speed in all trials.

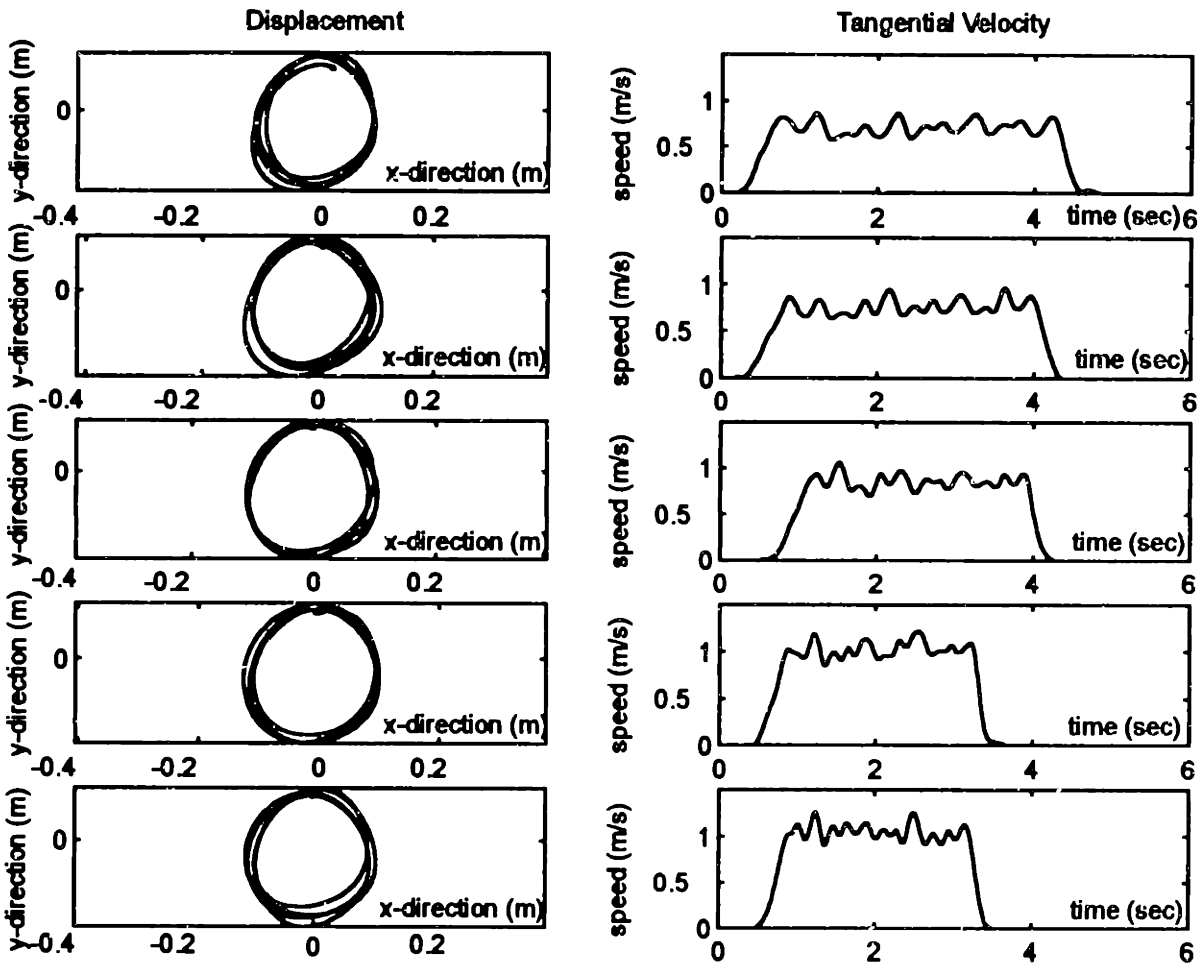

FIG.2.3. Subject B Drawing Four Circles at Constant Target Speed. Subject grasped the robot handle with the palm and was instructed to draw circles at constant speed. The trial was repeated until the subject considered himself/herself unable to maintain constant speed. The left column shows the circle traces and the right column shows the speed profiles at different target constant speeds. Note the oscillatory characteristic of the speed in all trials.

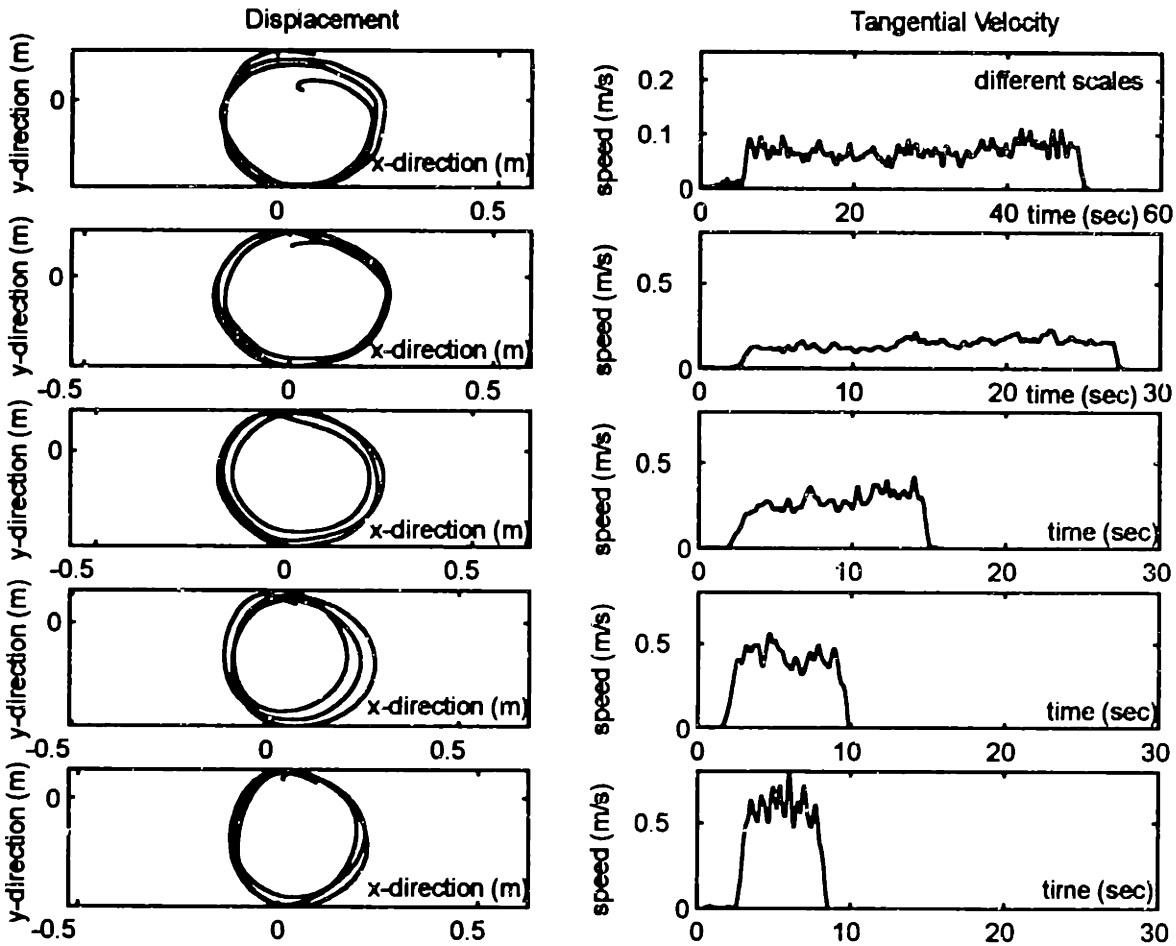

FIG.2.4. Subject C (Violinist) Drawing Three Circles at Constant Target Speed Subject grasped the robot handle with the palm and was instructed to draw circles at constant speed. The trial was repeated until the subject considered himself/herself unable to maintain constant speed. The left column shows the circle traces and the right column shows the speed profiles at different target constant speeds. Note the same oscillatory characteristic of the speed at comparable value with other subjects (lower row).

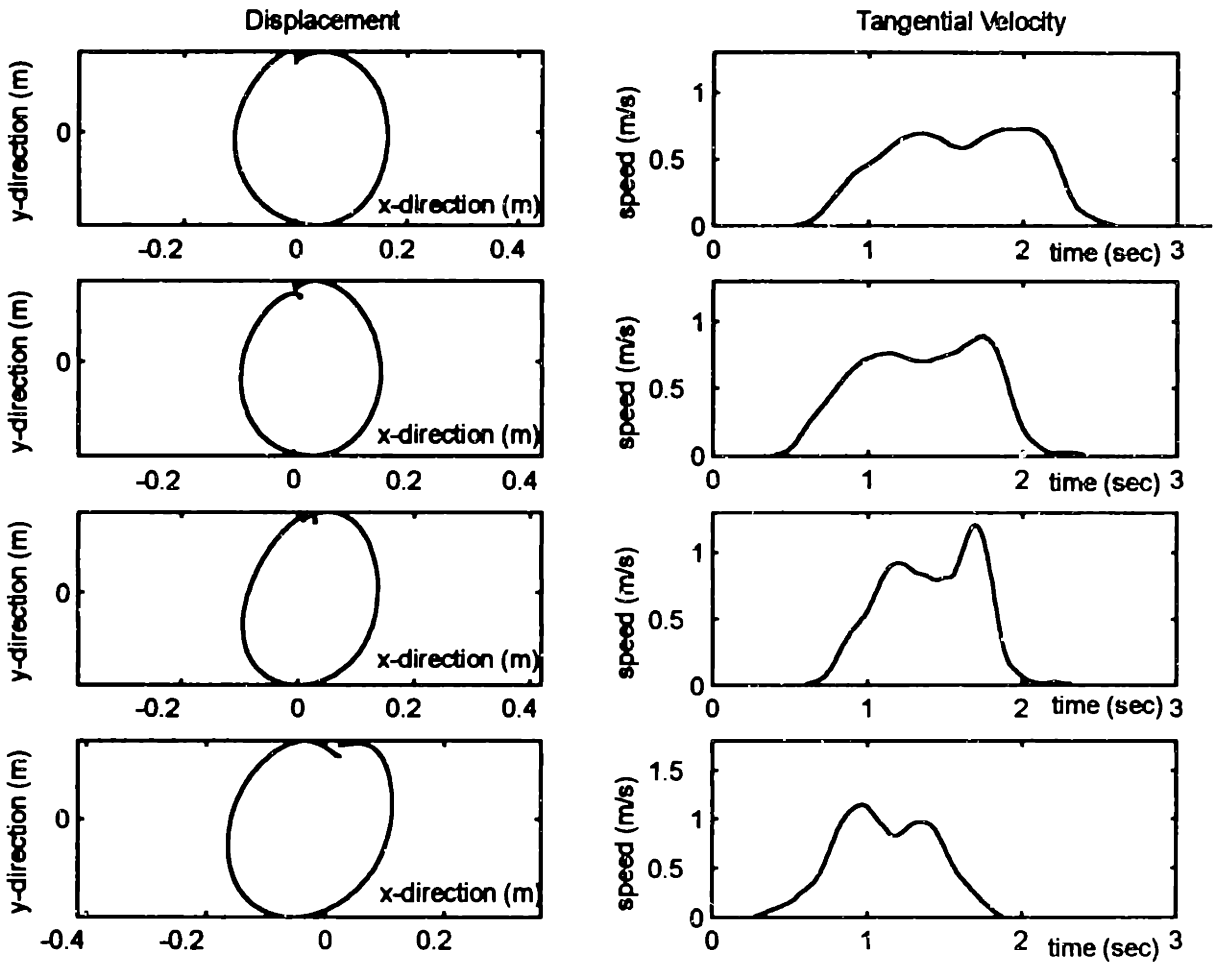

FIG.2.5. Subject A Drawing a Circle at Constant Target Speed (12 o'clock). Subject grasped the robot handle with the palm and was instructed to draw a circle at constant speed starting and ending at the same point. The trial was repeated until the subject considered himself/herself unable to maintain constant speed. The left column shows the circle traces and the right column shows the speed profiles at different target constant speeds. Note the oscillatory characteristic of the speed in all trials.

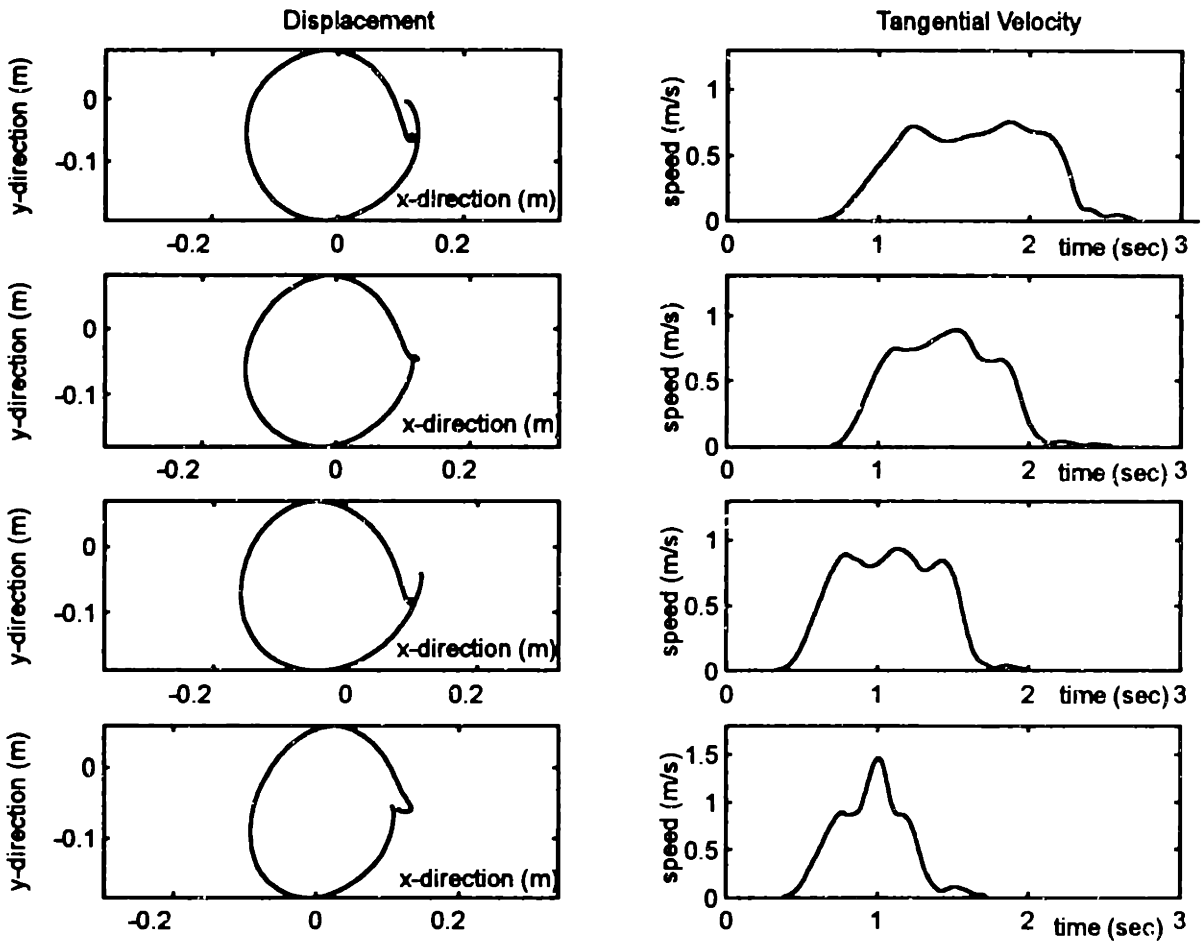

FIG.2.6. Subject A Drawing a Circle at Constant Target Speed (3 o'clock). Subject grasped the robot handle with the palm and was instructed to draw a circle at constant speed starting and ending at the same point. The trial was repeated until the subject considered himself/herself unable to maintain constant speed. The left column shows the circle traces and the right column shows the speed profiles at different target constant speeds. Note the oscillatory characteristic of the speed in all trials.

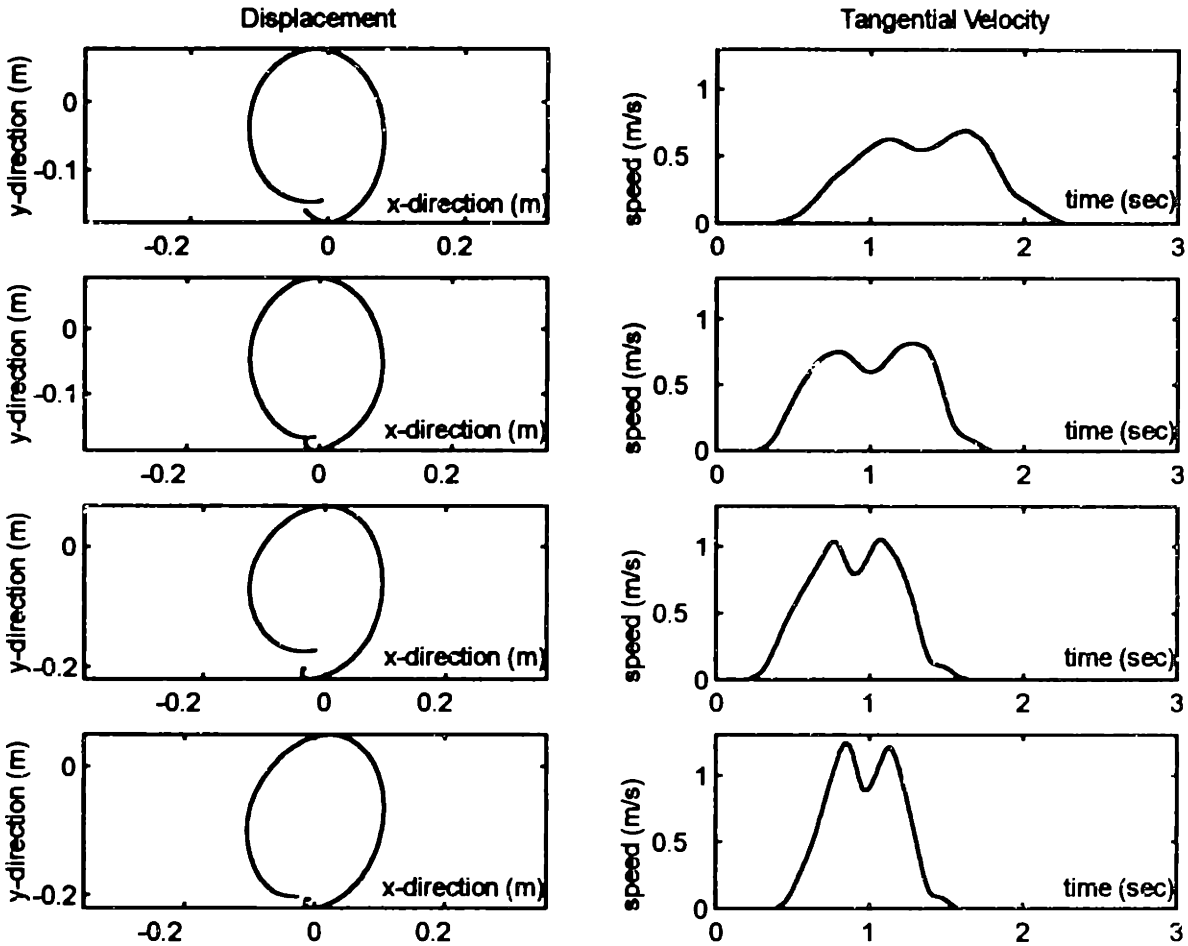

FIG.2.7. Subject A Drawing a Circle at Constant Target Speed (6 o'clock) . Subject grasped the robot handle with the palm and was instructed to draw a circle at constant speed starting and ending at the same point. The trial was repeated until the subject considered himself/herself unable to maintain constant speed. The left column shows the circle traces and the right colum shows the speed profiles at different target constant speeds. Note the oscillatory characteristic of the speed in all trials.

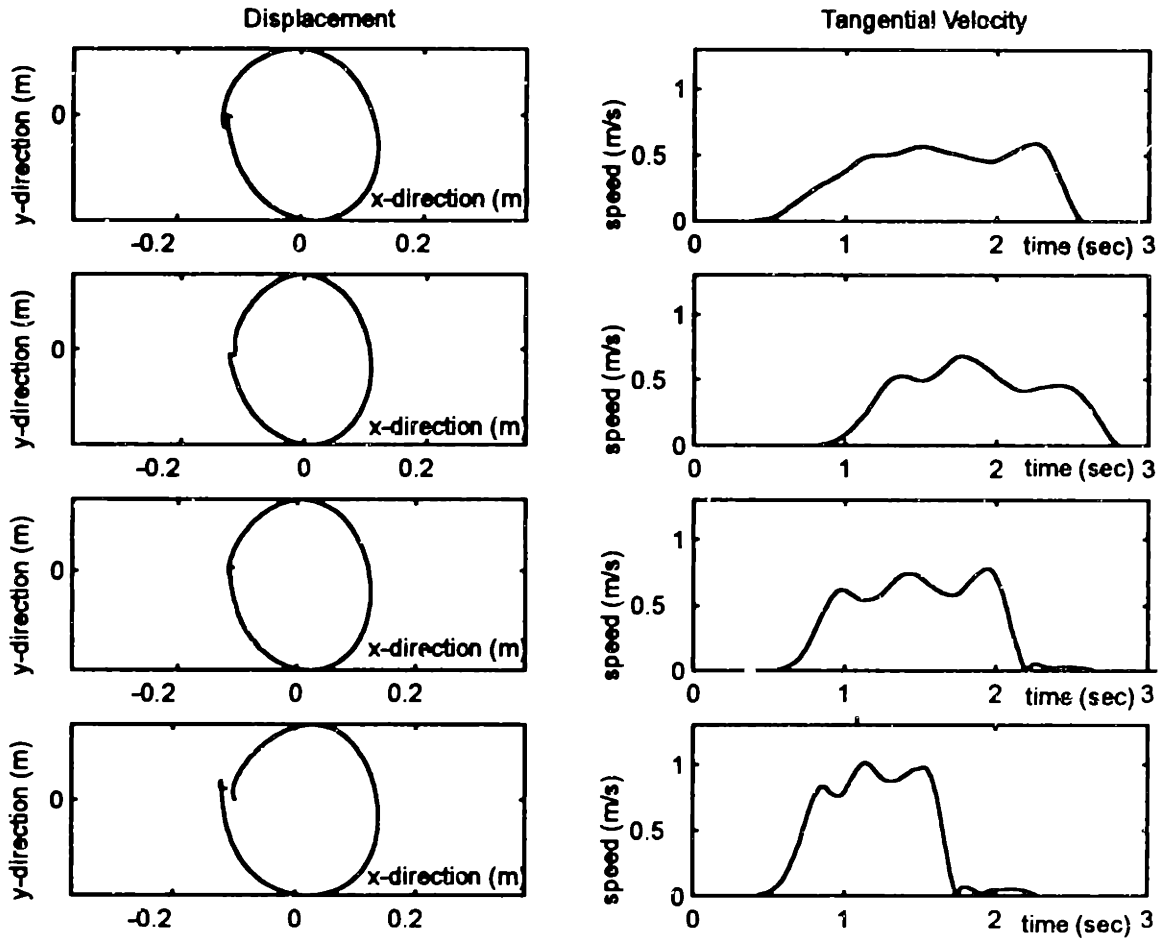

FIG.2.8. Subject A Drawing a Circle at Constant Target Speed (9 o'clock). Subject grasped the robot handle with the palm and was instructed to draw a circle at constant speed starting and ending at the same point. The trial was repeated until the subject considered himself/herself unable to maintain constant speed. The left column shows the circle traces and the right column shows the speed profiles at different target constant speeds. Note the oscillatory characteristic of the speed in all trials.

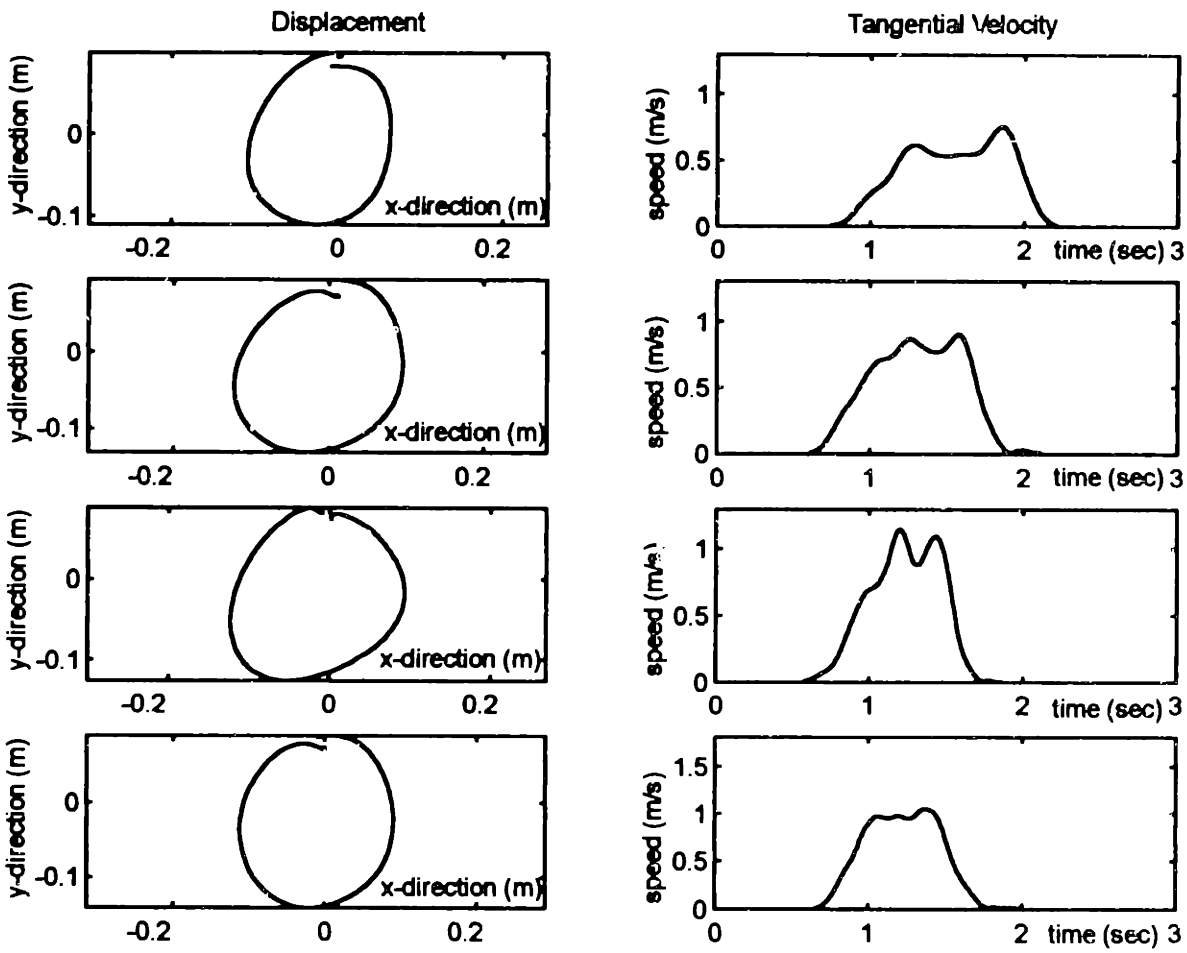

FIG.2.9. Subject B Drawing a Circle at Constant Target Speed (12 o'clock). Subject grasped the robot handle with the palm and was instructed to draw a circle at constant speed starting and ending at the same point. The trial was repeated until the subject considered himself/herself unable to maintain constant speed. The left column shows the circle traces and the right column shows the speed profiles at different target constant speeds. Note the oscillatory characteristic of the speed in all trials.

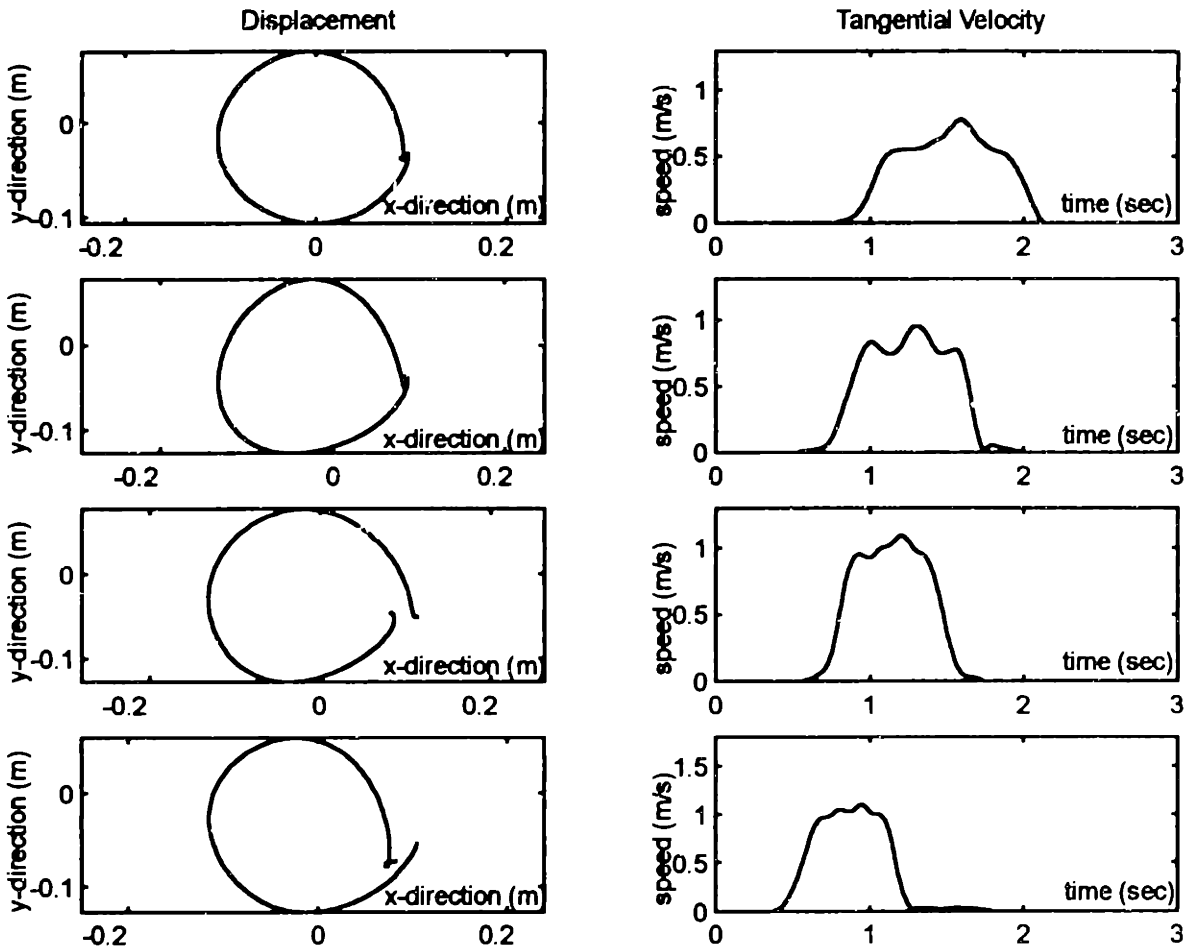

FIG.2.10. Subject B Drawing a Circle at Constant Target Speed (3 o'clock). Subject grasped the robot handle with the palm and was instructed to draw a circle at constant speed starting and ending at the same point. The trial was repeated until the subject considered himself/herself unable to maintain constant speed. The left column shows the circle traces and the right column shows the speed profiles at different target constant speeds. Note the oscillatory characteristic of the speed in all trials.

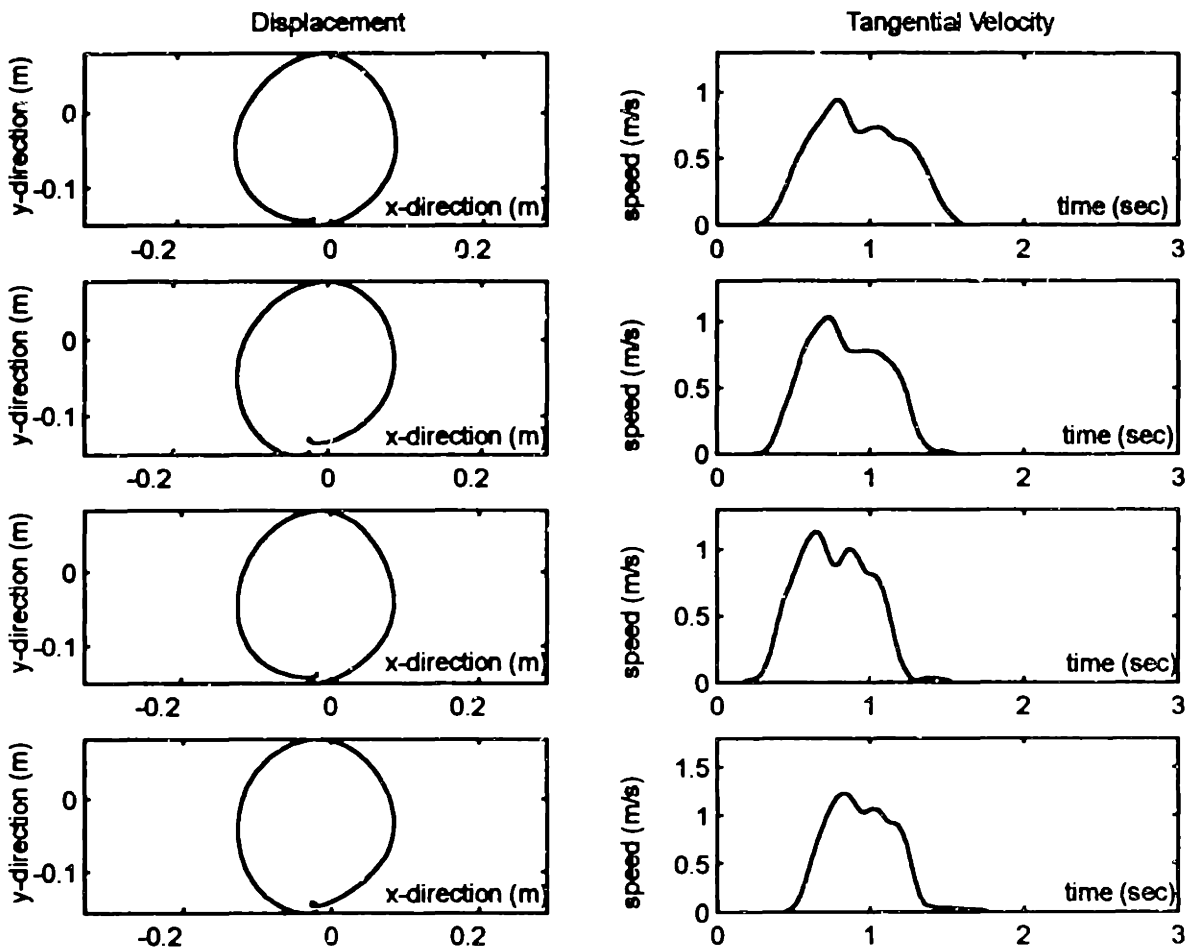

FIG.2.11. Subject B Drawing a Circle at Constant Target Speed (6 o'clock). Subject grasped the robot handle with the palm and was instructed to draw a circle at constant speed starting and ending at the same point. The trial was repeated until the subject considered himself/herself unable to maintain constant speed. The left column shows the circle traces and the right column shows the speed profiles at different target constant speeds. Note the oscillatory characteristic of the speed in all trials.

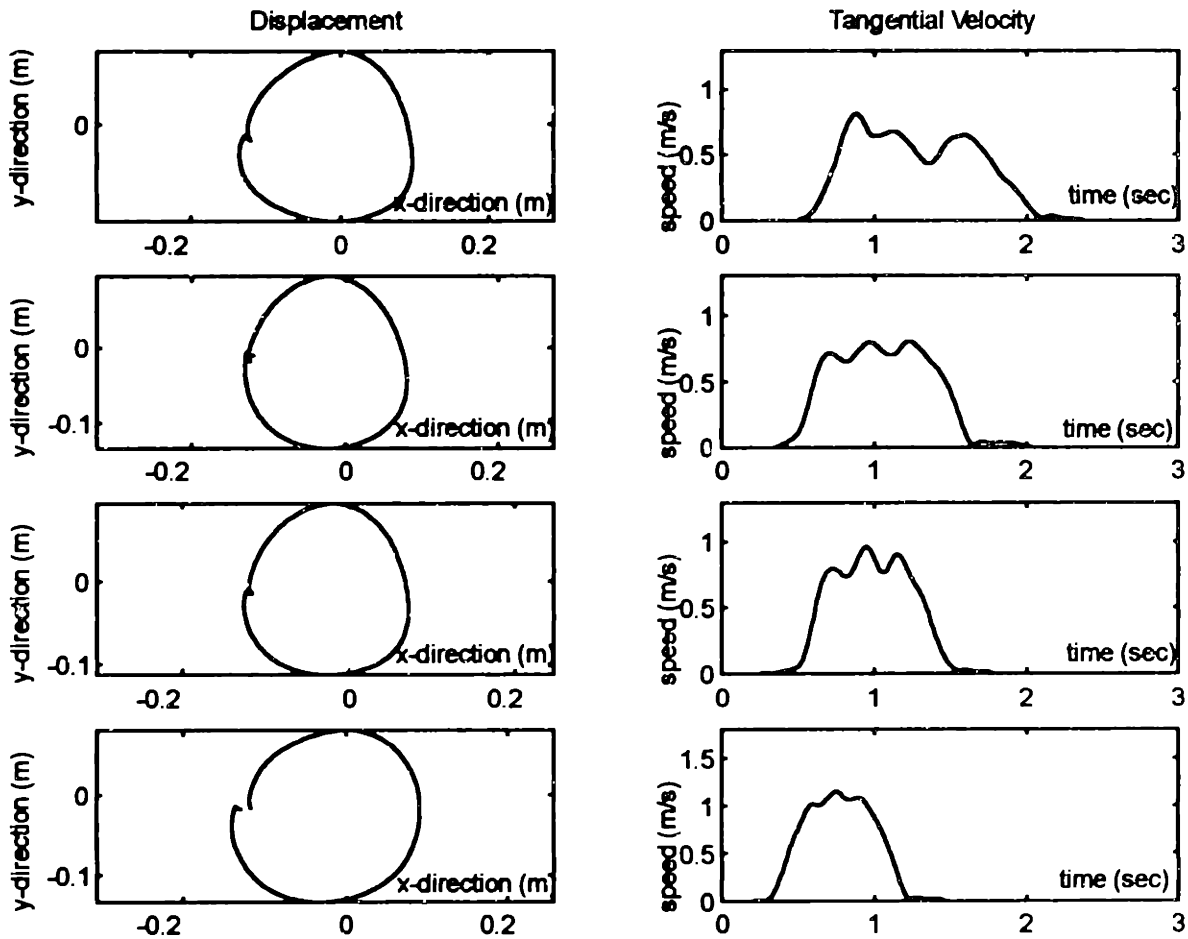

FIG.2.12. Subject B Drawing a Circle at Constant Target Speed (9 o'clock). Subject grasped the robot handle with the palm and was instructed to draw a circle at constant speed starting and ending at the same point. The trial was repeated until the subject considered himself/herself unable to maintain constant speed. The left column shows the circle traces and the right colum shows the speed profiles at different target constant speeds. Note the oscillatory characteristic of the speed in all trials.

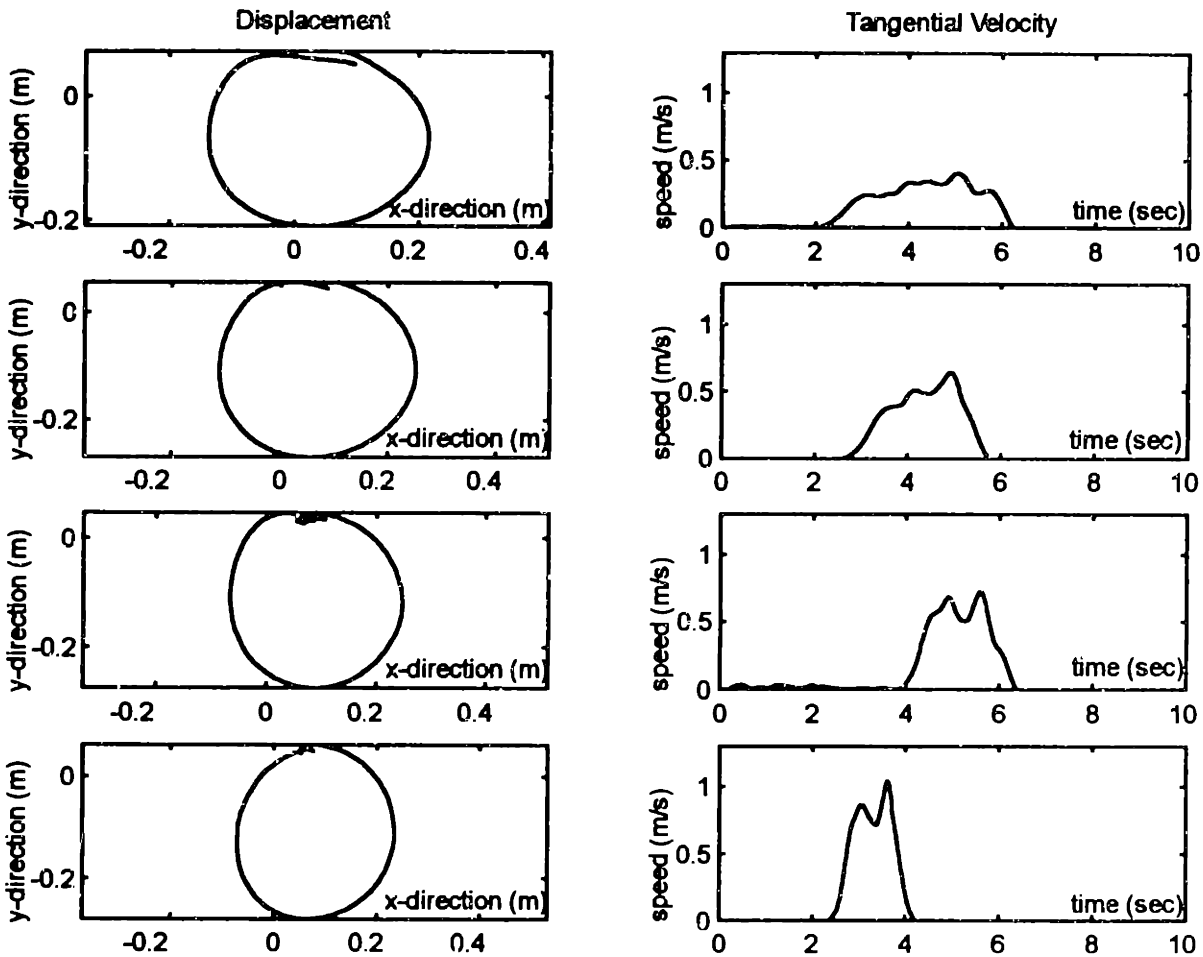

FIG.2.13. Subject C (Violinist) Drawing a Circle at Constant Target Speed (12 o'clock).

Subject grasped the robot handle with the palm and was instructed to draw a circle at constant speed starting and ending at the same point. The trial was repeated until the subject considered himself/herself unable to maintain constant speed. The left column shows the circle traces and the right colum shows the speed profiles at different target constant speeds. Note the oscillatory characteristic of the speed in all trials.

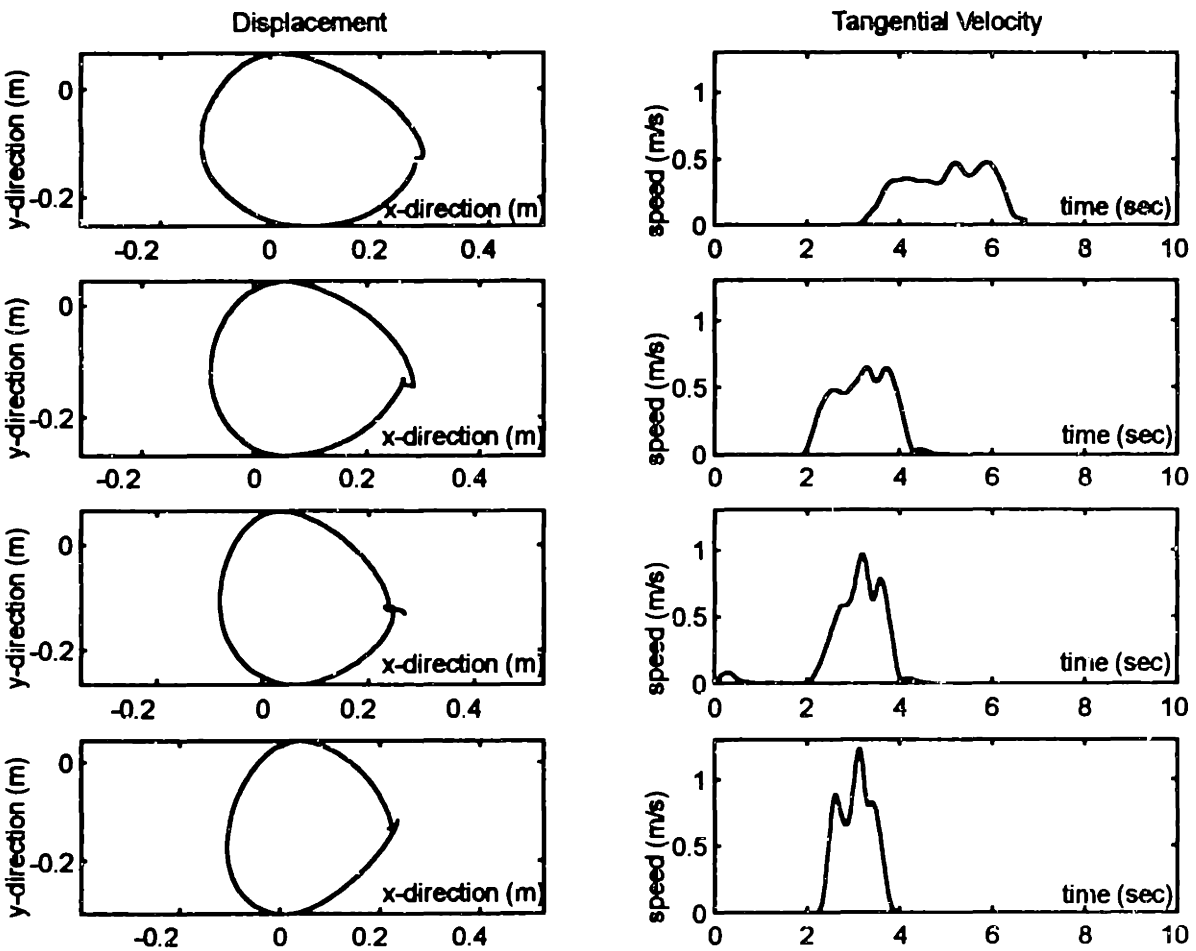

FIG.2.14. Subject C (Violinist) Drawing a Circle at Constant Target Speed (3 o'clock).

Subject grasped the robot handle with the palm and was instructed to draw a circle at constant speed starting and ending at the same point. The trial was repeated until the subject considered himself/herself unable to maintain constant speed. The left column shows the circle traces and the right column shows the speed profiles at different target constant speeds. Note the oscillatory characteristic of the speed in all trials.

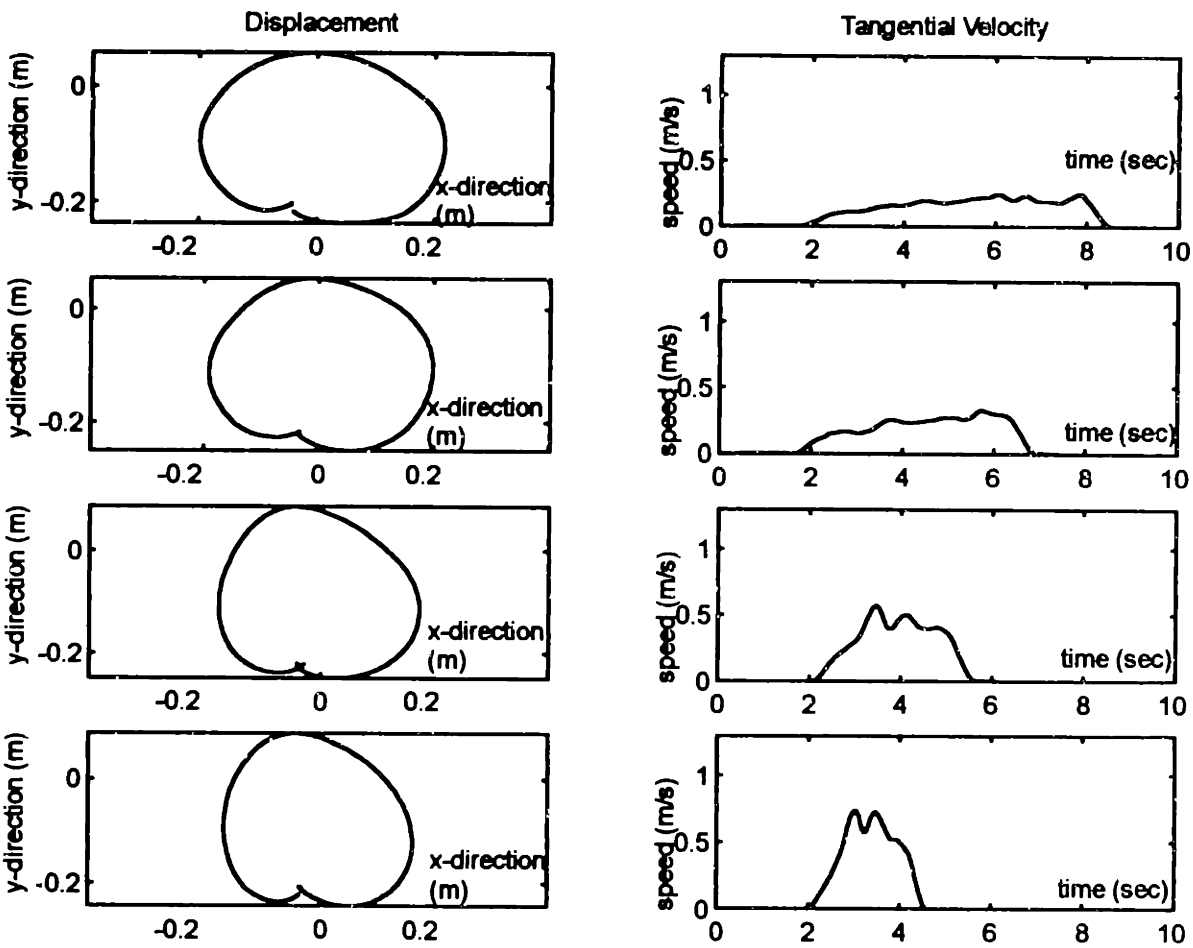

FIG.2.15. Subject C (Violinist) Drawing a Circle at Constant Target Speed (6 o'clock).

Subject grasped the robot handle with the palm and was instructed to draw a circle at constant speed starting and ending at the same point. The trial was repeated until the subject considered himself/herself unable to maintain constant speed. The left column shows the circle traces and the right column shows the speed profiles at different target constant speeds. Note the oscillatory characteristic of the speed in all trials.

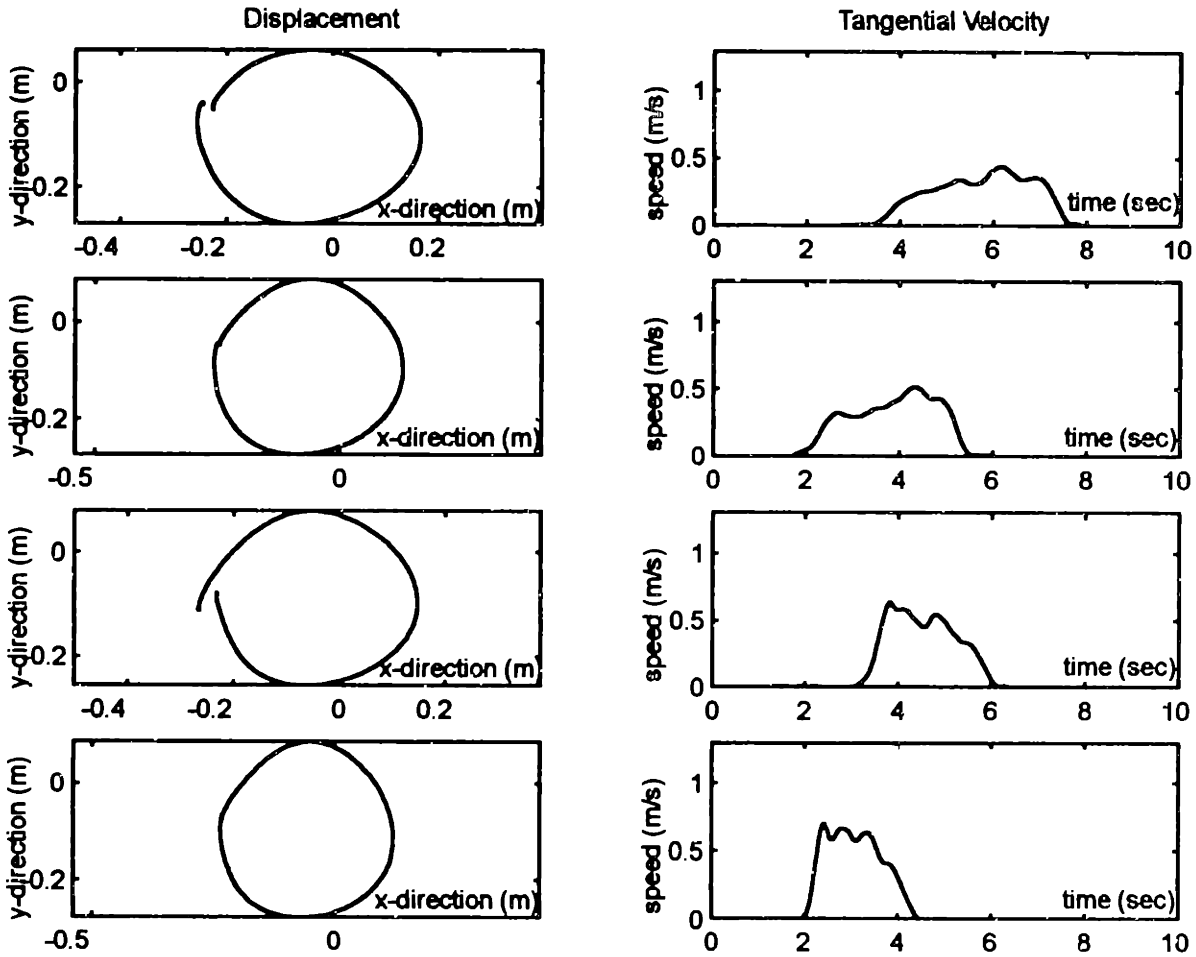

FIG.2.16. Subject C (Violinist) Drawing a Circle at Constant Target Speed (9 o'clock).

Subject grasped the robot handle with the palm and was instructed to draw a circle at constant speed starting and ending at the same point. The trial was repeated until the subject considered himself/herself unable to maintain constant speed. The left column shows the circle traces and the right column shows the speed profiles at different target constant speeds. Note the oscillatory characteristic of the speed in all trials.

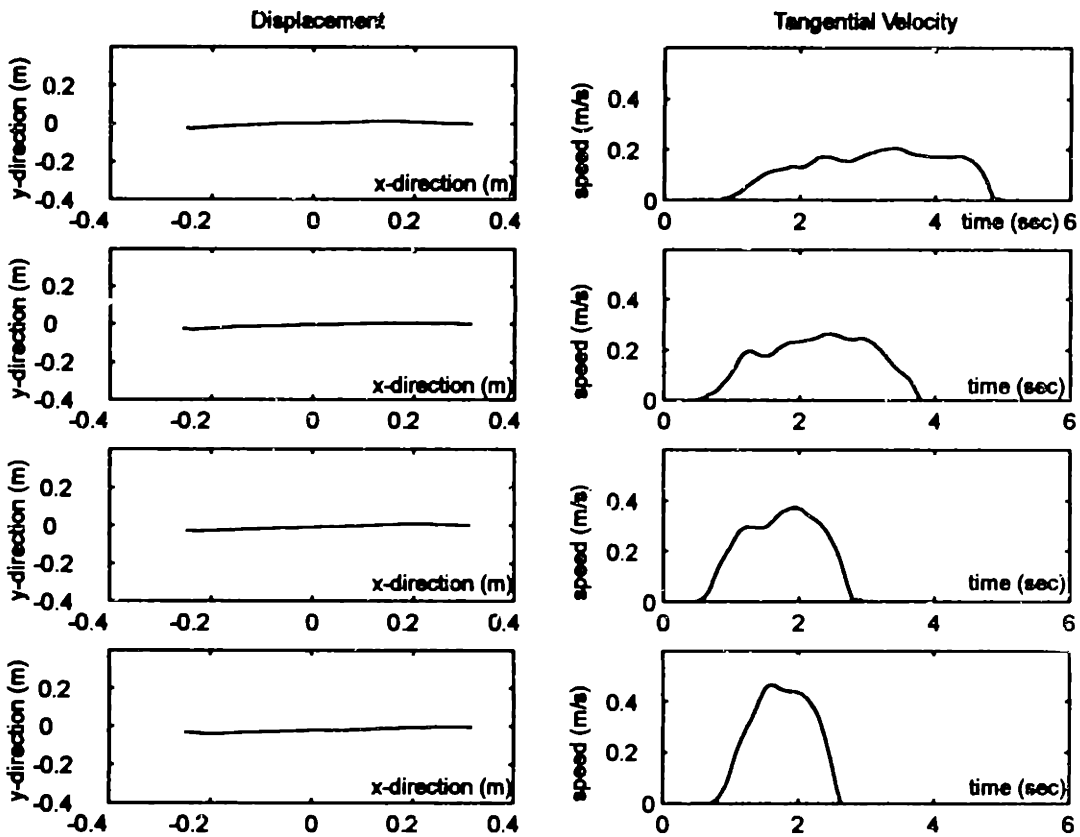

FIG.2.17. Subject B Drawing a Straight Line at Constant Target Speed from Left to Right. Subject grasped the robot handle with the palm and was instructed to draw a straight line at constant speed. The trial was repeated until the subject considered himself/herself unable to maintain constant speed. The left column shows the line traces and the right column shows the speed profiles at different target constant speeds. Note that the speed profile starts to resemble a bell-shape minimum-jerk curve characteristic of a point-to-point movement as target speed increases.

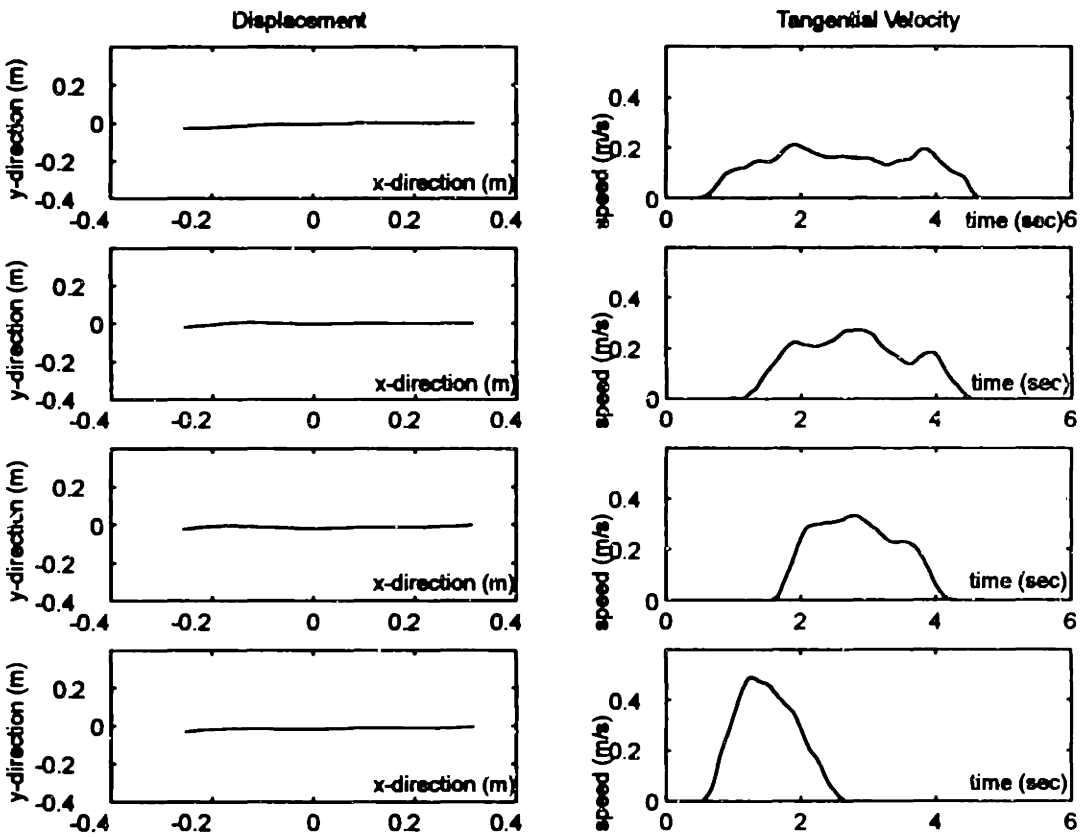

FIG.2.18. Subject B Drawing a Straight Line at Constant Target Speed from Right to Left. Subject grasped the robot handle with the palm and was instructed to draw a straight line at constant speed. The trial was repeated until the subject considered himself/herself unable to maintain constant speed. The left column shows the line traces and the right column shows the speed profiles at different target constant speeds. Note that the speed profile starts to resemble a bell-shape minimum-jerk curve characteristic of a point-to-point movement as target speed increases.

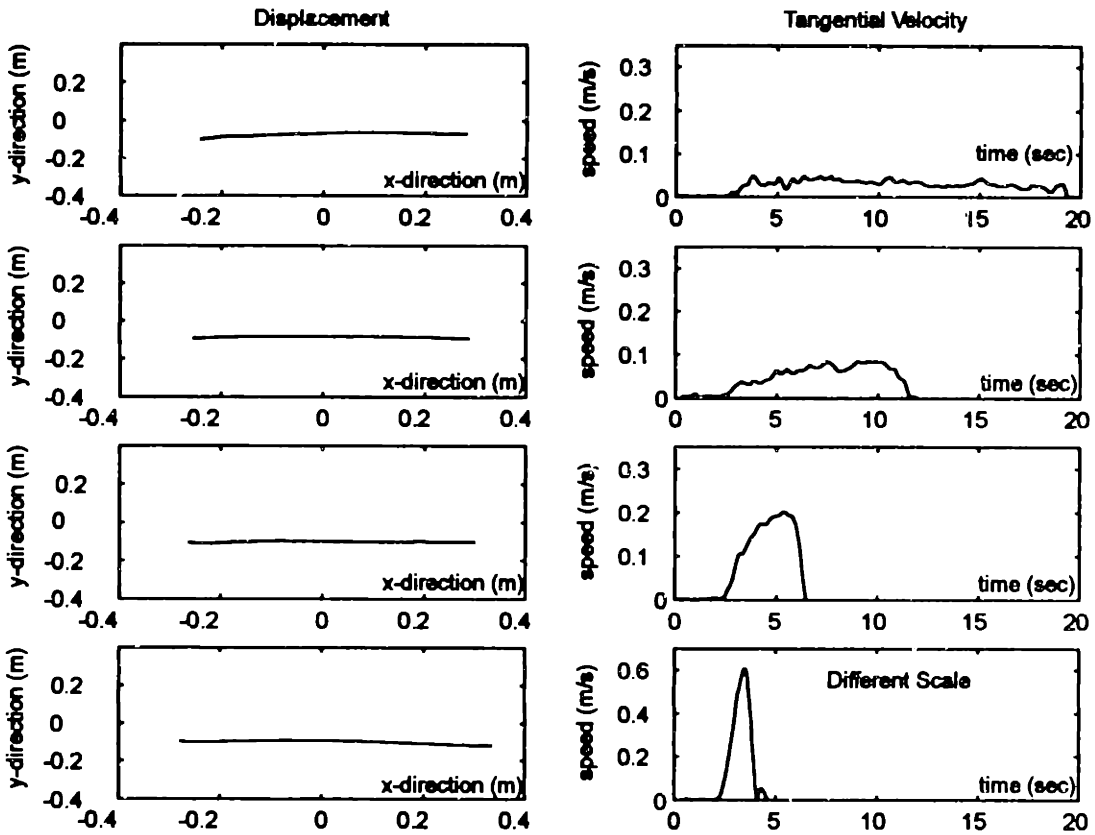

FIG.2.19. Subject C Drawing a Straight Line at Constant Target Speed from Right to Left. Subject grasped the robot handle with the palm and was instructed to draw a straight line at constant speed. The trial was repeated until the subject considered himself/herself unable to maintain constant speed. The left column shows the line traces and the right column shows the speed profiles at different target constant speeds. Note that the speed profile starts to resemble a bell-shape minimum-jerk curve characteristic of a point-to-point movement as target speed increases.

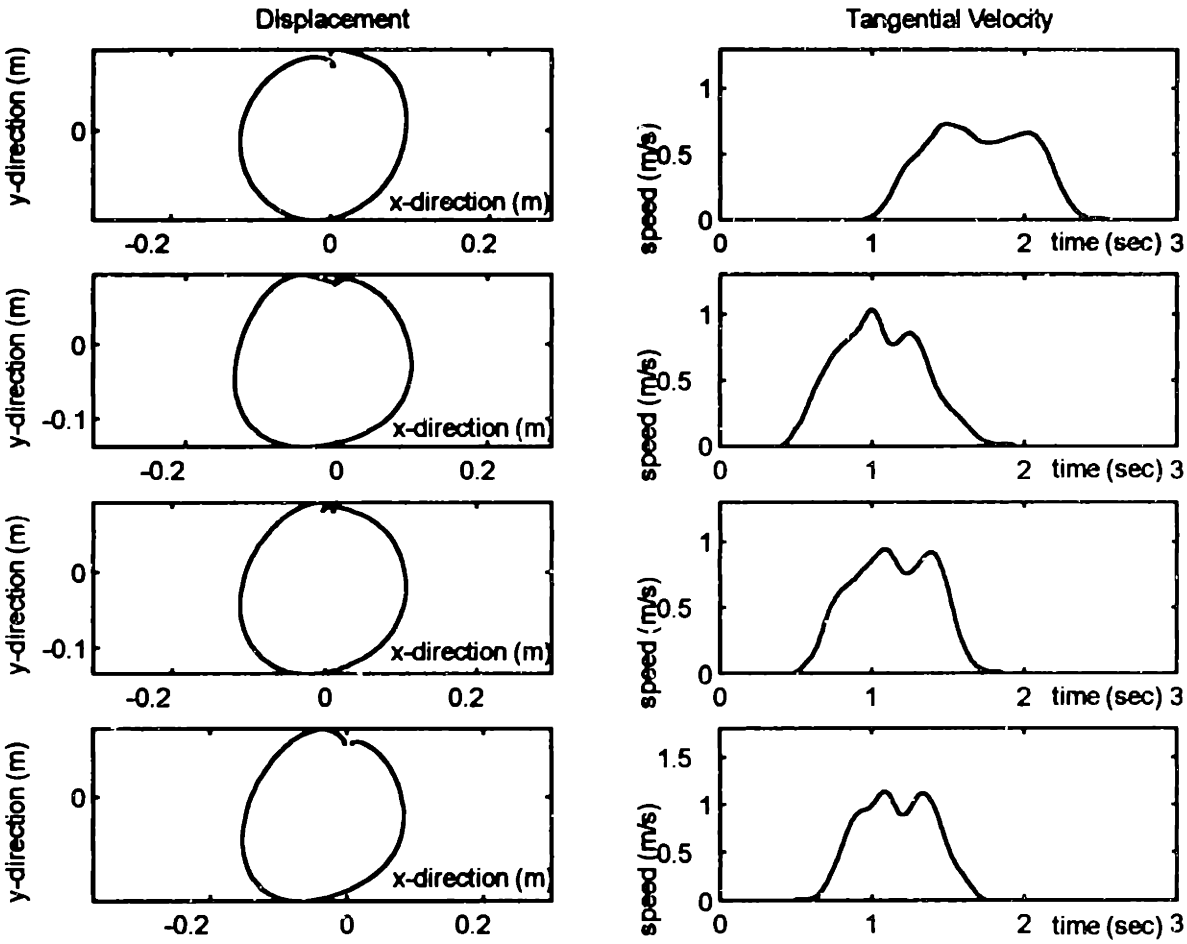

FIG.2.20. Subject B Drawing a Circle at Constant Target Speed (12 o'clock) - Counterclockwise from the Subject's View Point.
Subject grasped the robot handle with the palm and was instructed to draw a circle at constant speed starting and ending at the same point. The trial was repeated until the subject considered himself/herself unable to maintain constant speed. The left column shows the circle traces and the right column shows the speed profiles at different target constant speeds. Note the oscillatory characteristic of the speed in all trials.

2.2.3. Drawing at Increasing Speeds

The subjects were asked to draw at increasing speeds. They were instructed to draw the geometric form starting from a very low speed and increase the speed in a linear fashion. The movement continued until the subject considered himself/herself unable to fulfill the task requirements. Figure 2.21. shows the displacement, the tangential velocity and the angle plots of the amateur violinist drawing circles.This example will be revisited in the next section.

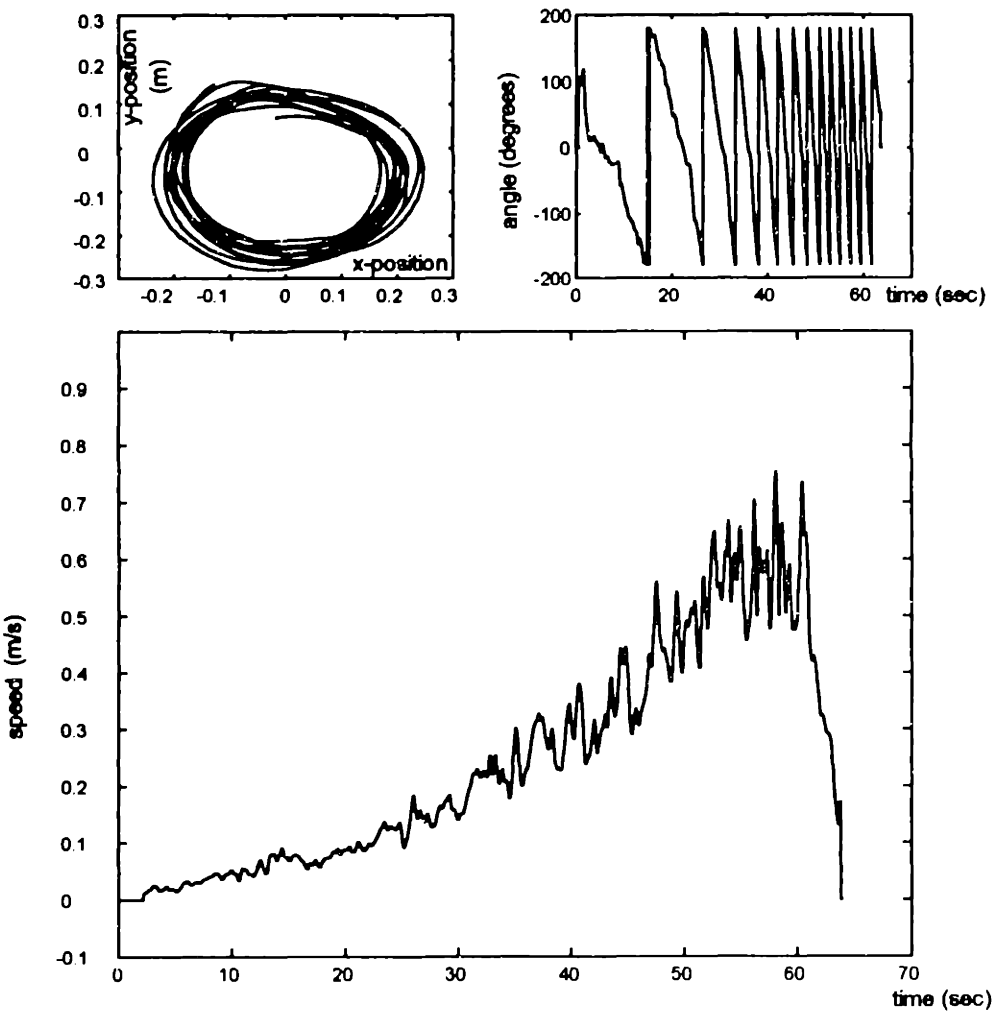

FIG.2.21. Subject C (Violinist) Drawing Circles at Increasing Target Speeds. Subject grasped the robot handle with the palm and was instructed to draw circles at increasing speeds. The trial continued until the subject considered himself/herself unable to increase the speed. The top row left shows the circle traces on the left and the speed angle on the right. The lower row shows the speed profiles at increasing target speeds. Note the oscillatory characteristic of the speed.

2.3. Movement Segmentation

The results in the previous session suggest that humans are not good at controlling velocity with the proprioceptive machinery, which includes force, position, and rate of change sensors. At very low speeds, the inertial effects are expected to be small, yet speed oscillations were observed. One might argue that the concept of submovement is a semi-tautological question, since it is hard to segregate the triggering moment of the segment from the system's oscillation due to the natural response and feedback loop. Therefore, it is fair to question the authenticity of the segments as real events, or artifacts from the experiments. Assuming that segmentation is a real event, the problem does not get simpler. Reliable and robust techniques to identify and segregate the segments, characterize their shape, and verify reproduceability must be found. Can the segments be identified and segregated from the kinematics ?

A spatial curve r(t) is determined by its instantaneous velocity, curvature, and torsion. In these two sections, I will address the questions using experimental results limited to the horizontal plane and examine the kinematic features of velocity and curvature.

Aligning the tangential velocity peaks and normalizing their peak values reveals a remarkable invariance of the shape for a subject and between subjects. Likewise the phase-plots have strong shape invariance. Figures 2.22.& 2.23. show data for subject A drawing a single circle starting and ending at 6 o'clock.

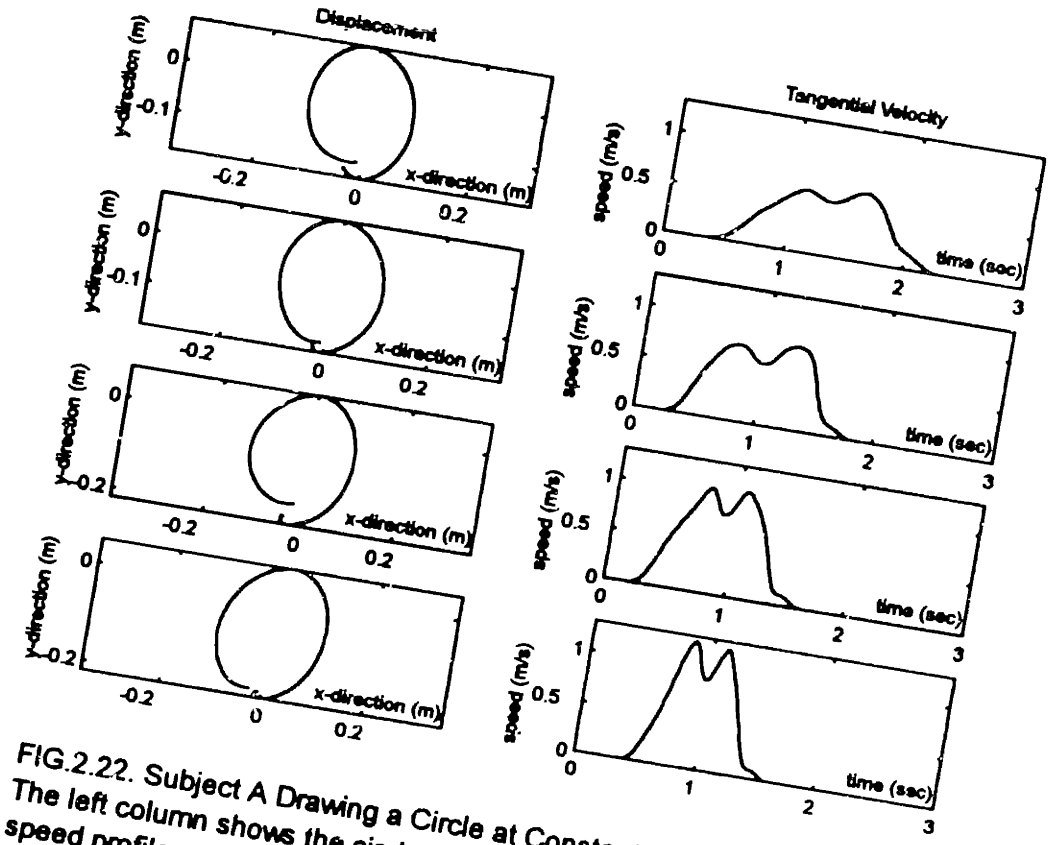

FIG.2.22. Subject A Drawing a Circle at Constant Target Speed (6 o'clock) . The left column shows the circle traces and the right column shows the speed profiles at different target constant speeds. Note that the task duration decreases by half and the speed profile retains characteristic.

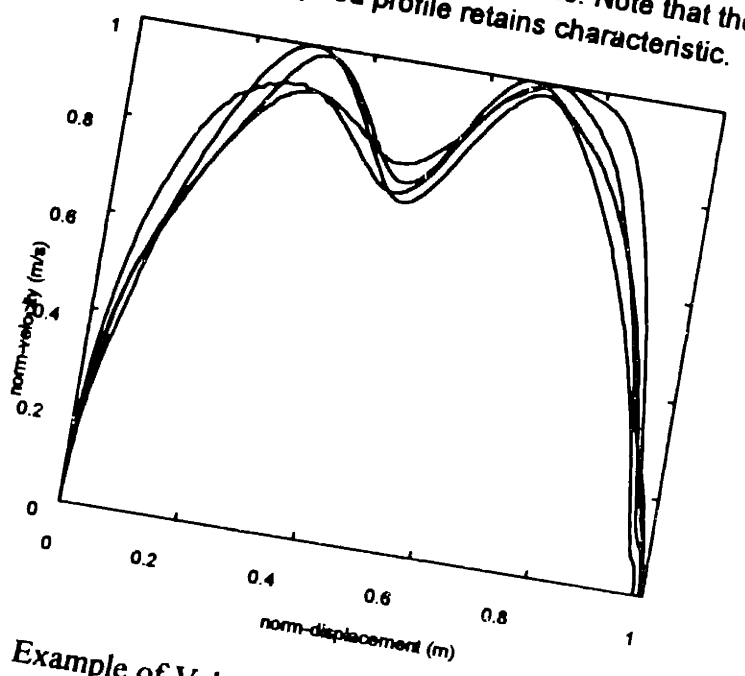

FIG.2.23. Example of Velocity Profile Normalization.
The maximum speed value for each of the trials in Fig.2.24. was normalized to unity. Also each of the circles had its displacement (circle length) normalized to unity. Note that the similarity of the resulting normalized speed profiles.

So far, raw data has been used without any significant mathematical manipulation. In what follows, a minor simplification is introduced. Humans cannot accurately perceive or draw circles. In fact, it has been shown that humans draw ellipses instead of circles [Fasse, 1992]. Nonetheless Fig. 2.24. to 2.26. present polar plots of the speed versus the displacement angle for repetitive circles (shown in Figs. 2.2. to 2.4.) around a center located at the mean value for x and y displacements. The two upper rows show the polar plots of the raw data, while the lower rows show the composite of all the plots (faster two plots for subject C). To compare all the plots, the speed was normalized at each plot by the plot's maximum speed, and the initial and final 90 degrees of the movement was not included, i.e. part of the movement accelerating from zero to the target constant speed and part of the movement decelerating to zero speed. Note that these results strongly suggest the kinematic, not temporal, characteristic of the speed profile and suggest the existence of the submovement phenomenon. To illustrate this aspect, note in the composites that the sample speeds within the angular range of $90° \pm 0.5°$ (subject A & B) and $120° \pm 0.5°$ (subject C) is statistically significant different than the $180° \pm 0.5°$ ($p < 0.05$, one-way ANOVA). Furthermore, note the strong suggestion of segmentation at the slowest speeds for subject C (Fig.2.26.- upper row). At these very low speeds, the inertial effects are expected to be negligible, yet the ubiquitous speed oscillations can be observed.

In order to apply a similar approach to the task of drawing circles at increasing speeds, the speed was "de-ramped". The raw data was smoothed with a 10 second rectangular moving average filter and translated by 0.2 m/s as shown in the upper row of Fig.2.27. The upper right plot shows the "de-ramped" speed between 30 and 50 seconds. The lower row shows the speed and 20 seconds of the "de-ramped" speed polar profiles. Note again the kinematic characteristic of the speed profile, and the evidence of submovements.

In agreement with the literature on submovements, it is argued here that the oscillation at low speeds is a marker, or signature, of the submovement phenomena.

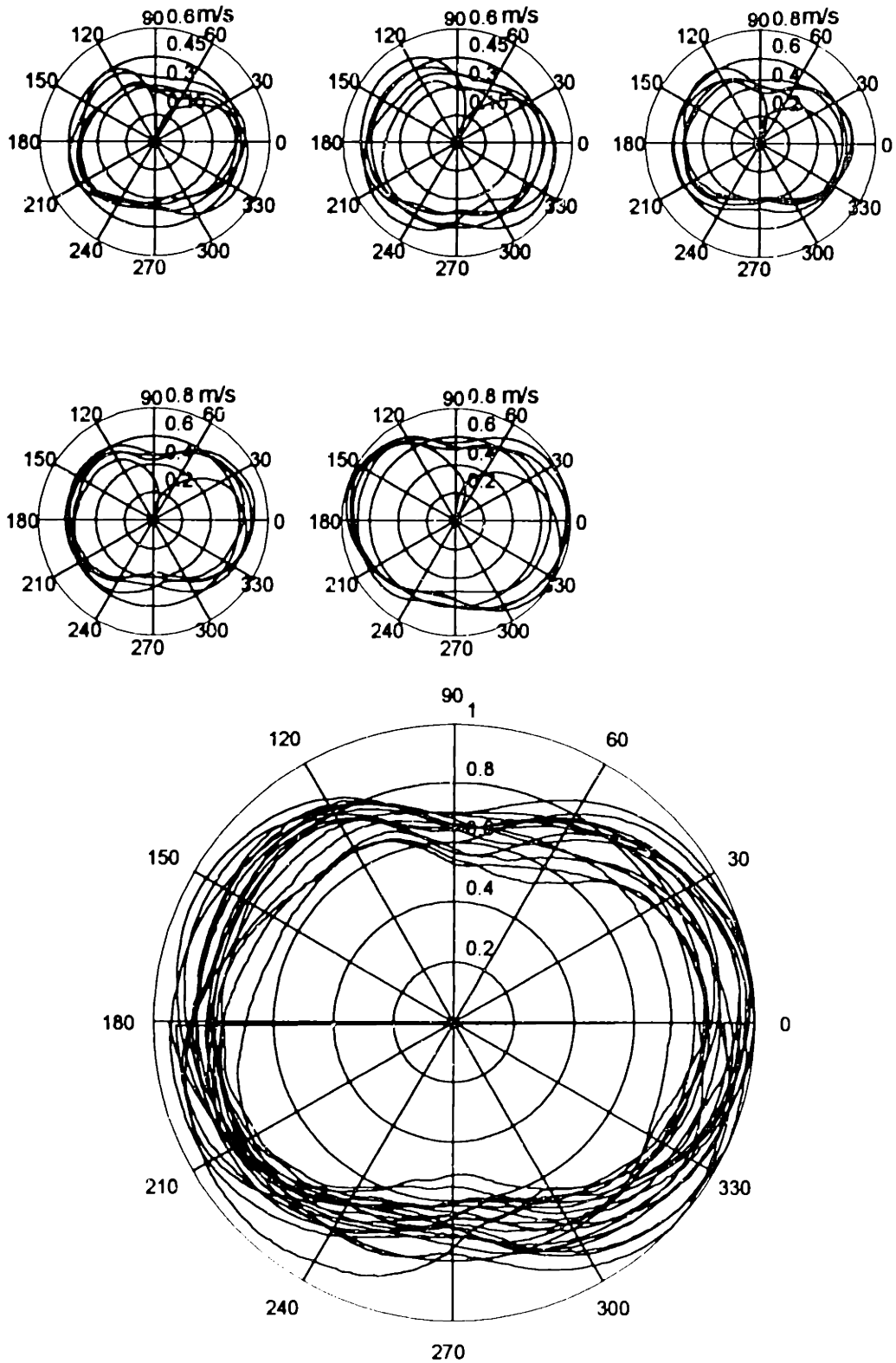

FIG.2.24. Polar Plots of Subject A Drawing Four Circles at Different Constant Target Speeds. The upper two rows show the plots for each of the trials shown in Fig.2.3. The lower plot shows the composite of the last two trials. The speed was normalized by the peak value in each case. Note the kinematic characteristic of the plot (not temporal). For example, points in the range 90 ± 0.5 degree are different than points in the range 180 ± 0.5 degrees (statistically significant with p = 0.0035).

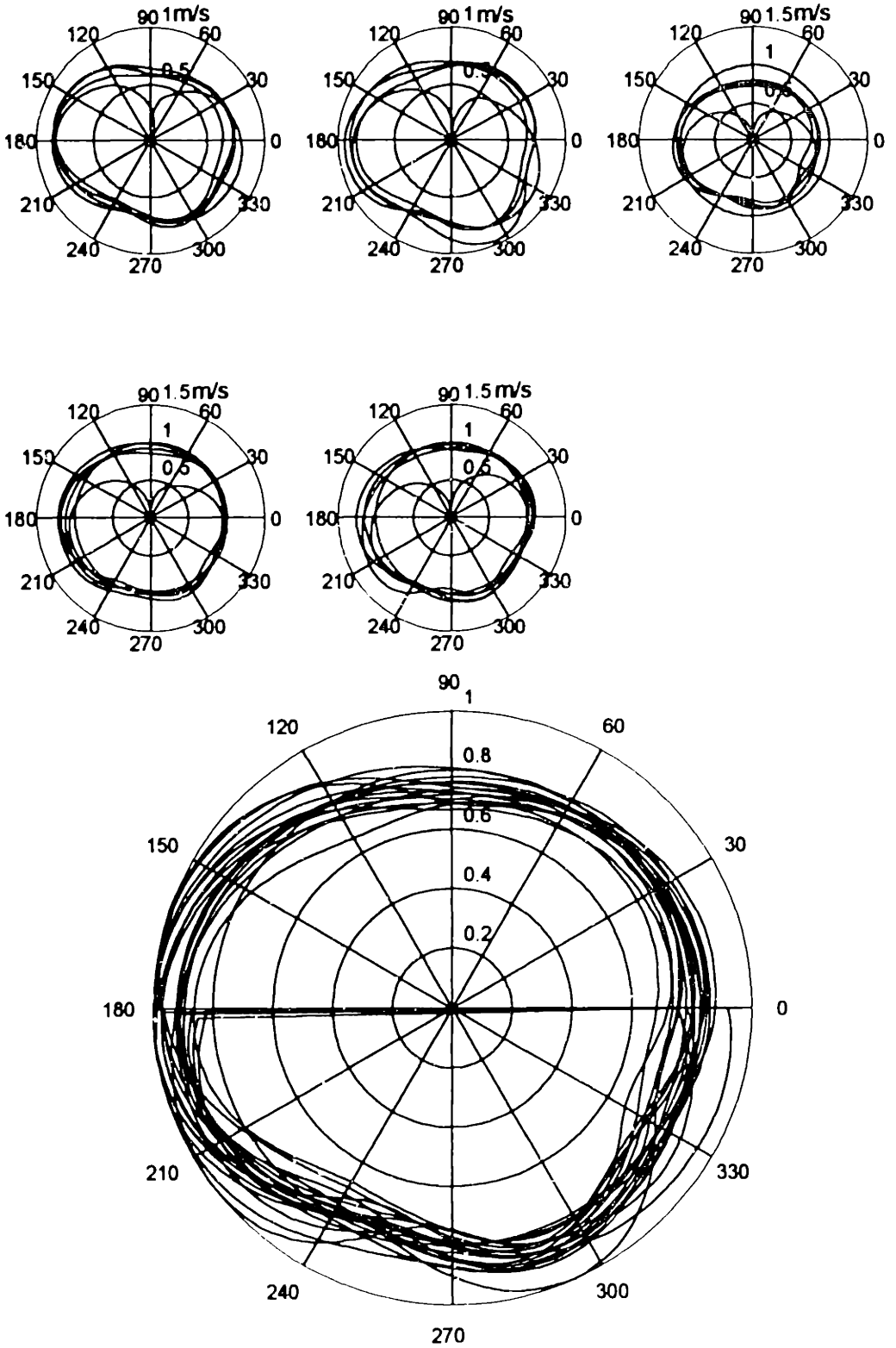

FIG.2.25. Polar Plots of Subject B Drawing Four Circles at Different Constant Target Speeds. The upper two rows show the plots for each of the trials shown in Fig.2.4. The lower plot shows the composite of the last two trials. The speed was normalized by the peak value in each case. Note the kinematic characteristic of the plot (not temporal). For example, points in the range 90 ± 0.5 degree are different than points in the range 180 ± 0.5 degrees (statistically significant with p = 0.0027).

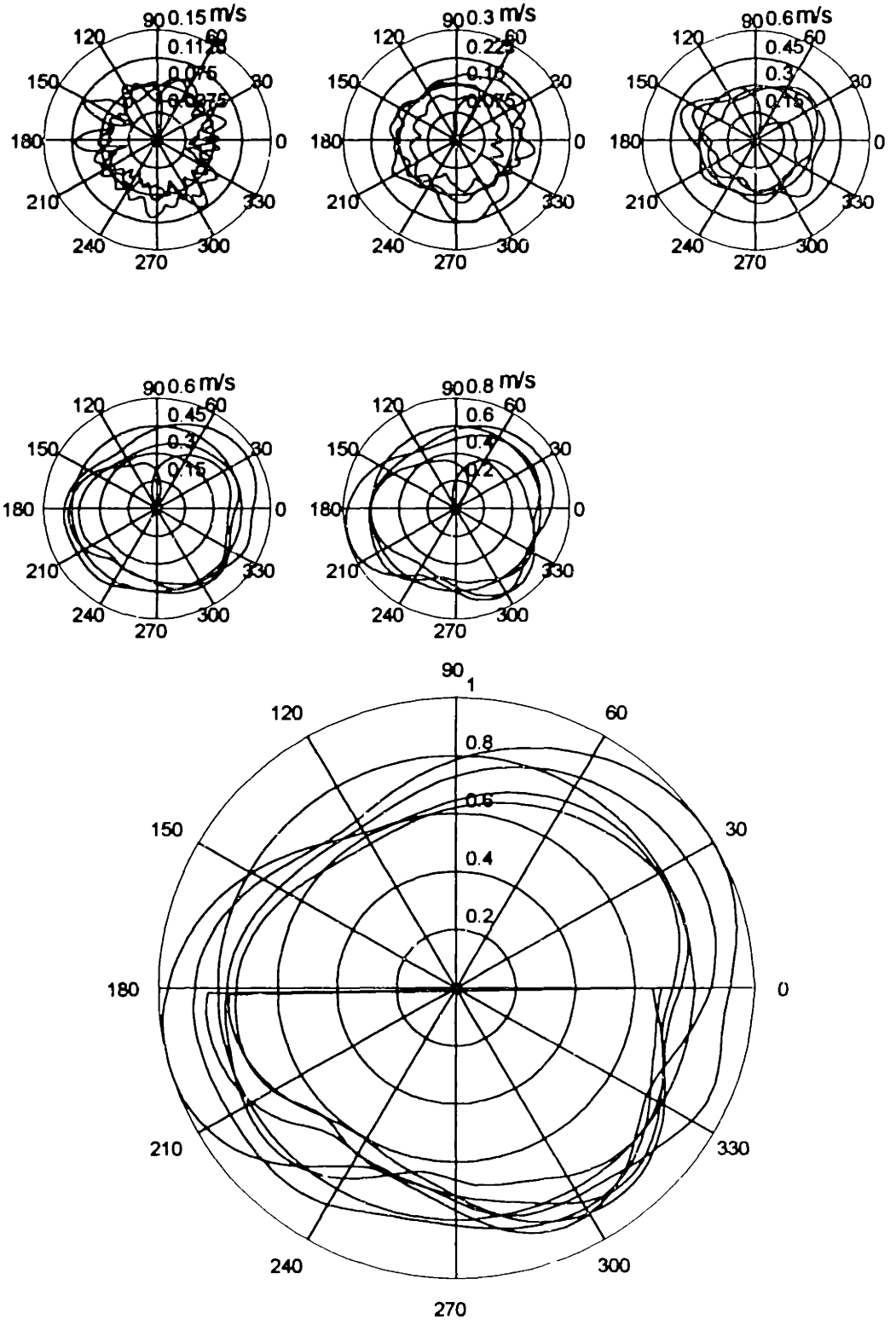

FIG.2.26. Polar Plots of Subject C (Violinist) Drawing Three Circles at Different Constant Target Speeds. The upper two rows show the plots for each of the trials shown in Fig.2.5. The lower plot shows the composite of the last two trials. The speed was normalized by the peak value in each case. Note the kinematic characteristic of the plot (not temporal). For example, points in the range 120 $\pm$ 0.5 degrees are different than points in the range 180 $\pm$ 0.5 degrees (statistically significant with p = 0.0005).

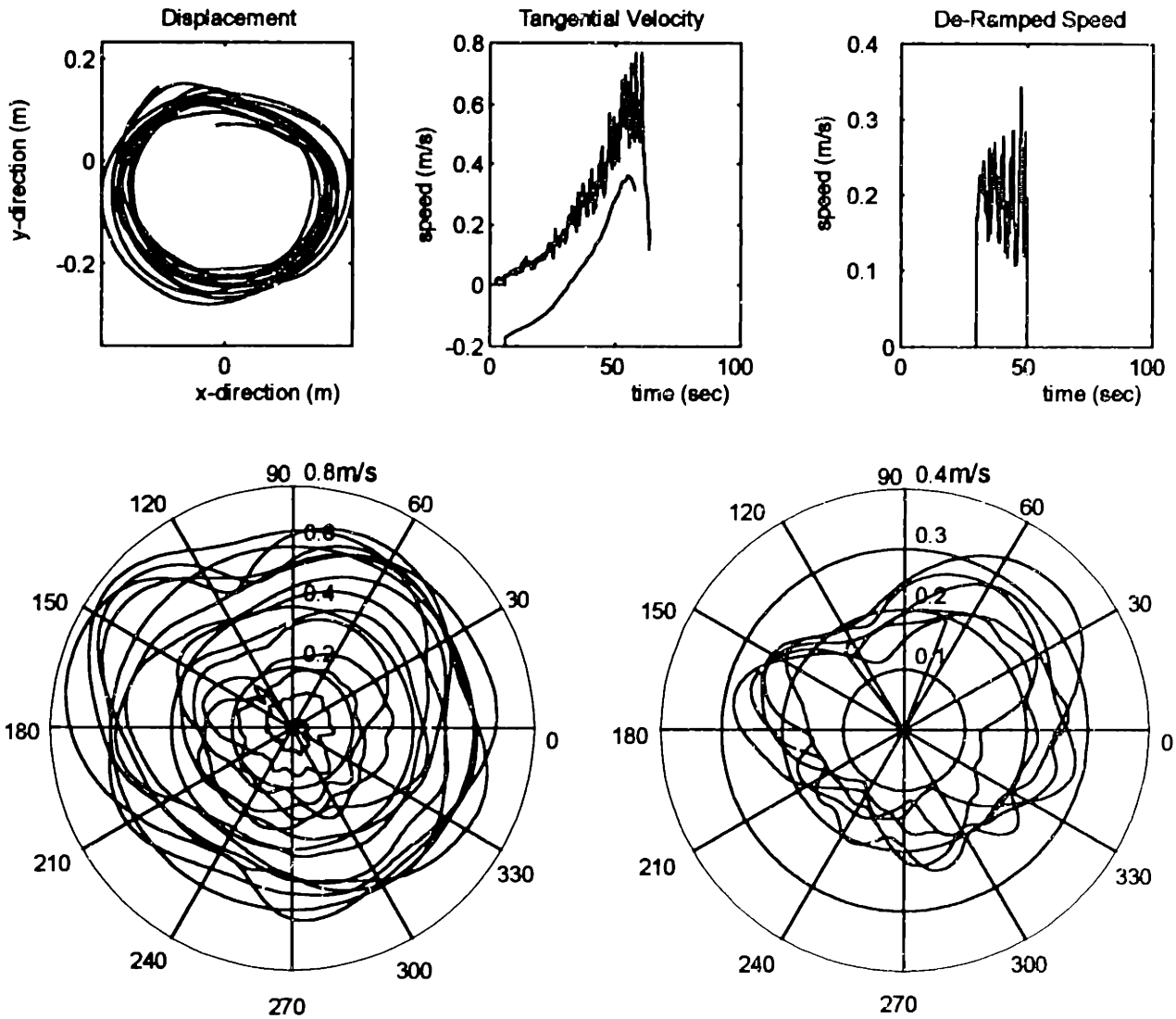

FIG.2.27. Polar Plots of Subject C (Violinist) Drawing Circles at Increasing Target Speeds.
The circles displacement is shown on the left side of the upper row (previously shown in Fig.2.22.). The center plot contains the speed, the filtered speed smoothed with a rectangular moving average window of 10 sec and translated downwards by 0.2 m/s. The right plot on the upper row shows the "de-ramped" speed, i.e. speed profile minus the translated and smoothed version of the speed. The lower row contains on the left side the polar plot of the speed. The right plot shows 20 sec of the "de-ramped" speed. Note the kinematic characteristic of the plot. For example, points in the range 120 $\pm$ 0.5 degrees are different than points in the range 180 $\pm$ 0.5 degrees (statistically significant with p = 0.0082).

2.4. Movement Curvature

Viviani & Terzuolo showed the correlation between tangential velocity and the radius of curvature of human movements [Viviani & Terzuolo, 1982]. There is a corresponding peak in curvature for each valley in tangential velocity. The curvature can be described by:

$$K(t) = \partial\theta/\partial s \qquad \text{(eq. 2.4.)}$$

where θ is the instantaneous velocity angle and s is the displacement. This formulation is equivalent to Frenet Formula:

$$K(t) = [(\vec{v} \bullet \vec{v})(\vec{a} \bullet \vec{a}) - (\vec{v} \bullet \vec{a})^2]^{\frac{1}{2}}/(\vec{v} \bullet \vec{v})^{\frac{3}{2}} \qquad \text{(eq. 2.5.)}$$

with v and a representing the first and second derivative, i.e. velocity and acceleration vectors of the curve r(t), and the multiplication symbol represents a dot product.

Similar to its companion tangential velocity, curvature is ambiguous. It can be an indicator of the submovement phenomena. For example, Fig.2.28. shows the same last four sets of circles drawn by subject A and previously shown in Fig.2.7. The instructions were to draw a circle of approximately a 10 inch diameter ring, starting and ending the movement at a pre-specified position with constant target speed. After drawing each circle, the clinician was requested to redraw the circle faster. The tangential velocity profiles show two peaks during the movement, while the corresponding curvature profile shows a peak at the dip in tangential velocity. However, using curvature as a marker to identify and segregate segments, has three weaknesses. (1) If humans were capable of generating precisely a straight line composed of two blended submovements resulting in two peaks, a dip in tangential velocity would be observed, but with no peak in curvature. (2) The peak in curvature is limited as a submovement counter, it cannot determine the submovement itself, only segregate the predominance of one segment or vibration mode over the other. (3) An oscillating mechanical system has the same curvature behavior with peaks in curvature that coincide with dips in the tangential velocity profile, e.g. second order mass-spring-damper system of Fig.2.29.

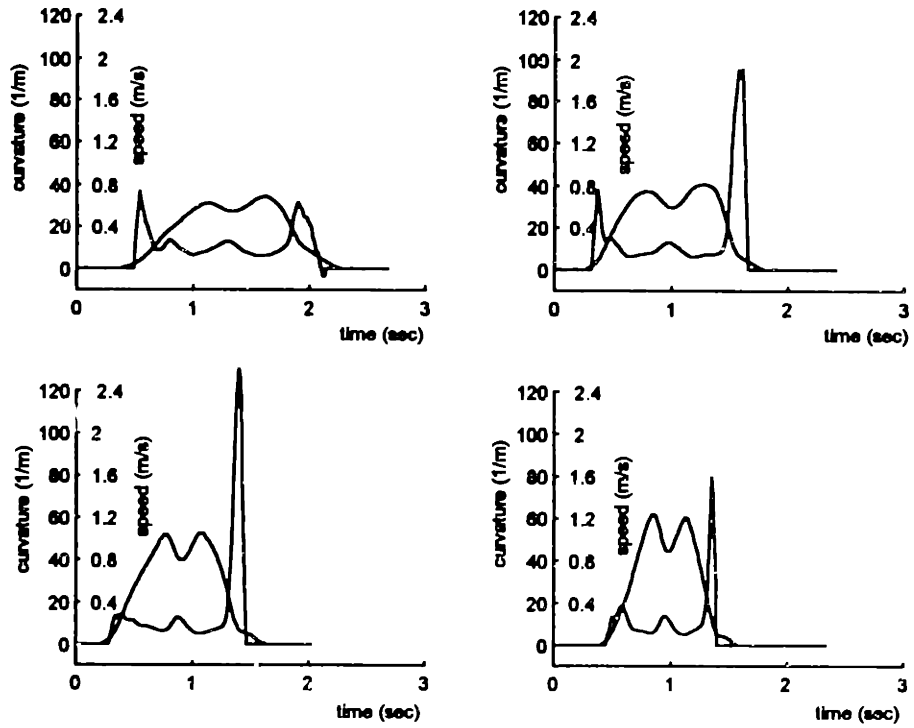

FIG.2.28. Curvature Correlates with Speed.
Illustrates the correlation between peaks in curvature and dips in arm movement speed using the example of subject A drawing circles starting and ending at 6 o'clock.

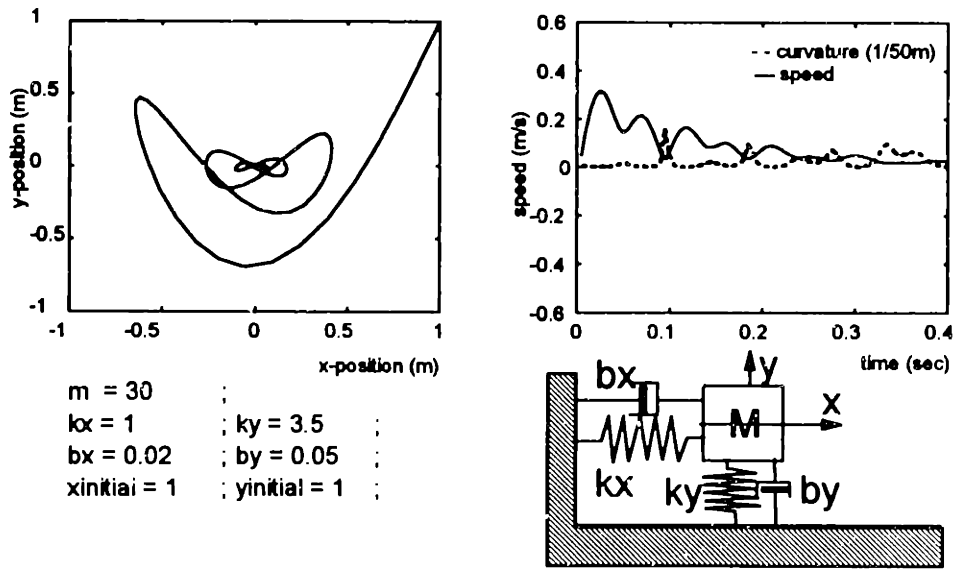

FIG.2.29. A Mass-Spring-Damping Mechanical System Speed vs Curvature.
Illustrates that an oscillating mechanical system can have the same speed vs curvature behavior as the human arm movement, i.e. peaks in curvature occur at dips of speed.

2.5. Working Model: Motor Control Hierarchy

The central theme of studies in human motor control is to understand how intentions are translated into actions. As mentioned in the Section 2.1., some researchers conjecture* that motor-control is hierarchically organized and that the top level appears to be exploiting the limbs' strong intrinsic stability properties and computing or predicting only the task kinematics, recruiting and modulating the proper sequence of motor primitives resident at the lower level, in particular in the spinal chord. Furthermore, the top level is stratified in different sublevels with distinct functions, activities, and time-scales, whose global performance index is to optimize the proper recruitment and modulation of the lower level and create an internal representation of the movement. This conjecture represents a remarkable simplification of the computational effort required to attempt to fully control the system dynamics. Therefore, the working model for the motor control hierarchy can be assumed to have two distinct levels: a) a symbolic or decision-making level described by discrete episodic events; and b) an energy-dominated physical level described by continuous processes. The symbolic level information needs to be compiled into a set of instructions to the energy-dominated physical level. Moreover these instructions can be generated in an asynchronous fashion. This episodic intervention will be called: "quantum". The task can be achieved by applying a parsimony of instruction events or "quanta" at selected times. "Quantum" has an energy-dominated dual. This dual movement is called "primitive", "submovement" or "segment", while some researchers refer to it as "stroke"**. As mentioned, the "submovement - quantum" concept is fundamentally a kinematic instruction. The desired operational stiffness of the arm during the task will be called: "stiffness function". The "natural response" is the measurable end-result for an unconstrained system operating with a "stiffness function" to "quantum" inputs. The fundamental value of the "submovement-quantum" concept is to unify and blend seamlessly the symbolic level with the energy-dominated physical level, which have hitherto been treated separately. "Submovements" represent a scientific conjecture. They constitute the primitives of the upper-limb movement and the building blocks of complex tasks.

* The conjecture is based on the views of many researchers, but there is no established consensus in the field.

**Original descriptive names can very scarce. Two different communities use the same word for completely unrelated descriptions: "Stroke" had been used by the medical community as a synonym of cerebral vascular accident. "Stroke" had been used by many in the motor control community to describe a segment of movement. For clarity purposes in this thesis, Stroke as used in the medical and popular verbatim sense is unaltered.

2.6. Working Hypothesis: Segments and Primitives of Arm Movement

I presented a literature overview and some evidence of the submovement phenomenon in the previous sections. To me, the evidence for the submovement phenomenon is overwhelming, and all the examples are in accordance with the submovement concept, but presently there are more open questions than answers. Within the hierarchy described in the previous section, segments or primitives of arm movement have generalizable characteristics that correspond to markers of the recruitment of the low-level controller.

In a nutshell, it is proposed that the system is controlled through episodic asynchronous instructions following the hierarchy described in the previous section. If the system response differs substantially from the predicted natural behavior, or if there is a change in the symbolic domain, a correction is expected. The correction can come in two forms: a) change in the parameters or gains of the local feedback closed-loop controller, i.e. change of the arm stiffness function via a local reflex or via a high-level "stiffness controller" instruction or b) corrective "submovement", each with a bell-shaped velocity profile.

2.7. Working Hypothesis: Minimum Action Unit Conjecture and Learning

In Section 2.5., it was mentioned that the top level controller is stratified in different sublevels, whose global performance index is to optimize the proper recruitment and modulation of the lower level. It was not specified what was meant by "proper" recruitment and modulation. The Russian physiologist Bernstein defined coordination as a problem of mastering the many degrees of freedom involved in a movement, and reducing the number of independent variables to control it. Similarly one may postulate that a repertoire of movement primitives, each with a bell-shaped velocity profile, constitute the building blocks of more complex tasks. In addition the motor learning task may be performed initially using a sequence of overlapping segments, which are then progressively "blended" as motor learning proceeds. This working hypothesis implies that one of the top level global objectives appears to be the minimization of the number of episodic interventions, i.e. the number of "submovements", or the economy of skilled movements [Nelson,

1983]. In other words, the human motor control and learning works towards simplification of the computational effort and dimensionality reduction, i.e. the number of submovements.

2.8. March of Progress - Chapter II

Chapter 2 presented a bibliographic overview on the submovement concept. This survey revealed that the idea is quite old, tracing it at least to end of the 19th Century with Woodworth's Ph.D. Thesis at Columbia University (1899). To me, the evidence for the submovement phenomenon is overwhelming, yet there is no established consensus in the field. Examples of three normal, unimpaired subjects performing simple tasks, such as drawing straight lines or circles, were explored in different manners to reveal the arm movement segmentation concepts. In particular, the results suggested that humans are not good at controlling velocity with the proprioceptive machinery, and that although at very low speeds, the inertial effects are expected to be small, speed oscillations were observed. In agreement with the literature on submovements, it is argued that these speed oscillations are markers, or signatures, of the segmentation phenomena. Moreover, the results suggested that the speed profile has kinematic not temporal "invariant characteristics" and that there is a correlation between speed and the radius of curvature of human movements. These ideas were summarized in three working models or hypothesis: Motor Control Hierarchy, Segments and Primitives of Arm Movement, and Minimum Action Unit Conjecture and Learning. The next chapter will explain how the speed profile was chosen and the details of the algorithm engine used for decomposition and encoding of the human arm movement

Apéritif : "I can resist anything, but temptation." -- Oscar Wilde

Why wait for the "wish-list" at the end of this document to entice the reader's craving. The circle drawing experiment raises interesting research questions. Subject A appears to be using a different submovement modal distribution than subjects B & C (four submovements or two pairs versus three submovements respectively). Subject A interpreted the instructions differently than subjects B & C and drew larger circles (approximately 0.4 m versus 0.2 & 0.3 m respectively).

Follow-up Hypothesis:

(1) The speed profile has kinematic not temporal "invariant characteristics."

(2) The apparent number of submovements changes with the hardware and its limitations.

Experimental Methods:

N subjects drawing consecutive circles at a constant target speed. Subjects repeat trials with:

(a) Increasing speeds

(b) Increasing circle diameters

(c) Grasping robot end-effector with the palm of the hand and with the tip of the fingers

(d) Clockwise and counterclockwise circles

Possible Outcomes:

Hypothesis 1 - Positive outcomes reinforce existing consensus in the motor control field that tasks are planned in terms of kinematics, and provides further evidence of submovements.

- Negative outcomes are a strong result indication that the field needs to reanalyze some of the basic assumptions.

Hypothesis 2 - Positive outcomes imply that the number of apparent submovements increase for the same shape with different sizes, decrease with a larger number of degrees of freedom of the "hardware" (palm of the hand vs finger grasping), kinematic characteristic is influenced by the "hardware" (human arm properties are not isotropic). It could lead to an insight into the ways motor planning is influenced by the "hardware".

- Negative outcomes imply that the central nervous system motor planning does not take into consideration the "hardware".

CHAPTER 3. A TASK-ENCODING SCHEME FOR HUMAN MOTION

"The great end of life is not Knowledge but Action."
– T.Huxley

"Knowledge is for Hungarians, Know-how is for Germans."
– anonymous (residing in Sao Paulo-Brazil)

3.1. Competent Description of Arm Movement

To discuss a language for arm movement requires the definition of what is considered a competent description. A competent description of arm movement retains the intrinsic information of the movement. In other words, the error between the original signal and the description is within an M-bound of a chosen norm (e.g. L2 or L-infinity norms). Therefore, a description in its most basic form could include a complete record of the movement, provided that the sampling accords with Shannon's sampling theorem allowing theoretically perfect reconstruction. On the other hand, the sampled signal could be transformed via Fourier analysis and synthesis equations. However, there is no dimensional reduction in the first case, and likewise the Fourier approach might increase the dimensionality of the problem depending on the transformed signal. Therefore a competent description should not only retain the intrinsic information in the data, but also project the data from the original dimensional space into a smaller subspace resulting in a dimensionality reduction.

Limiting the analysis to a particular set of data, the compromise between dimensionality reduction and intrinsic information could be achieved via Principal Component Analysis (PCA), also known as Karhunen-Loeve Transform [Papoulis, 1991]. The approach has been adopted in different unsupervised learning schemes in the neural networks community[e.g. Linsker, 1988; Bell & Sejnowski, 1995; Sanger, 1989]. They showed that performing PCA is equivalent to maximizing

the mutual information that the output of a processor contains of its input (Infomax). A similar approach has been adopted in filter design in the digital signal processing community, in the approximation theory, in the least-squares methods, in the singular-value decomposition, in the genetic algorithms, and in others. The approach adopted in this thesis is tailored in a similar fashion, but differs in that it is well suited to a class of data not just a particular one. It creates a biologically-based encoder with an appropriate choice of a basis function (or non-linear hidden unit in neural network parlance) well suited to human arm movement.

3.2. Best Basis Function

The previous chapter discussed working models of segmentation and submovements that permeate motor control and motor learning literature. In particular, it was postulated that a repertoire of movement primitives or submovements, each with a bell-shaped velocity profile, constitute the building blocks of complex tasks. In addition, it was proposed as a working model, that this kind of "quantization" is a basic feature of human motor behavior. Furthermore, the working model assumes that movement is a composition of asynchronous episodic submovements constructed from the same bell-shaped velocity profile. The submovement concept can be expressed via the following synthesis equation:

$$f(x) = \Sigma_{i=1}^{N} c_i \bullet (\Phi(\tfrac{x-b_i}{a_i})) \qquad \text{(eq. 3.1.)}$$

where Φ is the basis function.

In other words, it is desired to reconstruct f(x) by modulating, by translating, and by dilating a "mother" shape. The desired unsupervised algorithm to decompose f(x) represents the analysis equation, though the shape of the "mother" basis function remains an open issue. The fundamental questions are:

- Is it feasible to identify a unique basis function ?
- What are the criteria to choose the basis function ?

From a mathematical standpoint, it had been shown that the choice of a basis function is not unique considering a criterion that encompasses solely reproduction fidelity (L2 norm). For example, a compactly supported function f(x) can be approximated with infinite precision by ridge functions [Cybenko, 1989] [Hornik, 1989], by radial basis functions [Poggio & Girosi, 1990], or by an ideal reconstructor (sinc function) centered at each sample point. If the criterion is best approximation in the minimax sense (Linfinity norm), the fixed shape radial basis function has the best approximation property. Logistic functions do not have this property. Before further considering uniqueness, it is useful to note that the above result is limited in practice by the fact that there must be a fixed shape basis function centered at each sample. For example, an approximation given by the above synthesis equation with less radial basis functions than sample points, also known as generalized radial basis function (GRBF), does not satisfy the best approximation property in the minimax sense [Girosi & Poggio, 1989].

The adopted approach was to identify the basis function from experimental data, in particular from stroke patients' data. Since if as postulated: (a) submovement is a basic feature of human motor behavior, (b) movement is composed of a small number of these primitives, and (c) the process of learning and post-cerebral vascular accident recovery proceed by blending and overlapping segments, then the signature of the "mother" shape(s) should be identifiable by modulating, translating, and dilating experimental patient's data. Note that a positive outcome does not imply the correctness of the working model and choice of primitive shape, although failure would be conclusive evidence that the working hypothesis is false. Although it cannot be claimed unequivocally that the "mother" basis function of human movement can be identified, it can be claimed from a mathematical standpoint that a competent description of movement can be obtained. This approach for identification of the "mother" shape should hold equally with normal subjects. However in normal subjects, movement is very smooth and fluid. Therefore, the experimental procedures and measuring devices must be remarkably refined to isolate the submovements in these subjects, particularly since the translation and the dilation operations are non-linear. In these subjects, it is a hard inverse problem. The approach should be straightfoward with hemiplegic subjects or young babies, since in the first case, the motor control system has been broken down into its elementary components, and in the second case, the motor control

system is being built from its elementary components. In particular, it should be less difficult to deal with the non-linearity represented by the translation and dilation mathematical operations.

Going back to the relative value of pictures over words, Fig.3.1.1. is a representative raw data record of the movement of a patient, initially hemiplegic, who during the initial stages of recovery, regains movement and control towards the target. The top left plot shows a plan view of the patient's hand movement. The top right and bottom left plots show the movement's velocity in the x and y-directions respectively, with the last plot showing the tangential velocity. In the upper row of Fig.3.1.2., the record was shifted to align all peaks above an arbitrary threshhold of 20 percent of the highest peak to the same center (translation). These peaks were normalized to the same unit value (modulation). For clarity, in the center row, the signal is shown only until the first reversal. Finally, the resulting signal is interpolated-decimated (dilation) and for comparison purposes the centers of the resulting velocities (translation) are aligned. Only the normalized speed profiles with first reversals occurring under 0.5 m/sec (half the normalized speed peak) were interpolated and decimated to the same reference length, which corresponded to the shortest speed profile duration in the particular movement record. The ratio between interpolation and decimation was determined by the ratio between the particular speed profile duration and the reference length. Due to limitations on the interpolation operation, this ratio was rounded to a ratio of tens, e.g., 13/18 implying resampling the data at a higher rate of 13 times with a symmetric lowpass filter interpolation, followed by the decimation of the resulting data points by 18 [Oppenheim & Schafer, 1989]. The speed-displacement phase-plot is shown on the right side of the lower row. As in the interpolation-decimation case, only the normalized speed profiles with first reversals occurring under 0.5 m/sec were included. These operations were originally designed considering the possibility of a large variability of the speed profile durations within the same movement. As it turned out, the speed profiles within a particular record for stroke patients had almost the same duration. Therefore mean curves were calculated directly from the normalized speeds without any further mathematical manipulation, such as the interpolation-decimation (dilation) or the phase-plots described above. The next sequence of figures - Figs.3.2.1 & 2 - show the same patient's movement with the same orientation, but with a different starting point. The horizontal scale on Figs. 3.1.2. & 3.2.2. was modified from time (Figs. 3.1.1. & 3.2.1) to time duration, and

this scale was not aligned with the center of the highest peak. Similar results can be obtained for all patients who regained some movement, but were initially hemiplegic or hemiparetic. Figs.3.3.1. to 3.3.10 display two stereotypical movement samples for each of the twenty stroke patients enrolled in the robot-aided neuro-rehabilitation clinical trial described in Chapter 5. The task consisted of a point-to-point movement of 4 inches with no time constraints. These samples correspond to the initial weeks after the onset of the stroke (typically 4 weeks). The left columns consist of the hand trace on the horizontal plane (displacement), the middle columns show the hand speed profile, and the right columns show the speed peaks above 20 percent of the maximum speed normalized to unity and aligned around a common center. To unclutter the figures, the speed profiles are shown up to the first reversal. To be discussed later in Chapter 5, these twenty stroke patients had different lesions (type, size, location) and constitute a representative pool of acute stroke patients. Movements were chosen to show the directions that required predominantly elbow or shoulder movement. As a result, movements were recorded for all but one patient. Caution should be exercised since any movement in one direction in a single joint should not be misinterpreted as suggesting control of movement in the horizontal plane, as illustrated in Fig.3.4.

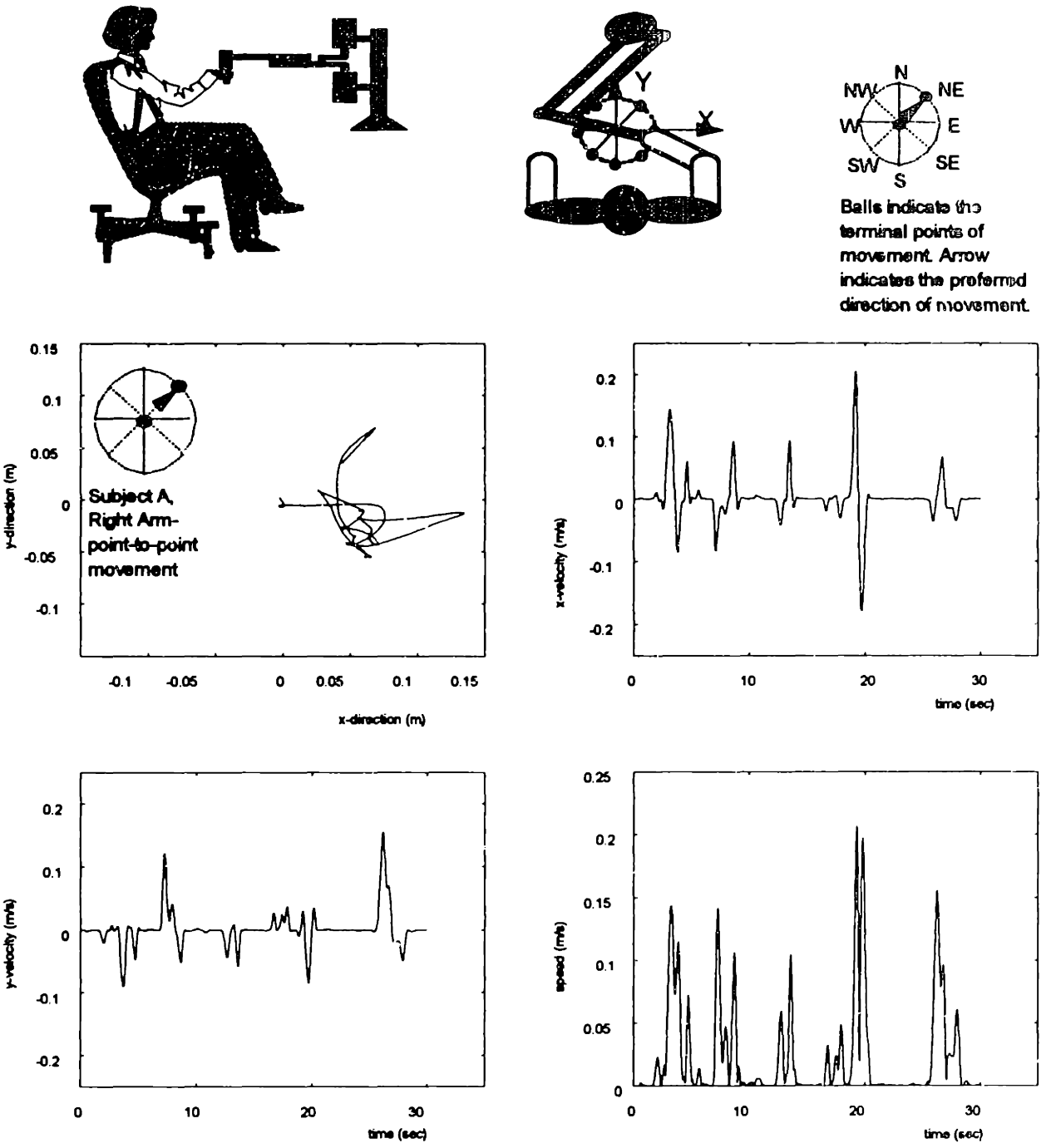

FIG.3.1.1.Kinematic Data of Subject A in a Point-to-Point Movement without Time Constraint.
The upper left plot shows the hand displacement in the horizontal plane with the upper right and lower left plots corresponding to the hand velocity in the x and y-directions respectively. The right lower plot shows the hand speed.

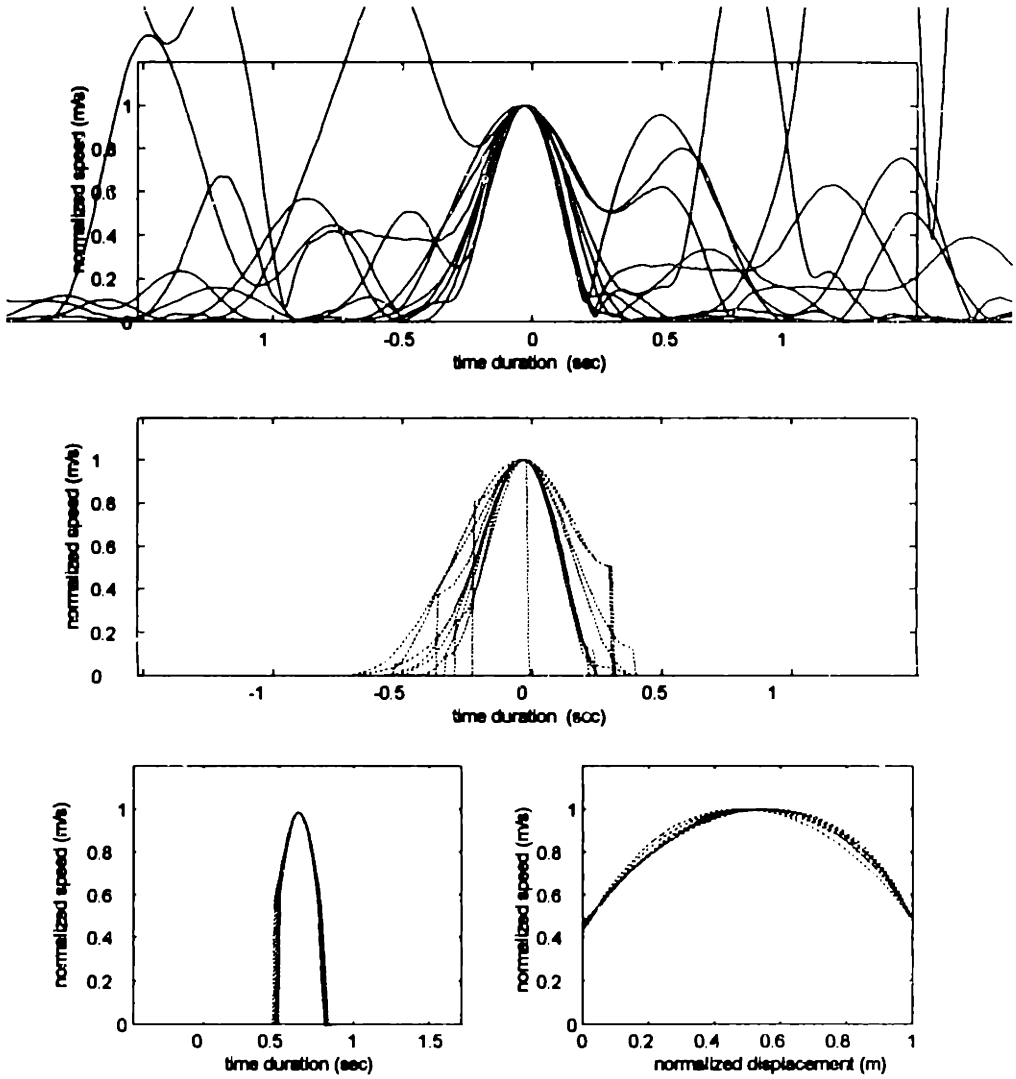

FIG.3.1.2.Kinematic Data of Subject A in a Point-to-Point Movement without Time Constraint. The plot on the upper row shows the hand speed peaks above 20% of the top speed, shifted to the same center (translation) and normalized to unity (modulation). The middle row shows the uncluttered view of the shifted & normalized speed up to the first reversal (vertical lines). The normalized speed profiles above 0.5 m/sec were dilated to the same length (interpolated and decimated) as shown in the lower left plot. The lower right plot shows the phase plot to normalized speed profiles above 0.5 m/sec.

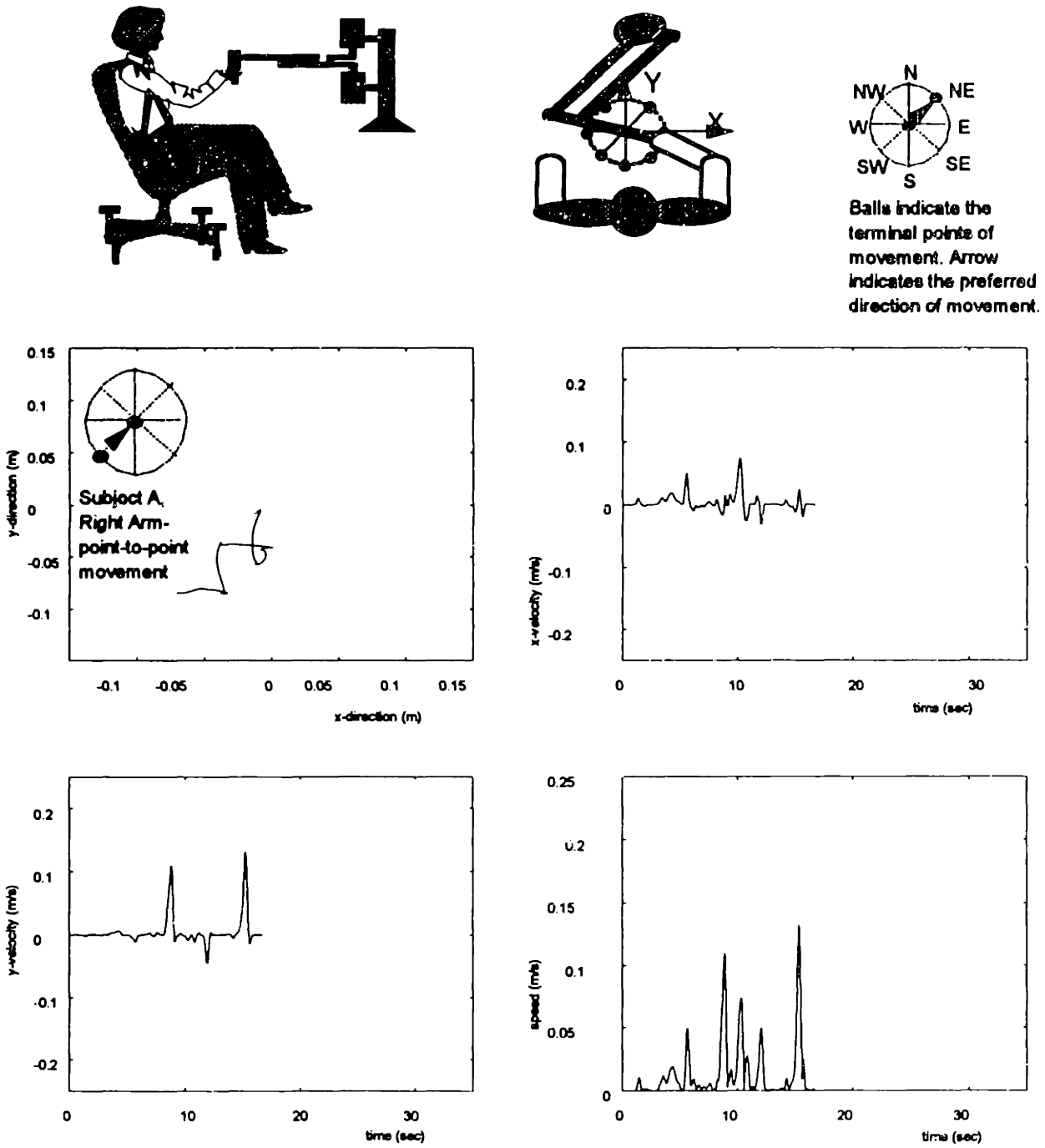

FIG.3.2.1.Kinematic Data of Subject A in a Point-to-Point Movement without Time Constraint.
The upper left plot shows the hand displacement in the horizontal plane with the upper right and lower left plots corresponding to the hand velocity in the x and y-directions respectively. The right lower plot shows th hand speed. Note that although the movement is in the same direction translated by 4 inches, the quality of movement is different from Fig.3.1. This result suggests that post-stroke movement is workspace dependent.

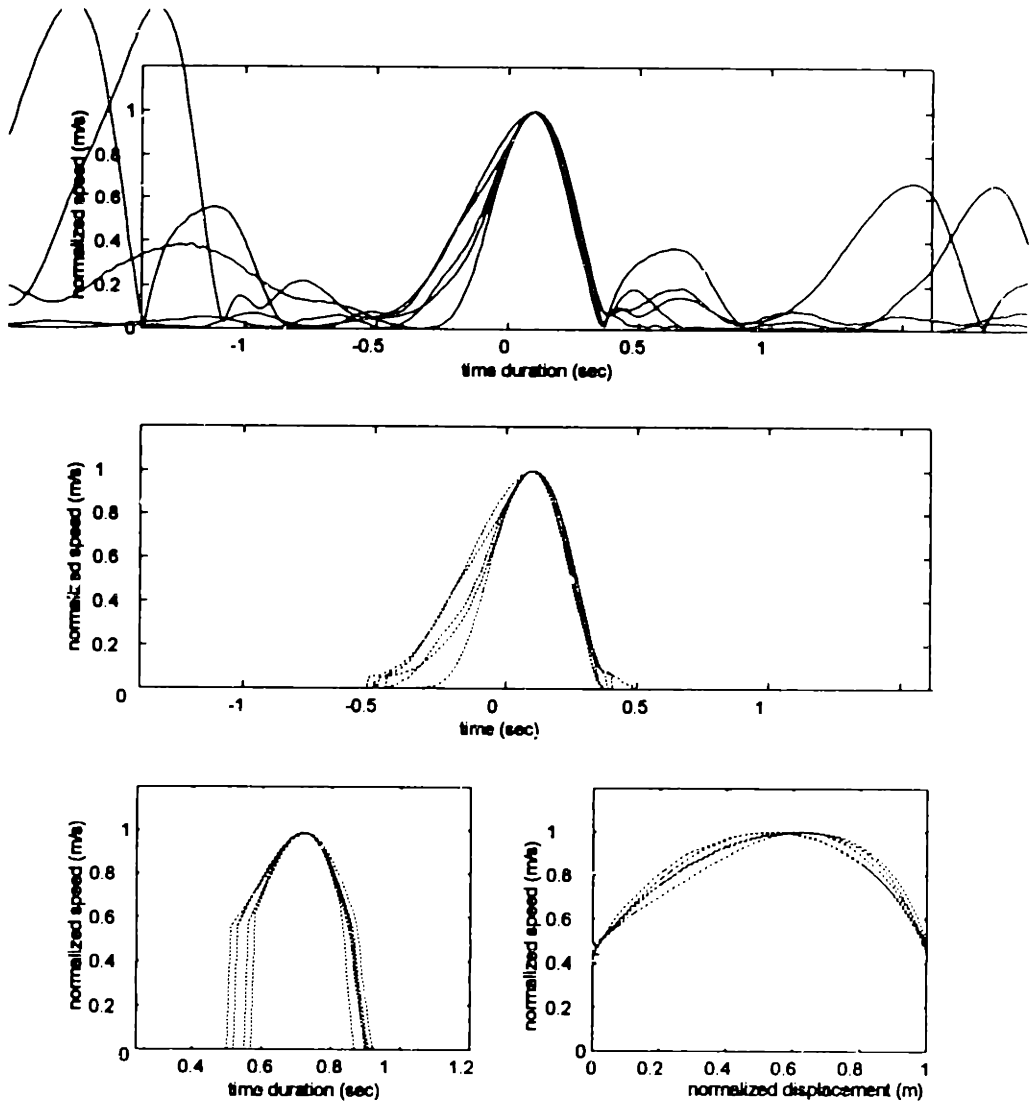

FIG.3.2.2.Kinematic Data of Subject A in a Point-to-Point Movement without Time Constraint. The plot on the upper row shows the hand speed peaks above 20% of the top speed, shifted to the same center (translation) and normalized to unity (modulation). The middle row shows the uncluttered view of the shifted & normalized speed up to the first reversal (vertical lines). The normalized speed profiles above 0.5 m/sec were dilated to the same length (interpolated and decimated) as shown in the lower left plot. The lower right plot shows the phase plot to normalized speed profiles above 0.5 m/sec.

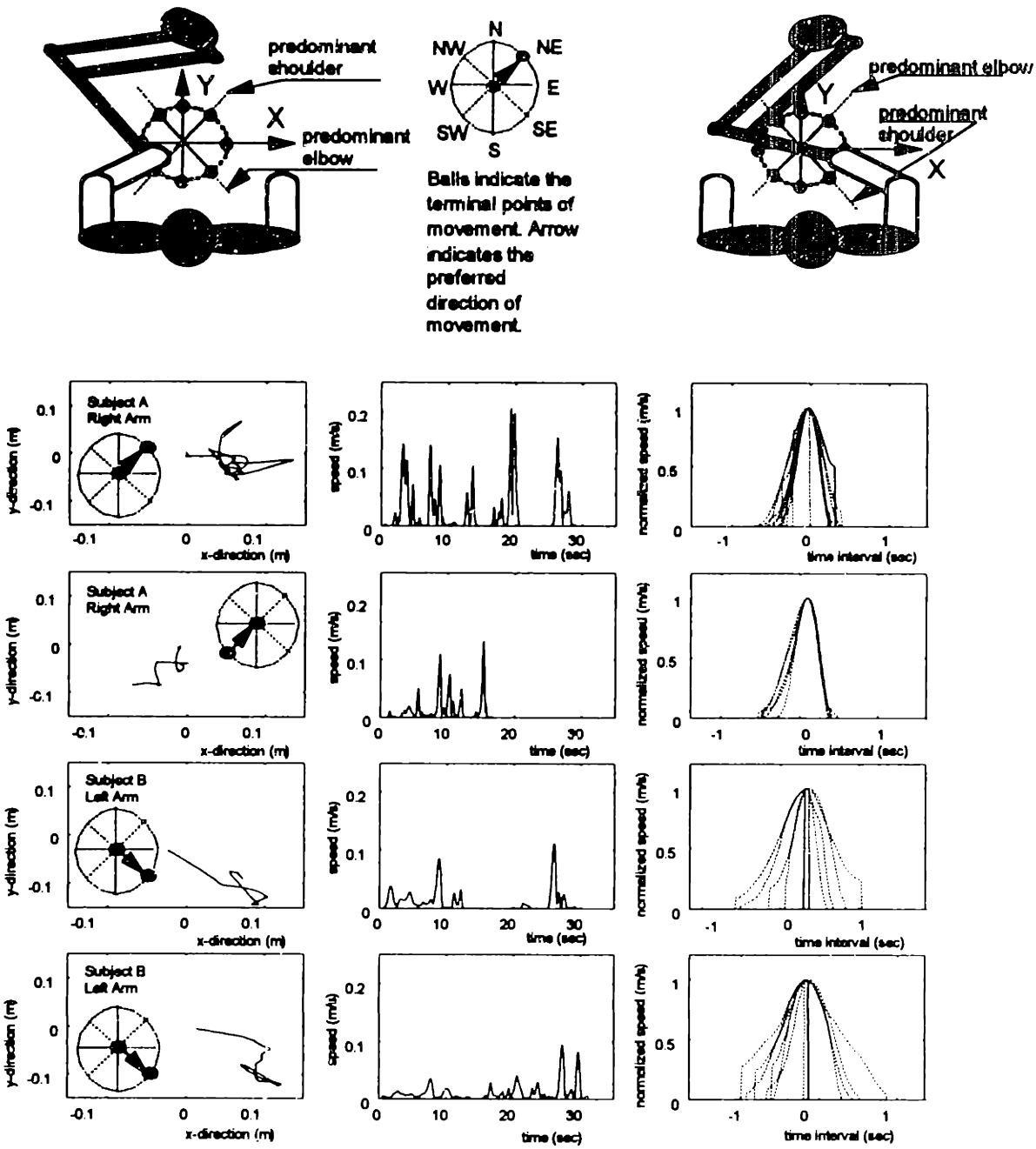

FIG.3.3.1. Two Samples of the Initial Post-Stroke Recovery Phase for Each of the 20 Patients Enrolled in the Clinical Trial. The task consisted of a point-to-point movement without a time constraint. The left column shows the hand displacement in the horizontal plane. The middle column shows the hand speed, and the right column shows the speed peaks above 20% of top speed up to the first reversal (vertical line), shifted to the same center and normalized to unity.

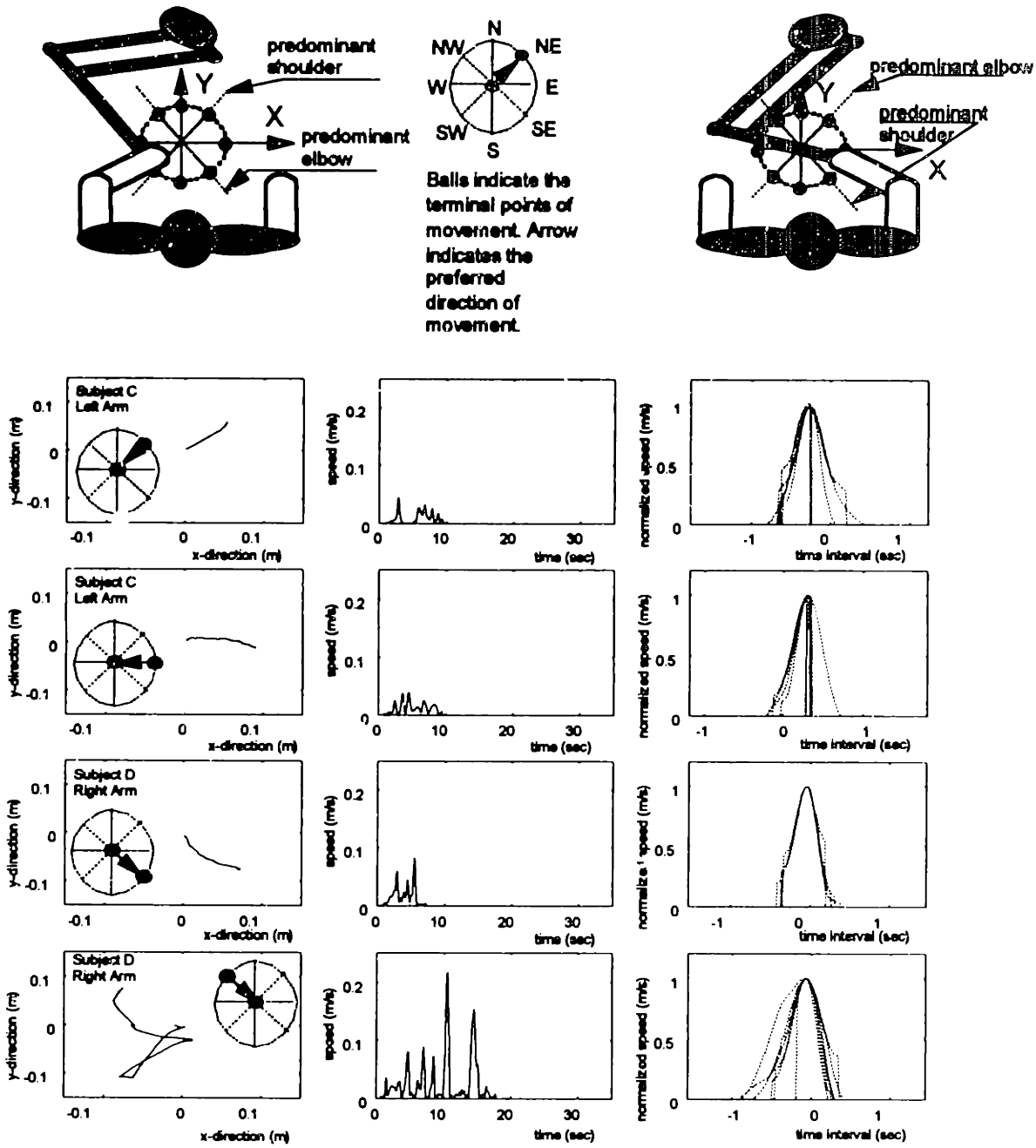

FIG.3.3.2. Two Samples of the Initial Post-Stroke Recovery Phase for Each of the 20 Patients Enrolled in the Clinical Trial. The task consisted of a point-to-point movement without a time constraint. The left column shows the hand displacement in the horizontal plane. The middle column shows the hand speed, and the right column shows the speed peaks above 20% of top speed up to the first reversal (vertical line), shifted to the same center and normalized to unity.

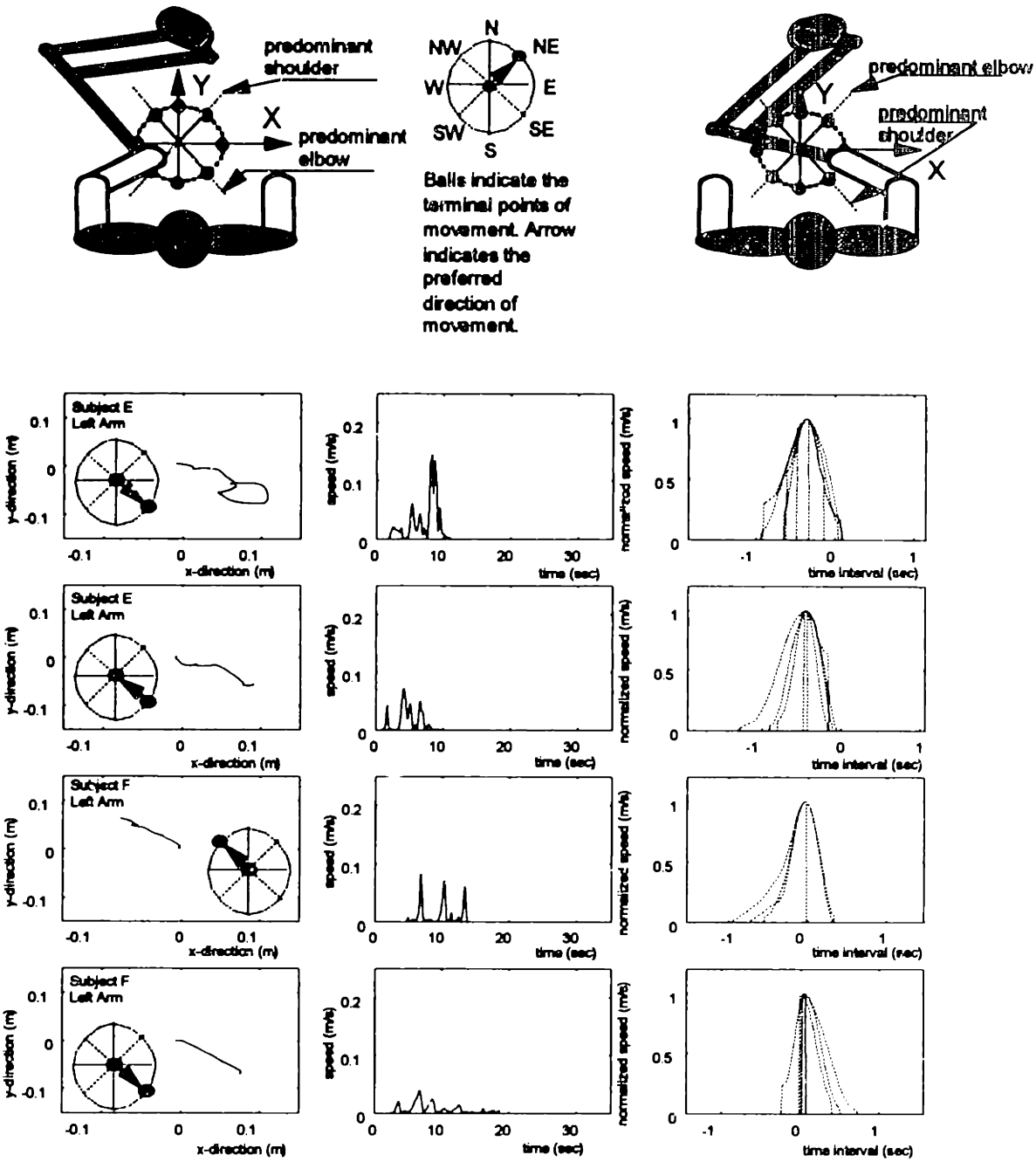

FIG.3.3.3. Two Samples of the Initial Post-Stroke Recovery Phase for Each of the 20 Patients Enrolled in the Clinical Trial. The task consisted of a point-to-point movement without a time constraint. The left column shows the hand displacement in the horizontal plane. The middle column shows the hand speed, and the right column shows the speed peaks above 20% of top speed up to the first reversal (vertical line), shifted to the same center and normalized to unity.

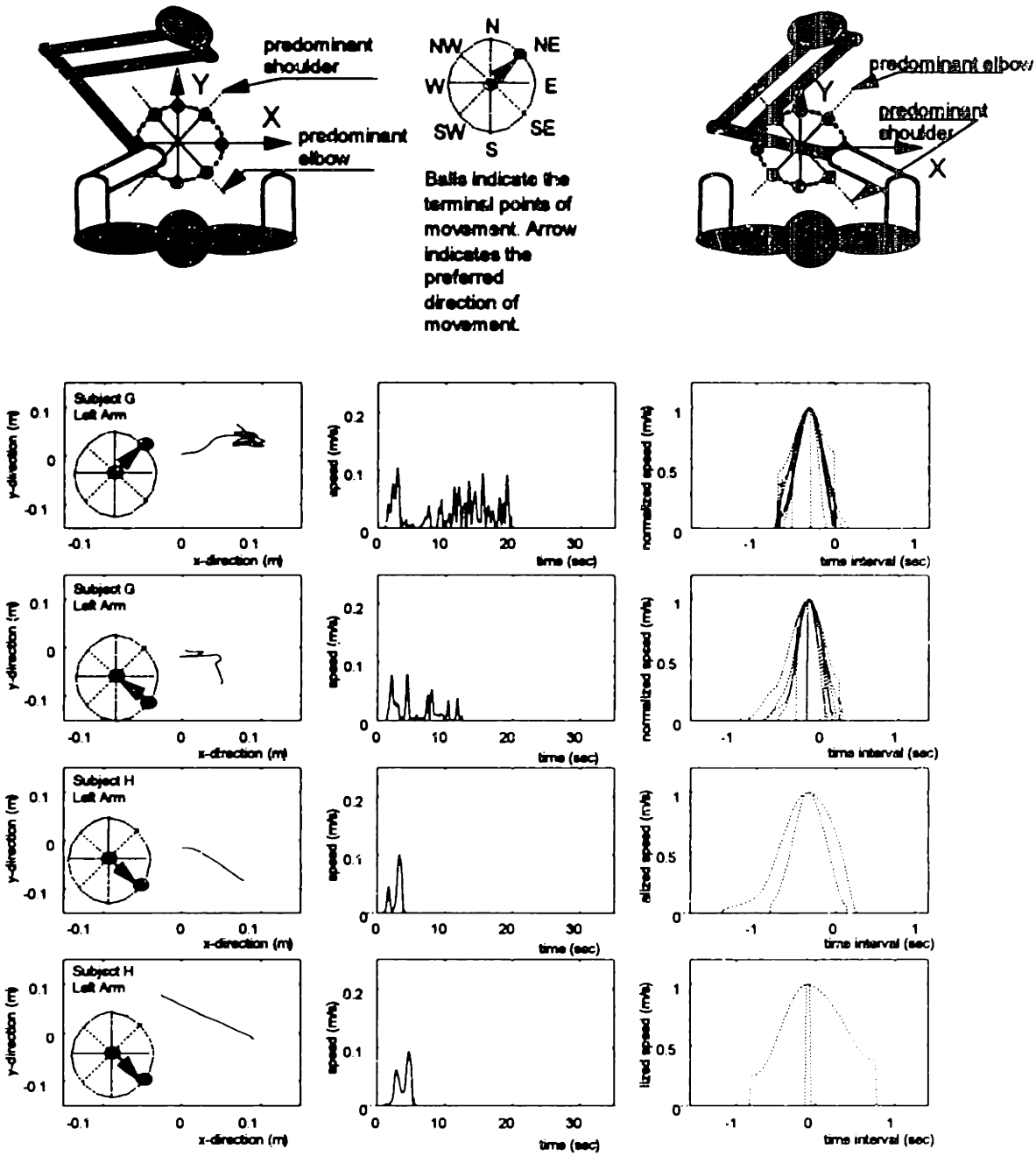

FIG.3.3.4. Two Samples of the Initial Post-Stroke Recovery Phase for Each of the 20 Patients Enrolled in the Clinical Trial. The task consisted of a point-to-point movement without a time constraint. The left column shows the hand displacement in the horizontal plane. The middle column shows the hand speed, and the right column shows the speed peaks above 20% of top speed up to the first reversal (vertical line), shifted to the same center and normalized to unity.

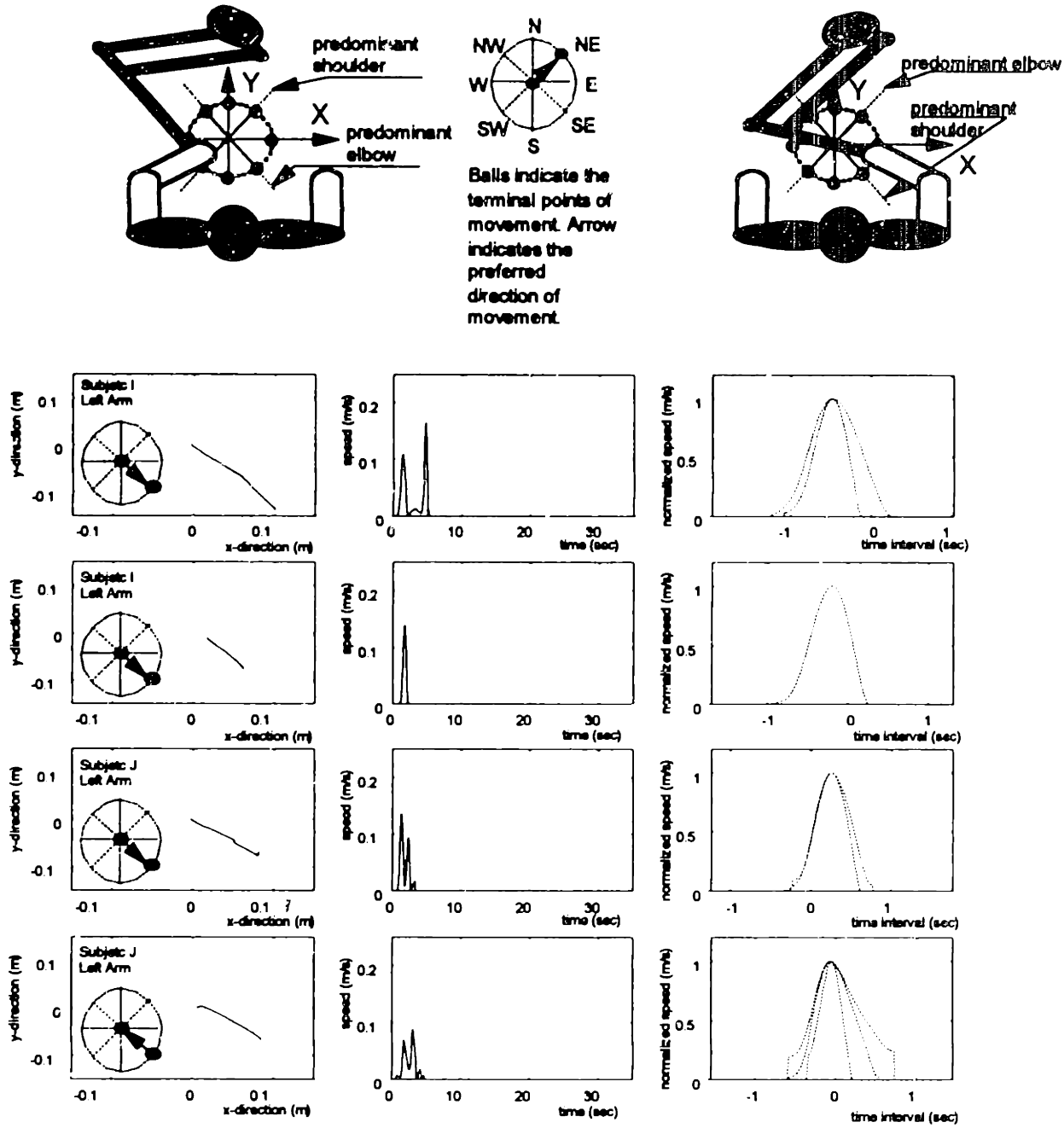

FIG.3.3.5. Two Samples of the Initial Post-Stroke Recovery Phase for Each of the 20 Patients Enrolled in the Clinical Trial. The task consisted of a point-to-point movement without a time constraint. The left column shows the hand displacement in the horizontal plane. The middle column shows the hand speed, and the right column shows the speed peaks above 20% of top speed up to the first reversal (vertical line), shifted to the same center and normalized to unity.

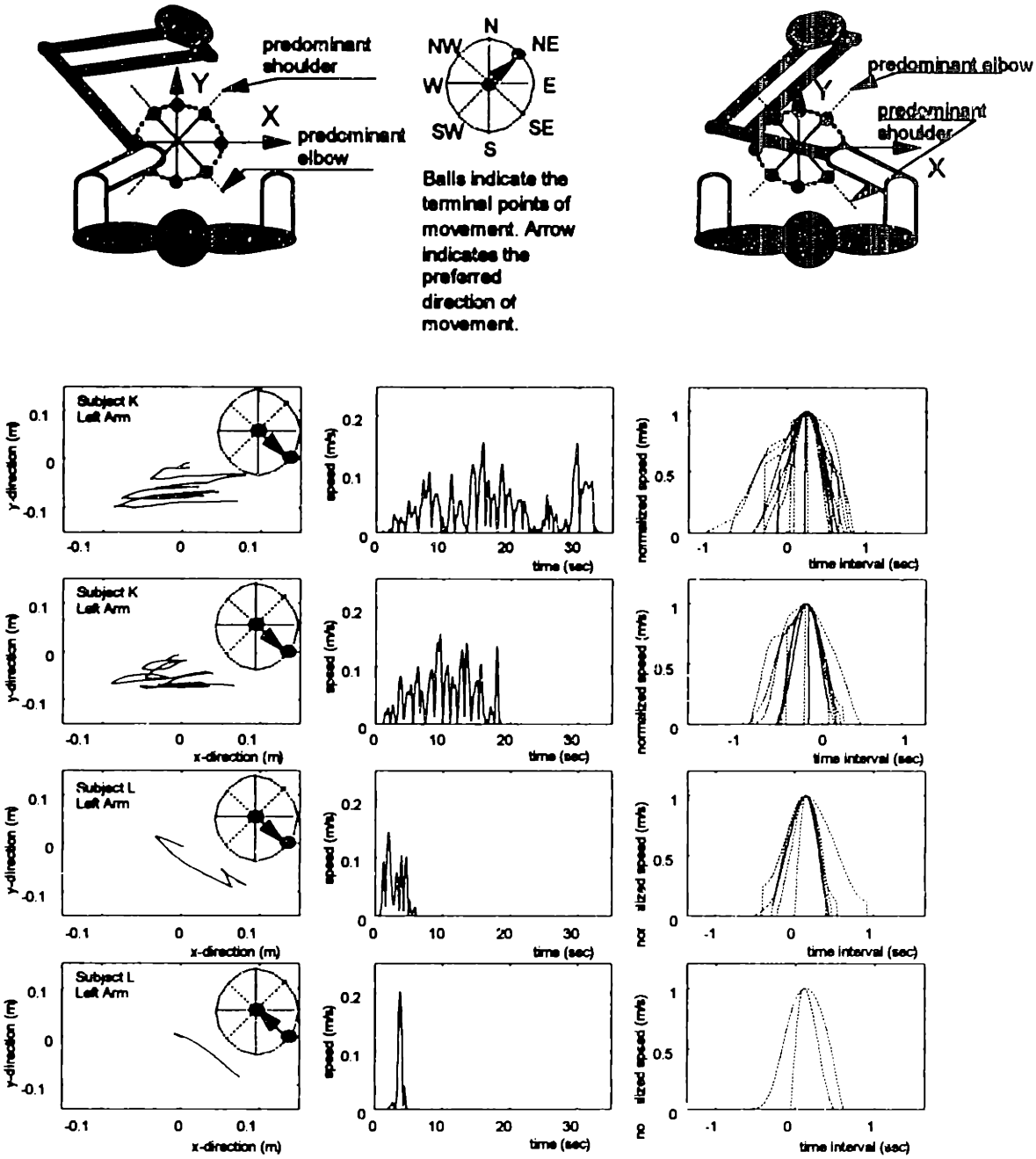

FIG.3.3.6. Two Samples of the Initial Post-Stroke Recovery Phase for Each of the 20 Patients Enrolled in the Clinical Trial. The task consisted of a point-to-point movement without a time constraint. The left column shows the hand displacement in the horizontal plane. The middle column shows the hand speed, and the right column shows the speed peaks above 20% of top speed up to the first reversal (vertical line), shifted to the same center and normalized to unity.

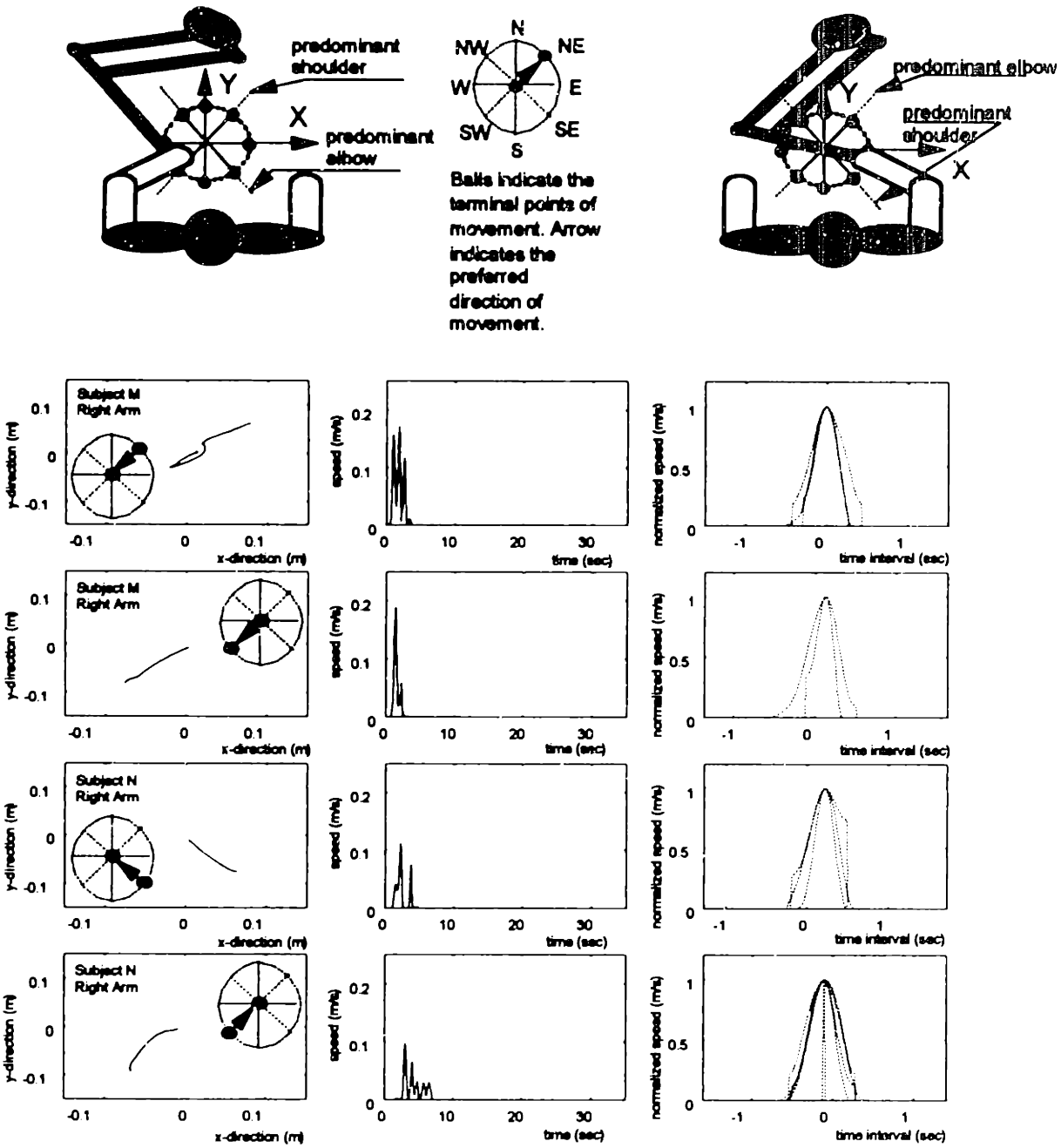

FIG.3.3.7. Two Samples of the Initial Post-Stroke Recovery Phase for Each of the 20 Patients Enrolled in the Clinical Trial. The task consisted of a point-to-point movement without a time constraint. The left column shows the hand displacement in the horizontal plane. The middle column shows the hand speed, and the right column shows the speed peaks above 20% of top speed up to the first reversal (vertical line), shifted to the same center and normalized to unity.

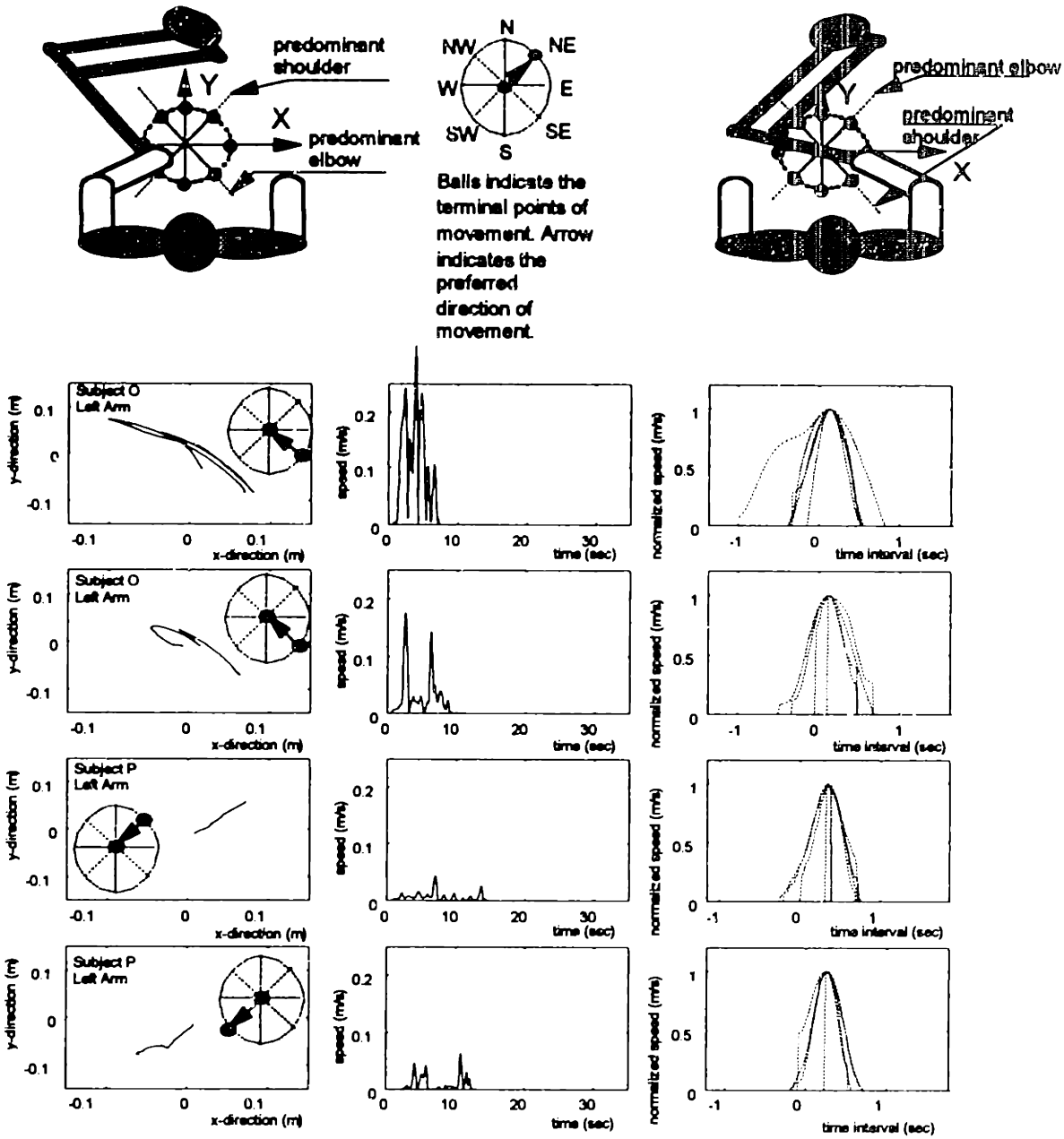

FIG.3.3.8. Two Samples of the Initial Post-Stroke Recovery Phase for Each of the 20 Patients Enrolled in the Clinical Trial. The task consisted of a point-to-point movement without a time constraint. The left column shows the hand displacement in the horizontal plane. The middle column shows the hand speed, and the right column shows the speed peaks above 20% of top speed up to the first reversal (vertical line), shifted to the same center and normalized to unity.

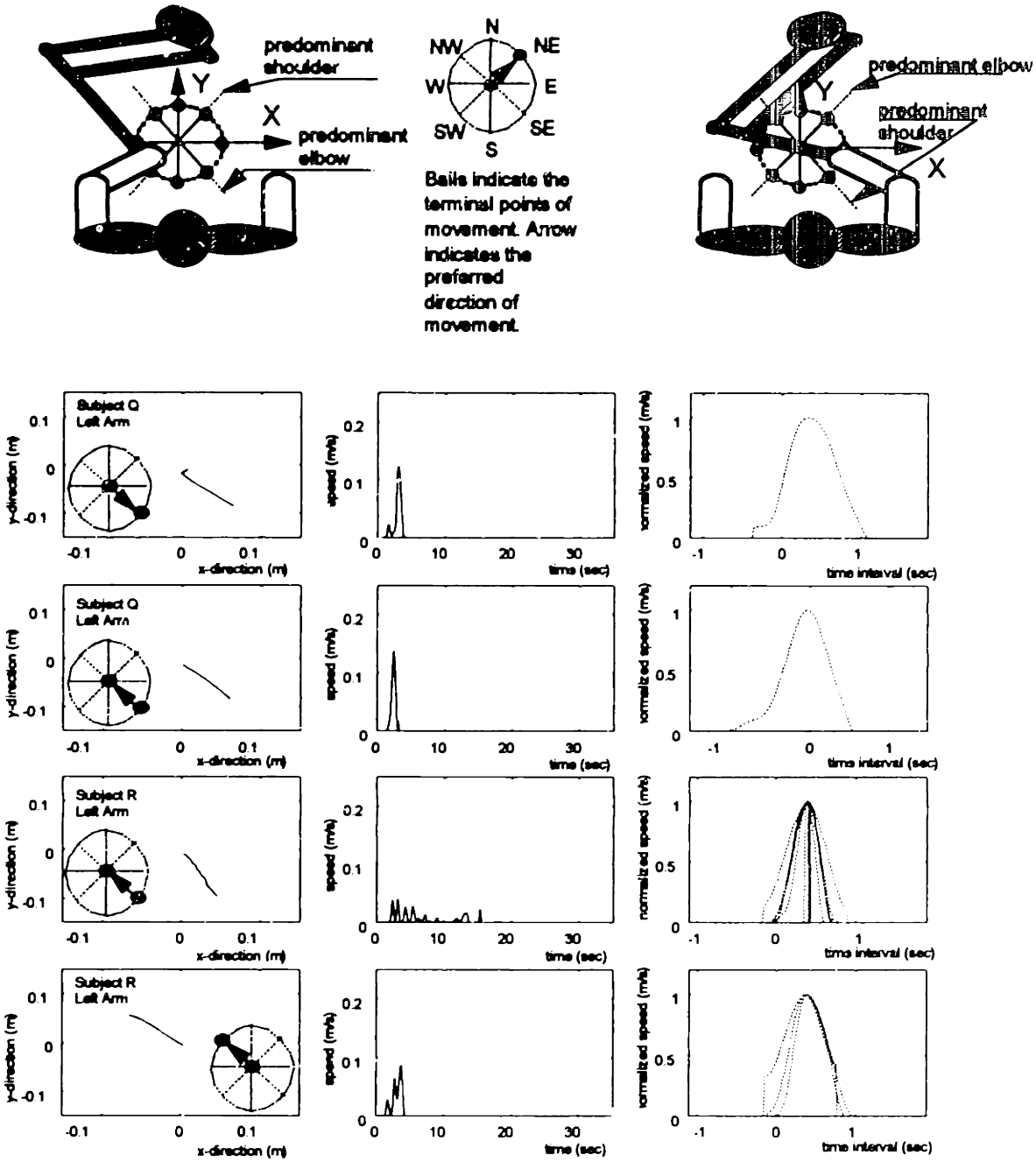

FIG.3.3.9. Two Samples of the Initial Post-Stroke Recovery Phase for Each of the 20 Patients Enrolled in the Clinical Trial. The task consisted of a point-to-point movement without a time constraint. The left column shows the hand displacement in the horizontal plane. The middle column shows the hand speed, and the right column shows the speed peaks above 20% of top speed up to the first reversal (vertical line), shifted to the same center and normalized to unity.

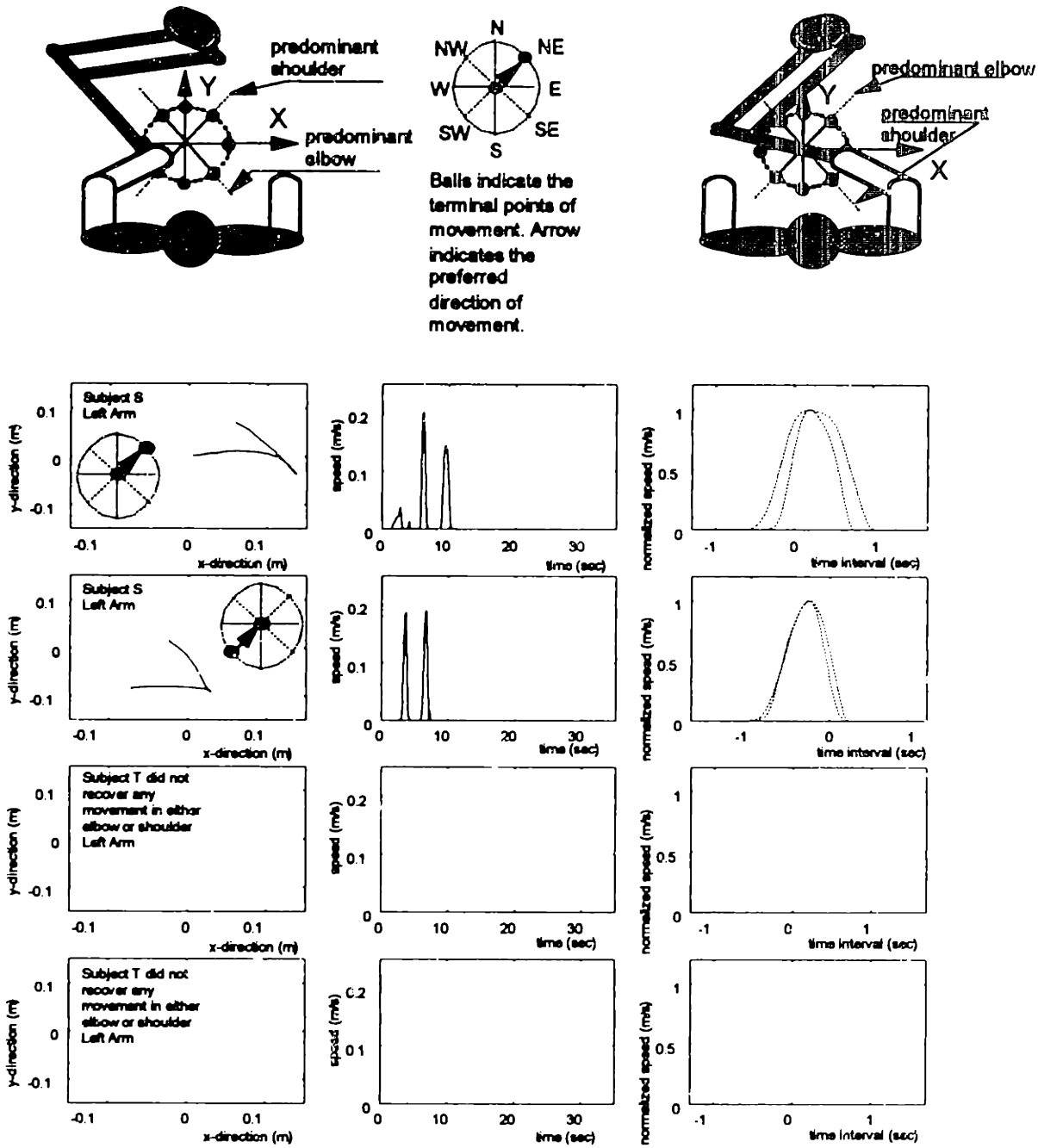

FIG.3.3.10.Two Samples of the Initial Post-Stroke Recovery Phase for Each of the 20 Patients Enrolled in the Clinical Trial. The task consisted of a point-to-point movement without a time constraint. The left column shows the hand displacement in the horizontal plane. The middle column shows the hand speed, and the right column shows the speed peaks above 20% of top speed up to the first reversal (vertical line), shifted to the same center and normalized to unity.

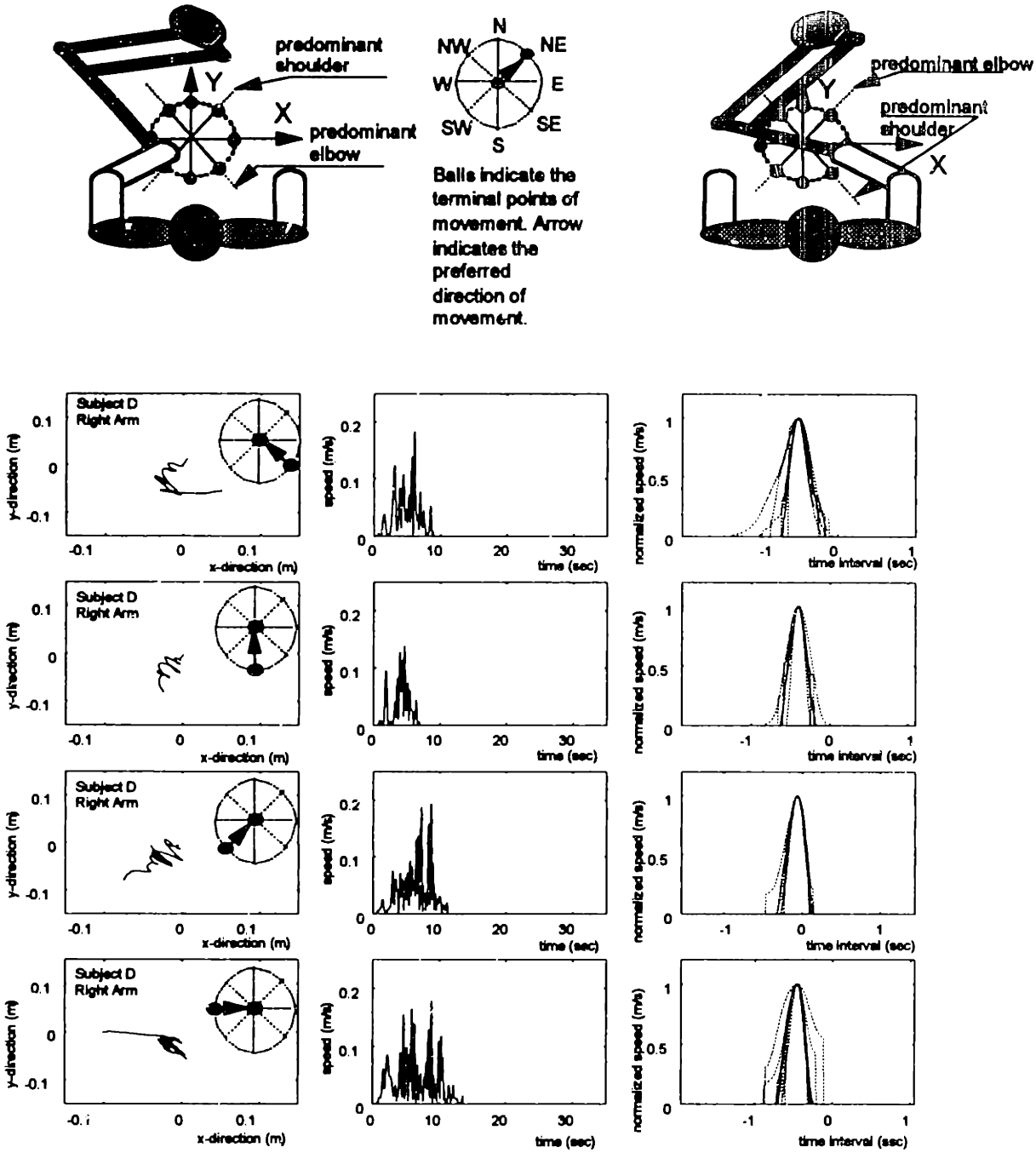

FIG.3.4. Kinematic Data of Subject D in a Point-to-Point Task without Time Constraint.
The left column shows the hand displacement in the horizontal plane. The middle column shows the hand speed, and the right column shows the speed peaks above 20% of top speed up to the first reversal (vertical line), shifted to the same center and normalized to unity. Not that subject D is capable of moving the shoulder and flexing the elbow joint, but incapable of extending the arm (see also Fig.3.3.2). These results suggest that movement is workspace and region dependent (see also Fig.3.1.1. and Fig.3.2.1.).

- How can the best basis functions be characterized analytically or geometrically ?

The most straightforward representation of the "mother" basis function is in the form of a look-up table with no mathematical manipulation, but the calculation of the mean value at different levels. Opting for a mathematically concise formulation of the isolated components of speed profile, the "mother" shape can be approximated by a Beta distribution function $f(t, \rho, \sigma)$, which has two adjustable parameters ρ and υ.

$$f(t, \rho, \sigma) = \frac{1}{B(\rho,\sigma)} \bullet t^{(\rho-1)} \bullet (1-t)^{(\sigma-1)} \qquad \text{(eq. 3.2.)}$$

where t is within the interval [0, 1] and $B(\rho, \sigma)$ is the Beta Function.

Proper choice of parameters results in a wide variety of shapes, e.g., symmetric, skewed, unimodal, bimodal, as illustrated in Fig.3.5. Mean curves were calculated for each of the normalized speed plots of Figs. 3.3. and 3.4. Each of these resulting mean curves were fitted by a Beta Function using standard techniques [Pratt, Raiffa, and Schlaifer, 1995]. Figure 3.6. shows the composite of all the previous plots expectations of the Beta function mean (p) and standard deviation (ps). Note the consistency of the expectation of the mean (intersubject) and standard deviation (scale). The resulting normalized Beta distribution density function approximation is shown in Fig.3.7. For comparison purposes, this figure displays a Gaussian with a standard deviation equal to half the span of the Beta function at the 0.67 level and a Minimum-Jerk profile with the same duration. The profiles peaks were centered at the same location.

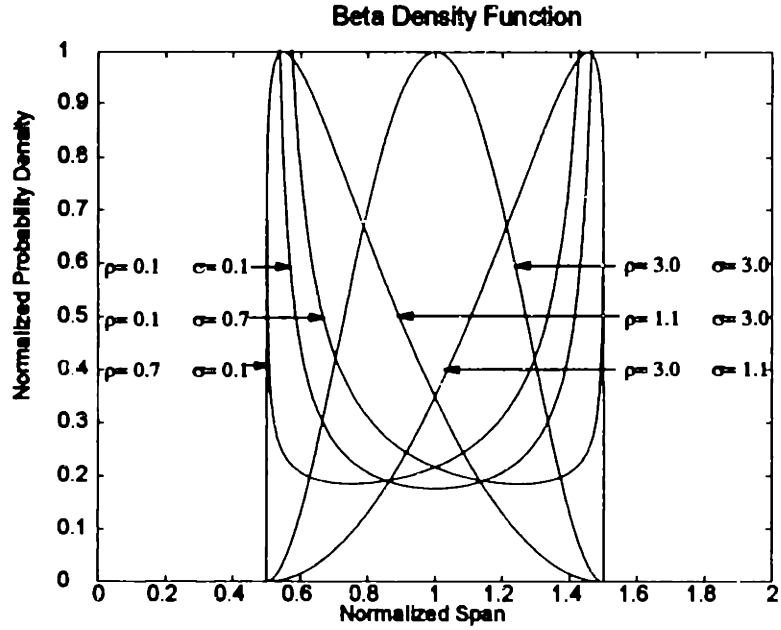

FIG.3.5. Examples of Normalized Beta Density Function for Different Values of ρ and σ. The figure shows that the proper choice of parameters leads to a wide variety of shapes, eg., symmetric, skewed, unimodal, bimodal.

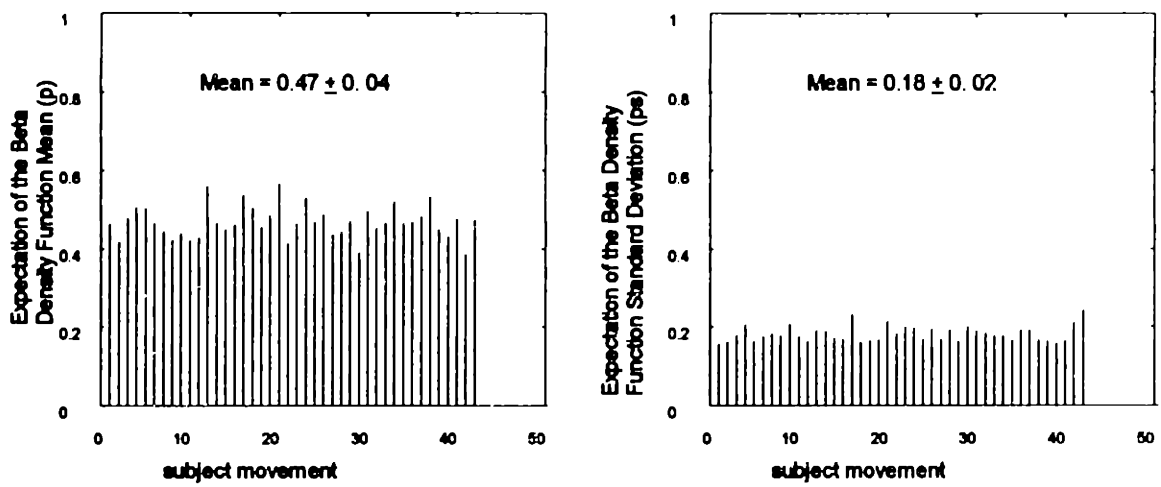

Beta Density Function

$\upsilon = p[1 - p] / ps - 1$	$\upsilon = 6.28$
$\rho = \upsilon . p$	$\rho = 2.96$
$\sigma = \upsilon - \rho$	$\sigma = 3.32$

FIG.3.6. Beta Density Function Parameters Determination.
The parameters for the Beta Density Function were estimated from all the movements in Fig.3.3. & 3.4. The parameters were estimated for each point-to-point task. The mean and standard deviation of these parameters are shown in the upper row, which shows on the left side the expectation of the mean (p), and on the right side the expectation of the standard deviation (ps) for each point-to-point task. The estimated parameters for the Beta Function are shown below (see Fig.3.7. for parameter explanation).

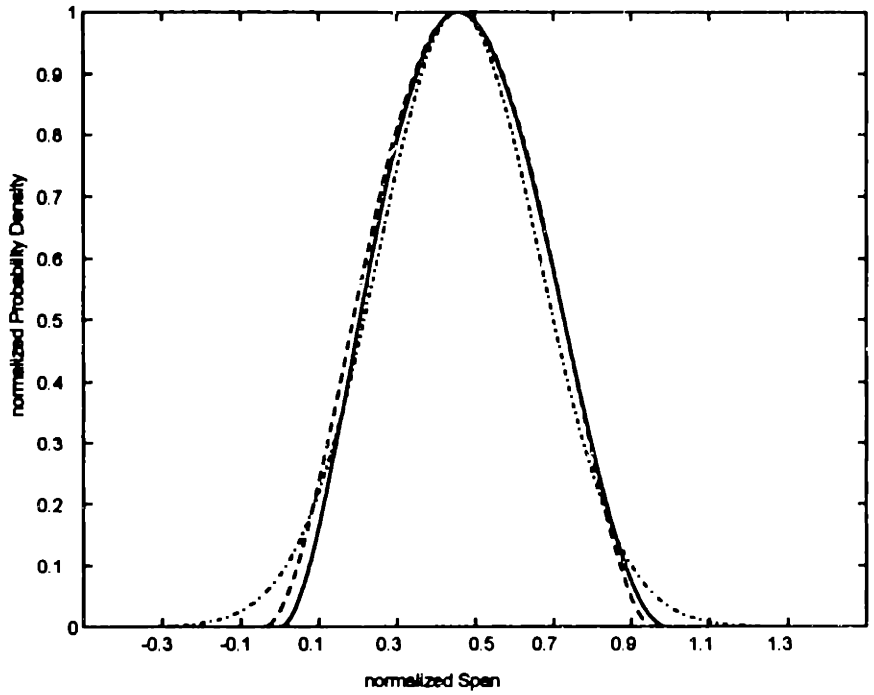

Minimum-Jerk
Error = $1.03.10^{-6}$(L2 sense)

Gaussian
Error = $2.69.10^{-6}$(L2 Sense)

Beta Approximation Function

$$f(p|\rho, \upsilon) = \frac{1}{B(\rho, \sigma)} . p^{(\rho - 1)} . (1 - p)^{(\sigma - 1)}$$

B is the Complete Beta Function

$0 \leq p \leq 1$

$\sigma = \upsilon - \rho$

$\rho, \sigma > 0$

FIG.3.7. Normalized Beta Density Function with υ of 6.28, ρ of 2.96 and σ of 3.32. The figure shows the estimated Beta Function for the point-to-point tasks shown in Fig.3.3. & 3.4. It also includes a Gaussian with standard deviation equal to half the span of the Beta at 67% and a Minimum-Jerk curve. The peaks of the curves are centered at the same point. Note that the Beta is not symmetric with a small degree of positive asymmetry, i.e. longer tail on the right side (skewness of 0.01). The Beta Function geometrical shape is platykurtic and resembles the Minimum-Jerk shape more than the Gaussian shape (kurtosis of -1.46 for the Beta versus -1.49 for the Minimum-Jerk and zero for the Gaussian).

- How can the best basis functions be computed numerically ?

The resulting fit suggests an almost symmetric "mother" shape. These results suggest that more tractable mathematical symmetric functions such as Gaussians or minimum-jerk profiles (fifth-order splines) could be used. The difference between bell-shaped curves is most pronounced in the curve's tail region. In Fig.3.6. the minimum-jerk velocity profile is a better match in the L2 sense and shape (kurtosis) than a Gaussian. Nonetheless, the difference in any case is quite small and does not differ for more than a fraction of a percentage point, e.g. 2.10^{-4} % and 5.10^{-4} % of the Beta approximation area. Moreover, most of the subjects' fitted data is concentrated near the peaks. Hence, differences in the tails have less meaning, and in what follows, a Gaussian or minimum-jerk profile is used as the "mother" shape. Note that using symmetric shapes for basis functions is an important simplification.

At the risk of being pedantic, this section is concluded by reiterating the working models and the importance of the "mother" shape. Movement was postulated as a composition of asynchronous episodic segments or submovements constructed from the same "mother" shape. These segments constitute the building blocks of more complex tasks and this type of "quantization" is a basic feature of human motor behavior. A single candidate was identified for the "mother" shape from the experimental data of 20 stroke patients during the initial stages of recovery. Although these patients had different lesions and impairment severity, there is a consistent "mother" shape, which allows the building of the biologically-based movement encoder in order to obtain a competent description of movement.

3.3. Regularization Theory Networks

The working model for human arm movement assumes that movement is a composition of asynchronous episodic submovements constructed from the same "mother" shape velocity profile by dilation, modulation, and translation. There are no well founded techniques to decompose a function f(x) by applying these three operations simultaneously. For example, radial basis function (RBF) style approach considers only modulation and translation of a single "mother" shape, while

wavelets considers only dilation and translation of a single "mother" shape. This Section reviews the well developed field known as Regularization Theory and its RBF techniques [Poggio & Girosi, 1990] and presents an extension, which considers simultaneously modulation, translation, and dilation operations, fashioned on Pyramidal Filtering, and named here: Irregular Sampling Radial Basis Function (ISRBF).

3.3.1. Radial Basis Function Networks (RBF)

Consider the inverse problem of finding f(x) given a set of data (x, y). Regularization Theory guarantees reproduction fidelity, but it additionally exploits smoothness leading to a solution obtained considering a performance index H[f] given by:

$$H[f] = \Sigma_{i=1}^{N}(y_i - f(x_i))^2 + \lambda\Psi[f] \qquad \text{(eq. 3.3.)}$$

The summation term gives the sum of the squared distance between the data and approximation function. This term represents a hard constraint if the summation is forced to zero guaranteeing perfect reconstruction (interpolation problem). The second term penalizes deviations from smoothness with a positive real number λ called the regularization parameter or stabilizer, and the smoothness deviation given by:

$$\Psi[f] = \|Pf\|^2 = \int_{R^d} \frac{|\tilde{f}(s)|^2}{\tilde{G}(s)}.ds \qquad \text{(eq. 3.4.)}$$

where P is an operator on f, and G is the Green's function of the self-adjoint operator $\tilde{P}$P. Depending on the choice of G, a non-empty null space might result. Assuming a symmetric $\tilde{G}(s)$ (Fourier Transform G(x) is real), the most general solution of the minimization problem is obtained as:

$$f(x) = \Sigma_{i=1}^{N} c_i.G(x - x_i) + p(x) \qquad \text{(eq. 3.5.)}$$

where p(x) is a polynomial lying in the null space of $\Psi(s)$. Considering a radial symmetric operator P (rotational and translational invariant), the solution involving radial basis functions results:

$$f(x) = \Sigma_{i=1}^{N} c_i . G(\|x - x_i\|) \qquad \text{(eq. 3.6.)}$$

This result indicates that an approximation composed by a sum of radial basis functions each centered at a distinct data point is a solution to the regularization problem. Moreover, this approximation can be formulated in terms of a multilayer neural network with one hidden layer as illustrated in Fig.3.8., and there are well-established algorithms to tune the network parameters. It provides a machinery to search and converge to the global minimum in the least-squares sense (fidelity of reproduction), while guaranteeing some degree of smoothness. There are several candidates for the radial basis function itself, e.g. quadrics, inverse quadrics, splines, and Gaussians.

This network approach is used as a guide and inspiration to the proposed movement encoder. The ideal arm movement encoder differs from the above regularization problem. The latter considers data fidelity and smoothness in its performance index. The former retains the intrinsic information in the data, but also aims at dimensionality reduction. Therefore, there is no space for an approximation function that requires a radial basis function centered at each distinct data point.

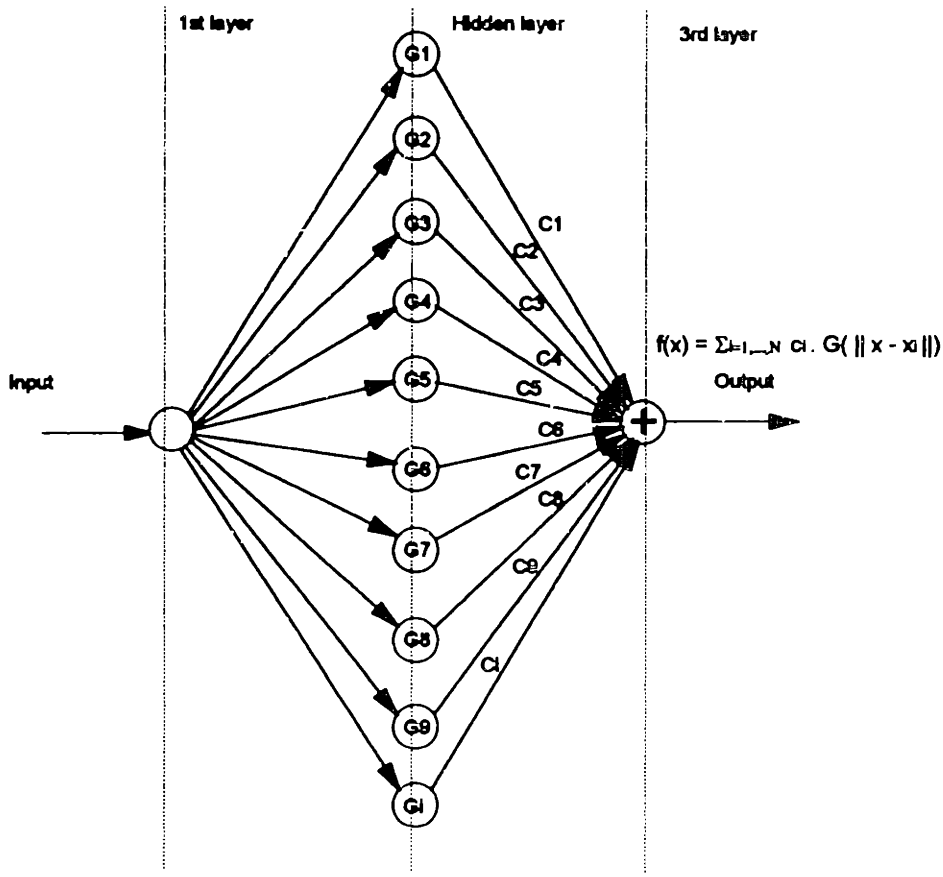

FIG.3.8. Multilayer Neural Network Structure

3.3.2. Generalized Radial Basis Function

The generalized radial basis function (GRBF) represents an attempt to solve the regularization problem with fidelity of reproduction and smoothness, while addressing the requirement to reduce the number of network units. Poggio & Girosi baptized the extension of the RBF to the case with movable centers as GRBF. Furthermore, they designed an heuristic approach that converges to a local minimum. In a nutshell, this heuristic approach consisted of finding an initial distribution of the radial bases with equal scales (variance in the case of Gaussians), and a gradient descent algorithm to search for a local minimum for the radial basis' centers (translation) and modulation of their coefficients. Consider the same cost functional and the approximation function:

$$H[f] = \Sigma_{n=1}^{N}(y_n - f(x_n))^2 + \lambda\|Pf\|^2 \qquad \text{(eq. 3.7.)}$$

$$f^*(x) = \Sigma_{i=1}^{N} c_i.\phi_i(x, t_i) \qquad \text{(eq. 3.8.)}$$

From variational calculus:

$$\partial H[f^*]/\partial c_i = 0 \qquad \text{(eq. 3.9.)}$$

$$\partial H[f^*]/\partial t_i = 0 \qquad \text{(eq. 3.10.)}$$

Leading to the update rate:

$$\partial H/\partial c_i = -2\,\Sigma_{n=1}^{N} \Delta_n h\left(\|x_n - t_i\|^2\right) \qquad \text{(eq. 3.11.)}$$

$$\partial H/\partial t_i = 4.c_i.\,\Sigma_{n=1}^{N} \Delta_n h\left(\|x_n - t_i\|^2\right)(x_n - t_i) \qquad \text{(eq. 3.12.)}$$

with $\Delta_n = y_n - f^*(x_n)$

The same approach can be further extended to include a class of non-radial basis functions, that result from the multiplication of a radial basis function by a non-radial function, e.g. an exponential term.

3.3.3. Shannon's Radial Basis Function (SRBF)

Although the previous GRBF approach might have its moments and reduce the problem dimensionality, it depends on the initial search vector which leads the network to converge to a local minima. Sanner & Slotine developed an alternative elegant framework to design the network with fewer units than input data based on Shannon's Sampling Theory, which is referred here as Shannon's Radial Basis Function (SRBF) [Sanner, 1993][Sanner & Slotine, 1992]. An equally spaced lattice of basis functions achieves a compromise between fidelity of reproduction, smoothness and dimensionality reduction. In particular, they opted for a Gaussian radial basis function reasoning that it attains the lower bound of the uncertainty relation (space-frequency

localization). They showed how to choose the Gaussian network parameters to approximate bandlimited functions based on bounds on errors, i.e. variance of the Gaussian basis, the mesh size of the lattice, and the truncation error. The choice of Gaussian network parameters become:

- Variance of the Gaussian Radial Basis:

$$\sigma^2 = \pi.\beta^2 \qquad \text{(eq. 3.13.)}$$

where σ is the variance and β corresponds to an estimate of the upper bound bandwidth.

- Size of the lattice mesh

$$\Delta = \frac{1}{2.\theta.\beta} \qquad \text{(eq. 3.14.)}$$

where Δ is the spacing of the lattice, and θ is an oversampling coefficient larger than one.

- Truncation error

$$\rho = n.\Delta \qquad \text{(eq. 3.15.)}$$

where ρ is the truncation, and n a multiplier larger than one.

- Total number of hidden units in the hidden layer

$$N = \frac{s}{\Delta} + 2.n.\rho + 1 \qquad \text{(eq. 3.16.)}$$

where s is the upper bound on the quantity.

To avoid the parameter drift instability phenomenon of the neural network, Sanner & Slotine designed a deadzone in the error function that stops the iteration.

3.3.4. Hyper Radial Basis Function (HRBF)

The SRBF approach considered only modulation and translation of a "mother" shape. It did not consider any dilation operation. The Hyper Radial Basis Function is an attempt in this direction by creating a network with bases of different scales. It consists of different hyperspaces (levels), each with a different dilation of the same mother shape, as illustrated in FIG.3.9.

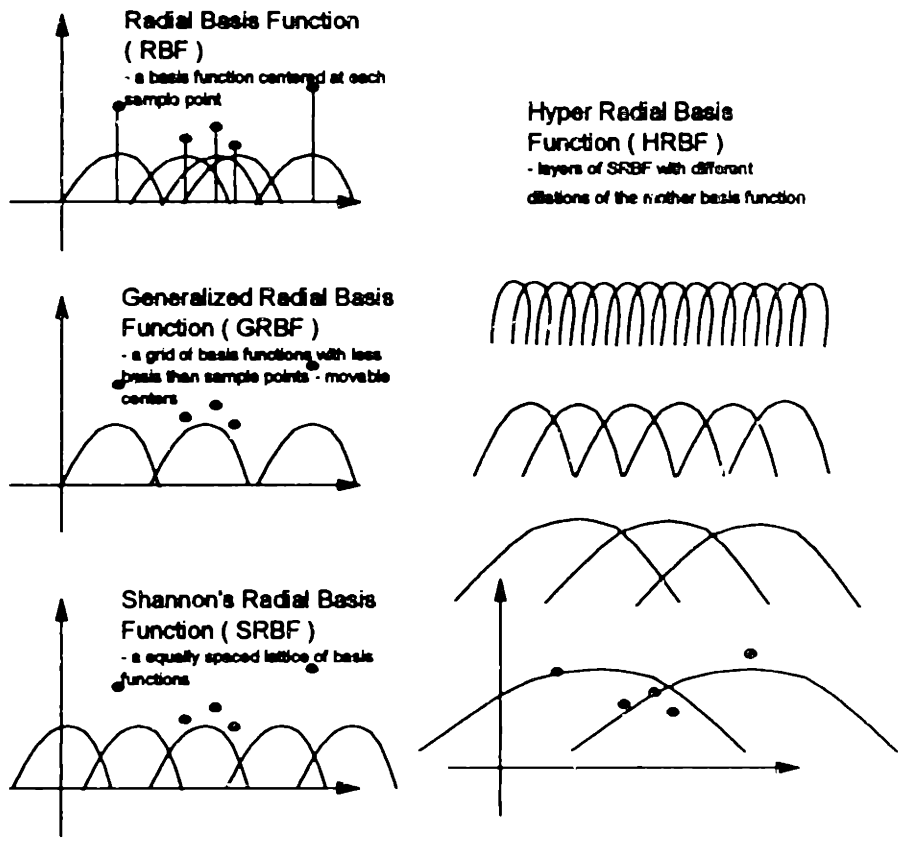

FIG.3.9. Sketches of Radial Basis Function, Generalized Radial Basis Function, Shannon's Basis Function, and Hyper Radial Basis Function

Poggio & Girosi indicated that it is rather difficult to derive rigorously this expansion form from Regularization Theory. Nonetheless, it looks rather tempting to establish an "heuristic" approach fashioned on multi-resolution techniques. In particular, using a multigrid algorithm that first tunes the spaces composed of bases with the larger scale (larger variance for the Gaussians), followed by tuning spaces with finer scales. In other words, the coarse grid is allowed to capture the coarse details of the function and then the finer mesh to capture the remaining finer details. The author is unaware of any particular established method to design an HRBF, and therefore uses an approach that is an adaptation of Sanner & Slotine's work with SRBF. First, a SRBF network is designed according to the previous section. The resulting network corresponds to the highest level of the HRBF, i.e. it corresponds to the finer mesh and last network to be tuned. In the next stage, the mesh size and basis scale (variance for the Gaussian) is doubled. This constitutes the

immediate lower level of the HRBF. The procedure of doubling the mesh size and basis scale continues until the lowest level has a single basis spanning over all the space. The hyperspaces are tuned in order: first the coarser mesh, followed by the next coarse mesh in-line. The tuning continues throughout the grid. Tuning is interrupted at each level by a corresponding deadzone designed in accordance to SRBF deadzone. Fidelity of data is verified at the end of each level's tuning phase, and the process is interrupted if the error bound has been achieved. There is no guarantee of reducing the dimensionality beyond the SRBF. Nonetheless, this might be achieved for classes of well behaved functions by eliminating from the approximation any bases corresponding to null weights. The algorithm is illustrated in Fig.3.10. This approach resembles a Pyramidal Laplacian filter [Simoncelli & Adelson, 1990]. A variation of this implementation using the same SRBF network structure at every hyperspace compresses the data, instead of changing the lattice grid of the radial basis function. The choice of the parameter for the relationship between consecutive levels of the HRBF was not totally arbitrary, but molded on wavelets as mentioned in the "apéritif" at the end of this chapter.

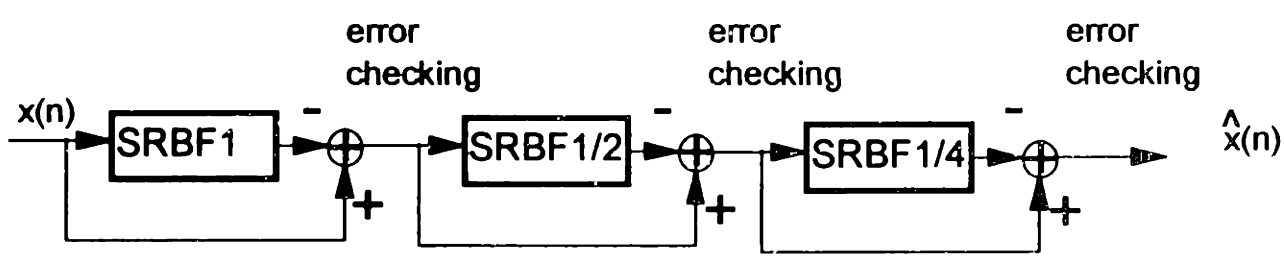

Fig.3.10. Hyper Radial Basis Function (HRBF) Multigrid Approximation
The figure illustrates the HRBF approach with a set of SRBF.
The last network scale was designed in accordance with Sanner & Slotine's SRBF. There is a relationship of 2 between the grid lattice spacing and scale for consecutives networks.

3.3.5. Irregular Sampling Radial Basis Function (ISRBF)

Before proceeding, a review of progress is in order. RBF locates a basis function for each sampling point, guaranteeing data reproduction and smoothness. GRBF attempts to reduce the dimension of the proolem by adopting an initial basis distribution and allowing the basis center and weights to float to the nearby local minimum. SRBF distributes the same basis over an equally spaced lattice. The grid spacing is determined via Shannon's Sampling Theorem guaranteeing data reproduction and smoothness, as well as some degree of dimensionality reduction. HRBF has a multigrid structure with each hyperspace described by an equally spaced grid and the same basis scale. The approach described here dilates by two the basis function scale and mesh size in consecutive levels of the multigrid. The HRBF might further reduce the dimensionality of the problem. Risking being pedantic, it is repeated that the working model for human arm movement assumes that movement is a composition of asynchronous episodic submovements constructed from the same "mother" shape velocity profile by dilation, modulation, and translation. This Section describes a "greedy" unsupervised algorithm named to maintain the tradition: Irregular Sampling Radial Basis Function (ISRBF).

3.3.5.1. Gaussian and Minimum-Jerk Compiler Engines

The unsupervised algorithm to design the scattered center radial Gaussian network uses a simple pyramidal decomposition scheme illustrated in Fig.3.11. At each pass, the maximum peak and adjacent symmetric region is fitted in a least-squares sense with a Gaussian (minimum-jerk) radial basis function. The symmetric region around the peak is determined by incrementally moving an equal step size Δx in both direction and bounding the relation between the function values at these $f(x+\Delta x)$ and $f(x-\Delta x)$ points. In this particular implementation, this relation was bounded to 5% differences. The fitted Gaussian (minimum-jerk) is subtracted from the data stream, and the remainder is iterated throughout the algorithm. The process ends when the remainder is within a pre-determined precision bound or the number of scattered centers reaches a pre-determined maximum center number (Cn). The Cn is determined for human arm movement based on the number of peaks of the movement curvature as discussed in the following subsection. There is a

minor operational difference between the two compiler engines. At each iteration of the minimum-jerk compiler engine, the peak value is first normalized to unity, and then fitted in the least-squares sense to a minimum-jerk profile. Furthermore, considering the particular application, any Gaussian with two standard deviations (2σ) smaller than 50 msec is eliminated from the approximation function, i.e. 95% of the gaussian duration lasts less than 100 msec. Likewise, any minimum-jerk with duration under 100 msec is eliminated.

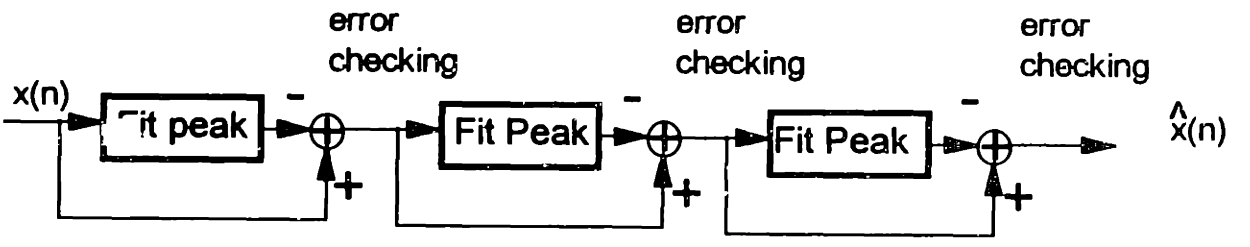

Fig.3.11. Irregular Sampling Radial Basis Function (ISRBF).
The figure illustrates the ISRBF approach. It resembles a pyramidal filter, in which a "mother" shape is fitted to the function's largest peak. If the remainder is above an error bound, and the number of bases does not surpass the upperbound limit obtained from the curvature analysis, the process is reiterated.

3.3.5.2. Upperbound on the Number of Bases

In the previous chapter, the movement curvature trait was discussed. It had been shown that there is a corresponding peak in curvature for each dip in speed. This trait is exploited to determine the maximum number of submovements or centers (Cn), as illustrated in the example at the end of this chapter (Figs.3.12. and 3.13.). This limit is imposed due to the nature of the problem, which is to decompose the human arm movement into segments or submovements. In a general approximation problem, the pyramidal decomposition method suffices in guaranteeing fidelity of

reproduction. Note that the curvature has a peak when the speed is close to null (see Fig.2.29.). Therefore a perfectly straight point-to-point movement (one submovement) has an infinite peak at the beginning and at the end of this movement (two peaks). To account for these edge peaks, the unsupervised algorithm does not count any peak occurring at the edges or outside the speed envelope (the curvature is kept null outside the speed envelope) , but adds one to the determined total number of peaks. The beginning and the end of a movement (speed envelope) is determined when the speed record surpasses 1% of the maximum speed peak or falls under this threshold. Moreover, to account for noise any peak under 5% of the maximum peak is not considered. Back to Fig.3.13., the left column shows an example of the curvature component of the unsupervised algorithm. Note that any peak under the 5% threshold is not counted, and in particular, due to the common speed dip (reversal) at the movement ending, some of the peaks occurring close to the edge are included and others not.

3.3.5.3. Gradient-Descent Refinement

The result of the movement decomposition by the pyramidal decoder with radial basis function suffices and it is used throughout the analysis in the subsequent chapters. A potential refinement of the technique stems from using the pyramidal decoder result as an initial search vector for a radial basis network with movable centers, i.e. translation and modulation of the bases, but no dilation. The gradient-descent algorithm obtained for the GRBF network shown in Section 3.3.2. was implemented. Yet, this approach did not show any substantial improvement in the decomposition (in the L2-sense, i.e. sum of the square of the error), and added computational time. Therefore, the ISRBF algorithm used for the analysis of Chapters 5, 6, and 7 did not incorporate this refinement.

This Subsection is concluded by showing the application of the ISRBF using Gaussian radial basis functions to the data shown in Fig.3.12. of a patient drawing a circle during the evaluation sessions in week 6, 7, 9, and 11. The patient was hemiplegic until week 5. The experimental setup and procedure was similar to the one previously described in Section 2.2.1., except that the patient had extensive experience with the robot from weekday therapy sessions lasting for an

hour. The patient's hand was connected to the robot via a hand-holder simulating a palmar grip of the robot end-effector. The patient was instructed to draw a smooth clockwise circle of approximately 8 inches of diameter with initial and final points at P2 (9 o'clock). The left column shows the circle traces and the right column shows the speed profiles. This is an extraordinary example, since it covers the whole spectrum of details encountered with patients involved in this trial. The circle traces suggests an initial kinematic planning indicated by the conspicuous displacement segments. The last plot of the circle trace (week 11) suggests the connectivity between the displacement segments. Similarly, the corresponding speed profiles on the right column covers a wide spectrum. Initially, there is minimal connectivity between segments, and the speed of the movement drops to a minimum. Note the shape of the almost isolated speed segments (symmetric and minimum-jerk bell-shape). These disconnected speed segments apparently evolved to conspicuous displacement segments with coalesced speed submovements. These successive observations of the patient's speed profile suggested that the movement was accomplished using a sequence of segments and, as training and recovery progressed, these segments appeared to become more overlapped or blended and began to resemble the profile of an unimpaired subject (see Figs. 2.9., 2.13., and 2.17.). Therefore it was postulated that the process of post-stroke motor recovery may be characterized and rigorously quantified by the pattern of timing and blending of these apparent segments. The results with the ISRBF algorithm implemented with Gaussians are illustrated in Fig.3.13. The left column corresponding to the curvature component was already discussed in the last Subsection, while the right column shows the speed profile decomposition (for detail see 3.13.a. to c.). The vertical spikes indicate the basis modulation coefficient, and they are located two standard deviation ahead of the basis center (Gaussian) indicating an estimate of the initialization of the submovement.

3.4. March of Progress - Chapter III

To decompose f(x) by modulating, translating, and dilating a "mother" shape required (a) the development of a methodology to decompose f(x) using these three operations concurrently, and (b) determine the "mother" shape. This Chapter presented the basis of the ISRBF decoding algorithm that achieves the desired decomposition (and presently is being further refined for

telerobotics applications), and the "mother" basis identified from a pool of twenty stroke patients' data. The data from these stroke patients was in the slow speed range of 0.1 m/s peak speed, and the identified "mother" basis proved to be remarkably close to the shape of normal subjects' arm movement in a point-to-point unconstrained task (typically in the range of 0.5 m/s peak speed), and to the identified shape in very fast involuntary movements caused by another neurological impairment (Section 5.5.2 -- 1.0 m/s peak speed).

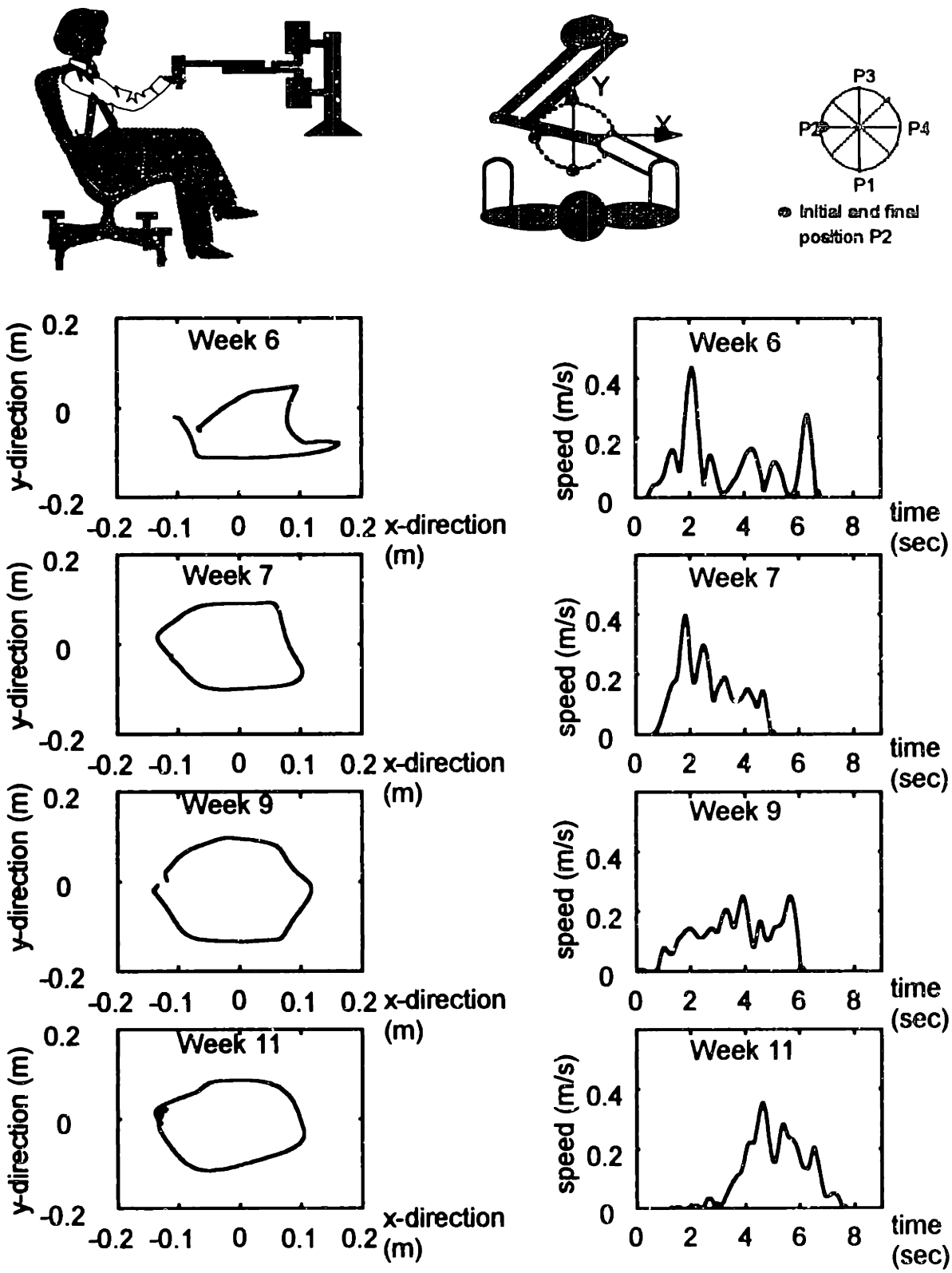

FIG.3.12. Patient (A) Drawing Clockwise Single Circles Starting and Ending at position P2 (9 o'clock) Patient is wearing a hand-holder that connects his/her palm to the robot end-effector and an elbow support to eliminate gravity. Patient was instructed to draw a smooth circle. The hand was within view, but no explicit feedback was provided.

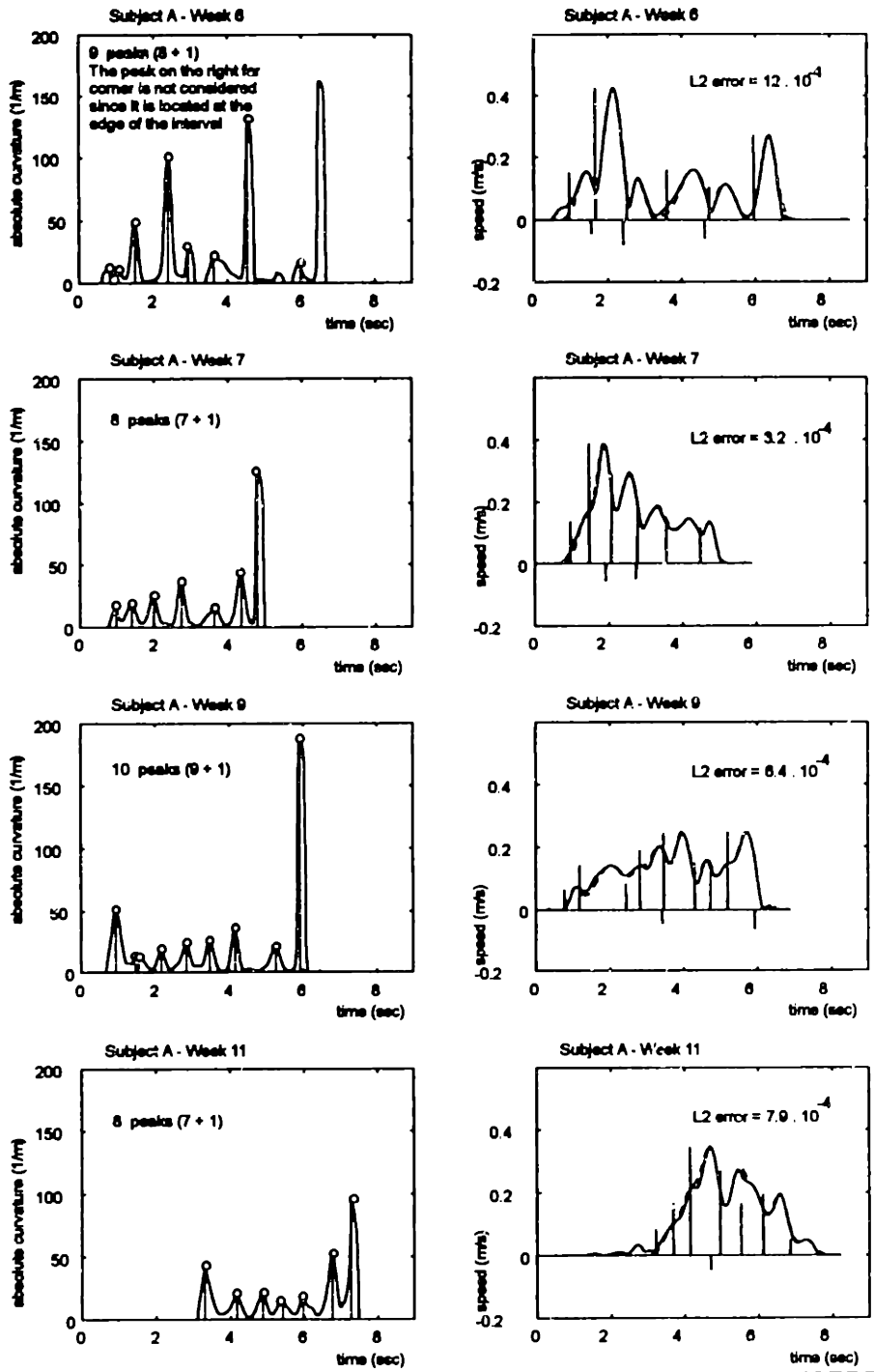

FIG.3.13. Application of the Irregular Sampling Radial Basis Function Algorithm (ISRBF) to the circles of Fig.3.12. In the first step (the left column), the maximum number of bases (Cn) is obtained from the peaks in curvature. Peaks at the edge of the interval and below 5 % of maximum peak are not considered, but an extra peak is added to Cn to account for the edges. Gaussians (min-jerk) are fitted to the symmetric regions around the peaks. The process stops if the error of the approximation is below a pre-determined threshold or the process uses Cn bases. The resulting approximation is shown in the right column. These distributions can be used as the starting point of a search for a local minimum using a gradient descent scheme.

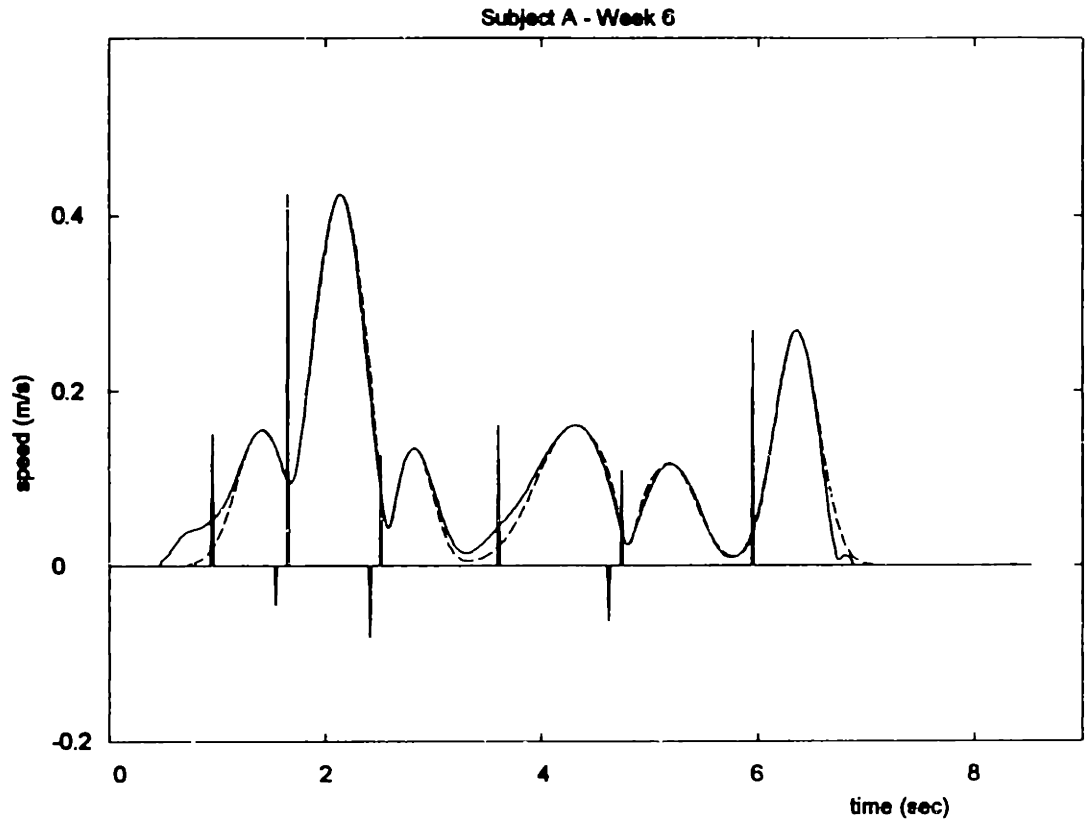

FIG.3.13.a. Detail of Approximation

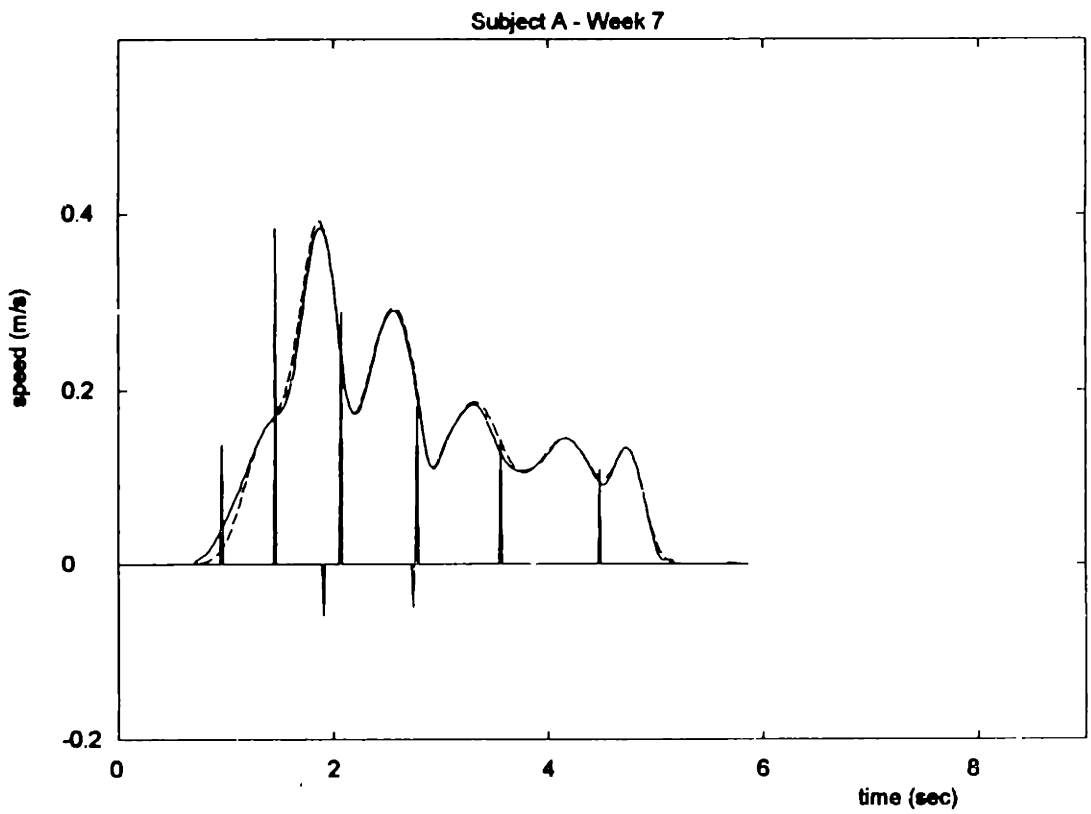

FIG.3.13.b. Detail of Approximation

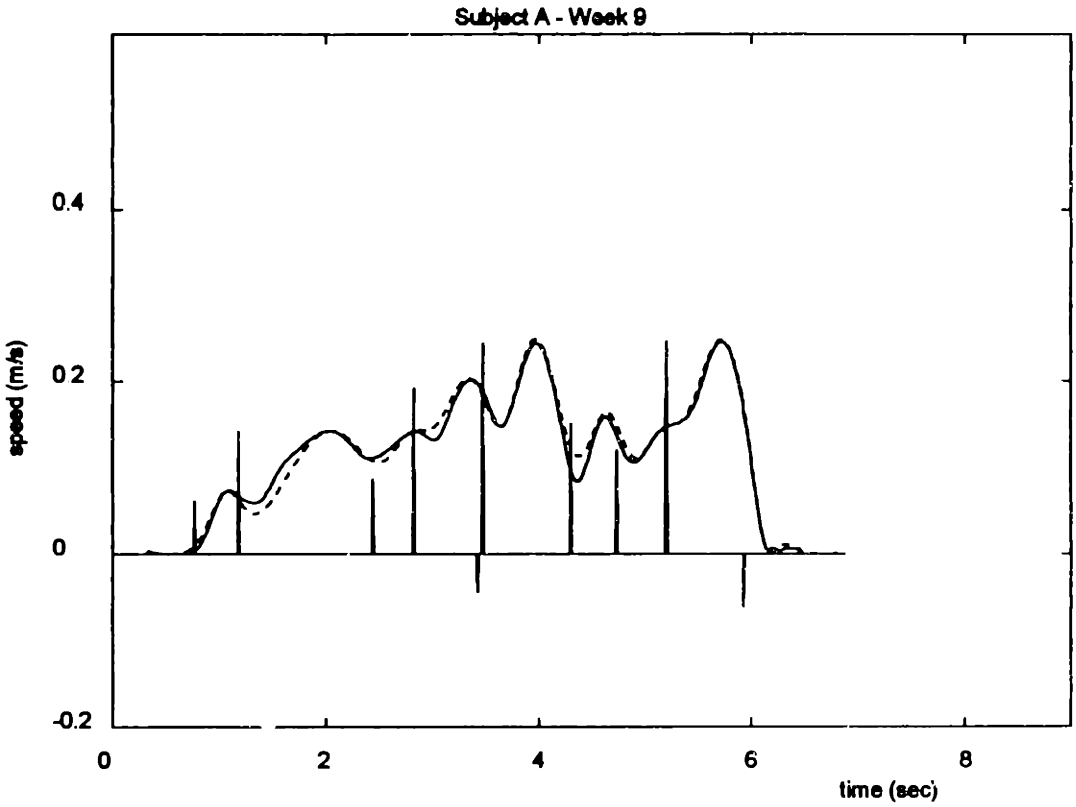

FIG.3.13.c. Detail of Approximation

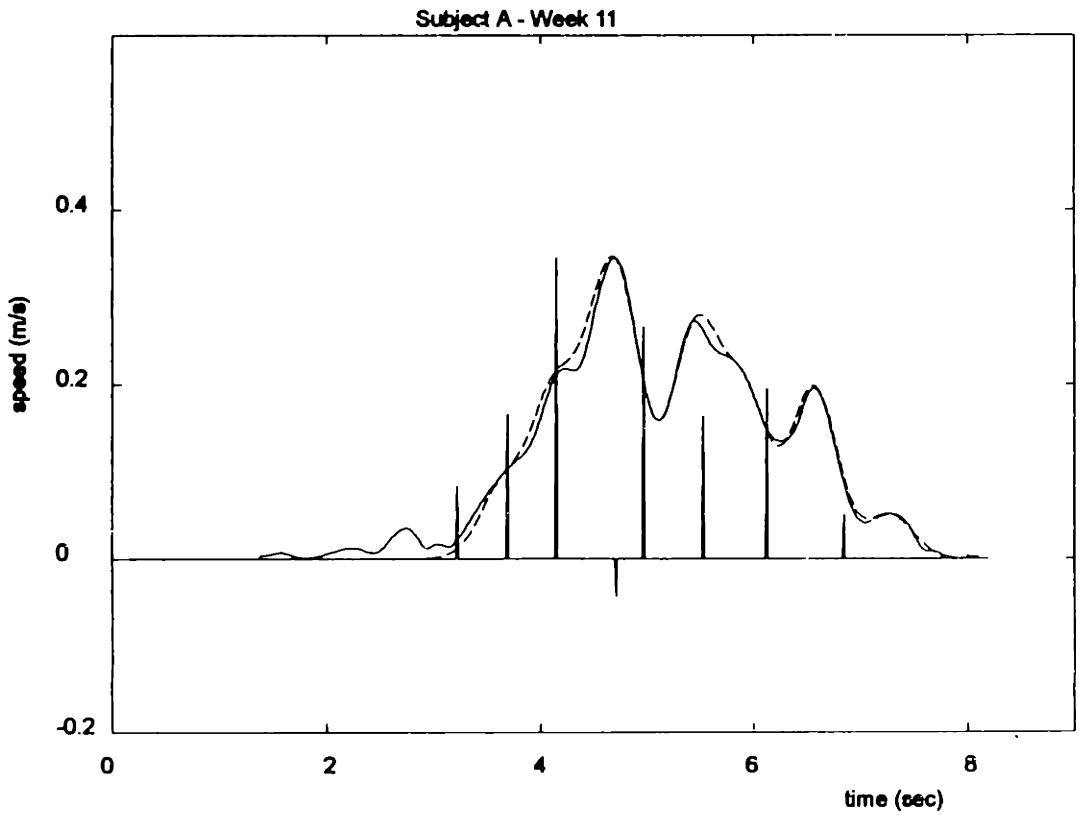

FIG.3.13.d. Detail of Approximation

Apéritif

1. <u>What is the best basis function ?</u>

In this Chapter, the "best" basis function was determined via experiments, i.e. data from recovering hemiplegic patients was used to identify and determine this basis function. Could the "best" basis function be identified from the mathematics ?

Consider the analog case of approximating a function f(x) by a polynomial and the Chebyshev Approximation Theorem [Davis], which states that for $f(x) \in C[a, b]$ with n a fixed integer. The problem of finding the minimax $| f(x) - (ao + a1\ x + ... + an\ x^n) |$ over the interval [a, b] has a solution that is unique. The solution is given by a Chebyshev polynomial Tn (f ; x) of degree $\leq$ n. The Chebyshev polynomial of the first kind is given explicitly by:

$$Tn(x) = \cos [n \arccos (x)] \quad \text{with } Tn(x) \in C[-1, 1] \qquad \text{(eq 3.17.)}$$

In other words, the above theorem states that the polynomial with the smallest degree that satisfies the minimax criterion is the Chebyshev polynomial. This theorem and the Chebyshev Equioscillation Theorem give a powerful tool. One of the best and most useful examples of application of this tool is in digital signal processing (DSP) in the design of optimal minimax finite impulse response filters (FIR) through Parks-McClellan Algorithm [Oppenheim]. Returning to the original motivation, consider the inverse problem of finding f(x) given a set of data (x, y). What is the best basis function Φ that approximates f(x) within an Lp norm and that minimizes the N number of bases ?

$$\{[f(x) - \Sigma_{i=1}^{N} c_i \bullet \Phi(\tfrac{(x-b_i)}{a_i})]^p\}^{\frac{1}{p}} < \varepsilon \qquad \text{(eq. 3.18.)}$$

2. Section 3.2. presented an estimate for the "best" basis function based on experimental data recorded during the initial stages of stroke recovery. In accordance with the working model, movement is composed of a superposition of segments or submovements, each with the "mother" shape ("best" basis function). Each submovement corresponds to a modulation, a translation, and

a dilation of the "mother" shape. Please review Fig.3.1.2. & 3.2.2. Note the remarkable invariance on the descent part the speed profiles falling to zero previous to the subsequent segment. It suggests that the subject may be unable to predict the movement and adopts a "waiting" strategy. The upside is an asymmetric with a longer tail. These speed profiles are a "mirror" image of normal subject's profiles. Typically in a point-to-point task, a normal subject's speed profile presents a degree of asymmetry of the descending side, suggesting corrections in the form of submovements. I speculate about the existence of an initial submovement on the ascending part of the profiles, perhaps due to some preceding trunk or arm submovement.

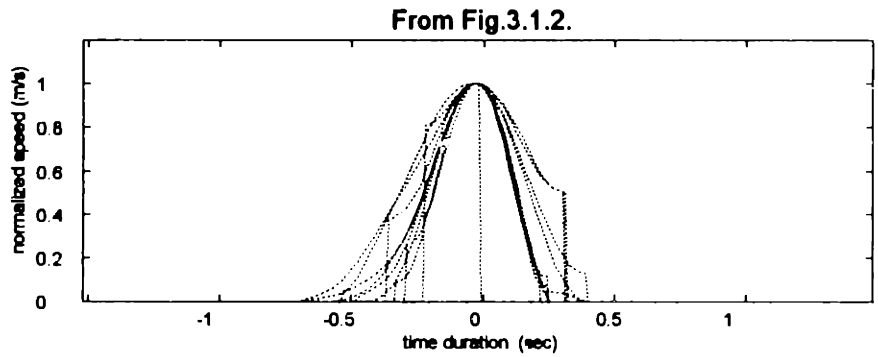

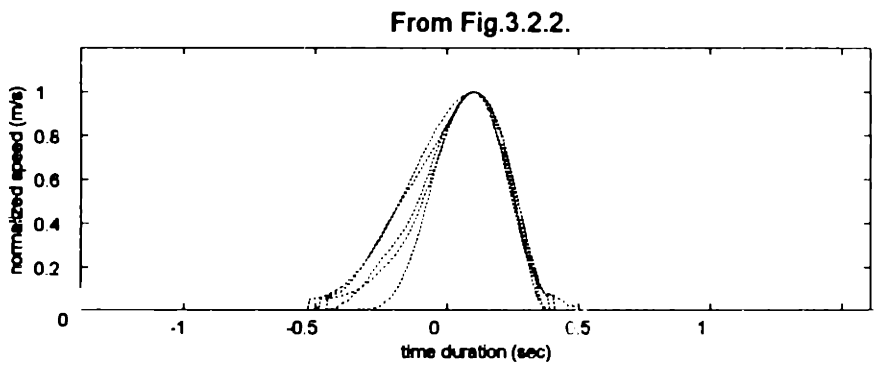

3. Minimum Jerk & "Mother" Shape:

A minimum-jerk curve appears to be quite a robust representation for arm movement. It was first suggested as a model for a point-to-point unconstrained movement in normal subject [Hogan, 1987] [Flash & Hogan, 1985]. It proved to be remarkably close to the "mother" shape identified from a pool of twenty stroke patients with different brain lesions. Professor Neville Hogan of MIT pointed out during an informal conversation that the minimum-jerk's robustness amazes him and

might eventually lead us to evolve from a phenomenologically concise mathematical representation to a deeper understanding of the motor system. Indeed, the first question stemming from the "mother" shape identified from the pool of stroke patients with different lesions, is regarding this primitive location in the system, i.e. is the pattern generator for the movement segment at the highest level of the central nervous system (CNS), or downstream ?

4. HRBF and Wavelets:

This chapter presented some of the techniques considered for extraction of arm movement segments. All of these techniques differ regarding choices for the basis function and approaches regarding modulation, translation, and dilation operations. The RBF style approach evolved from considering only modulation and translation of a single "mother" shape. Wavelets is an alternative approach that evolved from considering only dilation and translation of a single "mother" shape. In fact, there was a remarkable development of the field after Daubechies showed the link between wavelets and filter banks. In particular, an appropriate choice of the lowpass and highpass filters shown in the following figure leads to a recursive fast algorithm [Strang & Truong]. This approach recursively decomposes the function f(x) into a coarse approximation at a scale 2τ and a remainder containing the finer details at a scale τ. In this apéritif section, the author concludes by mentioning the path that he presently believes might be fruitful. The bell-shaped "mother" basis function identified in Section 3.2. should be identified with the scaling function, Φ, representing the coarse approximation, and not with the wavelet Ψ - French for small waves - containing the finer detail (Fig.3.14.). The later has to satisfy the vanishing moment(s) condition, while the associated scaling function must satisfy a weaker constraint.

$$\int_{-\infty}^{\infty} \Psi^n(t)\, dt = 0 \quad \text{valid at least for } n = 0 \qquad \text{(eq. 3.19.)}$$

$$\int_{-\infty}^{\infty} \Phi(t)\, dt = 1 \qquad \text{(eq. 3.20.)}$$

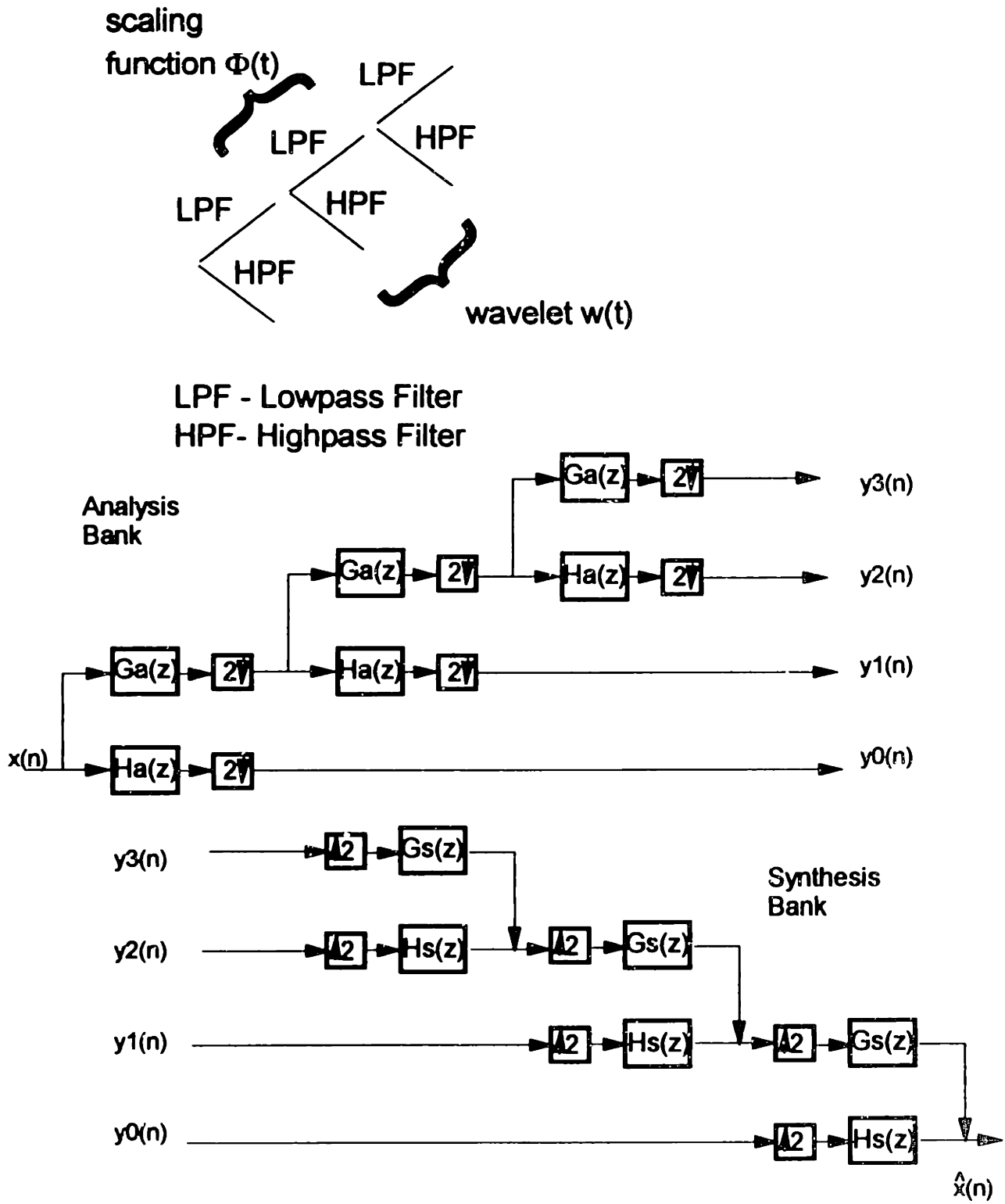

FIG.3.14. Filter Bank, Wavelet, and Scaling Function

CHAPTER 4. MIT-MANUS: A WORKSTATION FOR MANUAL THERAPY AND TRAINING

" I do not fear computers. I fear the lack of them."

— Isaac Asimov

This chapter provides an overview of the design and manufacture of the robotic workstation. It is a very concise summary of an enormous and focused effort. Several people at MIT were involved in one form or another in the design project. Jain Charnnarong's Master's thesis is a superb document summarizing the mechanical design efforts [Charnnarong, 1991]. The calibration procedures and the anti-aliasing filters were developed and manufactured in close collaboration with Christopher M. Minekime under the auspices of the UROP (Undergraduate Research Opportunities Program). For detailed information, C.M.Minekime's Bachelor's thesis is recommended [Minekime, 1994]. The video-games were developed in close collaboration with Amy Gorin under the auspices of UROP. Carol Cheung wrote some of the computer generated sound-tracks. The hand-holders were developed in close collaboration with Donna Louise Scott under the auspices of UROP. Carol Cheung and Eillen Liu also contributed during a summer. For detailed information, D.L.Scott's Bachelor's thesis is recommended [Scott, 1995].

The low-level functions of the software developed by my labmates Ernest Fasse and Anthony Hodgson for the fixed base manipulandums, and the A/D and D/A software from Professor William Durfee (analog-to-digital and digital-to-analog cards) were adapted to MIT-MANUS. Their efforts guided the development of the software for all the low-level functions, except for serial communication and digital-input-output. Documentation of the low-level functions, the experiment executives, and the video games are kept in the form of comments throughout the software.

4.1. Overview of Design Concept

The original goal of the project was to develop a robot-like machine that is competent to interact with humans. A robot that can interact with humans is novel, and to my knowledge the only robot with analogous characteristics in 1990 was our fixed-base manipulandum [Faye, 1986]. This precursor has limitations and could not be employed in our prime novel application: to serve as a robotic-aid to physical and occupational therapists. Presently, there exist very few applications of robotics that deliver physical or occupational therapy. Most such applications are limited to continuous passive motion or to no manipulation of the patient's limb, e.g. requiring the patient to hit a switch moved to different positions in space [Erlandson, 1990]. The project thus presents two novel characteristics: to interact with humans, and to deliver physical or occupational therapy. Deliberately the role of the robot was not defined precisely. Instead, the aim was to provide a stable machine that successfully interacts with unmodeled human(s), and to identify applications of the technology by working with the users, i.e. patients, therapists, and health-care providers. The broad technology philosophy was to develop haptic devices and combine them with audio-visual virtual environments. While audio-visual environments are advancing at a fast pace, innovative haptic devices are not. Therefore there are many opportunities to develop comparable haptic interfaces, which will complement audio-visual experiences, providing tactile, proprioceptive and kinesthetic sensori-motor experience.

Design spiral is a term often used in Naval Architecture and Marine Engineering to describe the process of design. Design is perceived as an interactive process. At every loop through the spiral, solutions are searched for and compromises are made between conflicting requirements. Economics dictates when this interactive process ends. Typically the starting point of the search loop is composed of the critical issues, where the designer perceives little space for compromise. The critical aspects for this project were within the user realm, i.e. the human-machine interface. This was not a capricious scientific obsession, but an emphatic engineering statement that the user represents the real performance index and theoretical illusions will be scrapped based on the human perception of the hardware. Therefore, the target working envelope for the robot was specified in terms of end-point properties. The following is a summary of my meeting minutes of

the design team between July and November of 1990, and my meeting minutes with my undergraduate collaborators. The opening paragraphs of this chapter referred to pieces of information that are superbly documented elsewhere. Only the key aspects of the design will be reported here, typically from the first loop of the design spiral. More detailed information will be added only when the cited sources do not provide a minimum account of the subject.

General Specifications for the Target Robot Envelope

(a) The robot must be backdriveable.

(b) The robot should be modular, allowing expansions and combinations of actuator packages.

(c) Actuators are to be of electromagnetic type.

(d) Controller platform will be digital - PC based. Previous experience showed that a digitally supervised analog loop is not necessary [Cary Abulhaj].

(e) All the sensors will be physically located in the drive package, i.e. position, velocity, and torque sensor. Previous experience regarding position sensor suggested that only absolute sensors should be considered. All the sensors should be off the shelf components and with the highest available resolution.

(f) Working surfaces should be kept free and uncluttered to allow maximum visibility and permit easy access to the users, i.e. patients and clinicians.

(g) The robot should be portable and its weight targeted to 70 pounds.

(h) The robot degrees of freedom will be limited in the present unit to the plane. Gravity compensation for a tridimensional unit requires large actuator packages and power supplies.

End-Point Specifications for the Target Robot Envelope

(i) Workspace area of 15" x 18".

(j) End-point static force of 10 lbf.

Motion control bandwidth of 1 Hz for a 6-inch amplitude motion was considered acceptable. (Consensus was that this would be easily achieved. It was not included within the target envelope, since this was not likely to be a limiting factor).

(k) End-point stiffness of 0 to 2 N/mm.

(l) From DC to 7 Hz the end-point impedance should behave primarily as viscous friction -- 7.11 Hz is the undamped natural frequency for a mass of 1 Kg with a stiffness of 2 N/mm with a 89 N.sec/m damping required for a critical damping ratio.

Significant anisotropy, especially in static friction, would cause the device to exhibit preferred directions of motion. Directional variation of any impedance parameter of 2:1 or less was deemed acceptable.

(m) End-point inertia and anisotropy should be within 2/3 Kg < I < 4/3 Kg.

(n) Static friction anisotropy should be within 56.7 grams < Fs < 113.4 grams.

4.2. Overview of Mechanical Design

The following configurations were discussed during the first loop through the design spiral: Cartesian, polar, double polar, gantry, spherical, marionette, motorized mouse, and SCARA. The chosen configuration was the SCARA (Selective Compliance Assembly Robot Arm). The other configurations were not considered satisfactory. A nutshell of the design team's experience summarized in the meeting minutes will be presented. Jain's thesis discusses in detail the pros-and-cons of most of these alternatives and documents with hard numbers the group's experience. The Cartesian configuration illustrated in the Fig.4.1. requires that for direct drive transmission, the first actuator carries the inertia of the second. A rough estimate suggested that the anisotropy would be around a 1:5 and typically linear sliding surfaces are hard to protect from dirt. Furthermore, the friction in bearings and actuators are reflected directly to the end-point. The polar and double configurations were ruled out due to the extra back-space requirement. The gantry configuration had similar problems as the Cartesian configuration. It also presented an additional disadvantage in terms of accessibility and visibility. The spherical configuration is tridimensional. Its main disadvantage was small payload near the workspace boundaries. The cable driven marionette and the motorized mouse could potentially interfere with objects on the working space.

Risking being redundant, some pieces of information regarding anthropometry and the adopted solution are described. Figure 4.2. shows the relevant distances for an average adult male sitting on a chair, the relevant pieces of information regarding the workspace, and the forces. It also summarizes information regarding hand sizes and movements.

Practice showed that these dimensions are reasonable for design purposes, but small difficulties were encountered with 10% of the patients involved during the clinical trials. Particularly, these dimensions do not seem to take into consideration what the author calls the "belly-effect", which is quite important in the graying population. The outreach seated dimension ignores the existence of a major protuberance (i.e. belly), that increases the sitting distance from the table top substantially. Though apparently anecdotal, it is an important limitation that seems to be pervasive in engineering designs. For example, patients with the "belly-effect" could not profit from important technological advances such as MRI, since they could not physically fit inside the scanners. While on one side one would feel the necessity to magnify some of the dimensions, on the other side a "small female" is oversized. Therefore the humanscale envelope should be slightly expanded in both directions to better fit most individuals. Fortunately in the robot-aided neuro-rehabilitation facility, these minor deficiencies were easily corrected via small "ad-hoc" adjustments in the carpentry.

Figure 4.3. shows an exploded view of the end result of the effort: the MIT-MANUS. It presently has two modules. The 2-dof consists of a direct-drive five bar-linkage SCARA mechanism, and it provides two translational degrees of freedom for elbow and forearm motion with a low intrinsic end-point impedance (i.e., be back-driveable), with a low and nearly-isotropic inertia and friction. It also permits a small range of passive vertical motion through a set of springs. The 2-dof final product is lightweight (88 lbs vs intended target of 70 lbs), with 16-bit high-resolution resolvers for position and velocity measurements. Redundant velocity sensing is provided by DC-tachometers with a range of 14 mV output at 0.008 rad/sec. Torque sensors with a range of 22.6 Nm are mounted on the brushless motor output shafts. The brushless motors are rated to 7.86 Nm of continuous stall torque. The mechanism is mounted on a tubular base that allows its vertical position to be adjusted. Note that a decision was made for an unusual

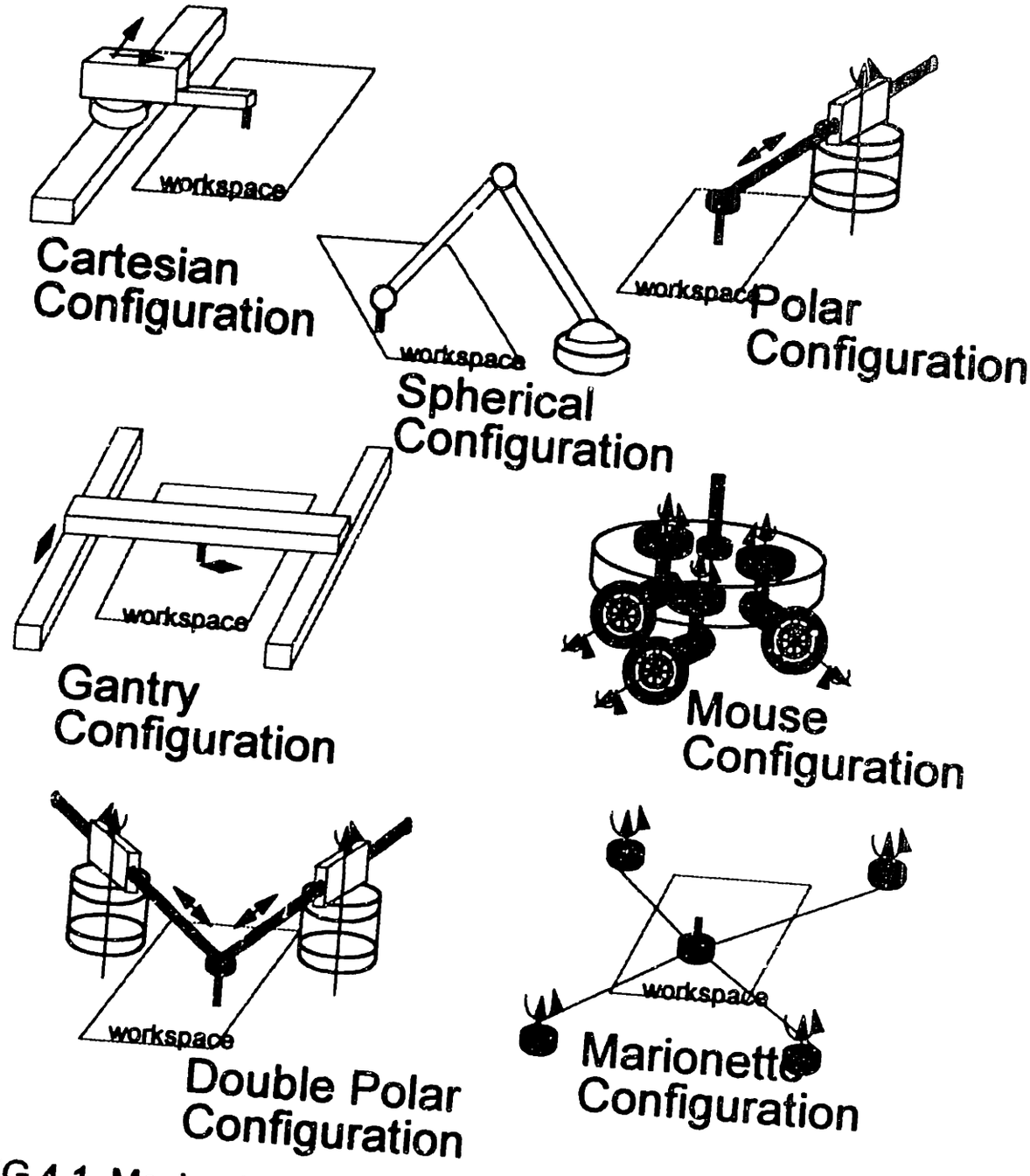

FIG.4.1. Mechanical Configurations.
Different configurations were examined during the design phase.
The configurations above failed to satisfy the design criteria.

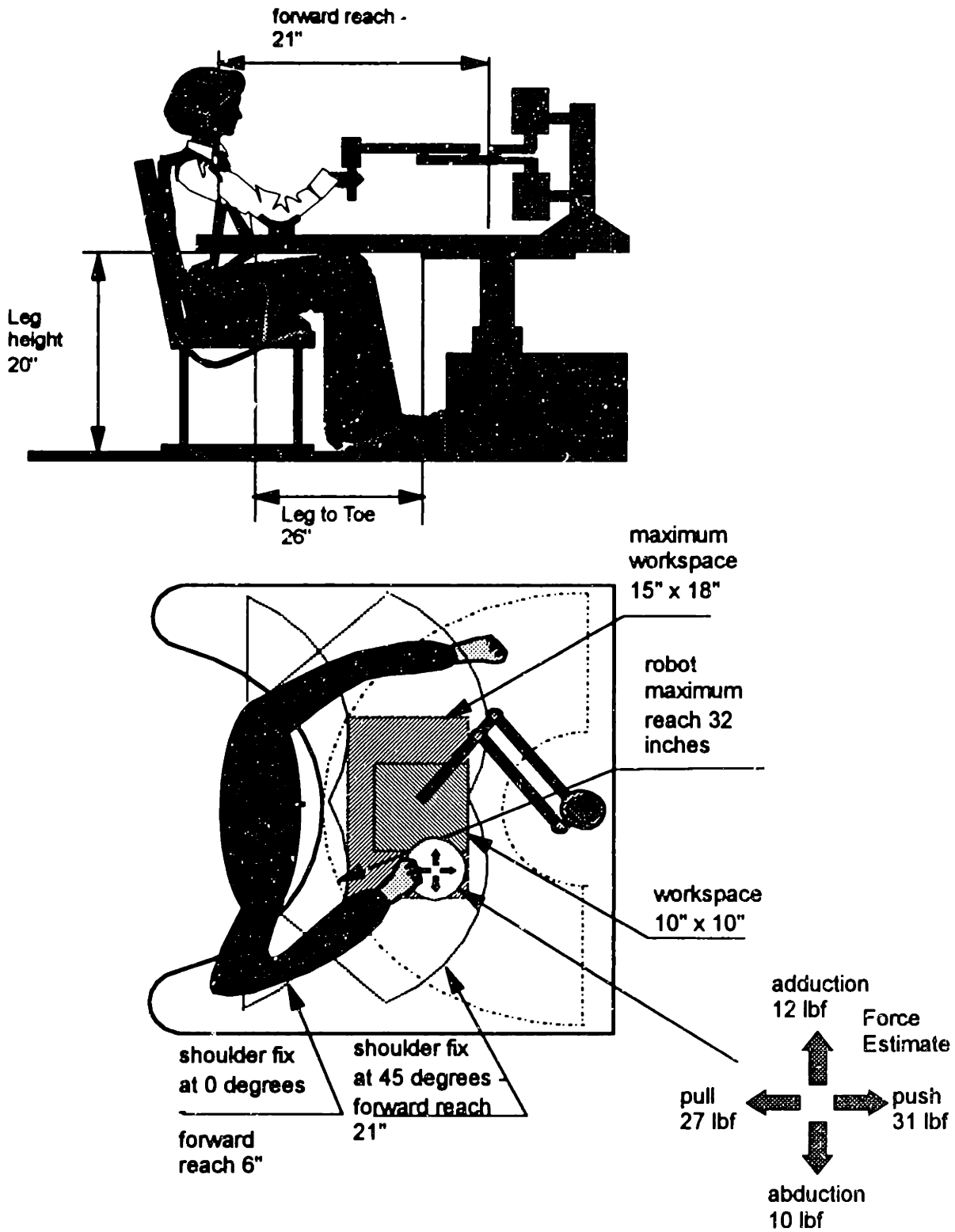

FIG.4.2.Estimated Dimensions and Forces During Design. The figure shows the anthropometric dimension and force estimates used during design and the resulting robot envelope

placement of the actuators' package. In a typical SCARA configuration, the actuator packages are placed in joint B which allows in a proper design to decouple the movement of the shoulder and elbow considering a fixed and known payload. Instead, the primary concern was to minimize the end-point friction. The reader is reminded that in a rotary configuration, the actuators and bearings' static friction is reflected at the end-point inversely proportional to the arm link length and the viscous friction is inversely proportional to the square of the link length. Therefore MIT-MANUS has the actuators sited in the farthest joint.

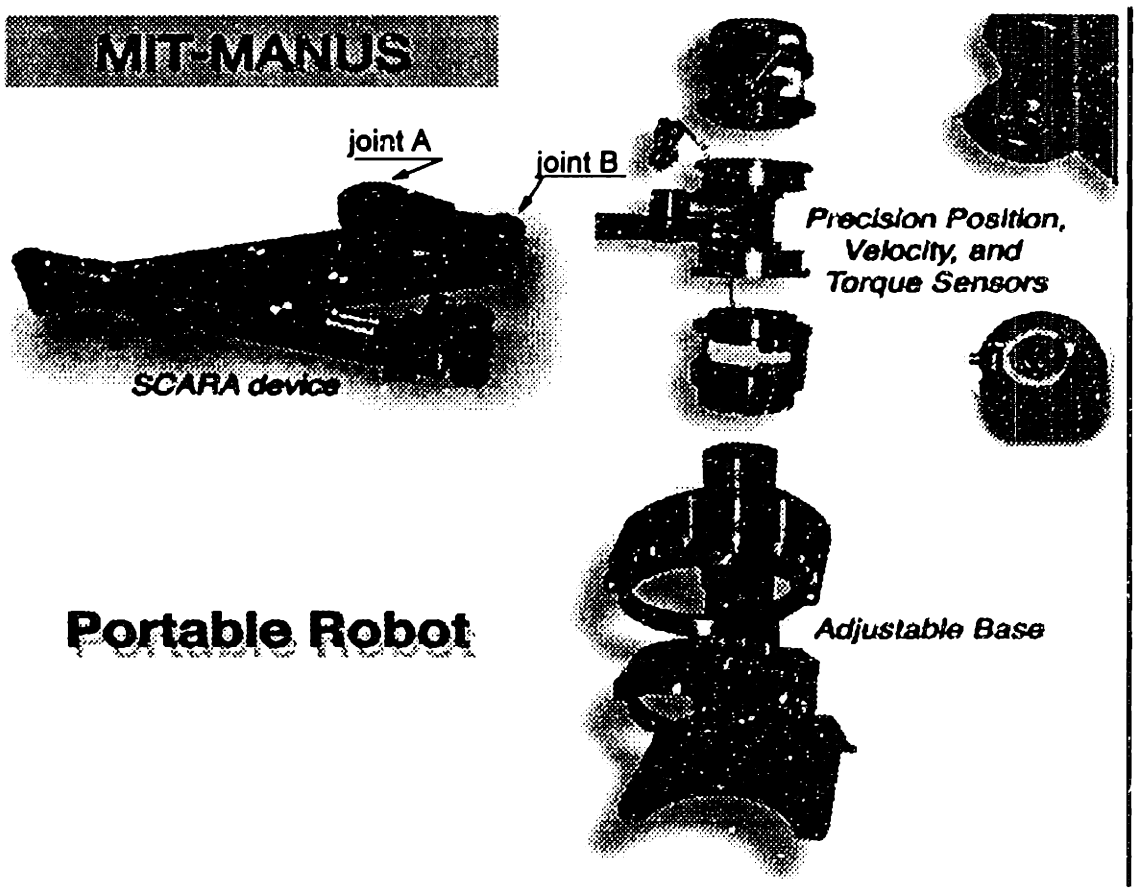

FIG.4.3. MIT-MANUS: Translational 2-dof package (degrees of freedom). Direct-drive SCARA mechanism was selected as the ideal robot configuration (Selective Compliance Assembly Robot Arm).

The 3-dof module provides three degrees of freedom for wrist motion and is shown in Fig.4.4. It consists of a differential mechanism mounted on a parallelogram linkage driven by three geared actuators. The geared actuators are rated to a peak torque of 0.108 Nm. Position sensing is provided by built-in precision potentiometers with 0.9 Kohm/rad. The actuator's package includes tachometers with a rated 0.07 volts/rad/sec sensitivity. The 3-dof hand-holder latches through a magnetic lock, allowing quick connection and disconnection. Since typically most of the patients in the acute rehabilitation hospital were discharged before any substantial movement was observed in the hand, the clinical trial was limited to shoulder and elbow movement not using this module. Although this module was put in operational condition and a suitable custom made hand holder was designed, I feel compelled to register my initial negative reaction while operating this module and therefore the unit might be redesigned. The primary deficiencies relate to two misconceptions incurred during the design phase. First, a typical therapy session lasts for a total of 30 minutes. Therefore it is critical to provide means to quickly harness the patient's hand. The present unit requires several minutes. The other misconception stems from the hypothetical task scenario of the patient inserting pegs in holes. An aim was to preserve the option of an operational "null" distance between the patient's hand and table top. Hemiparetic stroke patients requiring wrist exercises cannot move their fingers. Therefore the requirement to keep the space under the hand totally uncluttered is a fictitious constraint. In fact, I presently consider a dismissed version of the 3-dof wrist configuration to be ideal for stroke patients [Charnnarong, 1991]. The overall design is shown in Fig.4.5.

4.3. Carpentry Overview

As mentioned in the previous section, the robot is mounted on a column that allows vertical adjustments. For a user dedicated machine, this form of adjustment suffices. However, for a diverse population in consecutive therapeutical sessions lasting 30 minutes (60 minutes in the experimental procedure in this thesis), the time to adjust the vertical position of the SCARA mechanism makes this mode of adjustment prohibitive. The alternative was to mount the device on a table with a quick height adjustment. A table top was mounted on the hydraulic double cylinder frame of an old hospital bed, allowing up to 10" of vertical translation. The robot is a

portable device that can be fixed to any solid table. Neurologically impaired patients in general, and hemiplegic patients in particular, require elbow support to compensate for gravity during the acute and semi-acute phases of their disorder. Two different configurations were considered: (a) wheelchair mounted elbow rest, and (b) elbow skate on dedicated table top. Both configurations were considered satisfactory. The decision in favor of the latter for clinical trials stems from patients' comments during the pre-trial phase suggesting their familiarity with the idea of "working on a desk". The wheelchair bounded elbow rest does not preclude a table top extending close to the subject, but it does not require it. On the other hand, the construction of the variable height table made it advantageous to initially try the latter alternative. The table top is impregnated weekly with teflon dry lube and the skate sliding surface is made out of a teflon sheet. The approach was highly successful and presently no testimony can be made about the adequacy of the wheelchair bounded elbow rest configuration.

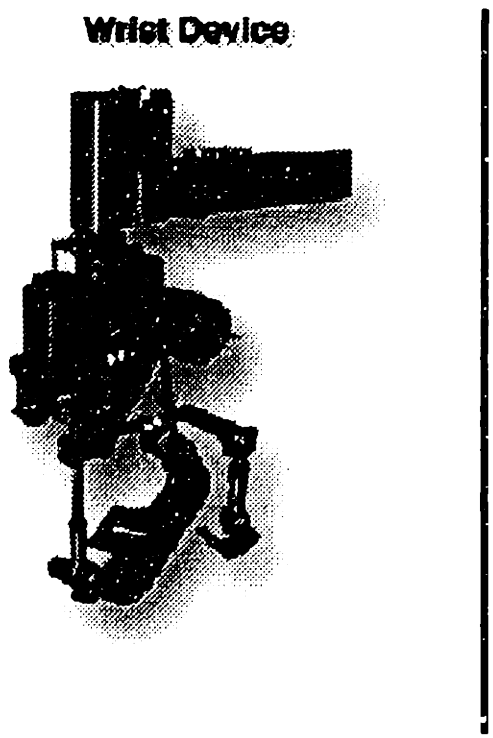

FIG.4.4. Wrist Device: 3-dof package(degrees of freedom).
It allows wrist rotation, flexion & extension, and abduction & adduction

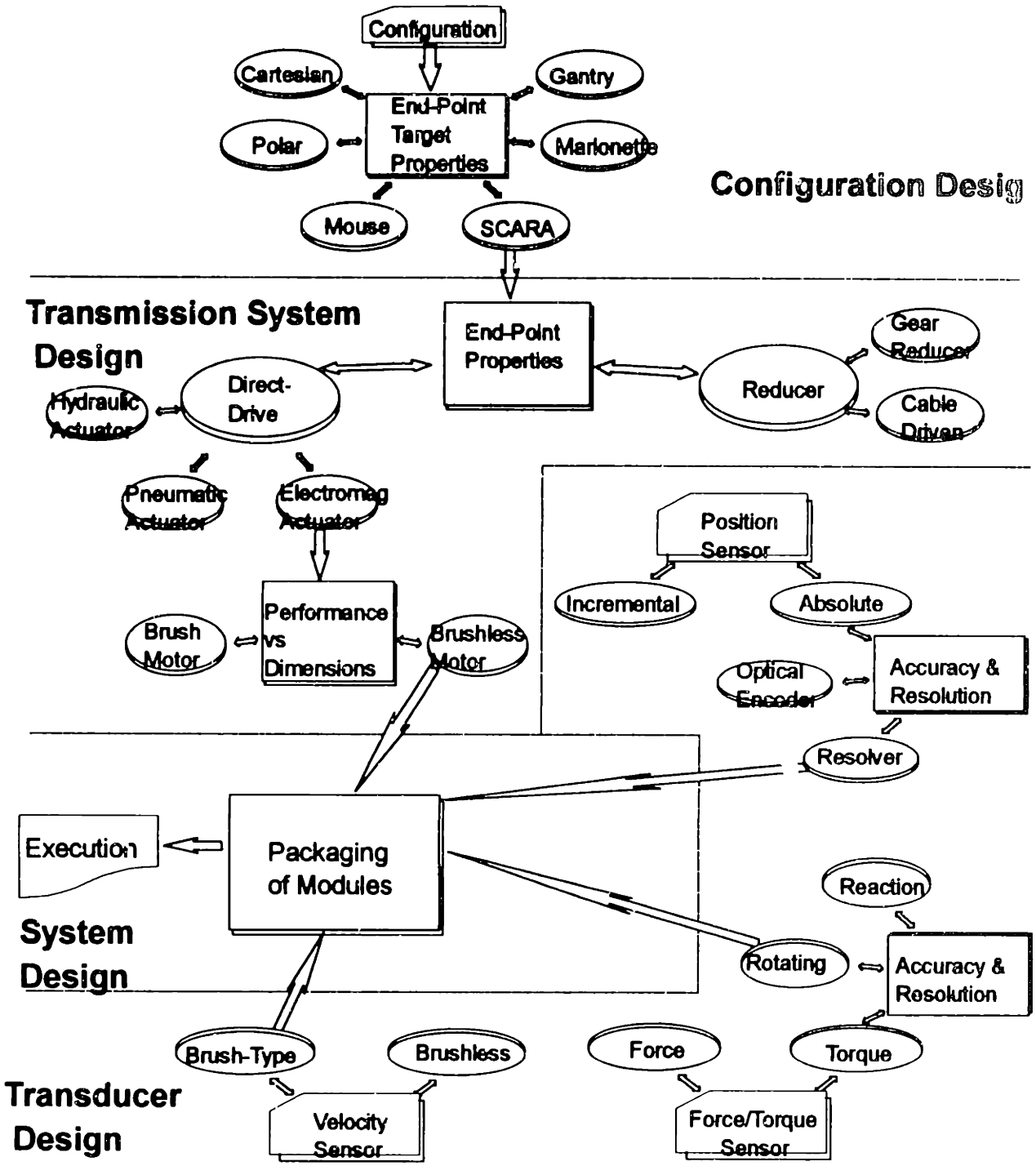

FIG. 4.5. Overview of Design Selections.
During the robot design, tradeoffs between different configurations, actuation, transmissions, and sensors were made and these choices were integrated and packaged together.

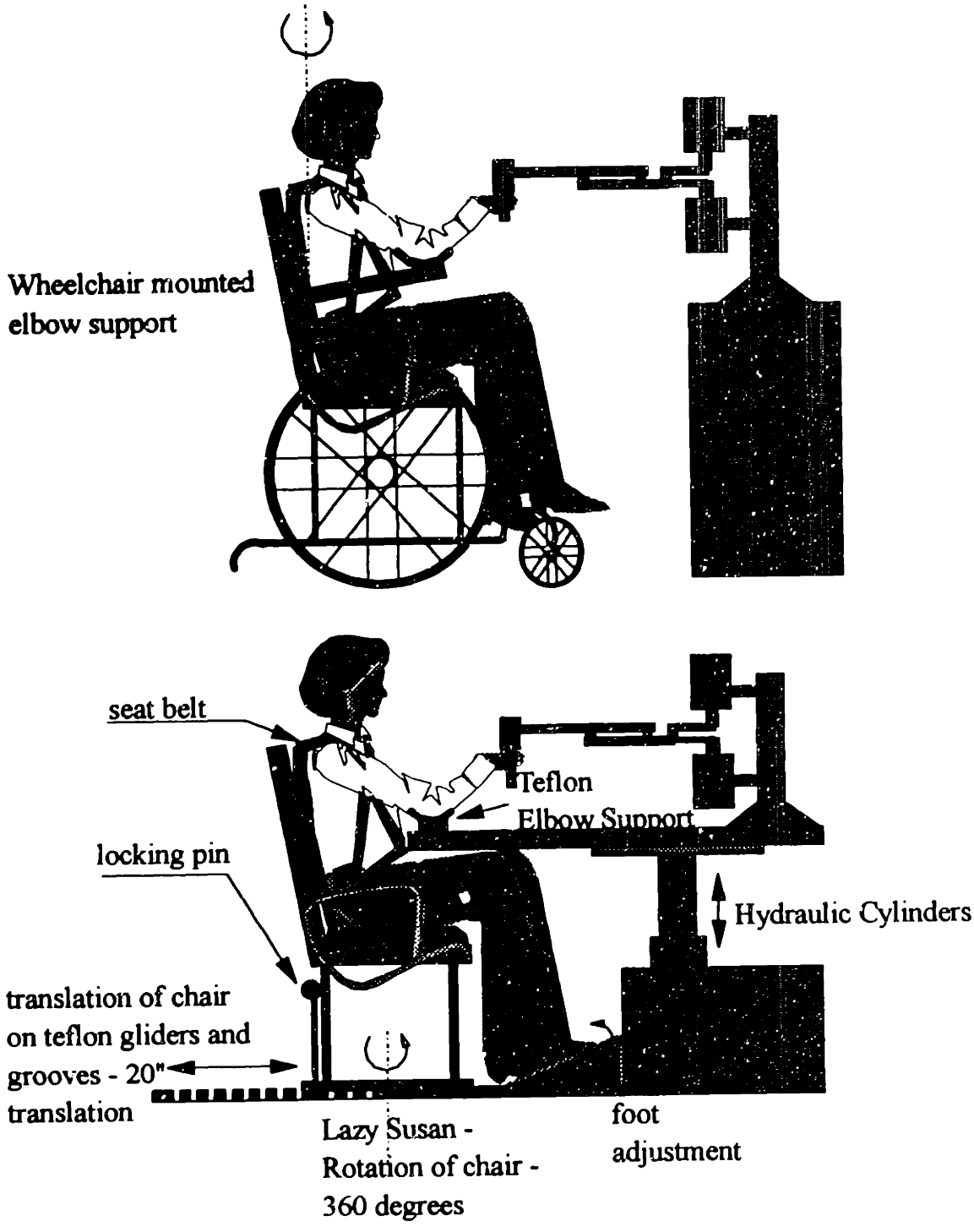

FIG.4.6. Carpentry Overview.
Most hemiparetic patients require gravity compensation.
Two different compensator configurations were considered:
wheelchair (upper sketch) or table-top (lower sketch).
Lower sketch also shows details of the carpentry.

Patients can perform the therapeutical session seated in their wheelchair. Typical quadriplegic patients use a motorized sturdy wheelchair with seat belts and brakes which can prevent the chair and the subject from moving. On the other hand, hemiplegic and paraplegic patients use a foldable wheelchair that adds an unrestrainable lateral degree of freedom. An alternative was provided in a rigid frame chair on a "Lazy-Susan" with a locking device and transfer the patients from their wheelchair, as sketched in Fig.4.6. The "Lazy-Susan" was mounted on teflon gliders, and it allows 360° rotation and 20" translation towards the table-top.

4.4. Overview of Electrical Design

So far, the different aspects regarding design envelope, end-point properties, configuration design, and component's specification have been described. Many of these details, including manufacturer's specification sheets, were documented in Charnnarong Master's thesis [Charnnarong, 1991]. These details correspond to the subsystem "robot" in Fig.4.7., which provides an overall picture for the 2-dof module. The 3-dof module has a similar architecture.

The subsystem "computer" acquires the measured quantities, calculates the appropriate control commands, and supplies the servo-amplifiers with the control command signals. The "computer" domain presently is composed of a dedicated ZEOS 486 CPU - 66 MHz for the robot control and a Dell 386 CPU - 33 MHz to display the video-games for the patients. The computer input-output (I/O) interface is accomplished by Analog-Devices' RTI-800 analog to digital (A/D) converter ISA card with 16 differential channels (32 single channels), Analog-Devices' RTI-802 digital to analog (D/A) converter ISA card with 8 channels and National Instruments' AT-DIO-32F digital input-output ISA card with 32 digital lines for the resolvers' signal.

The subsystem "chassis" powers the system and will be described in some detail. Figure 4.8. shows the basic electric circuit. The IEEE recommended practice for electric systems in health care facilities was followed [IEEE White Book, 1986]. The main requirement was to isolate the system from line ground. Previous experience with other applications that required isolated electrical system (e.g., ships and offshore oil platforms) suggested taking advantage of the

requirement for electrical isolation by adding a ground fault detector and protection. This was done by a ground fault interrupt (GFI) unit that detects a single ground fault and triggers interruption protection. It was also good practice to separate the power to the 2-dof translational module from the 3-dof module. Furthermore control and sensor signals were also segregated from the power cables. To avoid transients, time-delay relays were included so that the components are powered-up in an orderly fashion. Dynamic-braking was chosen to avoid abrupt stops of the end-effector interfacing with the human. Dynamic-braking implies that the dc-motors are normally in the "short-circuited" mode, and they can be enabled only by continuously energizing the solid-state relays of the safety circuitry.

Figure 4.9. presents the safety logic. Any failure of the power supplies, servo-amplifiers, R/D converters, limit switches actuation, or a computer crash, shuts down the system. It might be worthwhile to mention at this point that there is another safety layer in the software checking measured position, and velocity within the workspace.

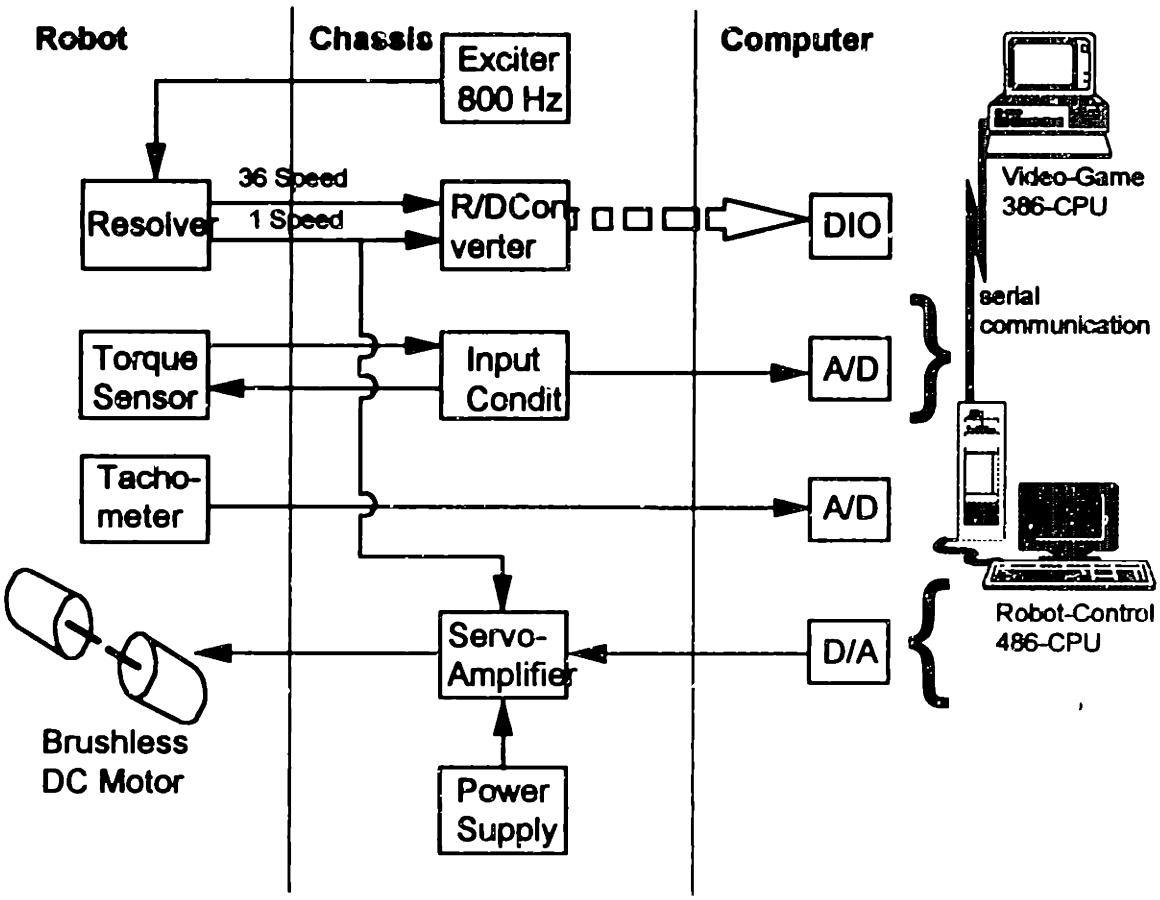

Fig.4.7. System Integration
The robot requires appropriate commands for the actuators. These servo-amplifiers commands receive instructions from the computer. The computer controller requires sensing position, velocity, and torques/forces.

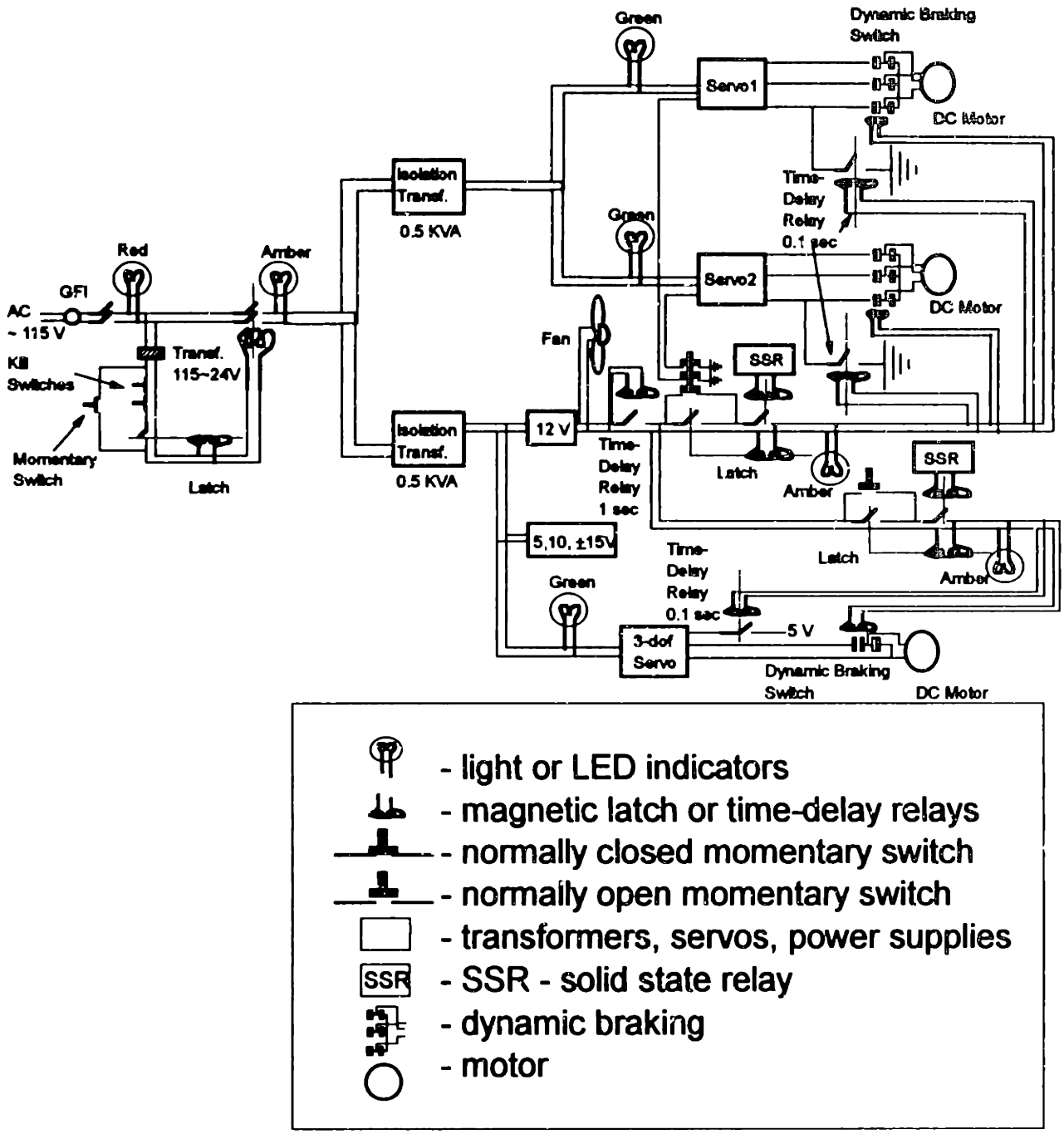

FIG.4.8. Power Circuit Logic.
Equipment intended for health care requires isolated circuitry (ANSI/IEEE Std 602-1986). A ground fault detector, and time-delay relays were included to avoid start-up transients. The system can be enabled only if safety checks are satisfactory (SSR).

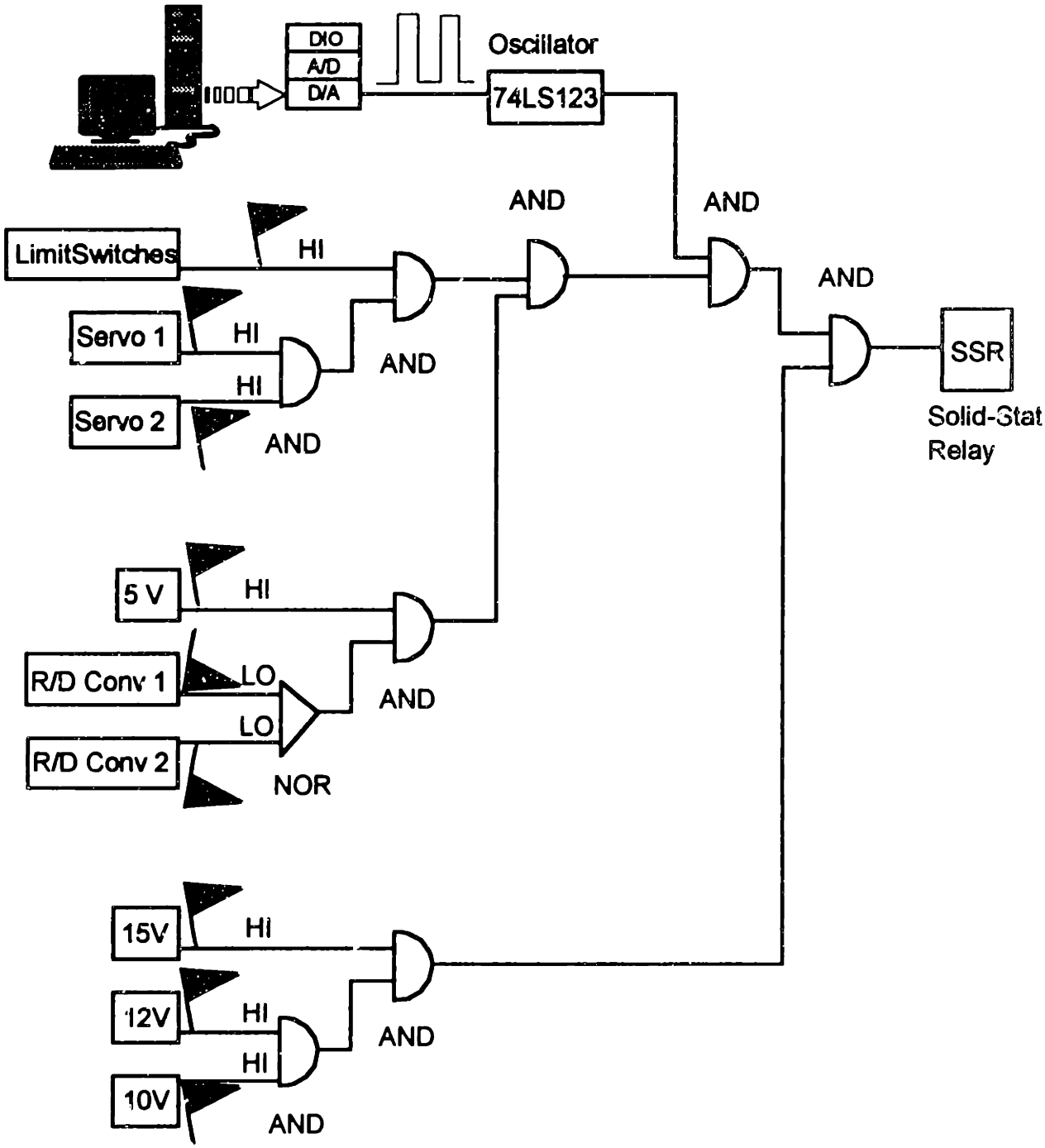

FIG.4.9. Safety Logic.
In the event of any failure of the computer, servo-amplifiers, R/D converters, power supplies, or triggering the limit switches, the SSR interrupts the enabling signal.

4.5. Overview of Software Design

The two main aspects to be considered were the operating system (OS) and the compiler language. The computer must be able to command the robot in real-time thus requiring a real-time OS. This ruled out OS/2 or Windows. In fact, there were very few alternatives for real-time OS, and the only two serious candidates were DOS and the real time version of UNIX. UNIX stands at the high end of the spectrum regarding user capability to manage the OS, and to run multiple processes. The capacity to manage directly the operating system can be critical in processes requiring high sampling rate, allowing no slack time between the duration of the computation, the OS operation, and the sampling events. Systems without direct managing access only allow optimization of the controller algorithm, but in UNIX the OS can be also tailored to the specific task. The main disadvantage in 1990 of real-time UNIX was the lack of support, expertise, and cost. On the other hand, DOS stands at the low end of the spectrum. It does not allow any managing or the ability to run multi-processes. In fact, the myth is that due to non-technical differences, Microsoft had to search for an alternative to CPM. They found QDOS, which stands for "Quick and Dirty Operating System". The "Q" was dropped due to phonetics. DOS' main advantages in 1990 were its vast support and expertise at no cost, therefore DOS was adopted.

Moore's Law states that computing power doubles every 18 months (Intel). This might suggest at least a comparable rate in software. However, previous experience with real-time systems suggested that the life span of software developed for these applications is at least a decade longer, and code documentation never suffices. The main concern was how to maintain and reuse generated code several years down the timeline. Procedural languages such as FORTRAN, PASCAL and C are accused of hiding the complexity under functions or subroutines. Once the code is operational, it should not be changed. The object-oriented language C++ was chosen, and whenever feasible, to reuse or adapt code developed by my labmates Anthony Hodgson (C++) and Ernest Fasse (C and Assembly) for the fixed base manipulandums, and Professor William Durfee (C) was either reused or adapted. Object-oriented language's strength proved to be also its weakness. The inheritance and overload operation that allows in C++ to reuse quickly and maintain software when the tracks are well marked, creates additional communication paths and

makes it rather difficult to reuse or maintain somebody else's code in the event of lack of documentation. Procedural languages in this respect were time consuming, but just required that the thread be continuously followed. This situation only changed after commercial packages such as Borland C++ 4.1. provided tools to allow clear visualization of these additional paths, such as illustrated in FIG.4.10. for one of the exercises.

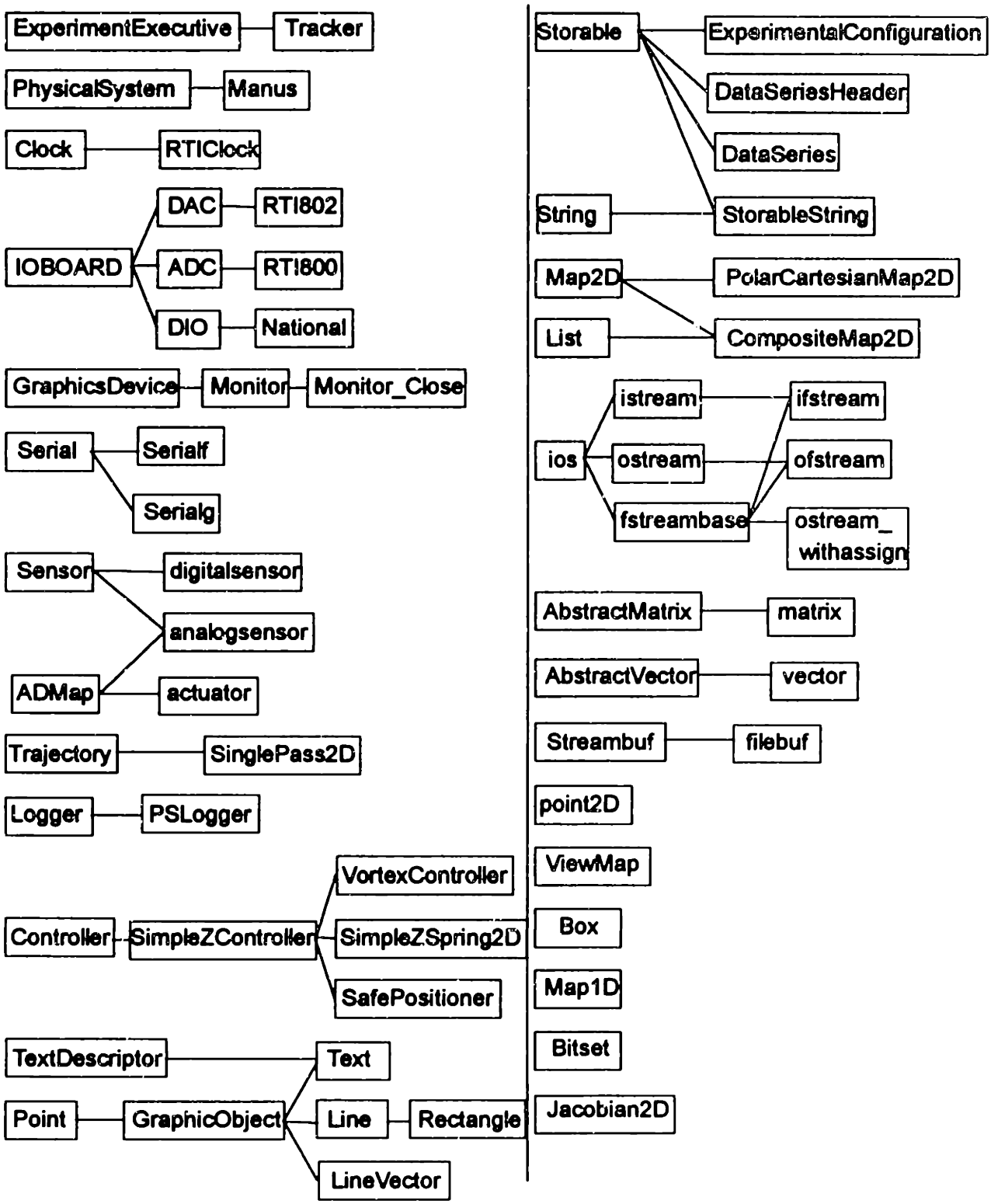

FIG.4.10. C++ Classes in a Video-Game Executable File.
Commercially available software packages presently allow the visualization of different classes & overloads in a particular executable file. Comments exist throughout the programs.

4.6. Overview of Hand-Holders

The two different designs of hand-holders, the Anti-Spastic and the Functional Splint, aim at different applications of the robot.

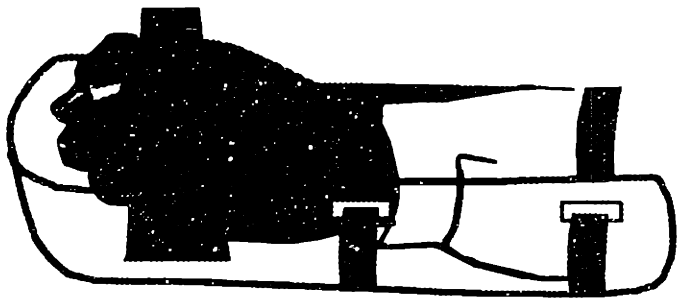

Anti-Spastic Splint

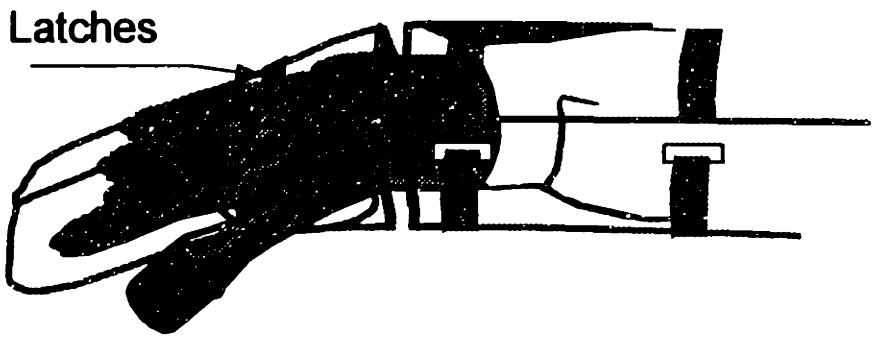

Functional Splint

FIG.4.11. Hand-Holder Design.
The anti-spastic splint is used in conjunction with a handle at the end of the 2-dof translation mechanism. The functional splint is used with the wrist device.

The Anti-Spastic Splint is used solely with the 2-dof mechanism, allowing exercises that involve the arm and forearm. Based on existing rehabilitation splint geometry intended for reducing spasticity in post-traumatic patients, this splint keeps the forearm supinated at 90°, as shown in Fig. 4.11. The fingers curl around a cone preventing the spastic posture of a tightly closed fist. The patient's arm rests on the splint harnessed with velcro bands at the wrist and forearm.

Contemplating applications involving patients with total paralysis and lacking any ability to grip, friction tape was placed in the splints at the forearm receptacle location, and therapy socks were prepared to keep the fingers curled around the splint's cone. Practice showed that the friction tape and velcro bands sufficed. The splint is connected to the 2-dof module via a threaded shaft. The shaft was machined with a flange matching the SCARA's end-effector. The splint's cone slides onto the shaft with a tapered off wooden cone that eliminates backlash, and the splint is secured with a nut type handle.

The Functional Splint is used in conjunction with the 3-dof mechanism, allowing exercises of the wrist in pronation-supination, in flexion-extension, and in adduction-abduction. In conjunction with the SCARA mechanism, it allows exercise in the specified five active degrees of freedom. The Functional Splint follows existing rehabilitation splint geometry used to immobilize the wrist and keep fingers laying flat open. The splint was manufactured in two stages. In the first stage a single piece splint and palm cover were molded, while in the second stage the single piece was cut around the wrist allowing wrist motion. The arm was held with velcro in the cuff part of the mold, and the hand was held enclosed between the hand and palmar cover through mechanical latches.

The prototypes were manufactured out of 1/8" thickness high-density polyethylene (HDPE). HDPE is suitable for this application due to its low melting point, high crystallization rate, rigidity, and impact compared to other plastics. Previous experience with this type of plastic demonstrated its suitability. The Anti-Spastic Splint was going to be extensively used during clinical trials, although manipulation of this splint raised questions about potential failures [Scott]. The base of the cone facing the wrist appeared to be prone to buckling or cracking. Although failure of the HDPE splints were considered unlikely due to the skate that harnessed the patient's elbow, the problem was addressed by: (a) visually inspecting the existing splints every other month, (b) manufacturing extra HDPE splints, and (c) manufacturing substitutes made out of carbon fiber. The choice of carbon fiber followed the similar rationale of the HDPE choice. Although in this case due to the opposite reasoning, it was chosen because the author had no previous experience with carbon-fiber.

The manufacturing procedure for the HDPE followed standard industry practices for thermo-forming plastics, with a male mold made out of air-cured commercial plaster. The molds have orifices for vacuuming the HDPE sheet during the draping operation. The sheet was framed and heated to 350° F for several minutes until it sagged. Draping while vacuuming followed. The manufacturing procedure with carbon fiber was substantially more extensive and elaborate. It required matched male and female plaster molds. These molds could not be recycled, therefore requiring a completely fresh start in the case of failure. Experiments were made with male-female molds of a cup in order to determine the adequate resin type and pressure. Results were very sensitive to the choices of resin type and to the applied pressure. The original expectation that the maximum pressure would be limited only by the structural properties of the plaster molds and that the higher the pressure the better final part, was incorrect. Bubbles dissolved the expectation (as well as that of the experts). Seven seas experience came to rescue in the form of a marine based epoxy resin, applied without any pressure, but gravity. The bulk of the forearm tray was manufactured out of a carbon fiber yarn braided at 45° with a 9" diameter mandrill. The cone and projections were manufactured out of carbon fiber yarn braided at 48° with a 3" diameter mandrill. The HDPE splints were manufactured at the facilities of Biotech Engineering - White Plains, NY and the carbon fiber splints were manufactured at the facilities of AC Products - Needham, MA.

Custom Made Hand-holder

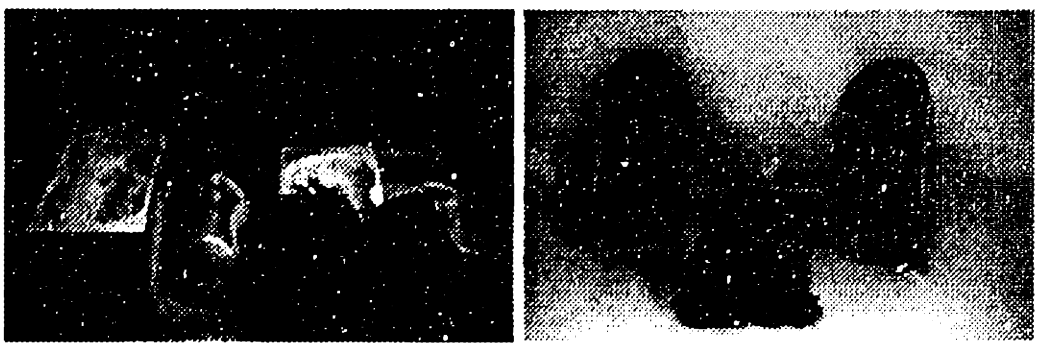

high density polyethylene or braided carbon-fiber

FIG.4.12. Hand-Holders Manufacture Process and Materials.

4.7. Overview of Video-Games

The robot-aided neuro-rehabilitation workstation involves more than proprioceptive feedback. The patients also receive visual and audio stimuli. This is achieved via two sets of video games. These games were intended to turn therapy into a fun activity. However, as any typical engineering design problem, the objective of challenging the patient cannot be carved separately from the whole. Neurologically impaired patients may have cognitive deficits therefore suggesting a simple implementation of the games. This approach of keeping it simple proved to be very wise. Practice had shown that some of the neurologically impaired patients had severe visual and/or cognitive deficits. For example, a representative share of the patients suffered from visual and proprioceptive neglect of "world" on one side of the midline centered at their body, creating a particular accident prone scenario. Though the computer monitor could be moved within the non-neglected field of view, it was recommended to keep it centered on the patient's midline as a potential additional therapeutical value. Patients were instructed to keep searching for the target which was present at all times. Another efficient approach was to force the cursor to travel from the non-neglected to the neglected field of view. Likewise, some of the patients suffered from severe cognitive deficits precluding them from initially understanding the coordinate transformation required from targets on the vertical monitor screen to the robot movement on the horizontal plane. Visually and auditory sophisticated games would hinder, not facilitate, therapy with these patients. Nonetheless these few examples show the streak of opportunities of robot-aided therapy and computer games with sensory and cognitive impaired patients. On the other hand, patients with pure motor deficit seemed to be sufficiently challenged by the task itself (i.e. movement) and did not seem to care for "arcade" quality video-games. The first set was extensively used during clinical trials at the Burke Rehabilitation Hospital. The set was conceived to exercise, evaluate, and document upper-limb movement involving the shoulder and elbow within the pre-determined workspace region. Some games required predominantly shoulder motion, while others required predominantly elbow motion. Other games required the coordination of both shoulder and elbow. All the games within this set were composed out of a subset of movements from a basic configuration shown in Fig. 4.13. This aspect is essential to generate meaningful statistics of patients' movement during the clinical trial experiments. It

allowed movements to be decomposed and re-combined according to their spatial orientation and temporal nature (i.e. timed versus open-ended games). Figure 4.14. illustrates the five variants of games used within the set.

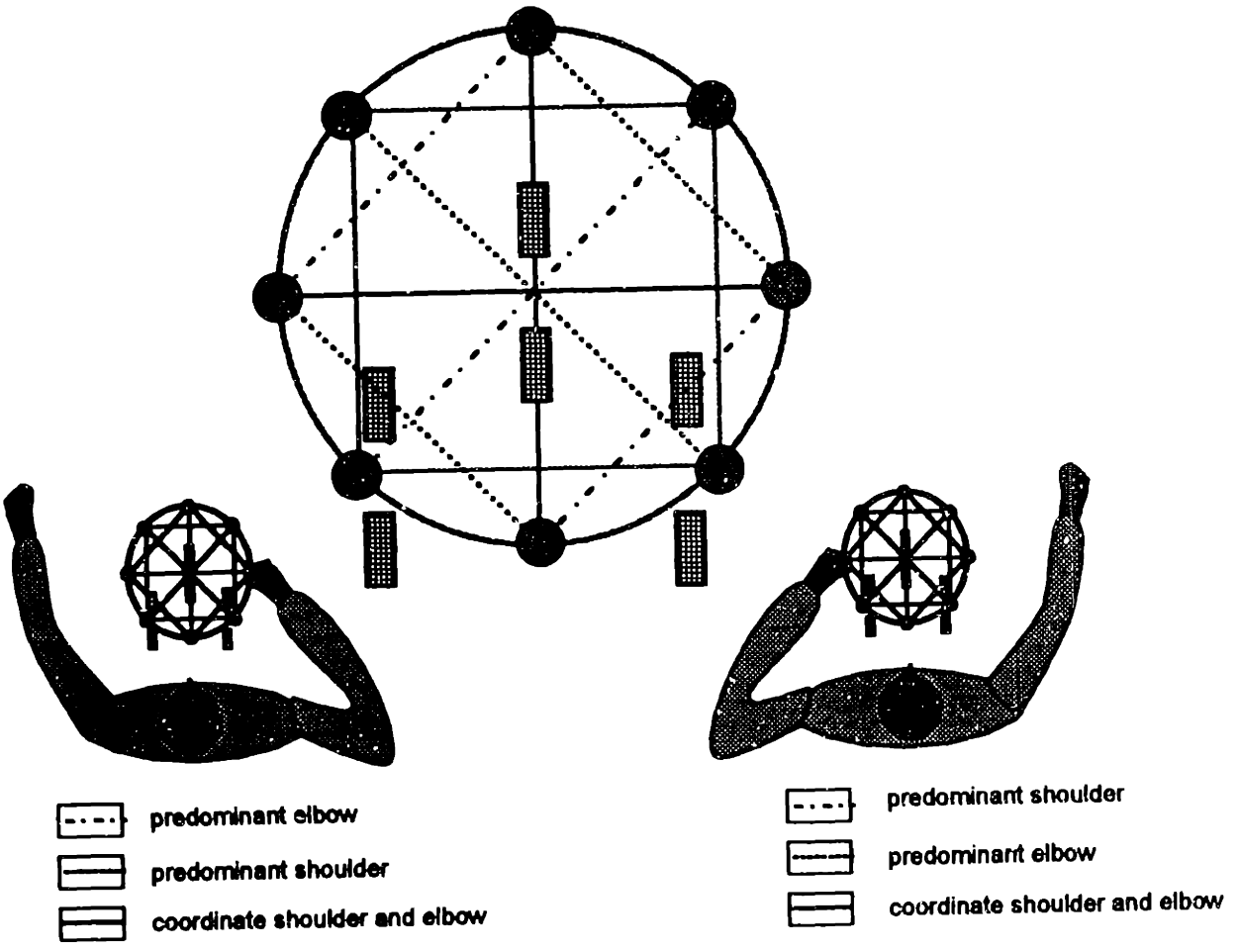

FIG.4.13. Basic Set for Elbow & Shoulder Exercise. All the games are a subset of the basic set, requiring movement of the elbow, shoulder, or both in extension and flexion.

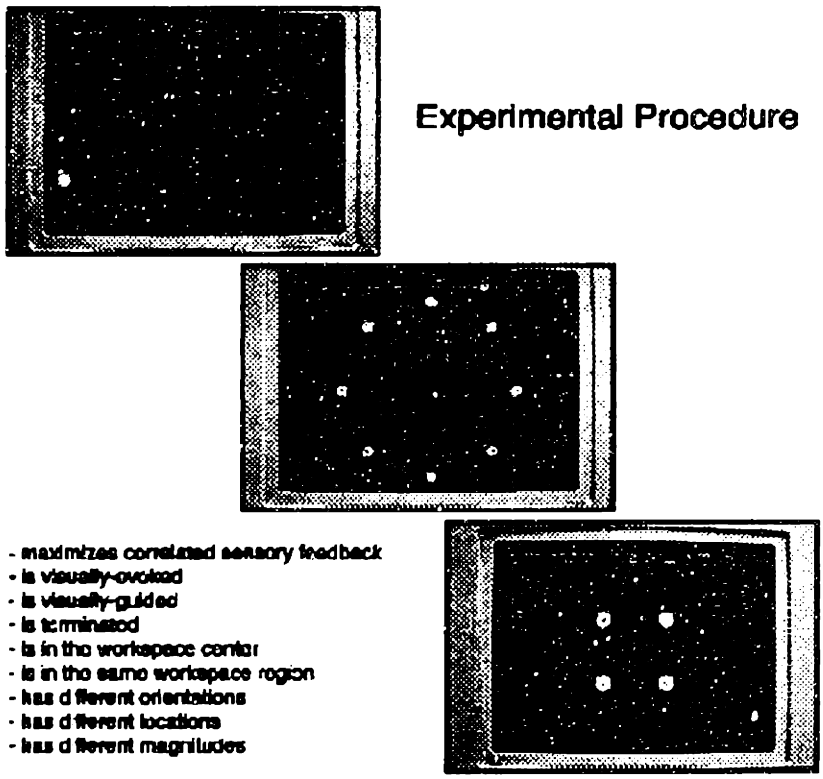

FIG.4.14. Video-Games.
The experimental procedure was presented in a form of video-games. All the games are a subset of the same basic set.

The second set was conceived to exercise, evaluate, and document upper-limb movement involving all five degrees of freedom of the design (2-dof from the SCARA mechanism plus 3-dof from the wrist mechanism). Similar to an insertion problem, it mirrors the concept of macro-micro manipulator for the human, requiring a point-to-point movement of the arm and forearm, and wrist movement. Fig.4.15. illustrates the game.

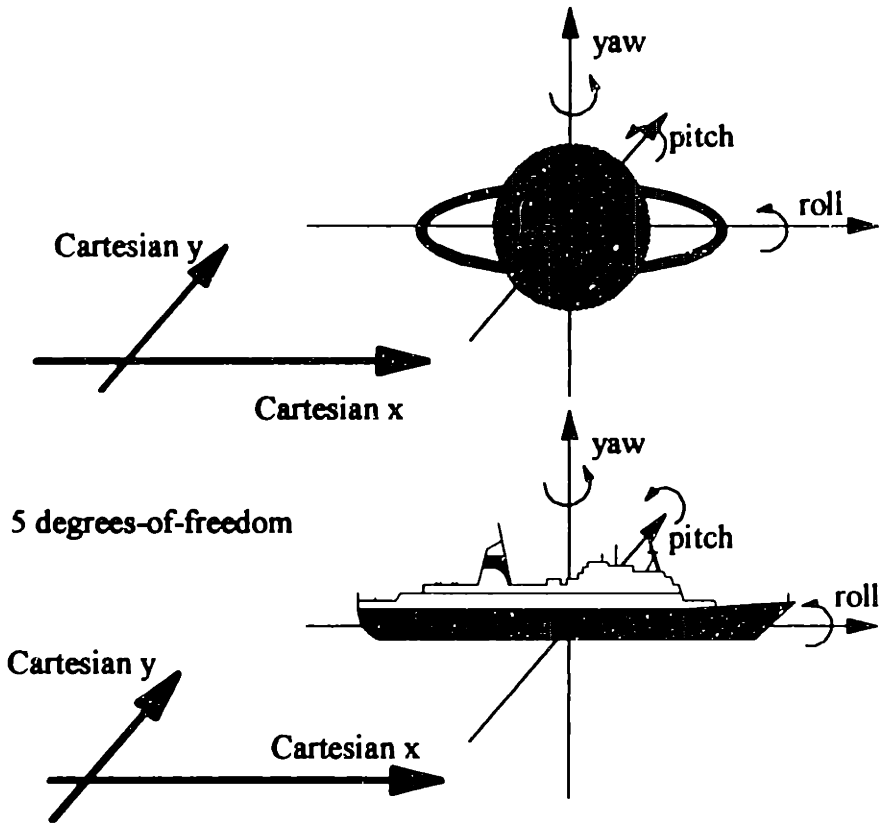

FIG.4.15. Video-Games for Elbow, Shoulder and Wrist.
The exercise for wrist is similar to peg-insertion. It requires translation of the 2-dof mechanism to approach the hole, and adjustments of the wrist attitude to insert the peg in the hole (spaceship into the docking area).

These games were intended as an operational prototype for the clinical trials and as an illustration of the concept. The software architecture was kept modular, segregating the games and the robot control program in two separate computers. Furthermore, since commercially available video-games' input devices are typically interfaced via a RS-232 (e.g. keyboard, mouse, and a few brands of joysticks), the robot control program sends the position of the robot-end effector via a serial-port allowing any plug-and-play video-games to be incorporated into the protocol.

CHAPTER 5: ROBOT-AIDED NEURO-REHABILITATION

"Most of what is regarded as high science in medicine is actually a set of technologies for diagnostic precision -- the CAT scan, NMR and many exquisite refinements of our methods for detecting biochemical abnormalities of one sort of another. But these have not yet been matched by any comparable transformation of therapy."

--Lewis Thomas -- 1992 -- The Fragile Species

5.1. Background on Cerebral Vascular Accident (CVA)

5.1.1. Brain Attack Overview

The human brain is 80% water, represents 2% of the total body weight, receives 15% of the cardiac output, and consumes 20% of the body's oxygen, with blood flow close to 1 liter/min. There are no significant energy reservoirs in the brain, therefore nutrients must be continuously supplied (e.g. oxygen, glucose) and waste products removed (e.g. carbon dioxide, lactic acid). Furthermore, an increase of activity in a particular brain region requires an immediate increase in nutrient supply, which is achieved by selective dilation of cerebral arteries. This dynamic, postulated almost a century ago by Roy and Sherrington [Roy & Sherrington, 1890], is the basis for functional imaging techniques either monitoring glucose or oxygen consumption (rCBF - regional Cerebral Blood Flow). In fact, new neural activity patterns can be detected within seconds after a change in motor activity. To guarantee the prompt delivery of nutrients, the brain circulatory system is highly developed and redundant. A single event failure of the circulatory system, i.e. cerebral vascular accident, can result in devastating consequences causing neurological symptoms within seconds, and irreversible neuronal damage within minutes. These accidents have several causes, but can be classified as (a) blood vessel occlusion (approximately

75% of the cases) and (b) blood vessel hemorrhage (approximately 25% of the cases). Examples of the first case include a blood clot formed somewhere in the body's circulatory system that migrates to the brain and momentarily disrupts the normal blood supply (e.g. embolism). Similarly, stenosis of the arteries will limit the supply of blood to the brain (e.g. carotid occlusion). This one-sided blood supply limitation is generally compensated by the redundancy in the system. The Circle of Willis interconnects all major arteries, so that stenosis or even a one-sided carotid occlusion does not cause a stroke. However, the occlusion does deplete the system of its redundancy and makes it more vulnerable to accidents. Hemorrhage occurs from the rupture of vessels and blood flooding the brain with the consequent hematoma. Note that normal brain is the only tissue in mammals that does not allow blood to permeate freely. The blood-brain barrier prevents blood from washing-out brain matter and regulates the delicate equilibrium between allowing the nutrients to flow into, and pollutants to flow out of the brain. Subsequent to the cerebral accident event itself. is an after-shock, the causes of which remain controversial, during which the blood is generally redirected to intracerebral areas distant from the infarct and glutamate is segregated annihilating neighboring cells. The ischemic area around dead tissue from the original event is called penumbra and it is at risk during the "after-shock".

Presently, preventive alternatives are limited to (a) surgical interventions for stenosis and carotid occlusion and cerebral angioplasty for middle cerebral and basilar arteries, and (b) antiplatelet agents and anticoagulants. Anticoagulants were recently recommended in FDA guidelines as a preventive alternative, though they may have detrimental consequences in one quarter of the stroke victims that have had hemorrhage accidents. For the acute phase, there are pharmacological drugs under development to provide effective neuro-protection of the ischemic cells in the penumbra region. These pharmacological attempts at neuro-preservation require immediate intervention within a small window of opportunity of one to six hours after the onset of the stroke. The drugs under development act either on the blood side of the blood-brain barrier, i.e. on the circulatory system destroying the clot or residue obstructing the normal blood flow (e.g. tPA, Trilizad, Heparin), or in the brain side of the brain-blood barrier lowering the energy and oxygen consumption by administration of powerful drug-poisons that temporarily knock-down the cells and limit the nutrient demands (e.g. Lubeluzol). Another generation of

drugs aims at reversing the effects of brain cell death and concentrates on plasticity and sprouting of synapses and connections, i.e. growth factors.

The robot-aided neuro-rehabilitation initiative in combination with different pharmacological interventions and imaging techniques might provide a quantification tool, as well as visual and proprioceptive experience required to reactivate the motor cortex, leading to sprouting of task related fibers and harnessing synapses.

5.1.2. Health Care Cost and Potential Savings

In the U.S. every year over half a million people will have a stroke. The consequences are devastating. 25 percent of the cases result in death, while 75 percent of the survivors are left with a permanent disability. The National Stroke Association (NSA) reports 550,000 cases in 1993 with 150,000 deaths, 350,000 disabled survivors, and 50,000 non-disabled survivors. These figures rank stroke as the third leading cause of death and the first leading cause of permanent disability in U.S. The National Stroke Association estimates total 1993 stroke costs at $30 billion, a conservative figure since, as a typical survivor spends 14 days in an acute hospital ($ 2,000 per diem) and 30 days in an acute rehabilitation hospital ($750 per diem), direct costs of $27.7 billion per year can be estimated. Indirect costs, e.g. losses of revenues and pensions, impose a much greater drag on the economy. The NSA direct cost figure represents roughly 0.5 percent of the American GDP and 3 percent of the health care cost, which presently overwhelms the system with a 13 percent share of the GDP. Graying of the population should aggravate the problem, since the relative incidence of the event in this age group roughly doubles for every decade after 55 years, and the leading edge of the baby-boomers is entering this age group. While structural changes can only be accomplished by the society as a whole, there are three potential modes of application of the robot-aided neuro-rehabilitation workstation that might contribute to the cost containment as illustrated in Figs.5.1. to 5.3. Figure 5.1. illustrates the potential cost savings by allowing a clinician to work with more than one patient at a time, e.g. a classroom of patients with a single therapist overseeing either directly or via a robot-aided workstation 3 or 4 patients. The next two figures in the sequence illustrate the option of meaningful self-therapy at home. Effective

home-based self-therapy may require "tele-mentoring" by a qualified clinician. This may be accomplished as depicted in Fig.5.2. by using existing communication resources (e.g., phone lines, cable TV lines, ISDN services) to establish a bilateral tele-operation link between the robot in the home and a robot in the clinic. Figure 5.3. illustrates another potential mode of self-therapy at home with the patient using his/her good limb to teach an exercise to the robot-aided workstation and then to exercise the impaired limb.

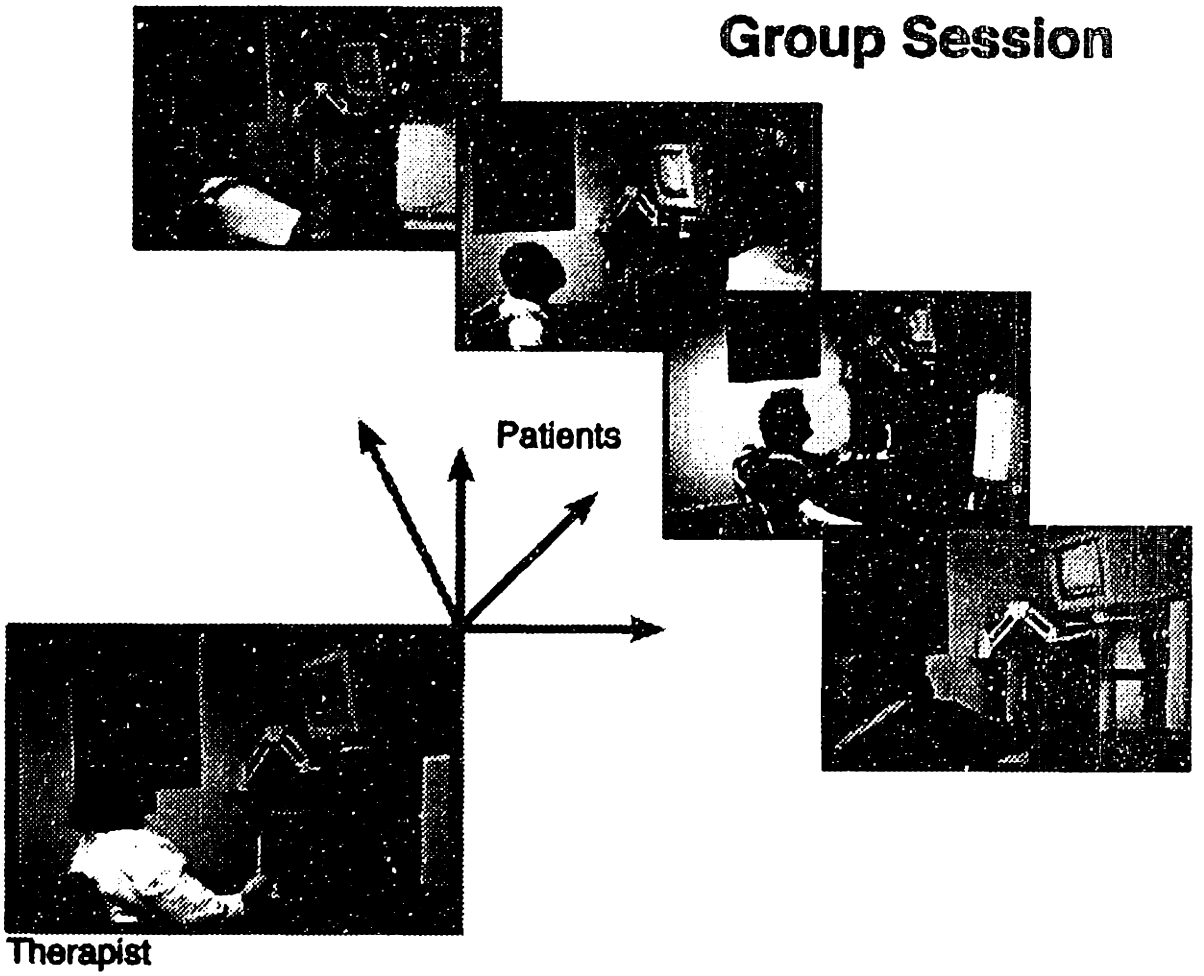

FIG.5.1. Robot-Aided Neuro-Rehabilitation: Classroom or Group Session. This figure illustrates the potential for cost-containment by allowing a clinician to work with more than one patient at a time. As depicted in this figure, the clinician is operating one robot-aided neuro-rehabilitation workstation, while selectively interacting with different patients. In another viable alternative, the clinician does not operate any workstation, but walks between patient's workstations.

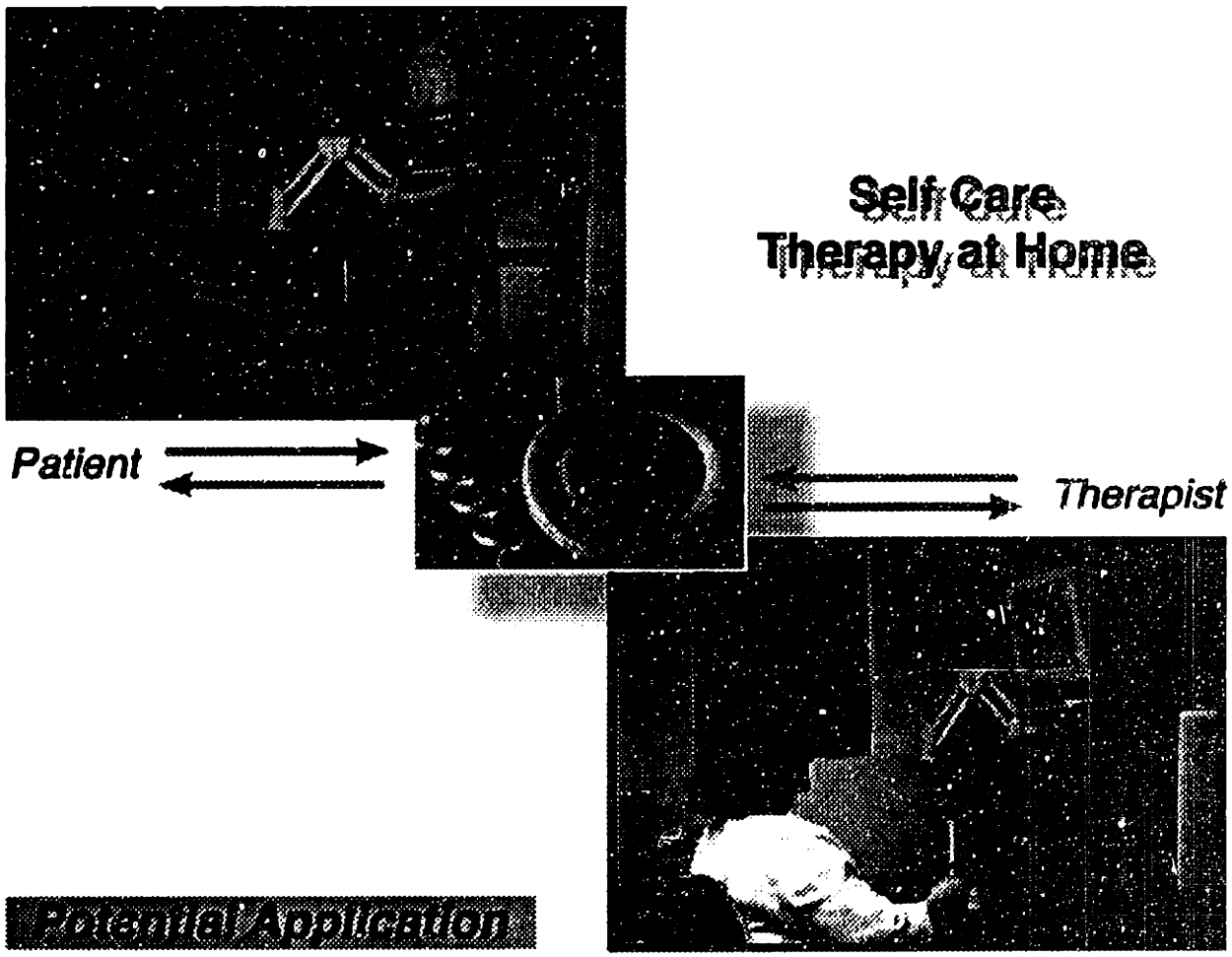

FIG.5.2. Robot-Aided Neuro-Rehabilitation: Self Care Therapy at Home. This figure illustrates the potential for telerobotics and telepresence. The clinician telementors an out-patient via a bilateral link between the robot in the home and the robot in the clinic.

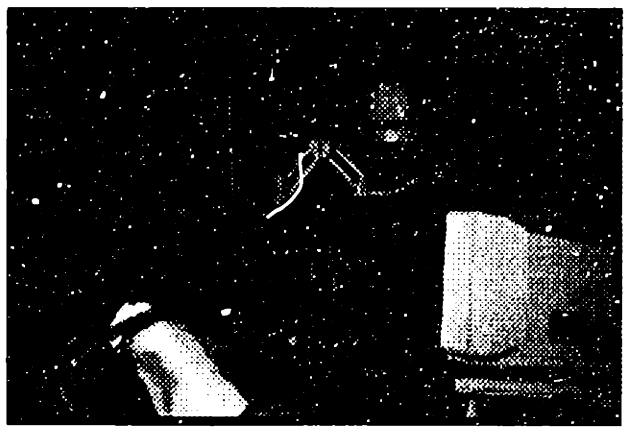

Normal Limb - Teach Mode

Self Instruction

Impaired Limb - Learning Mode

Potential Application

FIG.5.3. Robot-Aided Neuro-Rehabilitation: Self Instruction or Mirror Exercise. This figure illustrates the potential of self-therapy at home with the patient using his/her good arm to teach the robot an exercise and then to exercise the impaired limb.

In order to estimate the potential impact of the technology, rough estimates can be projected for the classroom application in which four patients interact under the supervision of a single therapist with an average salary plus benefits of $25 per hour or $200 per diem. This represents a quarter of the per diem cost in acute rehabilitation hospitals for stroke patients. In order to break even, the cost of the session with four robot-aids cannot be higher than $18.75 per hour per machine or roughly $37,500 per year, considering a weekly daily rate of utilization of 8 hours and 50 working weeks in a year. Considering that the piece of equipment has a lifespan of 5 years, this adds to $187,500. Present estimates of a small scale commercial production suggest a feasible cost per unit of under $35,000 with a $5,000 yearly maintenance cost. This back-of-the-envelope calculation suggests a potential best case scenario of savings close to 50 percent of the cost of a therapy session. Assuming a more conservative middle ground of 25 percent savings of the cost of a therapy session, and the bottom line is a cost containment of the acute rehabilitation per diem to $700 or 7 percent savings and a nationwide savings of $600 million per year. Coarse in nature, this estimate suggests the potential impact of this sort of technology to the society, hospitals, and insurance carriers. Even in a pessimistic scenario of no cost-containment without cost-expansion, the rehabilitation hospitals have a vested interest in differentiating themselves from the "herd" to attract more patients. Supply-and-demand in the field of rehabilitation is readily characterized by an over-supply of beds due to a significant decrease in the length of patient stay, coupled with a major expansion during 1985-1994 from 68 U.S. hospitals with 386 units and 18,500 beds, to 195 hospitals with 829 units and 35,500 beds (source: Kathleen Yosko - President and CEO of Schwab Rehabilitation Hospital and Care Network - Chicago, Illinois - The 3rd International Congress on Neurorehabilitation). The other "clients" of the technology include clinicians (e.g. therapists) and the patients. The research that follows was designed to allow assessment of the concept from the patient's perspective. This subsection concludes by citing highly positive feedback from therapists concerning the use of the technology, based primarily on their recognition of the major potential benefits of accurate and reliable quantification tools to validate and justify their professional experience.

5.1.3. Overview - Does Exercise Therapy Influence Brain Recovery ?

One goal of neuro-rehabilitation is to restore, as much as possible, the motor function of patients who have become disabled e.g. by a stroke. Past attempts at facilitating recovery of motor function have employed compensation strategies that target unaffected muscles. In these instances, recovery is measured in terms of improvement in patient's functional abilities rather than by the return of focal sensorimotor capacity. More recent attempts at the pharmacological management of spasticity have produced mixed results. The latest strategies target "at risk" brain tissue that surrounds focal ischemic areas. The so-called penumbra may provide a platform for brain rescue in the near future. Despite these recent new developments, current clinical practice attempts to decrease spasticity and facilitate functional motor abilities by passively moving a patient's paralyzed limb through the complete range of joint excursions. Furthermore, this practice continues by assisting the patient with voluntary movement to engage in function-oriented activities. The effectiveness of such treatment on the final functional motor ability of that limb is controversial. However, there is some recent evidence suggesting that genuine restoration of neurological function may be attainable, and that the environment may play a key role in this restoration, i.e. proper stimulus may enhance recovery, while the lack of it might constrain it. Functional imaging studies have shown the increase in the metabolism in ipsilateral hemisphere coincident with motor recovery in some hemiplegic patients [Chollet, 1991][Frackowiak, 1996]. Animal studies have suggested the role of stereotypical repetitive movement pattern in recovery when coupled with pharmacological intervention [Feeney, 1982]. More recently, cortical microelectrode studies in primates have shown that adjacent cortical tissue assumes the motor function of diseased tissue (experimentally induced stroke). The degree of reorganization in the cortex is significantly influenced by the environment via stereotypical movement patterns. Such findings indicate the potential for functional plasticity in the adult human cerebral cortex, and that the rehabilitation environment and practices might play a key role in influencing the outcome [Nudo, 1996]. Nonetheless, mainstream therapy philosophies upholding the validity of this form of treatment defend opposing approaches to the ideal process. For example, the Bobath approach for therapy, developed out of her work with children with cerebral palsy, defends the view that the use of synergies to complete the task at early stages of recovery is detrimental to the patient.

It defends the view that it is appropriate to restrain the movement until the proper sequence of muscles can be recruited. This approach claims that failing to wait for proper recruitment of the movement and stimulating the use of synergistic movements for short-term goals results in a long-term higher degree of disability [Bobath, 1990]. On the other hand, the Brunnstrom approach of therapy, based on the observation of cross-reflexes (upper extremity) and reciprocal reflexes (lower extremity) defends the opposite view. It recommends early exercise and stimulus for the use of synergistic movement in order to complete a task. It champions the view that early exercise with the impaired limb provides proprioceptive experience that helps the "rewiring" of the surviving tissue and promotes recovery [Brunnstrom, 1970].

Objective experimental studies of this problem have been hampered by the lack of an appropriate tool to quantify and control the amount of training and therapy (force, velocity, duration, repetition); and by the lack of accurate or reliable methods for quantifying and measuring patient response (strength, speed, accuracy). The robot-aided neuro-rehabilitation workstation permits (a) accurate measurement and control of motor activity delivered to a weakened or paralyzed limb, and (b) concurrent quantitative measurement of motor activity generated in the limb by the patient. The rest of this chapter is devoted to present some of the experimental results of a pilot clinical trial of the robot-aided neuro-rehabilitation addressing the key issue: Does Exercise Therapy Influence Brain Recovery ?

5.2. Patients

Consecutive patients with acute hemiparesis caused by a single computerized tomography (CT) verified cerebral vascular accident in the cortical or subcortical motor area served as subjects for the study. They were admitted to the same hospital ward at the Burke Rehabilitation Hospital and were assigned to the same team of rehabilitation professionals. A staggered pool of twenty subjects/patients participated in the study, in accordance with the guidelines and approval of the MIT-Committee on the Use of Humans as Experimental Subjects (Protocol # 2187) and Burke Rehabilitation Hospital Human Subject Committee (Protocol # 227), which can be found in Appendix A. Written consent was obtained from all subjects or designated guardians. Ten patients

were enrolled in a robot-aided therapy group (RT) and ten patients were enrolled in a standard therapy control group (ST). Both groups were well matched in terms of degree of impairment, number of men & women, time after the onset of the stroke, and length of stay in the rehabilitation hospital, as shown in Table 5.1. with an age range of 45 to 68 years for the experimental group and 38 to 72 years for the control group. It is unlikely in two pools of ten stroke patients to have well end-matched groups in terms of morphological brain lesion. Nonetheless, it turned out that the experimental and control groups formed comparable, though not identical pools (Tables 5.2.a&b). Both groups received conventional therapy, but the experimental group received an additional 4-5 hours per week of robot-aided therapy consisting of peripheral manipulation of the impaired limb correlated with audio-visual stimuli. The patients and clinical staff were not aware of which therapy group they had been assigned to (double blind study).

Group	Experimental (10 patients)	Control (10 patients)
Average Age (years)	58.40 ± 8.50	63.20 ± 10.59
Number of Male/Female	5 Men/ 5 Women	6 Men/ 4 Women
Average Admission at Rehab (weeks after stroke onset)	2.80 ± 1.11	3.20 ± 1.23
Average Discharge from Rehab (weeks after stroke onset)	9.25 ± 2.54	9.80 ± 2.53
Average Stay at Rehab (weeks at rehab hospital)	6.45 ± 1.96	6.60 ± 1.51

TABLE 5.1. Age, Sex, and Time Pieces of Information about the Trial's Groups

Patient	Sex	Age	Dominant Hand	Type of Stroke (hemisphere, shape or size, location)	Class of stroke location	Hospital Admition (wks aft onset)	Inclusion in Trial (wks aft onset)	Time Trial (wks aft onset)
M	M	45	Right	Left, wedge shaped, MCA Distribution	c	3	6	4
P	F	57	Right	Left, small, Lenticulo-Striate -- White Matter	s	5	6	7
R	F	68	Right	Right, wedge shaped, ACA/MCA	c	4.5	4.5	7
A	F	54	Left	Left, wedge shaped, MCA Distribution	c	2	2	5
L	M	57	Left	Right, small, Striato-Capsular - White Matter	s	2	2	2.5
E	F	66	Right	Right, large, deep Watershed -- White Matter	s	3	3	7
C	M	45	Right	Right, large, deep Watershed -- White Matter	s	2	2	7
S	F	62	Right	Right, entire, MCA distribution	sc	2	3.5	8
K	M	68	Right	Right, large, Pontine - Brain Stem		2	3	6
O	M	62	Right	Right, posterior wedge shaped, MCA Distribution	c	2.5	3.5	3.5

TABLE 5.2.a. Experimental Group Descriptive Data
MCA - Middle Cerebral Artery, ACA - Anterior Cerebral Artery
c - cortical, s - subcortical, sc - subcortical and cortical

Patient	Sex	Age	Dominant Hand	Type of Stroke (hemisphere, shape or size, location)	Class of stroke location	Hospital Admition (wks aft onset)	Inclusion in Trial (wks aft onset)	Time Trial (wks aft onset)
Q	F	69	Right	Right, small, Thalamic Hemorrhage -- deep White Matter	s	4	7	4
G	M	72	Right	Right, large, deep Watershed -- White Matter	s	2	2	7
H	M	71	Left	Right, large, deep Watershed -- White Matter	s	2	3	4
1	M	64	Right	Right, entire, MCA distribution	sc	5	9	4
J	F	70	Right	Right, small, Pontine -- Brain Stem		2	2	4
B	M	53	Left	Right, entire, MCA distribution	sc	5	10	4
D	M	38	Right	Left, small, deep Lenticulo-Striate distribution -- White Matter	s	3	5	5
T	F	69	Right	Right, wedge shaped MCA distribution	c	3	4	4
F	F	60	Right	Right, small, Thalamic Hemorrhage -- deep White Matter	s	4	5	6
N	M	66	Right	Left, small, deep Striato-Capsular -- White Matter	s	2	2	7

TABLE 5.2.b. Control Group Descriptive Data
MCA - Middle Cerebral Artery, ACA - Anterior Cerebral Artery
c - cortical, s - subcortical, sc - subcortical and cortical

5.3. Experimental Setup and Procedure

This study used the 2-dof module of a novel portable robot, MIT-MANUS, designed for clinical neurological applications. The 2-dof robot module, carpentry, layout, and video-games were described in some detail in Chapter 4. Patients sat facing the robot with their trunk movement partially restrained by seat belts, while the impaired arm was attached to the robot via the anti-spastic hand-holder with palm grasp. The sensory-motor training consisted of a set of "video-games", that were designed to create an exercise routine that focused on shoulder and elbow musculature with a restrictive rigid hand-holder at the wrist and hand. The games were used to evaluate the stroke patient's recovery of upper-limb motor function and to document and characterize stroke recovery in all of its phases. The games included drawing circles, stars, squares, diamonds, and navigating through "windows", as previously illustrated in Fig.4.14. The games were goal oriented and designed to maximize correlated sensory feedback, including visual, audio, and proprioceptive sensory stimuli; to be visually-evoked and visually-guided; to be terminated in the workspace center; and to occupy the same region of the workspace.

The procedure typically lasted for seven weeks, and in the case of the experimental group it consisted of an additional 4-5 hours per week of robot-aided therapy. The sensory-motor training for the experimental group required patients to move the robot end-effector according to the game's goals. If the patient could not perform the task, the robot assisted and guided the patient's hand. Therapy generally started with passive manipulation of the impaired limb during the initial weeks. It gradually evolved to active participation by the patient in an assisted phase and ended in an independent phase in which the robot's drive system was inactive. The menu-driven video-games allowed the clinician to choose different values for the impedance controller (null, very soft, soft, medium, hard, very hard). However, the same soft range (100 N/m, 2 N-sec/m) was used throughout the trial primarily due to patients' pre-trial preferences and to minimize any risk of exacerbating joint or tendon pain. For this trial, the impedance controller was implemented using nonlinear position and velocity feedback structured to produce a constant isotropic end-point stiffness and damping. Coupled to the highly back-driveable design, the stability of this controller is extremely robust to the uncertainties due to physical contact [Hogan][Colgate &

Hogan]. Each session consisted of an exercise with the normal limb followed by three packets of 20 repetitions of the daily exercise with the impaired limb. Each packet was preceded and succeeded by an active or manually guided exercise. Typical cumulative numbers for a seven week program were 25 sessions with 1500 repetitions of the game, 100 non-assisted repetitions, and 3 evaluation sessions.

The control group had a weekly session consisting of "sham" robot-aided therapy, and 3 evaluations sessions. Training for this group was similar to the experimental group, except that half of the one hour session consisted of playing the video games with the unimpaired arm and the other half of the session with the impaired arm with the robot passively taking a ride and providing visual biofeedback for the game. If the patient could not perform the task, he/she used the unimpaired arm to assist and complete the game, or the clinician assisted.

5.4. Primary Research Results

This section answers (or at least throws a dim light on) the three primary research questions of robot-aided neuro-rehabilitation: (1) Does robot-aided therapy have any detrimental effect on patients? (2) Does nurturing nature during the dynamic post-stroke acute recovery phase influence the outcome? (3) Can we develop better tools to evaluate and understand the mechanism of post-stroke recovery? To the best of my knowledge, robots have never been used so intensively and extensively in close physical contact with humans, let alone debilitated humans. As a background piece of information, close to 30 percent of stroke patients develop pain due to the so called shoulder-hand syndrome. Therefore, the first subsection addresses the potential unsalvageable question regarding pain, as well as the patient's acceptability of the robot-aided therapy. Therapy is unequivocally efficient in terms of functional recovery. Yet the value of nurturing on the course of nature remains controversial. In order for the results regarding the nurturing value to have any acceptability within the clinical community, the standard assessment procedures suggested by the clinical staff were used. These are described in the following subsection. In Chapter 3, I described the working hypothesis about movement segmentation and

motor learning. The results using the standard and robot-aided assessment procedures are used to answer the three working hypotheses.

5.4.1. Patients' Tolerance for the Procedure

A standard assessment procedure was used every other week to assess all patients (robot-aided therapy group and control group), and is found in Appendix B. The standard assessment was always performed by the same rehabilitation professional for all the patients involved in the study. This professional was not directly involved with the robot-aided therapy and did not know who was enrolled in the test group or control group (double blind study). The evaluation included the assessment of pain on the joint or tendon for shoulder, wrist, and hand, as well as shoulder-hand syndrome. The results were very comforting. There was no significant difference between groups. Joint or tendon pain occurred in 7 control and 5 experimental participants, and shoulder-hand syndrome occurred in 3 control and 4 experimental subjects. No adverse events occurred in an estimated 500 hours of operation in close contact with patients. A questionnaire administered during the bi-weekly standard assessment by the therapists showed that robot-assisted therapy was well accepted and tolerated by the patients. The average questionnaire result for the patients is summarized in Table 5.3. The last question was included specifically to assess the credibility of the questionnaire results, since a preference for the robot over a human therapist was considered extremely improbable.

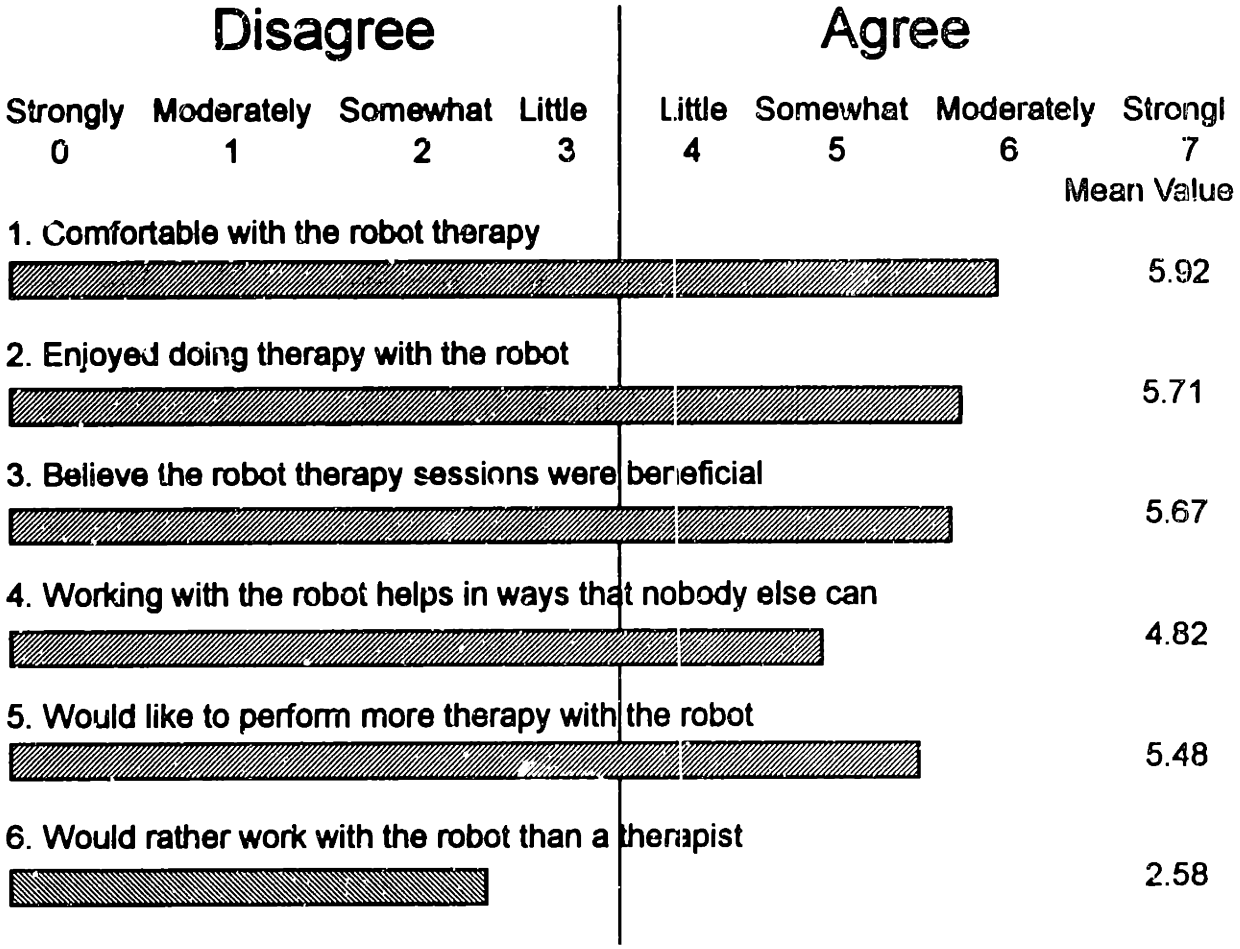

TABLE 5.3. Patients' Tolerance for the Procedure

5.4.2. Standard Assessment

To assess whether the supplemental 4-5 hours of robot-aided therapy had any significant impact on patient's outcome, the clinical team recommended the utilization of widely accepted assessment procedures. Three batches were used and are as follows:

Batch 1: To indicate consistency between the robot-aided therapy (RT) and standard therapy (ST) groups, evaluation scales in practice at the Burke Rehabilitation Hospital at admission and discharge were applied to assess functional status (FIM -- Functional Independence Measure) and motor impairment (F-M -- Fugl-Meyer Scale). Both scales are widely used in the US, and have

been shown to be valid and reliable to score different patients with an invariance for scoring by different therapists [Trombly, 1995][Fugl-Meyer, 1975]. These evaluations were performed by the patient's attending physical therapist. Based on the clinical research team's extensive experience, it was reasoned that the FIM is an adequate scale to measure competence in completing tasks such as dressing. However, its score does not depend solely on motor control, but also on intangible factors like patient's personality, pain, tone, depression state, and dependent attitude. Note that all the tasks involved are potentially achievable with a single hand (for upper-extremity related tasks). The Fugl-Meyer scale was developed considering a pattern of recovery for a typical patient with a nearly flaccid limb during the initial post-stroke phase. If any recovery occurs, Fugl-Meyer reasoned that the recovery pattern for the nearly flaccid patient shows characteristic milestones. The pitfalls of relying on the Fugl-Meyer scale subsection for the upper-extremity to assess the effect of supplemental therapy were that most patients were transferred to the acute rehabilitation hospital three weeks after the onset of the stroke, and intended robot-aided therapy would recruit essentially the shoulder/elbow/forearm. Therefore straight application of the Fugl-Meyer scale could potentially suffer from a decrease in resolution, since the return of reflex and synergistic movements, which represent a substantial component of the total score, might have taken place before the patients were admitted to a rehabilitation hospital. Instead of a broad range with 66 end-of-scale values for the upper extremity subscore, a range with 6 points for the shoulder/elbow/forearm isolated component was potentially expected.

Batch 2: To increase the number of isolated muscle groups assessed in the paretic limb, a scale based on the Fugl-Meyer approach, the Upper Extremity Motor Status Scale (MSS), was used. This scale includes ten shoulder movements, four elbow/forearm movements, three wrist movements, and twelve hand movements. The maximum score for the shoulder and elbow movements is 40, for the wrist is 6, and for the hand is 36. I will return to the wrist and hand movements in batch 3. A scale validated in other therapeutical trials [Aisen, 1995] assessed motor "power" (MP) in the biceps, triceps, anterior and lateral deltoid muscles. MP ranges to an end-of-scale value of 20. It is believed that there are no studies on the invariance of these scoring systems to different therapists. To control the variability due to different attending therapists, the same blinded therapist performed the evaluations of the MSS and MP. These evaluations were

typically performed biweekly and at least at admission and discharge. They were performed independently of the routine evaluation procedure of batch 1.

Batch 3: To assess the potential for generalization to other segments of the arm not exercised during the procedure, the three wrist and twelve hand movements of the Upper Extremity Motor Status (MSS) mentioned above were used.

5.4.3. Robot-Aided Assessment

In Chapter 1, an example of a language for human movement commonly used in dance was introduced (Labanotation). It subdivides the dancer's movement into body part, movement direction, speed, and muscular characteristic. The same three mechanical quantities are of interest to the clinician: accuracy, speed, and power (strength). At the outset of this research, there were no available assessment procedures that could be directly implemented with the robot. Therefore a general procedure was designed requiring different movements within the same workspace, and with different joints (i.e. predominantly shoulder motion, predominantly elbow motion, or both). This aimed at documenting and characterizing stroke recovery in all its phases and enlighting the path for the design of robot-aided assessment tools. Subsection 5.4.5. shows an example of a robot-aided assessment tool under development based on the kinematic data. Likewise, this kinematic data will be used to reveal new information based on submovement analysis.

5.4.4. Working Hypothesis: Exercise Therapy Influences Brain Recovery

There exists a long-standing dogmatic confrontation between determinism versus behaviorism views in almost every facet of society. Determinists believe that the inherited structure of the system fundamentally determines the outcome (e.g. Darwinism in Natural History), while the behaviorists believe that the environment significantly influences the outcome (e.g. Lamarckism in Natural History). In the case of cerebral vascular accidents, however, there is no such confrontation: nature overwhelms. Nonetheless, the question that is being posed relates to the

nurture potential during the highly dynamic phase following the stroke and neuronal reorganization, namely: Does exercise therapy influence brain recovery ?

Results in this pilot clinical trial suggest that robot-assisted therapy positively influenced patient recovery. Using the standardized clinical assessment procedures, the experimental group outranked the control group in all the assessments of the motor impairment involving the shoulder and the elbow (limb segments exercised with the robot-aided therapy). There was a trend in the F-M and MP scores favoring the experimental group ($p < 0.20$ and $p < 0.10$, one-tail t-test), and a statistically significant improvement in the MSS for shoulder/elbow ($p < 0.05$, one-tail t-test). Furthermore, the results' time history suggests that the control group did not improve after 6 weeks from the stroke onset, while seven patients in the experimental group continued to improve up to 8 weeks post-stroke, as shown in Fig.5.4. The timeline in these plots corresponds to the therapist evaluations and in some instances the initial evaluation occurred one week after the patient was enrolled into the program.

The results will be reviewed indicating (a) consistency between the robot-aided therapy (RT) and standard therapy (ST) groups via the FIM and upper extremity subsection of the Fugl-Meyer scales shown in Table 5.4.a.&b., (b) control of isolated muscles in the shoulder/elbow (MSS-shoulder/elbow) and power on the associated musculature (MP) shown in Table 5.5.a.&b., (c) generalization of the effect of the therapy on the wrist and hand (MSS - wrist and hand) shown in Table 5.6.a.&b.

The statistical analysis consisted of verifying significant differences between the control and experimental groups via a one-way ANOVA for the admission and discharge scores (error type I and II with null hypothesis "means are equal"), and verifying if the experimental group achieved a significantly better improvement than the control group via a one-tail t-test* (error type I with null hypothesis "mean of the experimental group improvement is greater than the mean of the control group improvement") with a significance level preset for all cases at $p \leq 0.05$.

* The t-test was used to be consistent with my neurologist colleagues' practices. To verify that the results' distribution was Normal, a one-way ANOVA was performed leading to similar significance levels.

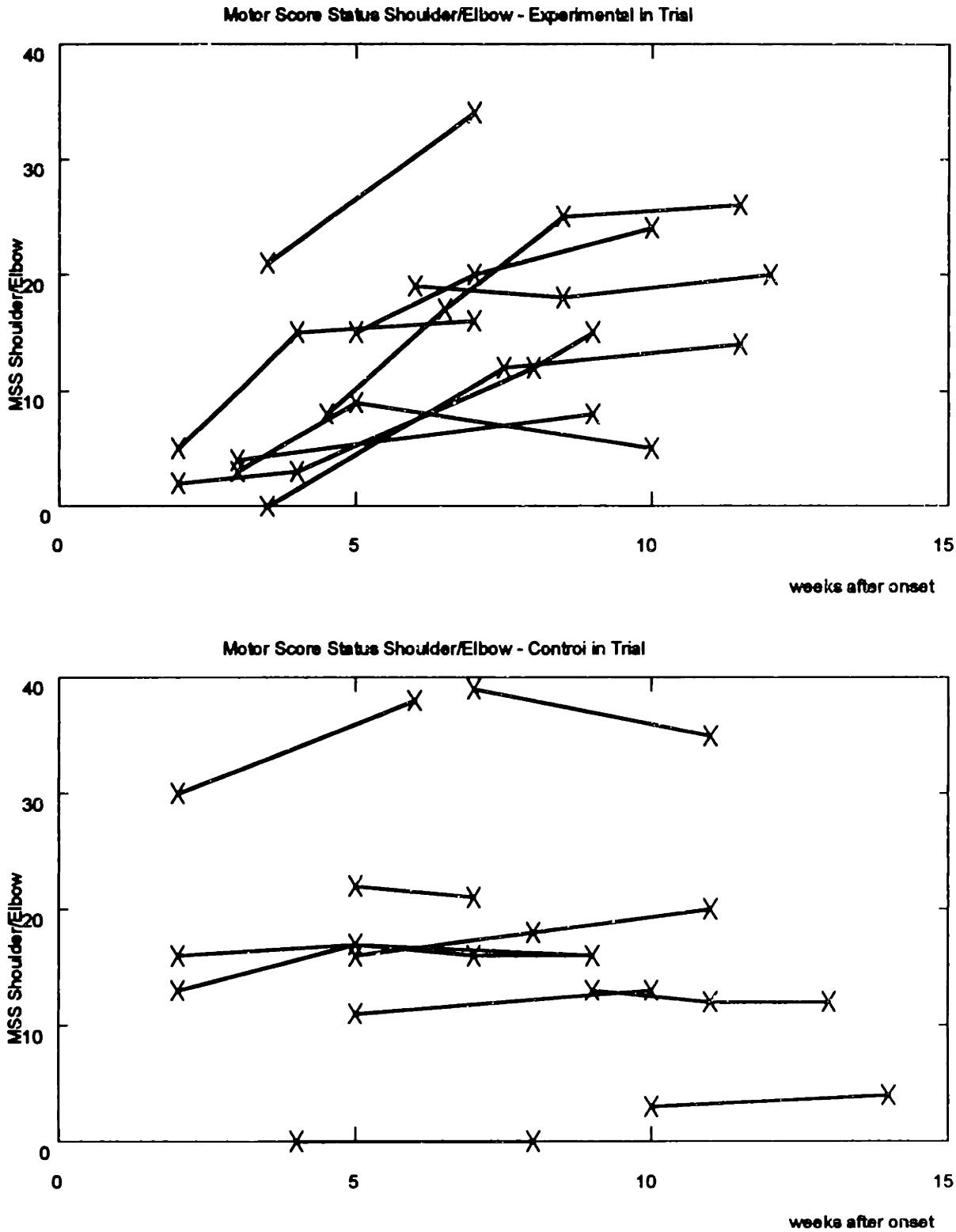

FIG.5.4. Time-Evolution of Shoulder/Elbow Motor Status Score of Trial's Groups
Note that a typical experimental patient continues to improve at least up to 8 weeks post-stroke, while a control patient's status stays unchanged after 5 weeks post-stroke.

Mean baseline admission FIM and Fugl-Meyer indicated no statistically significant differences between the control and experimental groups. Likewise, mean baseline admission for the MSS shoulder/elbow, wrist, hand, and MP indicated no statistically significant differences between groups, except for a strong trend in the MSS shoulder/elbow favoring the control against the experimental group, as shown in Table 5.7. At discharge, there were no statistically significant differences between the control and experimental groups. Mean baseline discharge FIM, Fugl-Meyer, MSS shoulder/elbow, wrist, hand, and MP indicated no statistically significant differences between groups, as shown in Table 5.8. Considering the sample size, these results should be taken with some caution, since another important indicator in comparing both groups is the lesion location and size. As mentioned in Section 5.2., the two groups of twenty consecutive patients formed a comparable, but not identical pool in terms of lesions.

The rehabilitation experience achieved its stated goal, with both the control and experimental group having a similar mean increase in the FIM score during their hospital stay, as summarized in Table 5.9. This is not surprising since both groups were equally trained regarding functional adaptation and compensatory techniques with the unimpaired limb. The MSS for the shoulder/elbow showed a statistically significant larger improvement for the experimental group versus the control group. Indeed, the degree of improvement in accuracy and degree of voluntary isolated movement in the specific muscle groups trained by the robot as reflected by the MSS shoulder/elbow is striking. Although not achieving statistical significance, the Fugl-Meyer and MP scores suggested a distinguishable trend for greater improvement in the experimental group against the control group. The potential for generalization of the exercise therapy effect to other segments of the arm not exercised during the procedure were evaluated via the MSS scores for wrist and hand. Notwithstanding the observable weak trend for wrist and hand, the experimental group outranked the control group significantly only in the joints that were directly involved in the robot-aided therapy.

The presentation of results will be completed by reviewing the MSS for shoulder/elbow time-history of Fig.5.4. and compare it with epidemiological stroke studies. The Copenhagen Stroke Study is an epidemiological study that traced the time-history of a large pool of several

hundred stroke patients and the analysis of several different aspects [Nakayama & Jorgensen, 1994]. In particular, a study involving 421 consecutive stroke patients traced the time history of upper extremity function recovery. It evaluated the patients on a weekly basis using standard assessment procedures like the Barthel Index subscores for feeding and grooming (functional activity) and the Scandinavian Stroke Scale. It concluded that within the study pool the best possible upper extremity function was achieved by 80 percent of the patients within 3 weeks after the onset of the stroke and by 95 percent of the patients within 9 weeks. In-patients with mild upper-extremity paresis, the best possible upper extremity function was achieved by 80 percent of the patients within 3 weeks after the stroke onset and by 95 percent of the patients within 6 weeks. In patients with severe upper-extremity paresis, the best possible upper-extremity function was achieved by 80 percent of the patients within 6 weeks and by 95 percent of the patients within 11 weeks. At the risk of making an inaccurate comparison, compare the epidemiological result from the Copenhagen Stroke Study for patients with severe upper extremity paresis with the time-history shown on Fig.5.4. The time-history of patients in the control group presents similar distribution to the findings of the Copenhagen Study with 2 patients showing some improvement in the upper extremity function after 6 weeks from the stroke onset, while 7 patients in the experimental group continued to improve after 6 week's post-stroke. In light of the results from the Copenhagen Study, it is an intriguing result that 7 out of 9 patients within the experimental group that stayed institutionalized for more than 6 weeks post-stroke onset fell into the latter group of the Copenhagen study, i.e., continued to improve after 6 weeks post-stroke. This result could be interpreted as suggesting that one of the exercise therapy modes of influencing brain recovery is by extending the effective acute recovery time-window.

In conclusion, results in this pilot clinical trial suggested that robot-assisted therapy positively influenced recovery of patients. A follow-up clinical trial is under way at the Burke Rehabiliation Hospital to confirm these results with a larger pool of stroke patients (30 patients in the experimental, and 30 patients in the control group). The inclusion criteria in this follow-up was sharpened to include only cortical and/or subcortical single lesions (no midbrain - pons or cerebellum lesions) with the time span between stroke onset and inclusion in the study less than 5 weeks.

Patient	Admission FIM / 126 pts	Discharge FIM / 126 pts	Admission F-M subsection UE /66 pts	Discharge F-M subsection UE /66 pts	Pain in Joints or Tendon	Shoulder/ Hand Syndrome
M	78	112	22	32	Yes	No
P	67	92	21	38	No	Yes
R	72	87	24	54	Yes	No
A	64	91	8	27	Yes	Yes
L	87	119	47	64	No	No
E	68	98	4	4	Yes	Yes
C	64	99	1	24	No	No
S	87	103	4	8	Yes	Yes
K	71	91	6	9	No	No
O	72	94	34	53	No	No

TABLE 5.4.a. Experimental Group FIM, Fugl-Meyer, and Pain Data

Patient	Admission FIM / 126 pts	Discharge FIM / 126 pts	Admission F-M subsection UE /66 pts	Discharge F-M subsection UE /66 pts	Pain in Joints or Tendon	Shoulder/ Hand Syndrome
Q	72	114	56	49	Yes	No
G	73	102	9	28	Yes	Yes
H	94	111	8	17	No	No
I	72	98	4	13	Yes	No
J	79	99	26	56	No	No
B	53	87	4	4	Yes	Yes
D	46	93	4	6	Yes	No
T	68	82	4	7	No	No
F	67	85	19	41	Yes	No
N	85	95	4	16	Yes	Yes

TABLE 5.4.b. Control Group FIM, Fugl-Meyer, and Pain Data

Patient	Admission Motor Power / 20 pts	Discharge Motor Power / 20 pts	Admission MSS for shoulder/ elbow / 40 pts	Discharge MSS for shoulder/ elbow / 40 pts
M	6.4	8.8	15	24
P	7.4	7.4	16	17
R	1.6	9.6	8	26
A	1.6	6.4	5	16
L	16.8	17.4	---	---
E	0	1.6	3	5
C	0	6.4	2	15
S	0	7.4	0	14
K	0	2.2	4	8
O	7.4	12.8	21	34

TABLE 5.5.a. Experimental Group Motor Power, and Motor Status Score for shoulder/elbow (--- not available)

Patient	Admission Motor Power / 20 pts	Discharge Motor Power / 20 pts	Admission MSS for shoulder/ elbow / 40 pts	Discharge MSS for shoulder/ elbow / 40 pts
Q	13.2	12.4	39	35
G	2.6	8.8	13	16
H	5.8	7.4	22	17
I	0	5.8	13	12
J	9.8	12.8	30	38
B	0	0	3	4
D	1.6	5.8	11	13
T	0	0	0	0
F	6.4	8.4	16	20
N	4.8	5.8	16	16

TABLE 5.5.b. Control Group Motor Power, and Motor Status Score for shoulder/elbow

Patient	Admission MSS for wrist / 6 pts	Discharge MSS for wrist / 6 pts	Admission MSS for hand / 36 pts	Discharge MSS for hand / 36 pts
M	0	4	0	12
P	3	3	11	17
R	5	5	35	36
A	1	2	1	1
L	---	---	---	---
E	0	0	0	0
C	0	3	0	18
S	0	0	0	1
K	0	0	0	1
O	3	3	12	14

TABLE 5.6.a. Experimental Group Motor Status Score for wrist and hand (--- not available)

Patient	Admission MSS for wrist / 6 pts	Discharge MSS for wrist / 6 pts	Admission MSS for hand / 36 pts	Discharge MSS for hand / 36 pts
Q	6	4	33	31
G	0	2	1	1
H	2	3	2	7
I	2	2	1	1
J	3	6	24	35
B	0	0	1	3
D	0	0	0	0
T	0	0	0	0
F	3	5	20	21
N	2	1	0	18

TABLE 5.6.b. Control Group Motor Status Score for wrist and hand

Group	Experimental (10 patients)	Control (10 patients)	ANOVA P-value (significant $p \leq 0.05$)
Admission FIM	73.0 ± 8.5	70.9 ± 14.0	0.69
Admission F-M -- UE subscore	17.1 ± 15.2	13.8 ± 16.7	0.65
Admission MP	4.1 ± 5.5	4.4 ± 4.5	0.89
Admission MSS - shoulder/elbow	8.2 ± 7.3 (*)	16.3 ± 11.7	0.09
Admission MSS - wrist	1.3 ± 1.9 (*)	1.8 ± 1.9	0.60
Admission MSS - hand	6.6 ± 11.8 (*)	8.2 ± 12.5	0.77

TABLE 5.7. Admission Scores: Mean, Standard Deviation, P-Value for the Trial's Groups with Standard Assessment Scales -- (*) indicates data available for 9 patients.

Group	Experimental (10 patients)	Control (10 patients)	ANOVA P-value (significant $p \leq 0.05$)
Discharge FIM	98.6 ± 10.2	96.6 ± 10.6	0.67
Discharge F-M -- UE subscore	31.2 ± 21.0	23.7 ± 18.9	0.41
Discharge MP	8.0 ± 4.7	6.7 ± 4.3	0.53
Discharge MSS - shoulder/elbow	17.7 ± 9.0 (*)	17.1 ± 11.9	0.91
Discharge MSS - wrist	2.2 ± 1.9 (*)	2.3 ± 2.2	0.93
Discharge MSS - hand	11.1 ± 11.9 (*)	11.7 ± 13.5	0.92

TABLE 5.8. Discharge Scores: Mean, Standard Deviation, P-Value for the Trial's Groups with Standard Assessment Scales -- (*) indicates data available for 9 patients.

Group	Experimental (10 patients)	Control (10 patients)	One-Tail t-test (significant $p \leq 0.05$)
Change FIM	25.6 ± 7.2	25.7 ± 12.2	0.51
Change F-M -- UE subscore	14.1 ± 9.7	9.9 ± 11.2	0.19
Change MP	3.9 ± 2.9	2.3 ± 2.4	0.10
Change MSS - shoulder/elbow	9.4 ± 5.9 (*)	0.8 ± 3.8	0.00065
Change MSS - wrist	0.9 ± 1.5 (*)	0.5 ± 1.5	0.29
Change MSS - hand	4.6 ± 6.4 (*)	3.5 ± 6.3	0.36

TABLE 5.9. Change During Acute Rehabilitation: Mean, Standard Deviation, P-Value for the Trial's Groups with Standard Assessment Scales -- (*) indicates data for 9 patients.

5.4.5. Automatization of Standard Assessment Procedures

In a typical standard evaluation session, it takes approximately 20 minutes to collect the MSS score alone. To illustrate the potential of developing robot-aided tools to automate patient status assessment with considerable time savings, consider the task of hitting eight targets equally distributed along a circle. Patients sat facing the robot restrained by a three point-seatbelt and were instructed to move the robot end-effector hitting eight targets equally distributed along a circle and the circle center. The targets were presented in a clockwise fashion starting at 12 o'clock. Subjects were instructed to hit all the targets as fast as possible. The task was considered successful only if the subject succeeded in hitting all the targets within 40 seconds (2.5 sec per move -- estimated five times slower than normals). Seven experimental and four control subjects were ever able to perform this task, as indicated in Fig.5.5. The figure shows the first recorded successful attempt in performing the task during an evaluation with the robot-aided procedure. Subsequent evaluation sessions continued to show successful attempts by these subjects. For the sole purpose of illustrating the feasibility of developing sets of robot-aided tools to automate patient status assessment, Fig. 5.5. also shows in the lower plot a regression curve for the eight patients with motor deficit (actuation side) that competently performed the task, with lesions in either the motor cortex (A, M, S), or basal ganglia (G, H, P), or lacunar and pons (L, J). The resulting correlation between the score of a standard evaluation procedure and the number of post-stroke days until the first competent performance of a robot-aided video-game should not be surprising. Both require a series of coordinated movements. Yet, there is virtually no available instruments to explored this untapped potential to develop fast and reliable tools to automate the assessment of patient status.

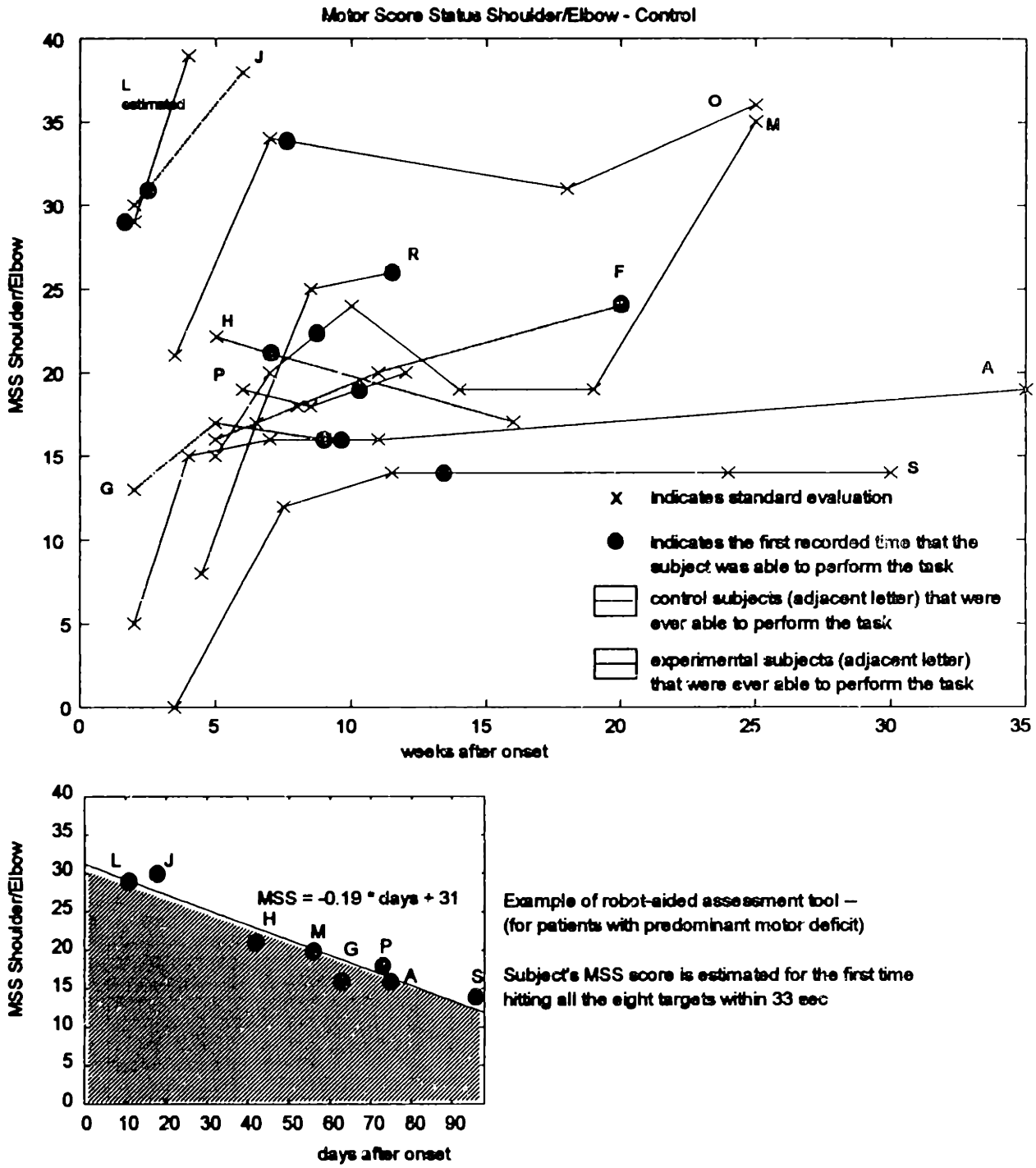

FIG.5.5. Robot-Aided Assessment Rose (1) Procedure versus Timeline of Motor Status Score
Top plot shows the timeline of the Motor Status Score for patients that successfully performed the procedure Rose (1) within 40 sec (seven experimental and four control patients). It also shows the first time they succeeded completing Rose (1) (robot-aided assessment and standard evaluation were performed independently and not in the same day). As an example of robot-aided tools, considering the eight subjects with motor impairment led to a regression correlating the value obtained in the MSS and days post-stroke (lower plot).

5.4.6. Working Hypothesis: Post-stroke sensorimotor behavior is more segmented than normal limb movements.

The application of a submovement decoding procedure can reveal new pieces of information. Consider the kinematic component of the task reported in the previous subsection, in which patients sat facing the robot restrained by a three point-seatbelt and were instructed to move the robot end-effector hitting eight targets equally distributed along a circle and the circle center. The targets were presented in a clockwise fashion starting at 12 o'clock. Subjects were instructed to hit all the targets as fast as possible. The task was considered successful only if the subject succeeded in hitting all the targets within 40 seconds (2.5 sec per move -- estimated five times slower than normals). Seven experimental and four control subjects were ever able to perform this task. The results of the submovement decomposition are depicted in Fig.5.6.a. to 5.6.h. The left column shows the hand displacement trace during the task with the dark arrow indicating whether the subject was still enrolled in the program or returned for an out-patient evaluation session. The center column shows the speed profile, while the right one indicates a histogram of the velocity phase $\left(\arctan\left(\frac{vx}{vy}\right)\right)$. The velocity phase indicates the subject's competence in making straight and aimed movements to the targets. To evaluate the subject's aiming performance, the standard deviation of the velocity phase histogram is used as a marker, i.e., larger value indicates the more accurate and better aimed movement. Since each of the examples of this task has a different time duration and a different number of sample points, the total number of bins in the velocity phase histogram was normalized to one thousand. Therefore, perfect performance in this task would result in a velocity phase histogram composed by eight spikes of 125 bins each, located at multiples of $\pi/4$, and a standard deviation of 18.4513. To the right side of the plots, a few quantities were compiled such as the total hand displacement, movement duration, velocity phase standard deviation, total number of submovements, submovement mean peak, duration, and the product of the total number by the mean duration of submovements.

Table 5.10. shows the statistical significance level of the sample composed by all the patients' data compared to the performance of a normal subject. One cannot but answer in the affirmative that post-stroke sensorimotor behavior is more segmented than normal limb movements (versus same

number of segments with longer duration). Indeed all the subjects performed the task with a larger number of submovements than a naive normal subject, though probably due to different pathologies. For example, patients A and S had a severe cortical lesions and while they seemed to be able to move at fast peak speeds, they had the poorest aiming score of all patients (actuation deficit). Patient M, with a less severe cortical lesion was far more better in aiming. Patients O and F have a strong sensory deficit (proprioceptive) with right parietal or thalamic lesions and were unable to perform the task without visual feedback, thus requiring a longer time to complete the task. This is particularly evident in subject's O first successful attempt. The difference between the movement duration and the product between the number of submovements and their mean duration, indicates a long down-time while acquiring visual information. Within the patients with slow submovement mean peak, patients O and F had strong sensory deficit, while patients P and H had a motor deficit (actuation) with lesions in the basal ganglia (putamen). Presently, the application of the submovement decoding procedure is being further refined to fully characterize the time-history of recovery, correlated with lesion location and degree of severity.

Group	A Normal Subject Performance	Patients Performance	One-Tail t-test P-value (significant $p \leq 0.05$)
Movement Duration (sec)	11.99	24.90 ± 5.43	$p \leq 0.01$
Velocity Phase Std	3.29	2.12 ± 0.27	$p \leq 0.01$
Number of Submovements	18	26.76 ± 4.02	$p \leq 0.01$
Submovement mean speed peak (m/s)	0.21	0.13 ± 0.02	$p \leq 0.01$
Submovement mean duration (sec)	0.65	0.78 ± 0.13	$p \leq 0.01$

TABLE 5.10. Rose Drawing Scores: Mean, Standard Deviation, P-Value for the Patient's

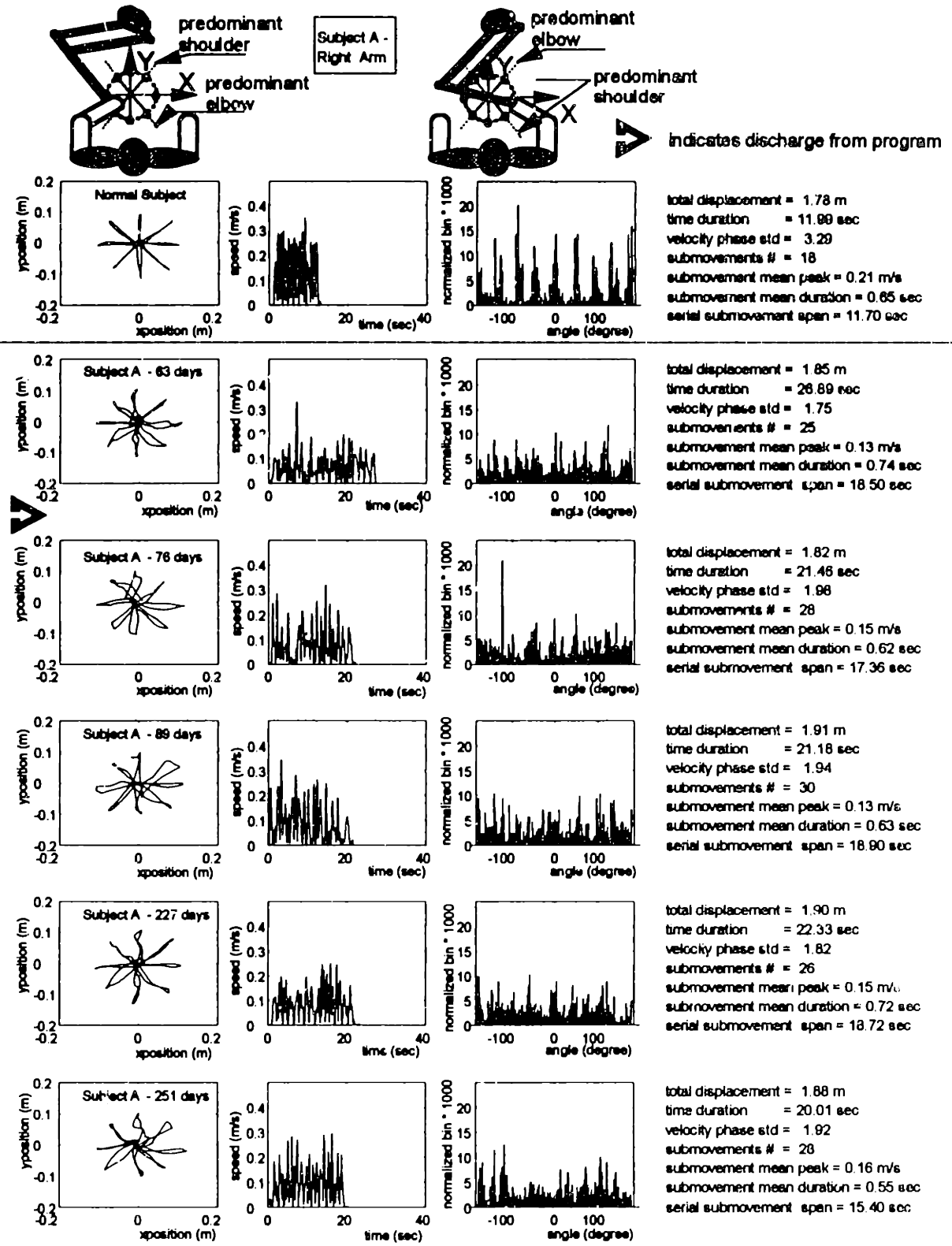

FIG.5.6.a. Robot-Aided Assessment Rose (1) Procedure

The left column shows the plan view of the hand displacement trace, while the center column shows the hand speed profile, and the right column shows the histogram of velocity phase (total number of bins normalized to 1000). The subject's hemiparetic arm is indicated on the top, and program discharge is indicated by the arrow. The movement displacement and duration, as well as the number of submovements, their mean peak speed and duration, and maximum submovement duration span is shown on the right.

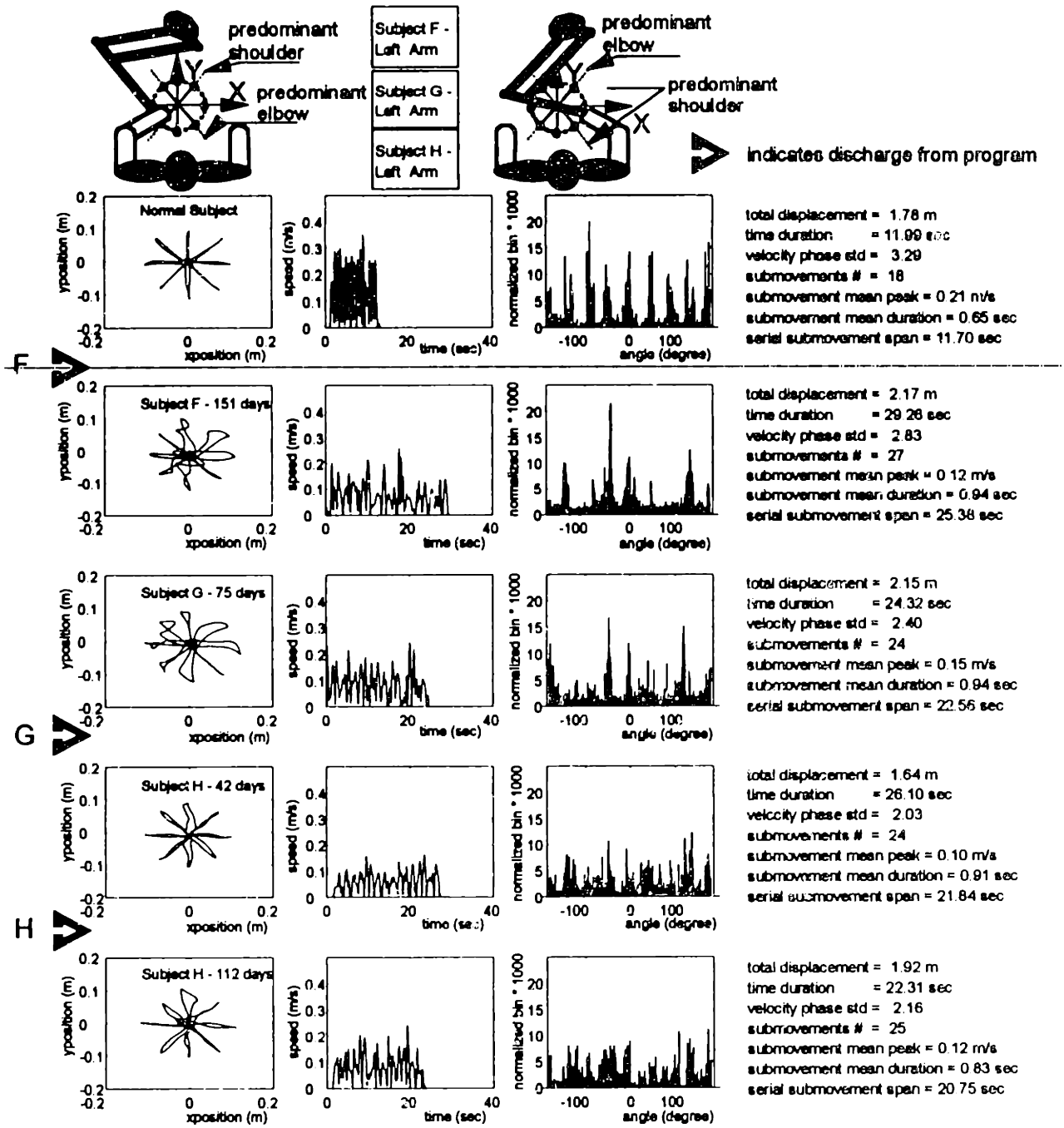

FIG.5.6.b. Robot-Aided Assessment Rose (1) Procedure
The left column shows the plan view of the hand displacement trace, while the center column shows the hand speed profile, and the right column shows the histogram of velocity phase (total number of bins normalized to 1000). The subject's hemiparetic arm is indicated on the top, and program discharge is indicated by the arrow. The movement displacement and duration, as well as the number of submovements, their mean peak speed and duration, and maximum submovement duration span is shown on the right.

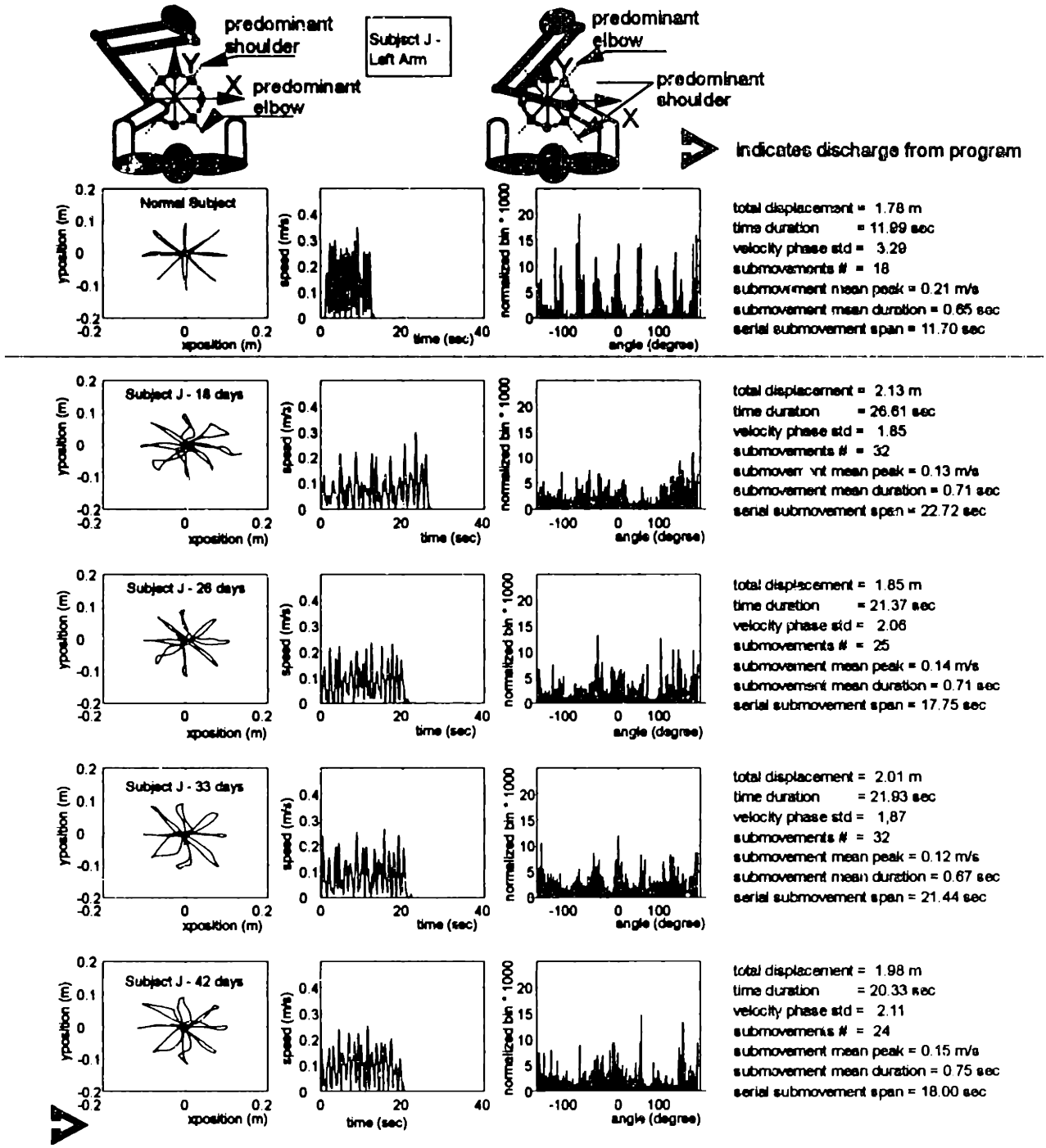

FIG.5.6.c. Robot-Aided Assessment Rose (1) Procedure

The left column shows the plan view of the hand displacement trace, while the center column shows the hand speed profile, and the right column shows the histogram of velocity phase (total number of bins normalized to 1000). The subject's hemiparetic arm is indicated on the top, and program discharge is indicated by the arrow. The movement displacement and duration, as well as the number of submovements, their mean peak speed and duration, and maximum submovement duration span is shown on the right.

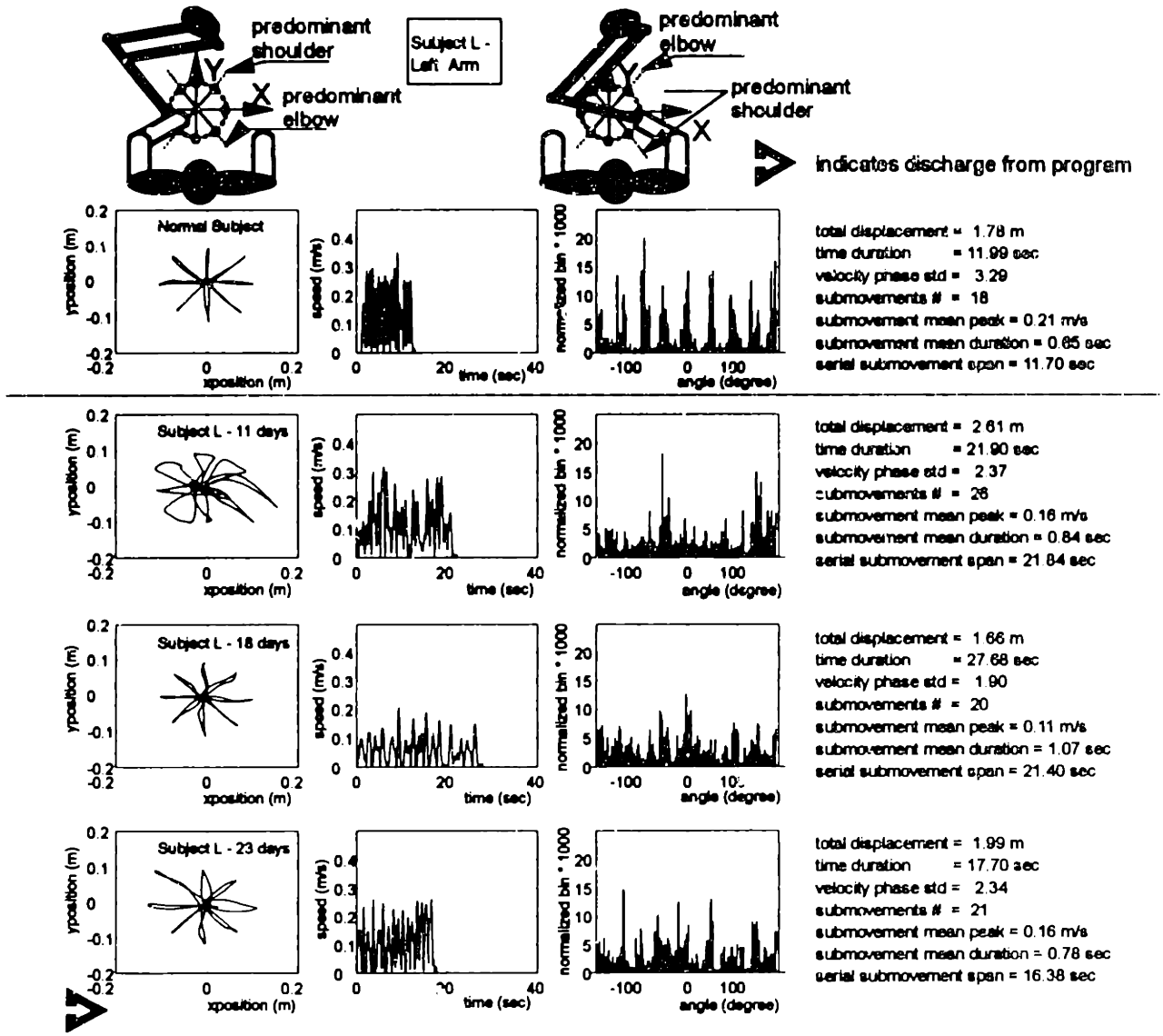

FIG.5.6.d. Robot-Aided Assessment Rose (1) Procedure

The left column shows the plan view of the hand displacement trace, while the center column shows the hand speed profile, and the right column shows the histogram of velocity phase (total number of bins normalized to 1000). The subject's hemiparetic arm is indicated on the top, and program discharge is indicated by the arrow. The movement displacement and duration, as well as the number of submovements, their mean peak speed and duration, and maximum submovement duration span is shown on the right.

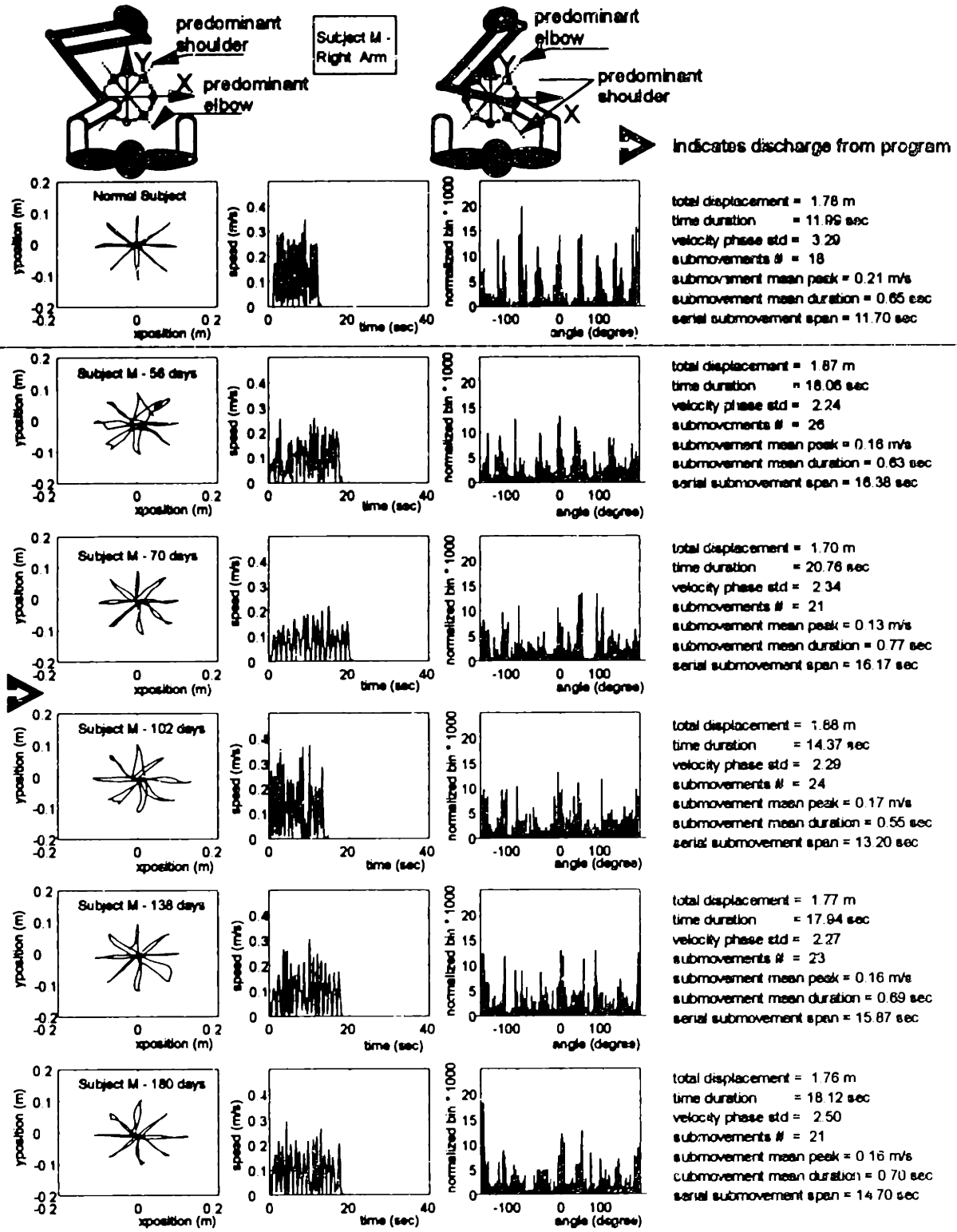

FIG.5.6.e. Robot-Aided Assessment Rose (1) Procedure

The left column shows the plan view of the hand displacement trace, while the center column shows the hand speed profile, and the right column shows the histogram of velocity phase (total number of bins normalized to 1000). The subject's hemiparetic arm is indicated on the top, and program discharge is indicated by the arrow. The movement displacement and duration, as well as the number of submovements, their mean peak speed and duration, and maximum submovement duration span is shown on the right.

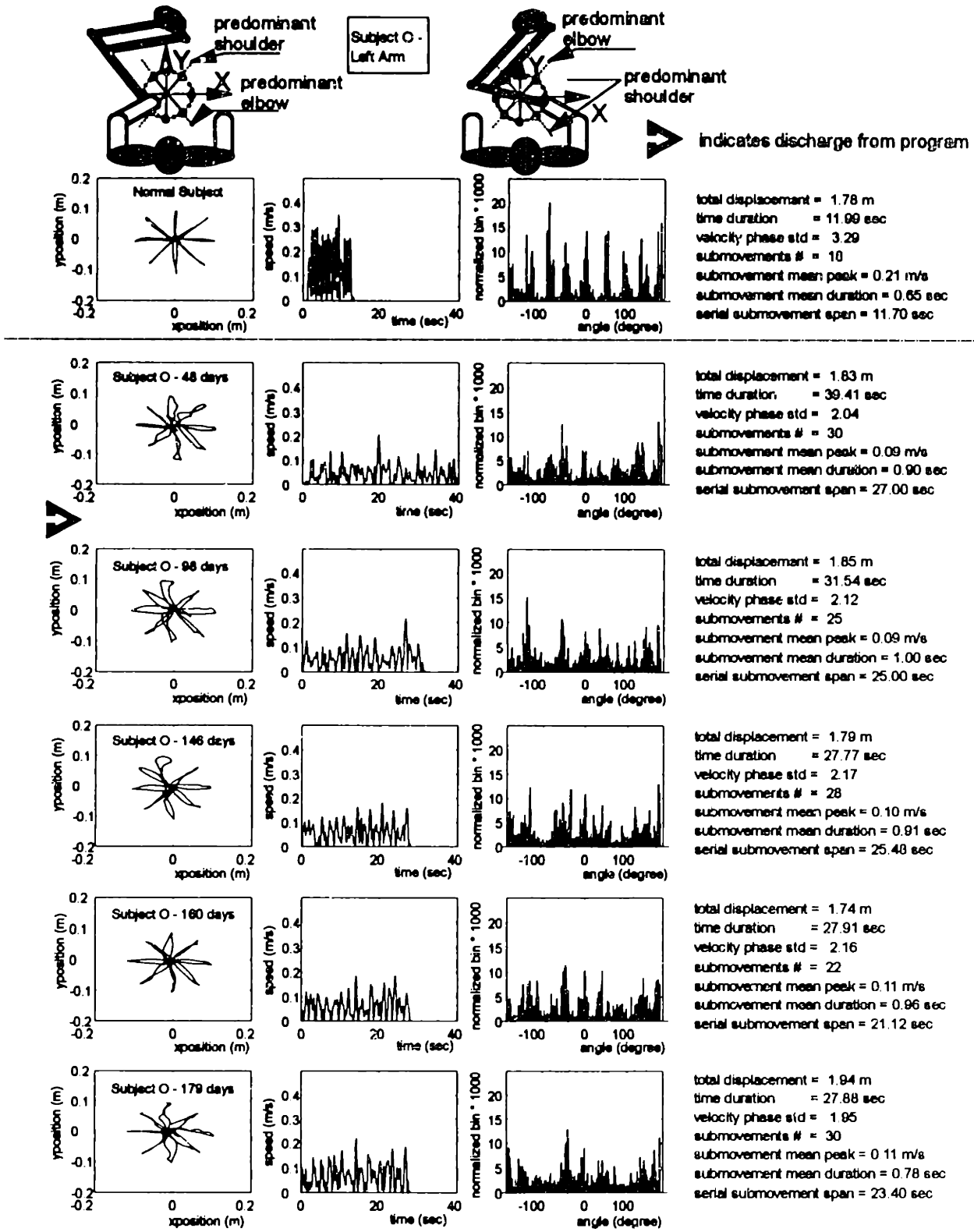

FIG.5.6.f. Robot-Aided Assessment Rose (1) Procedure

The left column shows the plan view of the hand displacement trace, while the center column shows the hand speed profile, and the right column shows the histogram of velocity phase (total number of bins normalized to 1000). The subject's hemiparetic arm is indicated on the top, and program discharge is indicated by the arrow. The movement displacement and duration, as well as the number of submovements, their mean peak speed and duration, and maximum submovement duration span is shown on the right.

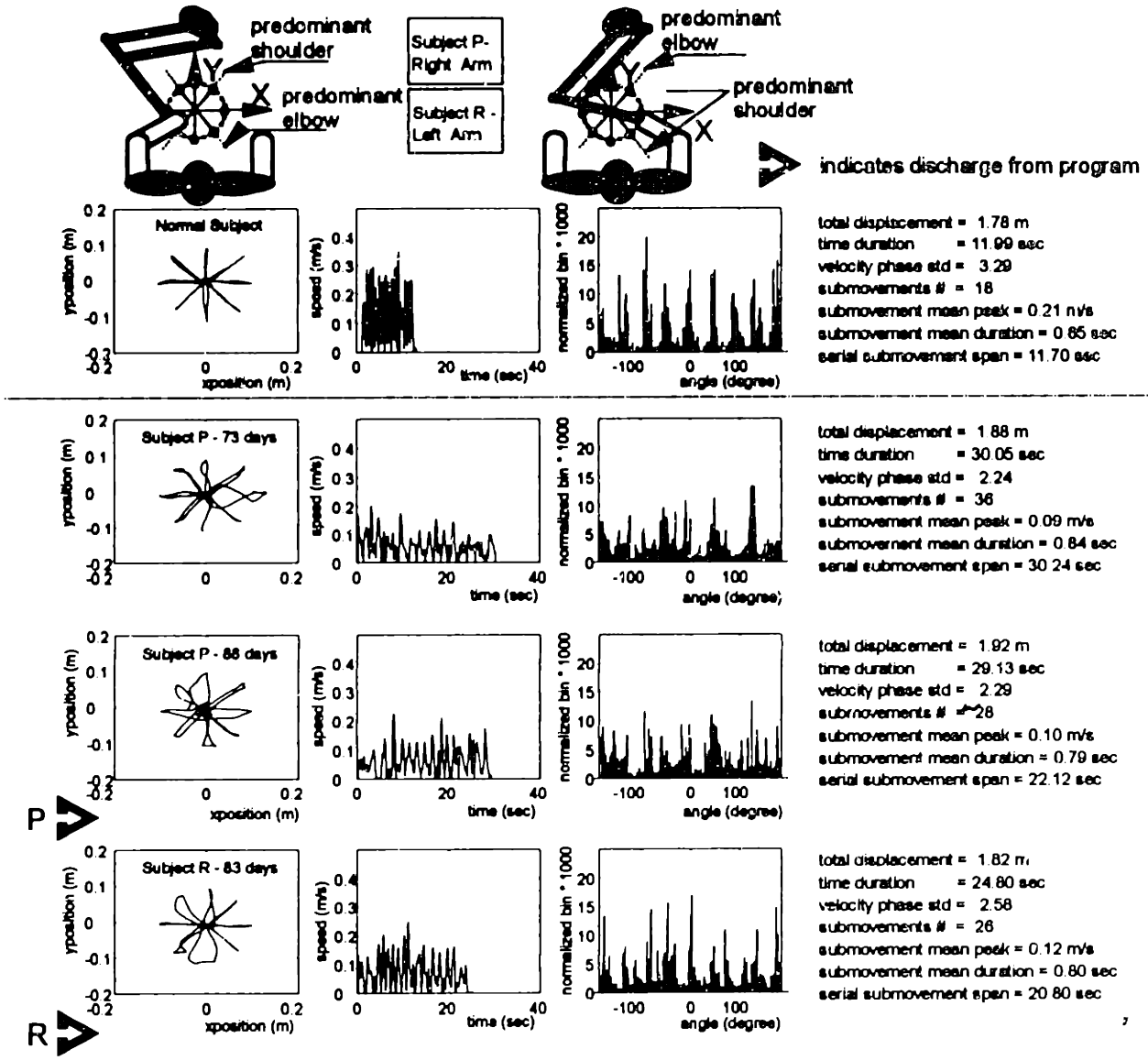

FIG.5.6.g. Robot-Aided Assessment Rose (1) Procedure

The left column shows the plan view of the hand displacement trace, while the center column shows the hand speed profile, and the right column shows the histogram of velocity phase (total number of bins normalized to 1000). The subject's hemiparetic arm is indicated on the top, and program discharge is indicated by the arrow. The movement displacement and duration, as well as the number of submovements, their mean peak speed and duration, and maximum submovement duration span is shown on the right.

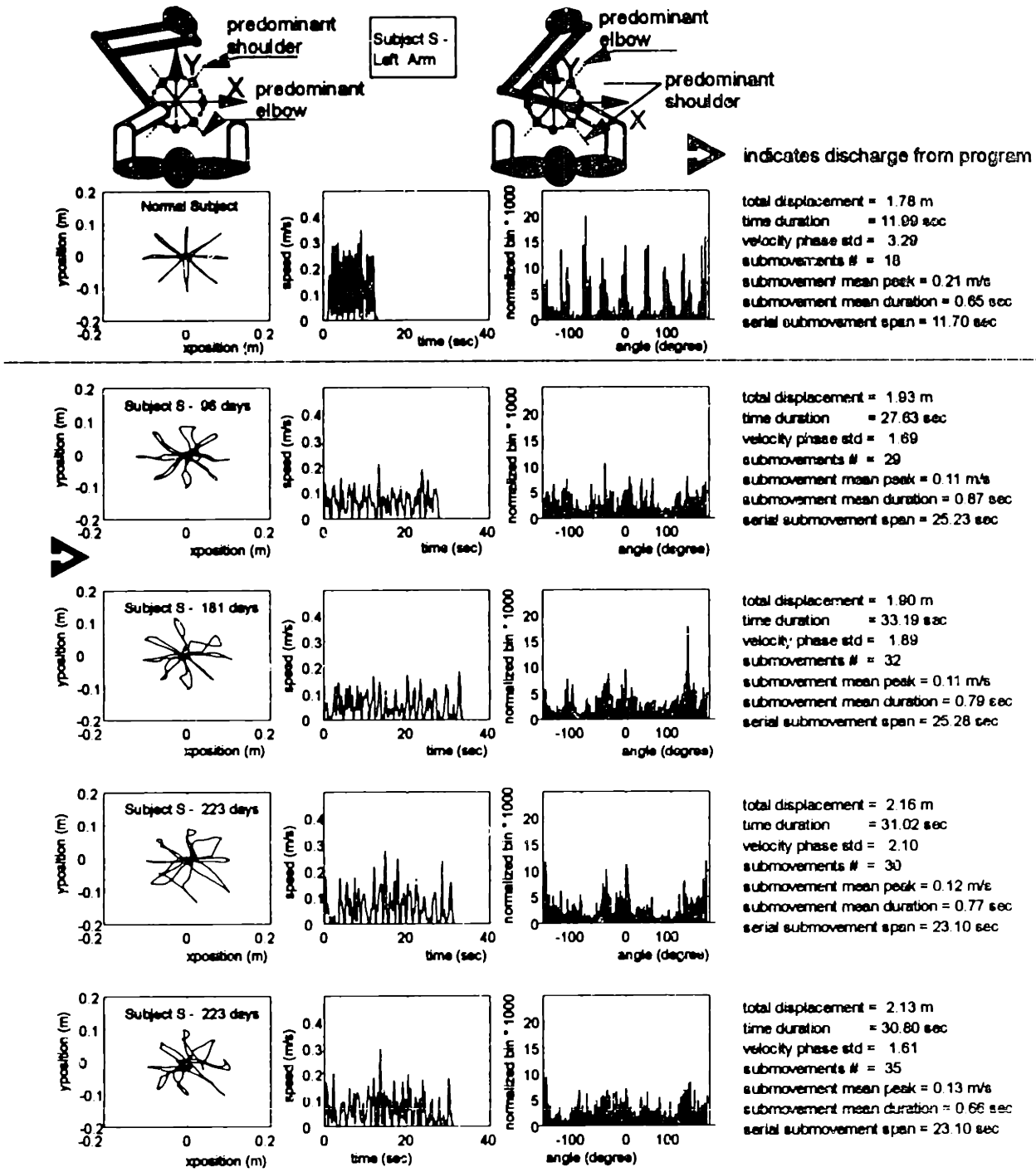

FIG.5.6.h. Robot-Aided Assessment Rose (1) Procedure

The left column shows the plan view of the hand displacement trace, while the center column shows the hand speed profile, and the right column shows the histogram of velocity phase (total number of bins normalized to 1000). The subject's hemiparetic arm is indicated on the top, and program discharge is indicated by the arrow. The movement displacement and duration, as well as the number of submovements, their mean peak speed and duration, and maximum submovement duration span is shown on the right.

5.4.7. Working Hypothesis: Exercise and Training Influence Movement Performance of Stroke Victims in the Stable Phase.

Subjects with the stroke in the motor strip (cortical Brodmann's areas 1 to 4, 6) volunteered for a study on the effect of learning and training several months after their discharge from the Burke Rehabilitation Hospital.(patients A, M, & S -- Fig.5.7.). They were originally assigned to the experimental group in the pilot-clinical trial and were intensively trained with the robot-aided neurorehabilitation workstation. In particular, two of the visually-evoked, visually-guided, workspace centered "video-games" required the patients to move the robot end-effector between the center target and outer targets equally spaced around a circle (rose) or to trace a circle. The subjects had repeated these games for at least 1500 times in the workspace center.

The novel task consisted of having the subjects move the robot end-effector from its initial position toward a target with their impaired limb. Unlike the previous training, the task center was translated on the x-axis first by 20 cm and then by 40 cm from the workspace center, as shown in Fig.5.8. Subjects were evaluated at the beginning of the trials (week 0). They were trained during the subsequent week on a daily basis for an hour with the games (rose and circle) centered at midline, 20 cm and 40 cm. They were then evaluated at the end of the week (week 1) and requested to return in two weeks time for a final evaluation (week 3). The mean-squared lateral deviation from a straight line for the subjects is shown in Figs.5.9. to 5.11. At the time of the experiment, subject M had a mild degree of upper extremity weakness (four-minus in a five motor power scale, where five corresponds to normal strength). Subject A had a greater impairment (two-plus in the same five scale) and Subject S had a more severe paresis (two-minus in the same five scale), as shown in Fig.5.7. Figure 5.9. shows that in the same session, subject M did not show any statistically significant change at the center position, consistent with the fact that the task was "over-trained" in this location. However, a statistically significant decrease of performance occurred when the task center was shifted by 20 cm and then by 40 cm from the center. For comparison purposes, results at the same task with a normal 25 year old male are also included in the figure. Likewise, performance at these task centers significantly improved with a week of training. Figure 5.10. shows subject A's performance during trial 2 in three evaluation

sessions at different task locations. For comparison purposes results of the same task during trial 2 with a normal 25 year old male are also included in the figure. Note the lack of performance improvement at the workspace location where this task was previously overtrained. Statistically significant performance deterioration occurred at the novel task locations, followed by improvement with training. It is noteworthy that there was no organized training between week 1 and week 3, suggesting that training had a lasting effect for this subject. Figure 5.11. shows subject S's performance during trial 2 in two evaluation sessions at different task locations. For comparison purposes, results of the same task during trial 2 with a normal 25 year old male are also included. Subject S had the most severe degree of paresis and could not perform the novel tasks during trial 1. The training for this subject was similar to the other subjects, but only the novel task translated by 20 cm is shown for week 1 (trial 2). After training, the subject was able to move the paretic arm within the target range centered at 20 cm and 40 cm, but not within the required time duration (at position 40 cm). The noticeable difference for this subject with the most severe degree of impairment was the trend for performance improvement also at the workspace location where this task was previously overtrained. It is rather dull to mention statistics for this subject, nonetheless there was a statistically significant performance deterioration at the novel task locations, followed by improvement with training

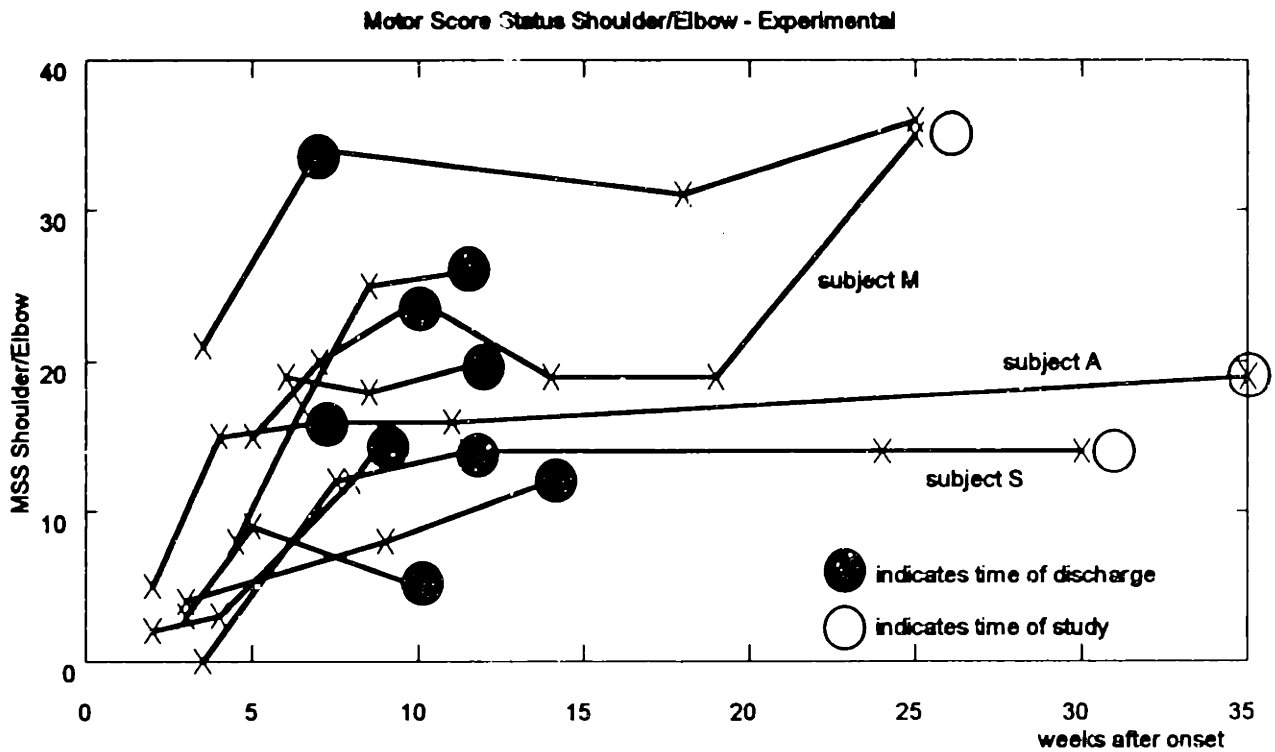

FIG.5.7. Time-Evolution of Shoulder/Elbow Motor Status Score on Selected Subjects After Hospital Discharge

Subjects living in the hospital neighborhood were invited to return for evaluations several months after their discharge. The plot shows the evolution of the three patients of the experimental group involved in the study of the effect of training and learning in the post-acute stroke phase. The three subjects have lesions involving the motor strip.

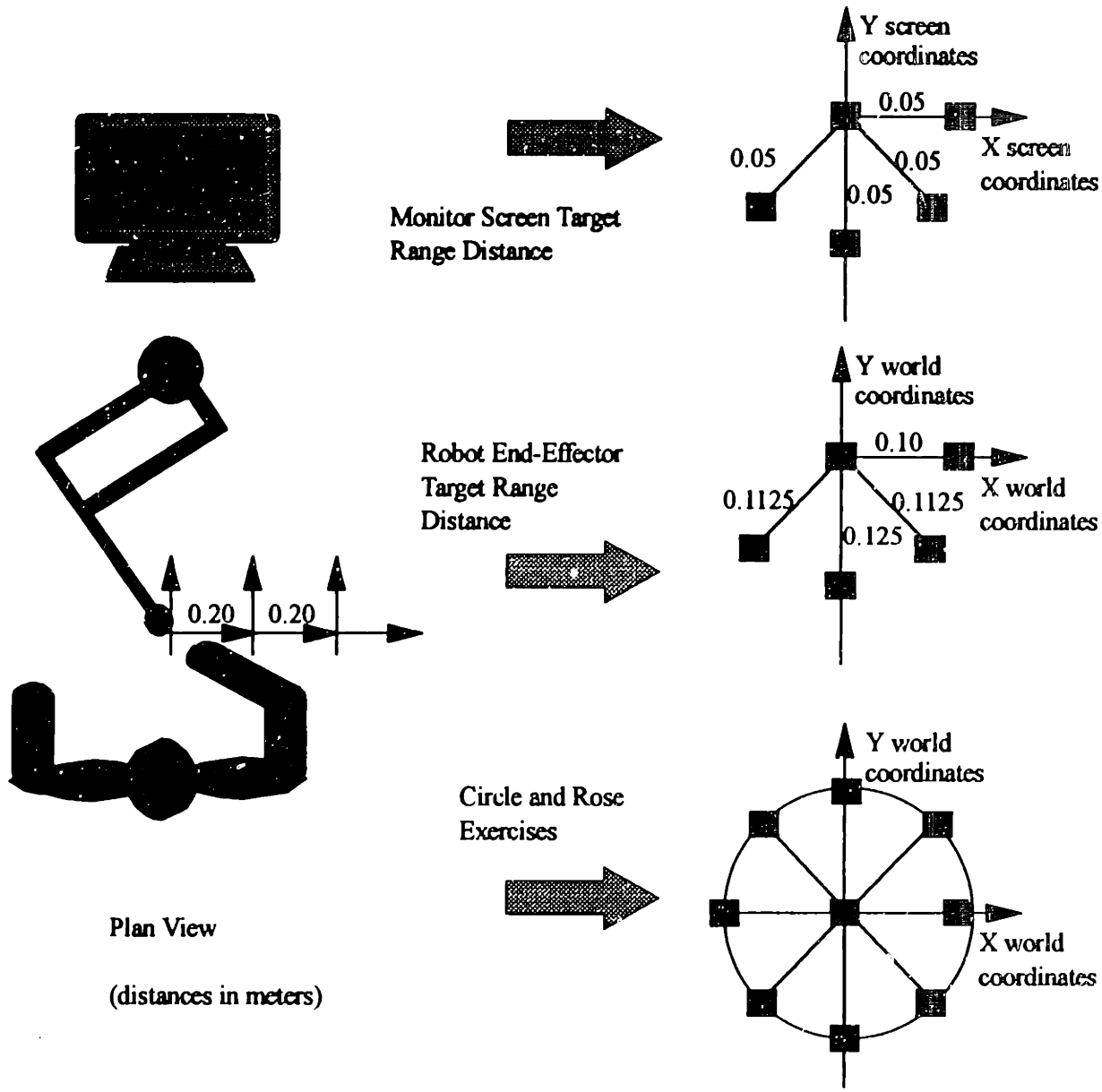

FIG.5.8. Visual and Spatial Exercise and Target Range During Training. Subjects were intensively trained and evaluated at the initial workspace region, while in acute rehabilitation. The workspace center was moved to the right (subjects A and M) and left (subject S) by 20 cm and 40 cm.

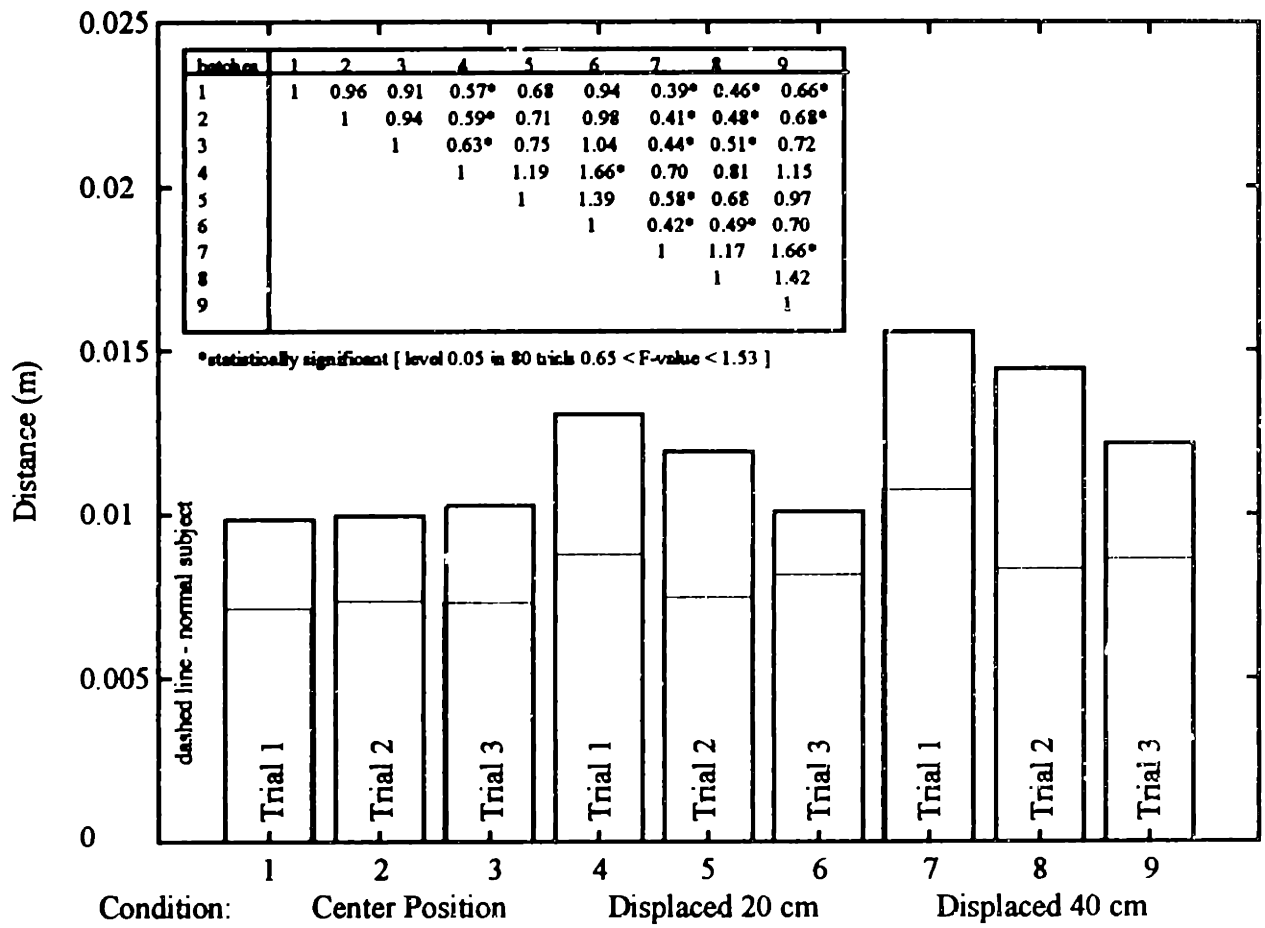

batches	1	2	3	4	5	6	7	8	9
1	1	0.96	0.91	0.57*	0.68	0.94	0.39*	0.46*	0.66*
2		1	0.94	0.59*	0.71	0.98	0.41*	0.48*	0.68*
3			1	0.63*	0.75	1.04	0.44*	0.51*	0.72
4				1	1.19	1.66*	0.70	0.81	1.15
5					1	1.39	0.58*	0.68	0.97
6						1	0.42*	0.49*	0.70
7							1	1.17	1.66*
8								1	1.42
9									1

*statistically significant [level 0.05 in 80 trials 0.65 < F-value < 1.53]

FIG.5.9.Mean Lateral Deviation from a Straight Line for Subject M
The plot shows the mean-squared deviation from the straight line thoughout the trials during week 1. This subject has a mild degree of paresis. The dashed line corresponds to the trials of the naive subject (subject did never work with the robot before). The table shows for reference a statistical test (F-test) to test the hypothesis that the means of different batches are equal.

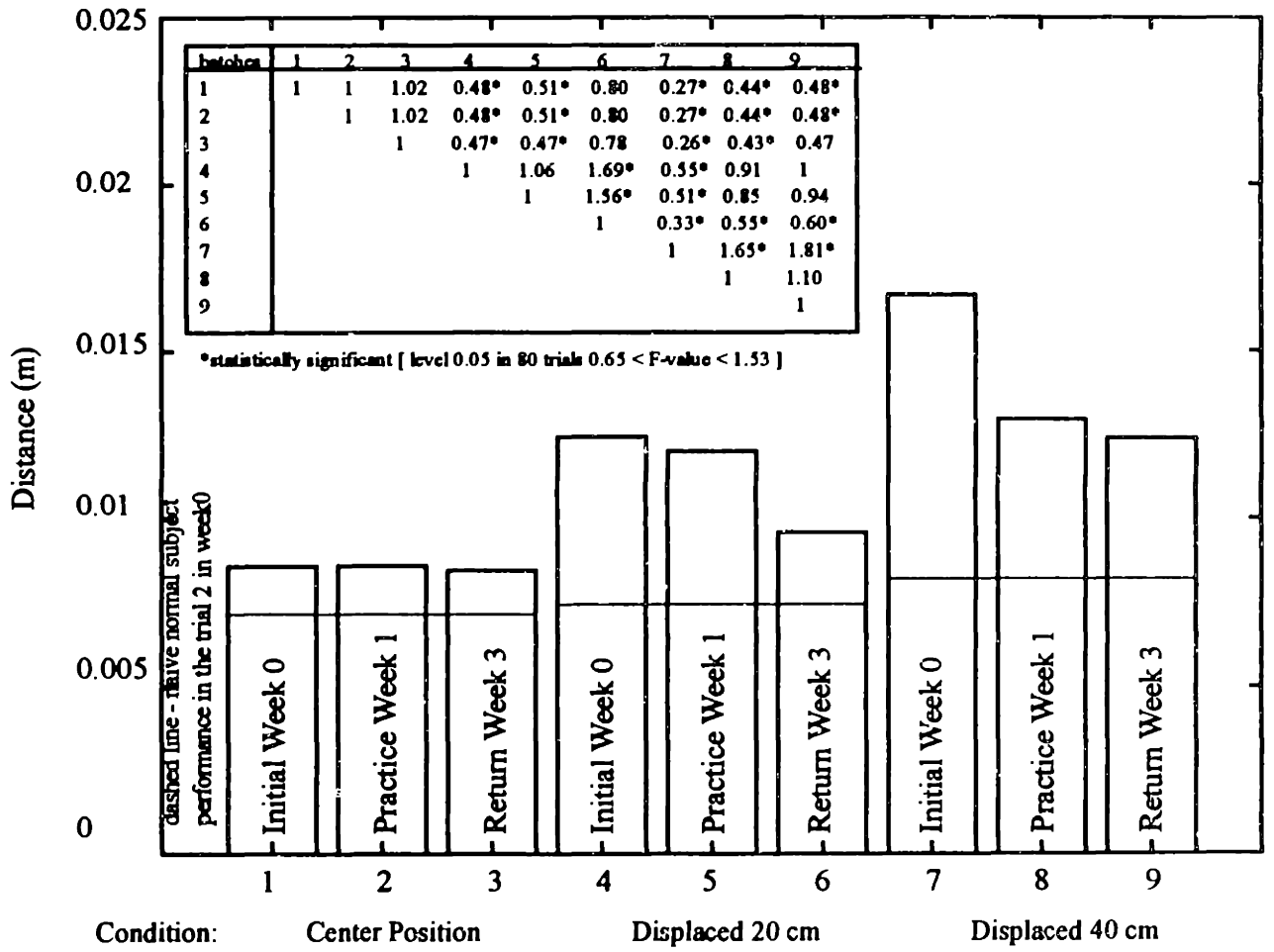

batches	1	2	3	4	5	6	7	8	9
1	1	1	1.02	0.48*	0.51*	0.80	0.27*	0.44*	0.48*
2		1	1.02	0.48*	0.51*	0.80	0.27*	0.44*	0.48*
3			1	0.47*	0.47*	0.78	0.26*	0.43*	0.47
4				1	1.06	1.69*	0.55*	0.91	1
5					1	1.56*	0.51*	0.85	0.94
6						1	0.33*	0.55*	0.60*
7							1	1.65*	1.81*
8								1	1.10
9									1

*statistically significant [level 0.05 in 80 trials 0.65 < F-value < 1.53]

FIG.5.10.Mean Lateral Deviation from a Straight Line for Subject A
The plot shows the mean-squared deviation from the straight line for the 2nd trial for each week. This subject has a severe paresis. The dashed line corresponds to the 2nd trial of the naive subject (subject did never work with the robot before). The table shows for reference a statistical test (F-test) to test the hypothesis that the means of different batches are equal.

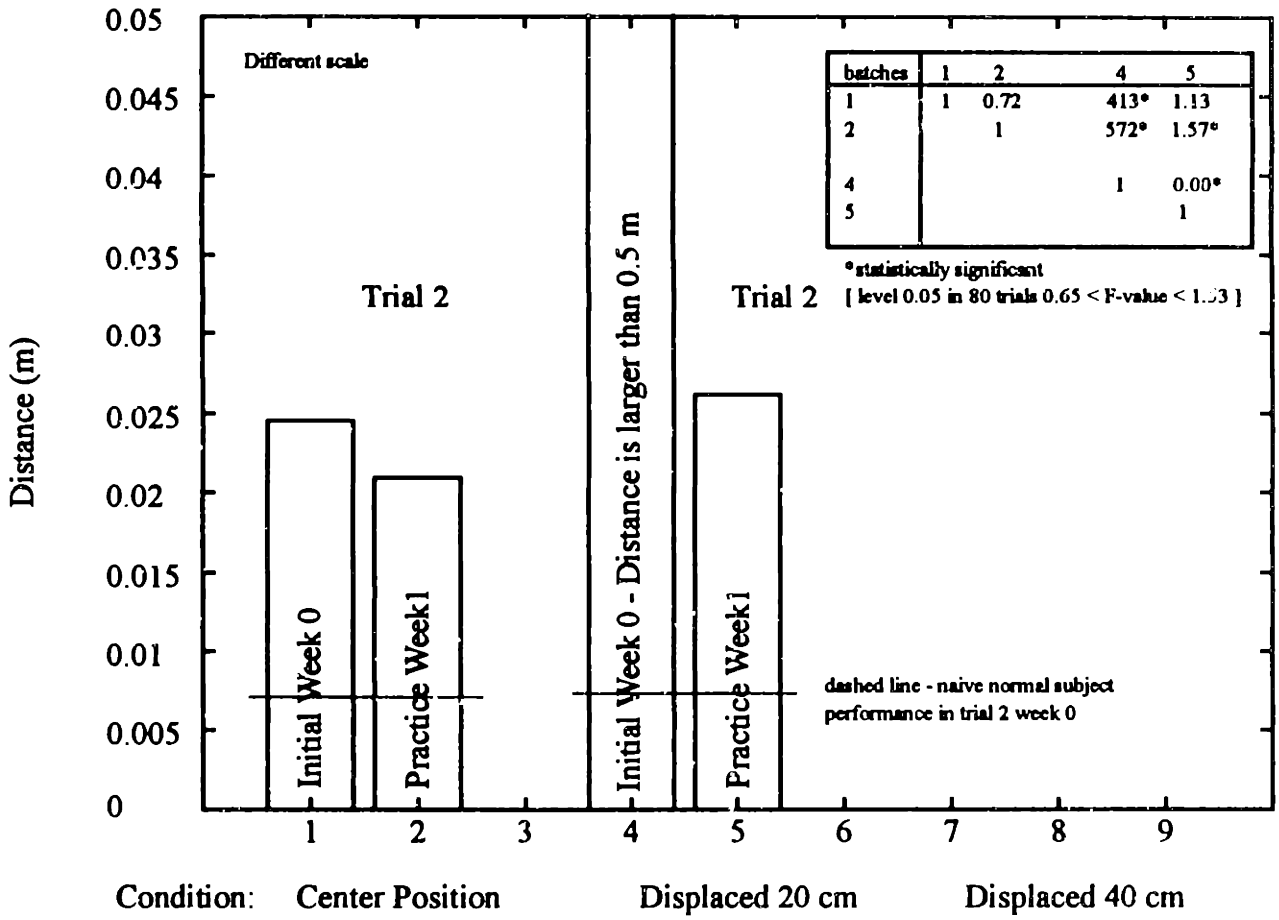

batches	1	2	4	5
1	1	0.72	413*	1.13
2		1	572*	1.57*
4			1	0.00*
5				1

*statistically significant
[level 0.05 in 80 trials 0.65 < F-value < 1.53]

FIG.5.11.Mean Lateral Deviation from a Straight Line for Subject S
The plot shows the mean-squared deviation from the straight line for the 2nd trial for each week. This subject has a very severe paresis. The dashed line corresponds to the 2nd trial of the naive subject (subject did never work with the robot before). The subject was unable to perform initially at the novel positions. After training at both new locations for a week, subject was able to move in both locations. Yet, subject could not complete the task within the predetermined time period in location 40 cm displaced from the midline. The table shows for reference a statistical test (F-test) to test the hypothesis that the means of different batches are equal.

The Copenhagen Stroke Study, mentioned earlier, suggested that further recovery of the upper extremity function should not be expected after 6 weeks for patients with mild paresis and 11 weeks for patients with severe paresis [Nakayama & Jorgensen, 1994]. Indeed, the possibility of a significant functional impact of the environment in the adult human brain during the stable phase, i.e. several months after the stroke, would appear rather remote. Nonetheless, the effect of learning and training in this post-acute phase was unknown. These preliminary results reported here demonstrate the potential for significant improvement of motor performance far beyond the acute and semi-acute phases following a cerebral vascular accident. In addition, they suggest the potential for deterioration in the most severe case. They suggest an important role of learning and training in the post-acute stroke phase with implications for general rehabilitation strategies and for the quality of life of stroke survivors.

5.5. Miscellaneous

In uncharted waters, temptation to explore prevails. During the clinical trial with stroke patients, a few case studies were performed to broaden the understanding of different neurological diseases of the central or peripheral nervous system. These included cases of spinal cord injury, myoclonus, meningioma, Parkinsonism, and multiple sclerosis. The following single-subject case studies with non-stroke related neurological diseases were chosen to illustrate other potential applications of the robot-aided neuro-rehabilitation workstation either as a measurement tool with or without pharmacological agents, or to deliver therapy. The first case study shows the potential of the device in conjunction with pharmacological agents and the second case study relates to an unusual movement disorder known as myoclonus.

5.5.1.Parkinson's Disease: Procedure for Evaluation of Pharmacological Effects on Motor Performance

Parkinsonism is a chronic, progressive, degenerative movement disorder that affects 85 to 187 in every pool of 100,000 people (race related ratio). It is characterized by bradykinesia (slowness in movement), tremor, rigidity, akinesia, and postural instability (righting ability) [Weiner & Lang,

1989]. Standard therapy consists of administration of dopamine. A single subject study of the effect of Sinemet (Levodopa) was performed in order to determine changes in motor performance early in the morning before the administration of the drug, 30 minutes, and 60 minutes after its administration.

The study used the robot-aided neuro-rehabilitation workstation described in Chapter 4. A 60 year old, left handed, male patient was enrolled in the study in accordance to the MIT-Committee on the Use of Humans as Experimental Subjects (Protocol # 2187) and the Burke Rehabilitation Hospital Human Subject Committee (Protocol # 227), which can be found in Appendix A. Written consent was obtained from the subject. The patient did not present either tremor or dementia symptoms. Nevertheless, he was classified by the attending neurologist as a Stage 5 in the Hoehn-Yahr scale with the scale ranging from 0 to 5. Stage 5 corresponds to the worst case with the patient either wheelchair bound or bedridden unless aided. The trials started in the early morning before the patient took his first daily dosage of Levodopa. The patient was instructed to grasp the robot's end-effector (palmar grasp) and hold the robot at a pre-specified position, while the robot was programmed to follow a desired trajectory consisting of three consecutive circles with the same diameter (30 cm), thus introducing a circular perturbation force (different direction and magnitude), as illustrated in Fig.5.12. For this trial, an impedance controller was implemented using nonlinear position and velocity feedback structured to produce a constant isotropic end-point stiffness and damping (50 N/m, 2 N-sec/m) which generated peak forces of 15 N. Kinematic data of the subject's movement for both hands was recorded early morning before Levodopa administration, 30 minutes and 60 minutes after. Results are shown in Fig.5.13.a. (before drug administration), Fig.513.b. (30 minutes after drug administration), and Fig.5.13.c. (60 minutes after drug administration). For comparison purposes, the results are shown with a normal subject in Fig.5.13.d. The left column shows the hand displacement and on the right column the speed profile. The submovement decoder was used as a tool to estimate the subject's motor performance via the mean basis time duration. This led to the estimates indicated in the figures for each condition with both hands. Note that before the drug administration, the subject showed a mean basis time in the left hand (dexterous hand) 40 percent longer than the right one. The results suggested a reduction in the mean basis time from 929 msec in the left hand

(663 msec in the right hand) to the 500 msec range in both hands after 30 minutes with the dexterous (most affected arm) outperforming the right one. This time range was sustained after 60 minutes. This single subject case illustrates the potential of the application of the robot-aided neuro-rehabilitation as a measurement tool in conjunction with pharmacological agents.

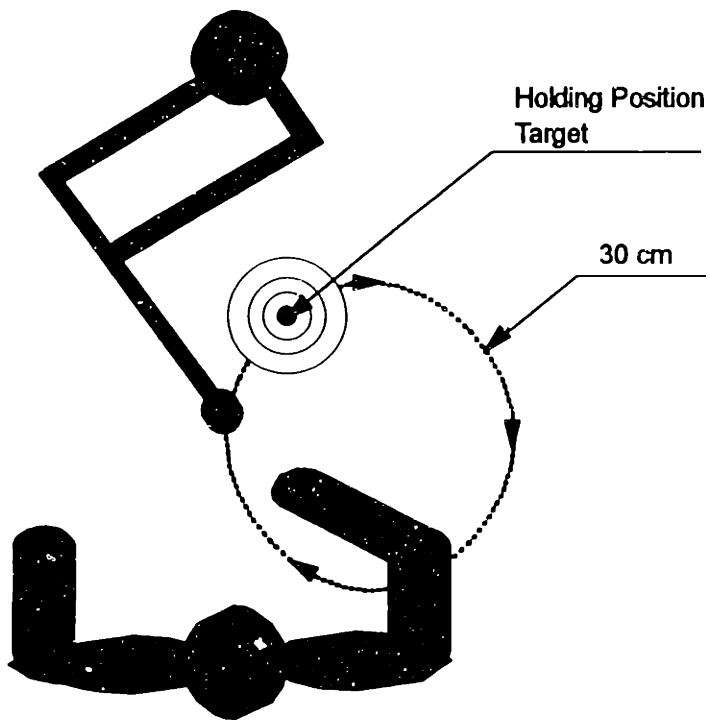

FIG.5.12. Holding Task for Parkinson Patient without Tremor
Subject was required to try to hold the robot end-effector position, while the robo was commanded by an impedance controller to perform three circles (50 N/m).

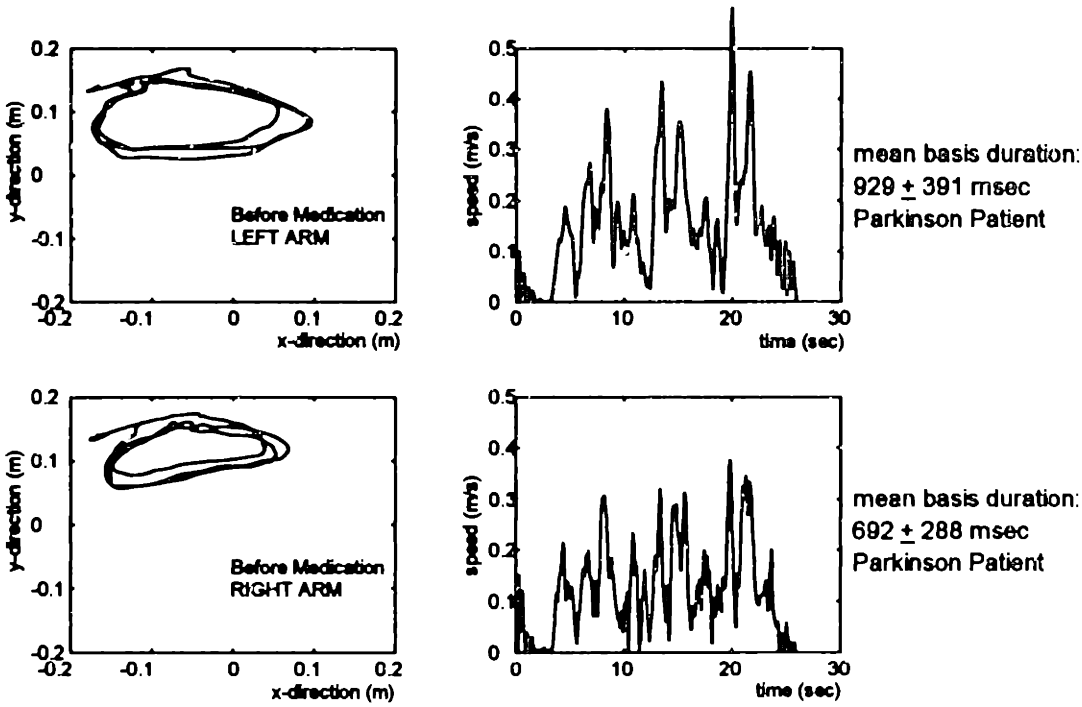

FIG.5.13.a. Parkinson Patient Holding Task Before Administration of Medication
The figure shows on the left column the hand displacement and on the right the speed. Note that subject is left handed and that the mean basis duration with that hand is 40 percent longer than with the right hand (see Fig.5.13.d. for significance levels).

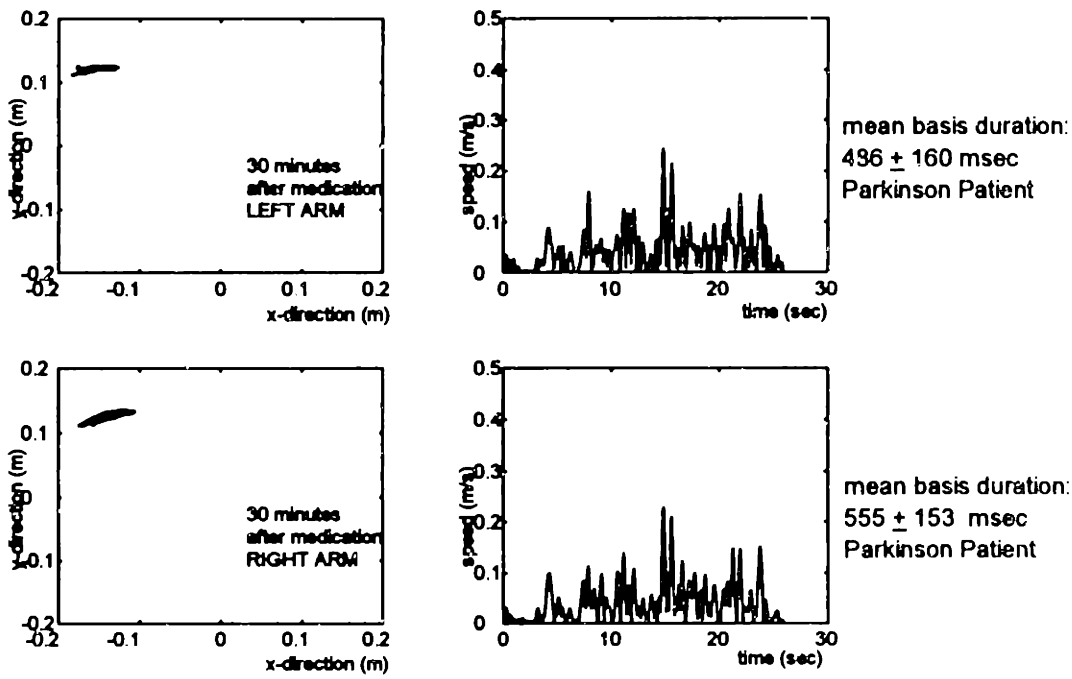

FIG.5.13.b. Parkinson Patient Holding Task 30 Minutes After Administration of Medication
The figure shows on the left column the hand displacement and on the right the speed. Note that subject's mean basis duration is much faster in both hands.

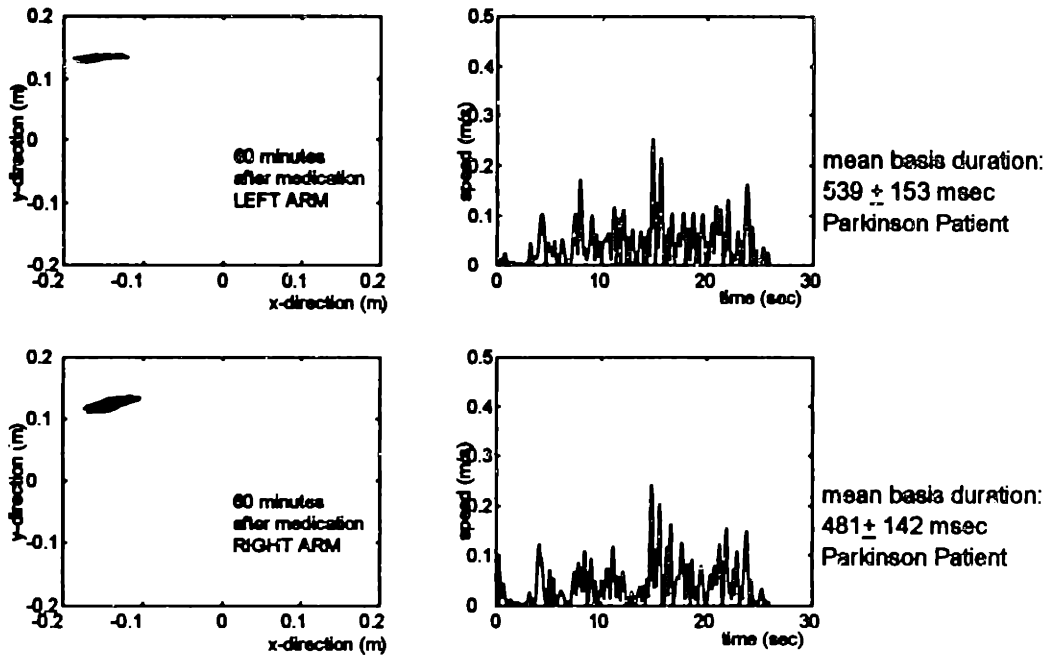

FIG.5.13.c. Parkinson Patient Holding Task 60 Minutes After Administration of Medication
The figure shows on the left column the hand displacement and on the right the speed.
Note that subject's mean basis duration is sustained in the same range.

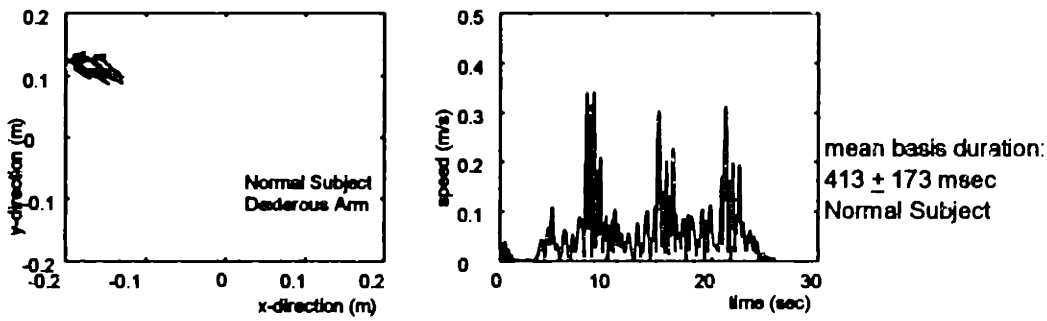

	Before - Left	Before-Right	30 mi - Left	30min-Right	60 min-Left	60min-Right	Normal
Before-Left	0	1	1	1	1	1	1
Before-Right		0	1	1	1	1	1
30 min-Left			0	0	0	0	0
30 min-Right				0	0	1	1
60 min-Left					0	0	1
60 min-Right						0	0
Normal Subject							0

FIG.5.13.d. Normal Subject Holding Task with Dexterous Arm
The figure shows on the left column the hand displacement and on the right the speed. Note that the subject displays larger speed corrections corresponding to maximum perturbation force. The table shows the hypothesis test (two-sided t-test) that the means of different experiments are equal (null hypothesis). It does not reject the null hypothesis (indicated by 0), or rejects the null hypothesis (indicated by 1) with statistical significance level of 0.05.

5.5.2. Myoclonus: Capturing a Shock-Like Movement

Myoclonic movements are brief, shock-like muscle jerks. Myoclonus is subdivided into cortical, subcortical, and spinal, and the movements are reported to last 10 to 50 msec occurring spontaneously or driven by anxiety or fatigue. In particular, Posthypoxic-Action Myoclonus is a temporary form of myoclonus typically occurring after anesthetic accidents and myocardial infarction resulting in coma [Weiner & Lang]. A single case study of this form of myoclonus investigated if the syndrome could be evoked by task-specific design aspects. The study used the robot-aided neuro-rehabilitation workstation described in Chapter 4. A 60 year old female patient suffering from an acute case of myoclonus lasting for several weeks after the comatose phase was enrolled in the study in accordance to the MIT-Committee on the Use of Humans as Experimental Subjects (Protocol # 2187) and the Burke Rehabilitation Hospital Human Subject Committee (Protocol # 227), which can be found in Appendix A. Written consent was obtained from the subject. The tasks were designed to try to evoke the shock-like muscle jerks by requiring fast movements, increasing the degree of difficulty of the fast movements, changing the goals during the execution, adding a perturbation force during movement, and changing from a single goal movement to a continuous multigoal movement. To avoid a startle, the subject was verbally and carefully informed of the different facets of each task. The tasks were performed within a week period (patient condition was improving fast) in the order mentioned below:

- Task 1. Fast Movements

The visually-evoked, visually-guided, and terminated task consisted of moving the robot end-effector from its initial position towards a target, in a point-to-point movement. The target set had a fixed number of positions in a horizontal 2D plane as shown in Fig. 5.14. The outward targets 1 to 4 were randomly presented. The inward homing target 0 was presented following each of the outward targets. Every outward target was presented an equal number of times (10 times for a total of 80 movements). The task required the subject to move her hand towards a randomly presented task within 0.8 sec. The subject had to wait after each movement during a short blackout period until the next target presentation.

- Task 2. Fast Movements of Large Amplitudes

Same as task 1, except that the magnitude of the displacement increased for outward targets lying on a circle of approximately 10 inches radius to 20 inches (Fig.5.14).

- Task 3. Change of Goal Position During Movement

Same as task 1, except that the outward target changed position during the execution in some random occasions (Fig.5.14).

- Task 4. Fast Movements in a Force Field

Same as task 1, except that a velocity dependent perturbation force field with characteristics similar to the one described in Chapter 6 was applied (Fig.5.14).

- Task 5. Random Continuous Task

The outward targets were randomly presented followed by deterministic movements back to the center. There is no waiting period as in task 1. The movement should be performed continuously.

- Task 6. Continuous Task

In this task, the randomness element was removed. All the targets were presented at the start of the trial (total 16 movements). The subject was instructed to hit all the targets in a clockwise fashion (Fig.5.14).

Results indicated that for this particular subject the shock-like muscle jerk could not be evoked in the single terminated movement tasks 1 through 4. However, it always occurred during task 5 and 6. I will not dwell on the results in the earlier group of tasks in this thesis. Some examples of the later group as exemplified in Figs.5.15. & 5.16 will be presented.

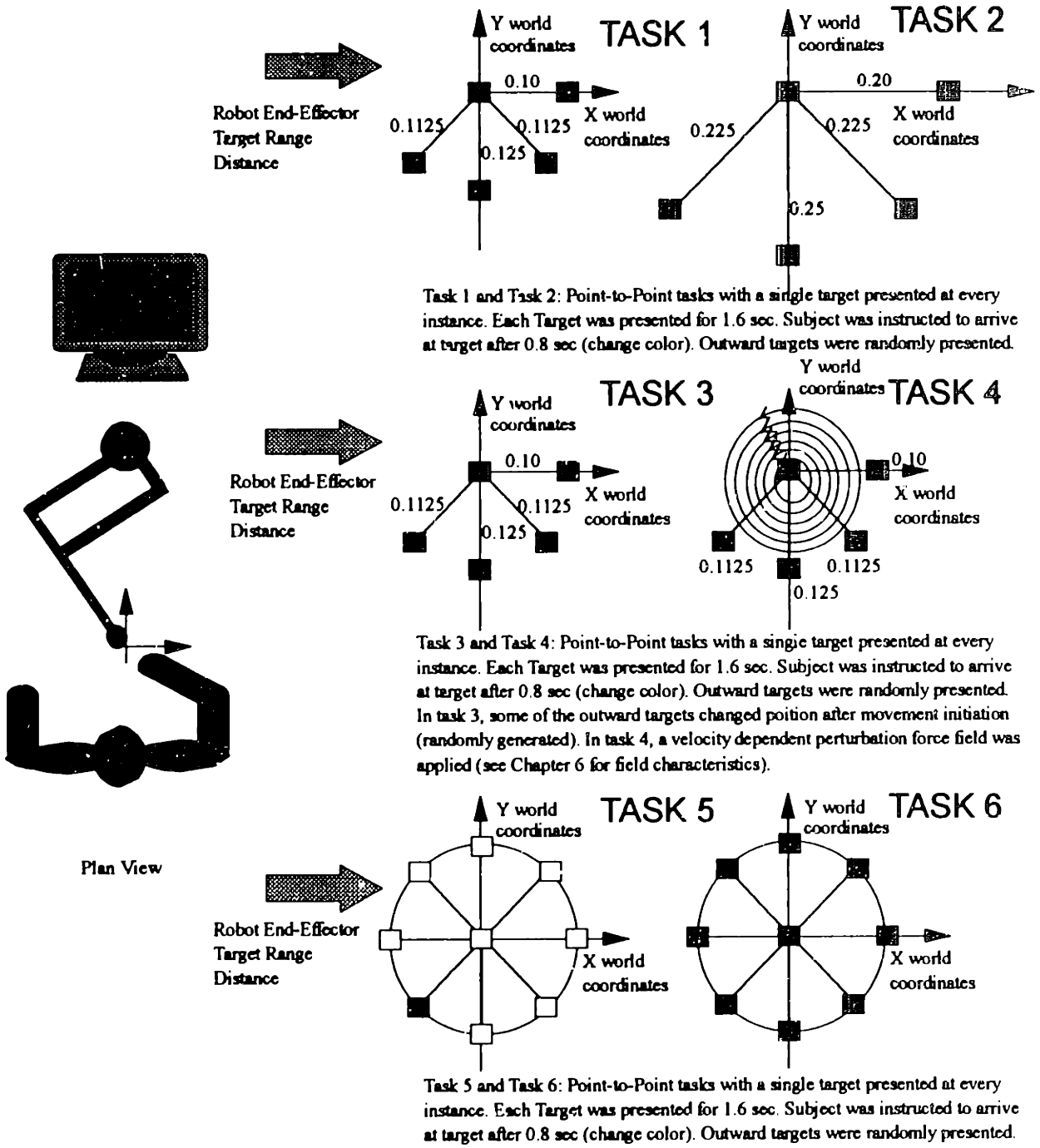

FIG.5.14. Target Range to Evoke Myoclonus

Tasks were fully explained to subject beforehand to minimize startling effect. Task 1 required fast point-to-point movements with movements completely terminated. Task 2 was similar to task 1, but required faster movements. In a few random instances, the outward target was changed after movement initiation in task 3. Task 4 was similar to task 1, except that a perturbation force field was applied. Task 5 presented one target at a time without any rest time in between. All the targets were presented at all times in task 6. Subject was required to hit them in a clockwise fashion. There was no time limit, and the movements did not have to be terminated in tasks 5 and 6.

Figure 5.15. shows examples of shock-like movements occurring during the execution of Task 5, while Fig. 5.16. shows an example of these movements occurring during the execution of Task 6. The left columns consist of the hand trace on the horizontal plane (displacement), the middle columns show the hand speed profile, and the right columns show the speed peaks above 0.3 m/sec. They were normalized to unity and aligned around a common center. To unclutter the figures, the speed profiles are shown up to the first reversal.

As for the stroke patients' data, I will try to obtain a mathematical concise formulation to describe the shock-like speed profile. The Beta distribution density function will be used to approximate the "mother" shape. Figure 5.17. shows the composite of all the previous plot expectations of the Beta function mean (p) and standard deviation (ps) for speed peaks above 0.3 m/s. Note the consistency of the expectation of the mean (intersubject), standard deviation (scale), and that the Beta function parameters are fairly close to the ones determined for the stroke patients. The resulting normalized Beta distribution density function approximation is shown in Fig.5.18. For comparison purposes, a Gaussian is shown in this figure with a standard deviation equal to half the span of the Beta function at the 0.67 level and a Minimum-Jerk profile with the same duration. The profiles peaks were centered at the same location.

The opportunity of capturing an "isolated" instance of movement is rather unique. Just as the impulse response in a linear system reveals the system transfer function, one might inquire "does the shock-like movement reveal the mother shape or the unit action ?" Most remarkable is the symmetry of these shock-like movements and their resemblance to the stroke patients' movement shape. Indeed, the speed range of the stroke group and the shock-like movements differ by an order of magnitude. One can not but ask again the question left in the apéritif section in Chapter 3 regarding this primitive shape location in the system, i.e. Is the pattern generator for the movement segment at the highest level of the central nervous system, or downstream ?

At the introduction of this subsection, it was mentioned that the literature suggests that shock-like movements last between 10 to 50 msec. The literature piece of information is based on recording of myoelectrical activity in muscles. Yet, here it was observed that in fact the movement itself

lasted an order of magnitude longer. This is an example of the technology application revealing new facets, and demonstrating for this patient that Posthypoxic-Action Myoclonus could not be evoked in a single goal presentation terminated point-to-point 2D movement, while it was always present in a multi-goal continuous point-to-point movement. I speculate that this form of myoclonus is related to the orderly "firing" of continuous movements or submovements. It also revealed a longer movement duration than previously reported and a "mother" shape for the shock-like movement that closely resemble the one identified for the stroke patients with speeds an order magnitude faster.

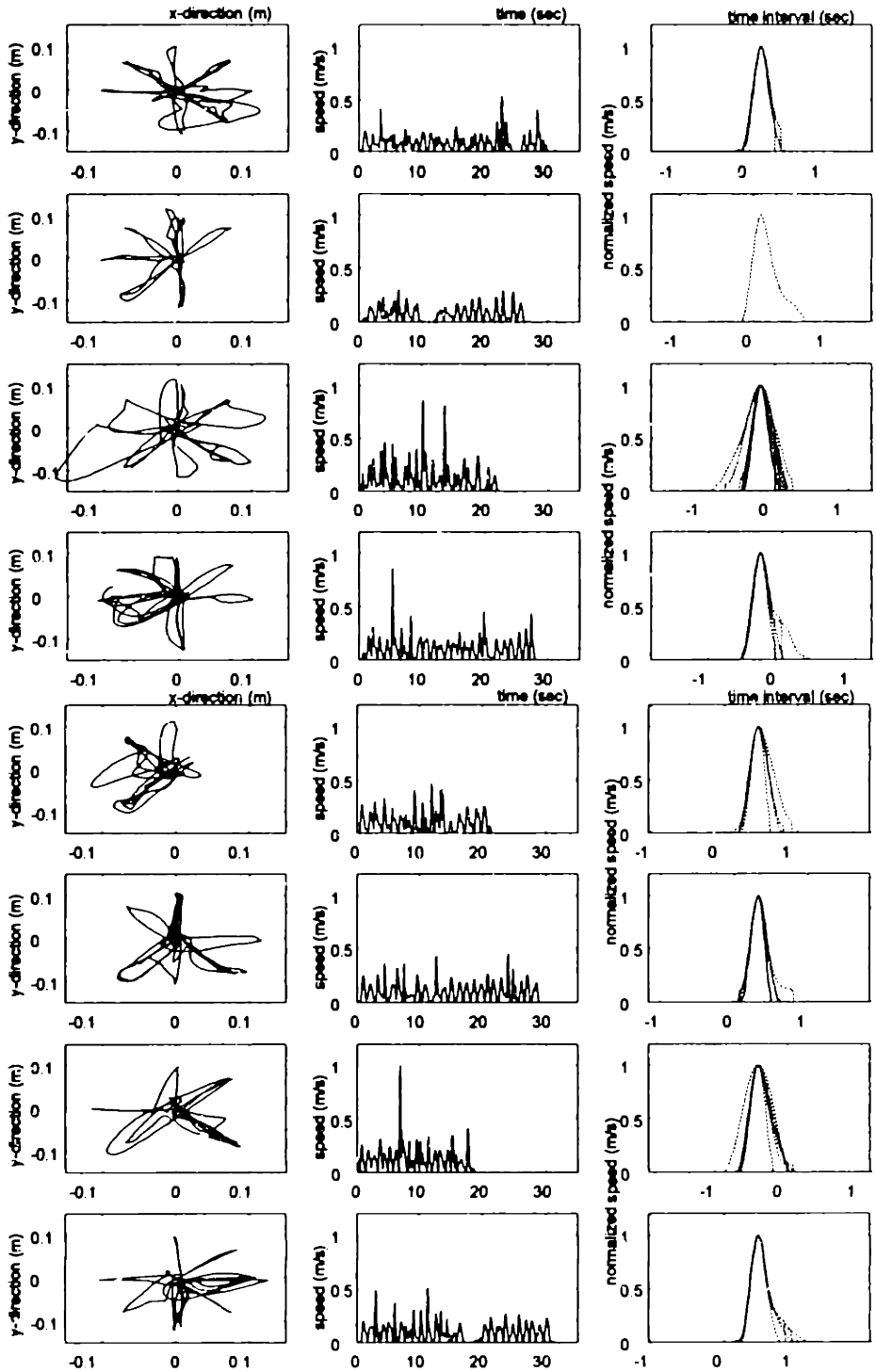

FIG.5.15.a. Kinematic Data of Myoclonus Subject in Task 5 without Time Constraint. The left column shows the hand displacement in the horizontal plane. The middle column shows the hand speed, and the right column shows the speed peaks up to the first reversal (vertical line), shifted to the same center and normalized to unity (range above 0.3m/s of top speed). This threshold was arbitrarily chosen to segregate the shock-like movements from the normal point-to-point movements. Note the remarkable resemblance of the shock-like movements for peak speeds ranging from 0.3 m/s to 1 m/s.

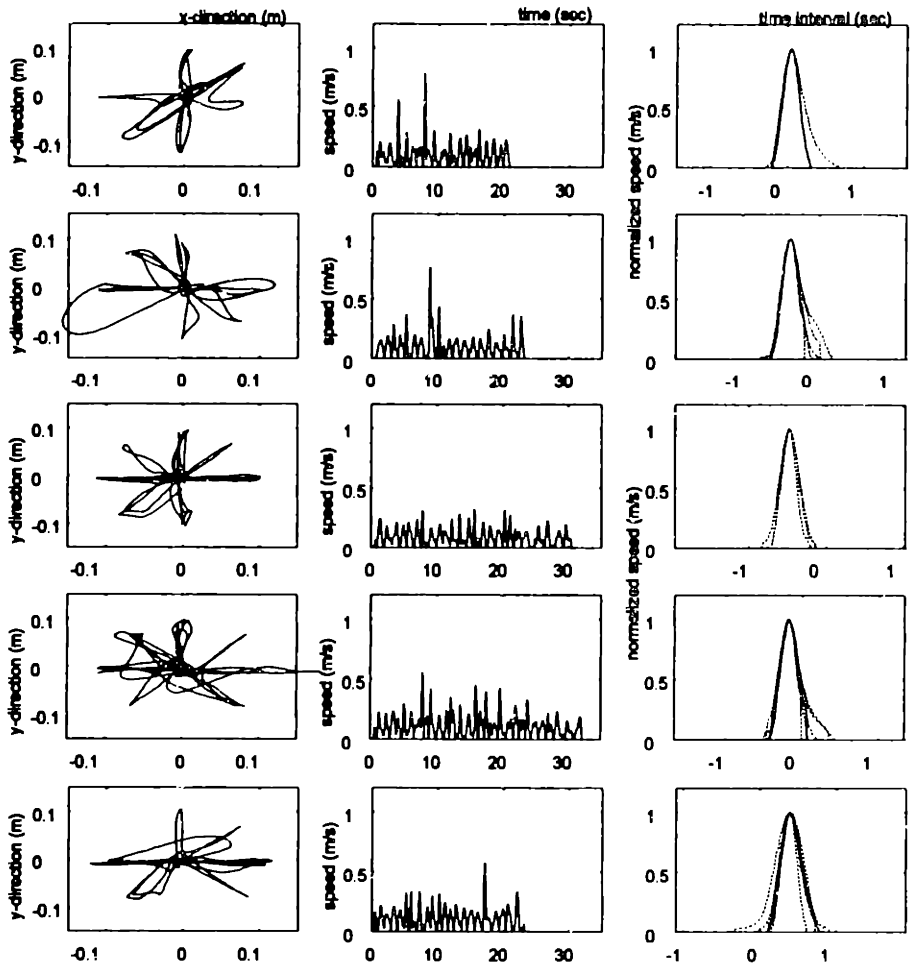

FIG.5.15.b. Kinematic Data of Myoclonus Subject in Task 5 without Time Constraint. The left column shows the hand displacement in the horizontal plane. The middle column shows the hand speed, and the right column shows the speed peaks up to the first reversal (vertical line), shifted to the same center and normalized to unity (range above 0.3m/s of top speed). This threshold was arbitrarily chosen to segregate the shock-like movements from the normal point-to-point movements. Note the remarkable resemblance of the shock-like movements for peak speeds ranging from 0.3 m/s to 1 m/s.

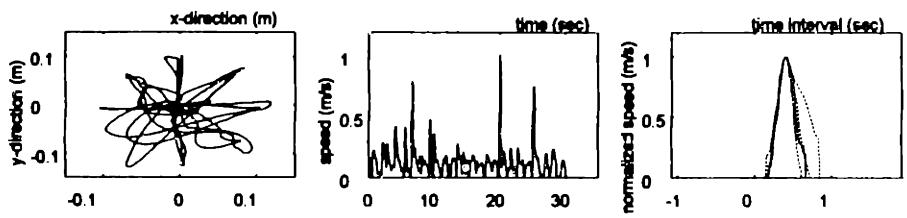

FIG.5.16. Kinematic Data of Myoclonus Subject in Task 6 without Time Constraint. The left column shows the hand displacement in the horizontal plane. The middle column shows the hand speed, and the right column shows the speed peaks up to the first reversal (vertical line), shifted to the same center and normalized to unity (range above 0.3m/s of top speed). This threshold was arbitrarily chosen to segregate the shock-like movements from the normal point-to-point movements. Note the remarkable resemblance of the shock-like movements for peak speeds ranging from 0.3 m/s to 1 m/s.

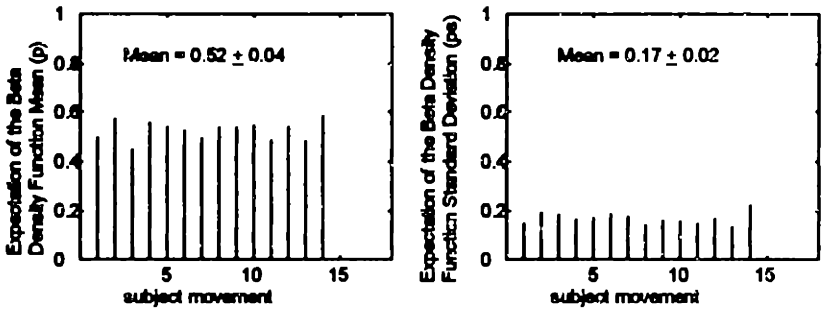

Beta Density Function

$\upsilon = p[1-p]/ps - 1$ $\qquad \upsilon = 7.64$

$\rho = \upsilon \cdot p$ $\qquad \rho = 3.97$

$\sigma = \upsilon - \rho$ $\qquad \sigma = 3.67$

FIG.5.17. Beta Density Function Parameters Determination for Myoclonus Shock-Like Movements
The parameters for the Beta Density Function were estimated from all the movements in Fig.5.13. The parameters were estimated for each speed section with peak above 0.3 m/s.

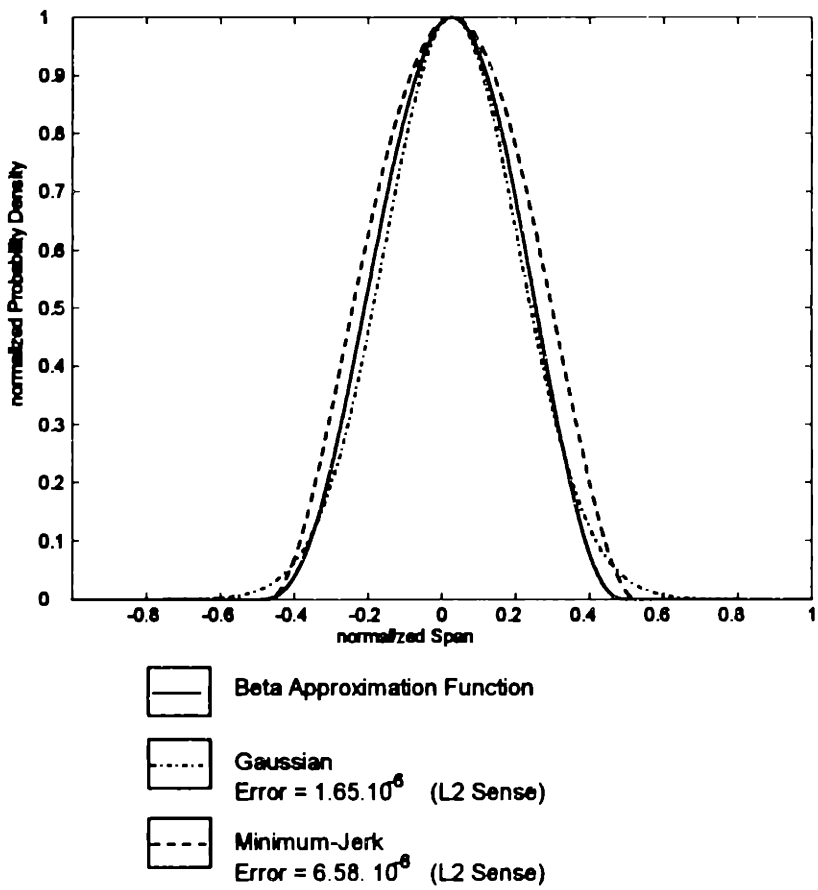

FIG.5.18. Normalized Beta Density Function for Myoclonus Shock-Like Movements
The figure shows the estimated Beta Function. It also includes a Gaussian with standard deviation equal to the Beta function span at 67% and a Minimum-Jerk curve. The peaks of the curves are centered at the same point. Note that the Beta is not symmetric with a small degree of negative asymmetry, i.e. longer tail on the left side (skewness = -0.01).

CHAPTER 6. ROBOT-AIDED FUNCTIONAL IMAGING: LEARNING A DYNAMIC TASK

It was six men of Hindostan,
To learning much inclined,
Who went to see the elephant,
(Though all of them were blind)
That each by observation
Might satisfy his mind.

The first approached the Elephant,
and happening to fall
Against his broad and sturdy side,
At once began to bawl:
"Bless me, it seems the Elephant
Is very like a wall".

The second, feeling of his tusk,
Cried, "Ho! What have we here
So very round and smooth and sharp?
To me 'tis mighty clear
This wonder of an Elephant
Is very like a spear."

The third approached the animal,
And happening to take
The squirming trunk within his hands,
Then boldly up and spake:
"I see, " quoth he, "the Elephant
Is very like a snake."

The fourth stretched out his eager hand
And felt about the knee,
"What most this mighty beast is like
Is mighty plain;" quoth he;
" 'Tis clear enough the Elephant
Is very like a tree."

The fifth who chanced to touch the ear
Said, "Even the blindest man
Can tell what this resembles most;
Deny the fact who can,
This marvel of Elephant
Is very like a fan."

The sixth no sooner had begun
About the beast to grope,
Than, seizing on the swinging tail
That fell within his scope,
"I see," cried he, "the Elephant
Is very like a rope."

And so the men of Hindostan
Disputed loud and long,
Each in his own opinion
Exceeding stiff and strong,
Though each was partly in the right
And all were in wrong.

— The Blind Men and The Elephant
— John Godfrey Saxe — 1816-1887

6.1. Background

Techniques for measuring and manipulating functional movements when correlated with neural activity would add a new dimension to basic and clinical research on neuro-motor function. Imaging technologies provide sensitive tools for measuring neural activity. Pharmaceutical interventions provide new and powerful ways to influence neural activity. To understand the functional motor consequences of neural activity, a comparable facility to measure and manipulate the motor system is needed. Robotic technology can serve that purpose.

This chapter reports on a novel application of robotic technology to functional brain imaging for the purpose of studying motor learning. The study examined neural activity underlying a dynamic motor learning task. In particular, the goals were: (a) to determine whether learning a motor task involves areas of the brain distinct from those involved in the performance of that task, (b) what changes in neural activity coincide with performance improvement, (c) to explore the different levels of organization of the putative higher level controller, and (d) to verify the competency of performance measurement tools based on the concepts of movement segmentation and submovements described in chapter 2.

Several individuals were involved in this particular implementation. Prof. Neville Hogan and I have been discussing this combination of technologies for at least half of my present stay at MIT. Dr. Robert H. Rubin provided the critical funding for the PET Scans via a grant from the MIT Clinical Research Center (GCRC Grant M01RR00088). Prof. Emilio Bizzi was the research "matchmaker". The force-field concept and learning paradigm were suggested by Dr. Reza Shadmehr (presently at John Hopkins University) from his work with Dr. Sandro Mussa-Ivaldi (presently at Northwestern University) [Reza & Sandro]. Dr. Alan J. Fischman (Massachusetts General Hospital - MGH) arranged for the weekend scans to allow the use of the same portable robot simultaneously in two different experiments 200 miles apart, and Dr. Nathaniel M. Alpert (MGH) granted us unrestricted access to imaging analysis tools. Dr. Scott L. Rauch (MGH) and Dr. Cary R. Savage (MGH) spent several weekends patiently teaching us how to process the images. Steve Weise (MGH) and John A. Correa (MGH) spent their leisure weekends running

the cyclotron and the PET camera. Last but not least, my colleague in this research, Dr. Thomas Brashers-Krug (presently at John Hopkins University), shared the responsibility for the experiments and imaging analysis, while primarily focusing on the motor memory field.

6.1.1. Functional Imaging

As stated in the previous chapter's introduction, there are no significant energy reservoirs in the brain. Nutrients must be continuously supplied (e.g. oxygen, glucose), and waste products removed (e.g.carbon dioxide, lactic acid). Any increase of activity in a particular brain region requires an immediate increase in the nutrients supplied through selective dilation of cerebral arteries, a fact postulated almost a century ago by Sherrington [Roy & Sherrington, 1890]. This process provides the basis for the functional imaging techniques that monitor consumption of glucose or oxygen; which are presumed to correlate with cellular activity in the brain. In fact, functional imaging devices can detect new patterns of neural activity within a few seconds after the change in associated activity, e.g. motor activity. Physical aspects behind the detection process are critical, and there exist a variety of functional imaging devices, e.g. SPECT (Single Photon Emission Computed Tomography), PET (Positron Emission Tomography), and NMR or MRI (Nuclear Magnetic Resonance or Magnetic Resonance Imaging).

6.1.2. Learning

Chapter 2 presented a bibliographic overview on the submovement phenomenon and its plausible connection with learning. Hofsten's experiments with 12 to 24 week old infants and Milner's peg-insertion experiments represent two examples of studies in the motor learning literature suggest the relationship between submovements and learning. However, two other elegant studies, incorporating an idea expressed by the Russian physiologist Bernstein, served as inspirational guides for this chapter. Bernstein suggested that since we cannot directly access the inputs to the human motor system, we have to fool it [talk comment -- 1994]. Bernstein's description preceded the forging of the term: "virtual environments". The first experiment by Shadmehr and Mussa-Ivaldi [Shadmehr & Mussa Ivaldi, 1994] used a robotic device, developed

by one of my laboratory predecessors [Faye, 1986], to generate a force field with the shape of a saddle that responded to the subjects' arm movements, thereby generating a "haptic virtual environment" that subjects learned to manipulate. The second experiment by Wolpert, Ghahramani and Jordan used a semi-silvered mirror and a computer controlled projector to generate a "visual virtual environment" increasing the perceived curvature [Wolpert, Ghahramani, & Jordan, 1994]. Both experiments required the subjects to make point-to-point movements to targets within the "virtual environments", and concluded in favor of kinematic planning (versus dynamic) for reaching movements. Furthermore, Shadmehr and Mussa-Ivaldi suggested that during learning, the motor controller composed an internal model of the force field. They expressed a view similar to Woodworth [Woodworth, 1899] against the concept that "corrective movements" (submovements) were involved during learning of this task, since in their task the subjects did not have any visual feedback of their hand during the movement execution, only proprioceptive. Rather, they attributed the speed oscillation only to the system's mechanical response of a "robust" control system implementing a single program.

6.2. Subjects

Eight subjects were involved in this study in accordance with the guidelines and approval of the MIT-Committee on the Use of Human Experimental Subjects and Massachusetts General Hospital Human Subject Committee. All the subjects were males, between 21 and 35 years old (mean 24), right-handed by the Edinburgh Inventory with a handedness quotient > 75% [Oldfield, 1971] , and native English speakers. The subjects were identified as normals (no neurological deficit). All subjects had no previous experience with the learning task.

6.3. Experimental Setup and Procedure

This study used the PET facility of the Massachusetts General Hospital which includes a GE Scanditronix PC4096 15-slices whole-body tomograph. Experimental subjects inhaled the tracer ^{15}O - CO_2 gas via a nasal cannula underneath a vacuum face mask to measure the regional cerebral blood flow, while performing a specified motor task. The transverse resolution after

reconstruction was 8 mm (hanning-weighted reconstruction filter). The radioactive tracer was synthesized via a cyclotron on-site. The 2-dof module of a novel portable robot designed for clinical neurological applications: MIT-MANUS was used. The 2-dof robot module is described in some detail in Chapter 4. A custom-made monitor hold was built to allow the subject's monitor to rest prone close to the ceiling above the PET table. This allowed the subject, while supine on the PET table, to view the monitor and access the handle on the robot end-effector (Fig.6.1. & 6.2.).

The visually-evoked and visually-guided task consisted of moving the robot end-effector from its initial position towards a target, in a point-to-point movement. The target set had a fixed number of positions in a horizontal 2D plane as shown in Fig.6.3. The outward targets 1 to 4 were randomly presented. The inward homing target 0 was presented following each of the outward targets. Every outward target was presented an equal number of times. Note that the hand coordinates were different from the visual coordinates, in order to compensate for the rectangularity of the monitor. The subject, while supine on the PET table, grasped a handle on the end-effector of the robot, as illustrated in Fig.6.4. He was instructed to move the end-effector to the presented target within 0.8 sec. The color of the target changed for the subsequent 0.8 sec, and a new target was presented. The monitor screen rested prone, therefore, moving the end-effector handle towards the subject's head corresponded to moving up on the monitor. The subject's movement was performed predominantly with the arm and forearm.

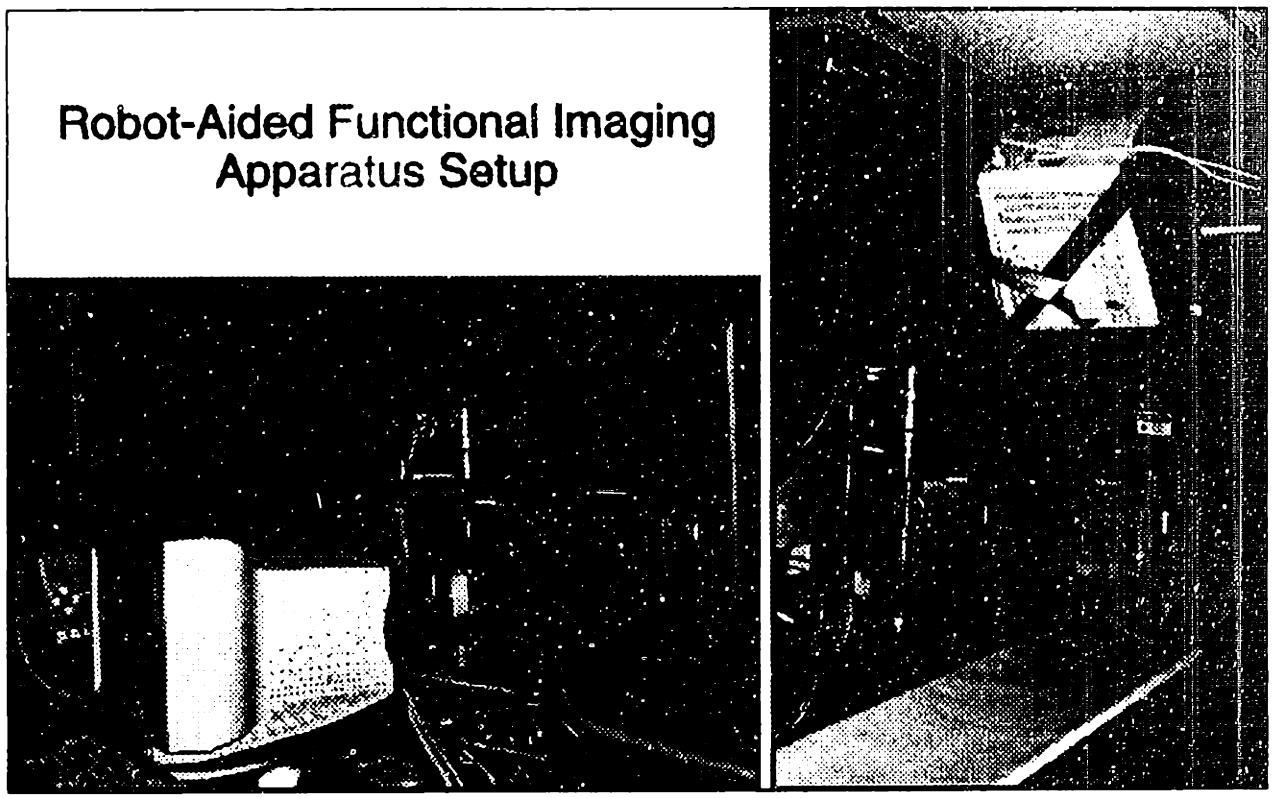

FIG.6.1. Robot-Aided Functional Imaging Apparatus Setup

This study used the PET facility of the Massachusetts General Hospital which includes a GE Scanditronix PC4096 15-slices whole-body tomograph. We used the 2-dof module of a novel portable robot designed for clinical neurological applications: MIT-MANUS. A custom-made monitor hold was built to allow the subject's monitor to rest prone close to the ceiling above the PET table.

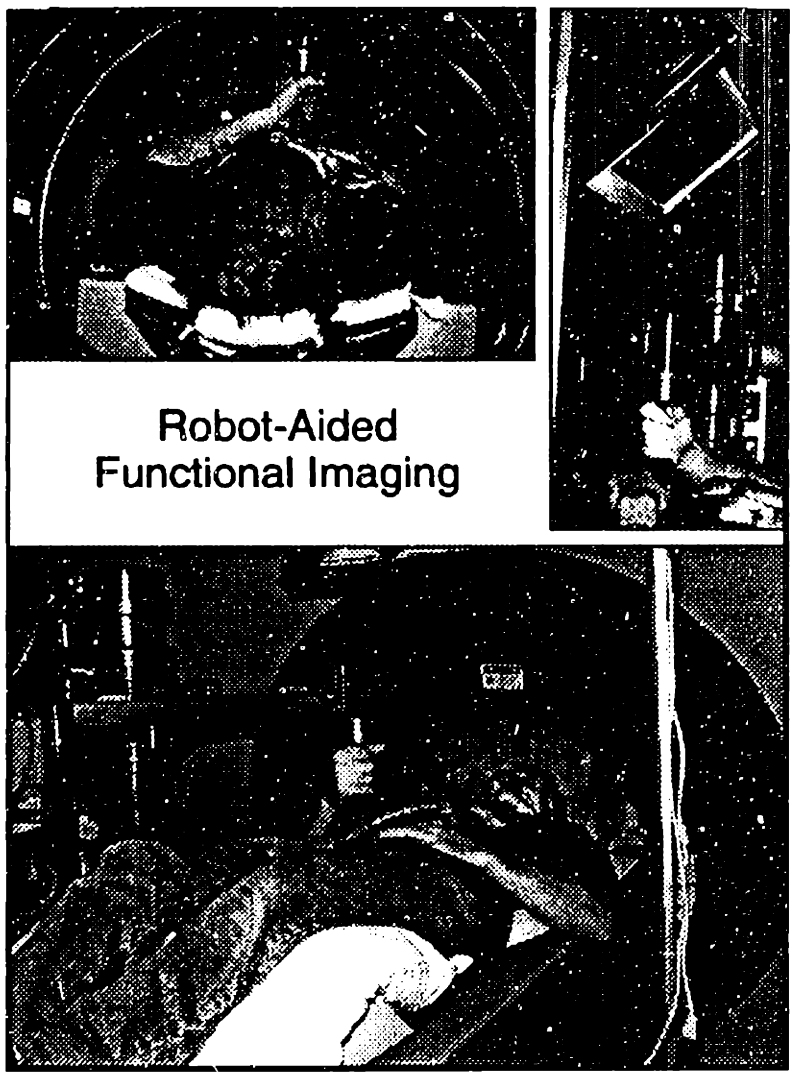

FIG.6.2. Robot-Aided Functional Imaging Setup with Subject
Experimental subjects inhaled the tracer O^{15}- CO_2 gas via a nasal cannula underneath a vacuum face mask to measure the regional cerebral blood flow, while performing a specified motor task. A custom-made monitor hold was built to allow the subject's monitor to rest prone close to the ceiling above the PET table. This allows the subject, while supine on the PET table, to view the monitor and access the handle on the robot end-effector.

The robot measured the kinematics and dynamics of the subject's hand motions, and imposed perturbation forces as follows:

Condition 1 - Motor Performance: The robot generated no perturbation but recorded the behavior of the subject (batches 1 & 2). The subject practiced as needed to become fully comfortable with the task.

Condition 2 - Early Motor Learning: The robot measured the behavior and also perturbed the movement of the subject (batches 3 & 4).

Condition 3 - Late Motor Learning: The robot measured the behavior and also perturbed the movement of the subject (batches 5 & 6). The subject had practiced the task as needed to become fully comfortable with it.

Condition 4 - Negative Transfer: The characteristic of the perturbation forces was reversed (batches 7 & 8).

The perturbation forces were velocity-dependent, generating a conservative force field ($\vec{F}' \bullet \vec{V} = 0$) according to the following relations:

$$\begin{bmatrix} Fx \\ Fy \end{bmatrix} = \begin{bmatrix} 0 & -B \\ B & 0 \end{bmatrix} \begin{bmatrix} Vx \\ Vy \end{bmatrix} \qquad \text{(eq. 6.1.)}$$

where B is a coefficient equal to 12 or -12 N.sec/m; the velocity in X-Y direction (Vx, Vy) are given in m/sec; and the forces in the X-Y direction (Fx, Fy) are in Newtons with X-Y directions indicated in Fig.6.3.

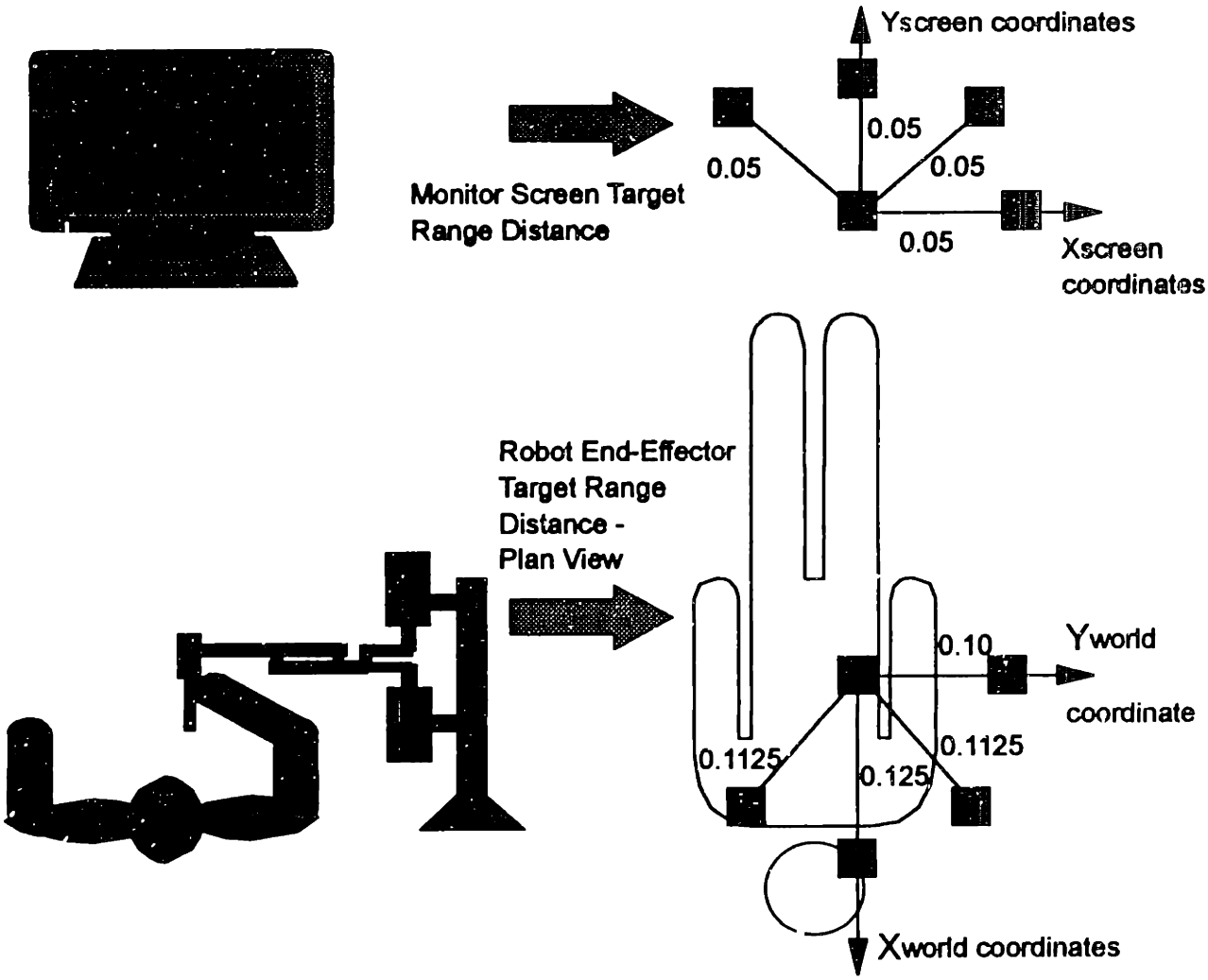

(distances in meters)

FIG.6.3. Visual and Spatial Target Range Subject while supine has to move robot's end-effector (world coordinates) to hit the targets shown on computer monitor.

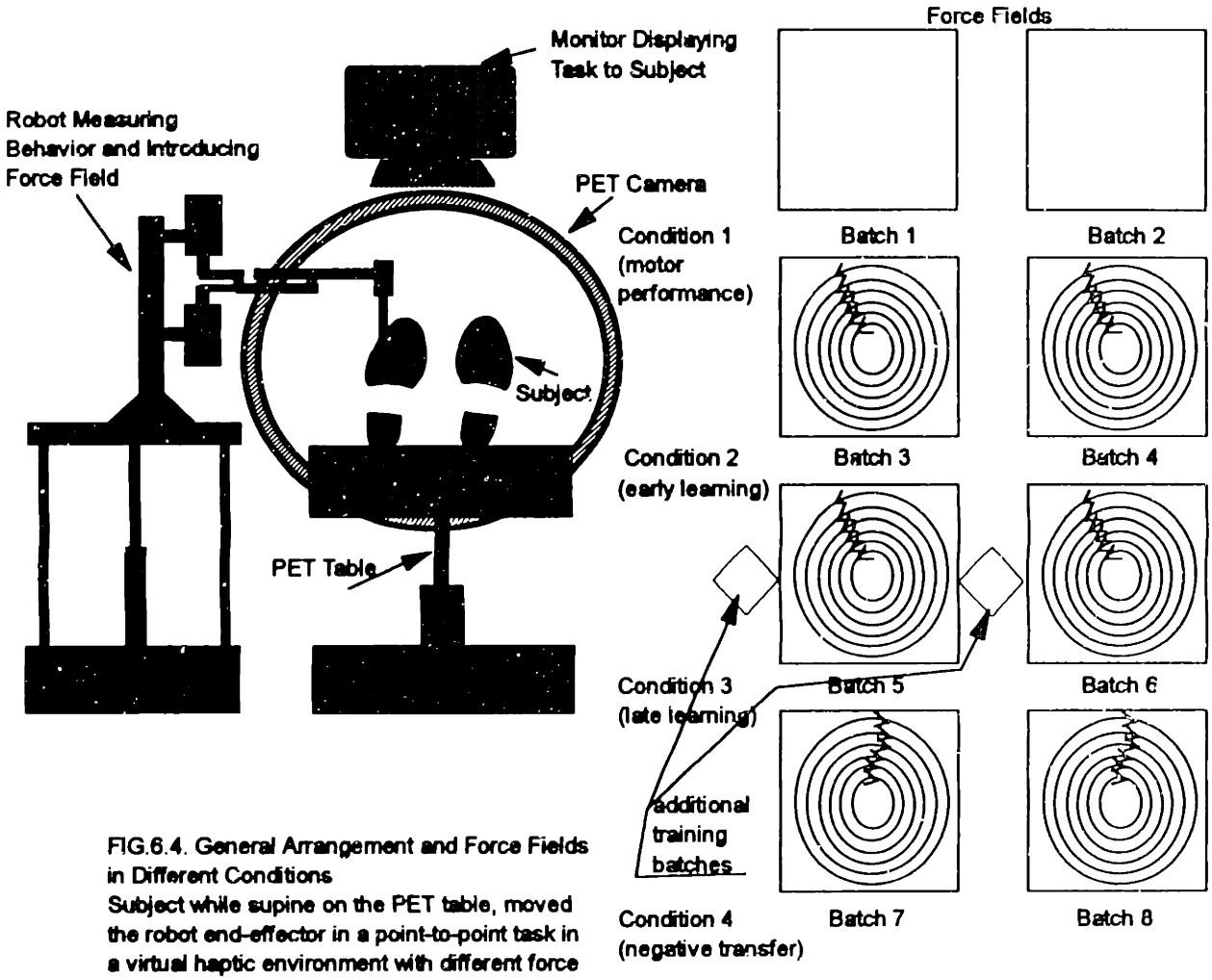

FIG.6.4. General Arrangement and Force Fields in Different Conditions
Subject while supine on the PET table, moved the robot end-effector in a point-to-point task in a virtual haptic environment with different force fields in each condition.

All conditions described above were divided into two batches. Each batch has a total of 80 movements (40 movements to the outward positions and 40 movements to the homing position). A PET scan began 30 seconds after the movement task was initiated. Scanning continued for 60 seconds. Frames in these 60 seconds of the scan were summed after reconstruction to form the rCBF images. Between the scans the subjects rested for 5 minutes and practiced as needed to become fully comfortable with the task. The PET 15-slice image set for each scan was generated using the Massachusetts General Hospital procedure [Rauch, Savage & Alpert, 1995]. The brain images were transformed to the standard 1988 Talairach's coordinate system using a least squares fitting program [Alpert, 1993] [Talairach, 1988]. The results depicted 30 horizontal slices located 4mm apart. The horizontal reference plane was at the Anterior-Posterior Commissural line

(AC-PC). Statistical parametric maps were generated with units in Z score. The threshold for significance was set at a $z = 3.0$, which corresponds approximately to a probability threshold of a false indication of $p < 0.001$. Subtractions were performed between each of the batches above. For the same activation in different horizontal planes, only the activation with the highest Z score is reported here.

6.4. Results

The novel combination of technologies provides a facility to measure and manipulate different facets of the same underlying phenomenon, i.e. it allows for the exploration of the different levels of organization of the higher level controller and the functional "outputs" of the neuro-motor system. The results were organized to report on the patterns of neural activity, as well as on the corresponding patterns of motor activity via a simple numerical measure of kinematic performance: the lateral deviation of the hand (end-effector) from the straight line connecting the homing target with the outbound target, and a performance measurement tool based on the concepts of movement segmentation and submovements.

6.4.1. Changes in Neural Activity

Kinematic data from a prior learning task experiment was also used to determine how to aggregate the PET scans to increase the number of degrees of freedom of the statistical parametric analysis. The batches of each condition were aggregated as follows: batch 1&2, 3&4, 5&6, 7&8. Motor Performance scans (baseline) were subtracted from the scans acquired in the Early Learning, Late Learning, and Negative Transfer conditions. These results indicated the areas with significant increases in rCBF during different phases of motor learning. Areas of neural activation, associated with specific stages in the acquisition of a complex motor skill, were identified via the PET results and behavioral measures of learning.

The Early and Late Learning conditions were both associated with bilateral increase of activation of parietal association areas and contralateral left hemisphere primary sensory cortex. As subjects

became skilled at the motor task, foci of activation increase shifted from ipsilateral right parietal association areas (Early Learning) to contralateral left motor and pre-motor cortex (Late Learning). As the characteristic of the perturbation force field was reversed (Negative Transfer), foci of activation on the contralateral left hemisphere continued to show an increase in activation in the primary sensory, pre-motor, and parietal cortex, although there was also bilateral increase in activation in the thalamus. Other areas showing differential activations included: bilateral ventral striatum, which showed a significant increases in rCBF in Early Learning; contralateral left ventral striatum, which showed a significant decrease in activation during Negative Transfer; contralateral left premotor area, which showed a significant decrease in activation in Early Learning, but showed a significant increase in activation in Late Learning and Negative Transfer; the ipsilateral right primary motor area, which showed a significant increase in activation during Negative Transfer; bilateral posterior cingulate, which showed a decrease in activation during Early Learning and Negative Transfer; contralateral left posterior cingulate, which showed a decrease in activation during Late Learning; and the ispilateral right cerebellar cortex, which showed a significant increases in Late Learning and Negative Transfer. Figures 6.5. to 6.7. summarize the regions with significant activations. Tables Activation.1.a.&b to Activation.5.a&b list the areas with significant activation (Appendix D).

The pattern of neural activity indicates that early implicit learning (Early Learning) involves the ipsilateral right striatum (figure 6) and right parietal cortex. The increase in activation in the ipsilateral right parietal area during Early Learning may be consistent with its suggested dominant role in spatial tasks [Mesulam, 1985]. Likewise, the increase in activation in the ipsilateral right ventral striatum is consistent with the findings in implicit sequence learning [Rauch, Savage & Brown, 1995]. Further experiments are required to determine if this finding is specific to the right hemisphere or due to details of our experimental design (e.g. a right handed task performed by right handed subjects). The pattern of neural activity also indicates a decrease of activity in the premotor area during Early Learning (naive subjects). It has been shown that the direction of the intended hand path is encoded by a task-related pool of neurons in the motor areas [Georgopoulos, 1984][Kalaska, 1989]. I speculate that during Early Learning the direction of the intended hand path is yet to be determined. As subjects became skilled at the motor task (Late

Learning), the pattern of neural activity shifted to the cortico-cerebello-cortical feedback loop. This result shows similarities with other studies on motor learning. For example, Grafton [Grafton, 1994] studied procedural motor learning in a pursuit rotor task (implicit motor learning). His comparison of three sequential scans during motor skill acquisition also showed an increase in the cortico-cerebello-cortical loop. The results in the Late Learning phase are consistent with the hypothesis that procedural learning takes place in the motor execution areas. Yet, these results also suggest the existence of different types of implicit learning (Early and Late Implicit Learning), occurring in an orderly fashion at different rates, and that distinct neural structures may be involved in these different stages. The cortico-cerebello-cortical feedback loop increase in activation persisted throughout the adaptation to the novel perturbation force field with reversed characteristic (Negative Transfer). The difference in the activation pattern during the novel task with a naive subject (Early Learning) and the novel task with an expert subject (Negative Transfer) suggests different learning mechanisms. The later one resembles the results in the Late Learning phase and is consistent with the hypothesis that procedural learning takes place in the motor execution areas. I speculate that expert subject learning (Negative Transfer) also involves the bilateral cortico-thalamic-cortical loop. A notable difference of our results from other studies is the lack of statistically significant differential activation in the supplementary motor area.

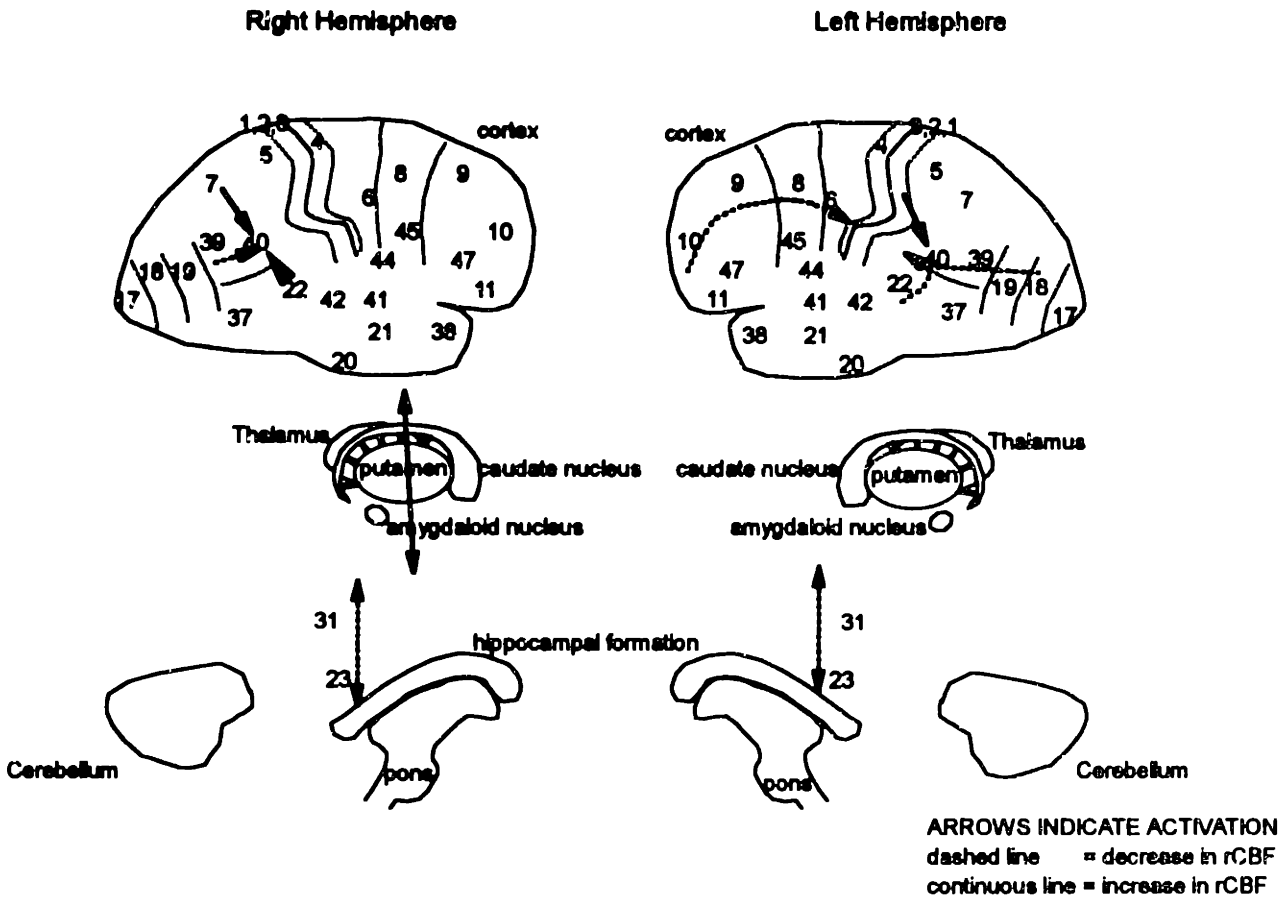

Fig.6.5. Early vs Baseline rCBF Activations
Summarizes areas with significant increase and decrease in rCBF during the Early Learning condition when compared with the Motor Performance condition (baseline)

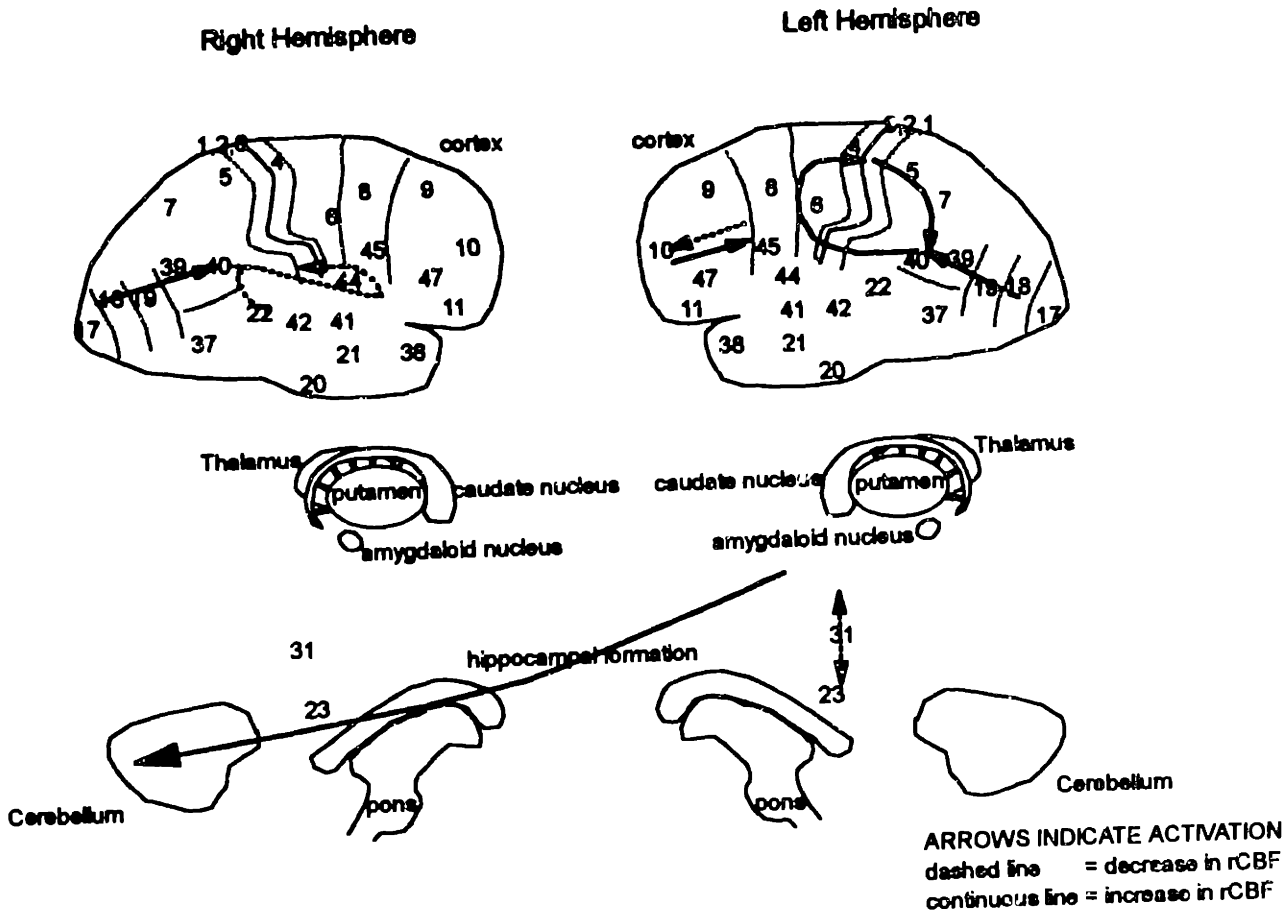

Fig.6.6. Late vs Baseline rCBF Activations Summarizes areas with significant increase and decrease in rCBF during the Late Learning condition when compared with the Motor Performance condition (baseline)

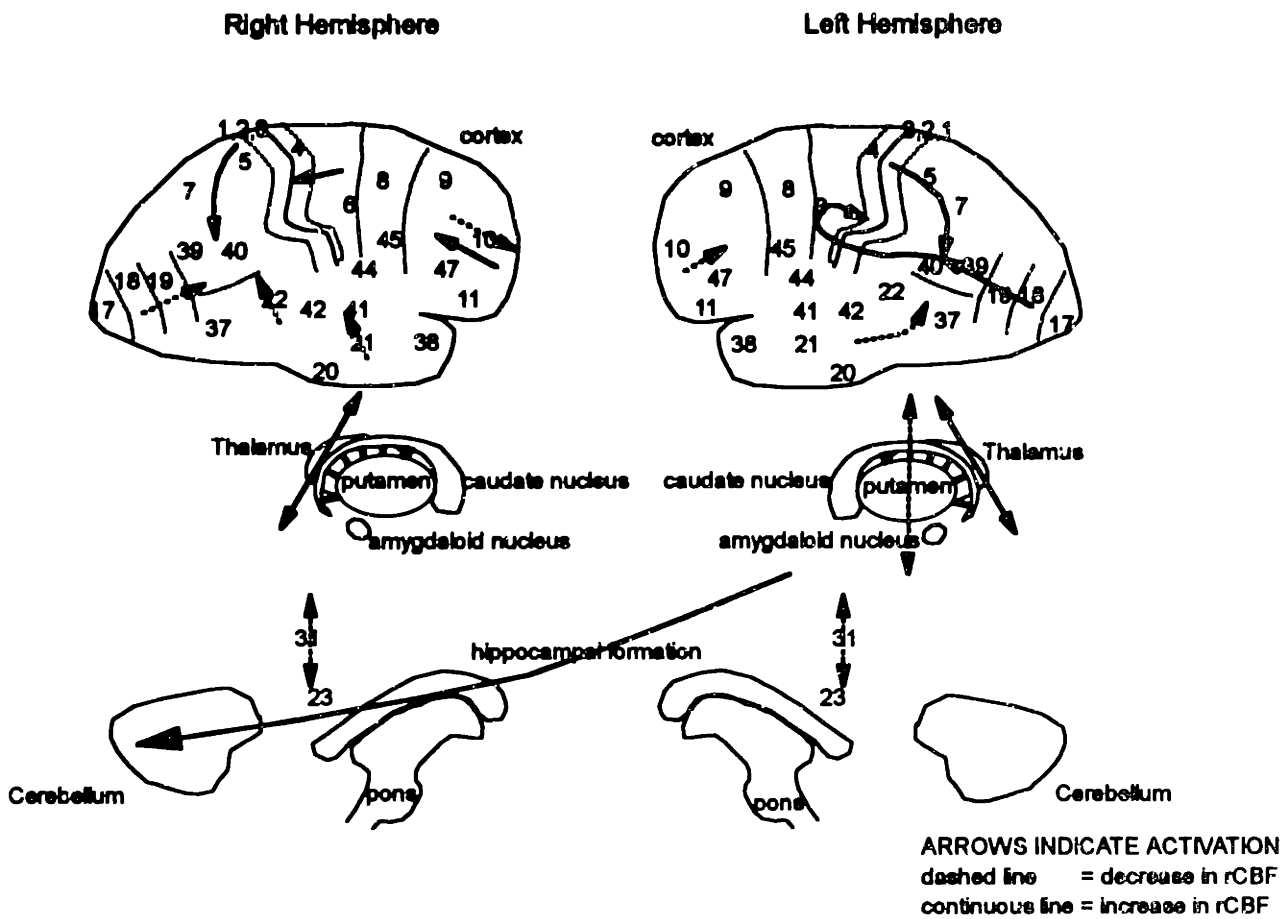

Fig.6.7. Negative Transfer vs Baseline rCBF Activations Summarizes areas with significant increase and decrease in rCBF during the Negative Trasfer condition when compared with the Motor Performance condition (baseline)

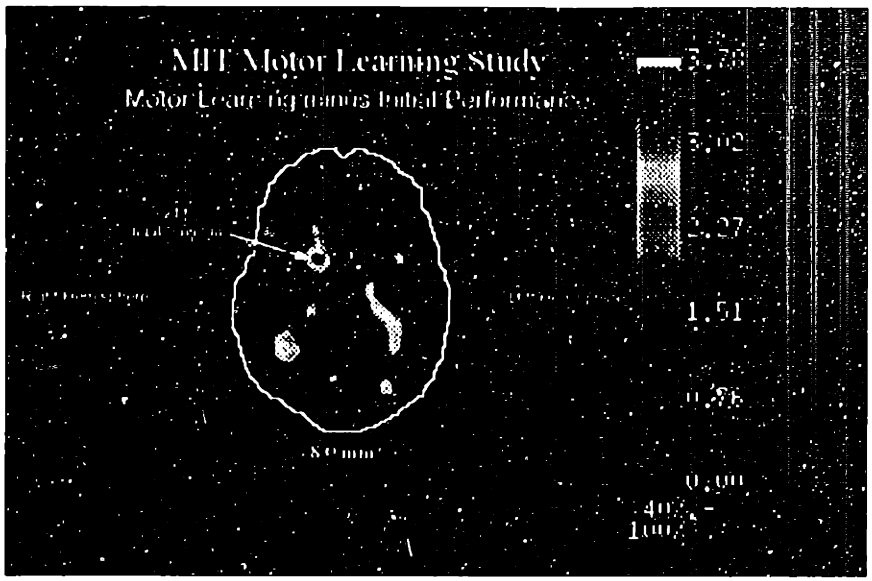

FIG.6.8. Example of Relative Increase in the Regional Cerebral Blood Flow during the Early Learning Phase (vs Baseline Motor Performance)
The readings indicated a relative increase in activity in the ipsilateral right ventral striatum during this task phase with right hand task (right handed subjects) in a virtual force field.

6.4.2. Kinematic Analysis via a Simple Motor Performance Index

The choice of a performance index is critical to revealing the different facets of the learning process. Normal subjects typically make point-to-point movements in approximately a straight line in an unconstrained environment, while evidence favors kinematic planning versus dynamic planning (see Chapter 2). For these reasons, one performance index chosen was the lateral deviation of the subjects' movements from a straight line connecting the targets. Using this index, the lack of evidence of a learning pattern would indicate that the consensus in the human motor control field regarding kinematic planning needed to be re-examined. Gathered kinematic data showed that, indeed, there is a consistent pattern of performance improvement while learning the task. Using the mean-squared lateral deviation as a numerical measure of performance, the baseline condition 1 (batch 1 & 2) was followed by deterioration of the performance as the force field was applied (batch 3). The subsequent results showed a progressive reduction on the lateral deviation mean, indicating learning (batch 4, training, batch 5, training, batch 6). Similar patterns can be observed as subjects were challenged with a new force field with reverse characteristics (batch 7 & 8). Figure 6.9. shows the mean-squared lateral deviation of the hand (end-effector)

from the straight line connecting the homing target with the outbound targets averaged across the eight subjects. At the risk of being pedantic, these results support the evidence favoring kinematic planning. This behavioral data also permits a quantitative measure of the rate of motor learning during each phase. Note in the figure that the learning rate can be assessed by the slope of the regression, with task difficulty measured by extrapolating the regression line to estimate performance at , e.g., 10th trial ($\log_{10}$ trial# = 1). Figures 6.10.a&b. to 6.17.a&b show all eight subjects' mean-squared deviation from the straight line connecting the homing target with the outbound targets. Part (a) of the sequence contains the average per batch and part (b) of the sequence contains the time-evolution within the batch. Even for this simple numerical measure of kinematic performance, the different movement phases can be clustered, i.e. Motor Performance, Learning, and Negative Transfer. As an example, for subject DD (Fig. 6.14.a.), batch 2 is statistically different from batch 3 and batch 6 likewise from batch 7, and there is a consistent trend within the Learning phase (Early plus Late Learning).

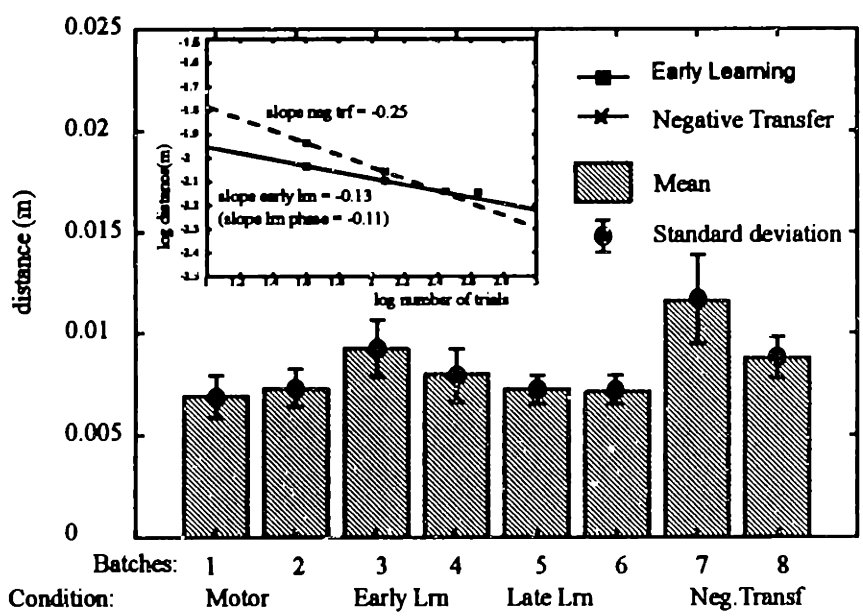

FIG.6.9. Mean Lateral Deviation from a Straight Line Averaged Across Eight Normal Subjects
The plot shows the mean-squared deviation for each batch with the inner plot showing the learning rate assessed by the slope of the regression during Early Learning and Negative Transfer, as well as for the overall Learning Phase (Early + Late) with task difficulty measured by extrapolating the regression line to estimate performance at, e.g. 10th trial ($\log_{10}$ trial# = 1).

Note that a faster learning rate in this task does not indicate the subject's skill. In fact in this task, subjects incurring large initial errors had faster learning rates. Therefore for this protocol, the task difficulty might be a better indicator of subject's skills. This subsection concludes with Table 6.1. which shows for each subject the mean value of the lateral deviation from the straight line during the last part of batch 7 (71st to 80th trial) and during the initial part of batch 8 (2nd to 11th trial). Note that there is discontinuity between the end of batch 7 and the beginning of subsequent batch 8. This difference is known in the motor control literature as motor consolidation. Learning a motor skill sets up a neural process that continues to evolve after practice (during the 5 minute break between batches). This is the area of research of the distinct group at MIT collaborating with us on this topic [Brashers Krug, Shadmehr & Bizzi, 1996].

Subject	Batch 7- Tail Mean Lateral Deviation (mm)	Batch 8 - Head Mean Lateral Deviation (mm)	Difference (mm)
CR	9.9	9.3	0.6
DB	9.7	7.7	2
DG	8.5	8.5	0
DS	9.5	6.3	3.2
DD	9.2	8.7	0.5
ES	9.8	9.7	0.1
MU	11.3	10	1.3
TH	7.8	7.3	0.5

TABLE 6.1. Example of Motor Consolidation
The Table highlights the phenomenon known as motor consolidation. Learning a motor skill sets a neural process that continues to evolve after practice (in this case during the 5 minute break). Note the discontinuity between the end and beginning of consecutive batches.

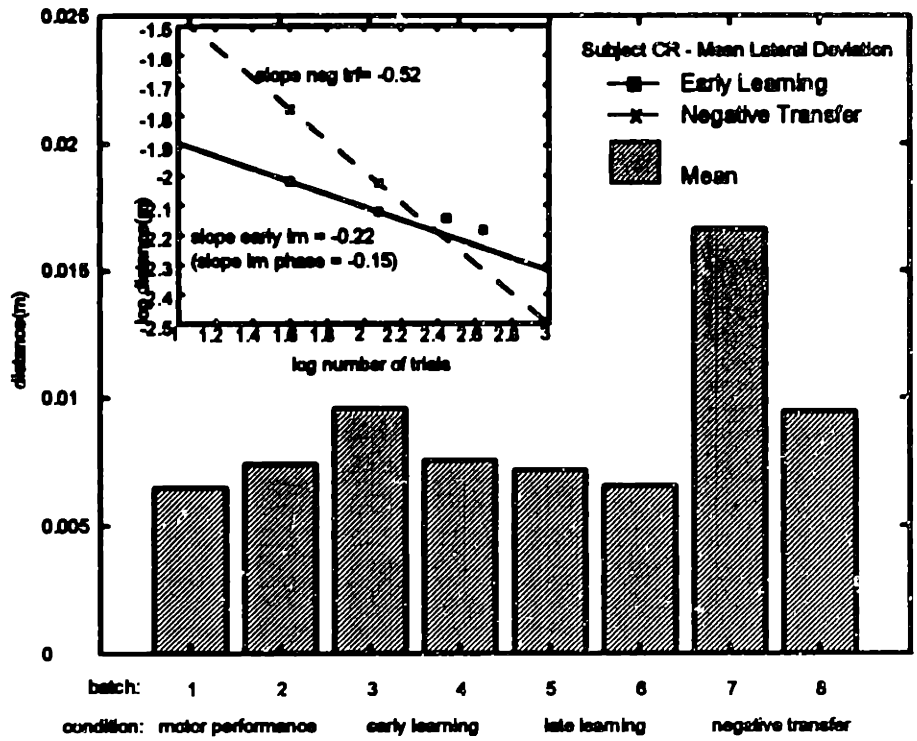

batch	1	2	3	4	5	6	7	8
1	1	0.76	0.46*	0.73	0.81	0.97	0.15*	0.47*
2		1	0.60*	0.96	1.06	1.27	0.20*	0.61*
3			1	1.60*	1.78*	2.13*	0.33*	1.03
4				1	1.11	1.33	0.21*	0.64*
5					1	1.20	0.19*	0.58*
6						1	0.16*	0.48*
7							1	3.10*
8								1

(*)Statistically significant [level 0.05 in 80 trials -- 0.65 < F-value < 1.53]

FIG.6.10.a. Mean Lateral Deviation from a Straight Line for Subject CR
The plot shows the mean-squared deviation for each batch with the inner plot showing the learning rate assessed by the slope of the regression during Early Learning and Negative Transfer, as well as for the overall Learning Phase (Early + Late) with task difficulty measured by extrapolating the regression line to estimate performance at , e.g., 10th trial ($\log_{10}$ trial# = 1). The table shows for reference a statistical test (F-test) to test the hypothesis that the means of different batches are equal.

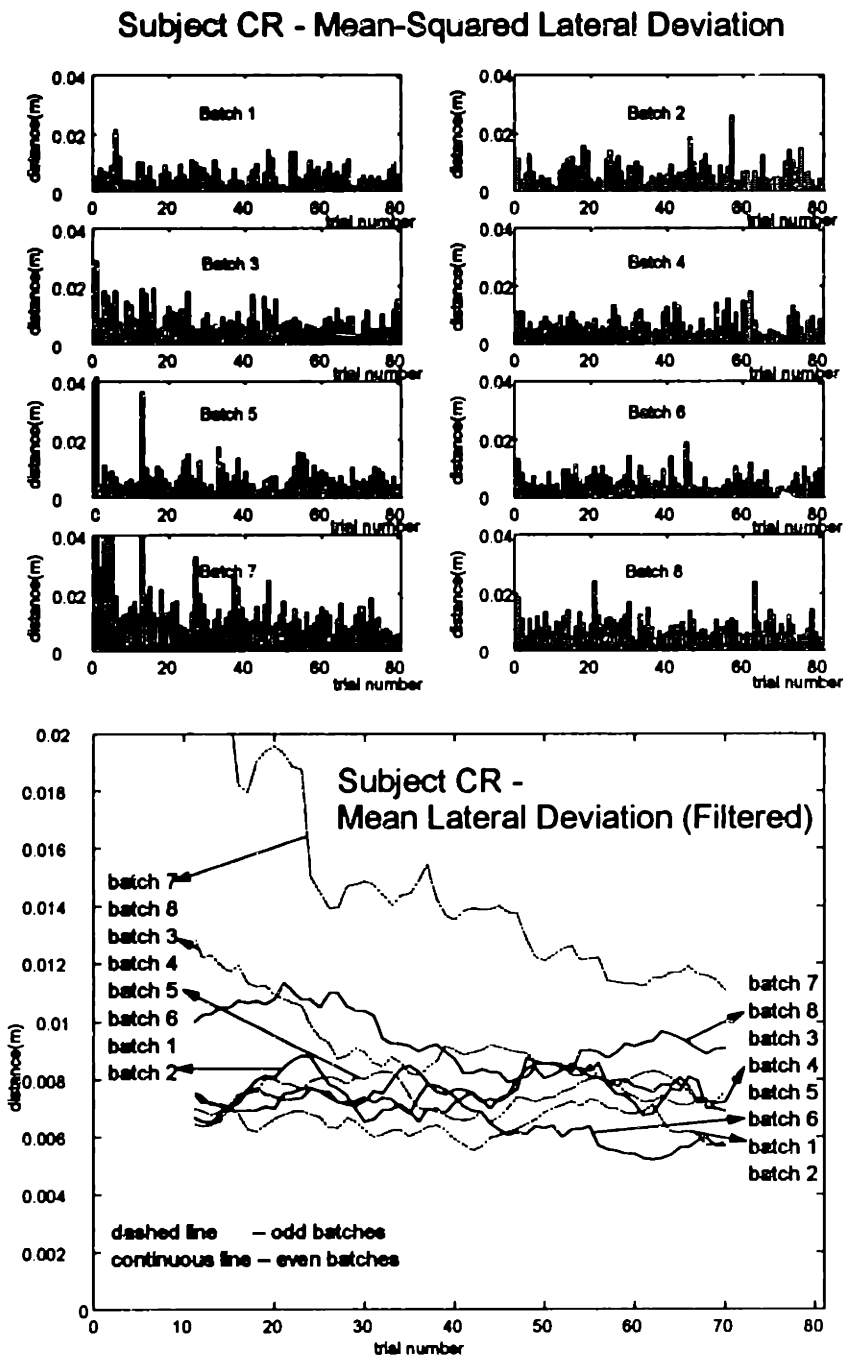

FIG.6.10.b. Mean Lateral Deviation from a Straight Line for Subject CR
The upper sequence of plots shows the mean-squared deviation for each of the 80 trials of each batch. The lower plot shows a composite of all the batches. The mean lateral deviation was filtered by a Moving-Average Filter with window equal to 20 trials to indicate trends.

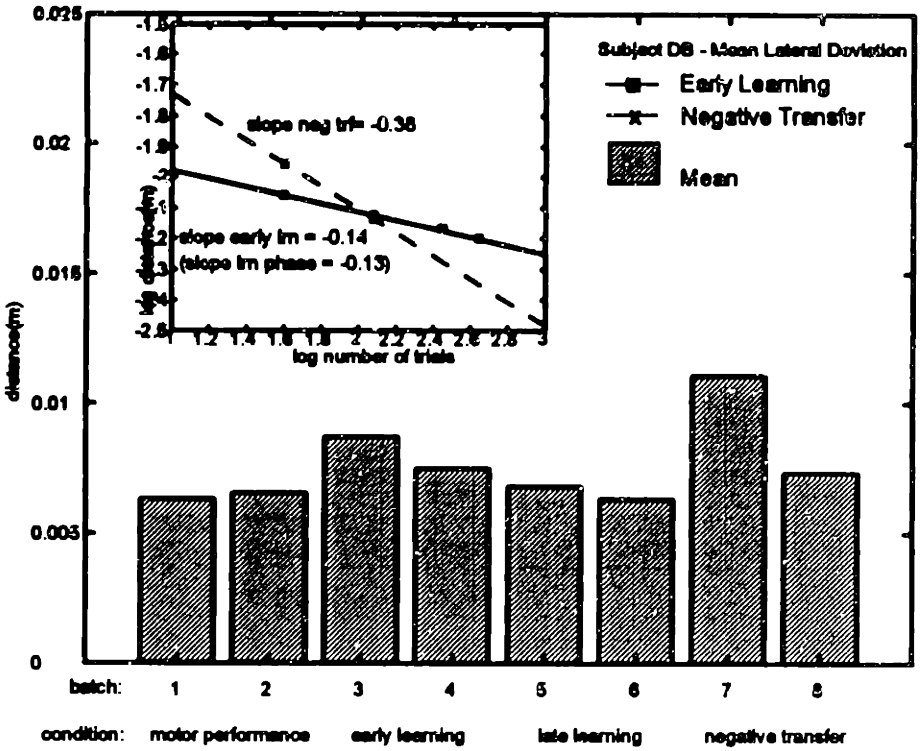

batch	1	2	3	4	5	6	7	8
1	1	0.93	0.52*	0.71	0.86	1.00	0.32*	0.74
2		1	0.56*	0.76	0.92	1.07	0.35*	0.80
3			1	1.35	1.64*	1.90*	0.62*	1.42*
4				1	1.22	1.41	0.46*	1.05
5					1	1.16	0.38*	0.86
6						1	0.33*	0.74
7							1	2.29*
8								1

(*) Statistically significant [level 0.05 in 80 trials -- 0.65 < F-value < 1.53]

FIG.6.11.a. Mean Lateral Deviation from a Straight Line for Subject DB
The plot shows the mean-squared deviation for each batch with the inner plot showing the learning rate assessed by the slope of the regression during Early Learning and Negative Transfer, as well as for the overall Learning Phase (Early + Late) with task difficulty measured by extrapolating the regression line to estimate performance at , e.g., 10th trial ($\log_{10}$ trial# = 1). The table shows for reference a statistical test (F-test) to test the hypothesis that the means of different batches are equal.

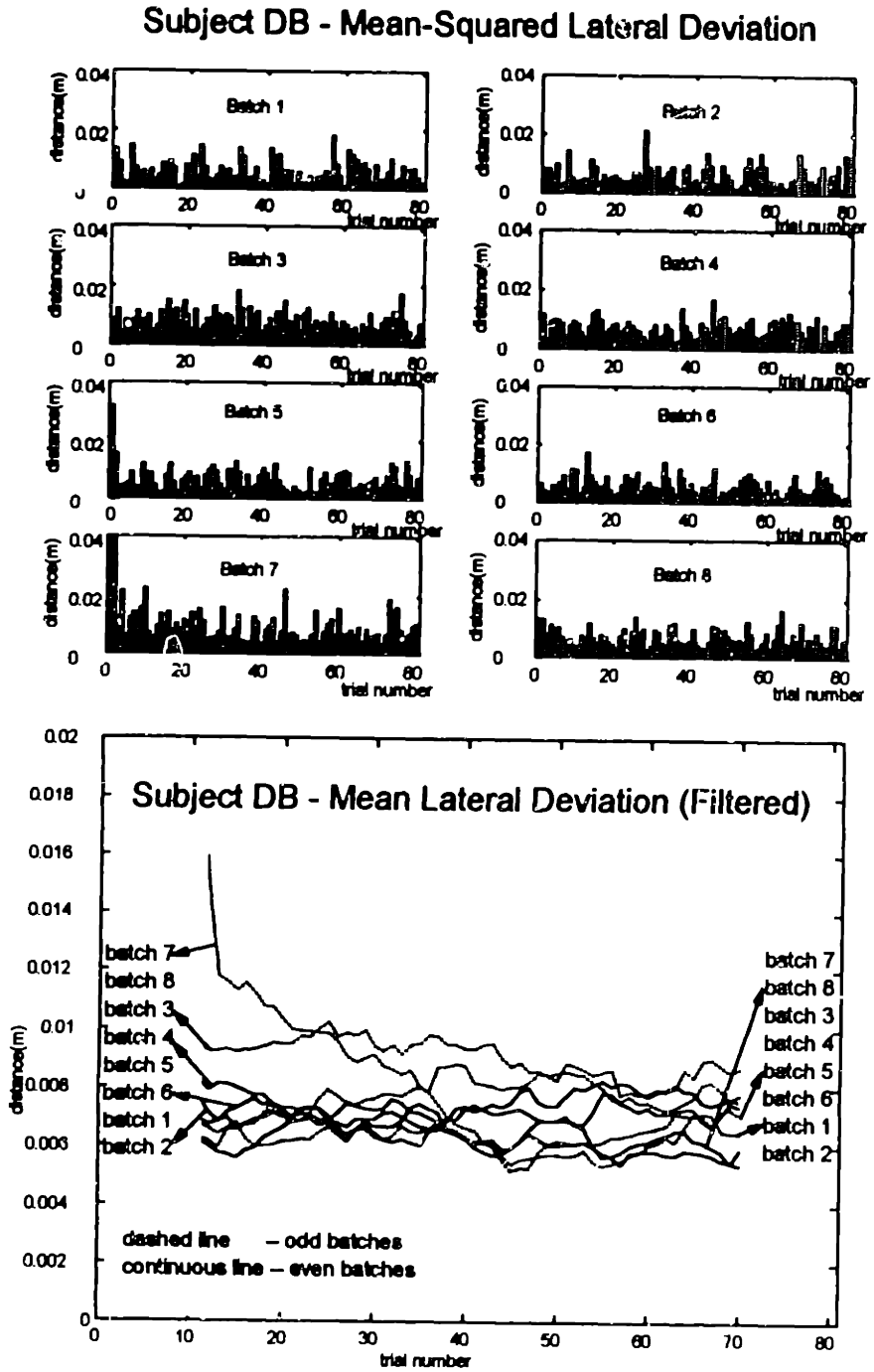

FIG.6.11.b. Mean Lateral Deviation from a Straight Line for Subject DB
The upper sequence of plots shows the mean-squared deviation for each of the 80 trials of each batch. The lower plot shows a composite of all the batches. The mean lateral deviation was filtered by a Moving-Average Filter with window equal to 20 trials to indicate trends.

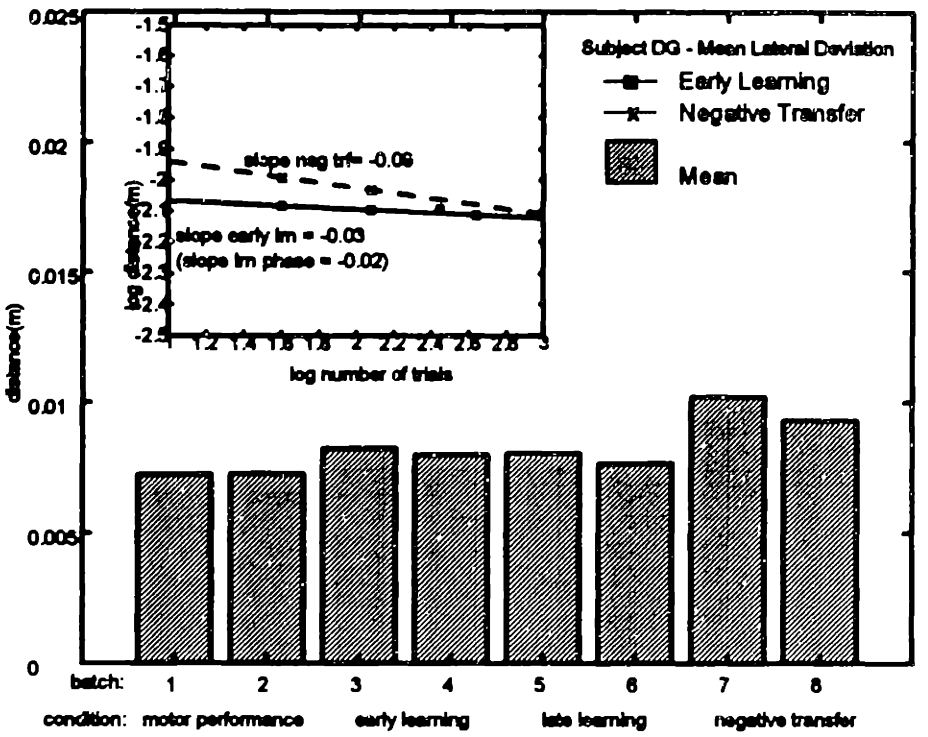

batch	1	2	3	4	5	6	7	8
1	1	0.99	0.77	0.82	0.81	0.89	0.50*	0.61*
2		1	0.77	0.82	0.92	0.89	0.51*	0.61*
3			1	1.06	1.05	1.15	0.65*	0.79
4				1	0.99	1.08	0.61*	0.74
5					1	1.09	0.62*	0.75
6						1	0.57*	0.68
7							1	1.21
8								1

(*)Statistically significant [level 0.05 in 80 trials -- 0.65 < F-value < 1.53]

FIG.6.12.a. Mean Lateral Deviation from a Straight Line for Subject DG
The plot shows the mean-squared deviation for each batch with the inner plot showing the learning rate assessed by the slope of the regression during Early Learning and Negative Transfer, as well as for the overall Learning Phase (Early + Late) with task difficulty measured by extrapolating the regression line to estimate performance at , e.g., 10th trial ($\log_{10}$ trial# = 1). The table shows for reference a statistical test (F-test) to test the hypothesis that the means of different batches are equal.

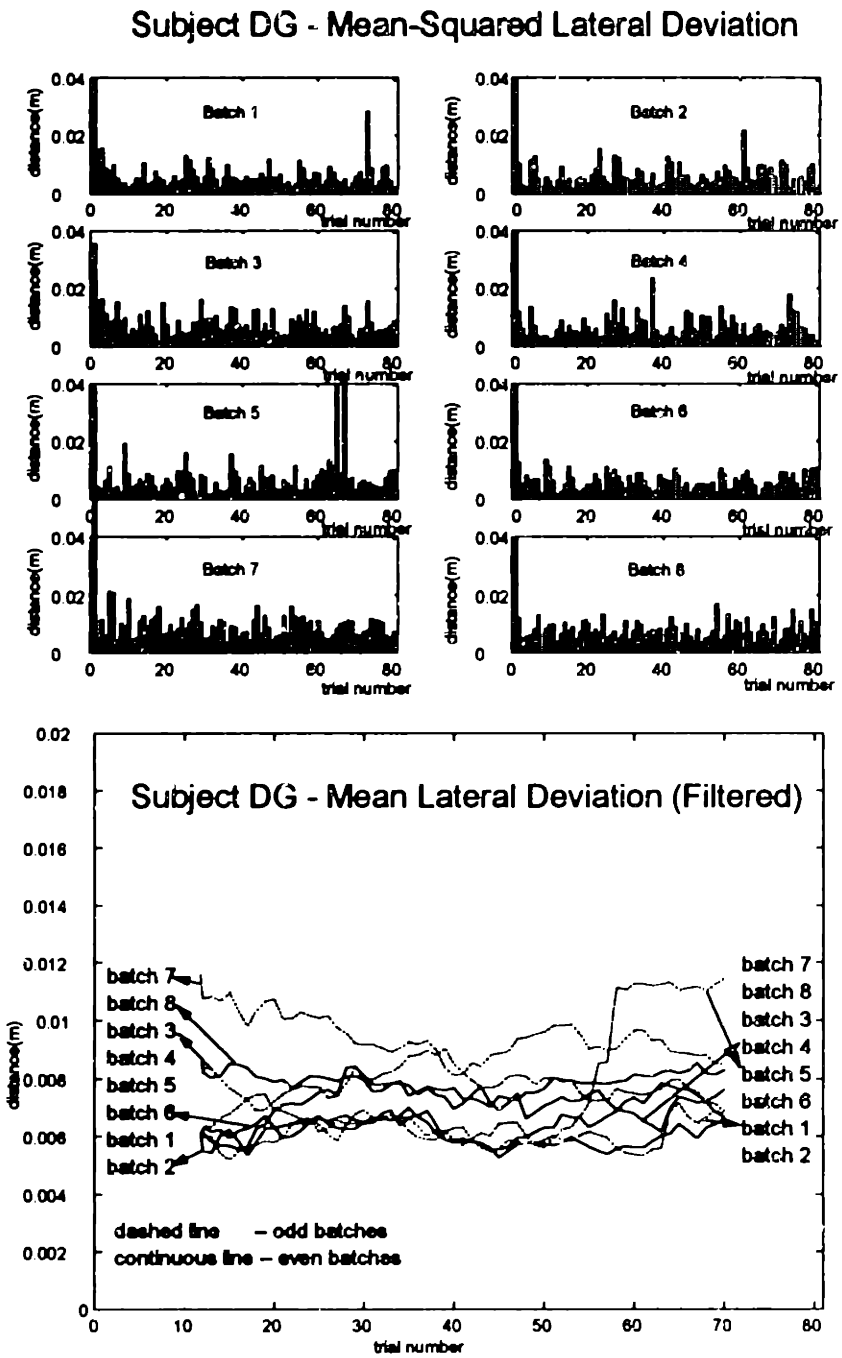

FIG.6.12.b. Mean Lateral Deviation from a Straight Line for Subject DG
The upper sequence of plots shows the mean-squared deviation for each of the 80 trials of each batch. The lower plot shows a composite of all the batches. The mean lateral deviation was filtered by a Moving-Average Filter with window equal to 20 trials to indicate trends.

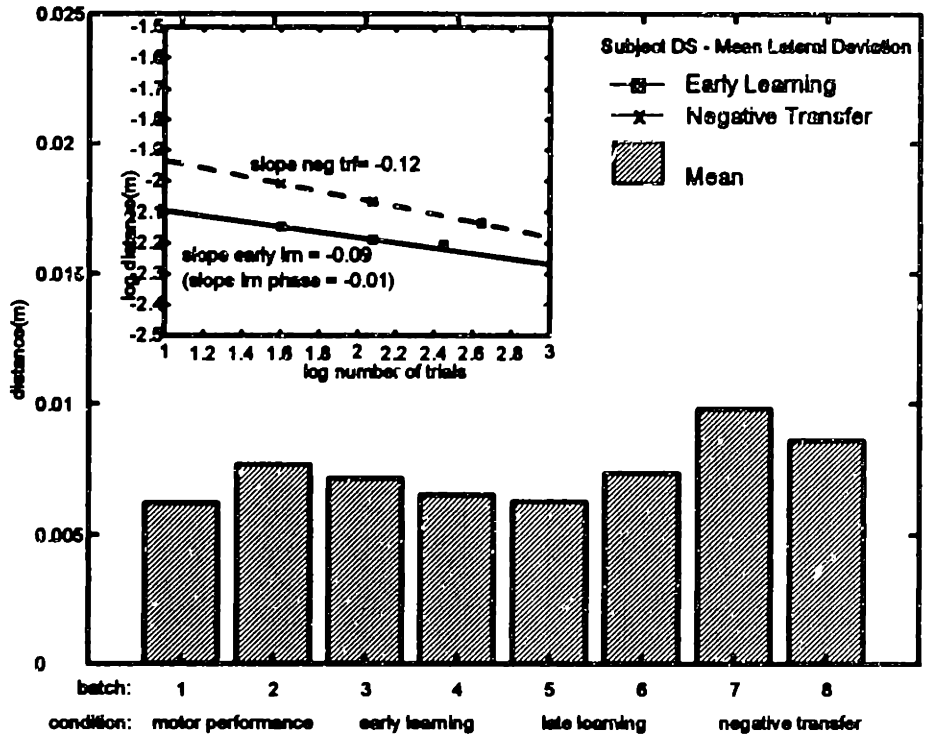

batch	1	2	3	4	5	6	7	8
1	1	0.66	0.75	0.91	0.99	0.71	0.40*	0.52*
2		1	1.15	1.39	1.51	1.09	0.61*	0.79
3			1	1.21	1.31	0.95	0.53*	0.69
4				1	1.09	0.78	0.44*	0.57*
5					1	0.72	0.40*	0.53*
6						1	0.56*	0.73
7							1	1.31
8								1

(*)Statistically significant [level 0.05 in 80 trials – 0.65 < F-value < 1.53]

FIG.6.13.a. Mean Lateral Deviation from a Straight Line for Subject DS
The plot shows the mean-squared deviation for each batch with the inner plot showing the learning rate assessed by the slope of the regression during Early Learning and Negative Transfer, as well as for the overall Learning Phase (Early + Late) with task difficulty measured by extrapolating the regression line to estimate performance at , e.g., 10th trial ($\log_{10}$ trial# = 1). The table shows for reference a statistical test (F-test) to test the hypothesis that the means of different batches are equal.

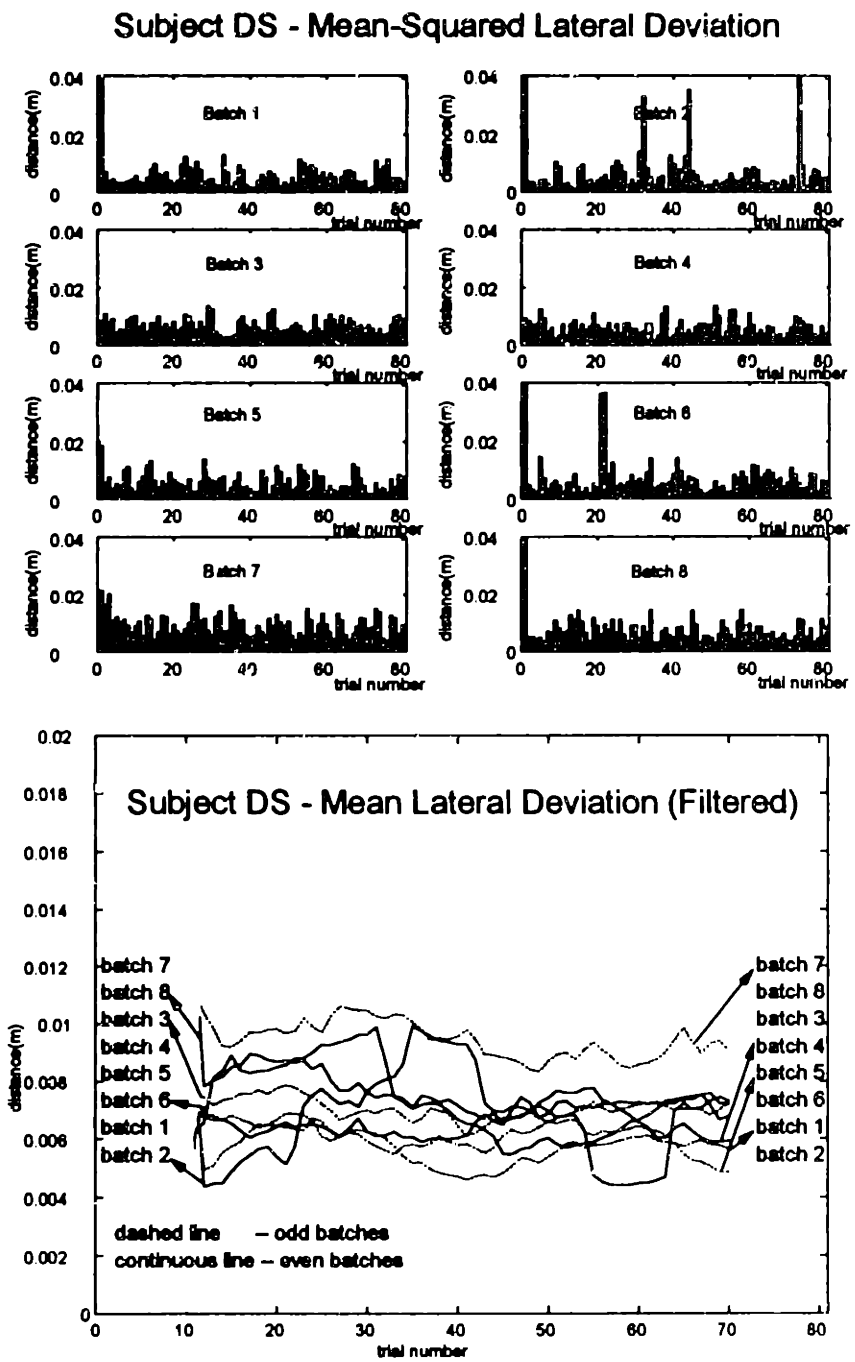

FIG.6.13.b. Mean Lateral Deviation from a Straight Line for Subject DS
The upper sequence of plots shows the mean-squared deviation for each of the 80 trials of each batch. The lower plot shows a composite of all the batches. The mean lateral deviation was filtered by a Moving-Average Filter with window equal to 20 trials to indicate trends.

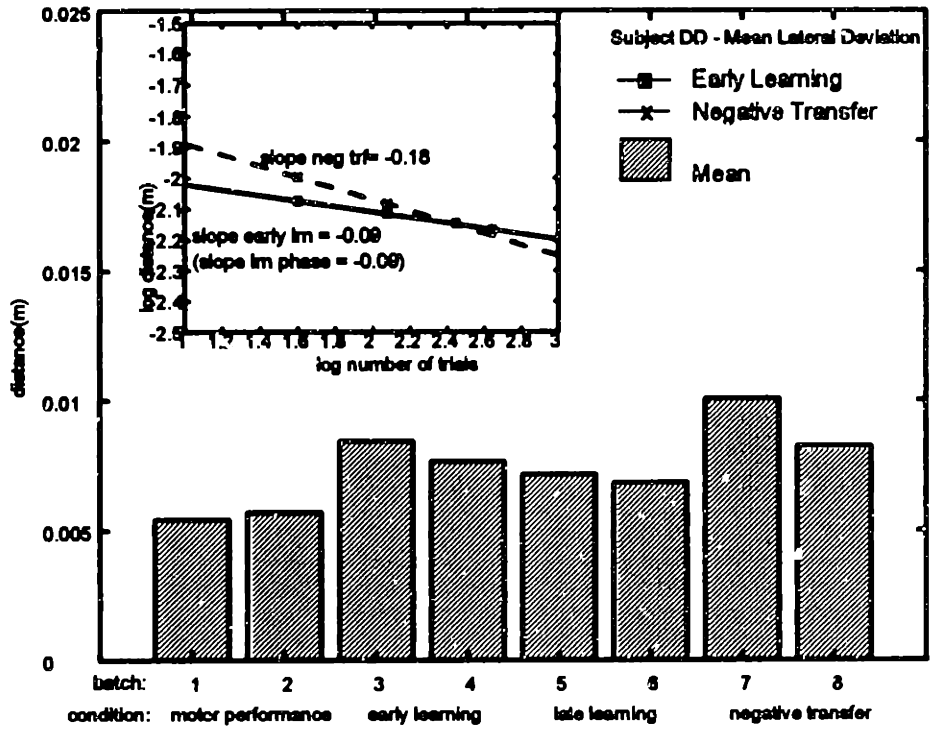

batch	1	2	3	4	5	6	7	8
1	1	0.91	0.41*	0.50*	0.57*	0.63*	0.29*	0.43*
2		1	0.45*	0.55*	0.63*	0.70	0.32*	0.48*
3			1	1.22	1.40	1.54*	0.70	1.05
4				1	1.15	1.26	0.58*	0.86
5					1	1.10	0.50*	0.75
6						1	0.46*	0.68
7							1	1.49
8								1

(*)Statistically significant [level 0.05 in 80 trials -- 0.65 < F-value < 1.53]

FIG.6.14.a. Mean Lateral Deviation from a Straight Line for Subject DD
The plot shows the mean-squared deviation for each batch with the inner plot showing the learning rate assessed by the slope of the regression during Early Learning and Negative Transfer, as well as for the overall Learning Phase (Early + Late) with task difficulty measured by extrapolating the regression line to estimate performance at , e.g., 10th trial ($\log_{10}$ trial# = 1). The table shows for reference a statistical test (F-test) to test the hypothesis that the means of different batches are equal.

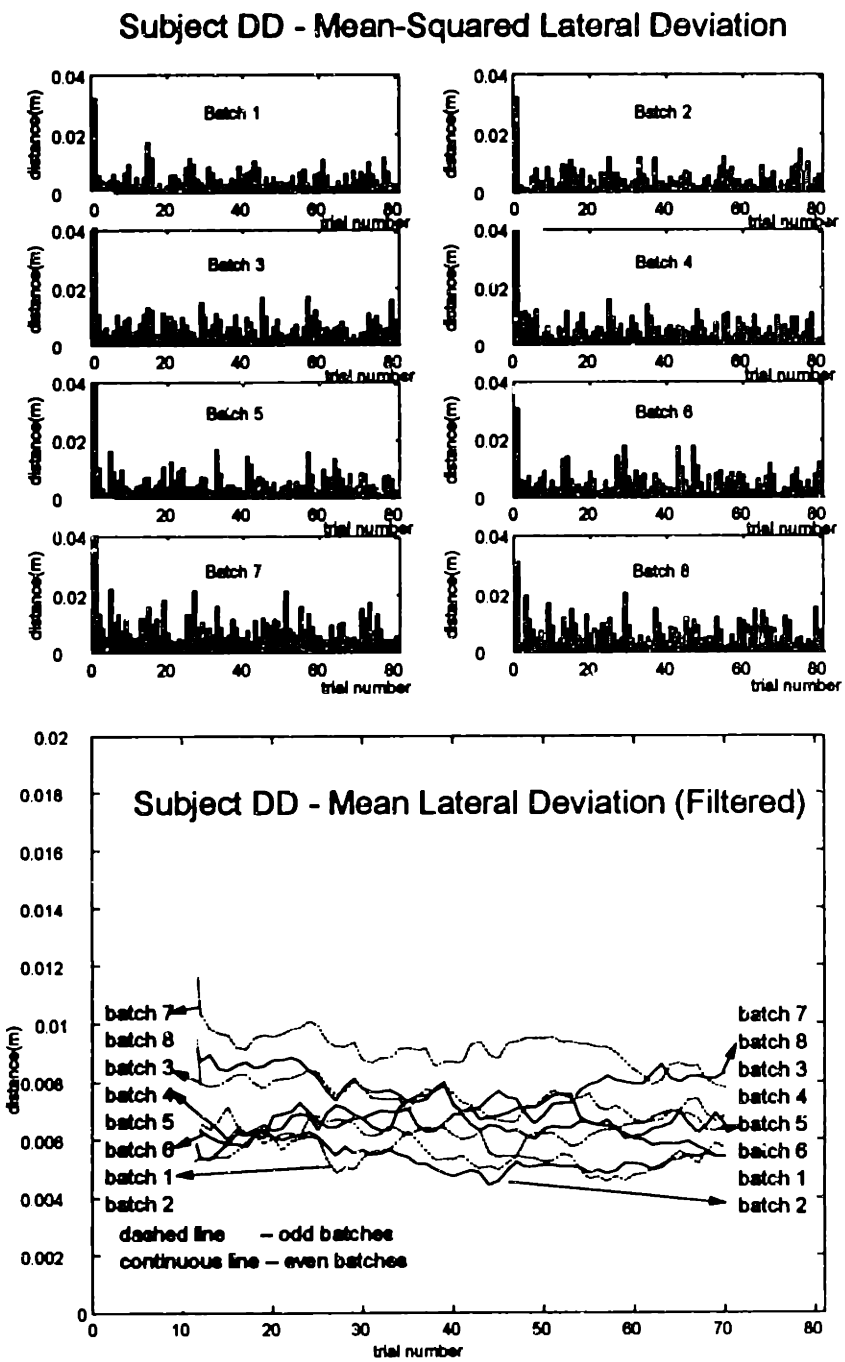

FIG.6.14.b. Mean Lateral Deviation from a Straight Line for Subject DD
The upper sequence of plots shows the mean-squared deviation for each of the 80 trials or each batch. The lower plot shows a composite of all the batches. The mean lateral deviation was filtered by a Moving-Average Filter with window equal to 20 trials to indicate trends.

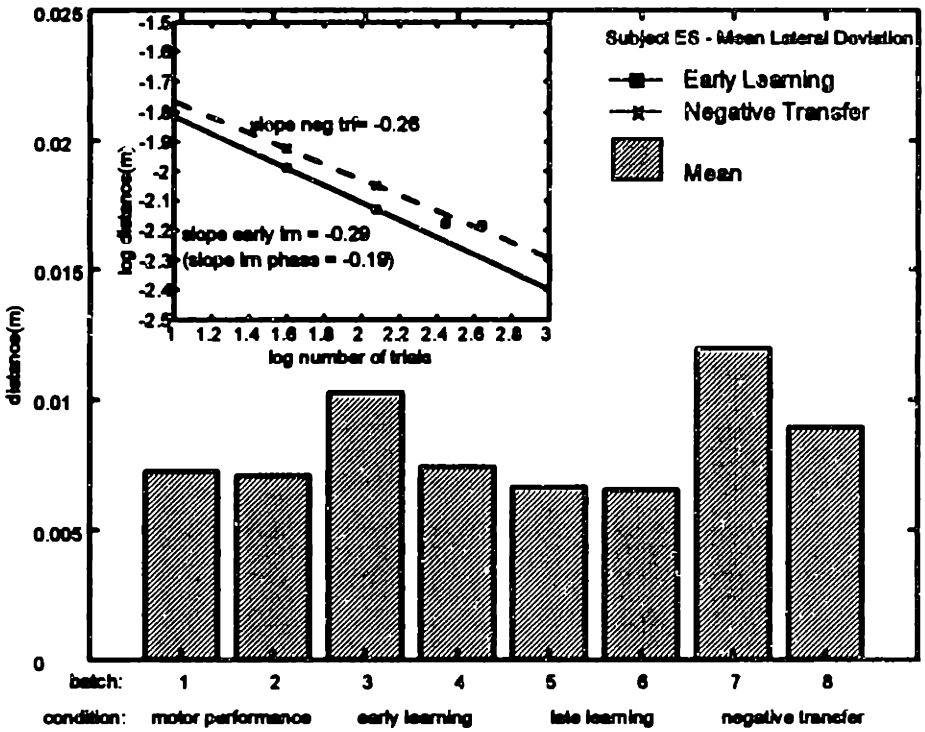

batch	1	2	3	4	5	6	7	8
1	1	1.04	0.50*	0.95	1.18	1.23	0.37*	0.66
2		1	0.48*	0.91	1.14	1.18	0.35*	0.63*
3			1	1.91*	2.38*	2.47*	0.74	1.32
4				1	1.25	1.29	0.39*	0.69
5					1	1.04	0.31*	0.55*
6						1	0.30*	0.54*
7							1	1.79*
8								1

(*)Statistically significant [level 0.05 in 80 trials – 0.65 < F-value < 1.53]

FIG.6.15.a. Mean Lateral Deviation from a Straight Line for Subject ES
The plot shows the mean-squared deviation for each batch with the inner plot showing the learning rate assessed by the slope of the regression during Early Learning and Negative Transfer, as well as for the overall Learning Phase (Early + Late) with task difficulty measured by extrapolating the regression line to estimate performance at , e.g., 10th trial ($\log_{10}$ trial# = 1). The table shows for reference a statistical test (F-test) to test the hypothesis that the means of different batches are equal.

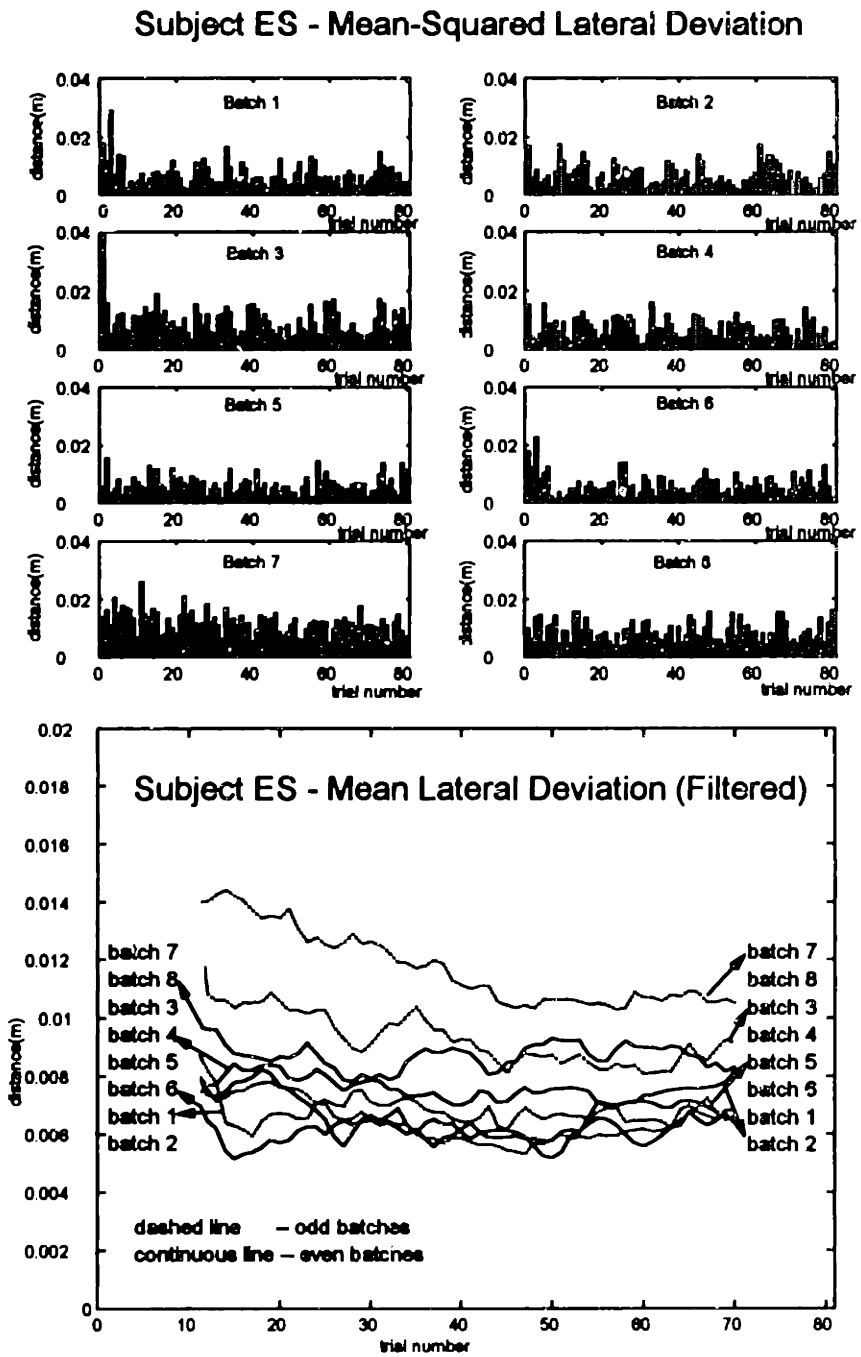

FIG.6.15.b. Mean Lateral Deviation from a Straight Line for Subject ES
The upper sequence of plots shows the mean-squared deviation for each of the 80 trials of each batch. The lower plot shows a composite of all the batches. The mean lateral deviation was filtered by a Moving-Average Filter with window equal to 20 trials to indicate trends.

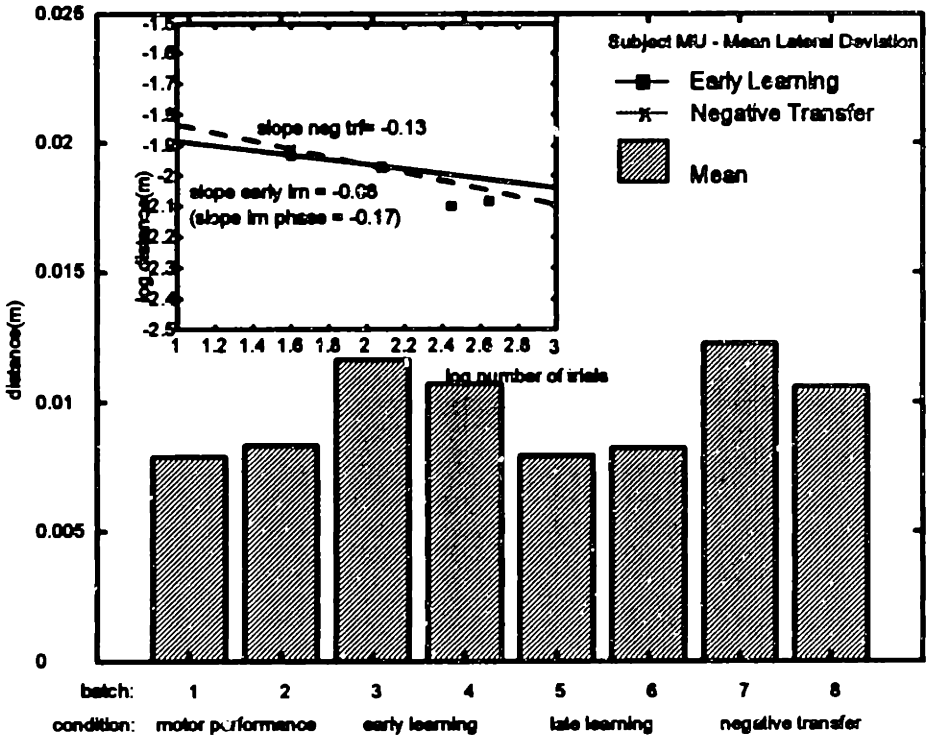

batch	1	2	3	4	5	6	7	8
1	1	0.89	0.46*	0.54*	0.99	0.92	0.41*	0.55*
2		1	0.51*	0.61*	1.11	1.03	0.46*	0.62*
3			1	1.18	2.16*	2.00*	0.90	1.21
4				1	1.82*	1.69*	0.76	1.02
5					1	0.93	0.42*	0.56*
6						1	0.45*	0.60*
7							1	1.34
8								1

(*)Statistically significant [level 0.05 in 80 trials – 0.65 < F-value < 1.53]

FIG.6.16.a. Mean Lateral Deviation from a Straight Line for Subject MU
The plot shows the mean-squared deviation for each batch with the inner plot showing the learning rate assessed by the slope of the regression during Early Learning and Negative Transfer, as well as for the overall Learning Phase (Early + Late) with task difficulty measured by extrapolating the regression line to estimate performance at , e.g., 10th trial ($\log_{10}$ trial# = 1). The table shows for reference a statistical test (F-test) to test the hypothesis that the means of different batches are equal.

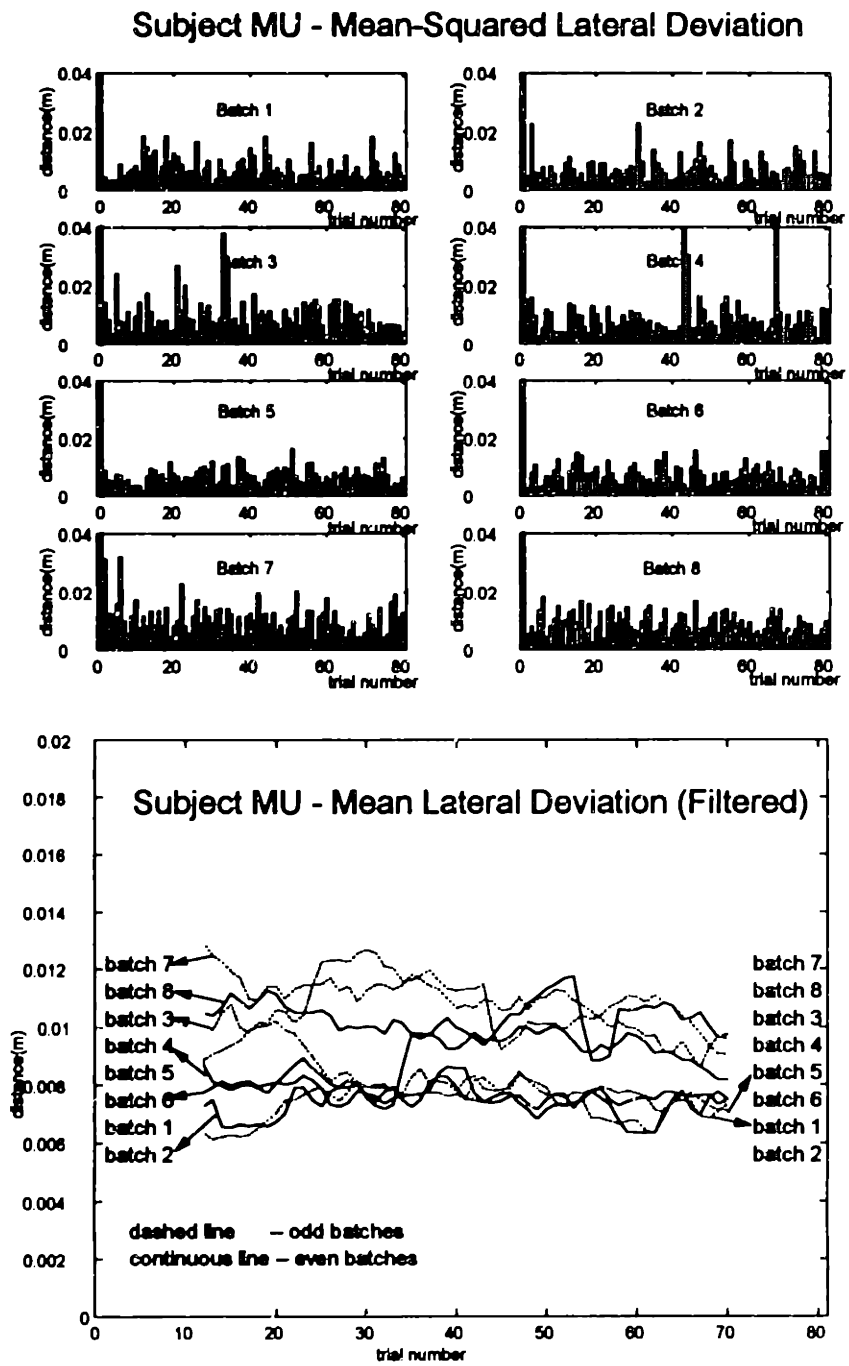

FIG.6.16.b. Mean Lateral Deviation from a Straight Line for Subject MU
The upper sequence of plots shows the mean-squared deviation for each of the 80 trials of each batch. The lower plot shows a composite of all the batches. The mean lateral deviation was filtered by a Moving-Average Filter with window equal to 20 trials to indicate trends.

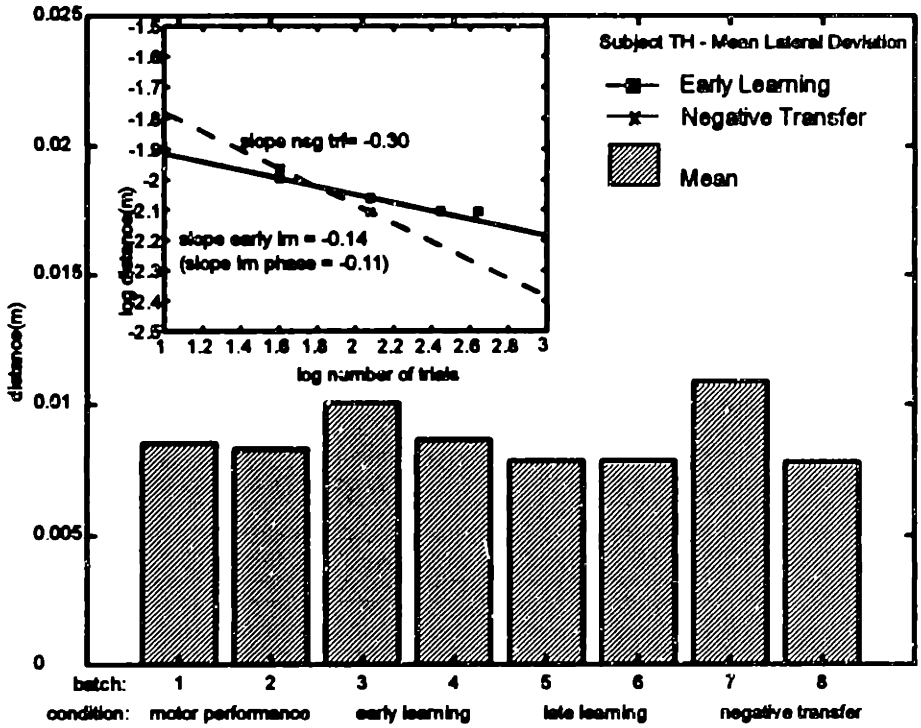

batch	1	2	3	4	5	6	7	8
1	1	1.06	0.72	0.97	1.18	1.19	0.62*	1.20
2		1	0.68	0.92	1.12	1.12	0.58*	1.14
3			1	1.35	1.64*	1.65*	0.86	1.67*
4				1	1.22	1.22	0.64*	1.24
5					1	1.00	0.52*	1.02
6						1	0.52*	1.01
7							1	1.94*
8								1

(*)Statistically significant [level 0.05 in 80 trials -- 0.65 < F-value < 1.53]

FIG.6.17.a. Mean Lateral Deviation from a Straight Line for Subject TH
The plot shows the mean-squared deviation for each batch with the inner plot showing the learning rate assessed by the slope of the regression during Early Learning and Negative Transfer, as well as for the overall Learning Phase (Early + Late) with task difficulty measured by extrapolating the regression line to estimate performance at , e.g., 10th trial ($\log_{10}$trial# = 1). The table shows for reference a statistical test (F-test) to test the hypothesis that the means of different batches are equal.

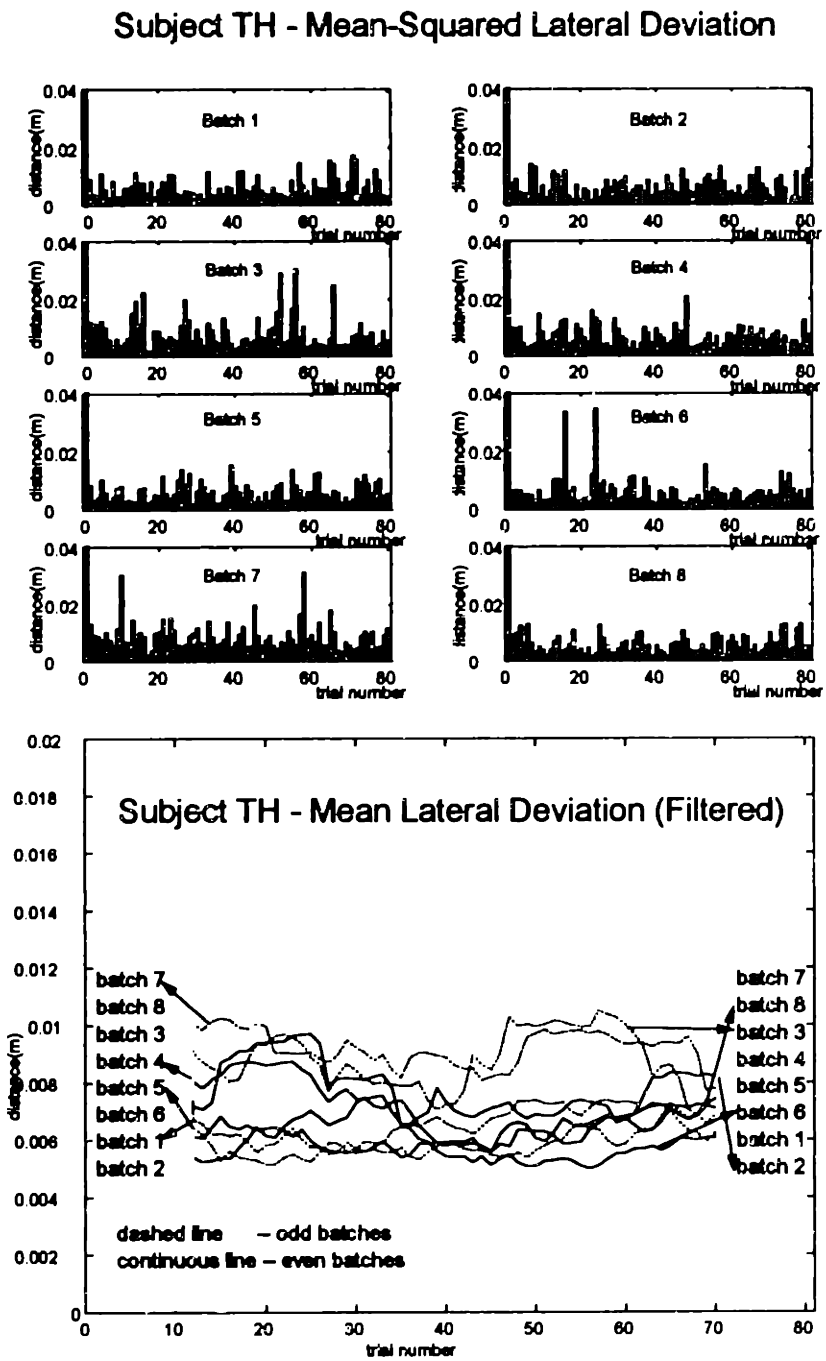

FIG.6.17.b. Mean Lateral Deviation from a Straight Line for Subject TH
The upper sequence of plots shows the mean-squared deviation for each of the 80 trials of each batch. The lower plot shows a composite of all the batches. The mean lateral deviation was filtered by a Moving-Average Filter with window equal to 20 trials to indicate trends.

6.4.3. Kinematics Analysis via the Submovement Motor Performance Index

In the previous subsection, a performance index was used that revealed several different facets of the task, such as learning, average deviation from the straight line, learning rate, and task difficulty. Examining the hand traces of subjects throughout the different batches, the adequacy of this performance index can be seen. Subjects drew straighter lines with learning. Figure 6.18. shows the trace records for subject CR throughout the experiment, while Figs.Trace.1 to Trace.8. shows the trace records for all the subjects only during the Negative Transfer condition (batches 7 & 8 -- see Appendix E). Subject CR has the most pronounced performance variation (see Fig. 6.10), and all the other subjects showed similar patterns. The figures on the left column show the traces for movements outward towards the targets, and on the right column, traces for movements inward towards the center. Likewise, the speed profiles suggested similar behavior. During Early Learning a multi-peaked velocity profile was evident that was quite different from the single-peaked profile seen in the unperturbed Motor Performance case. With learning, the secondary peaks become progressively less evident, starting to resemble the unperturbed case. A similar pattern can be observed during Negative Transfer. This observation led Shadmehr and Mussa-Ivaldi to use a different performance index in a similar experiment (saddle force field with no visual feedback). Their index corresponds to the correlation between the velocity in the unperturbed case and in the non-null force fields. Figure 6.19. shows the speed records for subject CR throught the experiment, while Figs.Speed.1. to Speed.8. show the speed records for all the subjects only during the Negative Transfer condition (batches 7 & 8 -- see appendix E). Again, subject CR has the most pronounced performance variation, and all the other subjects showed similar patterns with the left column registering the speed outward and the right column registering the speed inward to the center.

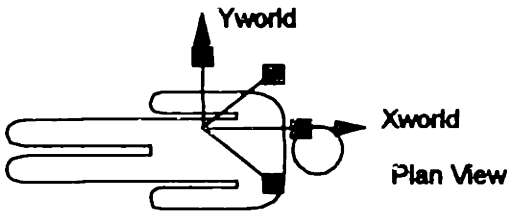

The inward movement traces were copied on the second column to allow better visualization of the end of the movement.

continuous bold line – first movement in the set
dashed bold line – last movement in the set

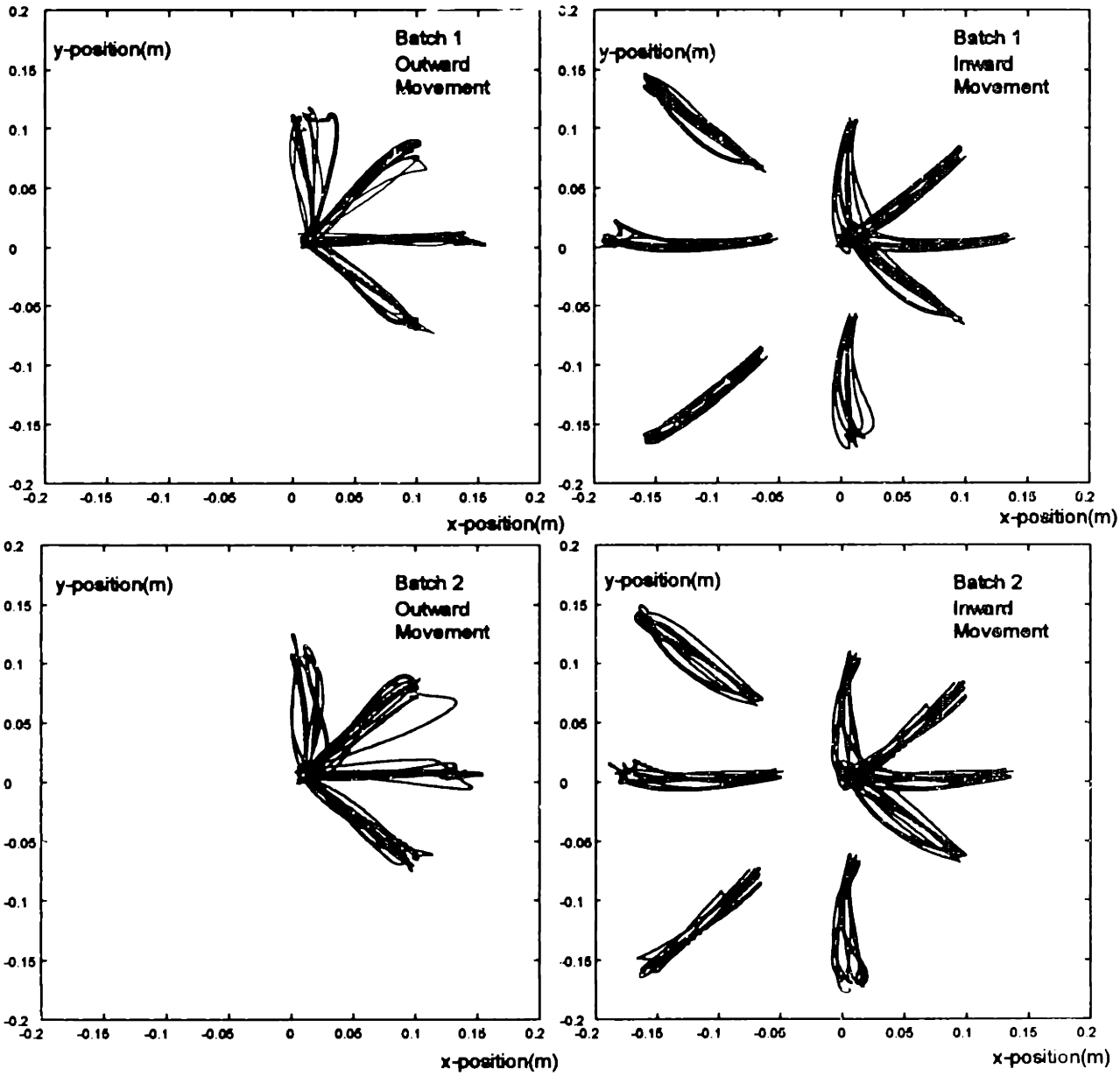

FIG.6.18.a. Trace Record for Subject CR - Batch 1 & 2

The upper row corresponds to batch 1 and the lower row to batch 2. Plots on the left column contain movements from the center to randomly presented outwards targets. The right column contains movements back to the center.

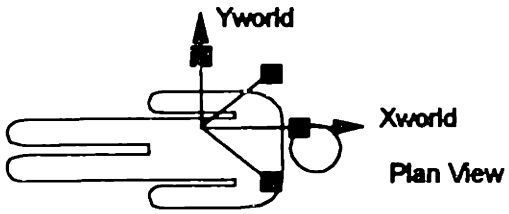

The inward movement traces were copied on the second column to allow better visualization of the end of the movement.

continuous bold line – first movement in the set
dashed bold line – last movement in the set

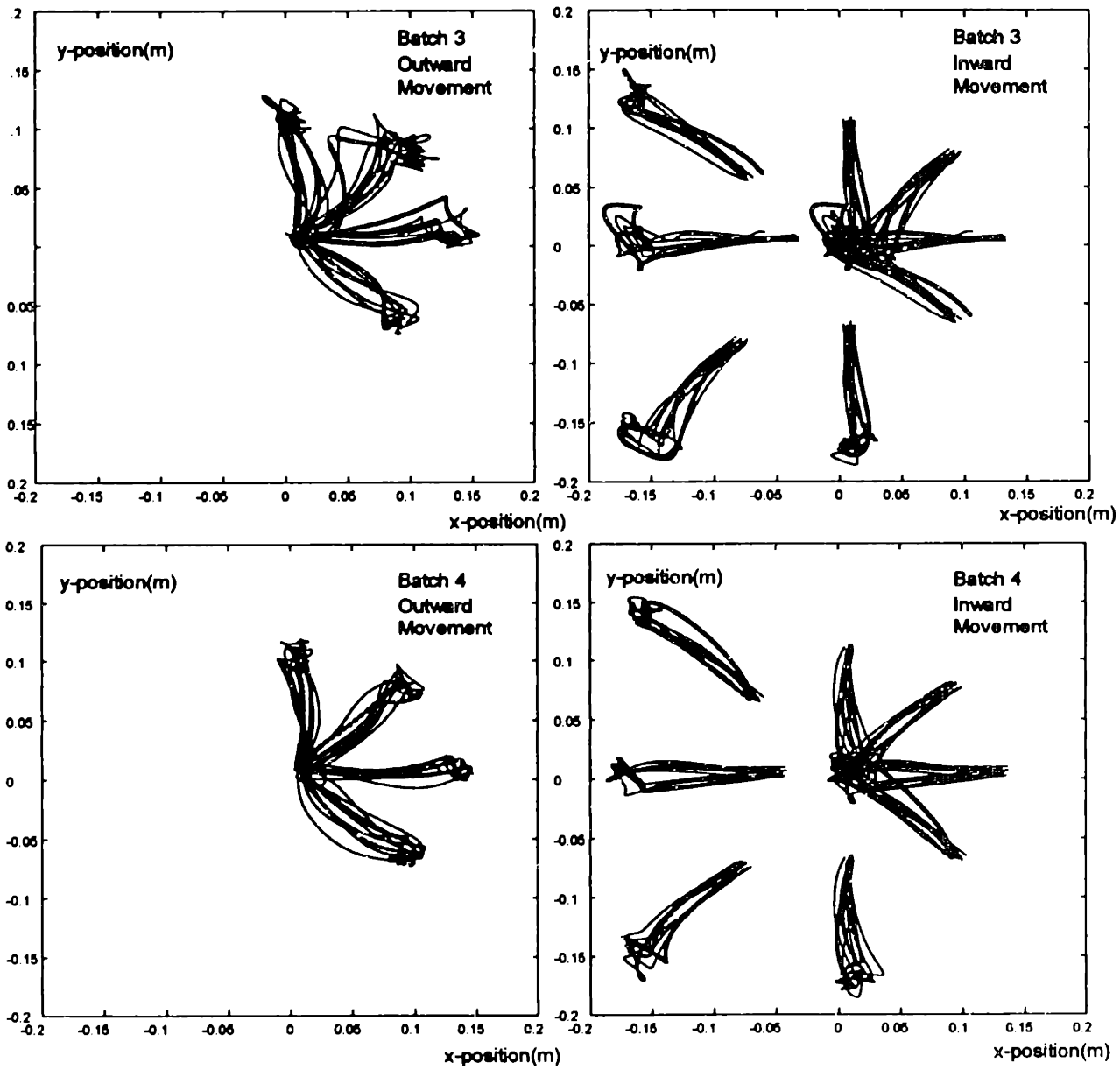

FIG.6.18.b. Trace Record for Subject CR - Batch 3 & 4

The upper row corresponds to batch 3 and the lower row to batch 4. Plots on the left column contain movements from the center to randomly presented outwards targets. The right column contains movements back to the center.

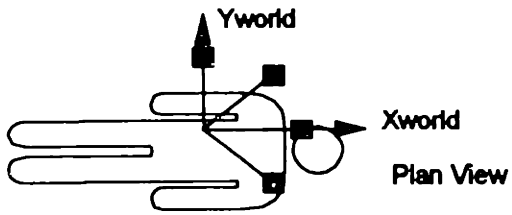

The inward movement traces were copied on the second column to allow better visualization of the end of the movement.

continuous bold line – first movement in the set
dashed bold line – last movement in the set

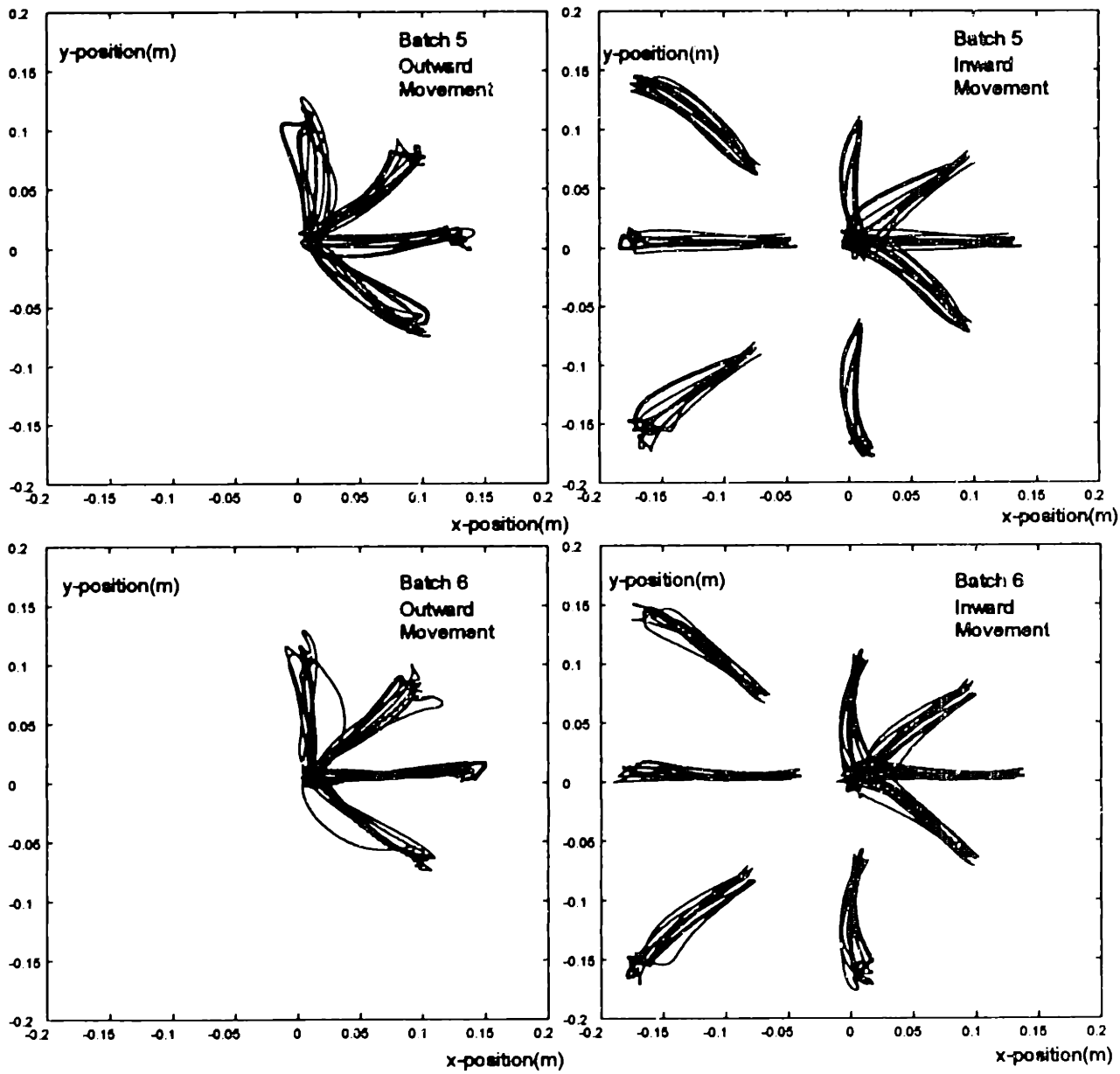

FIG.6.18.c. Trace Record for Subject CR - Batch 5 & 6

The upper row corresponds to batch 5 and the lower row to batch 6. Plots on the left column contain movements from the center to randomly presented outwards targets. The right column contains movements back to the center.

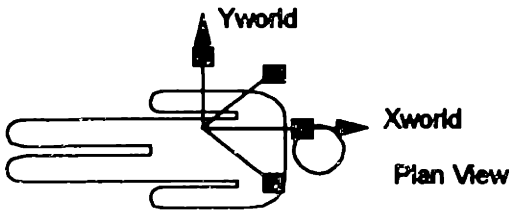

The inward movement traces were copied on the second column to allow better visualization of the end of the movement.

continuous bold line – first movement in the set
dashed bold line – last movement in the set

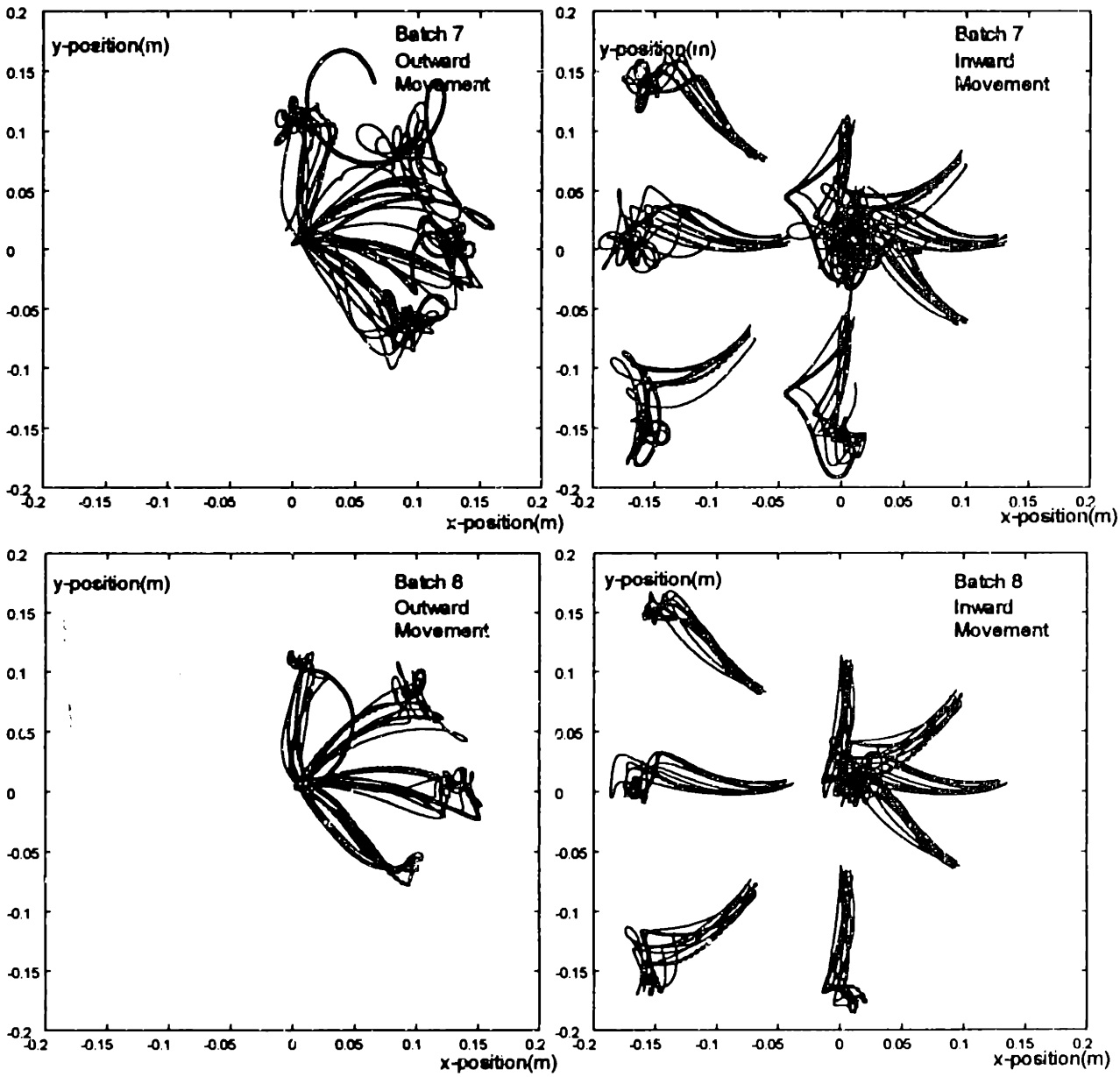

FIG.6.18.d. Trace Record for Subject CR - Batch 7 & 8

The upper row corresponds to batch 7 and the lower row to batch 8. Plots on the left column contain movements from the center to randomly presented outwards targets. The right column contains movements back to the center.

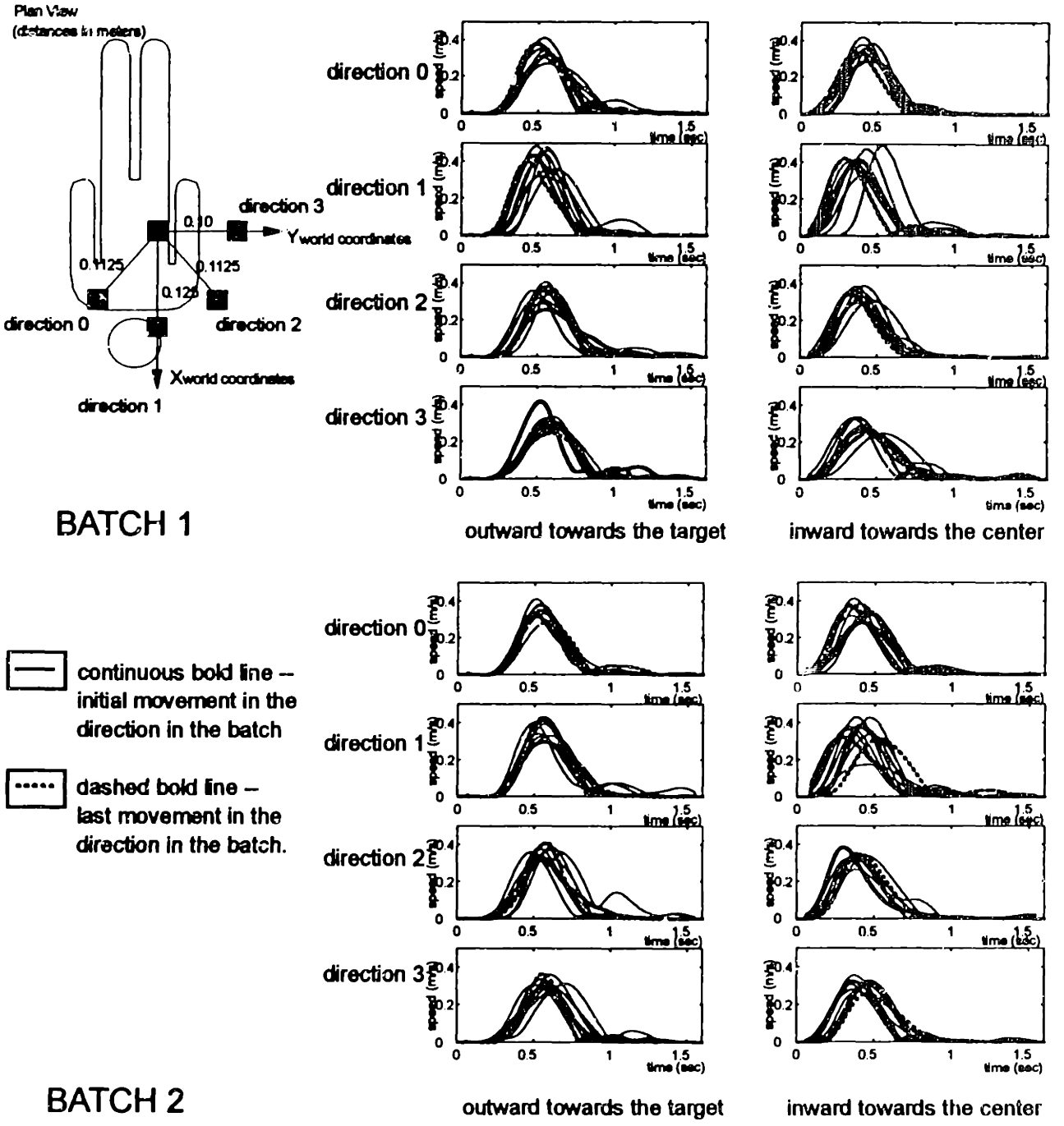

FIG.6.19.a. Speed Record for Subject CR - Batch 1 & 2
The figure shows two sets of speed records. The upper four rows correspond to batch 1 and the last four rows to batch 2. Plots on the left column contain movements from the center to randomly presented outwards targets. The right column contains movements back to the center.

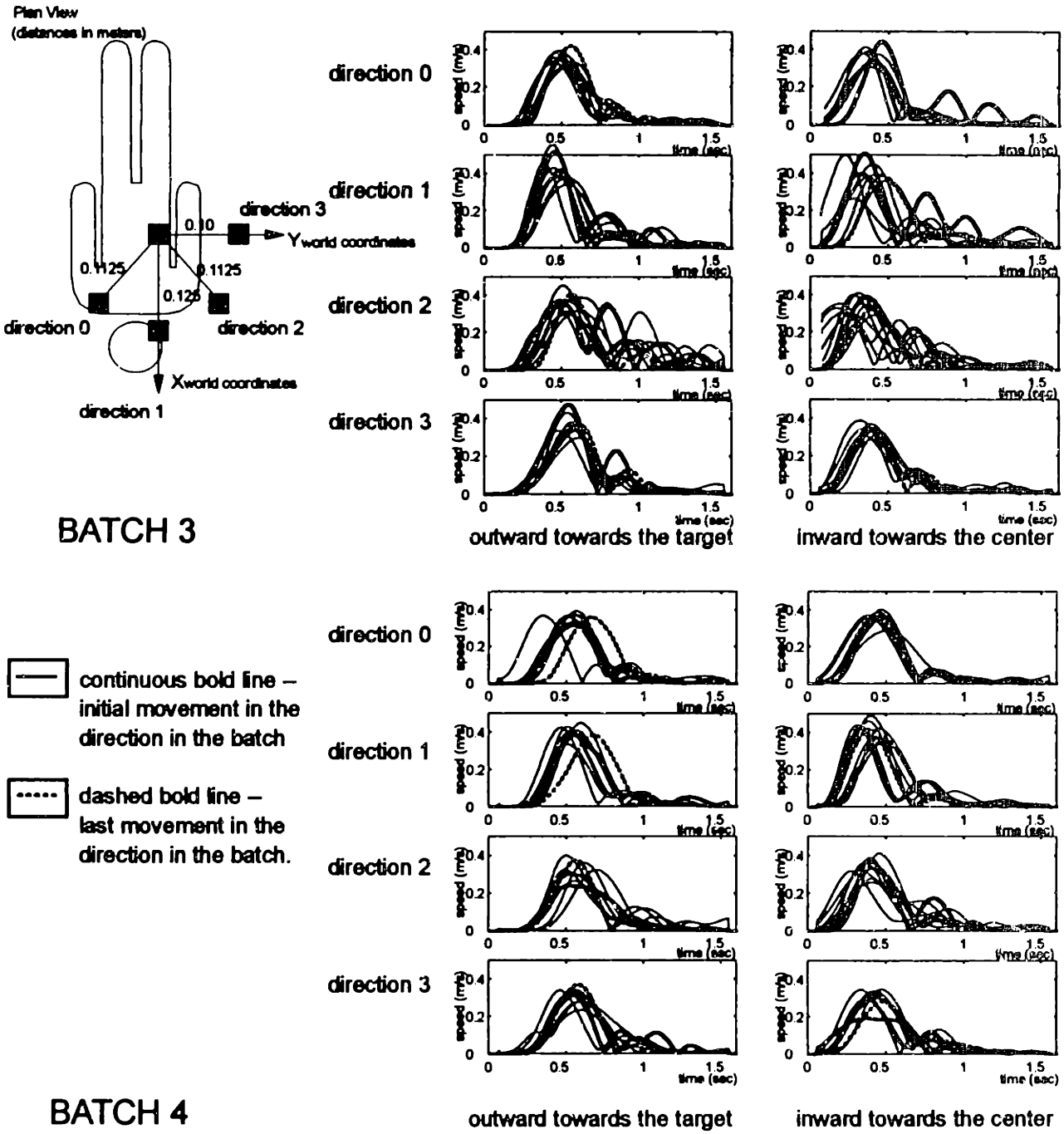

FIG.6.19.b. Speed Record for Subject CR - Batch 3 & 4

The figure shows two sets of speed records. The upper four rows correspond to batch 3 and the last four rows to batch 4. Plots on the left column contain movements from the center to randomly presented outwards targets. The right column contains movements back to the center.

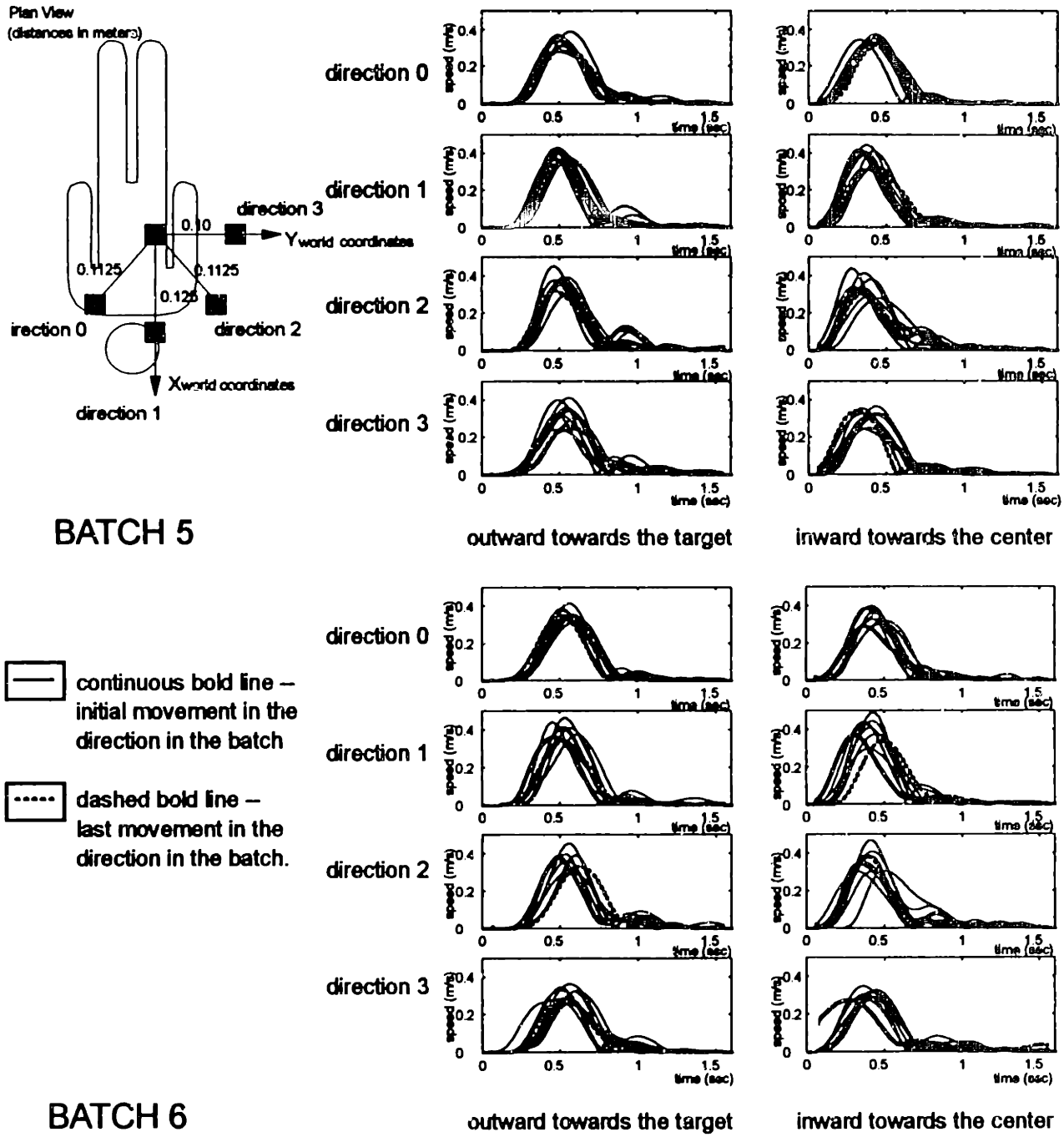

FIG.6.19.c. Speed Record for Subject CR - Batch 5 & 6
The figure shows two sets of speed records. The upper four rows correspond to batch 5 and the last four rows to batch 6. Plots on the left column contain movements from the center to randomly presented outwards targets. The right column contains movements back to the center.

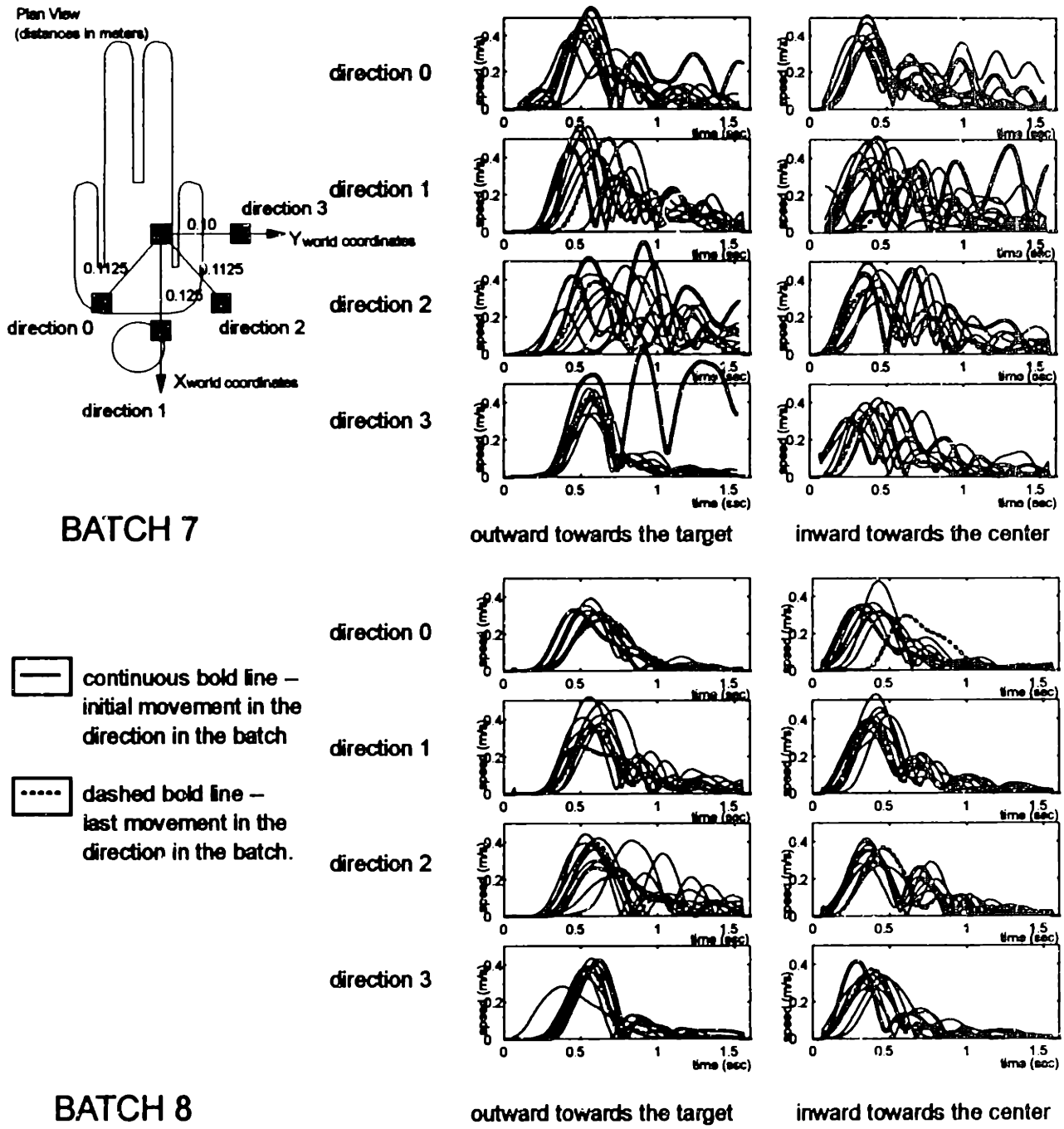

FIG.6.19.d. Speed Record for Subject CR - Batch 7 & 8
The figure shows two sets of speed records. The upper four rows correspond to batch 7 and the last four rows to batch 8. Plots on the left column contain movements from the center to randomly presented outwards targets. The right column contains movements back to the center.

In fact, both indices mentioned above are variations of the minimum-jerk hypothesis for point-to-point unrestricted planar movements [Flash & Hogan], which leads to "straight" lines (mean-squared deviation performance index) and bell-shaped speed profiles (performance index correlating the trial speed with the non-null field velocity with a minimum-jerk like velocity profile for the unperturbed case). The direct application of the jerk as a performance index leads to similar results, as illustrated with the mean jerk across the eight normal subjects in Fig.6.20. (data for all subjects can be found in Appendix E, Figs.Jerk_Index.1. to Jerk.8.). The figure shows in the upper plot the mean jerk magnitude for each batch. As with the mean lateral deviation, baseline condition (batches 1 & 2) was followed by deterioration of the performance as the force field was applied (batch 3). The subsequent results showed a progressive reduction on the mean jerk magnitude, indicating learning (batches 4 to 6). Similar patterns can be observed as subjects were challenged with a new force field with reverse characteristics (batches 7 & 8). For comparison, the insert plot shows the mean lateral deviation from the straight line of Fig.6.9. The lower plot shows the learning rate assessed by the slope of the regression during Early Learning and Negative Transfer, as well as for the overall Learning Phase (Early + Late). The insert plot shows the learning rate obtained with the performance index of Fig.6.9. Note the resemblance between the profiles of the index indicating the mean-squared lateral deviation from a straight line and the index indicating the jerk magnitude. One cannot but argue that for normal subjects, the different indices being proposed in the literature may represent different facets of a single global index: minimum-jerk.

Yet, the learning rate and inter-subject variability (standard deviation) differ between indices. While the mean-squared lateral deviation is the most invariant (smaller standard deviation), neither the deviation from the unperturbed trajectory or the velocity correlation with the unperturbed one might not serve as an appropriate index for different tasks. Indeed, these indices might suffer from lack of generalization which makes a global performance index tempting. By contrast, the observation of the grace and smoothness of human movement hints to the minimum-jerk as a possible global performance index. Likewise, experimental evidence points to movement segmentation, and in what follows, the conjecture of minimum number of interventions of Chapter 2 is used to design an index to measure learning in this task.

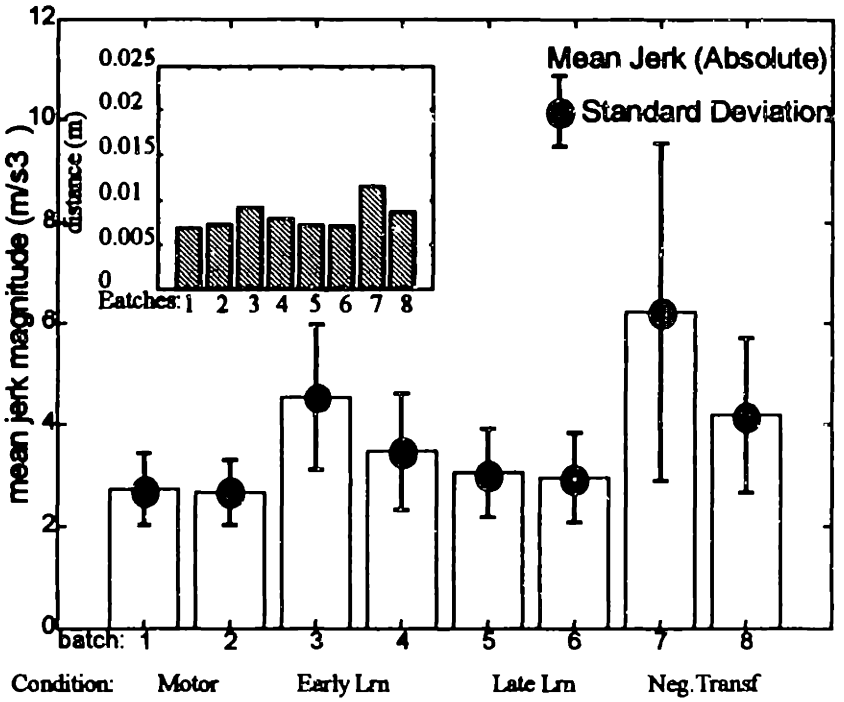

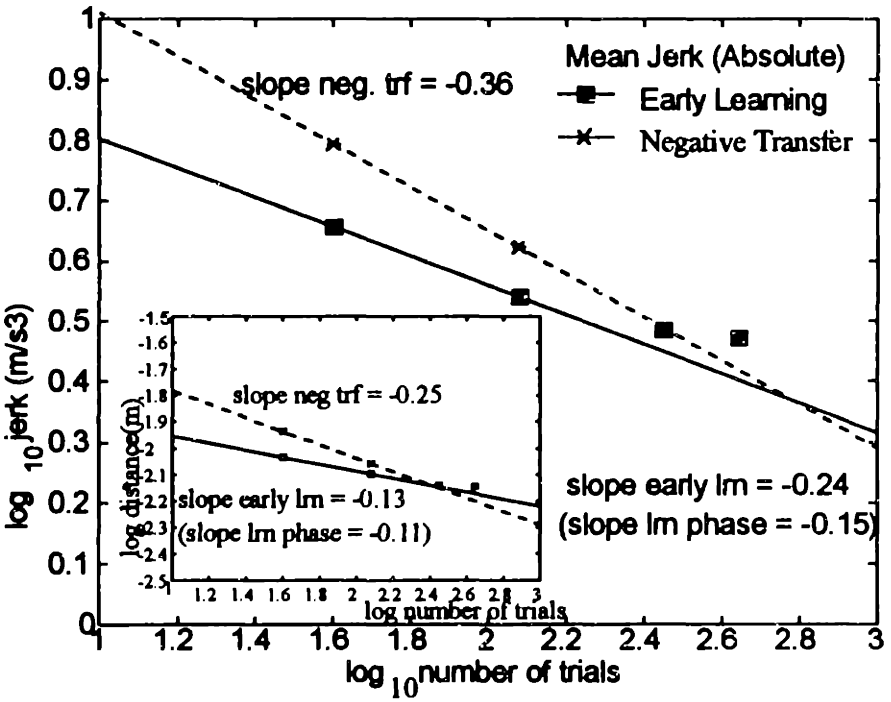

FIG.6.20. Mean Jerk Magnitude Across Eight Normal Subjects
The plots show the mean jerk magnitude for each batch with the insert plots showing the mean-squared deviation for each batch from Fig.6.9.

Consider the example shown in Fig.6.21. of one movement of subject DS at the beginning of each batch (the reason to choose this subject will become apparent later). The movement corresponds to the return movement from position (x,y)=(0.135, 0.01) in meters to the homing position (0.01, 0.01). As mentioned, during Early Learning a multi-peaked velocity profile is evident (right column, batch 3) that is quite different from the single-peaked profile seen in the unperturbed Motor Performance case (right column, batches 1 & 2). With learning, the secondary peaks become progressively less evident (right column, batches 4, 5 & 6). A similar pattern can be observed during Negative Transfer (right column, batches 7 & 8). This is consistent with the working hypothesis of Chapter 2 (Minimum Action Unit Conjecture and Learning). Therefore, the tools developed in Chapter 3 to analyze patient kinematic data were used in this learning context.

Figure 6.22. shows in the upper plot the mean number of basis functions for the eight normal subjects. There is a consistent pattern of reduction in the number of bases required to decompose movement while learning the task. The baseline condition (batches 1 & 2) was followed by deterioration of the performance as the force field was applied (batch 3). This is indicated by the increase in the mean number of bases. The subsequent results showed a progressive reduction in the mean number of bases, indicating learning (batches 4 to 6). Similar patterns can be observed as the subjects were challenged with a new force field with reverse characteristics (batches 7 & 8). For comparison, the insert plot shows the mean lateral deviation from the straight line of Fig.6.9. The lower plot shows the learning rate assessed by the slope of the regression with this index. The insert plot shows the learning rates obtained in Fig.6.9. Note that the number of basis functions during the baseline condition is close to 2 and this occurs due to the typical dip into the negative velocity values at the tail of fast point-to-point movements (mechanical oscillation). This is evident in the mean number of bases during the baseline condition (batches 1 & 2) and it can be easily observed in batch 1 of Fig.6.21.

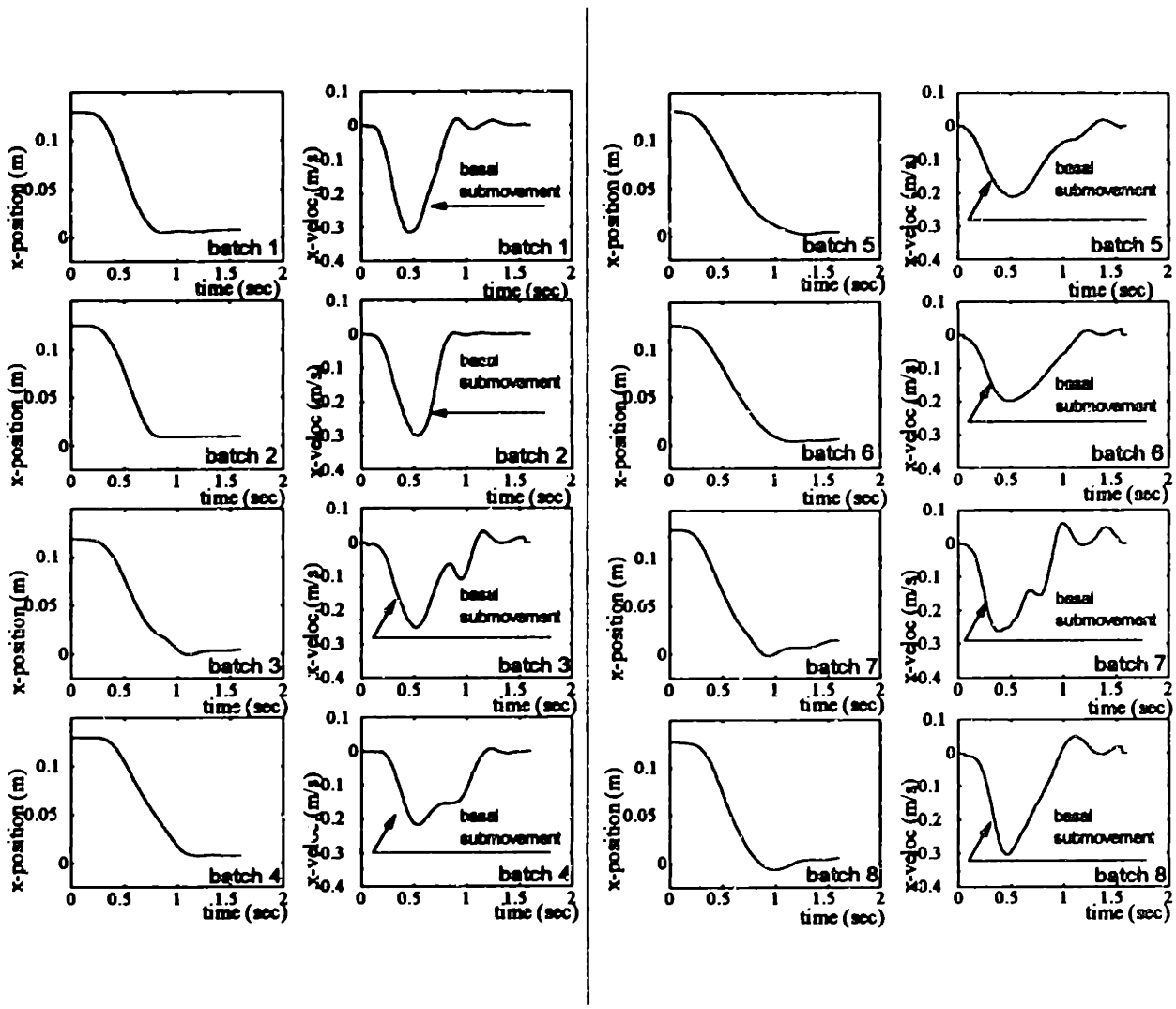

FIG.6.21. Example of Velocity Record for Subject DS

The figure shows the x-direction trace and velocity records at the beginning of each batch. The movement corresponds to the return movement from position (x,y) = (0.135, 0.01) in meters to the homing position (0.01, 0.01). Batches 1 through 4 are in the left, batches 5 through 8 on the right. The left columns show the x-direction trace and the right columns show the x-direction velocity.

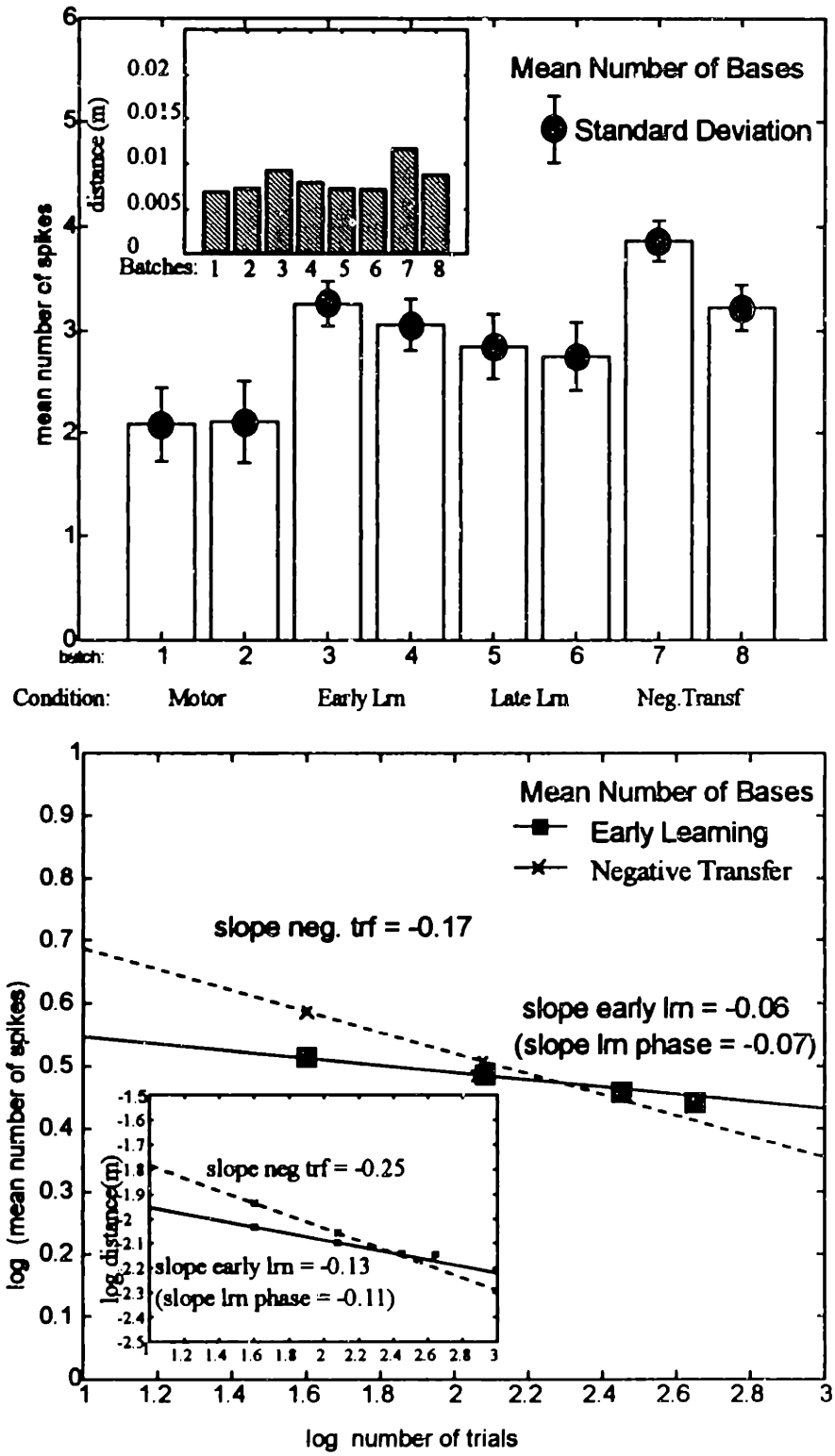

FIG.6.22. Mean Number of Basis Functions Across Eight Normal Subjects The plots show the mean number of basis for each batch with the insert plots showing the mean-squared deviation for each batch from Fig.6.9.

In this context the claim of a competent performance index can be made and at a first glance the number of basis functions looks like just another variation in indices based on the minimum-jerk hypothesis for point-to-point unrestricted planar movements [Flash & Hogan]. Additionally, this index can be used in a general sense, but the main criticism rises from questions regarding the working model for learning which suggests that this motor learning task may be performed initially using a sequence of overlapping segments, which are then progressively tuned and "blended" as motor learning proceeds. Moreover, in a protocol that exposed the subject's hand to disturbing forces, a method must be found to extract and segregate segments (submovements) from the system's mechanical response. In fact as mentioned in Subsection 6.1.2., Shadmehr and Mussa-Ivaldi expressed views similar to Woodworth against the concept that "corrective movements" (submovements) were involved during learning in their tasks, since the subjects did not have any visual feedback of their hand during the movement, only proprioceptive. They suggested that an internal model in-line with general views favoring kinematic planning of the force field would be composed, and subjects started "aiming better" compensating the force field. It is easy to follow the strength of their viewpoint by considering the simplest example of a point-mass following the same virtual trajectory of the unconstrained movement (reference) in a bidimensional plane, as shown in Fig.6.23. The forced trajectory presents the same sort of "hooks" at the end of the movement as many of the subjects' trajectories (see Appendix E, Figs.Trace.1. to 8.). In fact, one cannot but speculate that the "hooks" in the force field are the same mechanical "artifact" that causes the dip in velocity (reversal) in null-field.

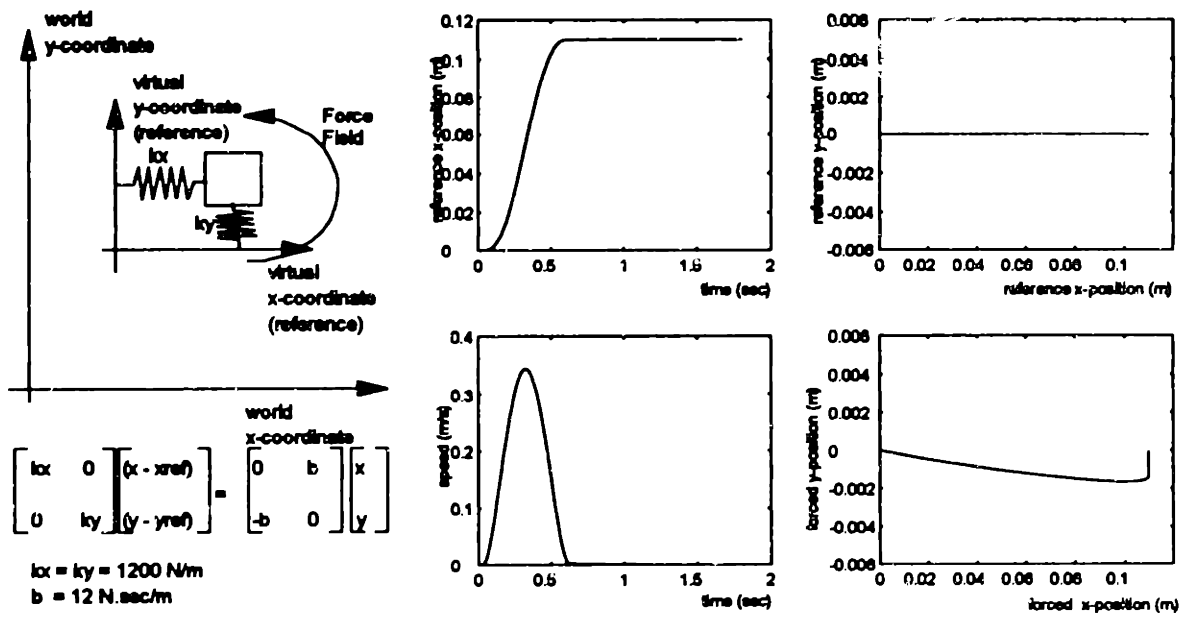

FIG.6.23. A Point Mass-Spring Mechanical System in the Force Field.
Illustrates the "hook" in the tail part of the hand trace of a mechanical system in a non-null force field. The virtual trajectory (reference) is the same as in the null force field (upper row). The speed and trace record of the system response is shown in the lower row. Note in the trace record the "hook" at the tail of the movement (lower right plot).

This dichotomy of views is not recent and it can be traced at least to the work of Woodworth a century ago (Chapter 2). It is the classical arguments between pure feedforward and feedforward plus feedback corrections. Shadmehr and Mussa-Ivaldi suggested a learning mechanism of non-intervention during the movement itself with updates of the internal model for subsequent movements (the oscillation is a consequence of the mechanics). The conjecture in this work that motor learning task may be performed initially using a sequence of overlapping segments, which are then progressively tuned and "blended" as motor learning proceeds, requires intervention during the movement to update the internal model for subsequent movements (submovements are centrally generated and masked in some instances by mechanical oscillations). In what follows, evidence will be shown indicating that while the "hooks" are most likely just mechanical artifacts at the tail of the movements in the force field, most subjects in this study did build the internal model in a fashion suggested by the working model of Chapter 2 and one subject probably built

the internal model predominantly in the non-intervention fashion. In summary, it is another instance of a colorful world. The evidence is based on the analysis of the basal first submovement (see Fig.6.21). Figures 6.24. through 6.31. show the basal submovement mean peak speed per batch (left upper row plot), the basal basis mean duration (right upper row plot), and the basal mean displacement (left lower row plot). The dashed horizontal line in the displacement plot is the mean distance to targets. The core of the analysis that follows is that in a conservative force field, a non-intervention strategy leads the forced case to equal or longer time duration for the basal submovement as compared to the null-field condition. At the risk of over-interpreting the data, the results for each subject are briefly discussed below:

- Subject CR (Fig.6.24.) interpreted the instructions in a more stringent form than the other subjects. During baseline conditions (batches 1 & 2), his basal submovement lasted 600 msec. Adding to it the typical 200-250 msec for reaction time, and the subject was trying to reach the target precisely when it changed colors (800 msec). Throughout the trial, the displacement of CR's basal submovement allowed him to hit the target in a single submovement. However, it can be concluded from these plots that CR did not adopt the non-intervention approach, since he tried to hit the targets with a faster submovement (mean time duration batch 3 and 7).

- Subject DB (Fig.6.25.) interpreted the instructions more loosely than the other subjects. During baseline conditions (batch 1), his mean basal submovement lasted well after the change of target colors and caught up later (batch 2). Subject DB showed signs of segmentation at least during the negative transfer phase. Even in the event that the mean displacement of the basal submovement occurred in a straight line, it fell short of the target mean distance.

- Subject DG (Fig.6.26.) showed signs of segmentation throughout the non-null force field phases of the trial. Even in the event that the mean displacement of the basal submovement occurred in a straight line, it fell short of the target mean distance.

- Subject DS (Fig.6.27.) apparently did not intervene during the learning phases. The mean time duration increased during the learning phase, although he intervened during the negative transfer phase trying faster basal submovements.

- Subject DD (Fig.6.28.) showed signs of segmentation throughout the non-null force field phases of the trial. Even in the event that the mean displacement of the basal submovement occurred in a straight line, it fell short of the target mean distance.

- Subject ES (Fig.6.29.) intervened during the early learning phases with a faster basal submovement and he showed signs of segmentation during the negative transfer phase. Even in the event that the mean displacement of the basal submovement occurred in a straight line, it fell short of the target mean distance.

- Subject MU (Fig.6.30.) showed signs of segmentation throughout the non-null force field phases of the trial. Even in the event that the mean displacement of the basal submovement occurred in a straight line, it fell short of the target mean distance.

- Subject TH (Fig.6.31.) showed signs of segmentation throughout the non-null force field phases of the trial. Even in the event that the mean displacement of the basal submovement occurred in a straight line, it fell short of the target mean distance.

In conclusion, the approach of observing to the basal submovement seems fairly robust and sheds light onto the long standing debate regarding subject's intervention and learning strategies during reasonably fast movements (800 msec). The mechanical response of the system made this problem particularly tough, but the conjecture of the existence of submovement corrections is upheld. At the risk of being pedantic, it is emphasized once more that the application of the tools developed in Chapter 3 might reveal different facets and learning strategies that otherwise would be concealed. For example, one possible interpretation of the basal submovement analysis is to cluster subjects based on adopted learning strategies during the learning phase (batches 3 to 6):

- Group A tried to hit the target with a single basal submovement.

- Group B did not try to hit the target with a single basal submovement, but instead adopted the "one-two punch" strategy, i.e. the basal submovement fell short and was followed by a corrective submovement.

This interpretation would suggest that Group A number of submovements during the learning phase would tend towards the number in the baseline condition (batches 1 & 2), while Group B number of submovements would tend towards the baseline condition plus one. Indeed, these trends can be observed as shown in Fig.6.32.A. which shows the number of basis for subjects in group A on the left side and for subjects in group B on the right side with statistical significance analysis shown in Fig.6.32.B. The mean number of submovements in the learning condition (batches 3 to 6) appears to tend to 2 submovements for Group A, and to 3 submovements for Group B. Furthermore, addressing the fact that in many instances the basal submovements were shorter, one cannot but argue that Shadmehr and Mussa-Ivaldi's suggested learning mechanism of non-intervention during the movement itself with updates of the internal model for subsequent movements does not hold. Most subjects did intervene to hit the targets. The conjecture in this work that motor learning task may be performed initially using a sequence of overlapping segments, which are then progressively tuned and "blended" as motor learning proceeds, requires intervention during the movement to update the internal model for subsequent movements. These results will be further discussed in the following Chapter 7 (imaging and kinematic analysis). Work must be done analysing not just the mean values, but the submovement time-history and statistics throughout the trials.

Subject CR - Basal Submovement

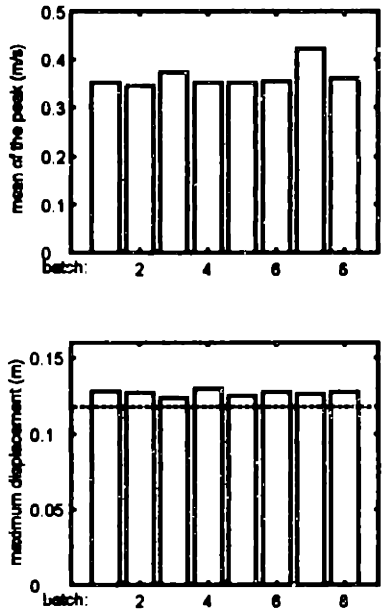

Hypothesis Test - Mean Duration

	1	2	3	4	5	6	7	8
1	0	0	1	0	0	0	1	0
2		0	1	0	0	0	1	0
3			0	1	1	1	1	1
4				0	0	0	1	0
5					0	0	1	0
6						0	1	0
7							0	1
8								0

- - dashed horizontal line indicates the distance to targets

FIG.6.24. Basal Submovement Mean Values for Subject CR

The left upper plot shows the mean peak velocity (m/s), the right upper plot shows the mean time duration (sec), and the left lower plot indicates the mean displacement (m) of the basal submovement per batch.The table shows the hypothesis test that the duration means of different batches are equal (null hypothesis). It does not reject the null hypothesis (indicated by 0), or rejects the null hypothesis (indicated by 1) with statistical significance level of 0.05.

Subject DB - Basal Submovement

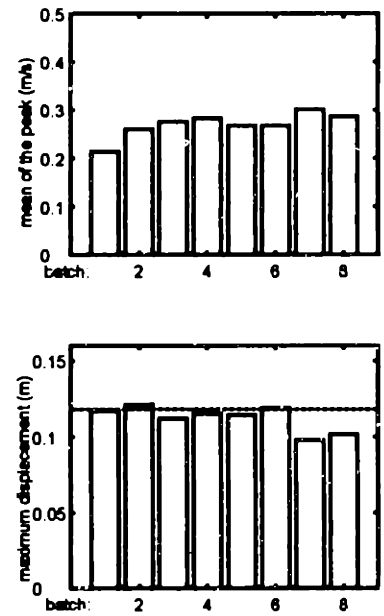

Hypothesis Test - Mean Duration

	1	2	3	4	5	6	7	8
1	0	1	1	1	1	1	1	1
2		0	1	1	1	0	1	1
3			0	0	0	1	1	1
4				0	0	1	1	1
5					0	0	1	1
6						0	1	1
7							0	1
8								0

- - dashed horizontal line indicates the distance to targets

FIG.6.25. Basal Submovement Mean Values for Subject DB

The left upper plot shows the mean peak velocity (m/s), the right upper plot shows the mean time duration (sec), and the left lower plot indicates the mean displacement (m) of the basal submovement per batch.The table shows the hypothesis test that the duration means of different batches are equal (null hypothesis). It does not reject the null hypothesis (indicated by 0), or rejects the null hypothesis (indicated by 1) with statistical significance level of 0.05.

Subject DG - Basal Submovement

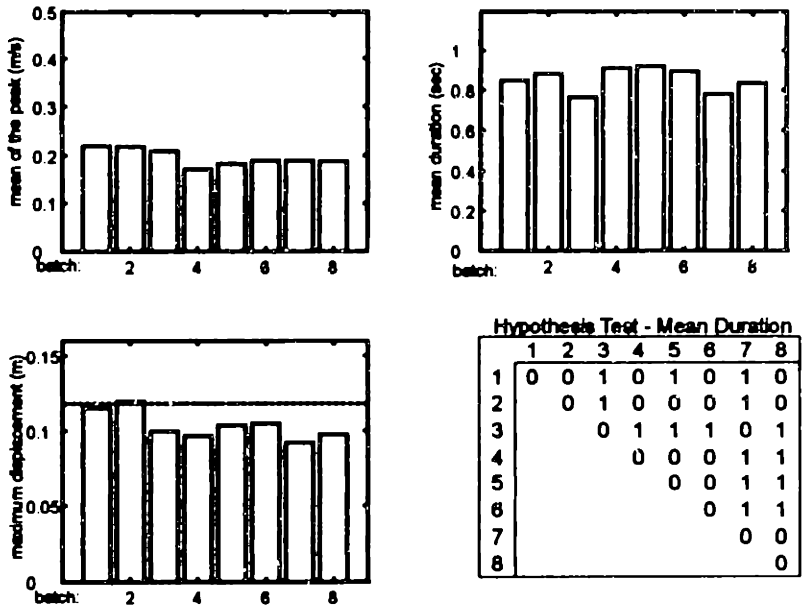

Hypothesis Test - Mean Duration

	1	2	3	4	5	6	7	8
1	0	0	1	0	1	0	1	0
2		0	1	0	0	0	1	0
3			0	1	1	1	0	1
4				0	0	0	1	1
5					0	0	1	1
6						0	1	1
7							0	0
8								0

- - dashed horizontal line indicates the distance to targets

FIG.6.26. Basal Submovement Mean Values for Subject DG

The left upper plot shows the mean peak velocity (m/s), the right upper plot shows the mean time duration (sec), and the left lower plot indicates the mean displacement (m) of the basal submovement per batch.The table shows the hypothesis test that the duration means of different batches are equal (null hypothesis). It does not reject the null hypothesis (indicated by 0), or rejects the null hypothesis (indicated by 1) with statistical significance level of 0.05.

Subject DS - Basal Submovement

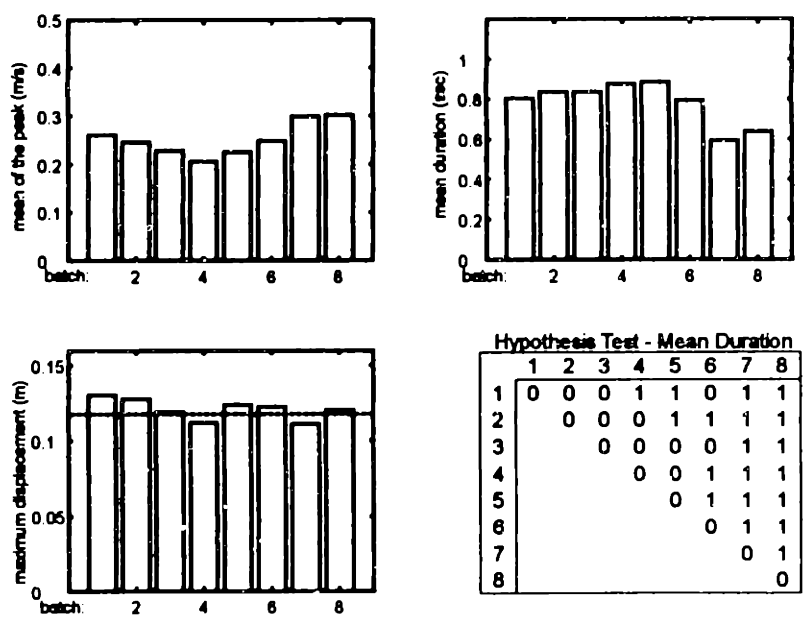

Hypothesis Test - Mean Duration

	1	2	3	4	5	6	7	8
1	0	0	0	1	1	0	1	1
2		0	0	0	1	1	1	1
3			0	0	0	0	1	1
4				0	0	1	1	1
5					0	1	1	1
6						0	1	1
7							0	1
8								0

- - dashed horizontal line indicates the distance to targets

FIG.6.27. Basal Submovement Mean Values for Subject DS

The left upper plot shows the mean peak velocity (m/s), the right upper plot shows the mean time duration (sec), and the left lower plot indicates the mean displacement (m) of the basal submovement per batch.The table shows the hypothesis test that the duration means of different batches are equal (null hypothesis). It does not reject the null hypothesis (indicated by 0), or rejects the null hypothesis (indicated by 1) with statistical significance level of 0.05.

Subject DD - Basal Submovement

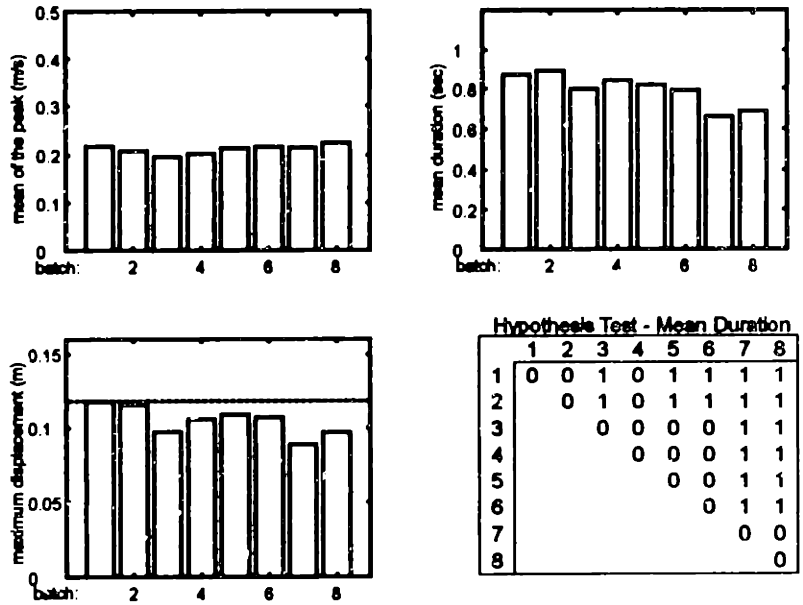

Hypothesis Test - Mean Duration

	1	2	3	4	5	6	7	8
1	0	0	1	0	1	1	1	1
2		0	1	0	1	1	1	1
3			0	0	0	0	1	1
4				0	0	0	1	1
5					0	0	1	1
6						0	1	1
7							0	0
8								0

- - dashed horizontal line indicates the distance to targets

FIG.6.28. Basal Submovement Mean Values for Subject DD

The left upper plot shows the mean peak velocity (m/s), the right upper plot shows the mean time duration (sec), and the left lower plot indicates the mean displacement (m) of the basal submovement per batch.The table shows the hypothesis test that the duration means of different batches are equal (null hypothesis). It does not reject the null hypothesis (indicated by 0), or rejects the null hypothesis (indicated by 1) with statistical significance level of 0.05.

Subject ES - Basal Submovement

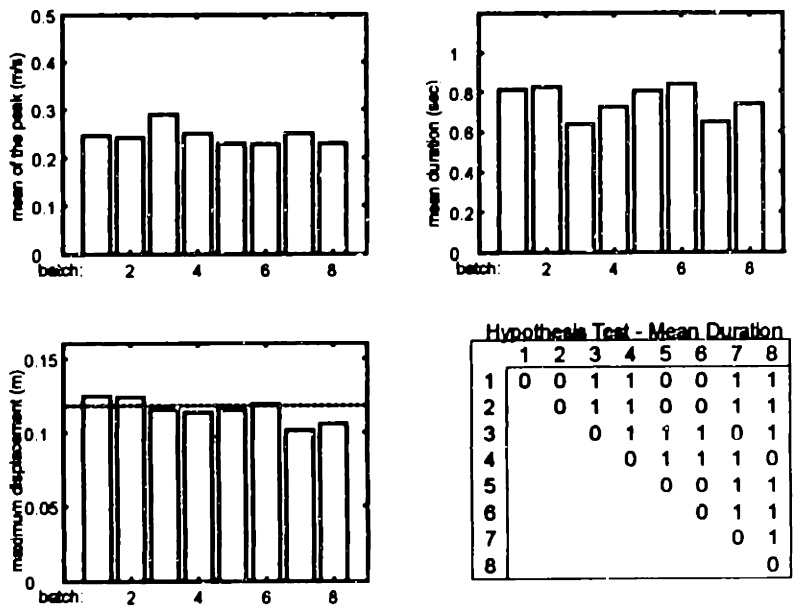

Hypothesis Test - Mean Duration

	1	2	3	4	5	6	7	8
1	0	0	1	1	0	0	1	1
2		0	1	1	0	0	1	1
3			0	1	1	1	0	1
4				0	1	1	1	0
5					0	0	1	1
6						0	1	1
7							0	1
8								0

- - dashed horizontal line indicates the distance to targets

FIG.6.29. Basal Submovement Mean Values for Subject ES

The left upper plot shows the mean peak velocity (m/s), the right upper plot shows the mean time duration (sec), and the left lower plot indicates the mean displacement (m) of the basal submovement per batch.The table shows the hypothesis test that the duration means of different batches are equal (null hypothesis). It does not reject the null hypothesis (indicated by 0), or rejects the null hypothesis (indicated by 1) with statistical significance level of 0.05.

Subject MU - Basal Submovement

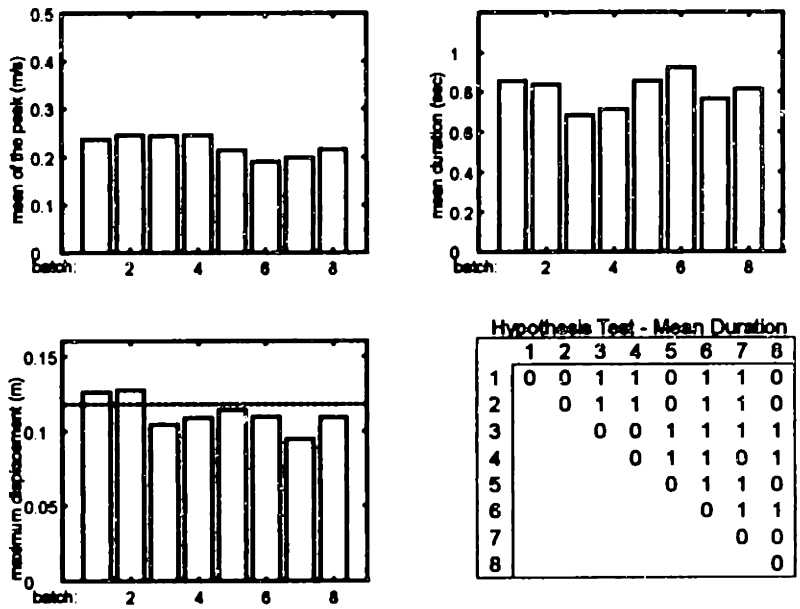

Hypothesis Test - Mean Duration

	1	2	3	4	5	6	7	8
1	0	0	1	1	0	1	1	0
2		0	1	1	0	1	1	0
3			0	0	1	1	1	1
4				0	1	1	0	1
5					0	1	1	0
6						0	1	1
7							0	0
8								0

- - dashed horizontal line indicates the distance to targets

FIG.6.30. Basal Submovement Mean Values for Subject MU

The left upper plot shows the mean peak velocity (m/s), the right upper plot shows the mean time duration (sec), and the left lower plot indicates the mean displacement (m) of the basal submovement per batch.The table shows the hypothesis test that the duration means of different batches are equal (null hypothesis). It does not reject the null hypothesis (indicated by 0), or rejects the null hypothesis (indicated by 1) with statistical significance level of 0.05.

Subject TH - Basal Submovement

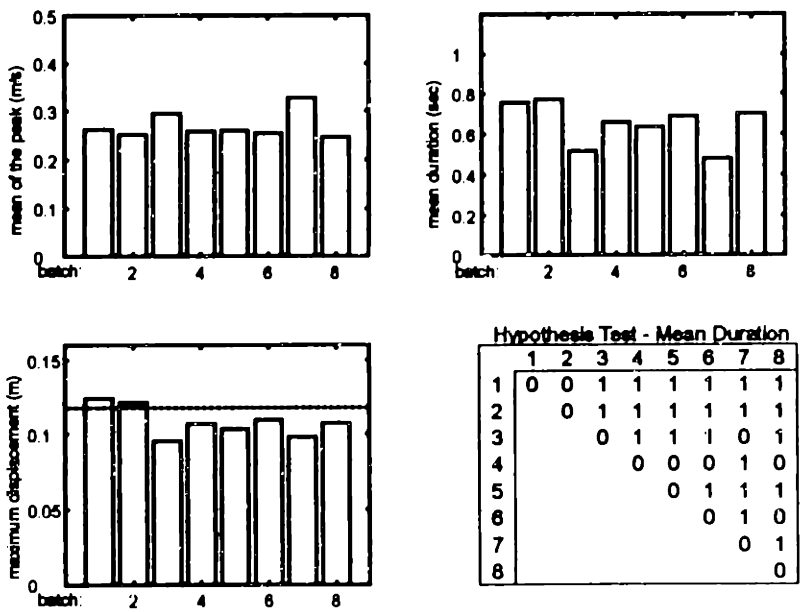

Hypothesis Test - Mean Duration

	1	2	3	4	5	6	7	8
1	0	0	1	1	1	1	1	1
2		0	1	1	1	1	1	1
3			0	1	1	1	0	1
4				0	0	0	1	0
5					0	1	1	1
6						0	1	0
7							0	1
8								0

- - dashed horizontal line indicates the distance to targets

FIG.6.31. Basal Submovement Mean Values for Subject TH

The left upper plot shows the mean peak velocity (m/s), the right upper plot shows the mean time duration (sec), and the left lower plot indicates the mean displacement (m) of the basal submovement per batch.The table shows the hypothesis test that the duration means of different batches are equal (null hypothesis). It does not reject the null hypothesis (indicated by 0), or rejects the null hypothesis (indicated by 1) with statistical significance level of 0.05.

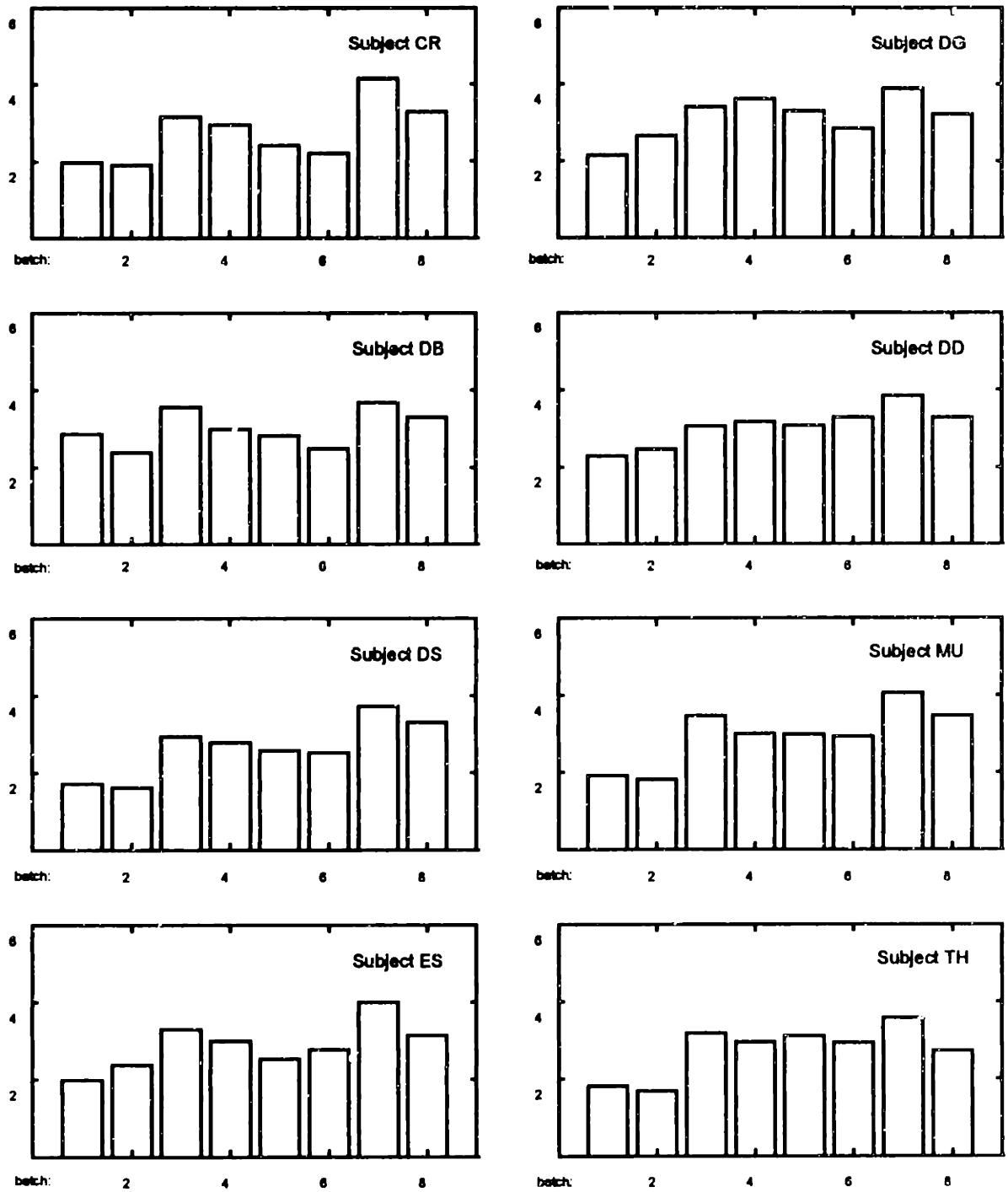

FIG.6.32.A. Mean Number of Basis for all Subjects
The plots show the mean number of bases for each subject per batch. Subjects on the left column had basal submovements that on average could reach the target in a straight line. Subjects on the right column have basal submovements that on average always fell short from the target.

Subject CR

	1	2	3	4	5	6	7	8
1	0	0	1	1	1	0	1	1
2		0	1	1	1	1	1	1
3			0	0	1	1	1	0
4				0	1	1	1	1
5					0	0	1	1
6						0	1	1
7							0	1
8								0

Subject DG

	1	2	3	4	5	6	7	8
1	0	1	1	1	1	1	1	1
2		0	1	1	1	0	1	1
3			0	0	0	1	1	0
4				0	0	1	0	0
5					0	1	1	0
6						0	1	0
7							0	1
8								0

Subject DB

	1	2	3	4	5	6	7	8
1	0	1	1	0	0	1	1	1
2		0	1	1	1	0	1	1
3			0	1	1	1	0	0
4				0	0	1	1	0
5					0	0	1	1
6						0	1	1
7							0	0
8								0

Subject DD

	1	2	3	4	5	6	7	8
1	0	0	1	1	1	1	1	1
2		0	1	1	1	1	1	1
3			0	0	0	0	1	0
4				0	0	0	1	0
5					0	0	1	0
6						0	1	0
7							0	1
8								0

Subject DS

	1	2	3	4	5	6	7	8
1	0	0	1	1	1	1	1	1
2		0	1	1	1	1	1	1
3			0	0	0	1	1	0
4				0	0	0	1	1
5					0	0	1	1
6						0	1	1
7							0	1
8								0

Subject MU

	1	2	3	4	5	6	7	8
1	0	0	1	1	1	1	1	1
2		0	1	1	1	1	1	1
3			0	1	1	1	1	0
4				0	0	0	1	1
5					0	0	1	1
6						0	1	1
7							0	1
8								0

Subject ES

	1	2	3	4	5	6	7	8
1	0	1	1	1	1	1	1	1
2		0	1	1	0	1	1	1
3			0	0	1	1	1	0
4				0	1	0	1	0
5					0	0	1	1
6						0	1	0
7							0	1
8								0

Subject TH

	1	2	3	4	5	6	7	8
1	0	0	1	1	1	1	1	1
2		0	1	1	1	1	1	1
3			0	0	0	0	0	1
4				0	0	0	1	0
5					0	0	1	0
6						0	1	0
7							0	1
8								0

FIG.6.32.B. Mean Number of Basis for all Subjects - Hypothesis Test (two sided t-test)
The tables show the hypothesis test that the means of different batches are equal (null hypothesis). It does not reject the null hypothesis (indicated by 0), or rejects the null hypothesis (indicated by 1) with statistical significance level of 0.05. Note that the variance for all the batches is approximately the same.

CHAPTER 7. TECHNIQUE TO INVESTIGATE IPSILATERAL FUNCTIONAL ACTIVATION IN MOTOR TASK

"Absence of evidence is not evidence of absence."

– M.Rees

7.1. Background

D'arcy Thompson in his remarkable book, "On Growth and Form", described living beings and their shapes from a functional perspective [Thompson, 1961]. One intriguing aspect of living beings described in D'arcy's book is symmetry. Symmetry is advantageous since it reduces the amount of information required to build a structure and it enhances stability around a particular axis. Therefore it is not surprising to find large numbers of structures and beings in nature with varying degrees of symmetry. Nonetheless, it is function, not symmetry, that is the paramount aspect of survival. For example, humans have two symmetric kidneys, but only a single liver. Similarly, the dichotomy between the left hemisphere of the brain controlling the limbs on the right side of the body, and the right hemisphere of the brain controlling the limbs on the left side is an oversimplification. Examining patient's handwriting with their "intact" dexterous hand after a stroke revealed clearly anomalous characteristics. Likewise robot-aided neuro-rehabilitation clinical trial observations revealed, unequivocally, deficiencies in the unimpaired arm. These deficiencies are generally attributed to the relative motion within the skull that the non-affected hemisphere is subjected to following the hematoma and swelling on the affected hemisphere. In fact, clinical studies have shown that the unimpaired limbs lose almost 30 percent of their strength during the initial post-stroke phase [Colebatch, 1989], and therapy attempts to restore and to train compensatory techniques with the unimpaired side. In general, these deficiencies and weaknesses subside with time. However, robot-aided functional imaging experiments (see Chapter 6) suggested that the ipsilateral hemisphere plays a role in learning a motor task that involves the ipsilateral arm. Specific motor neural processes might be taking place in a particular brain hemisphere, and such results would have implications for general rehabilitation strategies that

presently do not recognize this deficit. Therefore, hemiplegic subjects in the stable phase provide an opportunity to test: (a) the effect of cerebral lesions during motor learning and (b) whether the measured significant changes in neural activity during imaging experiments are not artifacts.

This chapter investigates three ipsilateral activations shown in the functional imaging experiments of the last chapter with the subjects' right dominant arm. During the learning phase of normal subjects with the right arm, there was a statistically significant increase in the regional cerebral blood flow in the ipsilateral temporoparietal, as well as in the ventral striatum (early learning). Likewise, there was a statistically significant increase in the ipsilateral primary motor area during the negative transfer phase.

7.2. Patients

Subjects with hemiparesis after a single CT verified stroke in the left motor strip (cortical Brodmann's areas 1 to 4, 6), right temporal area (Brodmann's areas 21, 22, 37), and right striatum (nucleus caudate and anterior putamen), volunteered for a study on the effect of learning and training several months after their discharge from Burke Rehabilitation Hospital (patients A, O, G respectively). The subjects had permanent severe motor deficit on their contralateral non-dominant limb and had been previously involved in the study described earlier (Chapter 5) that required manipulation of the robot, in accordance with the guidelines and approval of the MIT-Committee on the Use of Humans as Experimental Subjects (Protocol # 2187) and Burke Rehabilitation Hospital Human Subject Committee (Protocol # 227 - Appendix A). Prior written consent was obtained from all subjects.

7.3. Experimental Setup and Procedure

The study used the 2-dof module of a portable robot: MIT-MANUS. Its main features were discussed in some detail in Chapter 4. Subjects performed a visually-evoked and visually-guided task with their unimpaired dexterous arm, while facing a monitor. The task required holding the robot-end effector with a palmar grasp and moving it from its initial position towards a randomly

presented target (outward targets 0 to 3), while the robot generated a haptic virtual environment, as illustrated in Fig.7.1. Each target direction was presented an equal number of times. The subject was instructed to move the end-effector to the presented target in approximately 0.8 seconds. To indicate that 0.8 sec had elapsed, the color of the target changed. The target was visible another 0.8 sec and a new target was presented (blank screen for a few milliseconds). The robot generated no perturbation during motor performance (batches 1, 2, 11, 12), although it perturbed the subject's movement during learning and negative transfer conditions (batches 3 to 10). The characteristic of the perturbation force was reversed during negative transfer.

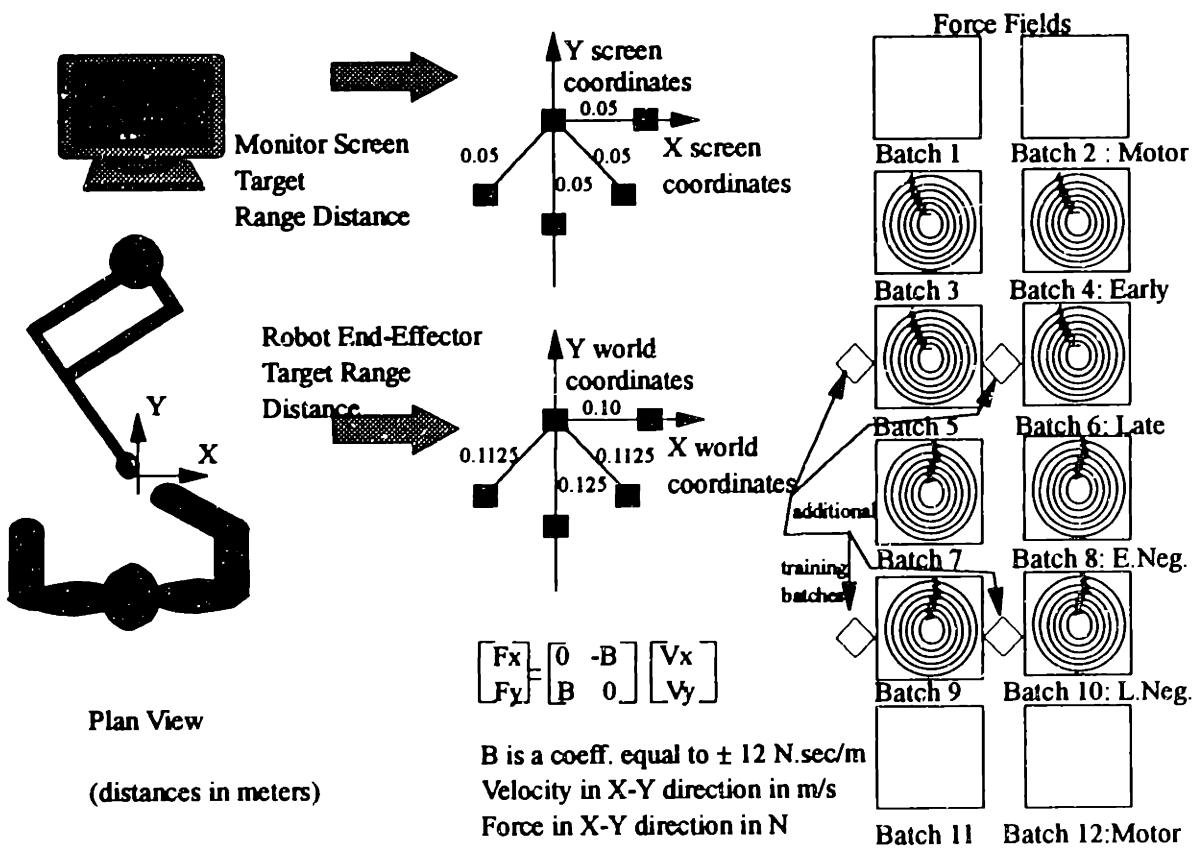

FIG.7.1. Visual and Spatial Exercise and Target Range

7.4. A Handful of Results

7.4.1. Kinematic Analysis via the Mean Lateral Deviation

The performance index of Subsection 6.4.2. was used to indicate learning, namely the lateral deviation of subject's movement from a straight line connecting targets. The mean lateral deviation from a straight line averaged across eight normal younger subjects, with no previous experience with the task is shown in Fig.7.2. The experiment with these subjects was limited to: motor performance, early learning, late learning, and early negative transfer conditions. Comparison of the performance of the intact controls with the three stroke subjects is also tallied in Fig.7.2. Subject A has a lesion in the left motor strip (Brodmann's areas 1 to 4, 6), Subject G has a lesion in the right ventral striatum area (nucleus caudate and anterior putamen), while Subject O has a lesion in the right temporal area (Brodmann's areas 21, 22, 37). The error bars indicate two standard deviations with the eight normal subjects.

Using the mean-squared lateral deviation as a numerical measure of performance, normal subjects' baseline condition 1 (batch 1 & 2) was followed by deterioration of performance as the force field was applied (batch 3). The subsequent results showed a progressive reduction in lateral deviation, indicating learning (batch 4 to 6). Similar patterns can be observed as subjects were challenged with a new force field with reverse characteristics (batch 7 & 8). The subject with the ipsilateral motor strip lesion (subject A) was able to learn at rates comparable to the intact subjects, and he continued to show reduction on the lateral deviation throughout the remaining negative transfer condition (batch 9 & 10). Using this performance index, there was no noticeable after-effect on removing the force field with the subject returning to baseline performance levels. The term "after-effect" refers to observable traces of a conditioning factor induced in subjects with training in a particular environment after the removal of the training constraints. The subject with an ipsilateral temporoparietal lesion (subject O) had a poorer motor performance than the intact subjects, particularly when the force field characteristics was reversed (negative condition, batches 7 to 10). The subject showed very slow improvement towards his baseline performance, although he had no evident signs of difficulty in returning to baseline performance levels with the removal

of the force field (after-effect). The subject with ipsilateral striatum lesion (subject G) also had a poorer motor performance than the intact subjects. This subject appeared to have marked difficulties in compensating for the after-effect of the force field removal, in contrast to the subjects with temporo-parietal or motor strip lesion.

These results suggest that the increase in activations in the ipsilateral right hemisphere (striatum and parietal region) is not an imaging artifact, but is consistent with the suggested dominant role of the right parietal cortex in spatial tasks and with the conjectures that the basal ganglia (striatum) plays an important role to preprogram ballistic movements. On the other hand, the ipsilateral primary motor area increase in activation appears to be an experiment artifact. The indication at [31.24 -20.79 52] in Talairach coordinates (see Table 6.3.a.) is close to the symmetrical activation on the contralateral side at [-41.44 -22.06 48] (see Table 6.2.a.) and near the PET facility resolution of 8 mm. Yet in view of the above results, the face value of the readings is considered accurate, suggesting that the ipsilateral right primary motor activation on a higher slice and closer to the center is an experiment artifact. This artifact might be caused by the subject(s) stiffening up the left leg or buttock to provide better support during the negative transfer condition. Likewise, it can be concluded that this case study provided some evidence that certain ipsilateral lesions affect the unimpaired arm, and that these deficiencies and weaknesses do not subside with time. These results have implications for general rehabilitation strategies that presently do not recognize this deficit

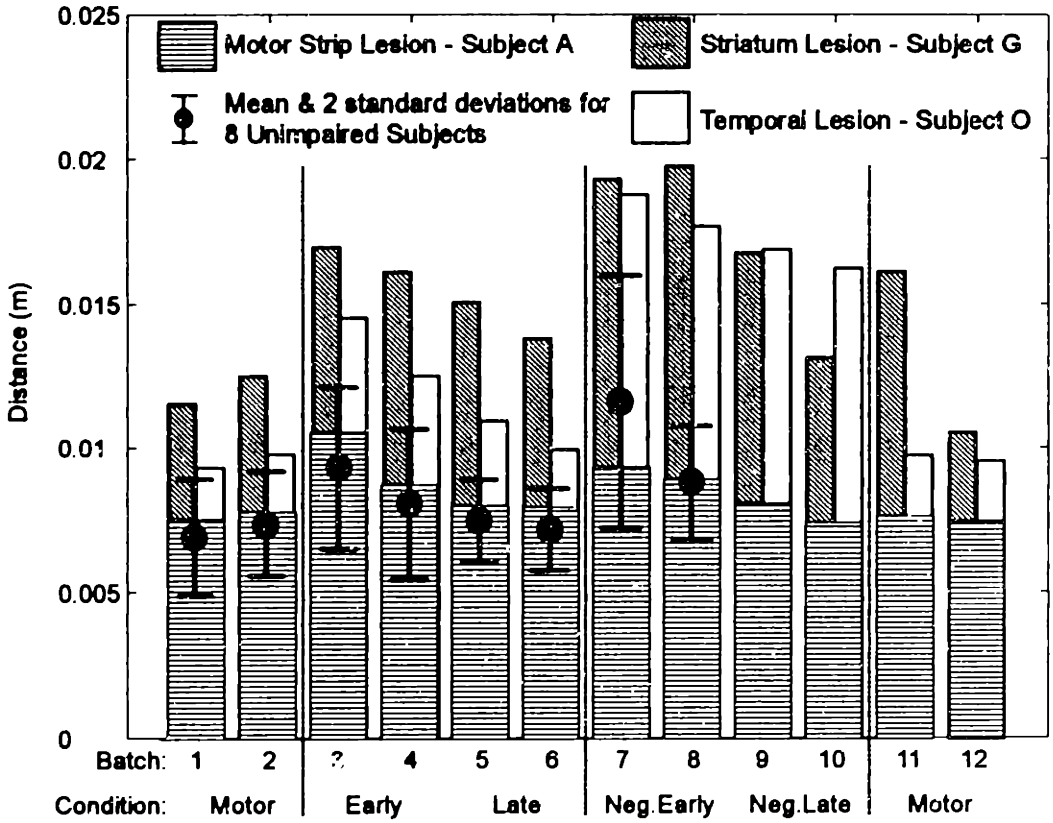

FIG.7.2. Mean Lateral Deviation from a Straigtht Line for the Unimpaired Arm of Three Hemiparetic Stroke Victims
Subjects have lesions in the motor strip (A), temporo-parietal (O), or striatum (G) areas. Mean and standard deviation for 8 younger unimpaired subjects are also shown (up to Negative Early Condition). Lesions on the motor strip do not seem to adversely affect motor learning with the unimpaired hand, while lesions on the temporal or striatum areas do.

7.4.2. Kinematics Analysis

The previous subsection discusses whether ispilateral brain structures play a role during motor learning, demonstrating that in this case study with three subjects, this was true for certain structures. This effect became apparent by using the mean-squared deviation from the straight line as the performance index. This subsection aims at demonstrating the value of the availability of different tools to analyse movement and reveal different kinds of information.

Figure 7.3. shows the mean results for the normal subjects and for the same three patients using the mean-jerk as the performance index. Using this index as a numerical measure of performance, the normal subject's baseline was followed by deterioration of performance as the force field was applied (batch 3). Subsequent results showed a progressive reduction of the mean jerk, indicating learning (batches 4 to 6). For normal subjects, note the resemblance between the index indicating the lateral deviation from a straight line and the index indicating the jerk magnitude (Appendix Jerk). As mentioned in Subsection 6.4.3., both indices mentioned above are variations of the minimum-jerk hypothesis for point-to-point unrestricted planar movements [Flash & Hogan],

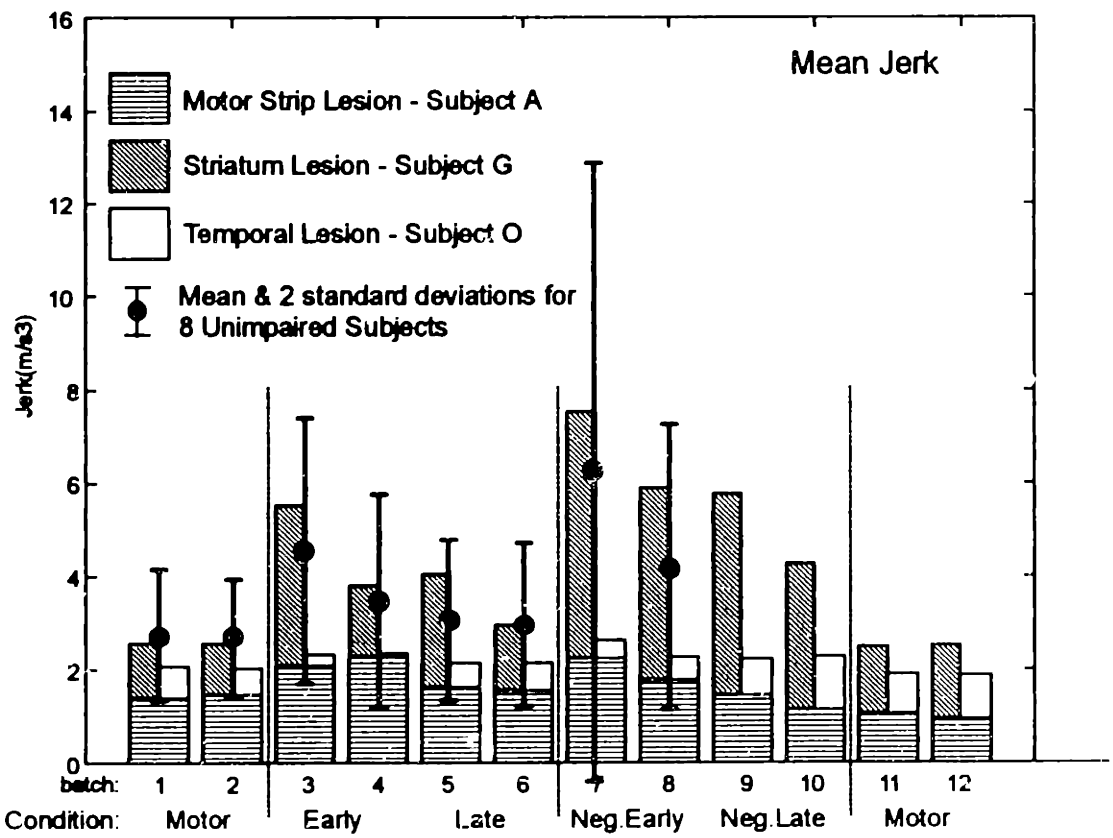

FIG.7.3. Mean Jerk for the Unimpaired Arm of Three Hemiparetic Stroke Survivors Subjects have lesions in the motor strip (A), temporo-parietal (O), or striatum (G) areas. Mean jerk for eight younger normal subjects (Chapter 6) is shown for comparison purposes.

which leads to "straight" lines (mean-squared deviation performance index) and bell-shaped speed profiles (performance index correlating non-null field velocity and the minimum-jerk like velocity profile for the unperturbed case). However, the performance index correlating the speed with the non-null field velocity for the unperturbed case or the mean-jerk failed to reveal any anomalous behavior in the patients data, illustrating the necessity of different tools to analyze movement.

To illustrate the advantages of different tools, this subsection uses some of the tools developed previously to better understand the subjects' performance. Figures 7.4. to 7.6. show hand trace records of the stroke survivors A, G, and O throughout the experiment during batches preceding and succeeding changes in the force field characteristics of the virtual environment (batches 2, 3, 6, 7, 10, and 11). The figures on the left column show the traces of outward movements towards the targets, and on the right column, traces of inward movements towards the center. A coarse analysis suggests that during non-null force field batches, some of the subjects tended to lock one of the joints in the direction that required predominantly movements in the other joint. Note also the "after-effect" trace discussed in the last subsection as the force field is neutralized (see batch 11), and the spread of the initial hand position during the non-null field conditions. Likewise, the speed profiles are shown in Figs. 7.7. to 7.9. for the same batches with the left column registering the speed outward and the right column registering the speed inward. Coarse analysis shows that although the task instructions and training batches without the force field were the same for all subjects, subjects' interpretation of the movement duration in the presence of the force field was quite elastic. For example, subject A initially performed within the expectation of movement duration on the order of 800 msec, but in subsequent trials slowed down due to the force field or to fatigue. Also, in many inward movements towards the center (there is no element of randomness), the subject did not follow the instruction to wait for the target presentation. Subject G on the other hand, waited for the visual presentation of the target. Yet his speed profile apparently did not converge to any repeatable pattern. As an explanatory remark, the plotting subroutine segregates the direction based on the initial and final position. Therefore, during trials in which the subject's hand initial or final position is out of the expected range, certain directions contain a smaller number of speed profiles than others (for example: subject G, batch 7). Subject

O presented an unusual pattern, appearing to change little throughout the whole trial and to stretch the movement duration to the total target presentation.

The decomposition of the trials into the basal submovement is shown in Fig. 7.10 to 7.12. They show the basal submovement mean peak speed per batch (left upper row plot), the basal basis mean duration (right upper row plot), the basal basis mean displacement (left lower row plot), and the basal basis mean starting instant (right lower row plot). The dashed horizontal line in the displacement plot is the mean distance to the targets. The basal analysis leads to similar comments of the coarse analysis of the hand traces and speed profiles. Subject A continuously decreased the mean basal submovement peak speed and increased the basal basis mean duration from the 800 msec to the 1250 msec range. On the other hand, subject G's mean basal basis duration is quite short. This subject took an exceedingly long time to initiate movement. In some instances, his mean initiation time (reaction) was above 600 msec and therefore he tried to compensate with short fast movements, making even faster movements to cope with the force field. These observations are rather anecdotal, but questions arise about the role of the striatum in the movement initiation. Subject O's basal submovement analysis did not reveal any unusual learning pattern with the subject's basal displacement falling short from the target with the force field. Yet, his mean movement initiation time roughly doubled from the 300 msec baseline to 500 msec with the force field. The presence of the force field did not influence normal subjects' movement initiation time.

In summary, this case study with three stroke survivors with distinct lesions provided some evidence that certain ipsilateral lesions affect the unimpaired arm, and that these deficiencies and weaknesses do not subside with time. Moreover, traces of these deficiencies cannot be detected in any index (Mean Lateral Deviation or Mean Jerk Indices), requiring a rich variety of tools such as the kinematic movement decoder of Chapter 3 to analyze and to enhance our understanding of motor control and neurological impairments.

Apéritif:

The indication that different lesion deficiencies might be revealed by some indices and not by others, prompts the old speculation that proper index exploitation might suggest the role of the living tissue destroyed during the cerebral vascular accident.

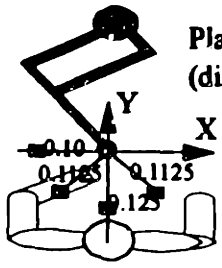

Plan View
(distances in meters)

The inward movement traces were copied on the second column to allow better visualization of the end of the movement.

continuous bold line – first movement in the set
dashed bold line – last movement in the set

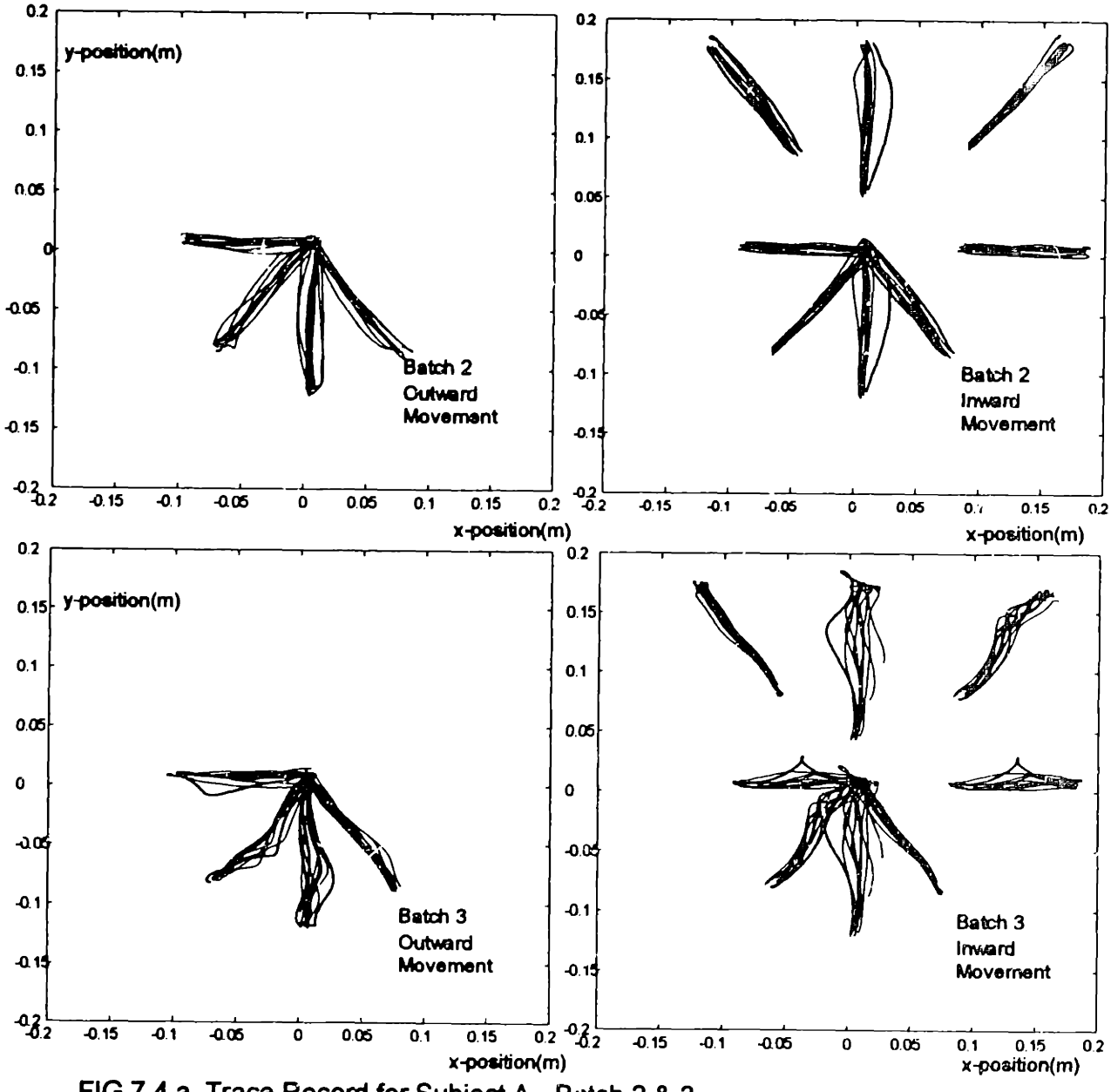

FIG.7.4.a. Trace Record for Subject A - Batch 2 & 3
The upper row corresponds to batch 2 and the lower row to batch 3. Plots on the left column contain movements from the center to randomly presented outward targets. The right column contains movements back to the center.

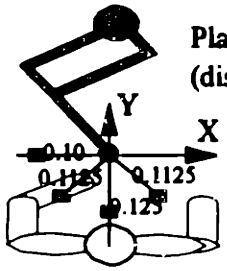

The inward movement traces were copied on the second column to allow better visualization of the end of the movement.

continuous bold line – first movement in the set
dashed bold line – last movement in the set

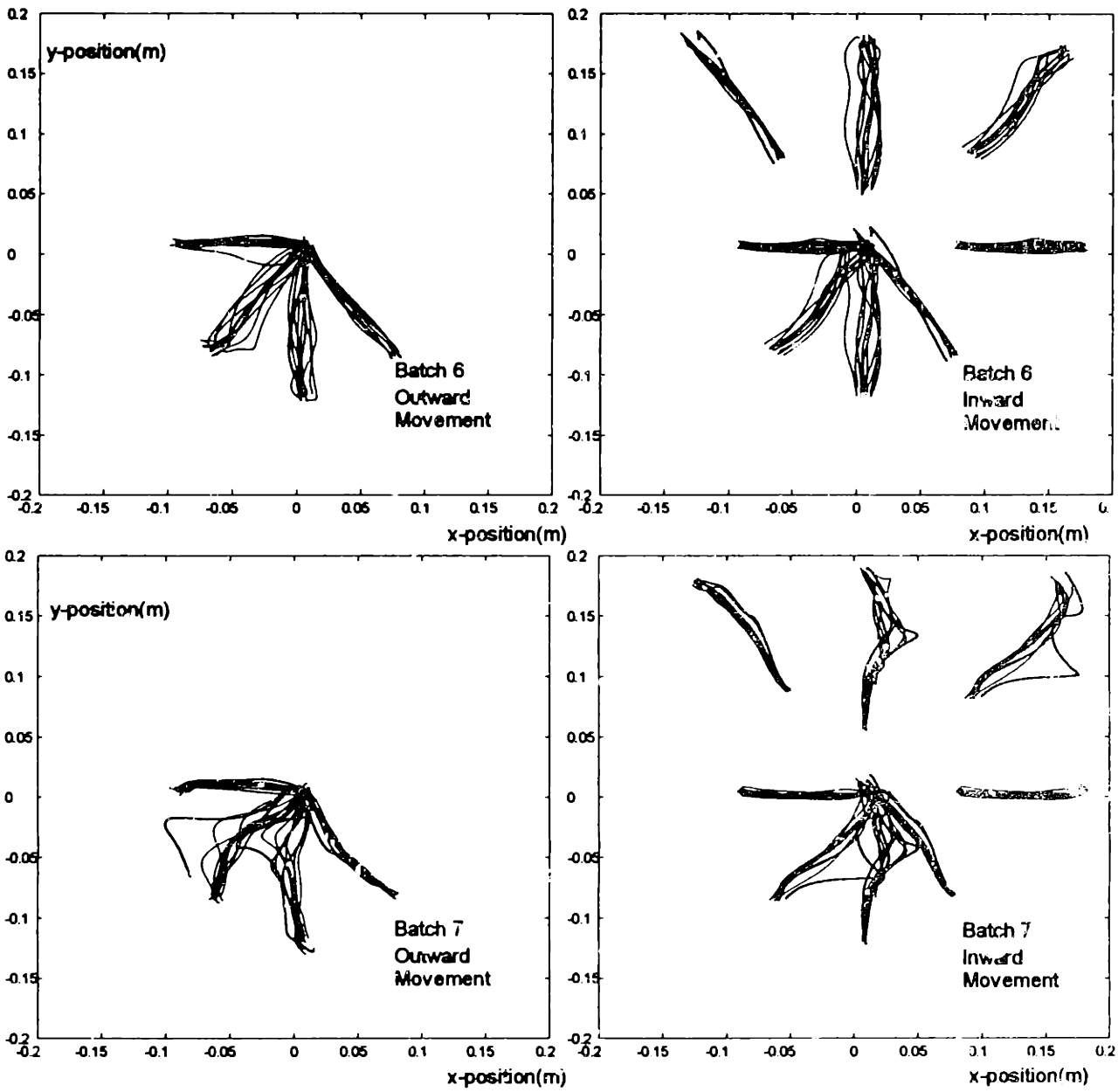

FIG.7.4.b. Trace Record for Subject A - Batch 6 & 7

The upper row corresponds to batch 6 and the lower row to batch 7. Plots on the left column contain movements from the center to randomly presented outward targets. The right column contains movements back to the center.

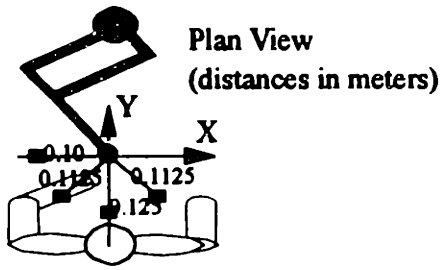

The inward movement traces were copied on the second column to allow better visualization of the end of the movement.

continuous bold line – first movement in the set
dashed bold line – last movement in the set

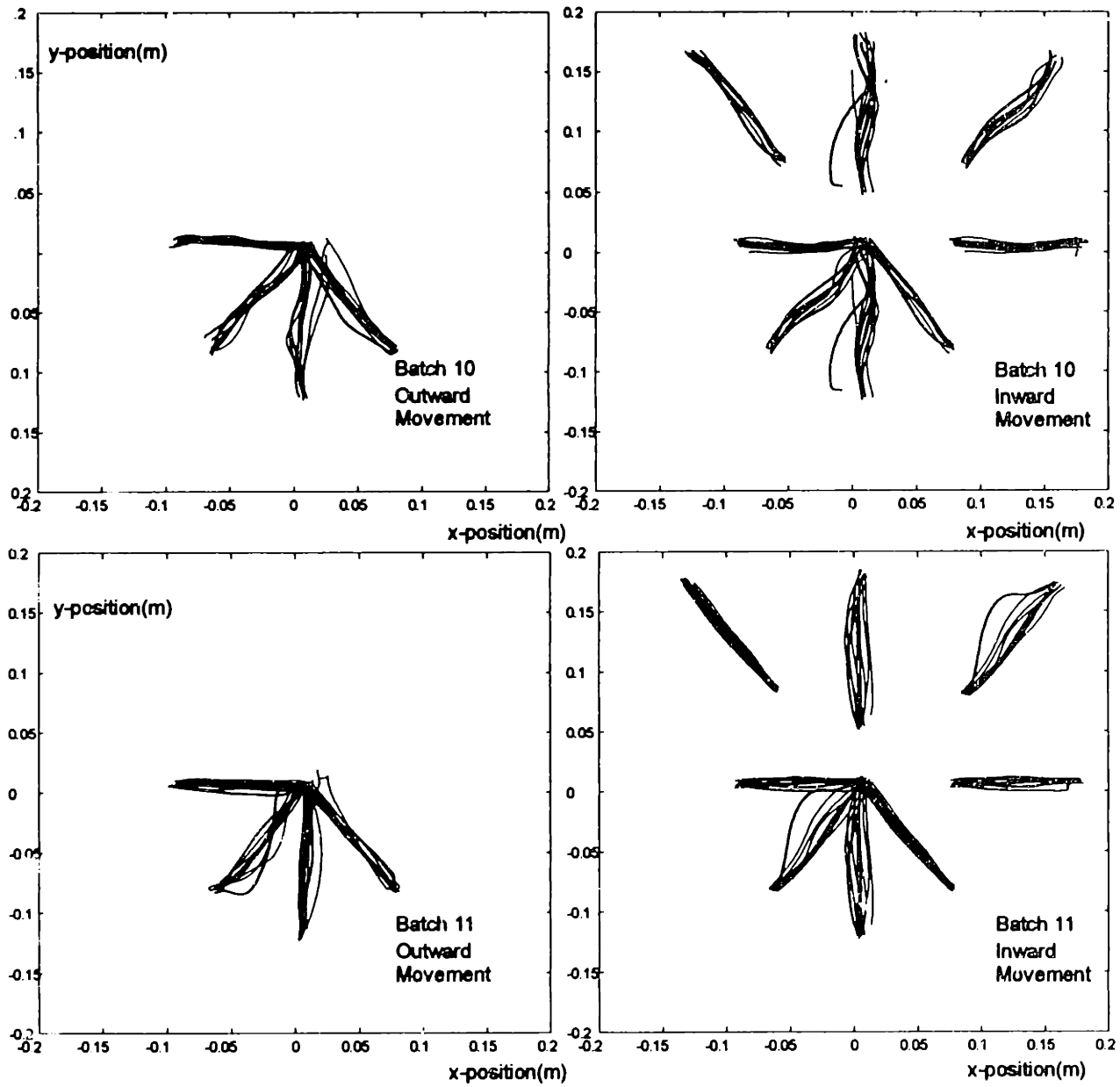

FIG.7.4.c. Trace Record for Subject A - Batch 10 & 11

The upper row corresponds to batch 10 and the lower row to batch 11. Plots on the left column contain movements from the center to randomly presented outward targets. The right column contains movements back to the center.

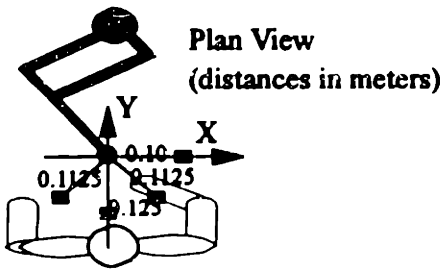

The inward movement traces were copied on the second column to allow better visualization of the end of the movement.

continuous bold line – first movement in the set
dashed bold line – last movement in the set

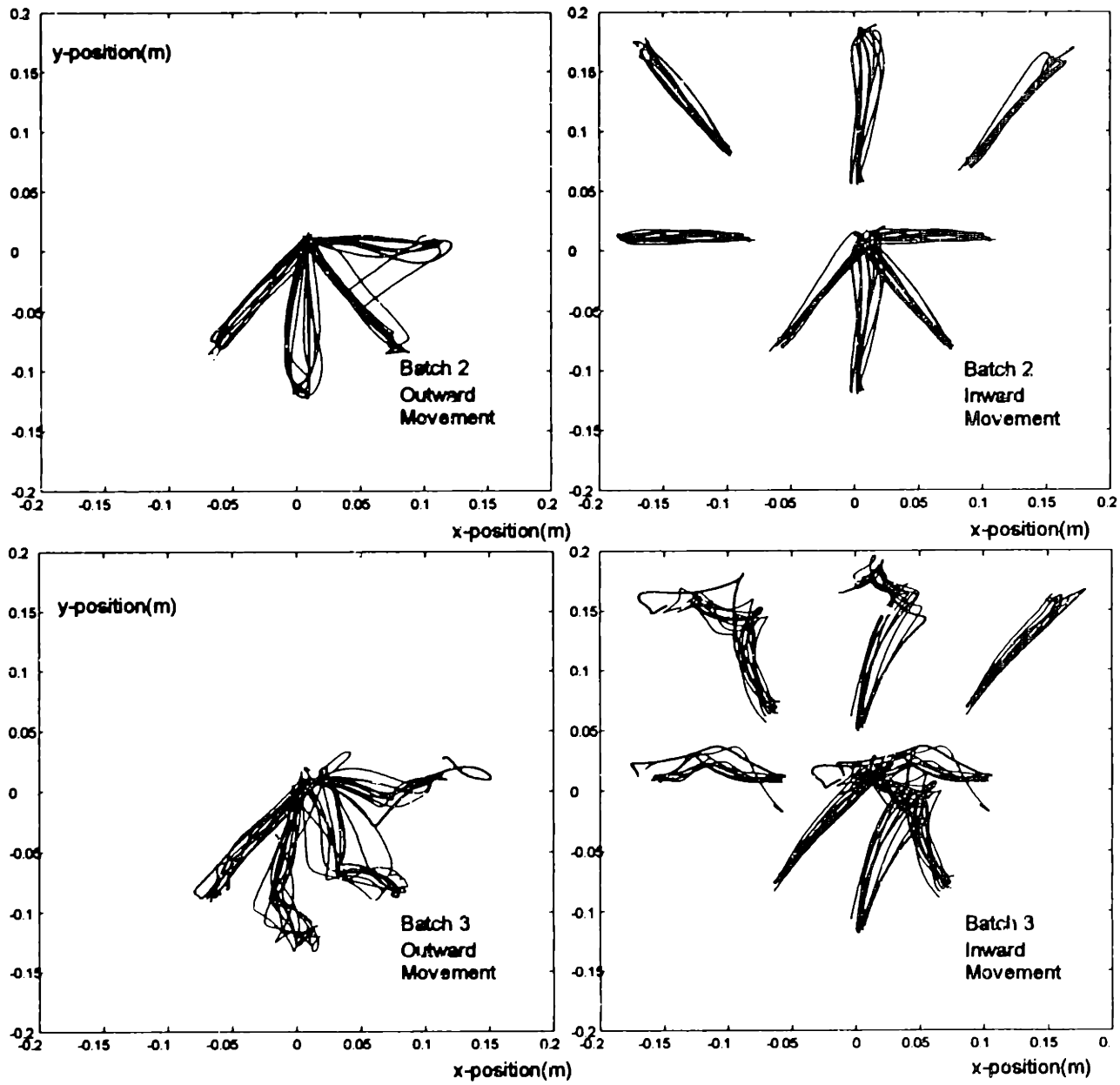

FIG.7.5.a. Trace Record for Subject G - Batch 2 & 3
The upper row corresponds to batch 2 and the lower row to batch 3. Plots on the left column contain movements from the center to randomly presented outward targets. The right column contains movements back to the center.

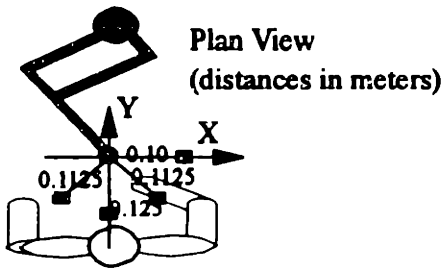

The inward movement traces were copied on the second column to allow better visualization of the end of the movement.

continuous bold line -- first movement in the set
dashed bold line -- last movement in the set

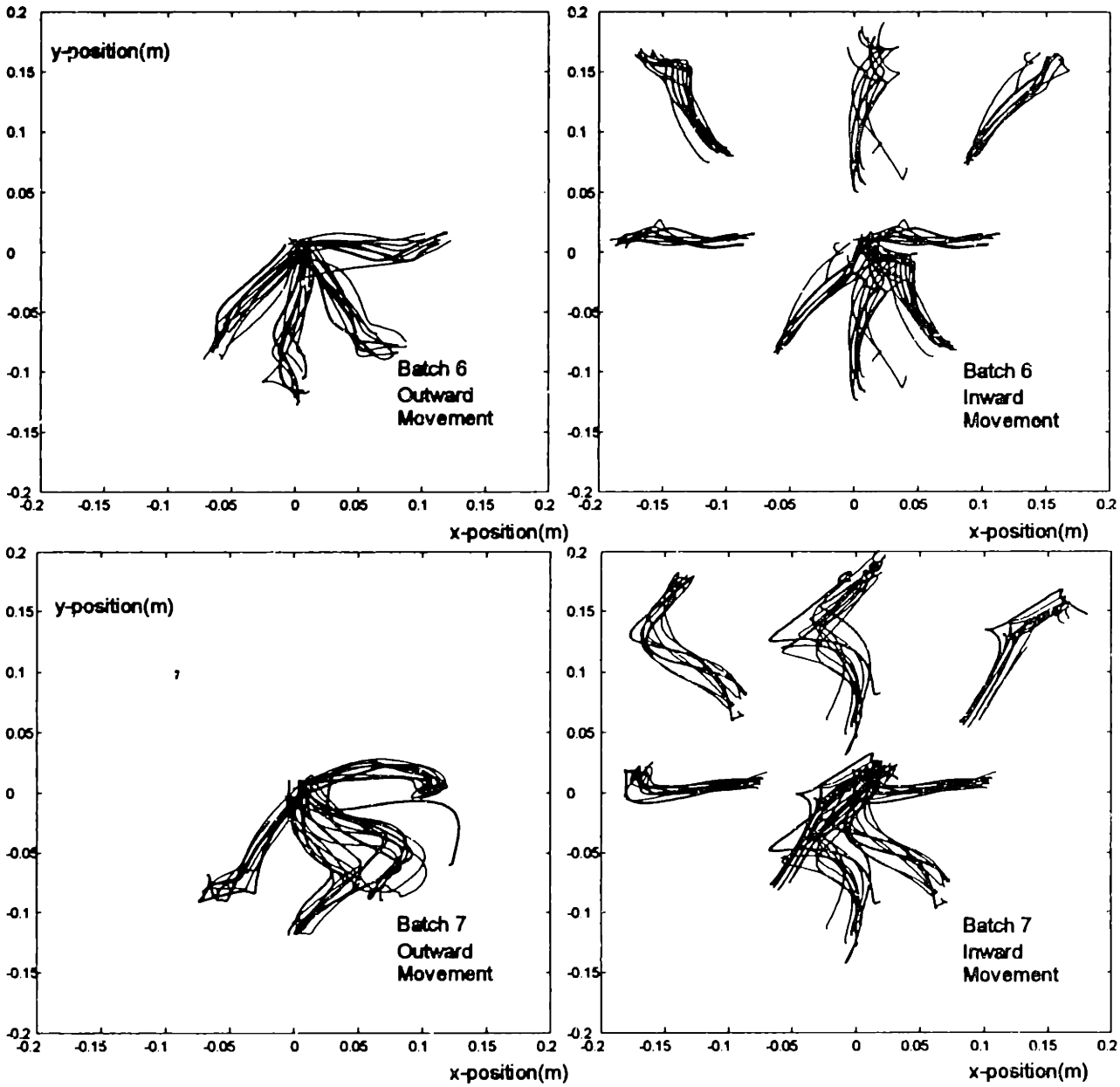

FIG.7.5.b. Trace Record for Subject G - Batch 6 & 7
The upper row corresponds to batch 6 and the lower row to batch 7. Plots on the left column contain movements from the center to randomly presented outward targets. The right column contains movements back to the center.

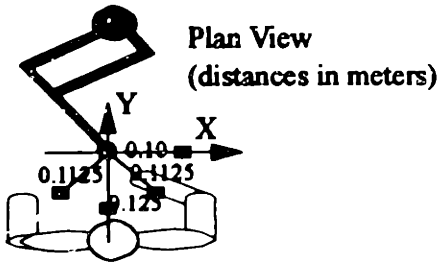

The inward movement traces were copied on the second column to allow better visualization of the end of the movement.

continuous bold line – first movement in the set
dashed bold line – last movement in the set

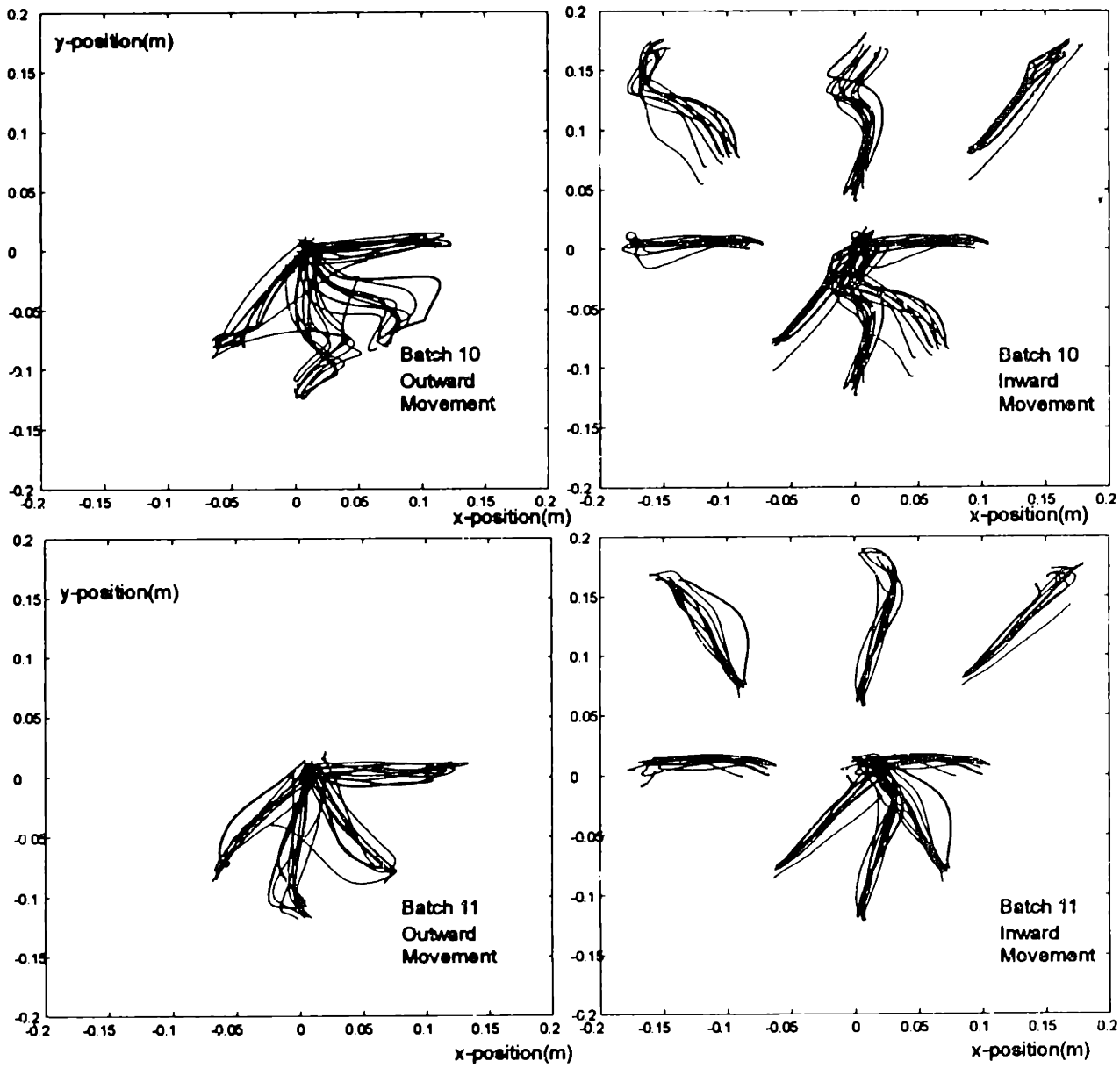

FIG.7.5.c. Trace Record for Subject G- Batch 10 & 11

The upper row corresponds to batch 10 and the lower row to batch 11. Plots on the left column contain movements from the center to randomly presented outward targets. The right column contains movements back to the center.

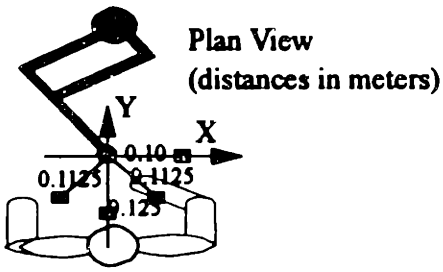

The inward movement traces were copied on the second column to allow better visualization of the end of the movement.

continuous bold line – first movement in the set
dashed bold line – last movement in the set

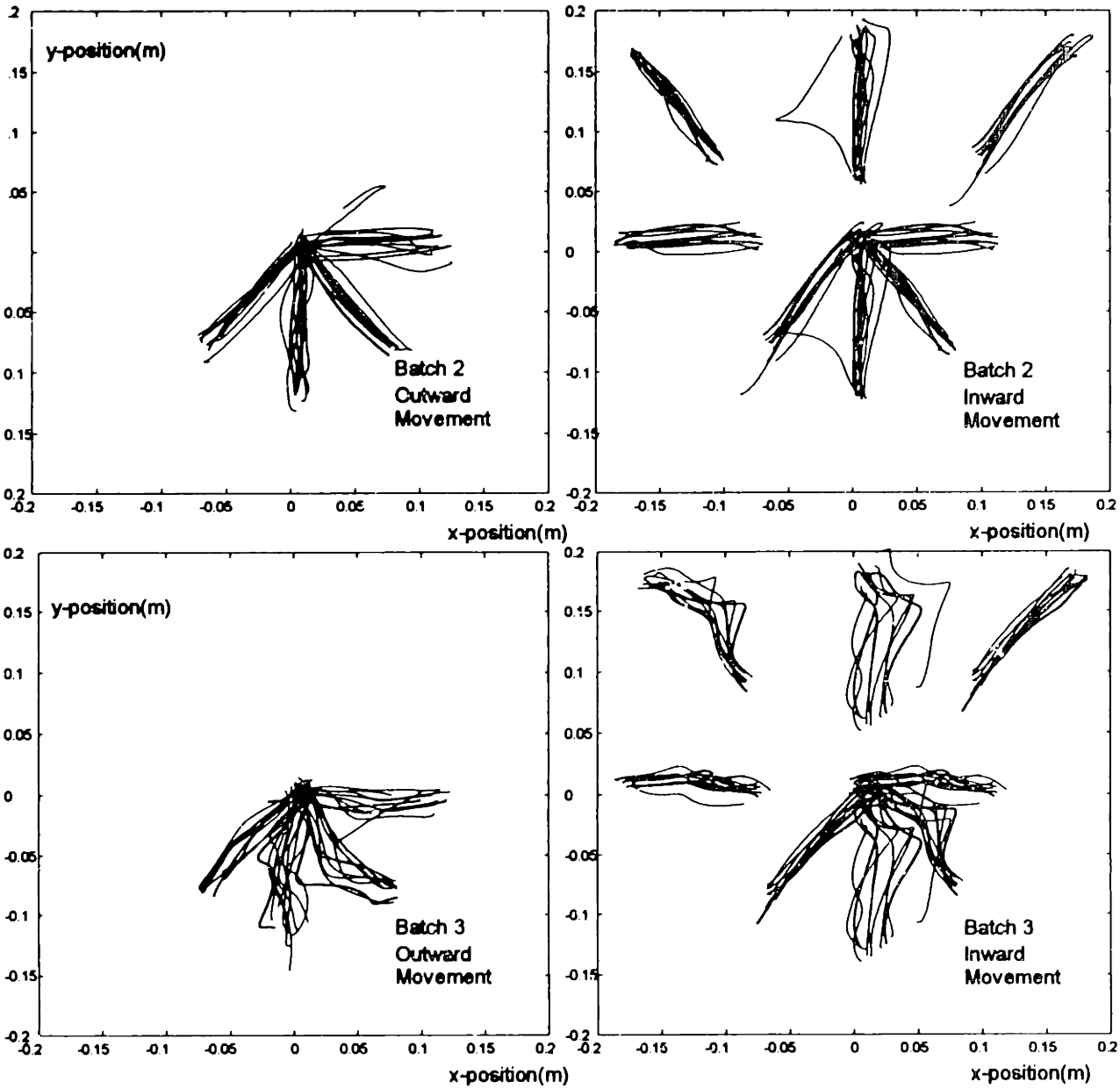

FIG.7.6.a. Trace Record for Subject O - Batch 2 & 3

The upper row corresponds to batch 2 and the lower row to batch 3. Plots on the left column contain movements from the center to randomly presented outward targets. The right column contains movements back to the center.

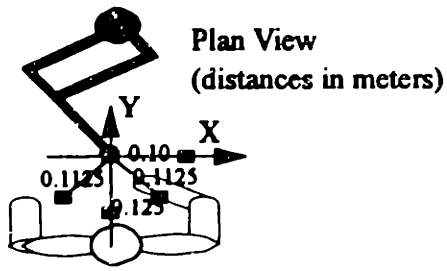

The inward movement traces were copied on the second column to allow better visualization of the end of the movement.

continuous bold line – first movement in the set
dashed bold line – last movement in the set

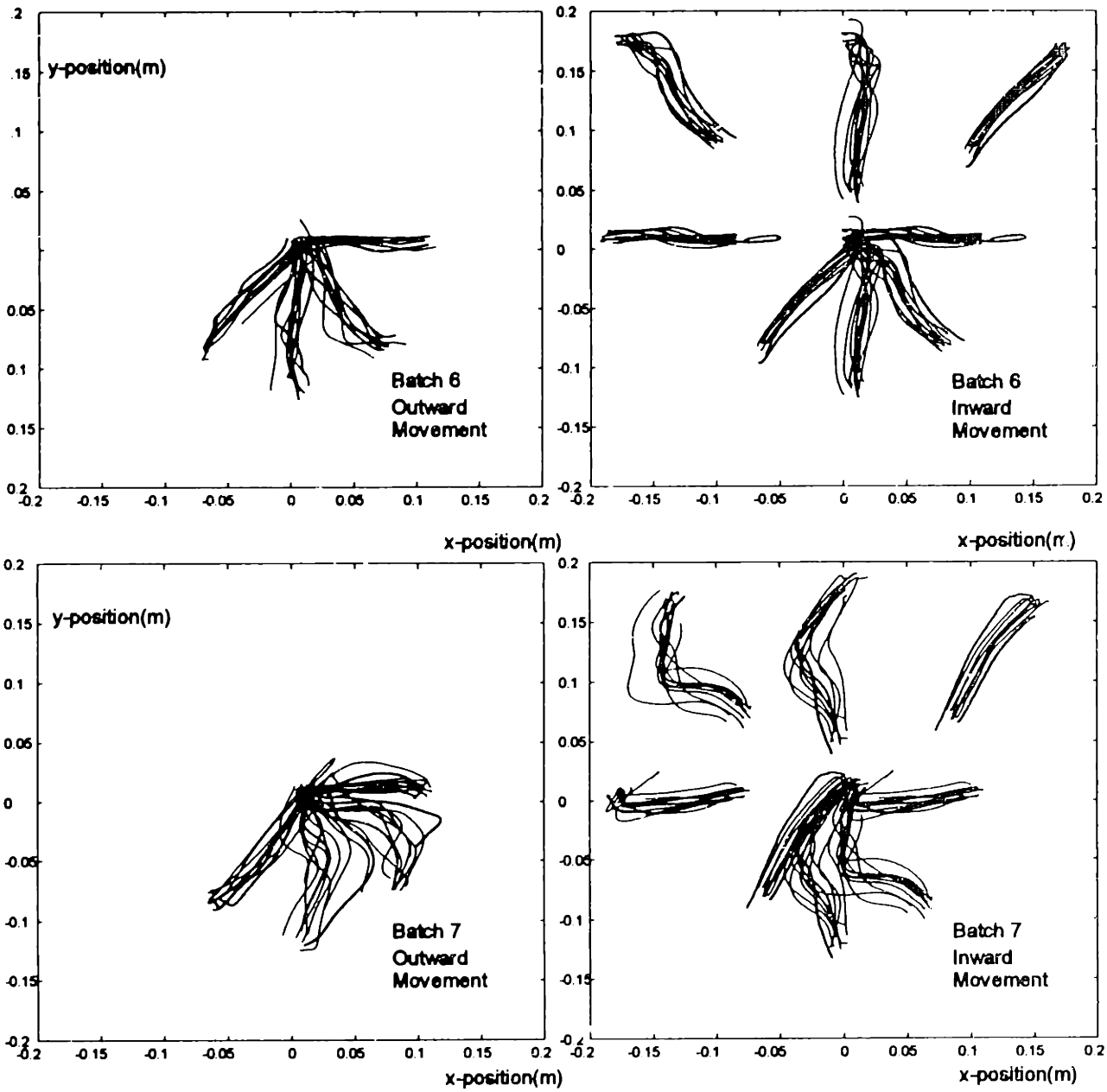

FIG.7.6.b. Trace Record for Subject O - Batch 6 & 7

The upper row corresponds to batch 6 and the lower row to batch 7. Plots on the left column contain movements from the center to randomly presented outward targets. The right column contains movements back to the center.

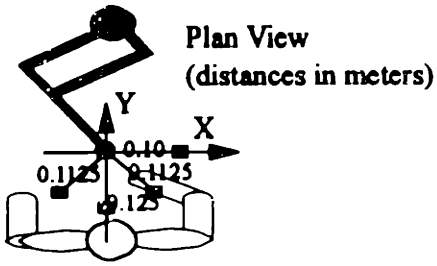

The inward movement traces were copied on the second column to allow better visualization of the end of the movement.

continuous bold line – first movement in the set
dashed bold line – last movement in the set

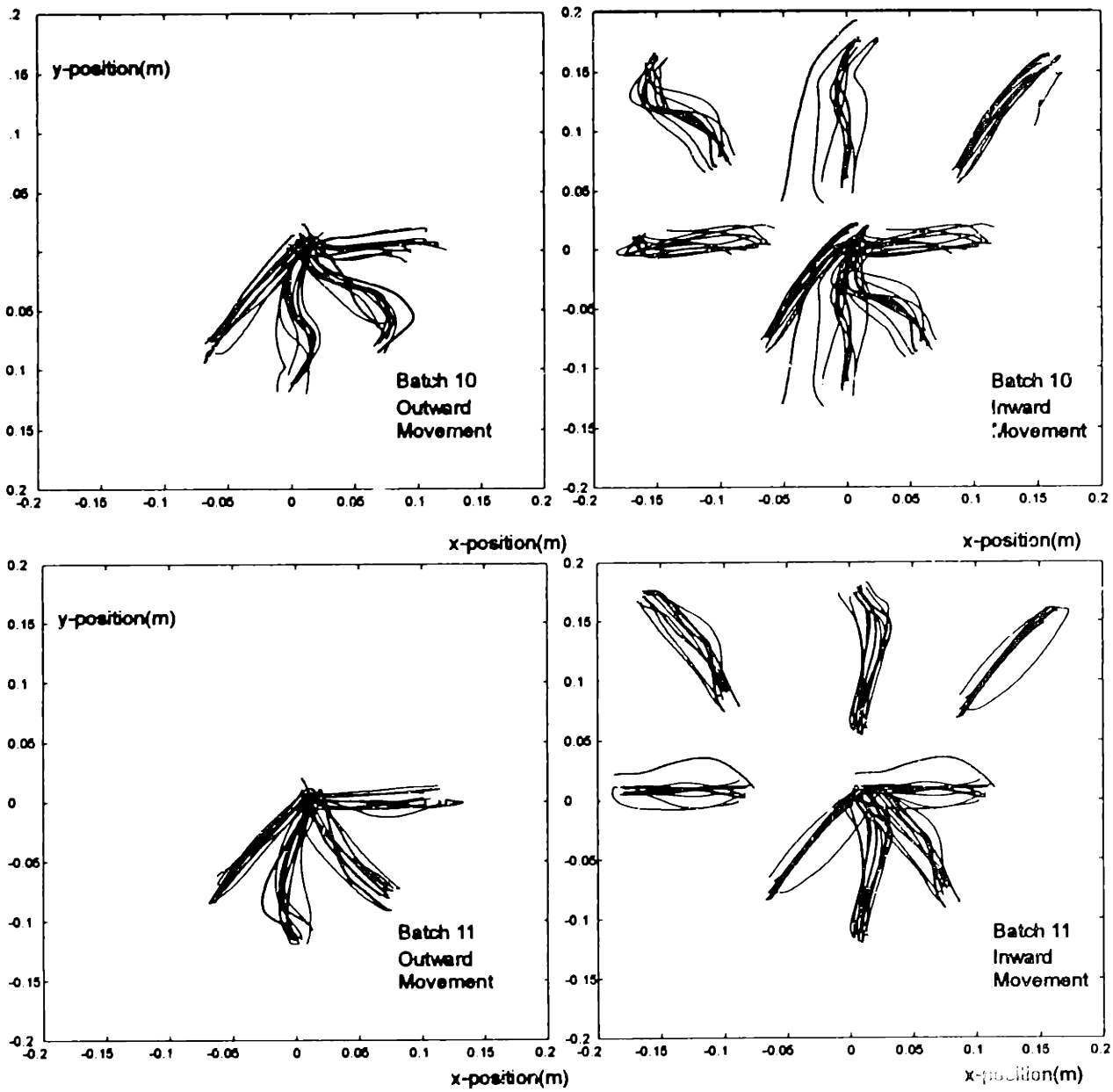

FIG.7.6.c. Trace Record for Subject O - Batch 10 & 11

The upper row corresponds to batch 10 and the lower row to batch 11. Plots on the left column contain movements from the center to randomly presented outward targets. The right column contains movements back to the center.

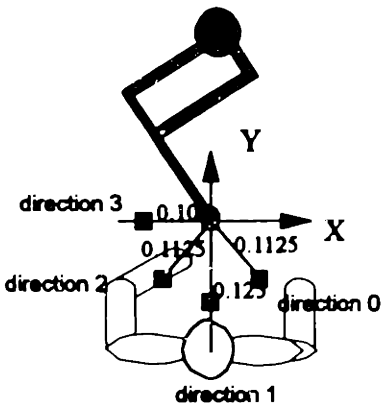

Plan View

(distances in meters)

BATCH 2

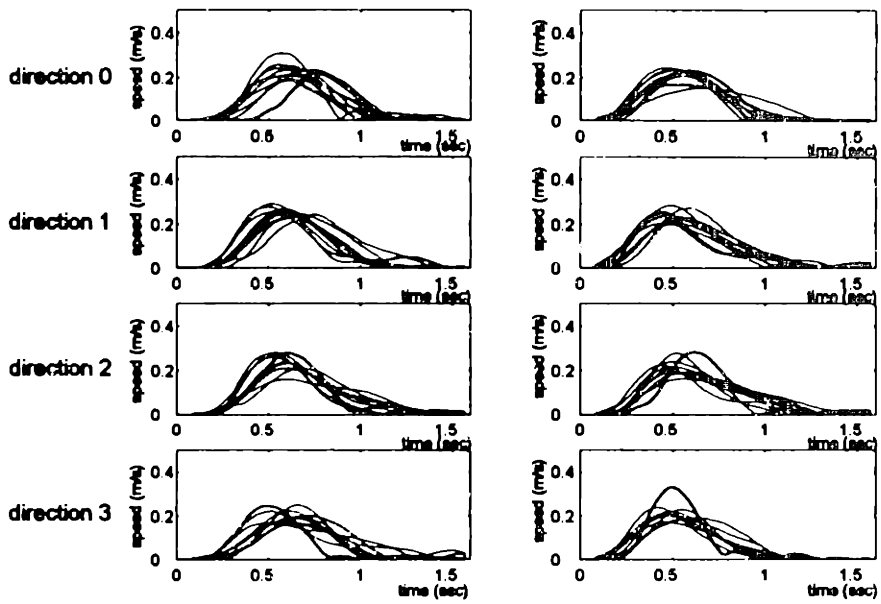

outward towards the target

inward towards the center

continuous bold line – initial movement in the direction in the batch

dashed bold line – last movement in the direction in the batch

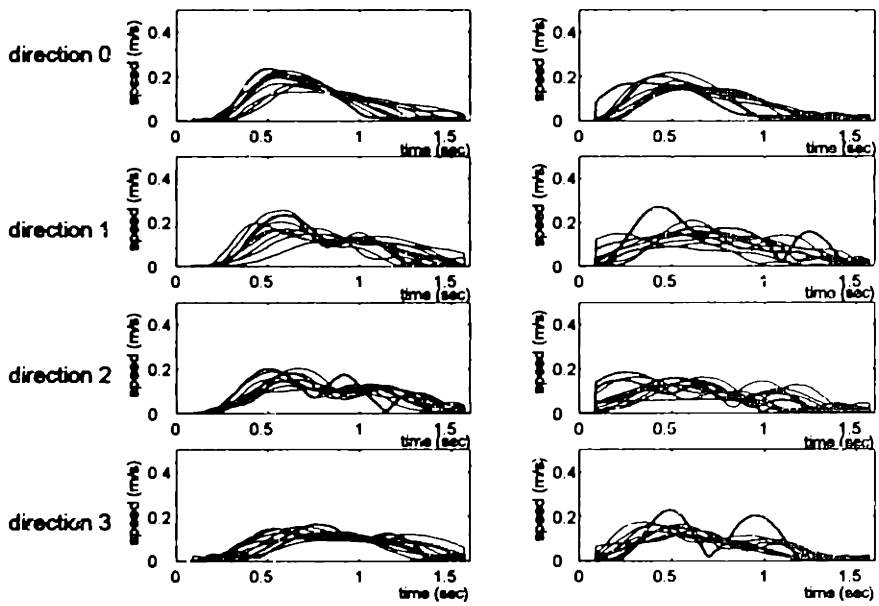

BATCH 3

outward towards the target

inward towards the center

FIG.7.7.a. Speed Record for Subject A - Batch 2 & 3

The figure shows two sets of speed records. The upper 4 rows correspond to batch 2 and the last 4 rows to batch 3. Plots in the left column contain movements from the center to randomly presented outward targets. The right column contains movements back to the center.

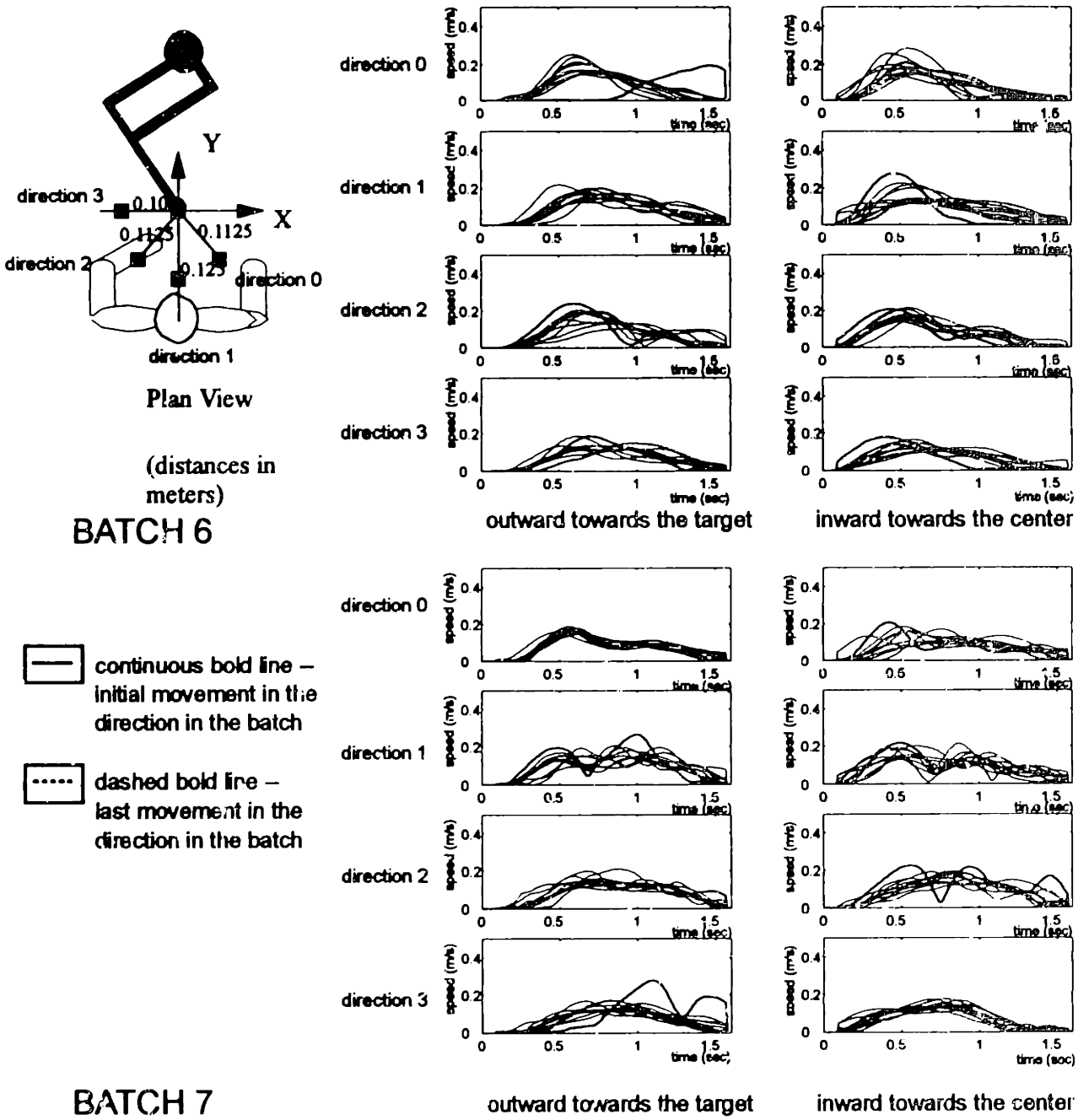

FIG.7.7.b. Speed Record for Subject A - Batch 6 & 7

The figure shows two sets of speed records. The upper 4 rows correspond to batch 6 and the last 4 rows to batch 7. Plots in the left column contain movements from the center to randomly presented outward targets. The right column contains movements back to the center.

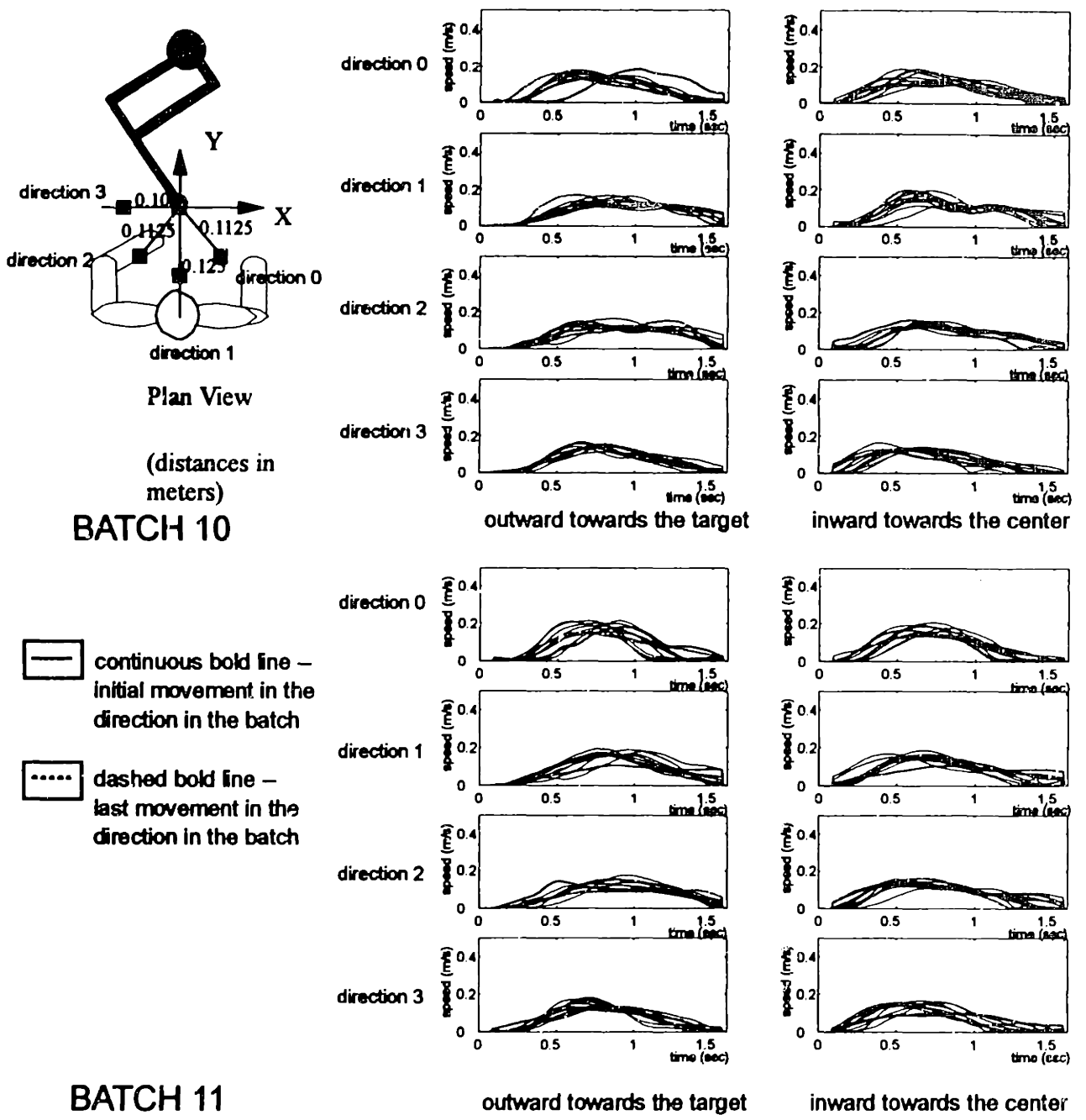

FIG.7.7.c. Speed Record for Subject A - Batch 10 & 11
The figure shows two sets of speed records. The upper 4 rows correspond to batch 10 and the last 4 rows to batch 11. Plots in the left column contain movements from the center to randomly presented outward targets. The right column contains movements back to the center.

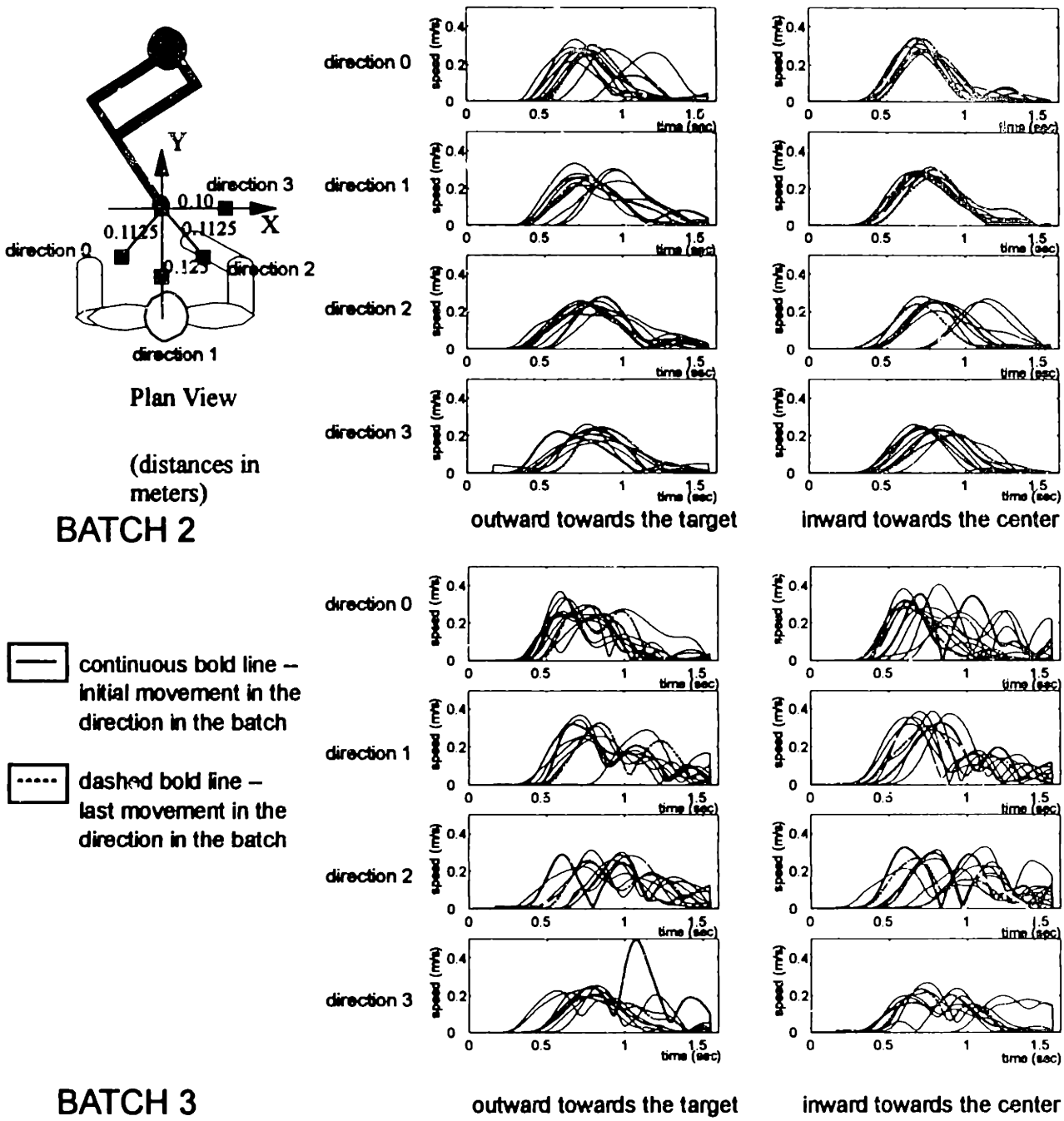

FIG.7.8.a. Speed Record for Subject G - Batch 2 & 3

The figure shows two sets of speed records. The upper 4 rows correspond to batch 2 and the last 4 rows to batch 3. Plots in the left column contain movements from the center to randomly presented outward targets. The right column contains movements back to the center.

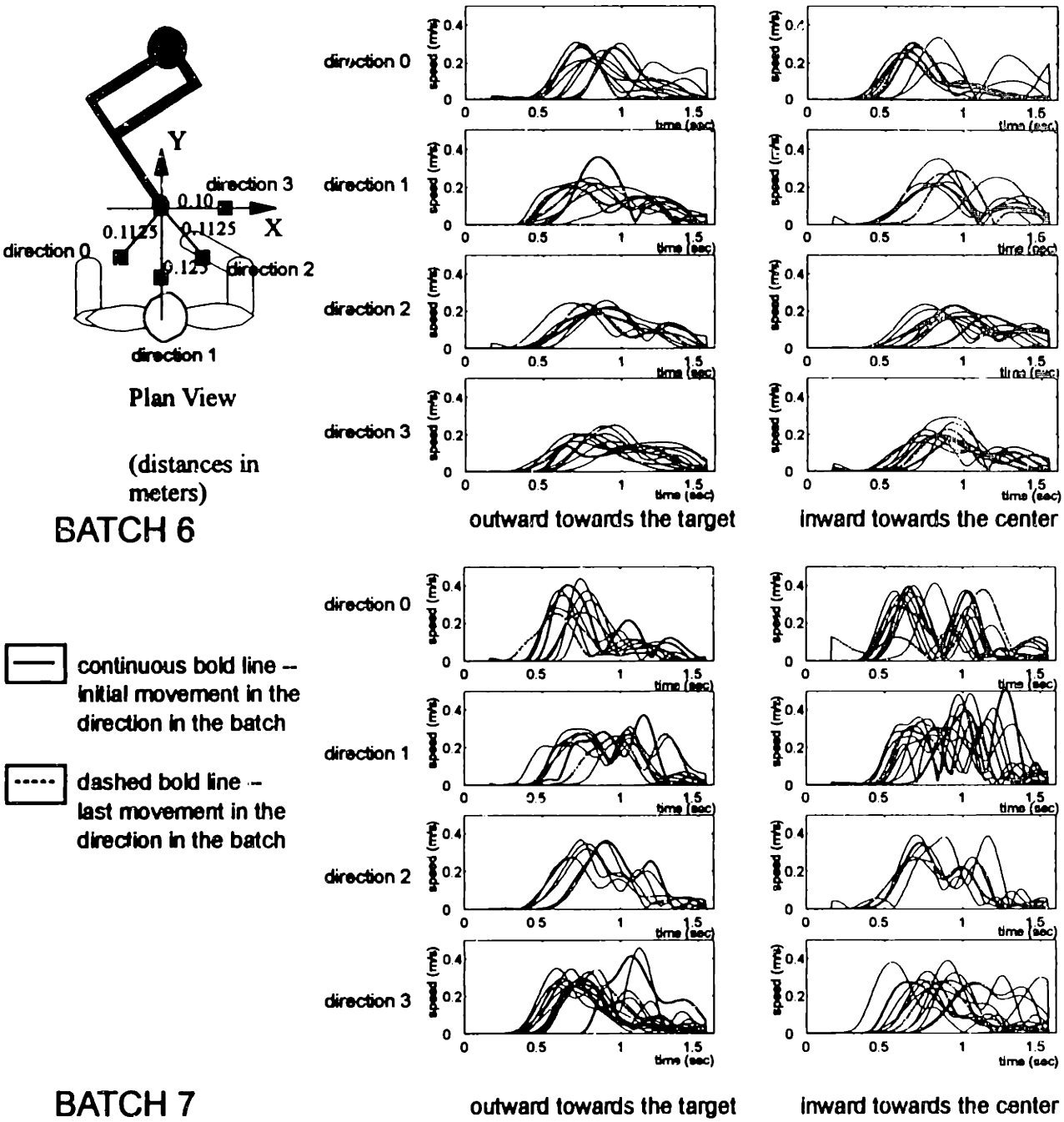

FIG.7.8.b. Speed Record for Subject G - Batch 6 & 7

The figure shows two sets of speed records. The upper 4 rows correspond to batch 6 and the last 4 rows to batch 7. Plots in the left column contain movements from the center to randomly presented outward targets. The right column contains movements back to the center.

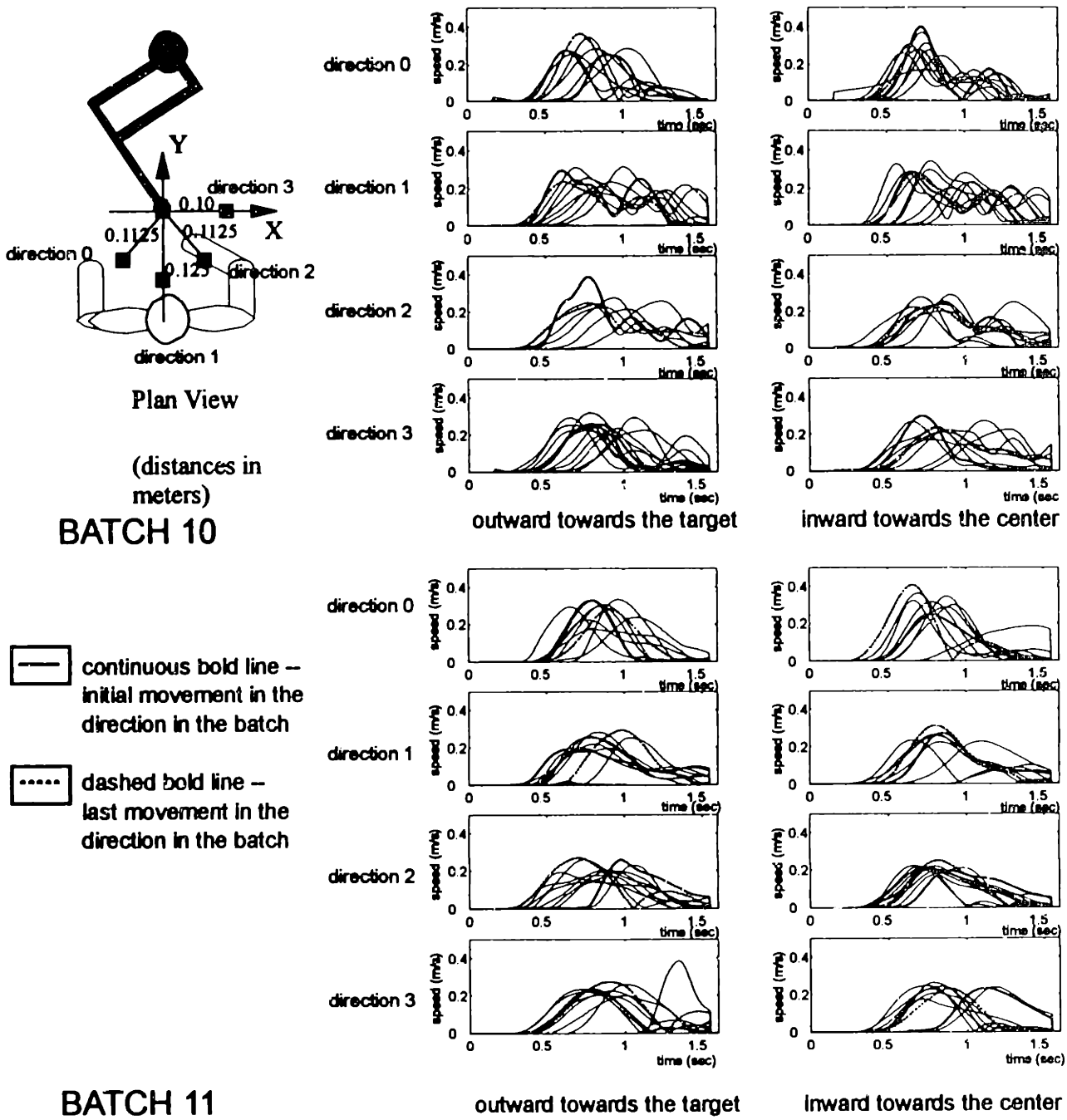

FIG.7.8.c. Speed Record for Subject G - Batch 10 & 11

The figure shows two sets of speed records. The upper 4 rows correspond to batch 10 and the last 4 rows to batch 11. Plots in the left column contain movements from the center to randomly presented outward targets. The right column contains movements back to the center.

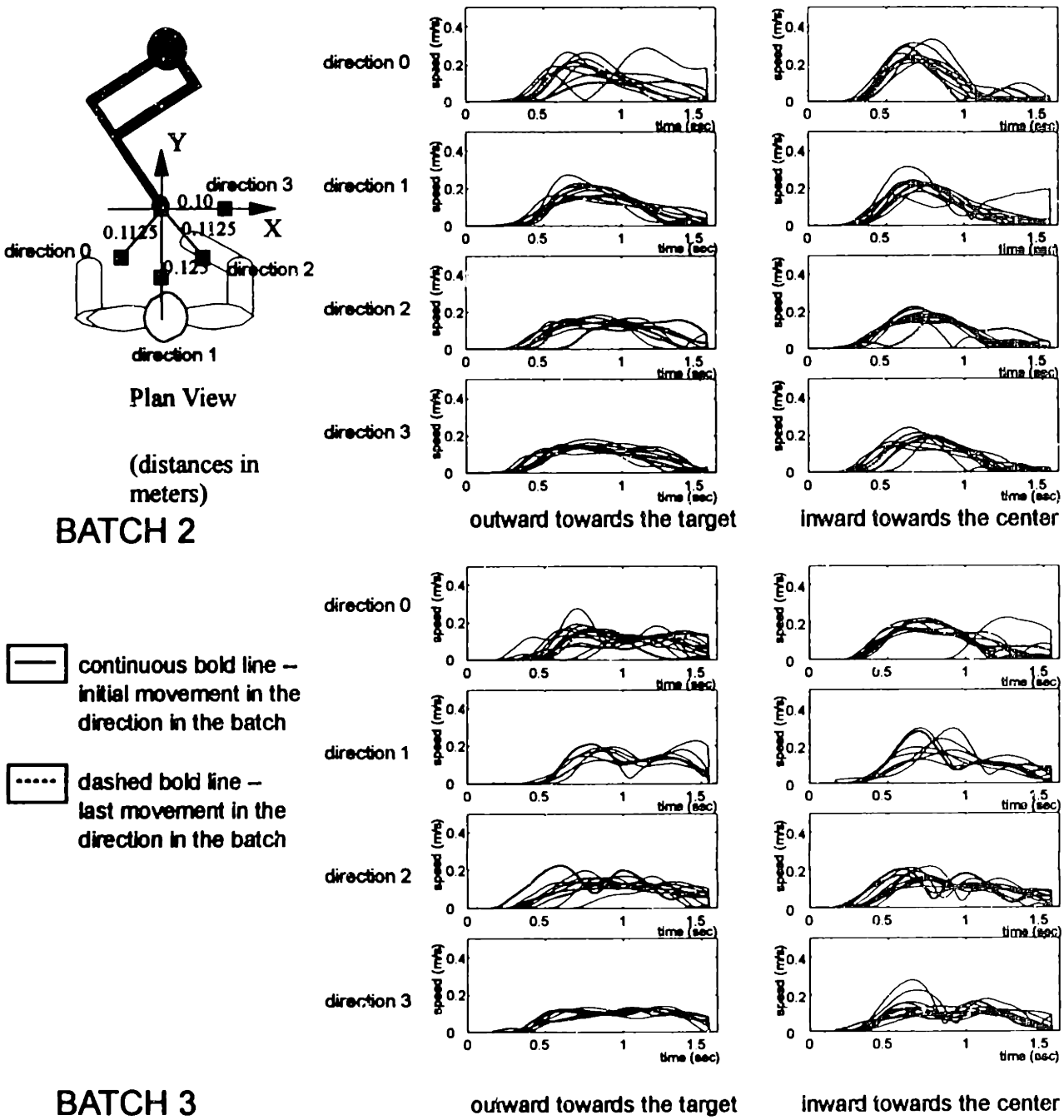

FIG.7.9.a. Speed Record for Subject O - Batch 2 & 3

The figure shows two sets of speed records. The upper 4 rows correspond to batch 2 and the last 4 rows to batch 3. Plots in the left column contain movements from the center to randomly presented outward targets. The right column contains movements back to the center.

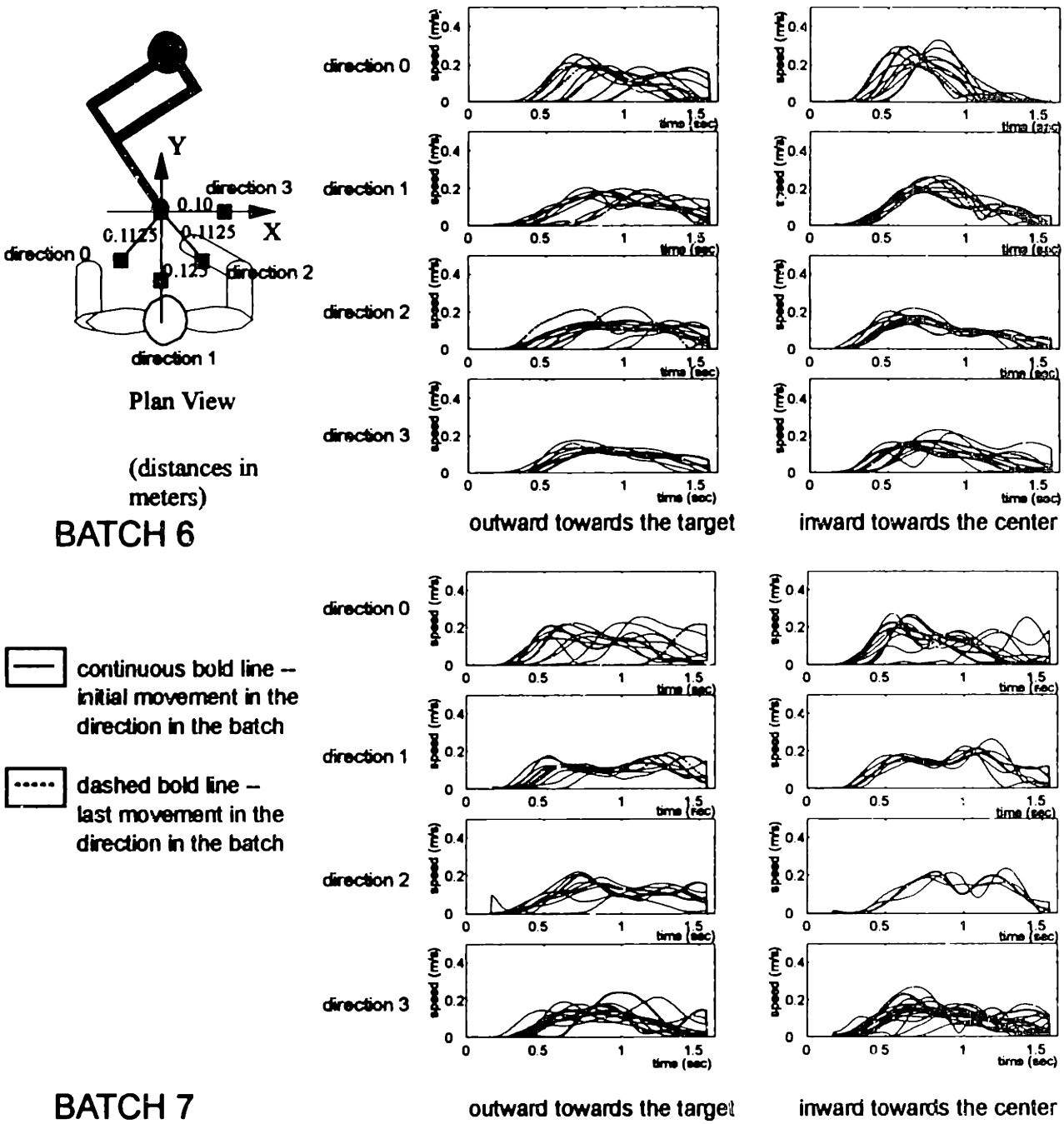

FIG.7.9.b. Speed Record for Subject O - Batch 6 & 7

The figure shows two sets of speed records. The upper 4 rows correspond to batch 6 and the last 4 rows to batch 7. Plots in the left column contain movements from the center to randomly presented outward targets. The right column contains movements back to the center.

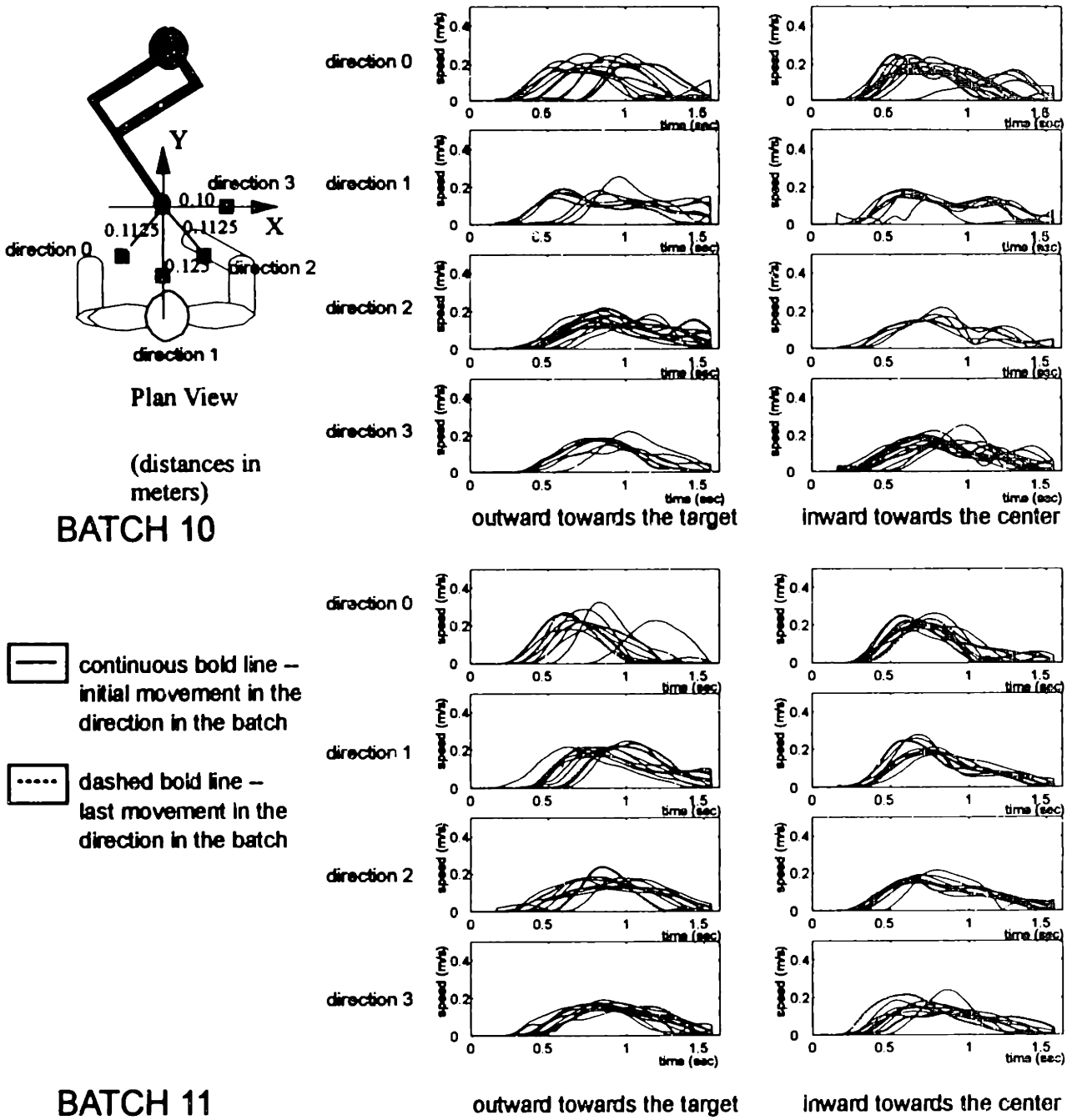

FIG.7.9.c. Speed Record for Subject O - Batch 10 & 11

The figure shows two sets of speed records. The upper 4 rows correspond to batch 10 and the last 4 rows to batch 11. Plots in the left column contain movements from the center to randomly presented outward targets. The right column contains movements back to the center.

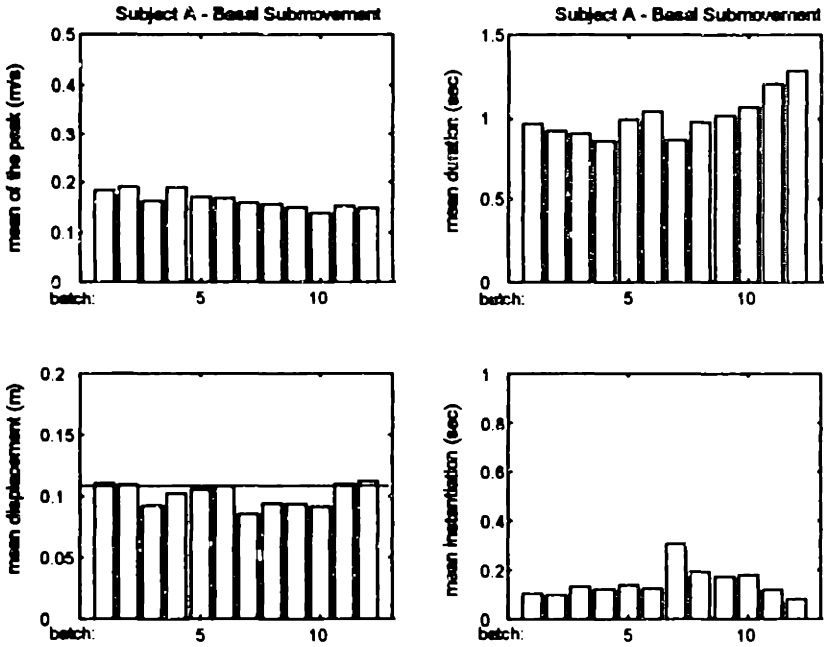

FIG.7.10. Basal Submovement Mean Values for Subject A
The left upper plot shows the mean peak velocity (m/s), the right upper plot shows the mean time duration (sec), the left lower plot indicates the mean displacement (m), and the right lower plot indicates the mean instantiation time of the basal submovement per batch.

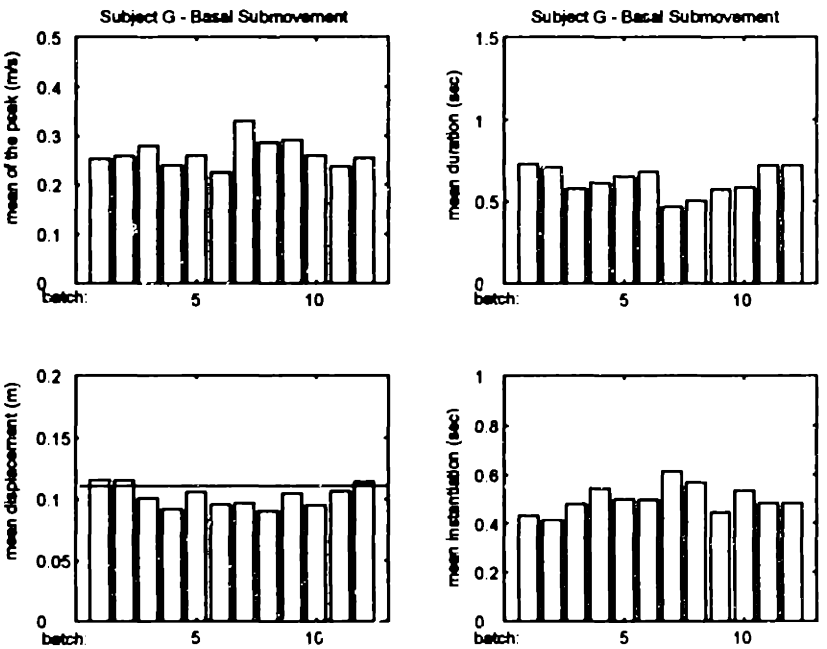

FIG.7.11. Basal Submovement Mean Values for Subject G
The left upper plot shows the mean peak velocity (m/s), the right upper plot shows the mean time duration (sec), the left lower plot indicates the mean displacement (m), and the right lower plot indicates the mean instantiation time of the basal submovement per batch.

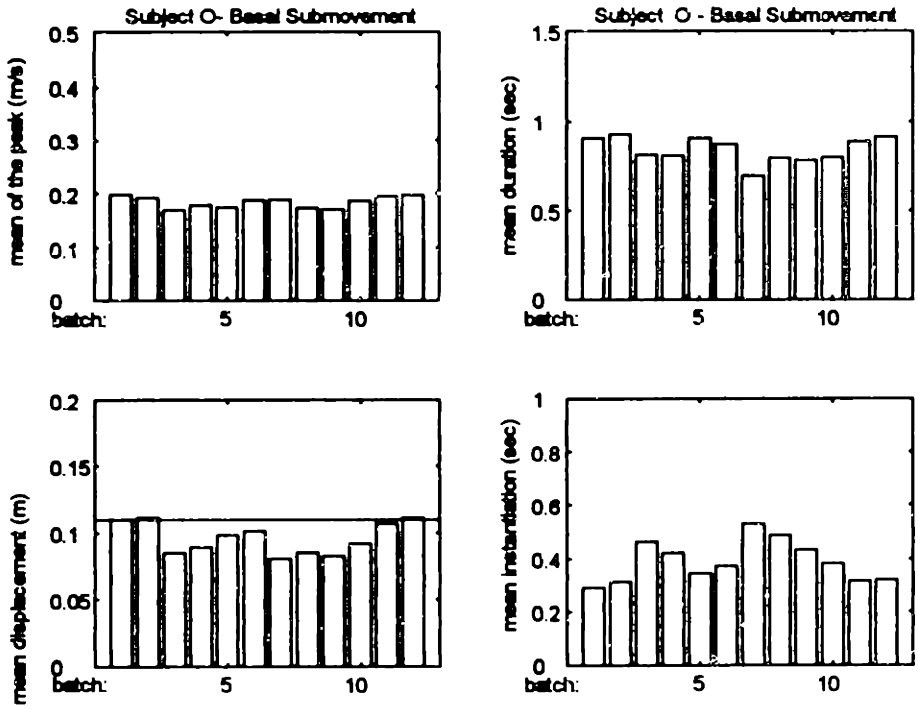

FIG.7.12. Basal Submovement Mean Values for Subject O
The left upper plot shows the mean peak velocity (m/s), the right upper plot shows the mean time duration (sec), the left lower plot indicates the mean displacement (m), and the right lower plot indicates the mean instantiation time of the basal submovement per batch.

CHAPTER 8. CONCLUSIONS AND FUTURE RESEARCH

" The market, and the market alone, rules."

– Lester Thurow - 1996 – The Future of Capitalism

" We will all be dead in the long run."

– Keynes

The most enjoyable facets of this research were its multidisciplinary character, and a key research theme that called for an adventuresome spirit. The results, too, yielded conclusions as well as avenues of future research that cut a wide swath through engineering, design, and medicine. To ensure an orderly flow of ideas, the remainder of this presentation combines conclusions with projected needs for future research.

- Nurture Influences Nature

The adventuresome spirit has paid off. Results from the pilot clinical trial involving stroke patients suggest that nurture positively influences nature i.e. patient's recovery during the highly dynamic neuronal reorganization post-stroke phase. Although a small sample size requires interpreting these results with caution, they are nevertheless highly encouraging. To paraphrase part of the Hippocratic oath of medicine: "First, do no harm." At the outset, it was unclear whether robot-aided therapy might actually impede recovery, or even have detrimental effects such as inducing pain. As a minimum, the results indicated that robot-aided therapy has no adverse effects on a patient's recovery. On a more positive note, at face value the results seem to have answered in the affirmative the crucial question: "Does robot therapy matter?." To my knowledge these results are the first objective data of its kind. To address the primary weakness of this study, a follow-up clinical trial is under way with a larger pool of 60 stroke patients.

- Tailoring Nurture I

A coarse analysis of the results suggests that the pilot clinical trial procedure did influence in particular the hemiplegic patients, i.e. patients with the most severe degree of impairment (see Fig.5.4.). Among patients with milder impairments, there were less distinguishable features of improvement. This does not necessarily indicate lack of value of nurture for the milder cases. More likely, it indicates the inadequacy of the procedure and the lesser challenge facing the mildly impaired. Even among severely-impaired patients who improve significantly, often showing much enthusiasm, boredom had to be occasionally shaken away by regimentation. This raises questions about tailoring therapy for different brain lesion locations, for degrees of severity, and for the particular stage of the neuronal recovery process. In fact, these questions had led rehabilitation to be labor intensive when therapy is customized to the patient. On the other hand, robotics constitutes the flexible arm of automation technology. These fields become the perfect match, and I invite the clinicians to engage and develop a set of therapies and training routines to tailor this flexible and programmable tool to the particular patient needs.

- Tailoring Nurture II

Likewise, a coarse analysis of the results suggest that patients that were intensively nurtured had the largest improvement in those body segments that were subjected to robot-aided therapy, i.e. shoulder and elbow (see Tab.5.8.). This raises questions about the generalization of improvement, i.e. does therapy focused on one limb or segment lead to a generalized improvement of function or is it specific to that limb or even to that specific action used in therapy? The present robot design is limited to the horizontal plane, althought there may be significant benefits to working simultaneously with many degrees of freedom, e.g., the fingers, the whole arm, the leg, or even the whole body. I fail to see any expedient way to address these questions, but learn by doing. Let's build the technology and tools, and deploy it.

- Tailoring Nurture III

In unchartered waters, the temptation to explore prevails. During the clinical trial with stroke patients, a few case studies were performed to broaden the understanding of different neurological diseases of the central or peripheral nervous system. These included cases of spinal cord injury, myoclonus, meningioma, Parkinsonism, and multiple sclerosis. One of the observations not reported in Section 5.5. refers to Parkinsonism. It is a well-known observation that Parkinson patients make tiny steps while approaching doors. They reestablish their normal walking pattern after passing through the "obstacle". It was rather intriguing to observe that one of the video-games, which requires the patient to navigate a balloon through "windows", produced the same behavior. It suggested that the pathological behavior could be reproduced in a simulated environment. This anecdotal observation suggests that the emerging "virtual environment" ("virtual reality") technologies may hold the promise of providing tools to address cognitive and sensory-motor deficits. Once again, to answer these questions, one must build the technology and tools and then learn by doing.

Of course, it is equally important to understand the outcome. Design synthesis complements scientific analysis and ideally both should progress symbiotically. At the risk of being ostracized to Antares (the brightest star of my childhood located in the Scorpius constellation), this aspect distinguishes the engineers from the scientists on one side and the engineers from the hackers on the other side.

- Understanding Nature I

If the ideal therapy for neurological recovery exists, contrary to dogmatic views, it is probably not unique. There may be several equally valid techniques. The early invitation to clinicians to develop and to customize therapy is based on the application of their expertise and practice. The adequacy of an approach can be established in principle via clinical studies. Nevertheless, recording quantities related to movement accuracy, to movement speed, to limb strength, and to gravity compensation mechanisms, may lead to a better understanding of the effect of the

particular brain lesion on the limbs functionality, thereby leading to a more "scientific" custom-built therapy. For example, recent results of a study at Burke Rehabilitation Hospital showed that against common expectations, patients with a larger lesion involving both the cortical and subcortical territories ranked better in terms of standing equilibrium than patients with a smaller lesion in the subcortical territory alone [Miyai, Blau, Reding & Volpe, 1996]. This type of observation falls out from the availability of data on balance. Similarly, the results of Section 5.4.5. suggested that post-stroke sensorimotor behavior is more segmented than normal limb movements and there might be a distinction between movement recovery patterns depending on the lesion location. For example, movement accuracy and speed recovery patterns may differ substantially for a cortical lesion when compared to a subcortical lesion (basal ganglia), and those differ from subcortical thalamic lesions. This in itself has scientific merit per se, but could also have practical consequences for adopting different training strategies involving more movement accuracy routines with one group, movement speed routines with the other group, and proprioceptive routines with the latter group. This path should be explored with clinical personnel to establish a clear characterization of lesion location and its movement time-history and consequences.

- Understanding Nature II

The central theme of studies in human motor control is to understand how intentions are translated into actions. This thesis adopted the approach of exploring this central theme to build a biologically-based language derived from present conjectures in the field. From the start, there was no intention of diving into human motor control per se. Yet, on two different occasions -- the stroke patients (Section 3.2) and myoclonus patient (Section 5.5.2.) -- an attempt was made to capture an isolated instance of the submovement "mother" shape. In both cases, the suggested shapes had a remarkable resemblance to each other and to normal subject point-to-point movements, even though the speed ranges differ by an order of magnitude. This invariance in itself is quite impressive, especially considering the extent of the patient's brain injury. I can not but ask myself about this primitive shape foci or circuitry, i.e. is the pattern generator for the movement segment at the highest level of the central nervous system or downstream (cerebellum,

midbrain, spinal cord, limb muscle and local feedback loop)? This question has scientific merit per se, and major consequences in designing therapy, in evaluation, and in developing diagnostic tools for patients.

- Understanding Nature III

Engineering is a synonym of tool development. Examples of this tool craftsmanship are imaging technologies which provide sensitive instruments for measuring neural activity, and pharmaceutical interventions which provide new and powerful ways to influence neural activity. To understand the functional motor consequences of neural activity, a comparable device to measure and to manipulate the motor system is needed. Robotic technology can serve that purpose. As an example of the practicality of this new tool, it allowed the manipulation of the environment in combination with pharmacological intervention and allowed the evaluation of a Parkinson patient motor performance (Section 5.5.1). Likewise, it allowed the robot to be used as a "haptic virtual environment", manipulating the motor system in new kinds of studies such as the one described in Chapter 6, exploring the different levels of organization of the putative higher level controller, and revealing that early learning of a motor task involves areas of the brain distinct from those involved in late procedural learning of that task (striatum and right parietal region vs cortico-cerebello-cortical feedback loop). Furthermore, the new tools based on the concepts of movement segmentation and submovements may reveal aspects of the subjects' different learning strategies that hitherto have been concealed. To my knowledge this combination of technologies and scientific results are the first of their kind.

Moreover, as suggested in Chapter 7, the results and the understanding of the human motor control can be refined by using the same "haptic virtual environment" with subjects with different cerebral lesions testing whether the measured significant changes in neural activity during imaging experiments are not artifacts, and identifying the effect of cerebral lesions during motor learning.

- Engineering I

At the outset of this document, the main objective of exploring the central theme of studies in human motor control was stated: To understand how intentions are translated into actions and to build a biologically-based movement encoder derived from present conjectures in the field. In particular, this work explored experimental evidence that arm movement is segmented with identifiable invariant movement characteristics. These segments or submovements constitute the primitives or building blocks of more complex movements. The scheme implemented was a simple "width-first search", which is very robust. It identifies the submovements from the speed peaks and the movement curvature with the critical feature residing in evidence that humans cannot suppress the speed peak occurrence, i.e. we cannot move at constant speeds, and of the symmetry of the invariant mother shape (see Sections 2.2.2, 3.2. and 5.5.2). The caveats of the approach stem from the lack of resolution of closely generated submovements, whose superposition forms a single peak in speed and the lack of resolution between smaller corrective submovements and the natural oscillatory response or tremor of the mechanical system. Nonetheless, this scheme allows an automatic movement assessment by estimating the number of submovements (number of basis), the modulation, the dilation, and the translation parameters of the mother shape. As shown in the various examples of application throughout Chapters 5, 6, and 7, these pieces of information provide different kinds of information with repeatability, reliability, objectivity, and potential for generalized application in diverse tasks or movements.

- Engineering II

Summoning attention to the episodic interventions and asynchronous character of the symbolic level or high-level controller, leads to considerations of a biologically-based scheme for human movement data-compression, for human-machine interface, and for communication in telerobotics. There are several questions that still need to be addressed. Namely, the proposed movement encoder requires other physical quantities to fully describe the motion. The telerobotic option has not been explored, except for a very crude demonstration of its feasibility using the MIT-MANUS and another two-degree of freedom robot in the laboratory. Nevertheless, the

initial direction and curvature might be the companion form for speed in the planar case (or may be the Cartesian tangential velocities in world coordinates), and to avoid drifting another physical quantity might be the submovement initial position. In other words, a planar submovement will be characterized for data compression by seven parameters: (1) the initial time, (2 & 3) initial position, (4) initial direction, (5) curvature, and (6 & 7) speed. In any event, the answer must be found to test the ideas on home-based self-therapy and group therapy.

- Engineering III

The 2-dof of the MIT-MANUS has been successfully in operation for over 1,000 hours in close contact with patients, proving the adequacy of the present design. Nonetheless, operation is presently limited to the horizontal plane. Units must be designed and deployed to test if there is significant benefit to working simultaneously with many degrees of freedom, e.g. the fingers, the whole arm, the leg, or even the whole body. Questions about the ideal configuration, actuators, and sensors, are inevitable, and is left as a challenge for engineers to engage and develop these robots.

I will conclude this step into the long journey stating my commitment for the tools of *"those magnificent men and their flying machines"*, and my enthusiasm to contribute for those tools into the next millenium. May we all live in interesting times ! (Chinese blessing and curse).

APPENDIX A: ROBOT-AIDED NEURO-REHABILITATION: CONSENT FORMS

MASSACHUSETTS INSTITUTE OF TECHNOLOGY

Title of Study: Development of Robot-Interactive Neuro-Rehabilitation

INFORMED CONSENT FORM

I understand that participation in the study of the "Development of Robot-Interactive Neuro-Rehabilitation" is completely voluntary and that I may withdraw my consent and discontinue my participation in the experiment at any time.

Description of the Procedure

The purpose of this research is to develop robot-interactive neuro-rehabilitation. You will be asked to perform several exercises with the robot. These exercises consist of moving or being moved by the robotic device. Some of the exercises might include a video-game enhancement to complete the exercise task, others none. Some exercises might include EMG data collection, others none. All the exercises are shown initially by the therapist guiding you and the robotic device. In a second phase, you will be asked to perform the exercise only with the robot. The training sessions with the robotic device are offered in addition to your standard therapy sessions. There would be no decrease in the amount of standard therapy being received by you. Every few weeks the robotic device will be used for evaluation of your progress.

Presently there are no known benefits to you from the study. Some subjects may find the procedure tiring. This effect should not be different from your standard therapy. You may ask us to stop the procedure at any time if you feel discomfort. You can also stop the exercises by pressing the red button next to you. This robotic device has several safety layers. However be aware that if the safety measure fails, you could be injured. Be sure to check with the therapist or operator any aspect of the exercise. We will be happy to answer any questions concerning the purpose of the research and the procedures.

You will be assigned a numerical code. All references to the information gathered during the procedure with you will be referred by this number. We will also video-tape all the procedures for analysis by the researchers. The video material will remain confidential and it might be disclosed only with your permission.

Having had the "Development of Robot-Interactive Neuro-Rehabilitation" explained to me, I would like to participate in this study which Dr. Hogan (M.I.T.), Dr. Volpe (Burke), Dr. Aisen (Burke), and Mr. Krebs (M.I.T.) are conducting at the M.I.T. - Department of Mechanical Engineering and at Burke Rehabilitation Hospital. I understand the risks and benefits to me, and that I am free to discontinue the project at any time for any reason.

In the unlikely event of physical injury resulting from participation in this research, I understand that medical treatment will be available from M.I.T. Medical Department, including first aid emergency treatment and follow-up care as needed, and that my insurance carrier may be billed for the cost of such treatment. However, no compensation can be provided for medical care apart from the foregoing. I further understand that making such medical treatment available, or providing it, does not imply that such injury is the Investigator's fault. I also understand that by

my participation in this study I am not waiving any of my legal rights. Further information may be obtained by calling the Institute's Insurance and Legal Affairs Office at (617) 253-2822.

I understand that I may also contact the Chairman of the Committee on the Use of Human as Experimental Subjects, M.I.T. (617) 253-6787, if I feel I have been treated unfairly as a subject.

_____

Date & Signature

Video Disclosure Statement:
Can we use part of the video images of the procedures for other purposes such as research presentations ?
( ) Yes
( ) No
( ) Would like to see the specific material, before disclosing it.

_____

Date & Signature

Witness:

_____

Date & Signature

DATE (MO., DY., YR.) | LOCATION | SERVICE

AGE | DOCTOR | IF NO PLATE, PRINT NAME, SEX, AND HISTORY NO.

THE BURKE REHABILITATION CENTER

Consent Form for Clinical Investigation

Project Title: The effect of interactive robotic manipulation on upper-limb paralysis

Subject: _____ **Research Project No.** 227

You are invited to participate in a study of use of robots in rehabilitation. Physicians of The Burke Rehabilitation Hospital hope to learn if robots help people regain more function. You were selected as possible participant in this study because you have a motor impairment which requires rehabilitation.

If you decide to participate, Dr. Aisen and her associates will have you perform exercises with the robot in addition to your regularly scheduled therapy, and measure changes in strength functioning and range of motion.

Your participation in the project involves the following risks: because this is a mechanical device, if the safety measure fails, you could be injured. Also, serial EMG tests will be performed. The EMG involves the use of a sterile needle that may cause mild bruising.

We may enhance your rehabilitation experience by improving your strength and range of motion. We cannot and do not guarantee that you will receive any benefits from this study.

Any information obtained during this study and identified with you will remain confidential and will be disclosed only with your permission.

Your decision whether or not to participate will not prejudice your future relations with The Burke Rehabilitation Hospital. If you decide to participate, you are free to discontinue participation at any time.

In accordance with Federal regulation, we are obligated to inform you about our policy in the event injury occurs. If, as a result of your participation, you experience injury from known or unknown risks of the research procedures as described, emergency medical care and treatment will be provided on our premises to the extent possible. We will assist you in obtaining additional medical care, as needed, but you will be responsible for the costs of such further medical treatment, either directly or through your medical insurance and/or other forms of medical coverage. No further monetary compensation will be available. Further information can be obtained from Dr. Aisen, 94-948-0050.

If you have any questions, please ask us. If you have any additional questions later, Dr. Aisen , The Burke Rehabilitation Hospital, 785 Mamaroneck Avenue, White Plains, NY 10605, 914-948-0050 will be happy to answer them.

You will be offered a copy of this form to keep.

45100
Rev. 8-75

(Use other side if necessary)

You are making a decision as to whether or not to participate. Your signature indicates that you have read the information provided above and have decided to do so. You may withdraw at any time without prejudice after signing this form should you choose to discontinue participation in this study.

Signature (Patient or next-of-kin)	Date	Time
Signature (Investigator)	Date	Time
Signature (Witness)	Date	Time

THE BURKE REHABILITATION HOSPITAL

785 Mamaroneck Avenue, White Plains. New York 10605 (914) 948-0050

I, _____

residing at: _____
Address State City Zipcode

hereby authorize the Winifred Masterson Burke Relief Foundation, (hereinafter "Burke") owning and operating The Burke Rehabilitation Hospital, and such assistants, photographers, and technicians as it may engage for this purpose, to take and use still and/or motion pictures, voice recordings, and videotape recordings made of me, my child, or my legal ward while a patient, employee, or visitor at Burke; including but not limited to the pictures and recordings taken during any procedure of treatment performed at Burke, together with a description of the diagnosis and treatment involved, as well as the identity of the patient; and together with the right to retouch or edit such pictures or recordings.

I authorize the use of these pictures and recordings in any publication, film, telecast or broadcast; and for instructional, educational and scientific purposes within Burke or other institutions, public relations, or any other purpose which Burke may deem appropriate.

I am over 18 years of age and have the legal right and authority to sign for myself and any minors named herein. I hereby release the Winifred Masterson Burke Relief Foundation and The Burke Rehabilitation Hospital, and its agents, servants, employees, attending physicians, and consultants from any claim or liability whatsoever in connection with either the taking or use of these pictures, recordings and accompanying disclosures.

My Name: _____
(Parent, Legal Guardian or Self)

Name & Age of Minor(s): _____

Witness: _____ Date: _____

Witness: _____ Date: _____

Please indicate if you are:

Inpatient ○

Outpatient ○

Non-patient ○

APPENDIX B: ROBOT-AIDED NEURO-REHABILITATION: CLINICAL SCALES

MANUS

Patient Name:_____

Age:_____ Sex:_____
Medical Record #:_____
Diagnosis:_____
Date of Onset:_____
Other CNS Disease:_____
MRI Result:_____

Date:_____
Assessment Week:_____

FIM SCORE

Patient Name:_____
Scored by:_____
Date:_____/_____/_____
Assessment Week:_____

I. Self care

Eating	_____
Grooming	_____
Bathing	_____
Dressing–Upper Body	_____
Dressing–Lower Body	_____
Toileting	_____

II. Sphincter Control

Bladder Management	_____
Bowel Management	_____

III. Mobility– Transfers

Bed, Chair, Wheelchair	_____
Toilet	_____
Tub, Shower	_____

IV. Locomotion

Walk/ wheelchair	_____
Stairs	_____

V. Communication and Social Cognition

Comprehension	_____
Expression	_____
Social Interaction	_____
Problem Solving	_____
Memory	_____

TOTAL: _____

COMMENTS:

ASHWORTH SCALE FOR MUSCLE TONE

Patient Name:_____
Scored by:_____
Date:_____/_____/_____
Assessment Week:_____

0 No increase in tone

1 Slight increase in tone giving a "catch" when the limb is moved in flexion or extension

2 More marked increase in tone but limb easily flexed

3 Considerable increase in tone, passive movement difficult

4 Limb rigid in flexion or extension

Muscle Group:	Ashworth Score: Left	Right
shld. internal rotators	_____	_____
elbow extensors	_____	_____
elbow flexors	_____	_____
pronators	_____	_____
supinators	_____	_____
wrist flexors	_____	_____
wrist extensors	_____	_____
digit flexors	_____	_____
digit extensors	_____	_____
TOTAL:	_____	_____

COMMENTS:

QUESTIONNAIRE

Patient Name:_____
Scored by:_____
Date:_____/_____/_____
Assessment Week:_____

Please circle the number that most closely describes how much you agree with each statement. The higher the number, the more you agree with the statement.

I DISAGREE				I AGREE			
Strongly	Moderately	Somewhat	A little	A little	Somewhat	Moderately	Strongly
0	1	2	3	4	5	6	7

1) I was comfortable with my robot therapy sessions.

0 1 2 3 4 5 6 7

2) I enjoyed doing therapy sessions with the robot arm.

0 1 2 3 4 5 6 7

3) I believe the robot therapy sessions were beneficial to me.

0 1 2 3 4 5 6 7

4) Working with the robot helps me in ways that nobody else can.

0 1 2 3 4 5 6 7

5) I would like to perform more therapy sessions with the robot arm.

0 1 2 3 4 5 6 7

6) I would rather work with the robot than a therapist.

0 1 2 3 4 5 6 7

TOTAL:_____

If you have any other comments you would like to share with us please write them in the space below:

UPPER EXTREMITY MOTOR STATUS

Patient Name: _____

Scored By: _____

Date: _____

Assessment: _____

Movement Scale:

0	no volitional movement or no contraction
1-	contraction or patient initiating first few degrees of movement
1	performs partly/incomplete or uncontrolled motion
1+	lacking last few degrees of motion
2-	completes full range, decreased control or timing
2	performs faultlessly (complete, controlled motion)

Synergy Scale:

0	synergy components begin with onset of movement
1	synergy components begin later in movement
2	no synergy components

0 = NO 1 = YES

Seated AROM (check w/c positioning)

Shoulder	**Mov't**	**synergy**
1. A. Shoulder flexion to 90, elbow 0, forearm neutral	_____	_____
B. If placed, can position be held	_____	X
0 = NO 1= YES		
2. A. Shoulder abd to 90, elbow 0, forearm pronated	_____	_____
B. If placed, can position be held	_____	X
3. A. Shoulder flex 90-150, elbow 0	_____	_____
B. If placed, can position be held	_____	X
4. A. Touch top of head	_____	_____
B. If placed, can position be held	_____	X

5. A. Touch small of back	____	____
B. If placed, can position be held	____	X
6. Scapula elevation	____	X
7. Protraction/retraction of the scapula arm supported on table or lap	____	X
8. A. Shoulder flex 0-30, elbow starts at 90	____	X
B. Return shoulder to 30 ext with elbow flex, forearm supported on table	____	X
9. A. Shld 0, elbow 90, shld internal rotation to abdomen	____	____
B. Shld 0, elbow 90, shld external rotation to abdomen	____	____
10. Touch opposite knee	____	____
Elbow/Forearm		
1. A. Forearm pronation from midposition shld 0, elbow 90	____	X
B. Forearm supination from midposition shld 0, elbow 90	____	X
2. A. Elbow 0, fully flex	____	____
B. If placed, can position be held	____	X
3. Full elbow flexion , extend to 0 (GE or AG)	____	____
4. Touch opposite shoulder	____	____
Wrist		
1. Wrist ext with shld 0, elbow 90, forearm pronated	____	X
2. Wrist flex with shld 0, elbow 90, forearm supinated	____	X
3. Wrist curcumduction shld 0, elb 90, forearm pronated	____	X
Hand		
1. Fingers - mass flexion (fingers to palm)	____	X
2. Fingers - mass extension	____	X
3. Hook grasp	____	X
4. Intrinsic plus position	____	X
5. Thumb abduction	____	X
6. Thumb adduction	____	X
7. Opposition to base of digit	____	X
8. A. Opposition to digit 2 (tip pinch)	____	X
B. Opposition to digit 3 (tip pinch)	____	X
C. Opposition to digit 4 (tip pinch)	____	X
D. Opposition to digit 5 (tip pinch)	____	X
9. A. Opposition to digit 2 (pad pinch)	____	X
B. Opposition to digit 3 (pad pinch)	____	X

C. Opposition to digit 4 (pad pinch)	_____	X
D. Opposition to digit 5 (pad pinch)	_____	X
10. Controlled grasp with soda can-grasp, place 2-4" away, release	_____	X
11. Pincer grasp with pen (sign name, date or 3 vertical lines)	_____	X
12. Lateral pinch with key	_____	X
Total movement scale	_____	
Total synergy scale	_____	

Edema Measurements:

0 No difference (no edema)

1 Trace

2 1+

3 2+

4 3+

	R	L
1. 4 cm proximal to wrist crease	_____	_____
2. 2 cm proximal to wrist crease	_____	_____
3. Wrist crease (distal to ulnar head)	_____	_____
4. Across palm at web space	_____	_____
5. Across palm at DPC	_____	_____
6. Base digit 1	_____	_____
Base digit 2	_____	_____
Base digit 3	_____	_____
Base digit 4	_____	_____
Base digit 5	_____	_____

Pain (with PROM)

0 No pain

1 Pain at end range

2 Pain at mid range

3 Pain at any motion

1. Shoulder	_____	_____
2. Wrist	_____	_____
3. Hand	_____	_____

Shoulder/Hand Rating

Definite:	distal limb pain	_____
	tenderness	_____
	swelling	_____
	vasomotor instability	_____
	Total rating (out of 4)	_____
Probable:	pain or tenderness	_____
	and	
	vasomotor instability or swelling	_____
	Total rating (out of 2)	_____
Possible:	limb pain	_____
	and	
	tenderness	_____
	Total rating (out of 2)	_____

Muscle Strength

Shoulder flexors	_____
Shoulder abductors	_____
Elbow flexors	_____
Elbow extensors	_____

BURKE REHABILITATION HOSPITAL
PHYSICAL THERAPY DEPARTMENT
CVA EVALUATION

Admission Discharge Date:_____
Date of Eval:_____
Initial Discharge
Patient's Age:_____

Patient's
Name:_____
MR#:_____
Treatment Unit:_____

S. Diagnosis:_____
Date of Onset:_____ Handedness:_____
CTT Scan/MRI Results:_____
Medical History:_____
_____
Precautions:_____
Medication:_____
Social/Family History:_____
_____

O: Mental Status:_____
Communication:_____
_____
Perception (functional):_____
_____
Vision/Hearing:_____
Vital Signs: Resting BP:_____ Resting HR:_____ Resting RR:_____
Respiratory Status:_____
Musculoskeletal Findings: (Structural/Postural)_____
_____

I. FUNCTIONAL ACTIVITIES: SCORE

Total A:	1	Min. A:	4	Modified I :	6	CG (4.5) used for P.T. will be considered score of 4 for research purposes.
Max. A:	2	*CG:	4.5	Complete I :	7	
Mod. A:	3	SV:	5	Not Appropriate:	N/A	

A. WHEELCHAIR PROPULSION: (Please ✓)
Endurance: Unable_____ <150'_____ ≥ 150'_____

WHEELCHAIR MANAGEMENT: SCORE
Footrests_____ Legrests_____ Lapboard_____ Brakes_____

B. TRANSFERS:

Stand Pivot:	TO LEFT	TO RIGHT
W/C --> mat	_____	_____
Mat --> W/C	_____	_____
W/C--> toilet	_____	_____
Toilet--> W/C	_____	_____
W/C--> bed	_____	_____
Bed--> W/C	_____	_____

Ambulatory: Devices: (Please circle) None / St. Cane / NBQC / WBQC / Hemiwalker / St. Walker / R. Walker

to low mat	_____	_____
to/from standard chair	_____	_____
to/from toilet	_____	_____
to/from bed	_____	_____

Floor--> low mat / furniture _____
Floor--> to stand _____

COMMENTS:_____
_____

C. POSITION CHANGES (Evaluated on a firm mat unless otherwise indicated)

	SCORE		SCORE
Roll to R from supine	_____	L sidelying---> sit	_____
Roll to L from supine	_____	Sit---> R sidelying --> supine	_____
R sidelying---> sit	_____	Sit---> L sidelying --> supine	_____

Comments: _____

II. SENSATION:

LIGHT TOUCH

0 - Anesthesia
1 - Hyperaesthesia/dyesthesia
2 - Normal

	Left	Right
1. Upper arm		
2. Palm of hand		
3. Thigh		
4. Sole of foot		
TOTAL		
	8	8

PROPRIOCEPTION

0 - No sensation
1 - Three quarters of answers are correct or considerable difference with positions on affected side.
2 - All answers are correct, little or no difference.

	Left	Right
1. Shoulder		
2. Elbow		
3. Wrist		
4. Thumb		
5. Hip		
6. Knee		
7. Ankle		
8. Toe		
TOTAL		
	16	16

Comments: _____

III. PROM/JOINT PAIN:

ROM Scoring

0 - Only a few degrees of motion
1 - Decreased PROM
2 - Normal PROM

	PROM		PAIN	
	Left	Right	Left	Right
Shoulder: Flexion				
Abduction to 90°				
External rotation				
Internal rotation				
Elbow: Flexion				
Extension				
Forearm: Pronation				
Supination				
Wrist: Flexion				
Extension				
Fingers: Flexion				
Extension				
TOTAL				
	24	24	24	24

PAIN Scoring

0 - Marked pain at end of range or pain through range
1 - Some pain
2 - No pain

	PROM		PAIN	
	Left	Right	Left	Right
Hip: Flexion				
Abduction				
External Rotation				
Internal Rotation				
Knee: Flexion				
Extension				
Ankle: Dorsiflexion				
Plantarflexion				
Eversion				
Inversion				
TOTAL				
	20	20	20	20

Comments: _____

IV. TONE:

Comments: _____

Patient's
Name: _____
MR #: _____

V. BALANCE:

	SCORE	BALANCE SCORING
A. Sit without support		0 - Cannot maintain sitting without support 1 - Can sit unsupported less than 5 minutes 2 - Can sit longer than 5 minutes
B. Protective extension: non-affected side		0 - Does not abduct shoulder or extend elbow 1 - Impaired reaction 2 - Normal reaction
C. Protective extension: affected side		0 - Does not abduct shoulder or extend elbow 1 - Impaired reaction 2 - Normal reaction
D. Supported standing		0 - Cannot stand 1 - Stands with maximum support of others 2 - Stands with minimum support of one for 1 minute
E. Stand without support		0 - Cannot stand without support 1 - Stands less than 1 minute or sways 2 - Stands with good balance more than 1 minute
F. Stand on unaffected side		0 - Cannot be maintained longer than 1-2 seconds 1 - Stands balanced 4-9 seconds 2 - Stands balanced more than 10 seconds
G. Stand on affected side		0 - Cannot be maintained longer than 1-2 seconds 1 - Stands balanced 4-9 seconds 2 - Stands balanced more than 10 second
TOTAL	14	

VI. MOTOR STATUS: UPPER EXTREMITY:

Score up to 2 points for each component of task (Maximum score = 66)

		SCORE	SCORING	TOTAL
A. Shoulder/ Elbow/ Forearm	1. Reflexes a. Biceps or Finger flexors_____ b. Triceps		*0 = No reflex elicited* *2 = Reflex Elicited*	4
	2. Flexor Synergy (Forearm supinated, bring affected arm to ipsilateral ear) a. Retraction _____ b. Elevation_____ c. Abduction_____ d. External Rotation_____ e. Elbow Flexion_____ f. Forearm Supination		*0 = Cannot perform at all* *1 = Perform partly* *2 = Perform faultlessly*	12
	3. Extensor Synergy (Forearm pronated and hand to contralateral knee) a. Adduction and internal rotation _____ b. Elbow extension_____ c. Forearm pronation		*0 = Cannot perform at all* *1 = Perform partly* *2 = Perform faultlessly*	6
	4. Mixed synergy patterns a. Hand to lumbar spine_____ b. Shoulder flexion to 90°, elbow @ 0°, forearm neutral_____ c. Forearm pronation - supination, shoulder @ 0°, elbow flexed @ 90°		*0 = Synergy components begin with onset of movement* *1 = Synergy components begin later in movement* *2 = No synergy components*	6

	SCORE	SCORING	TOTAL
	5. Isolated movements without synergy a. shoulder abduction to 90°, elbow @ 0°, forearm pronated_____ b. Shoulder flexion 90° - 180°, elbow @ 0°, forearm neutral_____ c. Forearm pronation - supination, shoulder flexion between 30° - 90°, elbow @ 0_____	0 = *Synergy components begin with onset of movement* 1 = *Synergy components begin later in movement* 2 = *No synergy components* 0 = *Cannot perform* 1 = *Performed partly* 2 = *Performed faultlessly*	6
	6. Score this section only if 5 was scored a perfect score of 6 a. Normal Reflex Activity: 1. Biceps, Finger Flexors, Triceps	0 = *2/3 Reflexes are markedly hyperactive* 1 = *1 Reflex is hyperactive or 2 are lively* 2 = *No more than 1 reflex is lively. None are hyperactive*	2
B. Wrist: (all tests with forearm pronated)	1. Wrist flexion/extension with elbow @ 90°, shoulder @ 0°_____	0 = *No volitional movement* 1 = *Wrist flexion/extension through partial range* 2 = *Controlled movement through full range*	10
	2. Wrist stability, with elbow @ 90°, shoulder @ 0°_____	0 = *Unable to extend wrist 15°* 1 = *Wrist extension to 15°, unable to take resistance* 2 = *Able to maintain wrist extension to 15° against minimal resistance*	
	3. Wrist flexion/extension with elbow @ 0°, shoulder at 0°_____	*Same as #1*	
	4. Wrist stability with elbow @ 0°, shoulder @ 0°_____	*Same as #2*	
	5. Wrist circumduction with elbow @ 90°, shoulder @ 0° or with elbow and shoulder at 0°_____	0 = *Unable to perform* 1 = *Incomplete or uncontrolled motion* 2 = *Complete, controlled motion*	
C. Hand	1. Fingers, mass flexion_____ 2. Fingers, mass extension_____	0 = *Cannot perform* 1 = *Performs partly* 2 = *Performs faultlessly*	14
	3. PIP - DIP hook grasp: MP Jts extended and PIPs + DIPs are flexed _____	0 = *Unable* 1 = *Performed weakly without resistance* 2 = *Performed with great resistance*	
	4. Thumb adduction with paper: All others jts @ 0° ____ 5. Pincer grasp with a pencil_____ 6. Cylinder grasp with small can_____ 7. Spherical grasp with tennis ball	0 = *Unable* 1 = *Able to hold with slight tug* 2 = *Hold firmly with tug*	
D. Coord./ Speed (Finger to nose 5x with eyes closed)	1. Tremor_____ 2. Dysmetria_____	0 = *Marked tremor or dysmetria* 1 = *Slight tremor or dysmetria* 2 = *No tremor or dysmetria*	6
	3. Time_____	0 = > 6 *seconds differ. b/w hands* 1 = 2-5 *seconds differ. b/w hands* 2 = < 2 *seconds differ. b/w hands*	
		TOTAL	66

Patient's
Name: _____
MR #: _____

VII. MOTOR STATUS: LOWER EXTREMITY: Score up to 2 points for each component of task (Maximum score = 34)

	SCORE	SCORING	TOTAL
A. Hip/ Knee/ Ankle	1. Reflexes a. Achilles_____ b. Patellar	*0 = No reflex elicited* *2 = Reflex elicited*	4
	2. Flexor Synergy (Patient supine, full flexion of all LE joints) a. Hip flexion_____ b. Knee flexion_____ c. Dorsiflexion	*0 = Cannot be performed* *1 = Perform partially* *2 = Performed faultlessly*	6
	3. Extensor synergy (Patient supine, limb extension from position of full flexion, resist motion) a. Hip extension_____ b. Hip adduction_____ c. Knee extension_____ d. Ankle plantarflexion	*0 = Cannot be performed* *1 = Perform partially* *2 = Performed faultlessly*	8
	4. Mixed synergy patterns (Patient seated) a. Knee flexion > 90°_____ b. Ankle dorsiflexion	*0 = Cannot be performed* *1 = Perform partially* *2 = Performed faultlessly*	4
	5. Isolated movements without synergy (Patient standing) a. Knee flexion to 90° with hip at 0°_____ b. Ankle dorsiflexion with hip at 0°_____	*0 = Synergy begins at onset of movement* *1 = Synergy begins later in movement or no synergy but decreased range of motion* *2 = Full motion without synergy*	4
	6. Score only if #5 had a perfect score of 4 a. Normal Reflex Activity: 1. Hamstrings, Patellar, Achilles	*0 = 2/3 reflexes are markedly hyperactive* *1 = 1 reflex is hyperactive or 2 are lively* *2 = No more than 1 reflex is lively and none are hyperactive*	2
B. Coord./ Speed (Heel to knee 5x Patient supine)	1. Tremor_____ 2. Dysmetria_____	*0 = Marked tremor or dysmetria* *1 = Slight marked tremor or dysmetria* *2 = No tremor or dysmetria*	6
	3. Time_____	*0 = > 6 second difference b/w lower extremities* *1 = 2 - 5 second difference b/w lower extremities* *2 = < 2 second difference b/w lower extremities*	
		TOTAL	34

VIII. MOTOR STATUS: TRUNK AND NECK: _____

IX. STRENGTH: MMT of Non-involved limbs, and movements on involved side that have been determined to be isolated. _____

X. AMBULATION:

A. Pre-Gait Activities: (For non-ambulatory patients only)

1. Device/Orthosis used: _____
2. Describe Standing Posture: _____
3. Time standing is tolerated: _____
4. Activities performed while standing: _____
5. Amt. of assistance:
   Total A ____ Max A ____ Mod A ____ Min A ____ CG ____ SV ____ Modified I ____ Complete I ____ V.C. ____
   Where assistance given: _____

B. Ambulation/Gait:

1. Devices: (Please circle) None / St. Cane / NBQC / WBQC / Hemiwalker / St. Walker / R. Walker / Hemibar
2. Orthosis: (Please circle) None / PLS / AFO / KAFO / Other _____
   Temporary _____ Permanent _____
3. Upper Extremity Support: Hemisling Yes ____ No ____
4. Amount. of assistance:
   Total A ____ Max A ____ Mod A ____ Min A ____ CG ____ SV ____ Modified I ____ Complete I ____ V.C. ____
   Where assistance given: _____
5. Distance: _____
6. Shoe Modifications: _____
7. Timed Walk: 1 minute timed walking test with above assist: _____
8. Step Length: Equal _____ Unequal _____
9. Base of Support: Increased _____ Decreased _____ Natural _____
10. Stance Time: Equal _____ Unequal _____
11. Weight Shift: Equal _____ Unequal _____
12. Cognitive/Safety factors: Safe Yes ____ No ____
13. Ability to ambulate over different terrain/inclines:

	Independent	Assist Required (Note Amount)	Not Able
a. Grass:	_____	_____	_____
b. Curb:	_____	_____	_____
c. Sidewalk:	_____	_____	_____
d. Inclines:	_____	_____	_____

C. Stair Negotiation:

Patient negotiates _____ (#) _____ (ht.) inch steps using _____ (# Rails and/or devices)

Patient ascends using a step over step/step to step pattern requiring _____ assistance.

Patient descends using a step over step/step to step pattern requiring _____ assistance.

Patient's
Name: _____
MR#: _____

I. GAIT ANALYSIS (CHECK ALL DEVIATIONS THAT APPLY)

FOOT and ANKLE

	STANCE PHASE Left	STANCE PHASE Right		SWING PHASE Left	SWING PHASE Right
Entire sole down			Toe Drag		
Toes first			Inversion		
Supination early stance			Increased dorsiflexion		
Supination throughout			Whip		
Pronation			Eversion		
Foot Slap			Vaulting		
			Toe Clawing		

KNEE

Knee buckles			Flexion Absent		
Hyperextension (mild)			Flexion Decreased		
Hyperextension (moderate)			Flexion Increased		
Hyperextension (severe)					
able in slight flexion					

HIP

Trendelenberg			Circumduction		
Increased External Rotation			Increased Flexion		
Decreased Hip Extension			Decreased Flexion		
			External Rotation		
			Increased Adduction		

PELVIS

Increase Ant. Tilt			Hiking		
Increase Post. Tilt			Dec. Forward Rotation		
Retraction					

TRUNK

Inc. Lat. Flexion			Inc. Lateral Flexion		
Inc. Foward Flexion			Increased Extension		
Inc. Extension			Increased Rotation		
Inc. Rotation			Inc. Forward Flexion		

UPPER EXTREMITY

Posturing		
Arm Swing Absent		
Arm Swing Decreased		

XI. MISCELLANEOUS/ADDITIONAL COMMENTS: _____

MAJOR PROBLEMS/ASSESSMENT:

SHORT TERM GOALS: ____ Same as on note dated _____, unless indicated.

GOALS ACHIEVED:

COMMENTS:

LONG TERM GOALS: ____ Same as on note dated _____, unless indicated.

GOALS ACHIEVED:

COMMENTS:

TREATMENT PLAN:

Treatment frequency:

_____ Therapeutic Exercise (ROM; Strengthening; Stretching)
_____ Functional Activity Training
- _____ Position Changes
- _____ W/C Activities
- _____ Transfer Training
- _____ Gait Training

_____ Orthotic Evaluation/Assessment
_____ Instruction in home exercise program
_____ Family Education
_____ Other:

_____ Treatment plan discussed with patient and family
_____ Discharge plan discussed with patient and family

Recommendations/Equipment on D/C:

Physical Therapist:

APPENDIX C: ROBOT-AIDED NEURO-REHABILITATION: PATENT

US005466213A

United States Patent [19]

Hogan et al.

[11] Patent Number: 5,466,213

[45] Date of Patent: Nov. 14, 1995

[54] INTERACTIVE ROBOTIC THERAPIST

[75] Inventors: Neville Hogan, Sudbury; Hermano I. Krebs, Somerville; Andre Sharon, Newton; Jain Charnnarong, Charleston, all of Mass.

[73] Assignee: Massachusetts Institute of Technology, Cambridge, Mass.

[21] Appl. No.: 178,182

[22] Filed: Jan. 6, 1994

Related U.S. Application Data

[63] Continuation-in-part of Ser. No. 87,666, Jul. 6, 1993, abandoned.

[51] Int. Cl.[6] A61H 1/00

[52] U.S. Cl. 601/33; 482/901; 482/4

[58] Field of Search 601/33, 34, 40; 414/5; 901/4; 482/1, 4–9, 901, 902, 900

[56] References Cited

U.S. PATENT DOCUMENTS

3,648,143	3/1972	Harper et al.	901/4
4,046,262	9/1977	Vykukal et al.	414/5
4,235,437	11/1980	Ruis et al.	482/137
4,689,449	8/1987	Rosen .	
4,740,126	4/1988	Richter	901/4
4,837,734	6/1989	Ichikawa et al.	901/4
4,936,299	6/1990	Erlandson	601/33
5,020,790	6/1991	Beard et al. .	
5,078,152	1/1992	Bond et al.	482/902
5,163,451	11/1992	Grellas	601/33
5,186,695	2/1993	Mangseth et al.	482/4
5,201,772	4/1993	Maxwell .	
5,391,128	2/1995	deBear	482/4

FOREIGN PATENT DOCUMENTS

676280	7/1979	U.S.S.R.	601/33
876131	10/1981	U.S.S.R.	601/33
9313916	7/1993	WIPO	901/4

OTHER PUBLICATIONS

Adelstein, B. D. and Rosen, M. J., "A Two Degree-of-Freedom Loading Manipulandum for the Study of Human Arm Dynamics," 1987 Advances in Bioengineering, The American Society of Engineers, pp. 111–112 (1987, Dec.).

Rosen, M. J. and Adelstein, B. D., "Design of a Two-Degree-of-Freedom Manipulandum for Tremor Research," Frontiers of Engineering and Computing in Health Care-1984, IEEE Engineering in Medicine and Biology Society, pp. 47–51 (1984, Sep.).

Adelstein, B. D. and Rosen, M. J., "A High Performance Two Degree-of-Freedom Kinesthetic Interface," Proceedings of the Eng. Foundation Conf. on Human Machine Interfaces for Teleoperators and Virtual Environments, 6 pages, (1990, Mar.).

Primary Examiner—Joe H. Cheng
Assistant Examiner—Jeanne M. Clark
Attorney, Agent, or Firm—Hamilton, Brook, Smith & Reynolds

[57] ABSTRACT

An interactive robotic therapist interacts with a patient to shape the motor skills of the patient by guiding the patient's limb through a series of desired exercises with a robotic arm. The patient's limb is brought through a full range of motion to rehabilitate multiple muscle groups. A drive system coupled to the robotic arm is controlled by a controller which provides the commands to direct the robotic arm through the series of desired exercises.

20 Claims, 20 Drawing Sheets

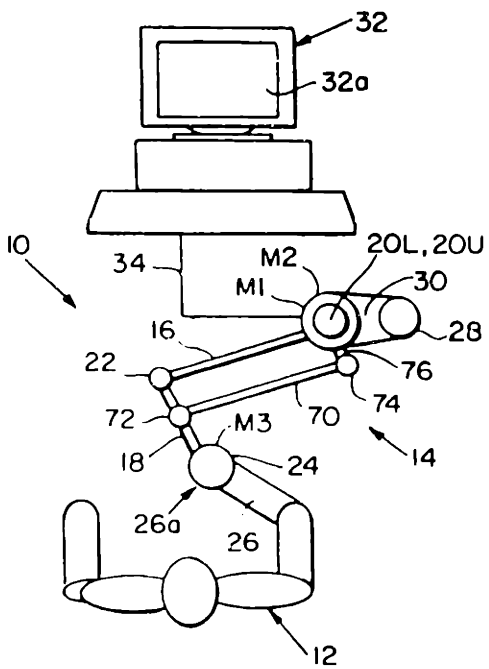

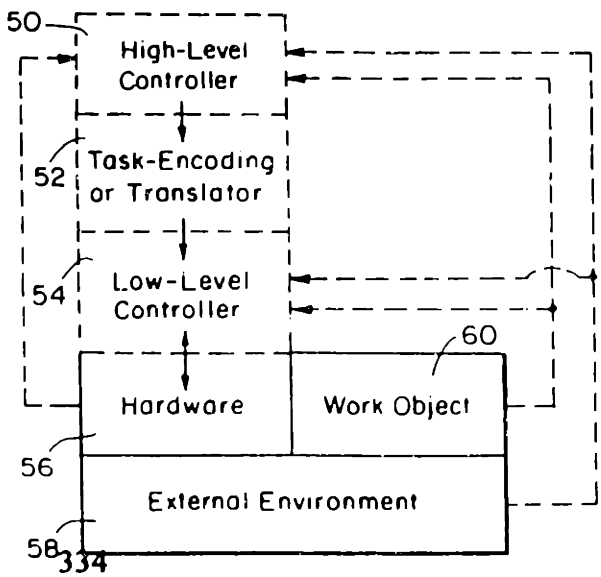

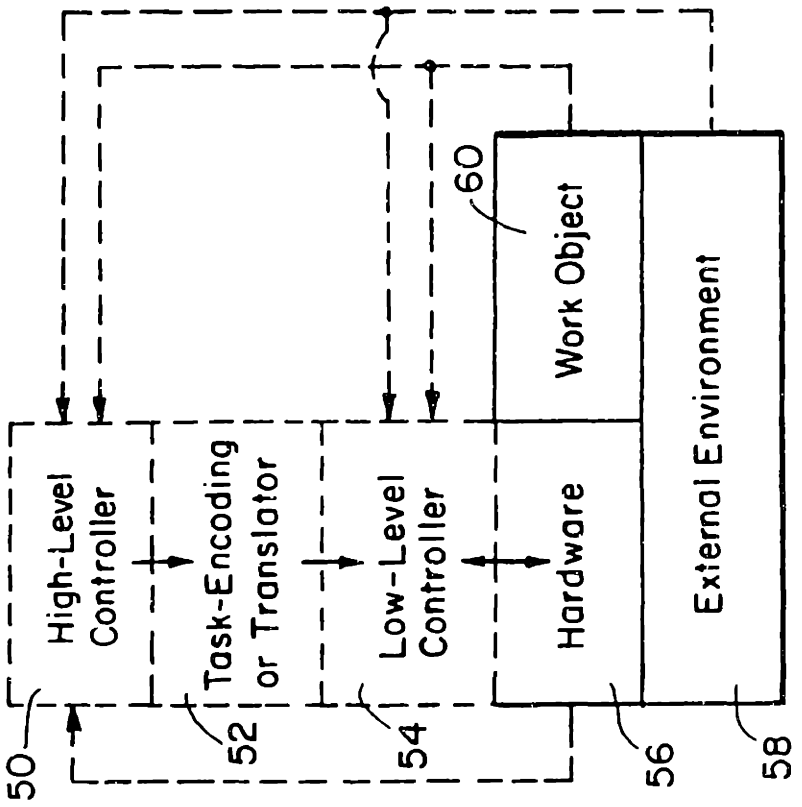
High-Level Controller
Task-Encoding or Translator
Low-Level Controller
Hardware
Work Object
External Environment
50
52
54
56
58
60

FIG. 2

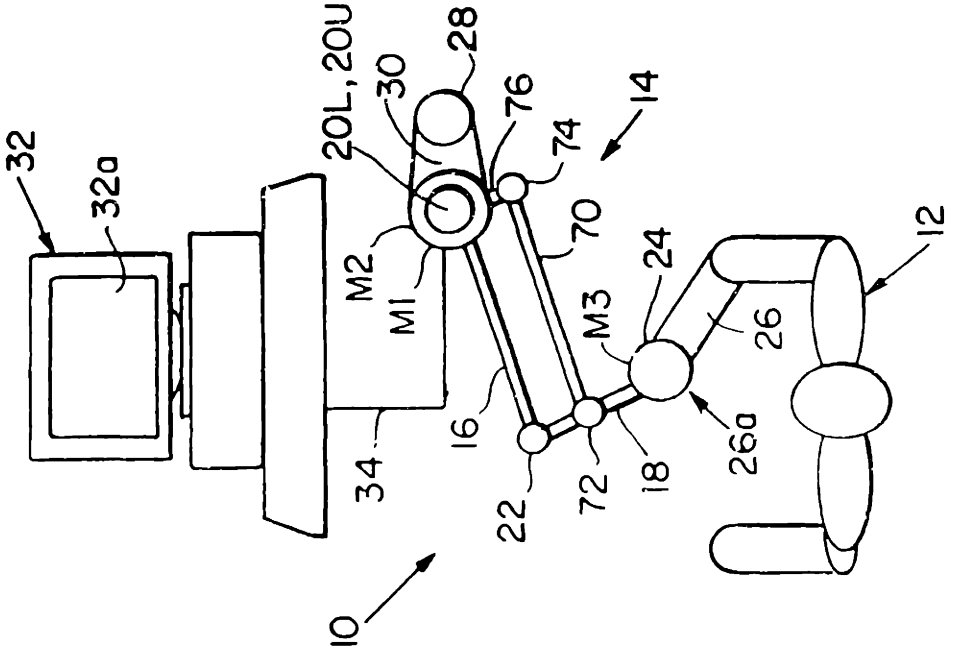
32
32a
20L, 20U
30
28
76
74
14
70
M2
M1
M3
24
26
26a
12
16
22
72
18
34
10

FIG. 1

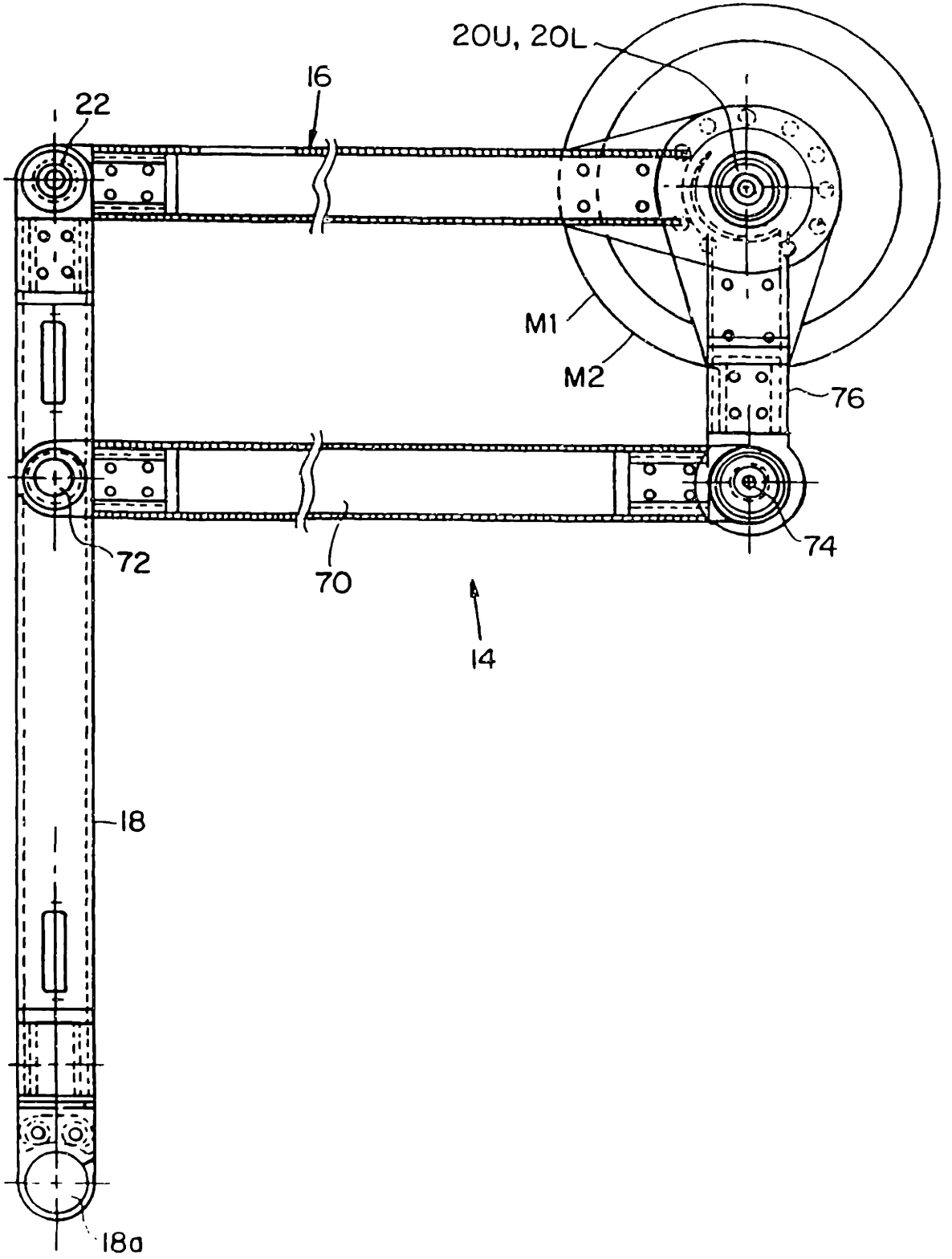

FIG. 3a

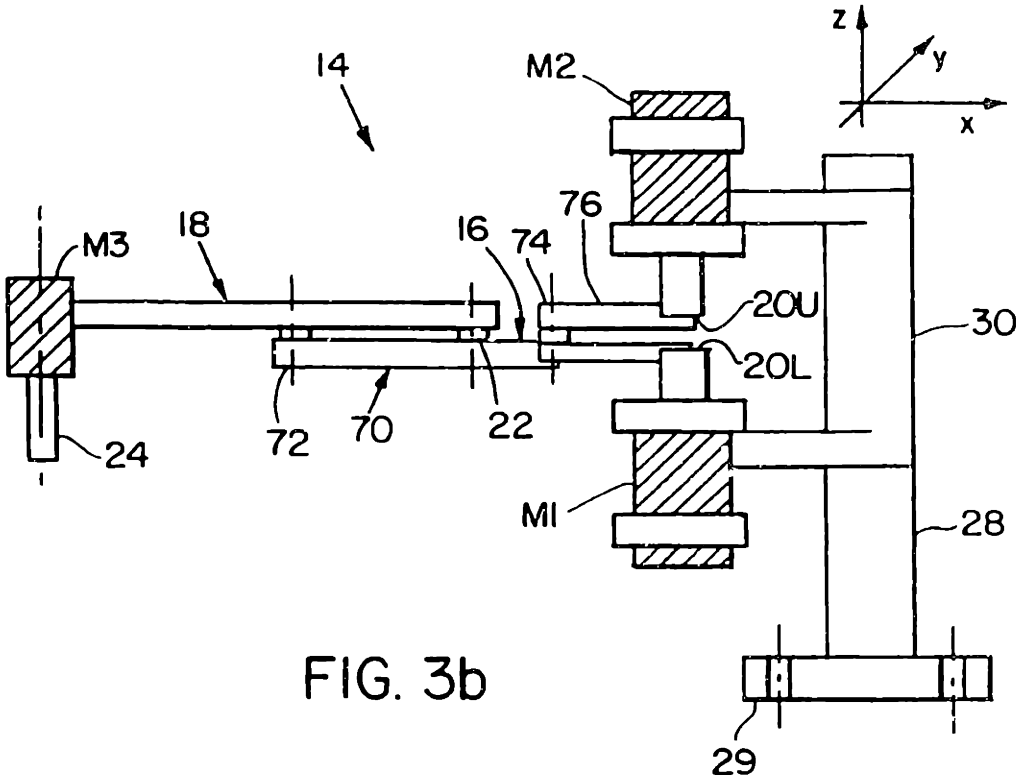
14
M2
z
y
x
76
M3
18
16
74
20U
30
20L
72
70
22
24
M1
28
29

FIG. 3b

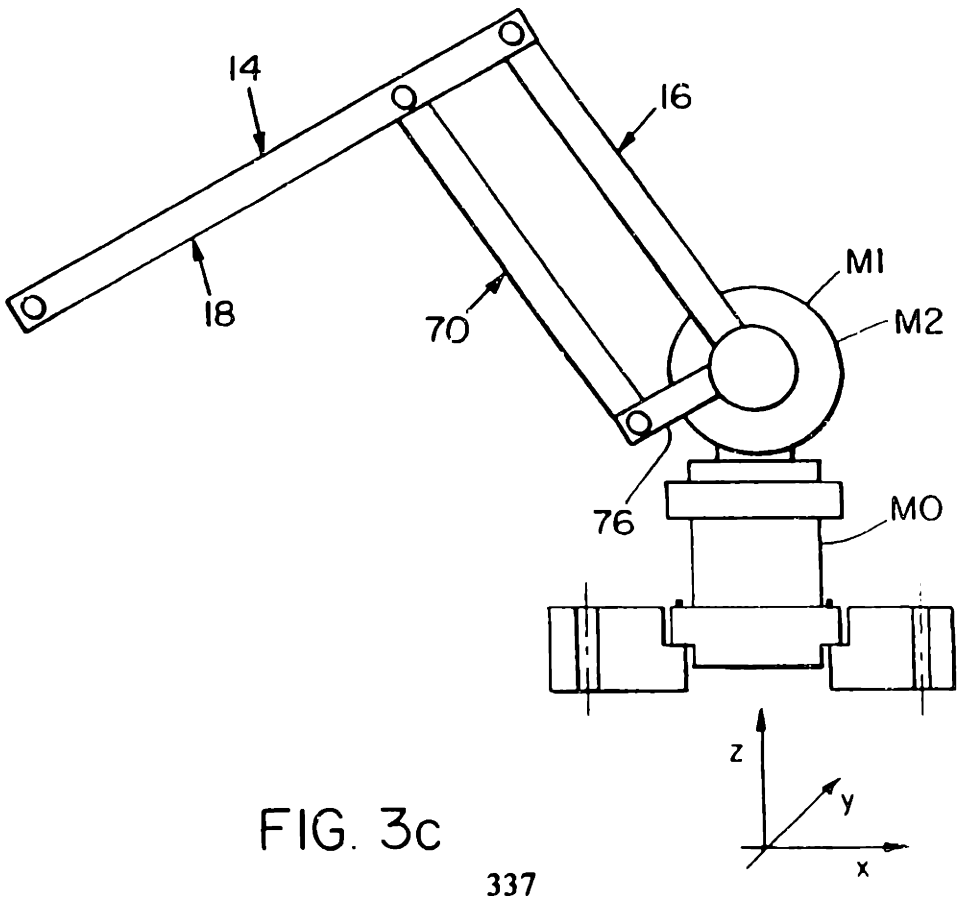
14
16
M1
18
70
M2
76
M0
z
y
x

FIG. 3c

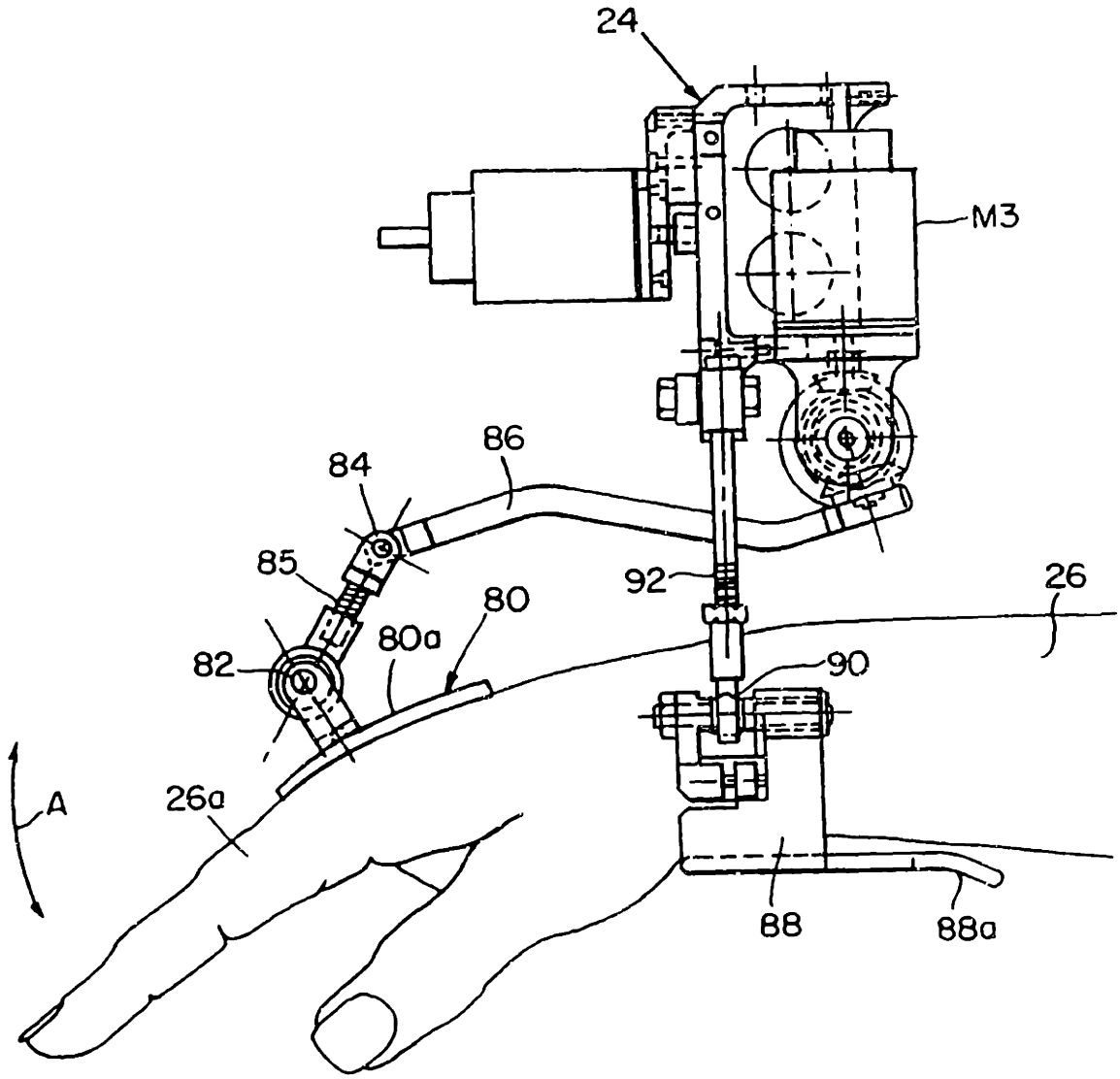

FIG. 4a

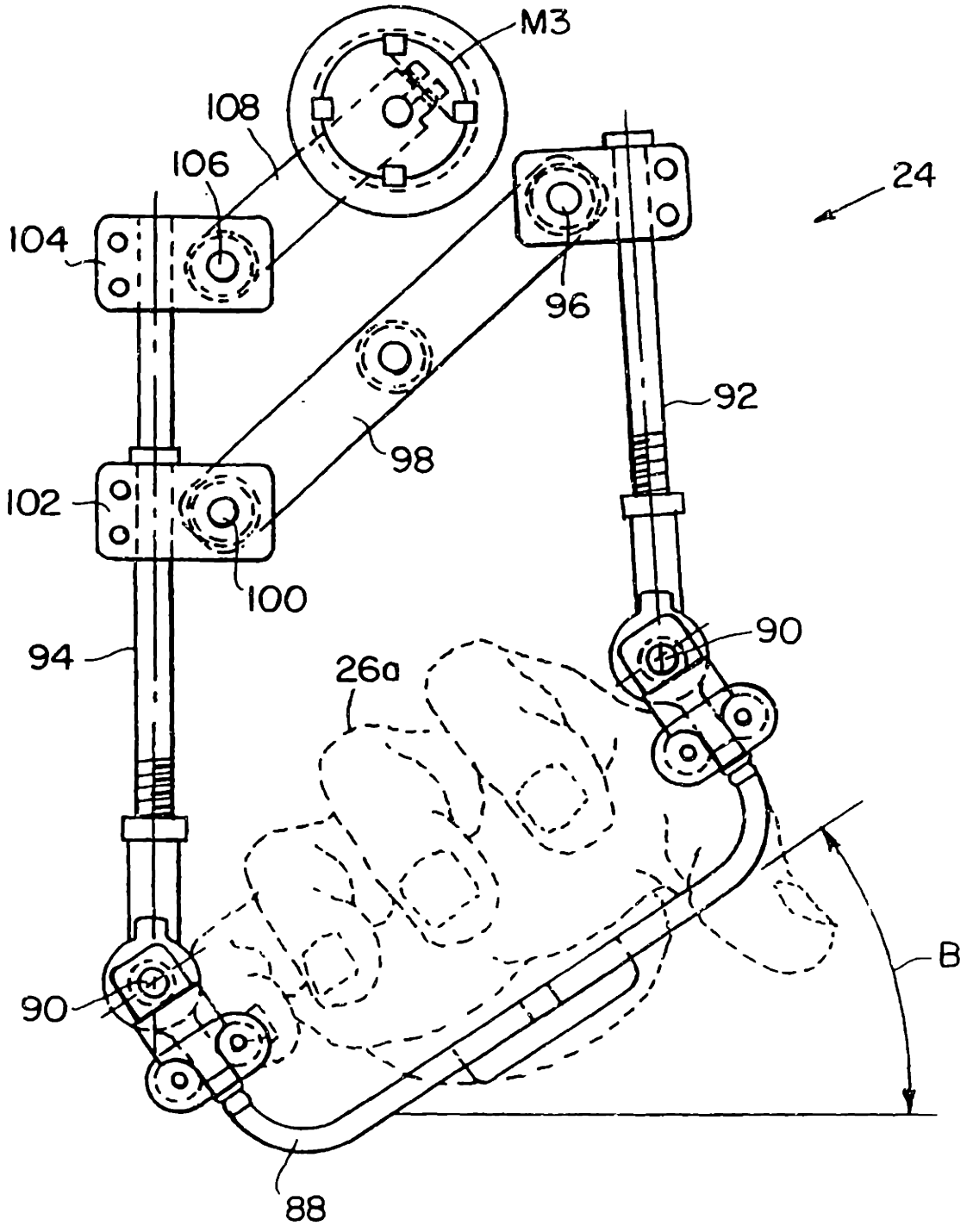

FIG. 4b

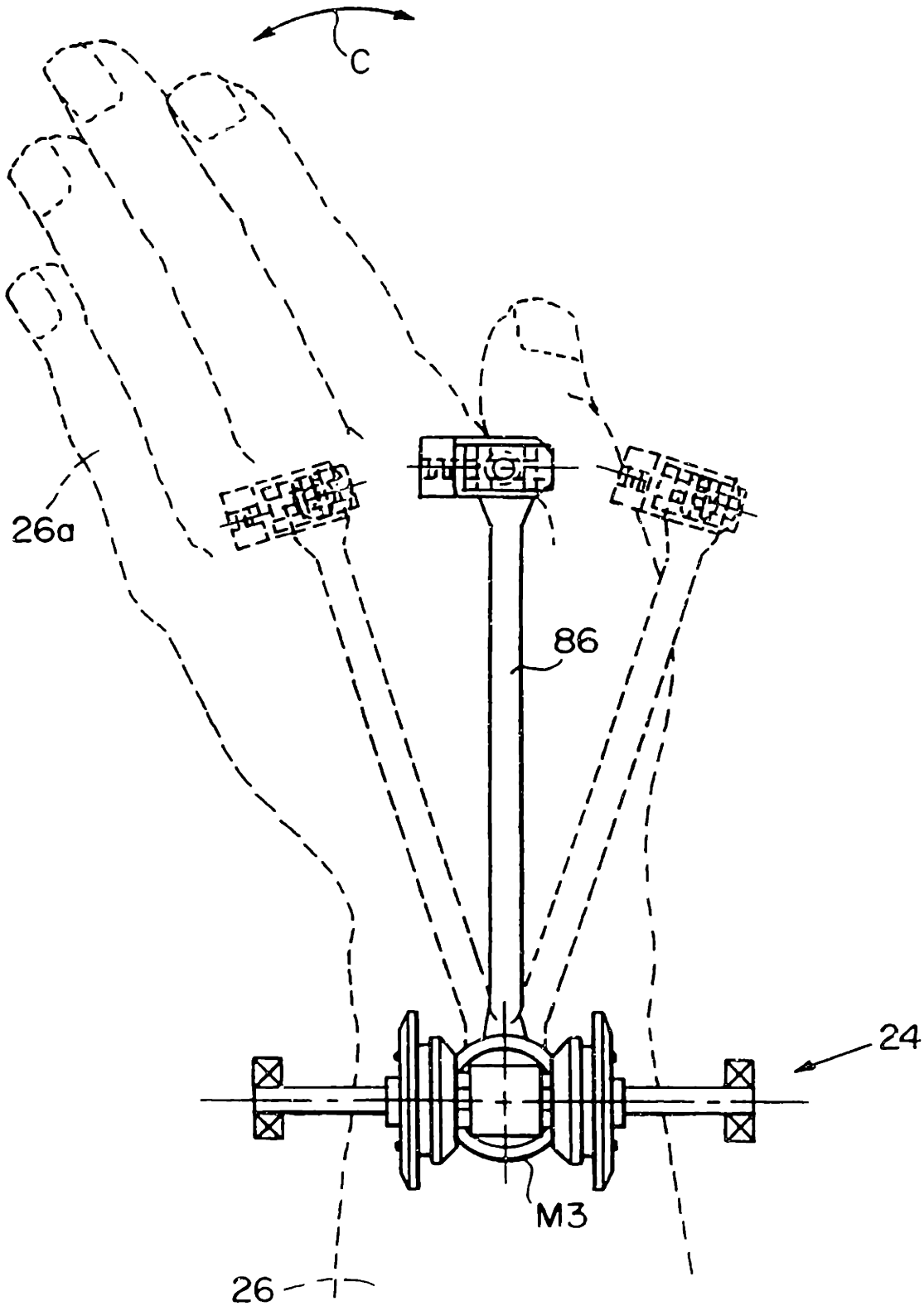

FIG. 4c

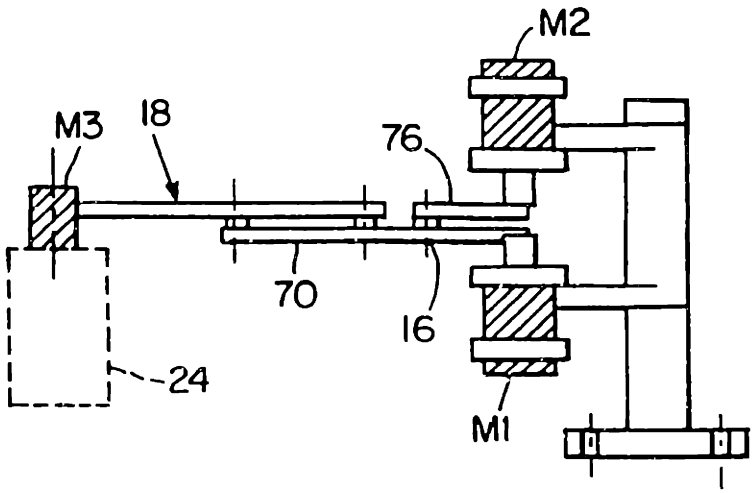

FIG. 4d

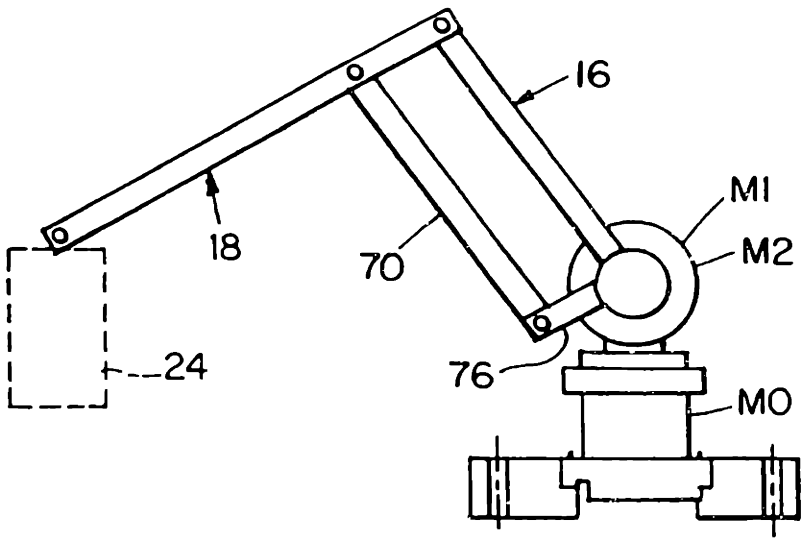

FIG. 4e

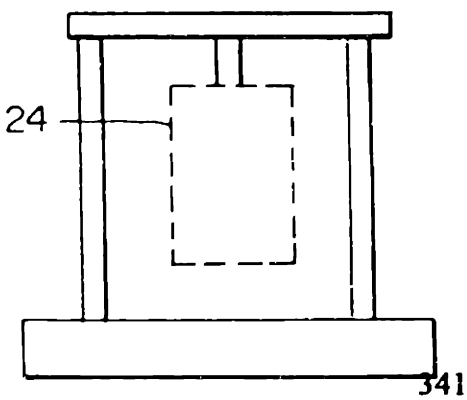

FIG. 4f

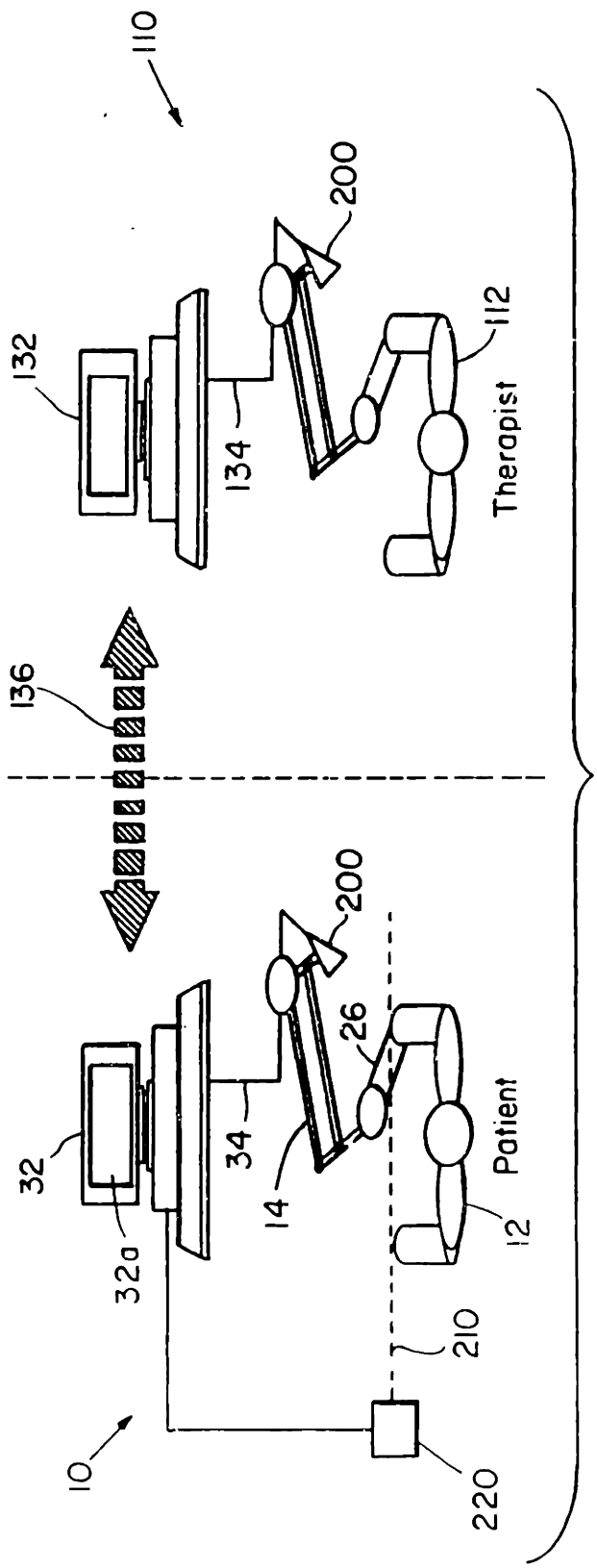
110
200
132
134
112
Therapist
136
200
26
32
34
14
Patient
12
32a
210
10
220

FIG. 5a

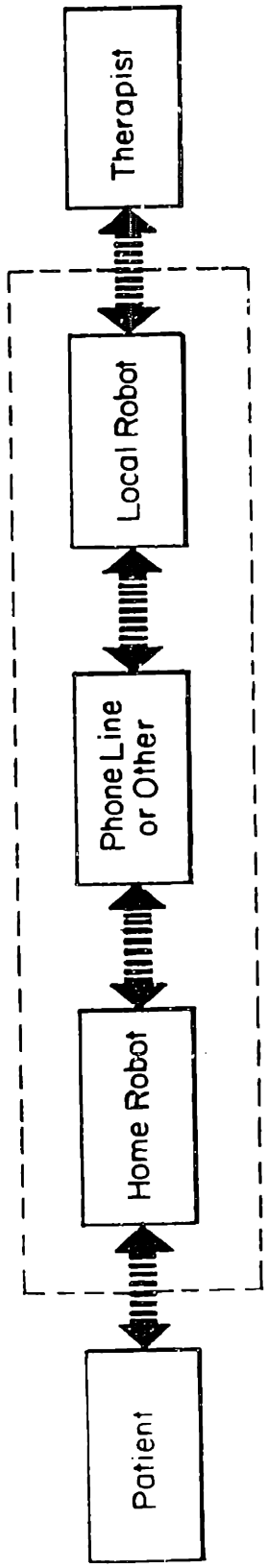
Therapist
Local Robot
Phone Line or Other
Home Robot
Patient

FIG. 5b

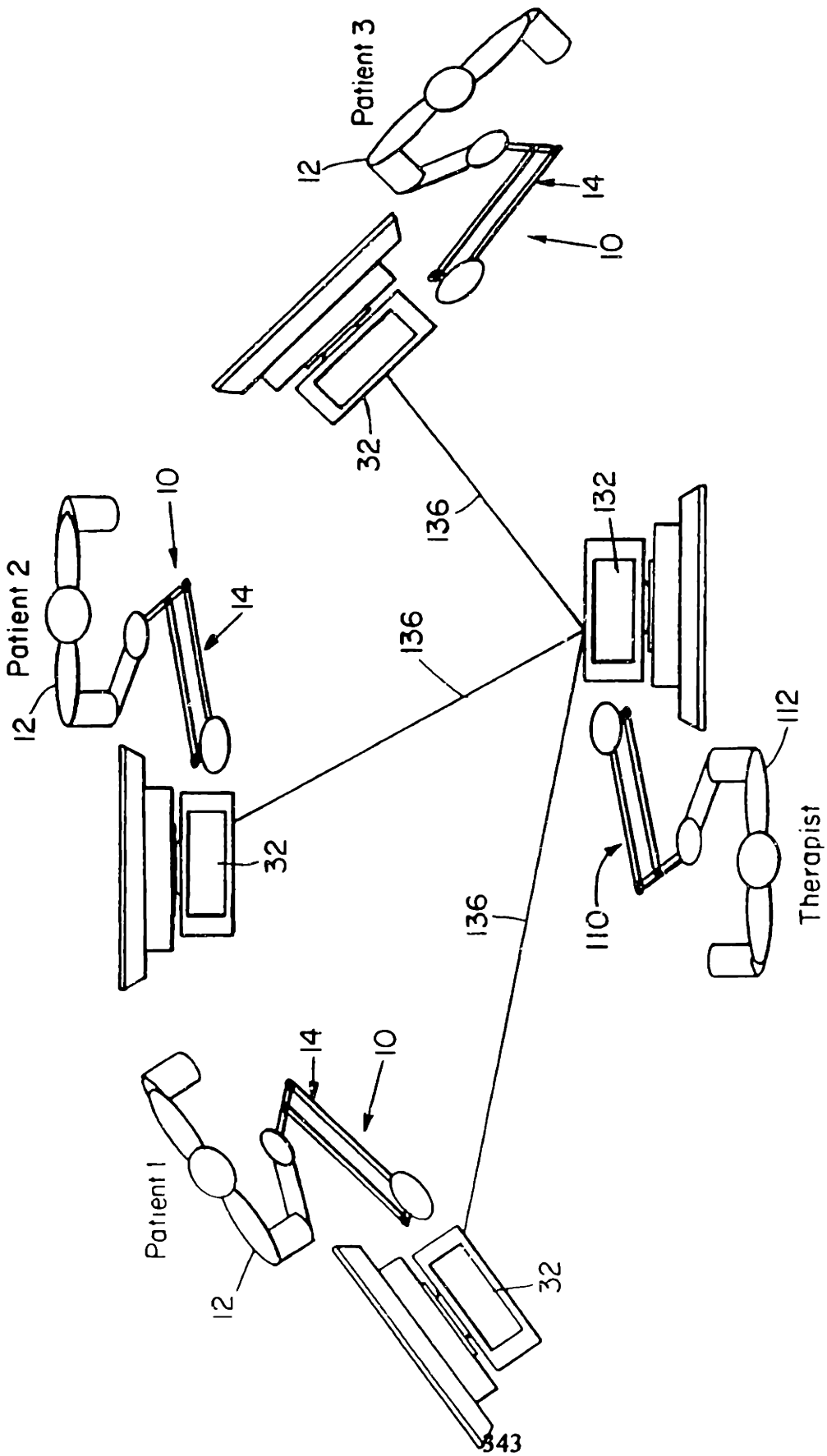
Patient 3
12
14
10
32
136
132
Patient 2
10
14
12
136
32
112
Therapist
110
136
14
10
Patient 1
12
32
343

FIG. 6

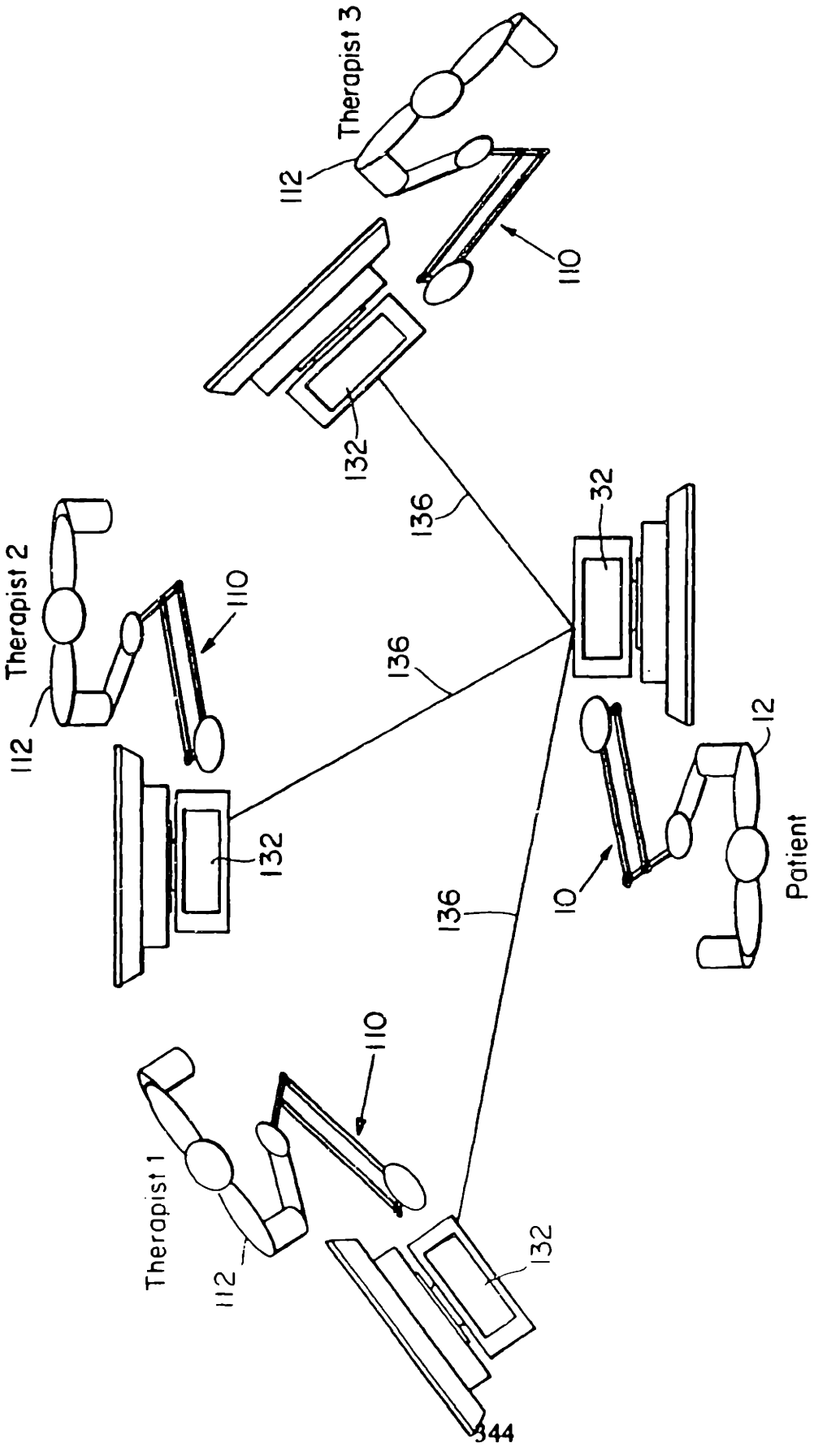
Therapist 3
112
110
132
136
32
Therapist 2
112
110
136
132
12
Patient
10
136
110
Therapist 1
112
132
344

FIG. 7

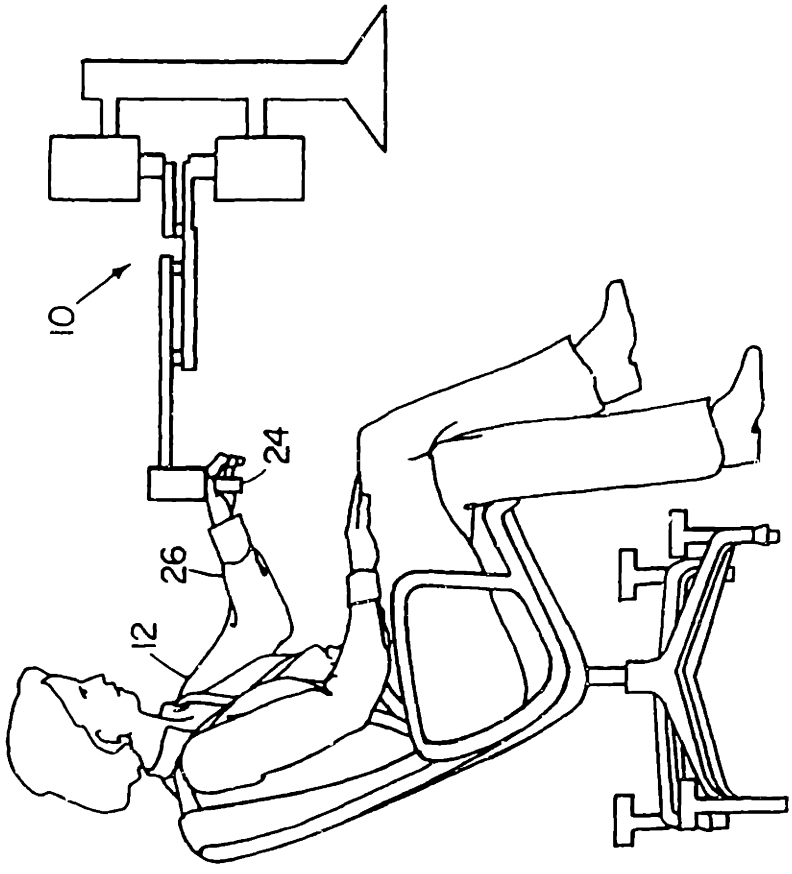

FIG. 8b

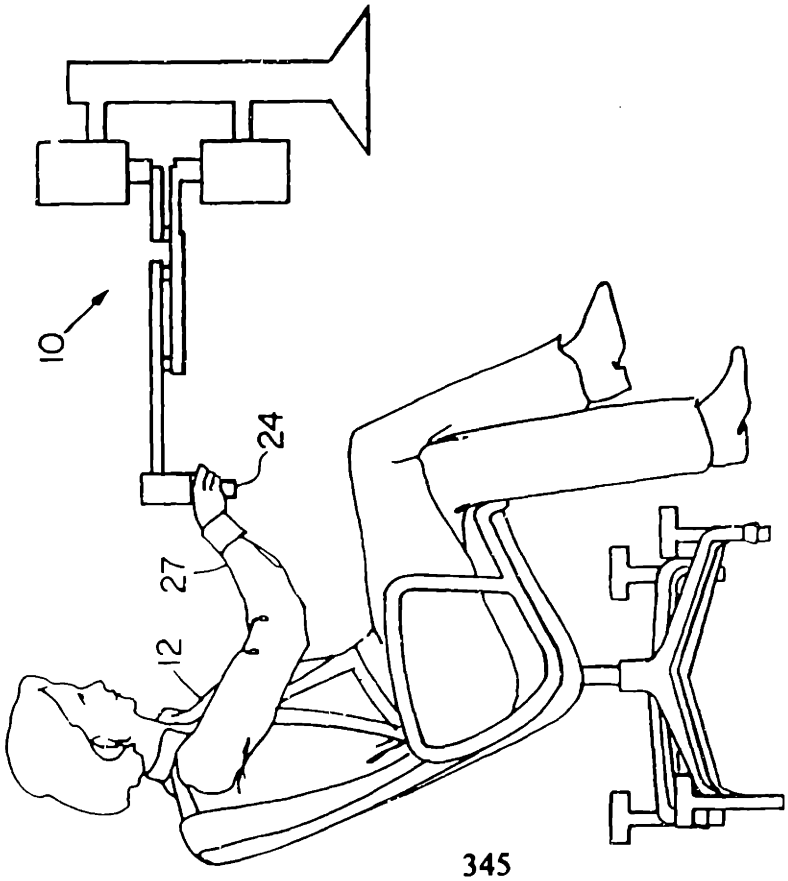

FIG. 8a

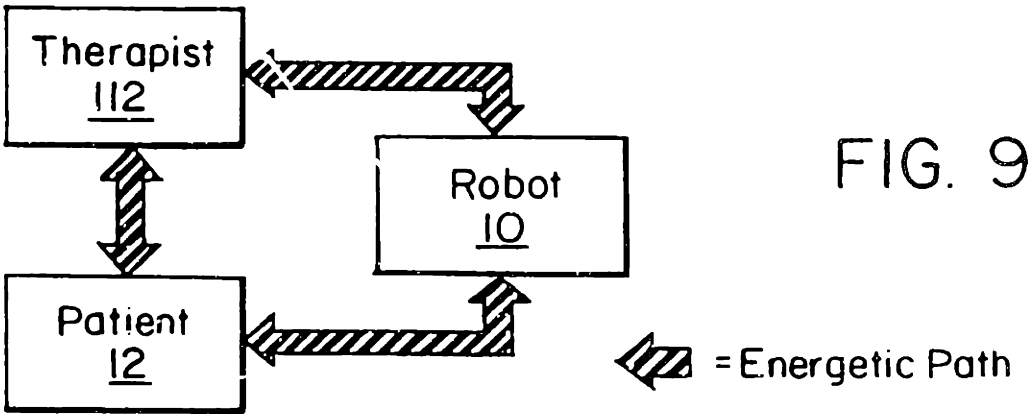

FIG. 9a

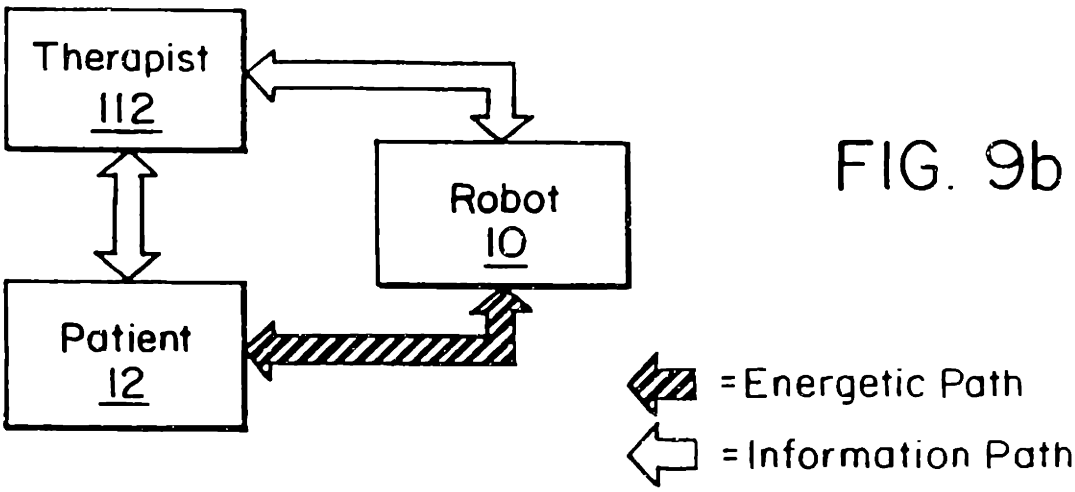

FIG. 9b

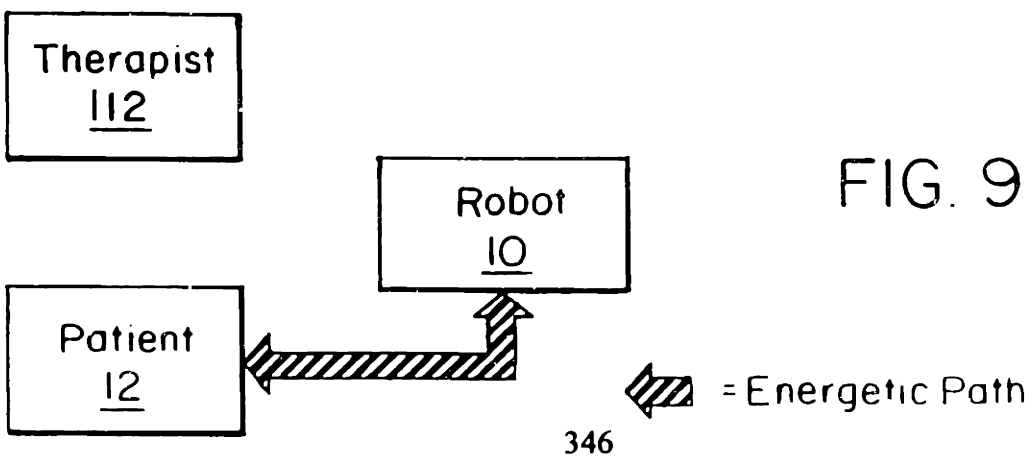

FIG. 9c

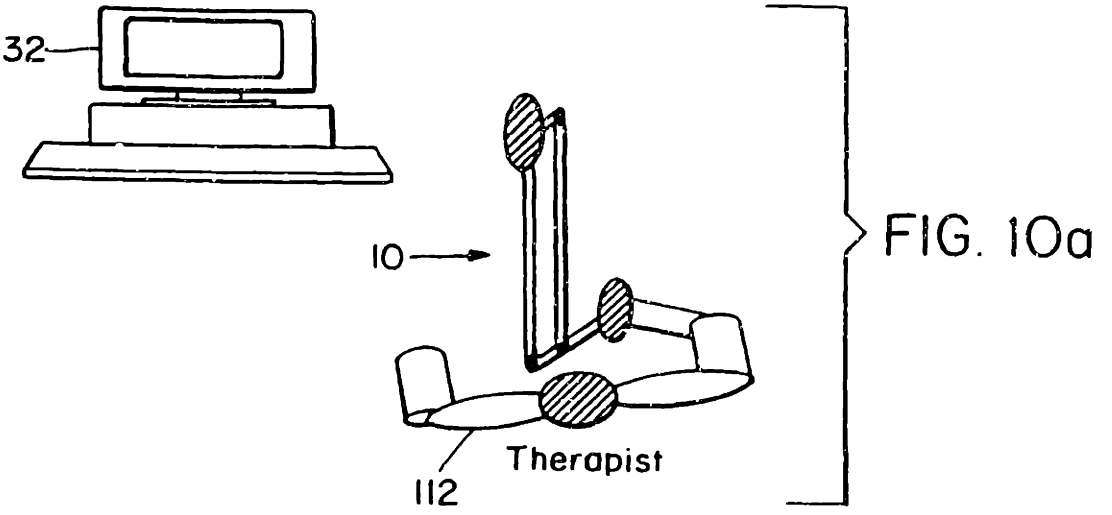

FIG. 10a

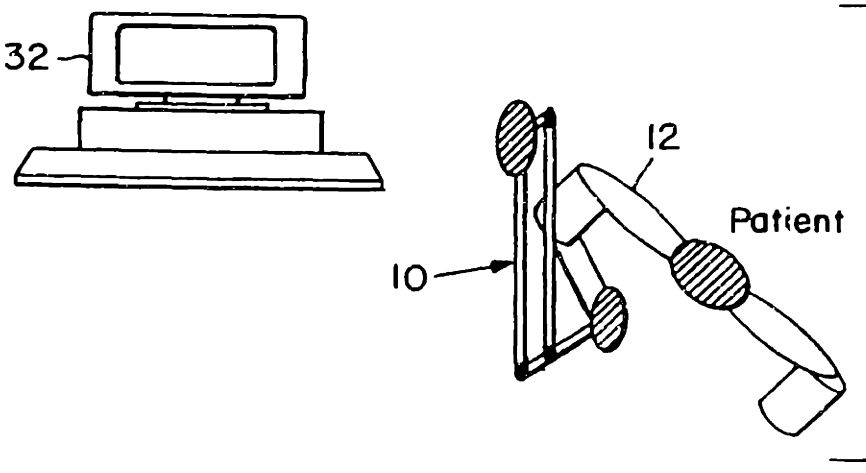

FIG. 10b

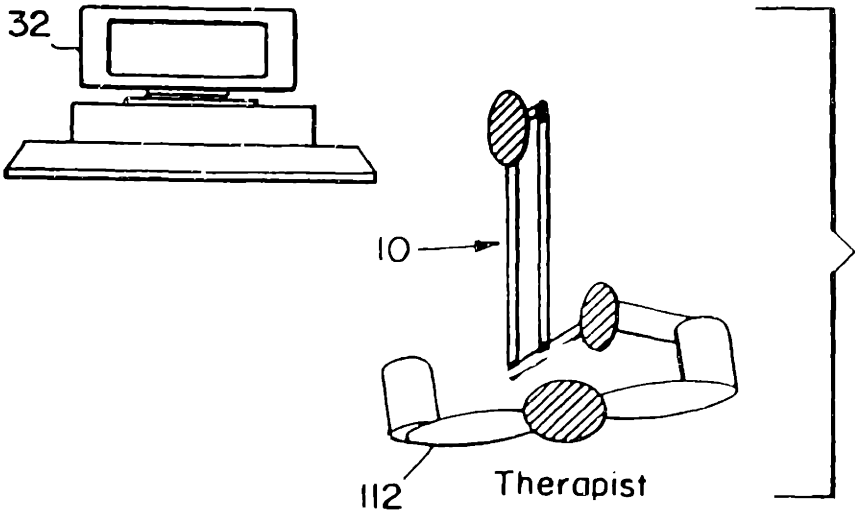

FIG. 10c

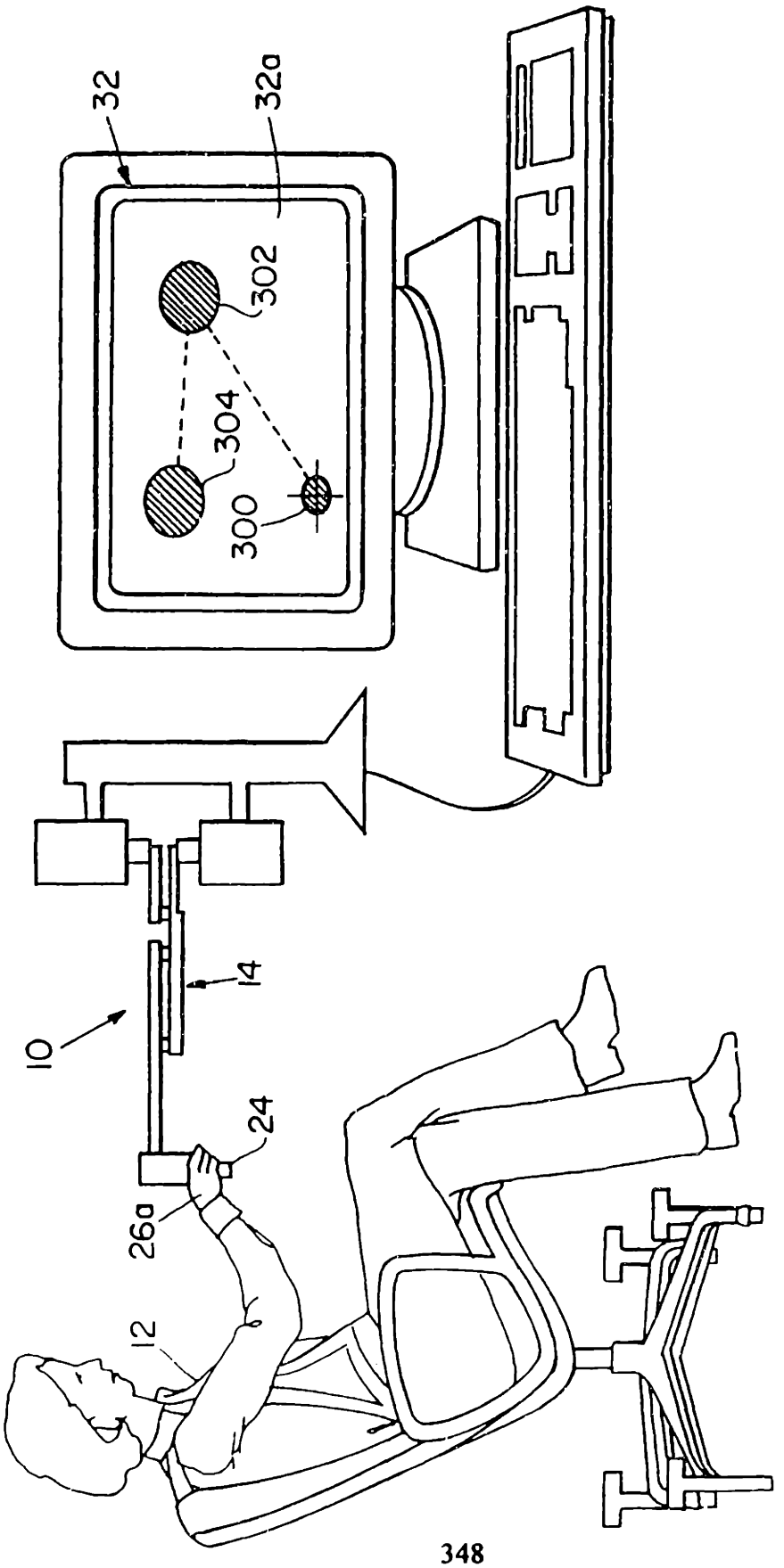

FIG. 11a

FIG. 11b

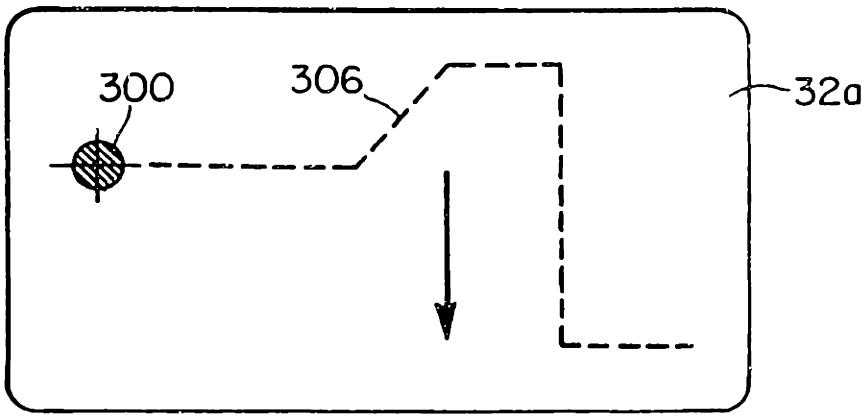

FIG. 11c

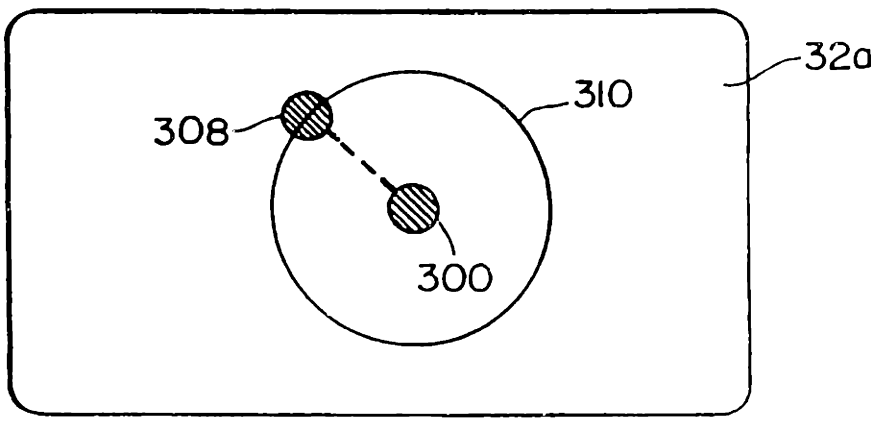

FIG. 11d

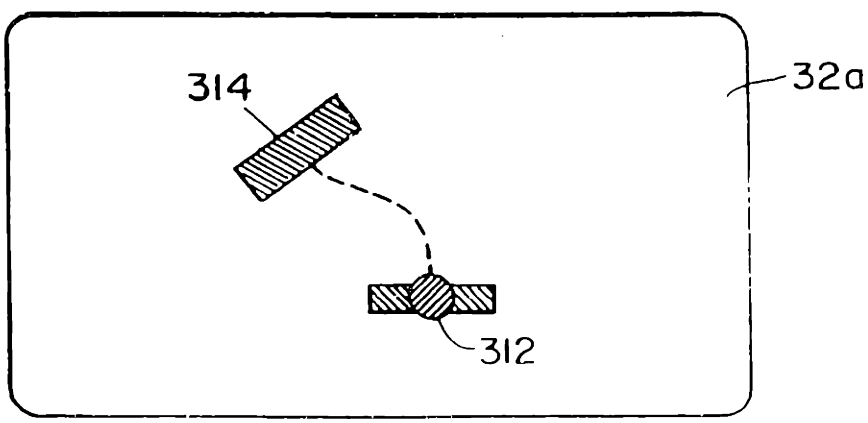

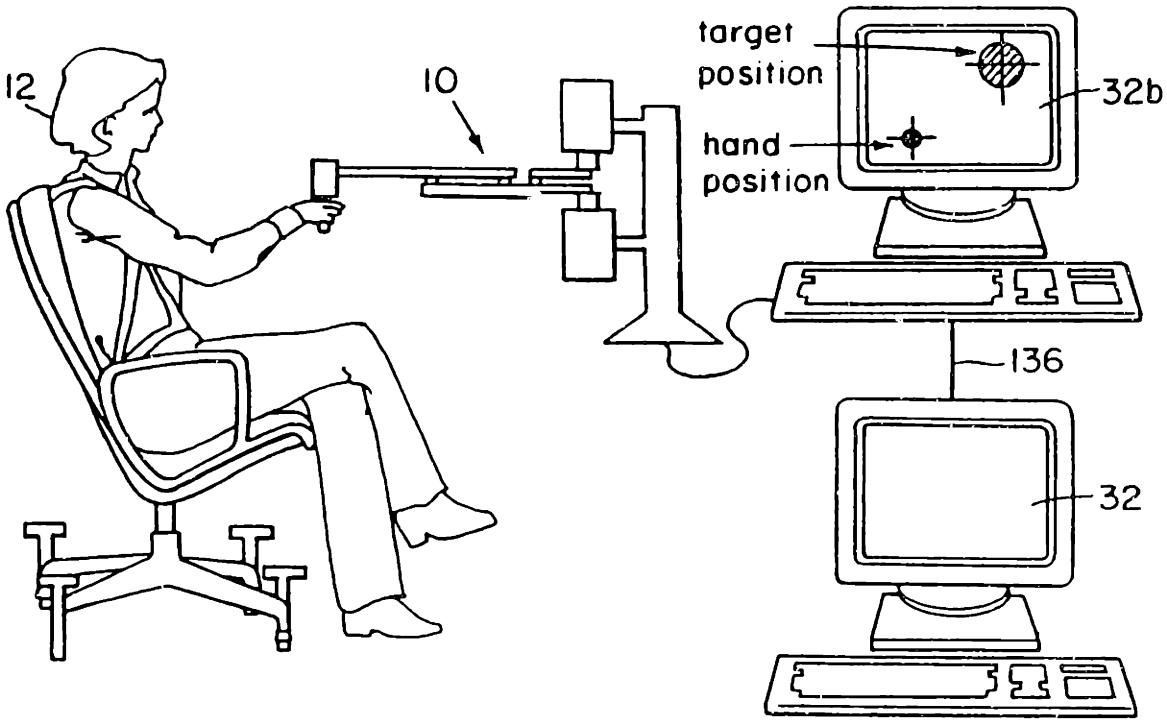

FIG. 12a

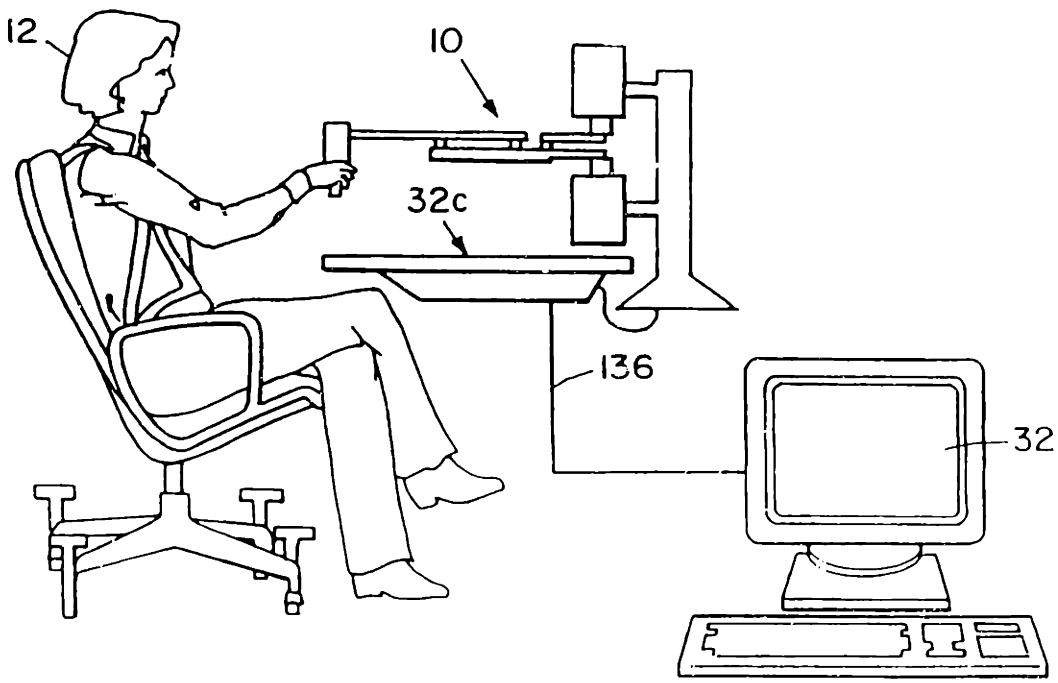

FIG. 12b

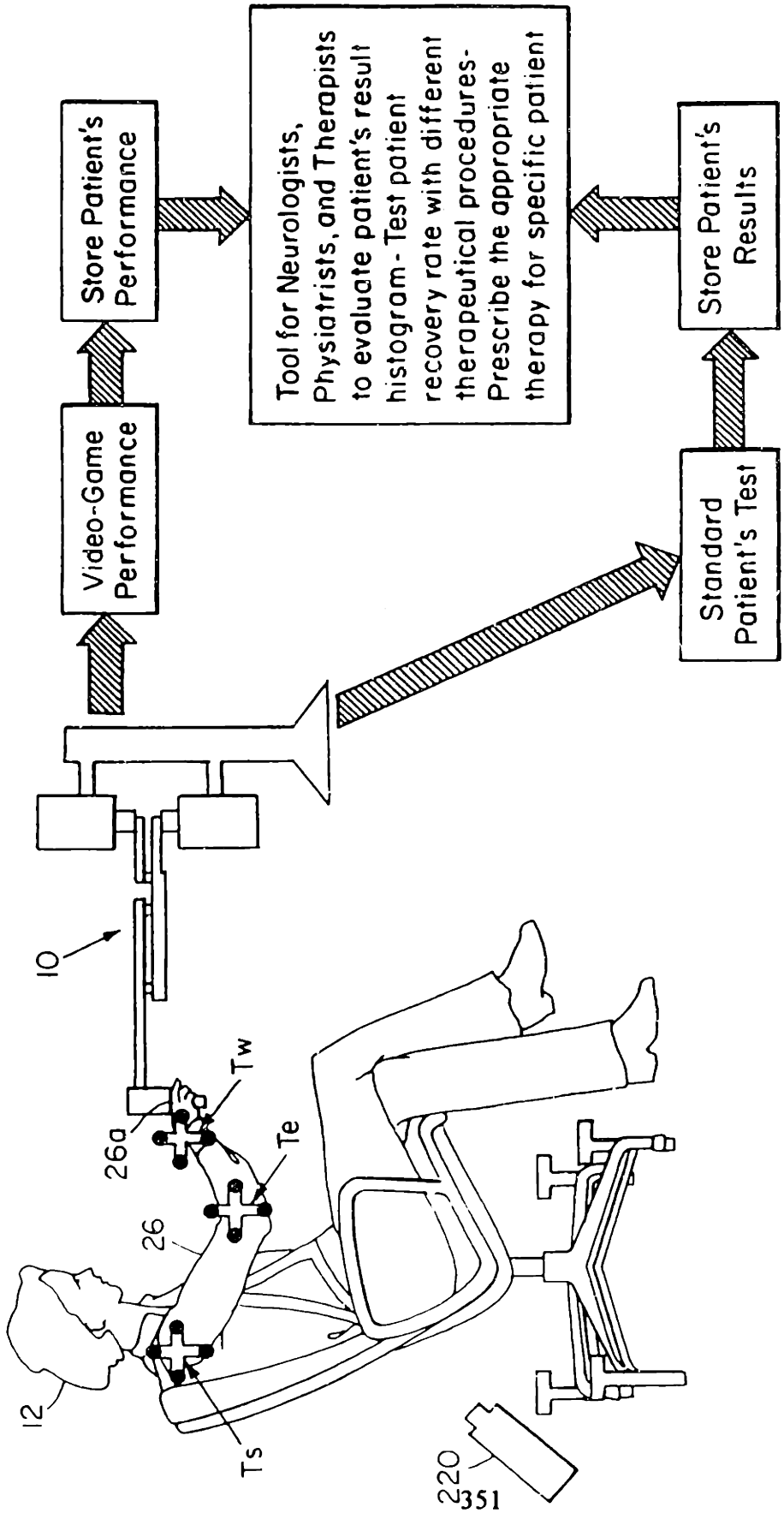
Store Patient's Performance
Video-Game Performance
Tool for Neurologists, Physiatrists, and Therapists to evaluate patient's result histogram - Test patient recovery rate with different therapeutical procedures - Prescribe the appropriate therapy for specific patient
Store Patient's Results
Standard Patient's Test
10
12
26
26a
Tw
Te
Ts
220
351

FIG. 13

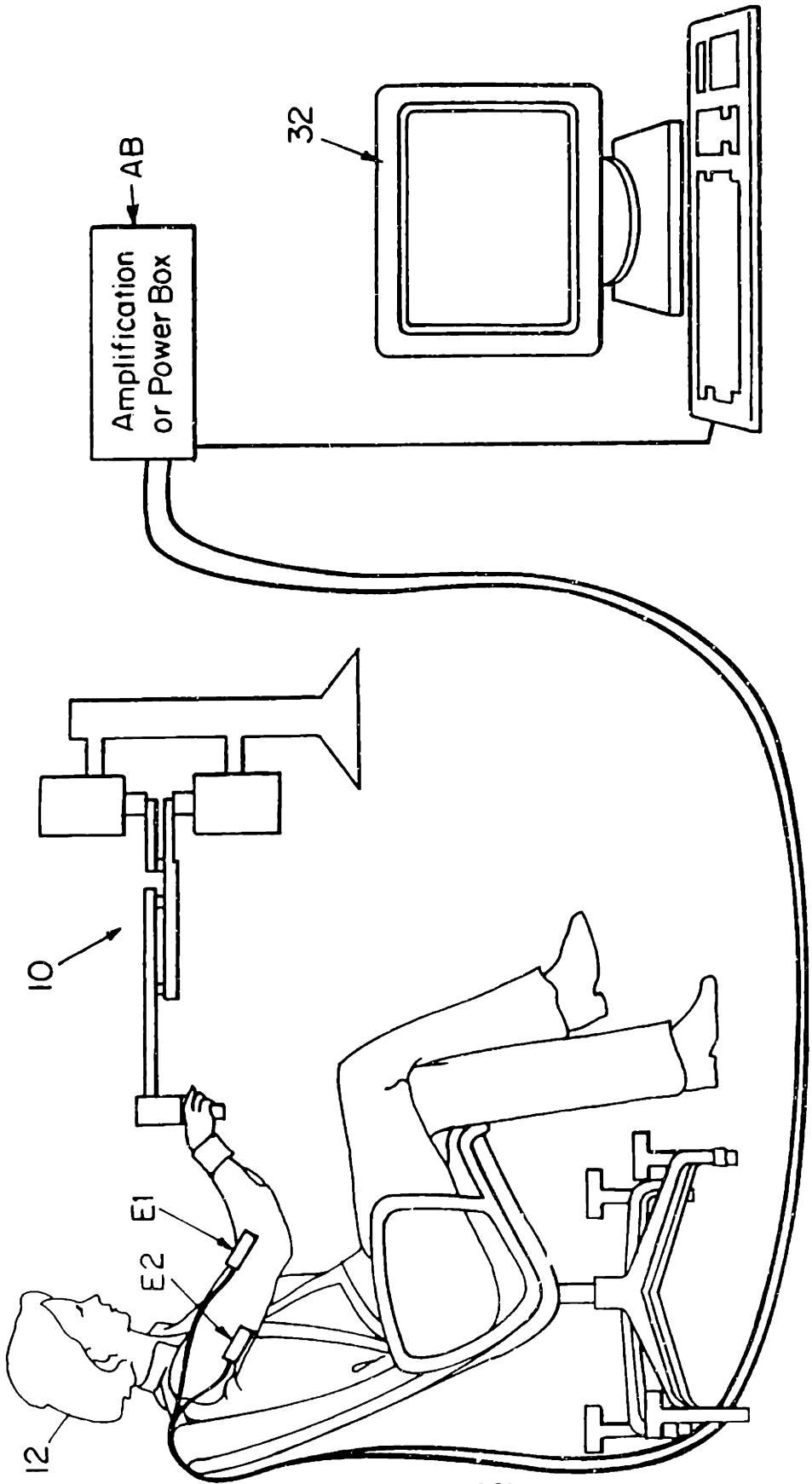

FIG. 14

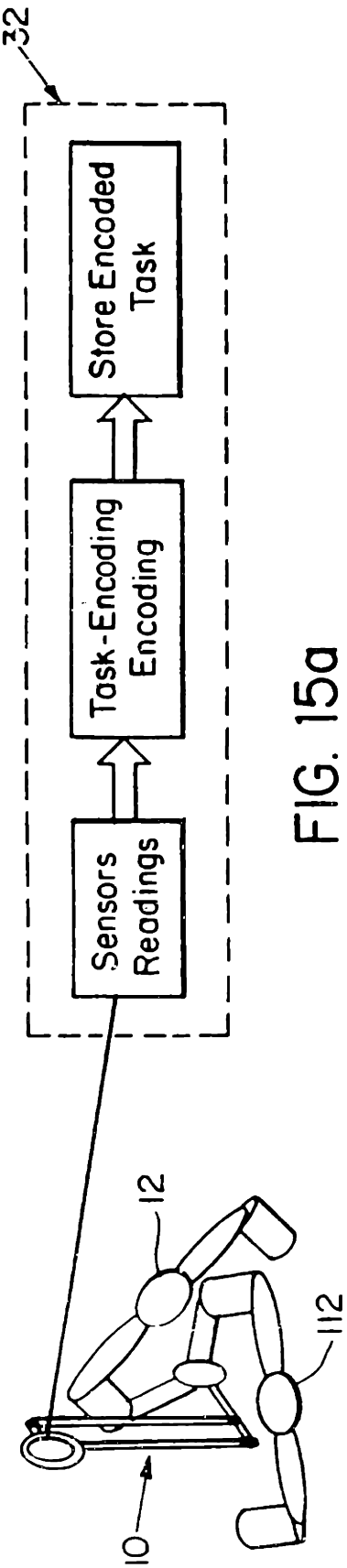

FIG. 15a

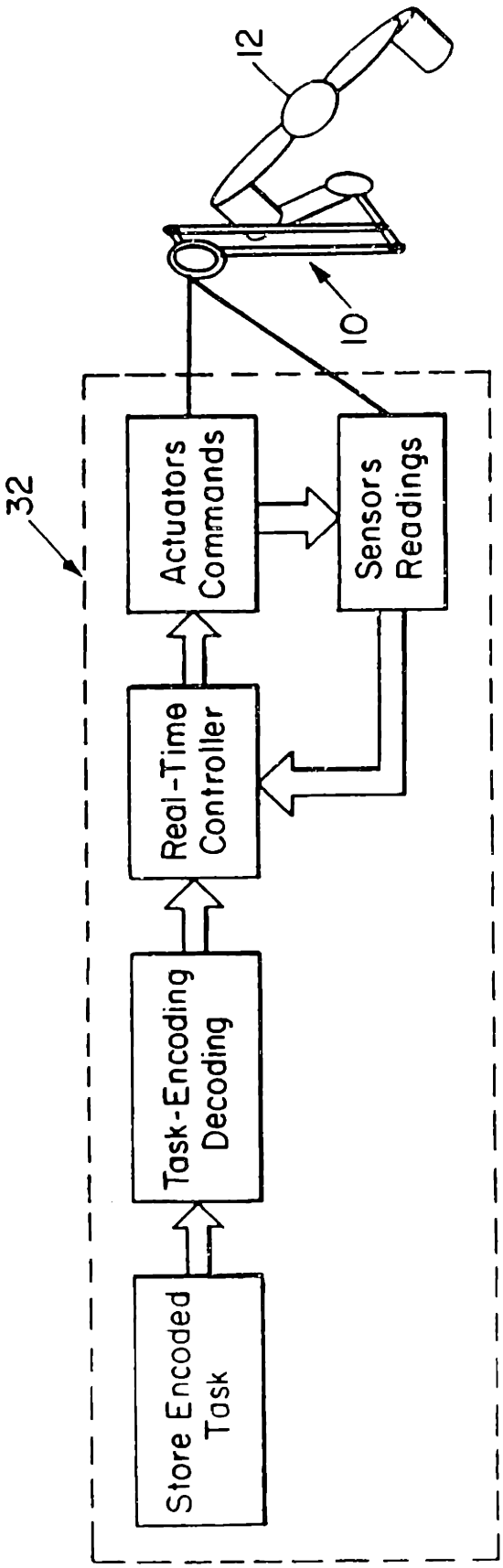

FIG. 15b

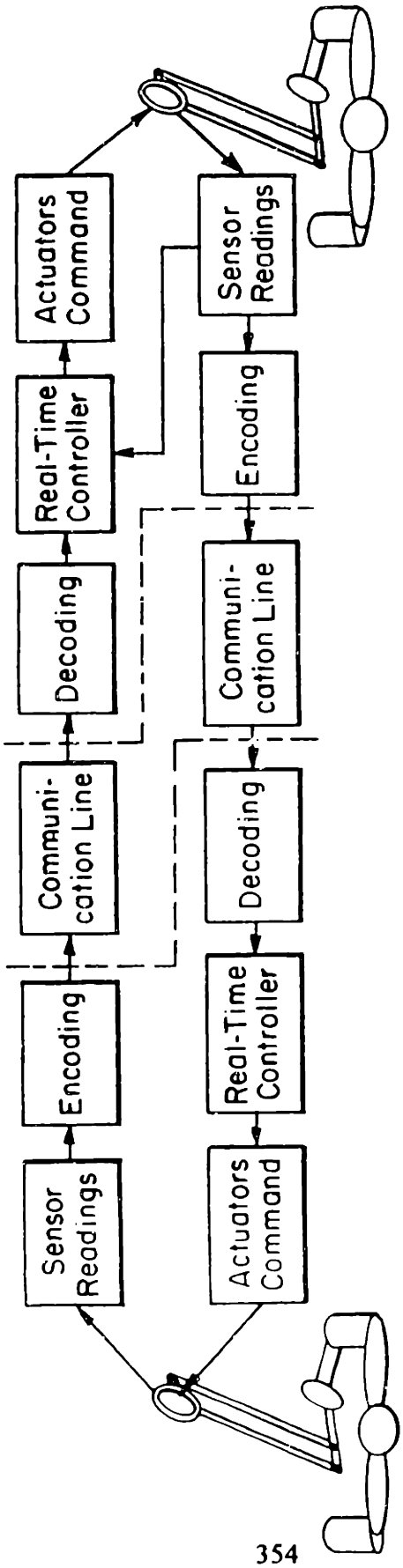
Sensor Readings
Encoding
Communi-cation Line
Decoding
Real-Time Controller
Actuators Command
Actuators Command
Real-Time Controller
Decoding
Communi-cation Line
Encoding
Sensor Readings

FIG. 16

INTERACTIVE ROBOTIC THERAPIST

This invention was made with government support under Grant Number 8914032-BCS awarded by the National Science Foundation. The government has certain rights in the invention.

RELATED APPLICATION

This application is a Continuation-in-Part of U.S. patent application Ser. No. 08/087,666 filed on Jul. 6, 1993 now abandoned.

BACKGROUND OF THE INVENTION

When a patient undergoes massive trauma such as a stroke, head injury, or spinal cord injury, the patient's motor skills in multiple muscle groups are impaired and the patient loses the full range of motion in the limbs. The patient must undergo physical and occupational therapy (from now on referred as therapy) in order to rehabilitate the impaired motor skills. Current therapy machines having one degree of freedom for rehabilitating single muscle groups are limited in the rehabilitation process because the range of motions needed for rehabilitation require the rehabilitation of multiple muscle groups (Functional Rehabilitation). The therapist must interact one-on-one with the patient and lead the patient through exercises having full range of motion.

SUMMARY OF THE INVENTION

The problem with employing a therapist to work one-on-one with a patient is that the therapist can only work with one patient at a time and must physically lead the patient through the exercises. Additionally, during a session, the therapist must be physically present at all times when the patient requires therapy. Furthermore, a patient's progress is very difficult to determine and quantify. Accordingly, there is a need for a therapy apparatus which allows a therapist to rehabilitate multiple patients at once, train therapists, permit remote sessions or autonomous recapitulation of a session, does not require the therapist's attention at all times during therapy, and quantifies the patient's performance and progress, permitting the session to be tailored to the patient's needs using the therapeutical procedure that maximizes the rate of recovery.

The present invention provides an interactive robotic therapist and method including a moveable member for interacting with a patient to shape the patient's motor skills. The moveable member is capable of guiding a patient's limb through a series of desired exercises. The moveable member is driven by a drive system which is coupled to the moveable member. The power output of the drive system is controlled so that the patient can alter the path of the series of exercises guided by the moveable member. The drive system is controlled by a controller which provides the commands to direct the moveable member through the series of desired exercises.

In preferred embodiments, the moveable member is a robotic arm which has a series of moveable joints. The patient's arm is secured to the robotic arm. The drive system comprises at least one drive motor coupled to at least one joint in the robotic arm. The robotic arm is capable of guiding the person's arm through more than one degree of freedom. The desired series of exercises are predetermined and are entered and stored into the memory of the controller by guiding the robotic arm through a series of motions. The exercises can then be replayed to interact with a patient.

The present invention provides an interactive robotic therapist and method which allows a therapist to rehabilitate multiple patients at one time and does not require the physical presence or continuous attention of the therapist. Additionally, the therapist can provide a patient with therapy by controlling the robotic therapist with a remotely located robotic therapist.

The present invention provides an interactive robotic therapist and method which allows a simultaneous diagnosis or training of therapists through the interaction with a patient.

The present invention provides an interactive robotic therapist and method which allows the quantification of the patient recovery and progress. This is a fundamental tool to evaluate different therapeutical procedures and tailor the therapy to the patient needs.

BRIEF DESCRIPTION OF THE DRAWINGS

The foregoing and other objects, features and advantages of the invention will be apparent from the following more particular description of the drawings of the preferred embodiments. Reference characters refer to the same parts throughout the different drawings. The drawings are not necessarily to scale, emphasis instead being placed on illustrating the principles of the invention.

FIG. 1 is a schematic drawing of a patient interacting with the present invention interactive robotic therapist.

FIG. 2 is a flow chart for a preferred control system for the present invention.

FIGS. 3*a*–3*c* are preferred embodiments of the robotic arm for planar motion version (two dimensions -2D) or spatial motion version (three dimensions - 3D).

FIGS. 4*a*–4*f* show a patient's hand secured to an end-effector in various positions as seen from the side, front and top, as well as different possible attachment locations for the end-effector.

FIGS. 5*a* and 5*b* are schematic drawings of a first interactive robotic therapist controlled by a second interactive robotic therapist.

FIG. 6 is a schematic drawing of a classroom of therapy patients interacting with individual interactive robotic therapists which are controlled by a single interactive robotic therapist.

FIG. 7 is a schematic drawing of a classroom of therapists interacting with individual interactive robotic therapists and interacting with a single interactive robotic therapist attached to a patient.

FIGS. 8*a* and 8*b* are side views of a patient using his/her intact limb to teach the interactive robotic therapist an exercise, which is mirrored by the device and played back to the impaired limb of the patient.

FIGS. 9*a*–9*c* are schematic drawings of different modes of therapy for the therapy.

FIGS. 10*a*–10*c* are schematic drawings of the procedure for asynchronous diagnosis of patients.

FIGS. 11*a*–11*d* show different educational video-games to motivate and register patient performance during the exercise. FIGS. 11*a*–11*d* show the implemented concepts for range of motion, force, direction and dexterity exercises.

FIGS. 12*a* and 12*b* are side views showing different options for the video game screen position such as a standard vertical monitor or a horizontal monitor to facilitate the patient's visualization of the exercise and his/her hand.

FIG. 13 is a schematic drawing showing the interactive robotic therapist as a quantification and measuring device.

FIG. 14 is a schematic drawing showing the interactive robotic therapist as a quantification and measuring device with the additional Electromyographic implementation feature and with a Functional Electric Stimulation Implementation feature.

FIGS. 15*a* and 15*b* are schematic drawings showing the modules used during the teaching (intimate mode) and playback phases (autonomous and monitored modes).

FIG. 16 is a schematic drawing showing the modules used in telerobotic implementation.

DETAILED DESCRIPTION OF THE PREFERRED EMBODIMENTS

In FIG. 1, interactive robotic therapist 10 2D-version has a robotic arm 14 which is controlled by direct drive motors M1, M2 and M3. Robotic arm 14 is secured to a column 28 by bracket 30. Column 28 provides robotic arm 14 with vertical adjustment. Bracket 30 is secured to motor M1, which controls motion of shoulder joint 20L. Robotic arm 14 comprises an arm member 16, which is connected to the forearm member 18 by elbow joint 22, which in turn is connected to an end-effector 24. Bracket 30 is also secured to motor M2, which controls motion of the joint 20U. Joint 20U is connected to member 76, which is connected to member 70 by joint 74. Member 70 is connected to the forearm member 18 by the elbow actuation joint 72. Shoulder joint 20L and elbow joint 22 provide robotic arm 14 with motion having two degrees of freedom.

Motor M2 controls movement at elbow actuation joint 72, and is secured to bracket 30 along the same vertical axis as motor M1 in order to reduce inertia effects on the movement of robotic arm 14. Alternatively, motor M2 can be located at elbow joint 22 or other suitable locations. The forearm 26 and hand 26*a* of patient 12 is secured to end-effector 24. End-effector 24 has three degrees of freedom and can exercise the full range of motion of the wrist of patient 12. End-effector 24 is driven by motor M3 which is mounted to end-effector 24.

Motors M1, M2 and M3 are preferably direct drive high torque DC motors, which are not connected to gear reducers but alternatively can be other suitable types of motors including motors connected to gear reducers or cables. Additionally, velocity, position and force sensors are located within joints 20U and 20L, as well as within end-effector 24 for providing feedback to controller 32. Controller 32 controls the motion of robotic therapist 10 and is connected to motors M1, M2 and M3 by electrical cable 34.

Presently, the position, velocity and force of the translational degrees of freedom of robotic arm 14, as well as the end-effector are measured by standard off-the-shelf components. The controller 32 is a personal computer which for example can be a 80486 CPU having standard 16 bit A/D and D/A cards, as well as a 32 bit DIO board.

Typically, in operation, the patient is first secured to robotic therapist 10. The human therapist then teaches the robotic therapist a series of motions by moving the robotic arm 14 and end-effector 24 through simple exercises such as stretching the arm and rotating the wrist. Robotic therapist 10 records the desired movements and stores them in memory within controller 32. Robotic therapist 10 can then replay the recorded motions while guiding patient 12 with varying degrees of firmness during which the human therapist may or may not choose to be present. The varying firmness can be programmed into and controlled by controller 32 and patient 12 can override or alter the programmed path of robotic arm 14 by exerting his or her strength on robotic arm 14. To promote learning, as motor skills are acquired, firmness may be progressively reduced, thereby reducing the degree of guidance and assistance provided to the patient. As the patient 12 regains lost motor skills, the dependence on the robotic interactive therapist 10 becomes reduced. Controller 32 can keep a record of a patient's performance at each session so that the patient's progress can be followed.

Referring to FIG. 2, the control system for robotic therapist 10 is composed of a sequence of layers. The control system is organized in a hierarchy with each layer interacting with the immediately adjacent layer. The highest layer corresponds to the designated high level controller 50 followed by a layer designated as task encoding or translator 52. The lower layer designated as low level controller 54 interacts with the hardware 56. A layer on the same level of the hardware corresponds to the work object 60 and both the hardware layer and the work object layer are deposited on the external environment layer 58. The arrows show the flow of information and energetic interaction.

Referring to FIG. 3*a*, one preferred embodiment of robotic arm 14 is a parallelogram linkage including arm member 16 which is connected to forearm member 18 by joint 22. Joint 20U is connected to arm member 76 which connects to forearm member 18 via joint 74, connecting member 70 and elbow actuation joint 72. Movement of arm member 16 is controlled by motor M1 and the movement of elbow actuation joint 72 is controlled by motor M2 via arm member 76, joint 74 and connecting member 70. End-effector 24 is secured to robotic arm 14 at end 18*a* of forearm member 18.

Referring to FIGS. 3*b* and 3*c*, the preferred embodiment of the robotic arm 14 of FIG. 3*a* has a modular concept. It can be assembled for 2D horizontal movement, in which case the arm 14 is assembled in the horizontal plane and the base 29 is fixed with respect to column 28 and bracket 30. It can also be assembled for 3D movement, in which case the arm 14 is assembled in the vertical plane and the base is a controlled rotational base with the motor M0.

Referring to FIG. 4*a*, the forearm 26 of patient 12 is secured to end-effector 24 by splint holder 88 and splint 88*a*. Splint 88*a* is made of plastic, carbon fiber (or Kevlar™) and foam. The user can remove his or her forearm 26 by pulling the splint holder out of the connector 90. Alternatively, patient 12 can pull his forearm 26 free from the splint holder 88 by unscrewing the butterfly of splint 88*a*. A wrist flexion/extension mechanism 80 is connected to hand 26*a*. Pad 80*a* rests upon the top of hand 26 and is connected to motor M3 via joint 82, member 85, joint 84 and member 86. The wrist flexion/extension mechanism 80 is capable of moving a patient's hand 26*a* in flexion and extension postures as shown by the arrows A.

Referring to FIG. 4*b*, hand 26*a* is capable of being moved in pronation/supination postures as indicated by the arrows B. Motor M3 has a built in potentiometer and tachometer and drives an eccentric crank 108. Crank 108 is connected to a four bar mechanism comprising vertical rods 92 and 94, horizontal beam 98 and splint holder 88. Splint holder 88, rod 92, rod 94 and beam 98 are moveably connected by joints 90, 96 and 100.

Referring to FIG. 4*c*, end-effector 24 is capable of moving the wrist in abduction and adduction postures as indicated by the arrows C. Member 86 is driven by motor M3 which

moves hand 26*a* in the direction of the arrows.

Motor M3 is composed of a set of multiple motors or actuators capable of moving the wrist in 3 degrees of freedom. Additionally, end-effector 24 can be of other suitable configurations which can provide 3 degrees of freedom at the wrist.

Referring to FIGS. 4*d*, 4*e* and 4*f*, end-effector 24 was built according to a modular concept. It can be assembled in the 2D version, in the 3D version and in the stand-alone version.

Referring to FIGS. 5*a* and 5*b*, the robotic therapist 10 to which patient 12 is secured, can be controlled by a human physical therapist 112 who is interacting with robotic therapist 110. Robotic therapist 110 is connected to computer 132 by line 134 and computer 132 is connected to computer 32 by line 136 which can be a phone line or other communication medium. As a result, therapist 112 can remotely guide the patient 12.

Robotic therapists 10 and 110 can optionally include cameras and sound systems 200 so that patient 12 and therapist 112 can see and talk to each other. Additionally, robotic therapist can include a range system 220 for shutting down robotic therapist 10 if a portion of the body of patient 12 other than forearm 26 crosses plane 210, thereby providing a safety feature. The same system 220 can be also used as a measuring device providing space position information of the patient's arm. Referring to FIG. 6, a single human therapist 112 operating a robotic therapist 110 can teach a classroom of patients 12 by connecting multiple computers 32 to computer 132 via lines 136.

Referring to FIG. 7, several human therapists 112 operating robotic therapists 110 can be trained simultaneously by a human therapist instructor 112 interacting with a patient 12 connected to the robotic therapist 10 by connecting multiple computers 132 to computer 32 via lines 136.

Referring to FIGS. 8*a* and 8*b*, a patient 12 can exercise alone with the interactive robotic therapist 10 by teaching the robotic therapist 10 an exercise with his/her intact limb 27. The robotic therapist 10 creates a mirror exercise for the patient's impaired limb 26 and plays it back to the patient 12.

Referring to FIGS. 9*a*, 9*b* and 9*c*, the standard teach and playback procedure (intimate, monitored and autonomous modes) is illustrated. In the intimate mode the human therapist 112 teaches an exercise to the patient 12 with the robotic therapist 10 attached. The robotic therapist 10 plays back the exercise to the patient 12 with the therapist 112 still physically connected but not interfering (monitored mode). The robotic therapist 10 plays back the exercise with the therapist 112 only overseeing (autonomous).

Referring to FIGS. 10*a*, 10*b* and 10*c*, the robotic therapist 10 can be used for asyncronous diagnosis and evaluation of the patient 12. In the teach mode, the human therapist 112 preprograms an exercise for robotic therapist 10. In the autonomous mode, the robotic therapist 10 plays the exercise back and registers the patient 12 reaction. In the diagnosis mode, the robotic therapist 10 plays the patient reaction to the therapist 112. The therapist 112 can diagnose or evaluate the patient 12 performance.

Referring to FIG. 11*a*, several educational video-games can be used for the patient 12. The games have several purposes: motivation for continuing exercising, cognitive exercise, and recording patient performance during exercise. Several educational video-games were developed for range of motion, force, direction and dexterity control. The patient performance can be stored and evaluated.

One example of a game for developing the range of motion of a patient is depicted in FIG. 11*a*. Icon 300, representing the position of the hand 26*a* of patient 12, is positioned on screen 32*a*. Two targets 302 and 304, respecively, are located at positions away from icon 300. By moving hand 26*a* and attached robotic arm 14, patient 12 can move icon 300 over targets 302 and 304 (or be moved). The range of motion of patient 12 can be increased by locating more targets on screen 32*a*, by changing the target size, or by spacing the targets further apart.

FIG. 11*b* depicts one example of a game for developing force control. Patient 12 maneuvers icon 300 along a path 306 by moving robotic arm 14, while robotic arm 14 applies a variable force against hand 26*a* in the direction of the arrow.

FIG. 11*c* depicts one example of a game for developing direction control. A target 308 is located in a predetermined direction away from icon 300. Patient 12 must maneuver icon 300 with robotic arm 14 in the direction of target 308 and place icon 300 over target 308. Target 308 can be located anywhere on circle 310 to develop directional control in all directions.

FIG. 11*d* depicts one example of a game for developing dexterity. Icon 312 designates the location of the hand 26*a* of patient 12. Icon 312 has a shape which allows the rotational orientation of icon 312 to be seen. A target 314 having a shape indicating rotational orientation is positioned away from icon 312. In order for icon 312 to be placed over target 314, icon 312 must be moved and rotated by patient 12, so that icon 312 is placed over target 314 in the same rotational orientation as target 314.

Although several video games have been described for developing the range of motion, force, direction and dexterity control of patient 12, there are countless possibilities for video games. The patient's performance in the games can be quantified and stored for patient's evaluation.

Referring to FIGS. 12*a* and 12*b*, the interactive robotic therapist 10 can have only one computer screen or monitor. However, the preferred embodiment has two separate monitors. One for the robot control system 32 and one for the educational video-game 32*b* or 32*c*. The video-game monitor can be the standard 14" computer screen 32*b*, or it can be a 21" screen 32*c* mounted horizontally just below the patient workspace to facilitate and permit the patient at look simultaneously to his/her arm and video-game screen.

Referring to FIG. 13, the interactive robot therapist 10 can be used as a measuring device for therapy quantification. It provides position, velocity, force information at the patient's hand 26*a*. It can also provide the patient's arm position information through the off-the-shelf range system 220 and targets, which are located at the shoulder (Ts), elbow (Te), and wrist (Tw). It can register the patient 12 performance and permit the evaluation of different therapy procedures.

Referring to FIG. 14, the interactive robotic therapist 10 can also incorporate off-the-shelf electromyographic system for measuring muscle contraction, or off-the-shelf functional eletrical stimulation system to stimulate specific muscles. Both systems are illustrated by the electrodes E1, E2 and amplification or power source AB.

Referring to FIGS. 15*a* and 15*b*, the system flow chart is shown for the intimate and autonomous/monitored modes of FIGS. 9*a*–9*c*. In the intimate mode the sensor readings are encoded through a set of human-like motion primitives and stored. In the autonomous or monitored modes, the stored information is decoded and the desired motion characteristic is reconstructed. This desired motion characteristic is target motion that the real-time controller tries to achieve by

sending commands to the actuators and using the sensors feedback to calculate the new set of commands.

Referring to FIG. 16, the system flow chart is shown for the telerobotic implementation. The sensor readings are used in two forms: to provide feedback for the local real-time controller and to encode the motion into human-like primitives, sent through a transmission line. At the other side of the transmission line, the message is decoded and the desired motion characteristic is used by the real-time controller to send commands to the actuators, and using the sensors feedback to calculate the new set of commands.

The interactive robotic therapist tries to mimic the human therapist. The controller schemes illustrated in the previous figures incorporate psycho-physical experimental results and hypothesis on primate motor control (humans and monkeys). This prior knowledge of human motor control is incorporated in different forms into the robotic therapist. The preferred controller of FIG. 2 incorporates the concept that motor behavior is hierarchically organized in the sequence of layers: volitional or object domain, kinematic domain (mapping of the task), and torque/force domain. The human-like motion primitives mentioned in the encoding scheme of FIGS. 15a through 16 incorporates the concept of encoding movement via a virtual trajectory. The virtual trajectory for unconstrained motions minimizes jerk, and the arm trajectory modification scheme incorporates the concept of virtual trajectory superposition. The resulting virtual trajectory and impedance estimates are then coded in a sequence of minimum jerk type components (or similar basis function, such as Gaussian or Wavelet functions). The concept of "stroke" will be used to aggregate these components. Stroke can be loosely defined as an action unit. A stroke will be represented by an episodic burst of information, whenever a new action is required.

Equivalents

While this invention has been particularly shown and described with references to preferred embodiments thereof, it will be understood by those skilled in the art that various changes and form and details may be made therein without departing from the spirit and scope of the invention as defined by the dependent claims. For example, various types of motors and actuators can be substituted for motors M0, M1, M2 and M3. Additionally, motors M0, M1, M2 and M3 can be positioned at other suitable locations and robotic arm 14 can be of various configurations. Furthermore, robotic therapist 10 can be employed to rehabilitate other parts of a patient's body such as the legs. Also, end-effector 24 does not have to provide three degrees of freedom at the wrist, but can be of other suitable configurations such as a handle which the patient grips.

What is claimed is:

1. An interactive robotic therapist system comprising at least one interactive robotic therapist including:

a robotic moveable member for interacting with a patient to shape the patient's motor skills, the moveable member including an end-effector with a limb coupler for securing a patient's limb to the moveable member at the end-effector, the moveable member being capable of guiding the patient's limb along a desired path through a series of desired exercises;

a drive system coupled to the moveable member for driving the moveable member, the drive system being configured such that force exerted by the patient's limb on the moveable member is capable of altering the desired path of the moveable member while the moveable member is guiding the patient's limb through the exercises without changing the series of the desired exercises wherein the patient can be safely connected with the moveable member since the patient can temporarily alter the desired path of the moveable member; and

a controller coupled to the drive system for providing the drive system with commands to direct the moveable member through the series of desired exercises.

2. The robotic therapist of claim 1 in which the moveable member is a robotic arm having a series of moveable joints.

3. The robotic therapist of claim 1 in which the controller has programming means for programming the series of exercises are.

4. The robotic therapist of claim 2 in which the drive system comprises at least one drive motor coupled to at least one joint in the robotic arm.

5. The robotic therapist of claim 1 in which the controller has memory means for storing the desired series of exercises.

6. The robotic therapist of claim 2 in which the robotic arm has more than one degree of freedom.

7. The robotic therapist of claim 1 in which the robotic therapist is a first robotic therapist and further comprising a second robotic therapist for controlling the movements of the first robotic therapist through command signals communicated over a communication line.

8. The robotic therapist of claim 1 further comprising educational video-games displayed on a monitor and playable by the patient through manipulation of the moveable member.

9. The robotic therapist of claim 1 in which the controller includes means for measuring and quantifying motor skill performance of the patient.

10. The robotic therapist of claim 1 in which only the end-effector has means for securing the patient's limb.

11. A method of shaping a patient's motor skills comprising the steps of providing an interactive robotic therapist system comprising at least one interactive robotic therapist including a robotic moveable member, a drive system coupled to the moveable member and a controller coupled to the drive system;

guiding a patient's limb along a desired path through a series of exercises with the moveable member secured to the patient's limb, the moveable member being driven by the drive system coupled to the moveable member;

controlling the drive system with a controller, a controller providing commands to direct the moveable member through the desired series of exercises; and

altering the desired path of moveable member while the moveable member is guiding the patient's limb through the exercises by exerting force on the moveable member with the patient's limb without changing the series of the desired exercises wherein the patient can be safely connected with the moveable member since the patient can temporarily alter the desired path of the moveable member.

12. The method of claim 11 further comprising the steps of:

teaching a series of exercises to the interactive therapy apparatus by guiding the moveable member through a series of motions; and

storing the guided series of motions in memory in the controller.

13 The method of claim 11 in which the series of exercises are predetermined.

14. The method of claim 11 in which the patient's limb is an arm.

15. The method of claim 13 in which the patient's arm is guided by the moveable member through a full range of motion.

16. The method of claim 11 further comprising the step of providing educational video games displayed on a monitor and playable by the patient through manipulation of the moveable member.

17. The method of claim 11 further comprising the step of measuring and quantifying motor skill performance of the patient with the controller.

18. The method of claim 11 in which the patient's motor skills are shaped with a first robotic therapist, the method further comprising the step of controlling the movements of the first robotic therapist with a second robotic therapist through command signals communicated over a communication line.

19. The method of claim 11 further comprising the step of providing the moveable member with more than one degree of freedom.

20. The method of claim 11 further comprising the step of coupling at least one drive motor to at least one joint in the moveable member to form the drive system.

* * * * *

APPENDIX D: ROBOT-AIDED FUNCTIONAL IMAGING: TABLES OF SIGNIFICANT ACTIVATION

Coordinates relative to AC-PC Line (in mm) X	Y	Z	Significance of Result z-Score (z > 3.0)	Right Hemisphere Region of Activation	Left Hemisphere Region of Activation
14.66	5.99	-8	3.78	Ventral Striatum	
-23.59	-27.16	-4	3.71		Hippocampal Formation
35.06	28.94	12	3.20	Insula	
49.09	-23.34	16	3.36	PostCentral Gyrus(area 40)	
47.81	-41.19	16	4.21	Superior Temporal Gyrus (area 22)	
-50.36	-22.06	24	3.15		Supramargianal Gyrus (area 40)
-45.26	-23.34	48	3.00		Postcentral Gyrus (area 1 & 2)
13.39	-48.84	60	4.06	Precuneus (area 7)	

Table Activation.1.a. Early Motor Learning Minus Motor Performance Pet Activation (batches 3 & 4 minus batches 1 & 2)

Coordinates relative to the AC-PC line (mm) X	Y	Z	Significance of Result z-Score (z > 3.0)	Right Hemisphere Region of Activation	Left Hemisphere Region of Activation
-24.86	44.24	-12	3.99		Superior Frontal Gyrus (area 11)
60.56	-42.46	-8	3.27	Middle Temporal Gyrus (area 21)	
-61.84	-46.29	-8	3.90		Inferior Temporal Gyrus (area 37)
-7.01	-73.06	0	4.13		Lingual Gyrus (area 18)
-49.09	-37.36	4	3.25		Middle Temporal Gyrus (area 22)
-18.49	62.09	8	4.00		Superior Frontal Gyrus (area 10)
-7.01	-37.36	24	3.24		Posterior Cingulate (area 23)
-31.24	50.61	24	4.12		Middle Frontal Gyrus (area 10)
0.64	-27.16	28	3.39	Posterior Cingulate (area 23)	
-10.84	-53.94	28	3.25		Posterior Cingulate (area 31)
-18.49	37.86	32	3.25		Superior Frontal Gyrus (area 9)
38.89	-64.14	32	3.04	Angular Gyrus (area 39)	
-36.06	-65.41	36	4.11		Angular Gyrus (area 39)
8.29	-34.81	36	3.04	Posterior Cingulate (area 31)	
-18.49	7.26	56	3.44		Superior Frontal Gyrus (area 6)

Table Activation.1.b. Motor Performance Minus Early Motor Learning Pet Activation (batches 1 & 2 minus batches 3 & 4)

Coordinates relative to the AC-PC line (mm) X	Y	Z	Significance of Result z-Score (z > 3.0)	Right Hemisphere Region of Activation	Left Hemisphere Region of Activation
-21.04	-18.24	-8	3.37		Hippocampal Formation
4.46	-61.59	-4	3.03	Cerebellum	
1.91	-81.99	-4	3.96	Lingual Gyrus (area 18)	
-31.24	42.96	0	3.19		Mid.FrontalGyrus(area10)
-23.59	-61.59	4	3.26		Lingual Gyrus (area 18)
1.91	-71.79	12	4.11	Cuneus (area 17)	
60.56	-22.06	16	3.01	PostCentral Gyrus(area40)	
29.96	-84.54	20	3.50	Middle Occipital Gyrus (area 19)	
-49.09	-13.14	40	3.76		PreCentral/PostCentral Gyrus (area 3/4)
-41.44	-22.06	48	4.93		PostCentral Gyrus (area 1/2/3)
-35.06	8.54	48	4.04		Mid. Frontal Gyrus (area 6)
-36.34	-33.54	52	3.73		Inferior Parietal Lobule (area 40)
-8.29	-24.61	52	3.36		ParaCentral Lobule (area5)
-4.46	-47.56	60	3.90		Precuneus (area 7)
-23.59	-22.06	60	4.20		PreCentral Gyrus (area 4)

Table Activation.2.a.. Late Motor Learning Minus Motor Performance Pet Activation (batches 5 & 6 minus batches 1 & 2)

Coordinates relative to the AC-PC line (mm) X	Y	Z	Significance of Result z-Score (z > 3.0)	Right Hemisphere Region of Activation	Left Hemisphere Region of Activation
28.69	35.31	-12	3.36	Middle Frontal Gyrus (area 47/11)	
-21.04	42.96	-8	3.04		Medial Frontal Gyrus (area 32/10)
47.81	-50.11	-8	3.24	Middle Temporal Gyrus (area 37)	
42.71	-69.24	-4	5.29	Middle Occipital Gyrus (area 19)	
42.71	13.64	0	3.16	Insula	
51.64	-55.21	0	3.72	Middle Temporal Gyrus (area 37)	
43.99	-70.51	0	3.36	Inferior Temporal Gyrus (area 19)	
37.61	4.71	4	3.51	Insula	
-36.34	5.99	4	3.13		Insula
-32.51	58.26	8	3.15		Middle FrontalGyrus(area10)
45.26	12.36	8	3.03	PreCentralGyrus(area 44)	
52.91	-47.56	8	3.85	Middle Temporal Gyrus (area 21)	
37.61	-69.24	8	4.25	Middle Occipital Gyrus (area 19/39)	
51.64	-39.91	12	3.74	Superior Temporal Gyrus (area 22)	
42.71	-64.14	12	3.87	Middle Temporal (area 39/19)	
54.19	-53.94	20	4.62	Superior Temporal Gyrus (area 39/22)	
50.36	-55.21	24	3.51	Inferior Parietal Lobule (area 39/40)	
-22.31	45.51	28	3.22		Superior FrontalGyrus(area9)
-3.19	-43.74	32	3.73		Posterior Cingulate(area31)

Table Activation.2.b. Motor Performance Minus Late Motor Learning Pet Activation (batches 1 & 2 minus batches 5 & 6)

Coordinates relative to the AC-PC line (mm) X	Y	Z	Significance of Result z-Score (z > 3.0)	Right Hemisphere Region of Activation	Left Hemisphere Region of Activation
17.21	51.89	-8	3.02	Superior Frontal Gyrus (area 10)	
7.01	-52.66	-8	3.05	Cerebellum	
-15.94	-19.51	-4	3.18		Pyramidal Pathway - Midbrain
-15.94	-46.29	0	3.07		Lingual Gyrus (area 19)
1.91	-2.94	0	3.20	Hippocampal Formation	
4.46	-4.21	4	3.39	Thalamus	
-15.94	-28.44	4	3.25		Thalamus
17.21	-33.54	8	3.36	Thalamus	
-13.39	-33.54	8	3.37		Thalamus
-41.4	-25.89	44	3.25		PostCentralGyrus (area 2 / 40)
-41.44	5.99	44	3.44		Middle Frontal Gyrus (area 6)
-4.46	-39.91	48	3.17		ParaCentral Lobulus (area 5)
-41.44	-28.44	48	3.96		PostCentral Gyrus(area 40)
31.24	-20.79	52	3.19	ParaCentral (area 4)	
21.04	-43.74	52	3.15	Precunneus (area 7)	
-4.46	-29.71	52	3.33		ParaCentral Lobulus (area 5)
-40.16	-30.99	52	3.70		PostCentral Gyrus(area 40)
26.14	-27.16	56	3.24	ParaCentral Gyrus(area 4)	
-1.91	-29.71	56	3.21		Paracentral Lobulus(area 7)
-19.76	-43.74	56	3.34	Precunneus (area 7)	
12.11	-39.91	60	3.78	Paracentral Lobulus (area 5 / 7)	

Table Activation.3.a. Negative Transfer Minus Motor Performance Pet Activation (batches 7 & 8 minus batches 1 & 2)

Coordinates relative to the AC-PC line (mm) X	Y	Z	Significance of Result z-Score (z > 3.0)	Right Hemisphere Region of Activation	Left Hemisphere Region of Activation
-28.69	39.14	-8	3.34		Middle Frontal Gyrus (area 10/47)
-52.91	-25.89	-8	3.29		Middle Temporal Gyrus (area 21)
-60.56	-43.74	-8	3.33		Middle Temporal Gyrus (area 21 / 37)
58.01	-48.84	-4	4.28	MiddleTemporalGyrus(area21)	
56.74	-48.84	0	3.93	MiddleTemporalGyrus(area21)	
50.36	-67.96	0	4.15	Inferior Temporal (area 19/37)	
-50.36	-75.61	4	3.34		Middle Occipital Gyrus (area 37/19)
-64.39	-48.84	4	3.41		Middle Temporal Gyrus (area 21)
-32.51	-1.66	4	3.20		Putamen
0.64	55.71	8	3.27	SuperiorFrontalGyrus(area 10)	
55.46	-52.66	8	4.16	Middle Temporal Gyrus (area 21/37)	
-50.36	-52.66	8	3.70		Middle Temporal Gyrus (area 21/37)
-12.11	56.99	12	4.55		Superior Frontal Gyrus (area 10)
47.81	-51.39	12	4.98	Superior Temporal (area 22)	
49.09	-62.86	16	3.54	Middle Temporal (area 39)	
24.86	-85.81	20	3.13	Middle Occipital Gyrus (area 18/19)	
14.66	-84.54	24	3.46	Cunneus (area 18)	
-5.74	-81.99	28	3.45		Cunneus (area 19)
-5.74	-47.56	28	3.11		PosteriorCingulate (area 31)
1.91	-43.74	32	3.47	Posterior Cingulate(area 31)	
1.91	-43.74	36	3.46	Posterior Cingulate (area 31)	
24.86	20.01	52	3.01	SuperiorFrontalGyrus(area 8)	

Table Activation.3.b. Motor Performance Minus Negative Transfer Pet Activation (batches 1 & 2 minus batches 7 & 8)

Coordinates relative to the AC-PC line (mm) X	Y	Z	Significance of Result z-Score (z > 3.0)	Right Hemisphere Region of Activation	Left Hemisphere Region of Activation
5.74	-73.06	-12	2.999*	Cerebellum	
-59.29	-27.16	-12	3.25		Middle Temporal Gyrus (Area 20)
0.64	-83.26	-8	3.54	Lingual Gyrus (area 18)	
-54.19	-41.19	-8	3.79		Middle Temporal Gyrus (area 21)
-3.19	-83.26	-4	3.78		Lingual Gyrus (area 18)
-59.29	-48.84	-4	4.03		Middle/Inferior Temporal Gyrus (area 21)
-64.39	-46.29	0	3.44		Middle Temporal Gyrus
5.74	-65.41	8	3.13	Cunneus (area 31)	
5.74	-74.34	12	3.16	Cunneus (area 17)	
-15.94	-65.41	16	3.05		Cunneus (area 18/31)
35.06	12.36	36	3.92	Middle Frontal Gyrus (area 9)	
-35.06	16.19	40	3.22		Middle Frontal Gyrus(area9/8)
15.94	13.64	48	2.99	Superior Frontal Gyrus (area 8/6)	
-17.21	4.71	52	3.03		Medial Frontal Gyrus (area 6)
-26.14	8.54	56	3.51		Middle Frontal Gyrus (area 6)

* Marginally below the z-Score of 3.0

Table Activation.4.a. Late Motor Learning Minus Early Motor Learning Pet Activation (batches 5 & 6 minus batches 3 & 4)

Coordinates relative to the AC-PC line (mm) X	Y	Z	Significance of Result z-Score (z > 3.0)	Right Hemisphere Region of Activation	Left Hemisphere Region of Activation
12.11	55.71	0	3.53	Cinguli Gyrus (area 32)	
42.71	-47.56	8	3.07	Middle Temporal Gyrus (area 37 /21)	
46.54	20.01	12	3.39	Inferior Temporal Gyrus (area 44/45)	
47.81	-47.56	12	3.58	Superior Temporal Gyrus (area 22)	
43.99	17.46	16	3.13	Inferior Temporal Gyrus (area 44 /45)	
51.64	-30.99	16	3.30	Superior Temporal Gyrus (area 42 /22)	
47.81	-50.11	16	3.42	Superior Temporal Gyrus (area 22)	
50.36	-27.16	20	4.75	PostCentral Gyrus (area 40)	
51.64	-27.16	24	4.64	PostCentral Gyrus (area 40)	
49.09	-27.16	28	3.62	Inferior Parietal Lobule (area 40)	

Table Activation.4.b. Early Motor Learning Minus Late Motor Learning Pet Activation (batches 3 & 4 minus batches 5 & 6)

Coordinates relative to the AC-PC line (mm) X	Y	Z	Significance of Result z-Score (z > 3.0)	Right Hemisphere Region of Activation	Left Hemisphere Region of Activation
52.91	-22.06	-16	3.47	Inferior Temporal Gyrus (area 20)	
-60.56	-43.74	-8	3.13	Middle Temporal Gyrus (area 21)	
1.91	-79.44	-4	3.08	Lingual Gyrus (area 18)	
-12.11	-19.51	-4	4.26		Pyramidal Pathway/ Midbrain
-4.46	-13.14	4	3.50		Thalamus
-31.24	-71.79	28	3.83		Occipital Gyrus (area 19)
-32.51	-69.24	32	4.18		Occipital Superior Gyrus (area 19/39)
-29.96	-65.41	36	3.78		Precuneus (area 19)
-24.86	-61.59	40	3.68		Precuneus (area 19)
1.91	23.84	44	3.10	Medial Frontal Gyrus (area 8)	
-0.64	22.56	48	3.20		Superior Frontal Gyrus (area 8)
-8.29	-32.26	56	3.64		ParaCentral Lobule (area 4 / 7)

Table Activation.5.a. Negative Transfer Minus Early Motor Learning Pet Activation (batches 7 & 8 minus batches 3 & 4)

Coordinates relative to the AC-PC line (mm) X	Y	Z	Significance of Result z-Score (z > 3.0)	Right Hemisphere Region of Activation	Left Hemisphere Region of Activation
17.21	7.26	-4	3.54	Putamen	
59.29	-36.09	0	3.83	Middle Temporal Gyrus(area21)	
54.19	-36.09	4	3.74	Middle Temporal Gyrus(area22)	
49.09	-59.04	4	3.06	Middle Temporal Gyrus(area37)	
54.19	-37.36	8	3.98	Superior Temporal Gyrus (area22)	
49.09	-51.39	8	3.50	Middle Temporal Gyrus (area21/37)	
49.09	-38.64	12	5.30	Superior Temporal Gyrus (area22)	
51.64	-56.49	12	3.99	Middle Temporal Gyrus(area39)	
54.19	-47.56	16	4.84	Superior Temporal Gyrus (area22)	
23.59	-84.54	16	3.79	Middle Occipital Gyrus (area19)	
42.71	-30.99	20	3.51	Insula	
59.29	-46.29	20	3.41	Superior Temporal Gyrus (area22)	
22.31	-85.81	20	4.49	Middle Occipital Gyrus (area 19/18)	
38.89	-23.34	24	3.57	Insula	
21.04	-84.54	24	4.10	Cunneus (area 19)	
15.94	-76.89	28	3.67	Cunneus (area 19/18)	
-7.01	-46.29	36	3.76		Precunneus (area 31)

Table Activation.5.b. Early Motor Learning Minus Negative Transfer Pet Activation (batches 3 & 4 minus batches 7 & 8)

APPENDIX E: ROBOT-AIDED FUNCTIONAL IMAGING: TRACE, SPEED, AND JERK RECORDS

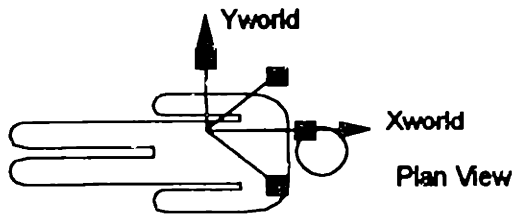

The inward movement traces were copied on the second column to allow better visualization of the end of the movement.

continuous bold line – first movement in the set
dashed bold line – last movement in the set

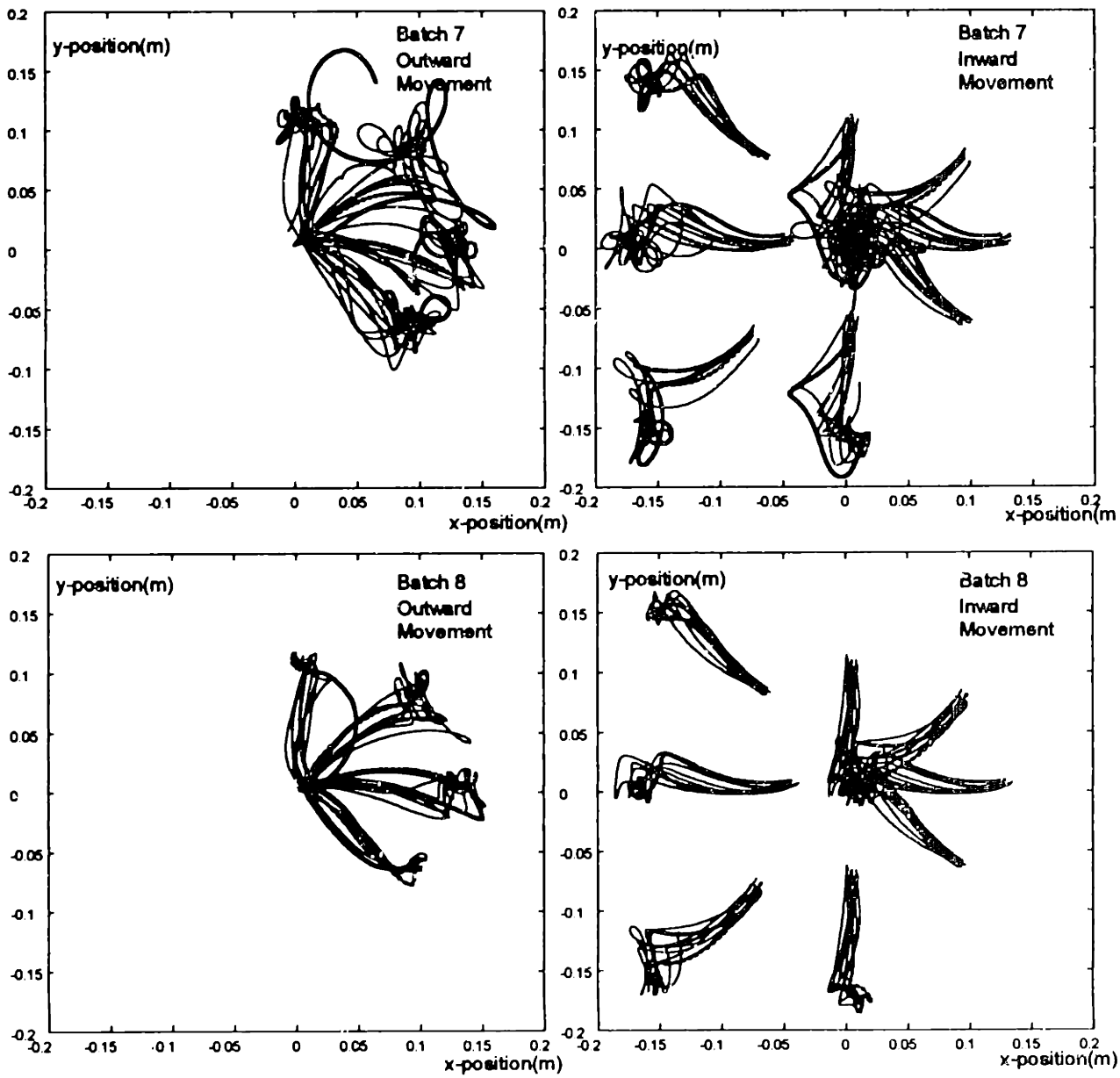

FIG.Trace.1. Trace Record for Subject CR - Batch 7 & 8

The upper row corresponds to batch 7 and the lower row to batch 8. Plots on the left column contain movements from the center to randomly presented outwards targets. The right column contains movements back to the center.

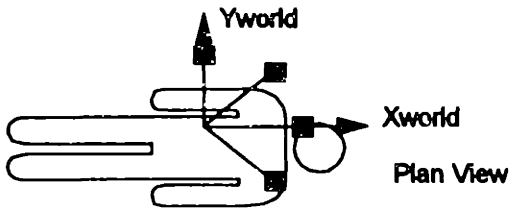

The inward movement traces were copied on the second column to allow better visualization of the end of the movement.

continuous bold line -- first movement in the set
dashed bold line -- last movement in the set

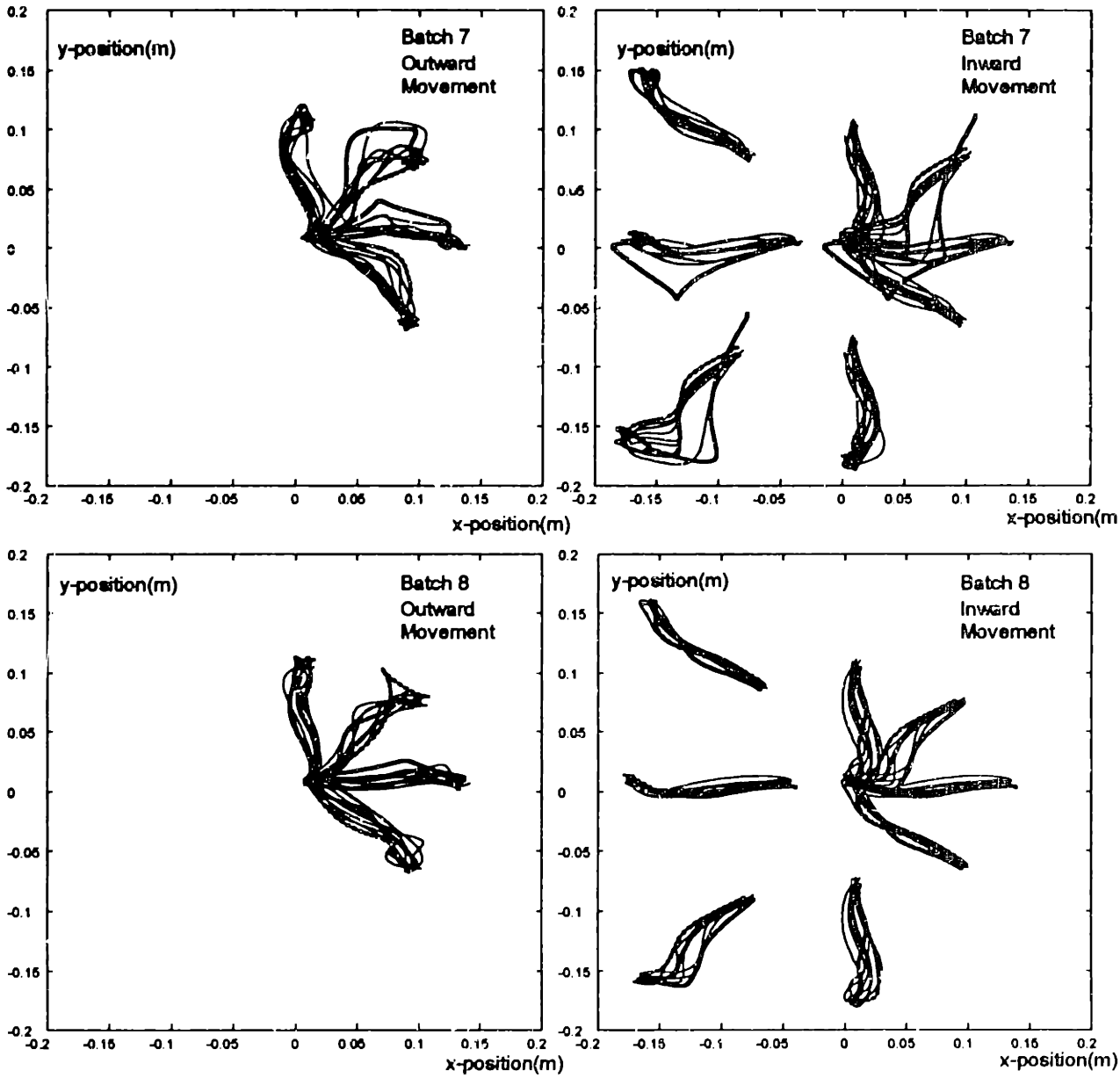

FIG.Trace.2. Trace Record for Subject DB - Batch 7 & 8

The upper row corresponds to batch 7 and the lower row to batch 8. Plots on the left column contain movements from the center to randomly presented outwards targets. The right column contains movements back to the center.

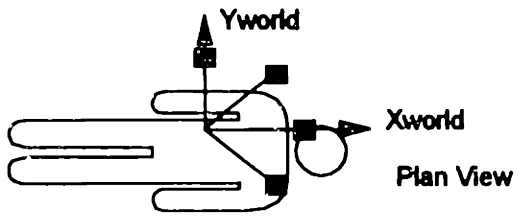

The inward movement traces were copied on the second column to allow better visualization of the end of the movement.

continuous bold line – first movement in the set
dashed bold line – last movement in the set

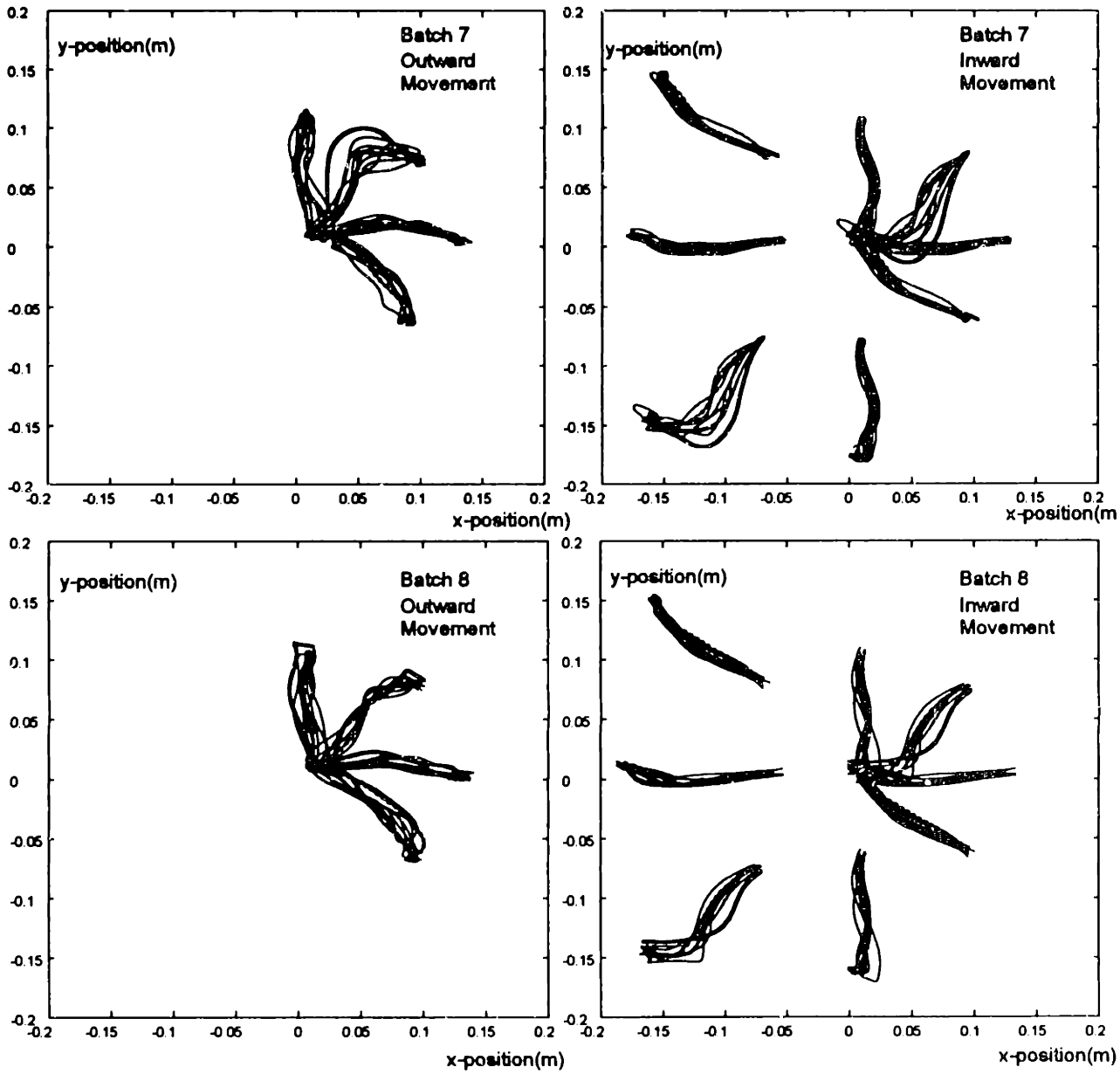

FIG.Trace.3. Trace Record for Subject DG - Batch 7 & 8

The upper row corresponds to batch 7 and the lower row to batch 8. Plots on the left column contain movements from the center to randomly presented outwards targets. The right column contains movements back to the center.

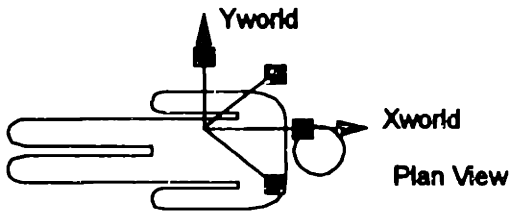

The inward movement traces were copied on the second column to allow better visualization of the end of the movement.

continuous bold line – first movement in the set
dashed bold line – last movement in the set

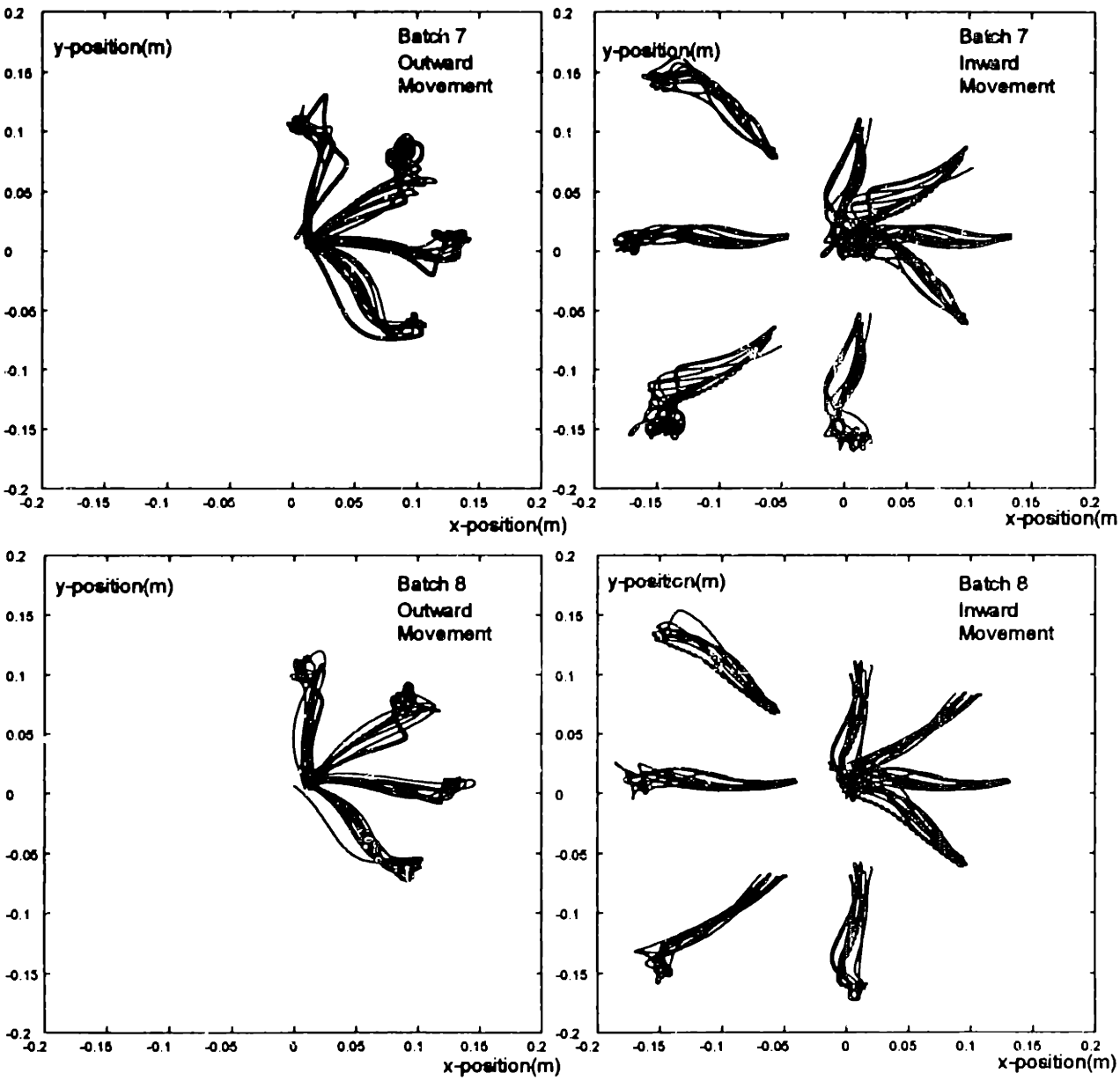

FIG.Trace.4. Trace Record for Subject DS - Batch 7 & 8

The upper row corresponds to batch 7 and the lower row to batch 8. Plots on the left column contain movements from the center to randomly presented outwards targets. The right column contains movements back to the center.

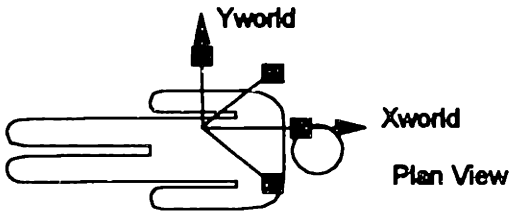

The inward movement traces were copied on the second column to allow better visualization of the end of the movement.

continuous bold line -- first movement in the set
dashed bold line -- last movement in the set

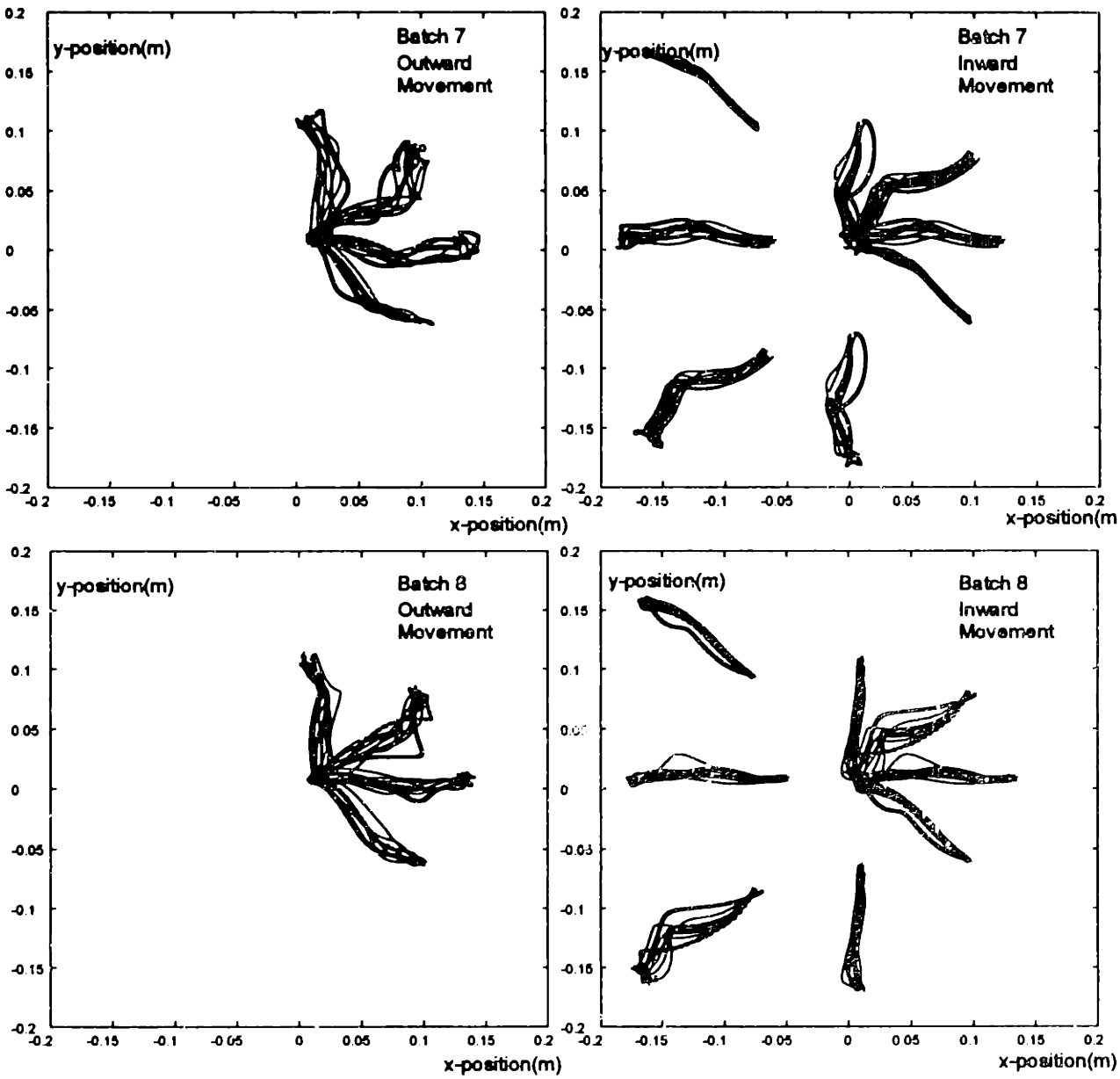

FIG.Trace.5. Trace Record for Subject DD - Batch 7 & 8

The upper row corresponds to batch 7 and the lower row to batch 8. Plots on the left column contain movements from the center to randomly presented outwards targets. The right column contains movements back to the center.

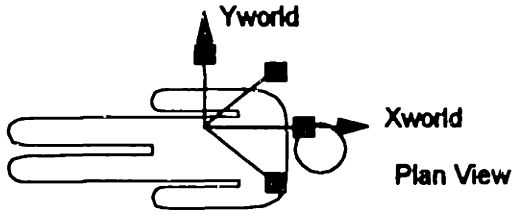

The inward movement traces were copied on the second column to allow better visualization of the end of the movement.

continuous bold line – first movement in the set
dashed bold line – last movement in the set

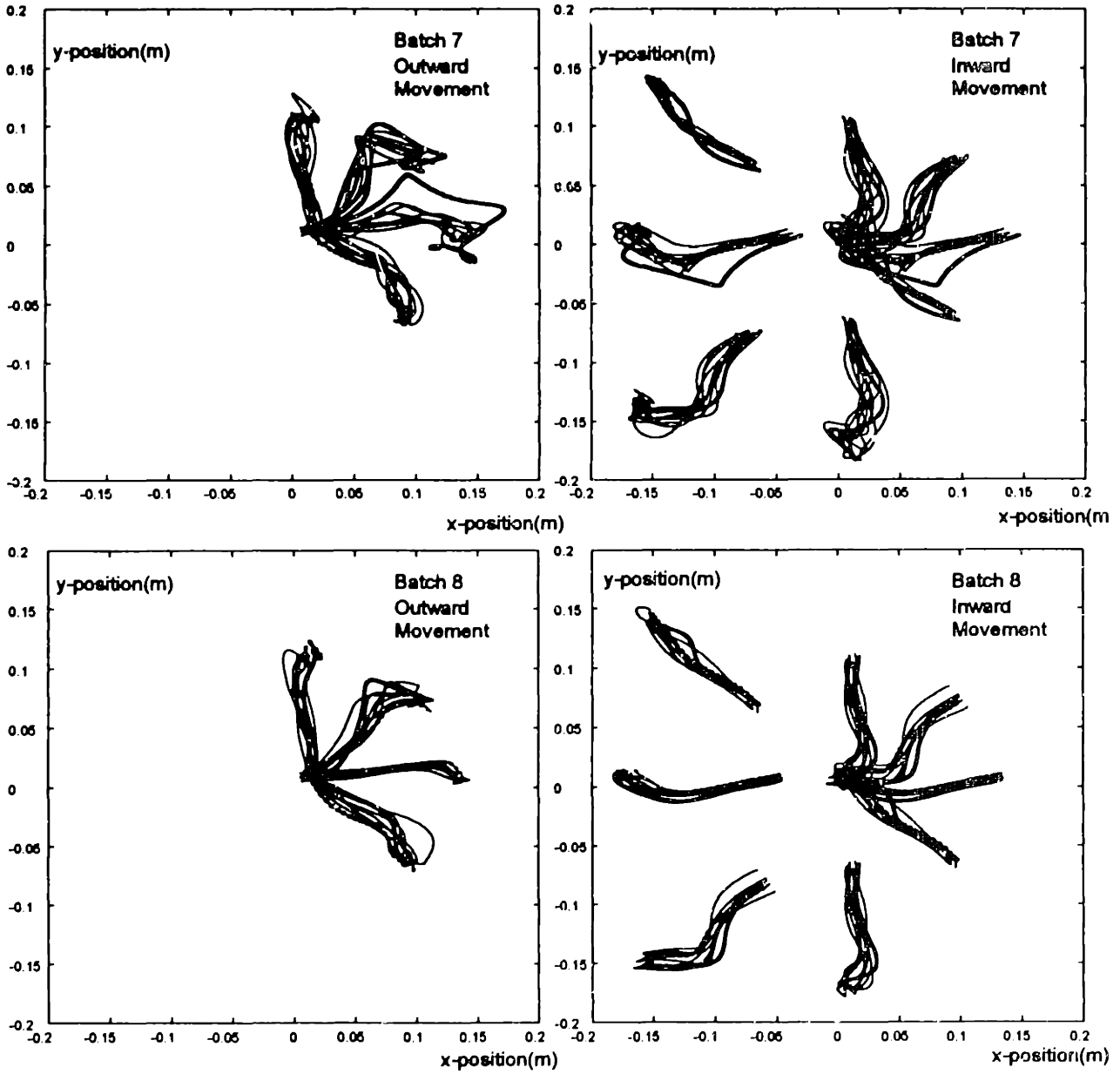

FIG.Trace.6. Trace Record for Subject ES - Batch 7 & 8

The upper row corresponds to batch 7 and the lower row to batch 8. Plots on the left column contain movements from the center to randomly presented outwards targets. The right column contains movements back to the center.

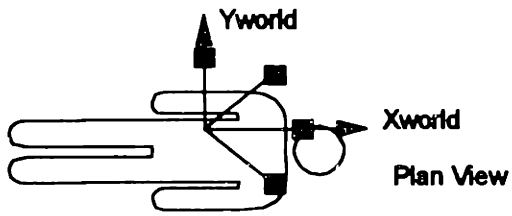

The inward movement traces were copied on the second column to allow better visualization of the end of the movement.

continuous bold line – first movement in the set
dashed bold line – last movement in the set

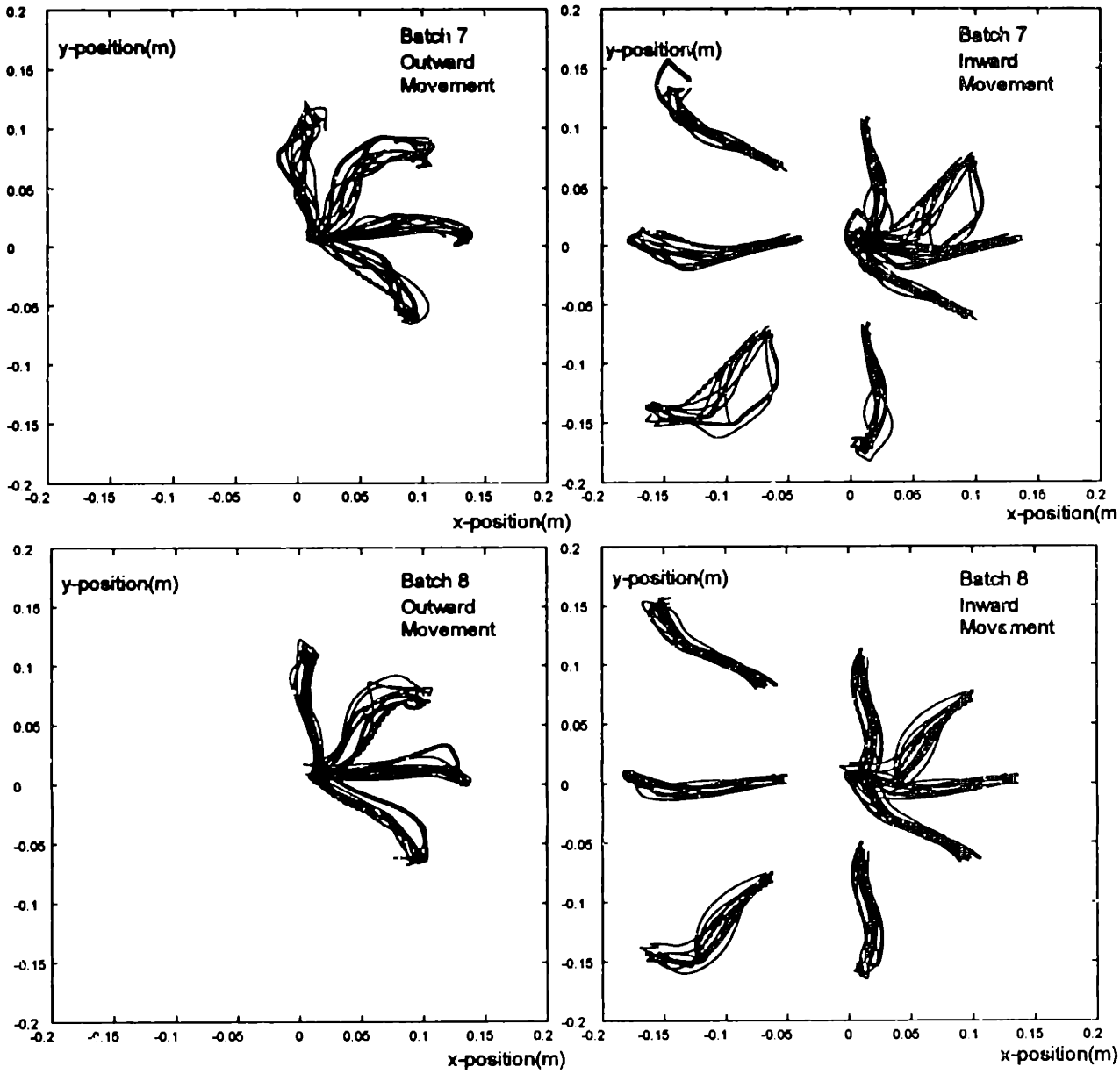

FIG.Trace.7. Trace Record for Subject MU - Batch 7 & 8

The upper row corresponds to batch 7 and the lower row to batch 8. Plots on the left column contain movements from the center to randomly presented outwards targets. The right column contains movements back to the center.

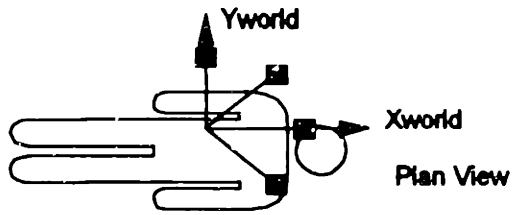

The inward movement traces were copied on the second column to allow better visualization of the end of the movement.

continuous bold line – first movement in the set
dashed bold line – last movement in the set

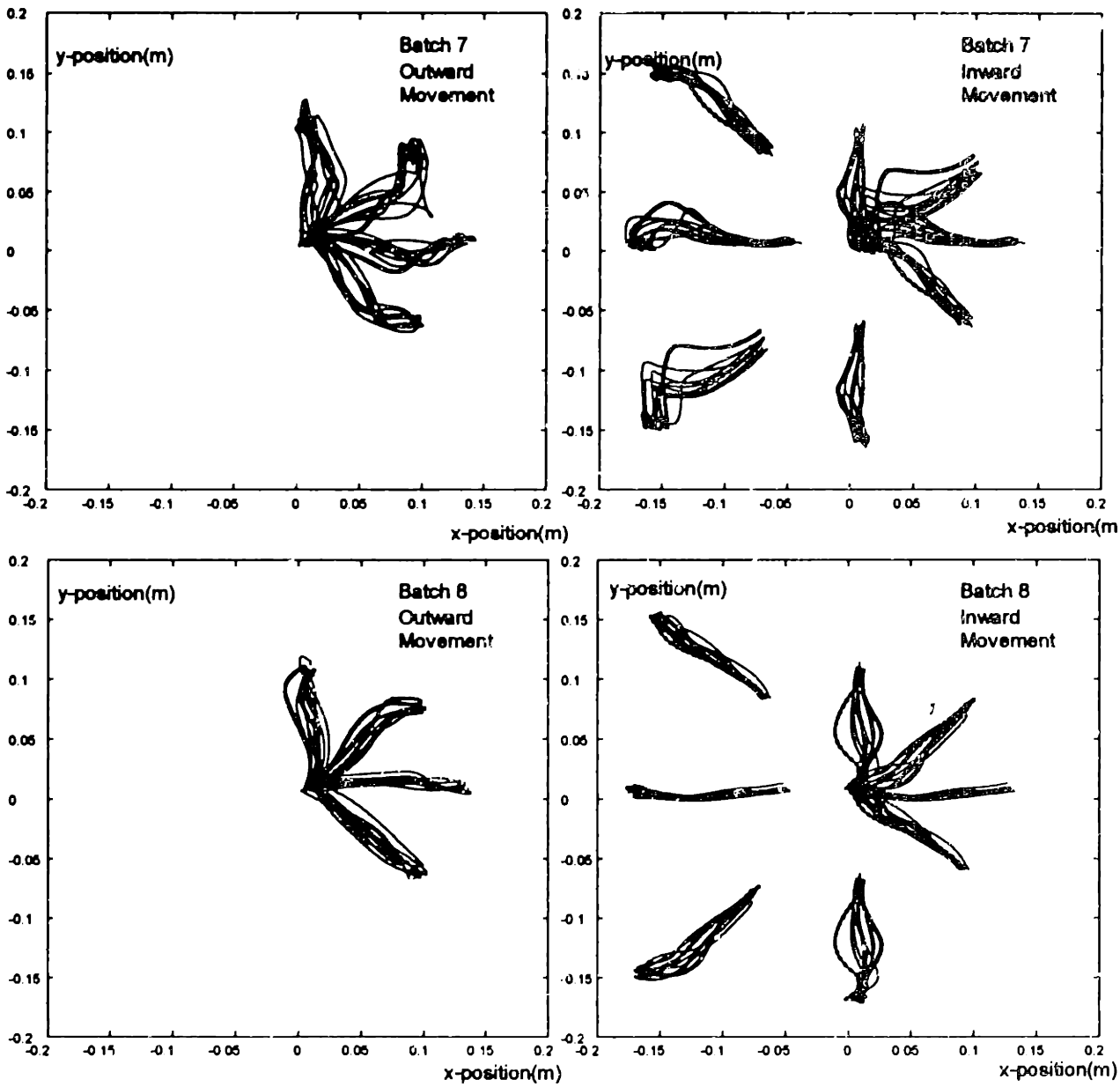

FIG.Trace.8. Trace Record for Subject TH - Batch 7 & 8

The upper row corresponds to batch 7 and the lower row to batch 8. Plots on the left column contain movements from the center to randomly presented outwards targets. The right column contains movements back to the center.

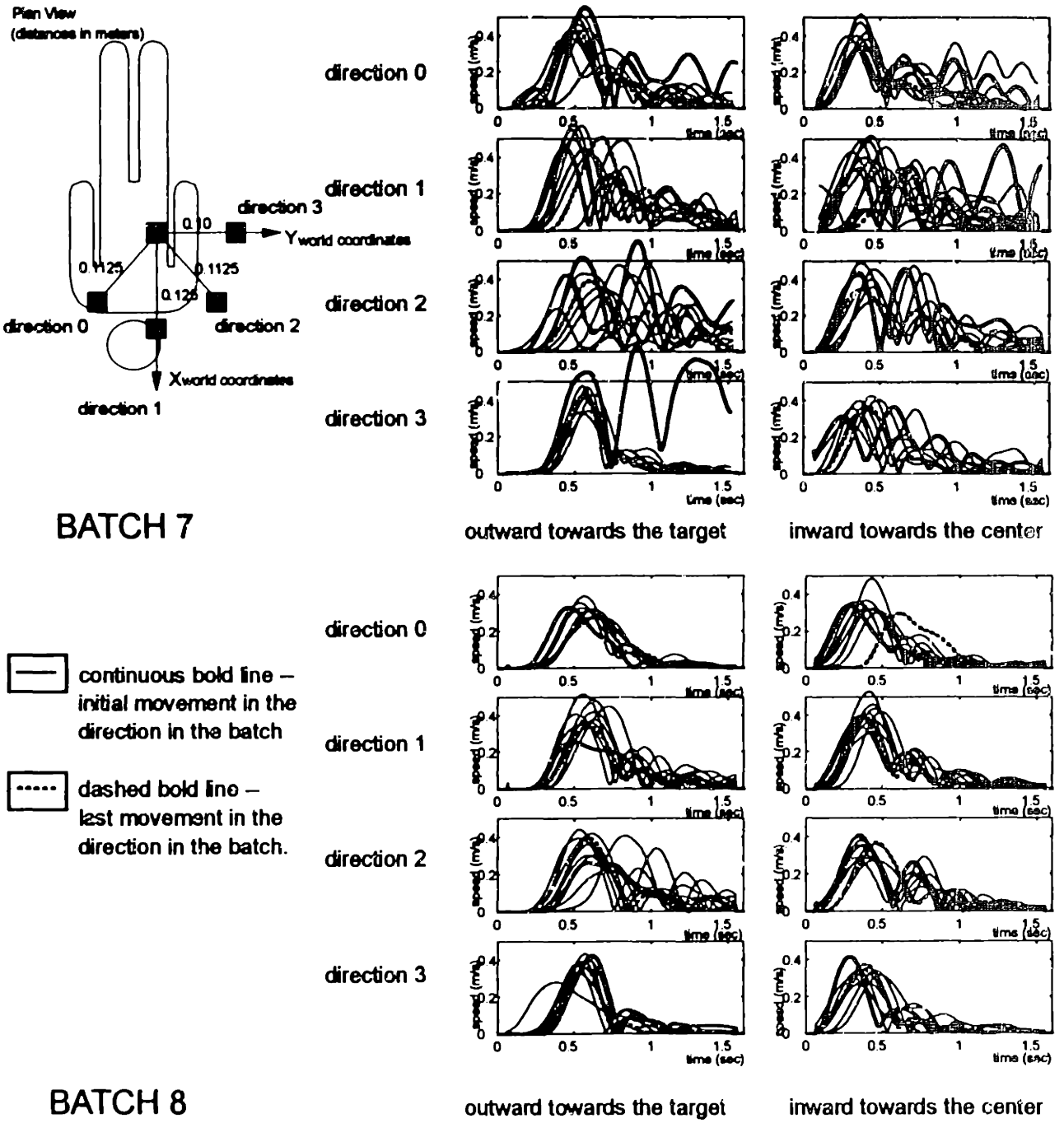

FIG.Speed.1. Speed Record for Subject CR - Batch 7 & 8
The figure shows two sets of speed records. The upper four rows correspond to batch 7 and the last four rows to batch 8. Plots on the left column contain movements from the center to randomly presented outwards targets. The right column contains movements back to the center.

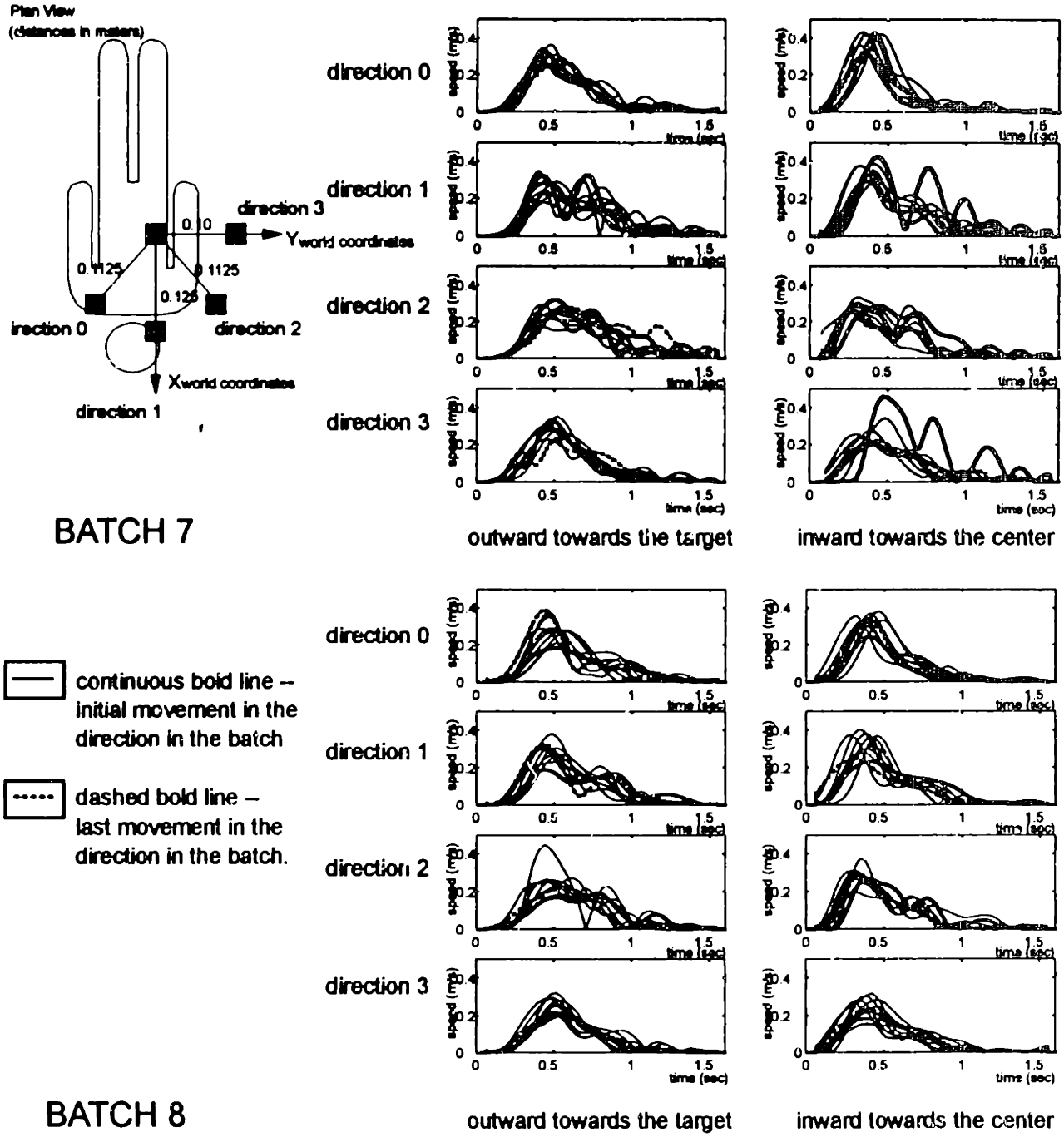

FIG.Speed.2. Speed Record for Subject DB - Batch 7 & 8

The figure shows two sets of speed records. The upper four rows correspond to batch 7 and the last four rows to batch 8. Plots on the left column contain movements from the center to randomly presented outwards targets. The right column contains movements back to the center.

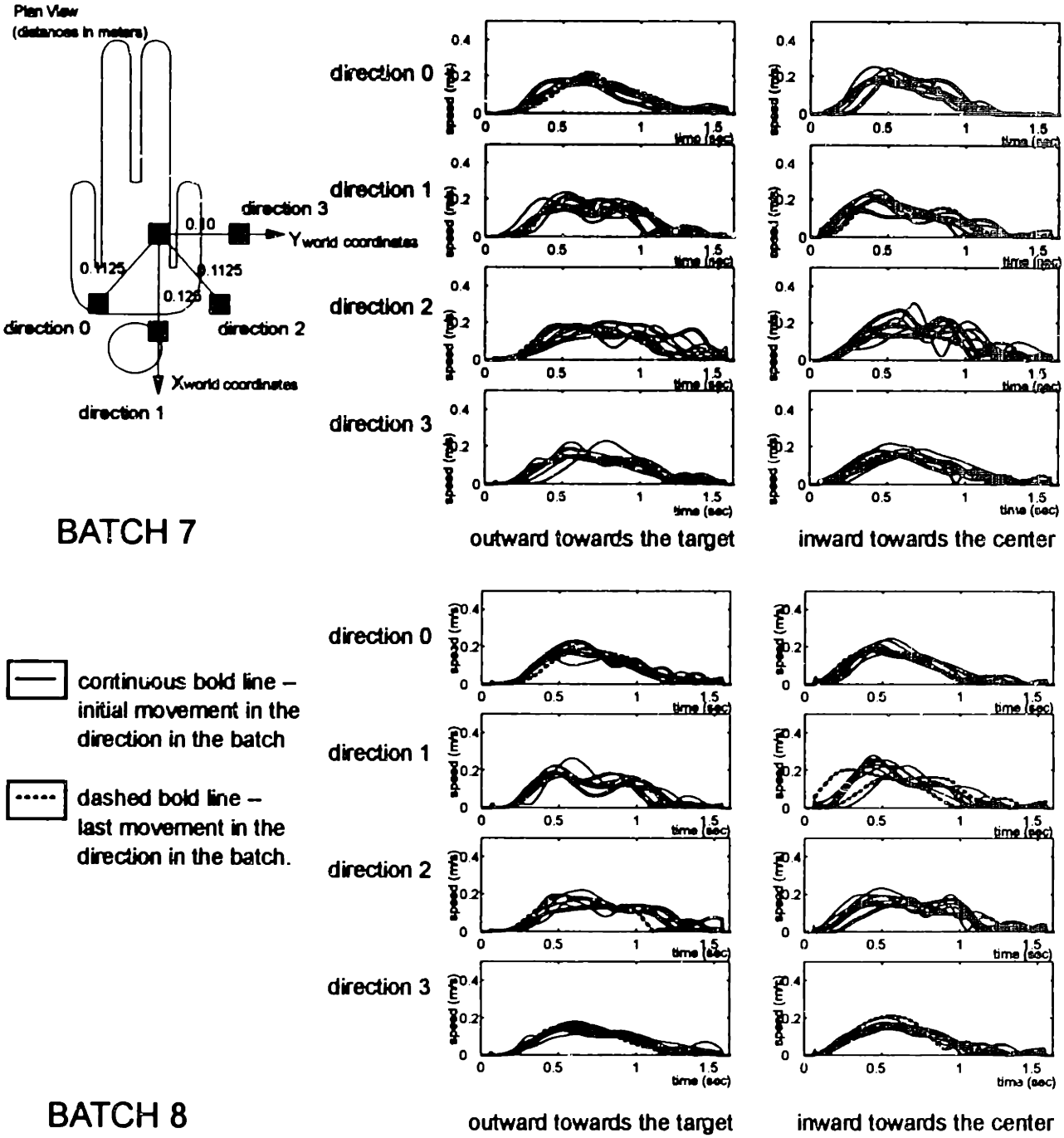

FIG.Speed.3. Speed Record for Subject DG - Batch 7 & 8

The figure shows two sets of speed records. The upper four rows correspond to batch 7 and the last four rows to batch 8. Plots on the left column contain movements from the center to randomly presented outwards targets. The right column contains movements back to the center.

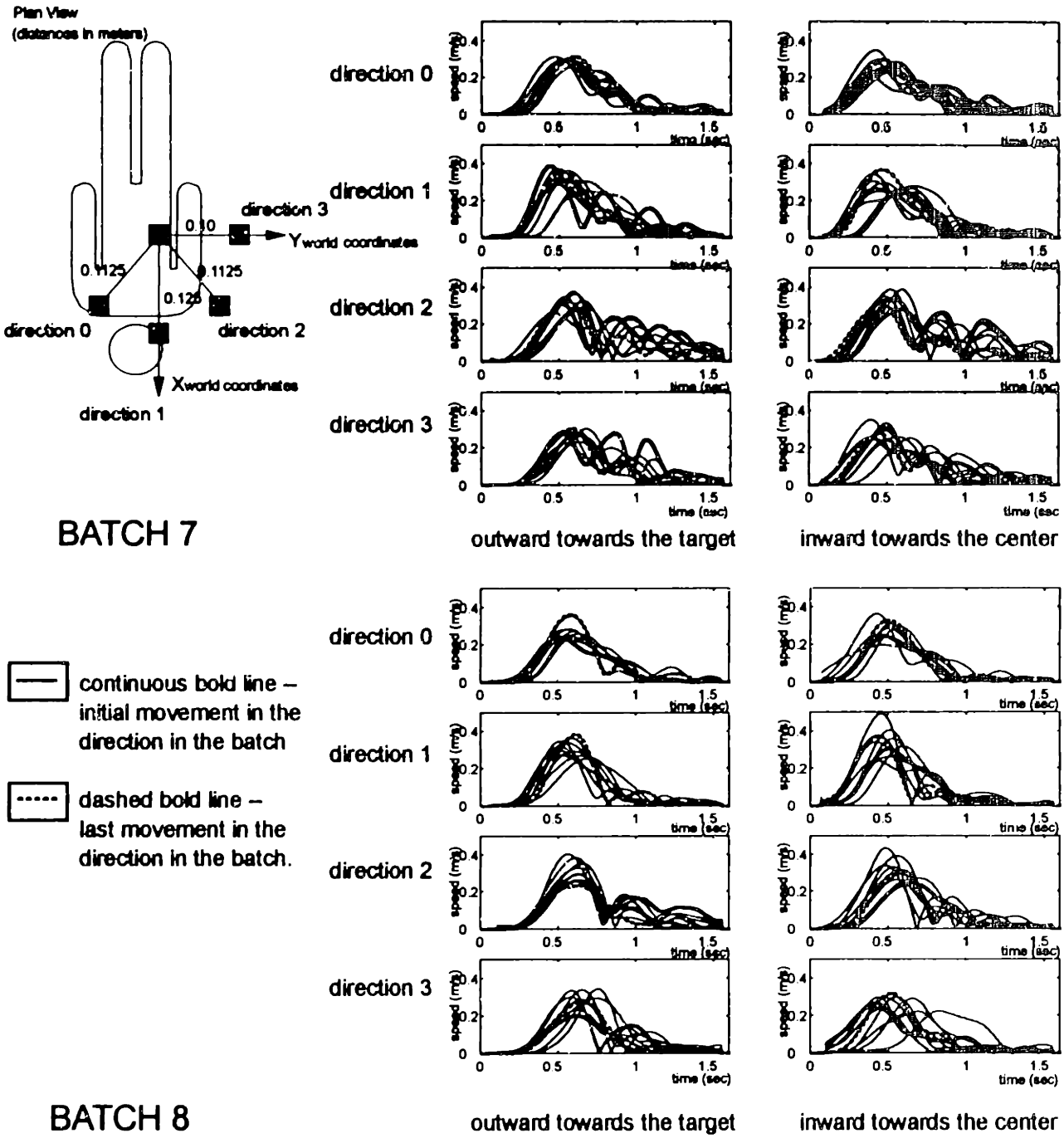

FIG.Speed.4. Speed Record for Subject DS - Batch 7 & 8
The figure shows two sets of speed records. The upper four rows correspond to batch 7 and the last four rows to batch 8. Plots on the left column contain movements from the center to randomly presented outwards targets. The right column contains movements back to the center.

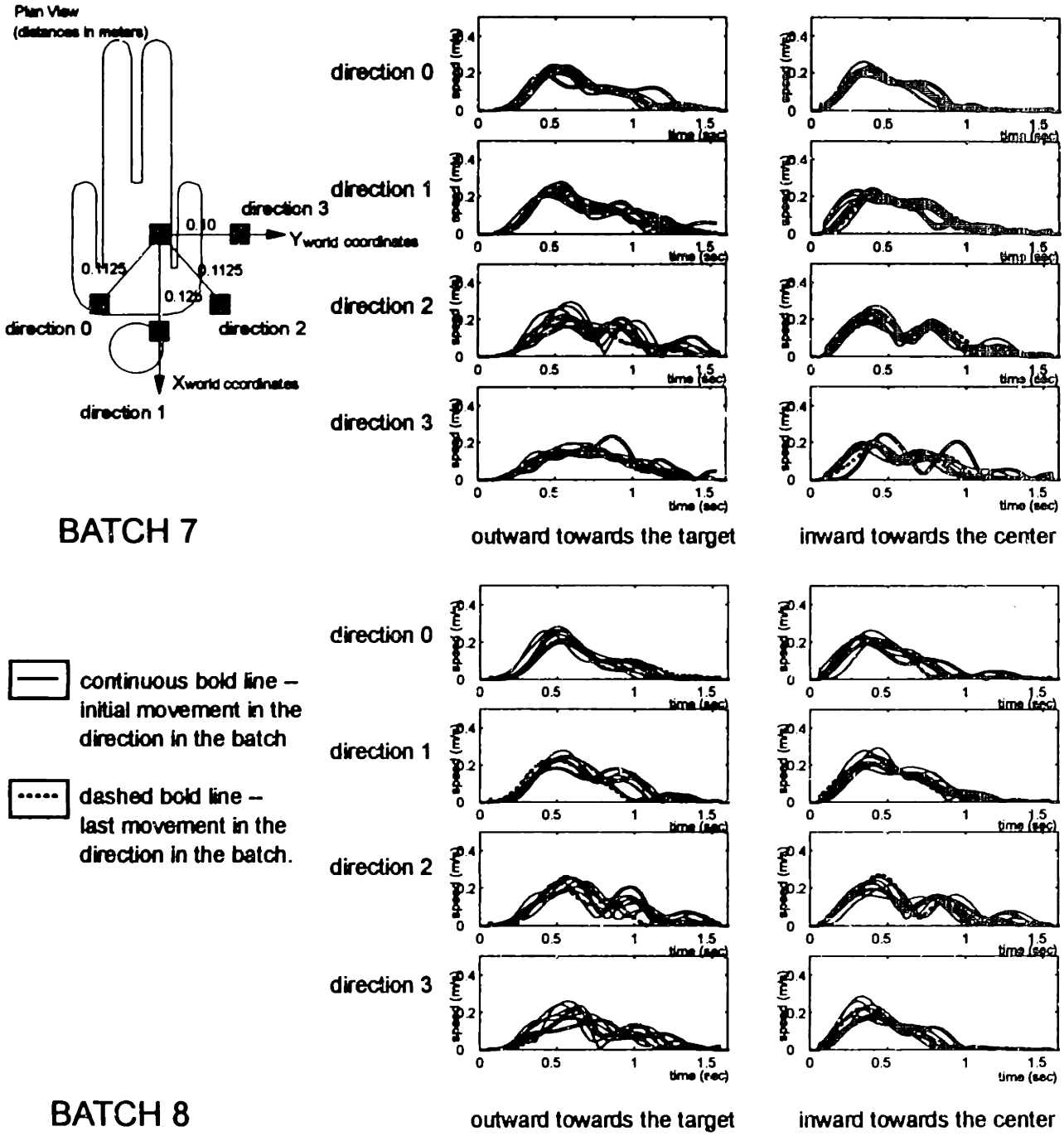

FIG.Speed.5. Speed Record for Subject DD - Batch 7 & 8

The figure shows two sets of speed records. The upper four rows correspond to batch 7 and the last four rows to batch 8. Plots on the left column contain movements from the center to randomly presented outwards targets. The right column contains movements back to the center.

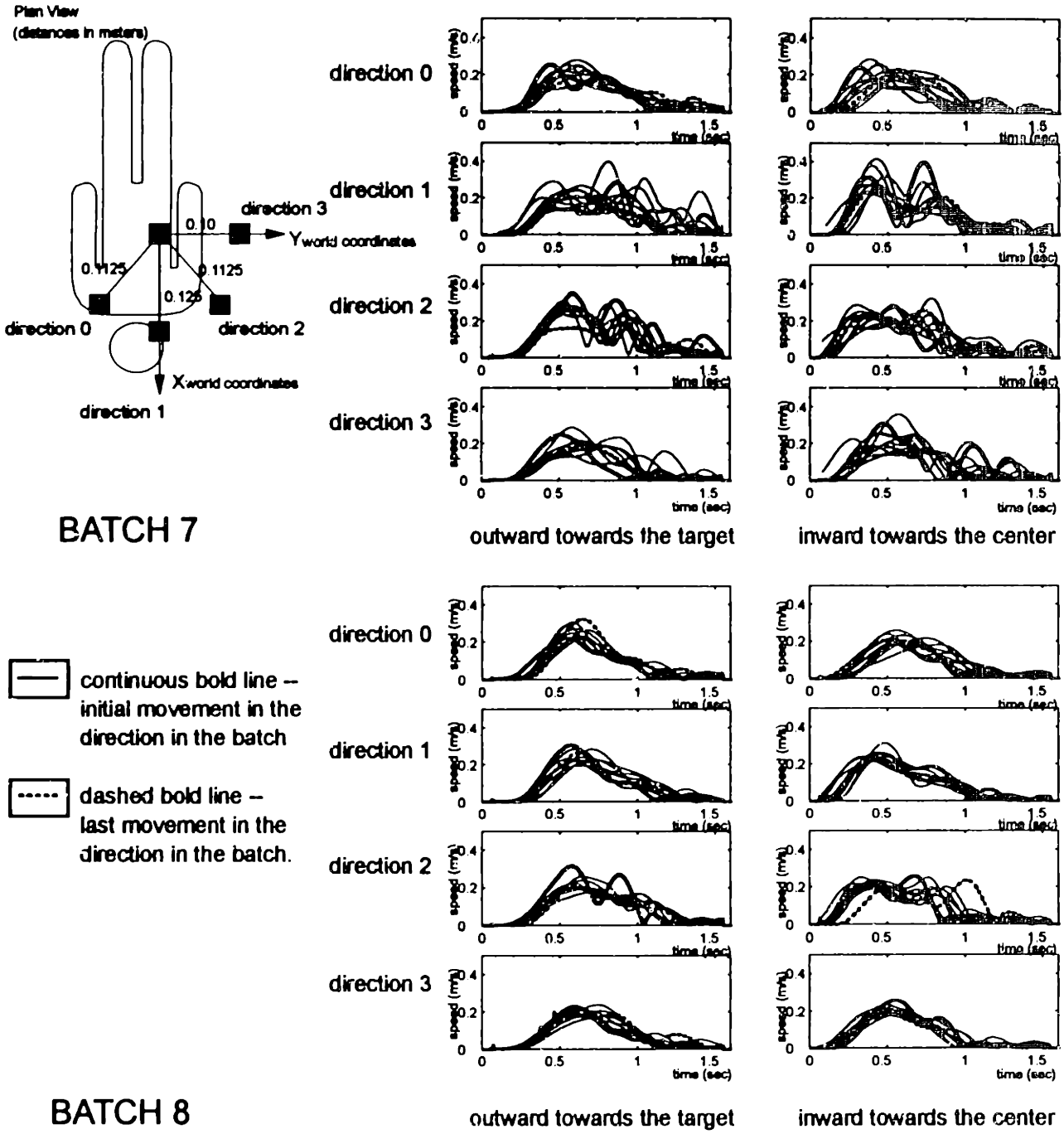

FIG.Speed.6. Speed Record for Subject ES - Batch 7 & 8
The figure shows two sets of speed records. The upper four rows correspond to batch 7 and the last four rows to batch 8. Plots on the left column contain movements from the center to randomly presented outwards targets. The right column contains movements back to the center.

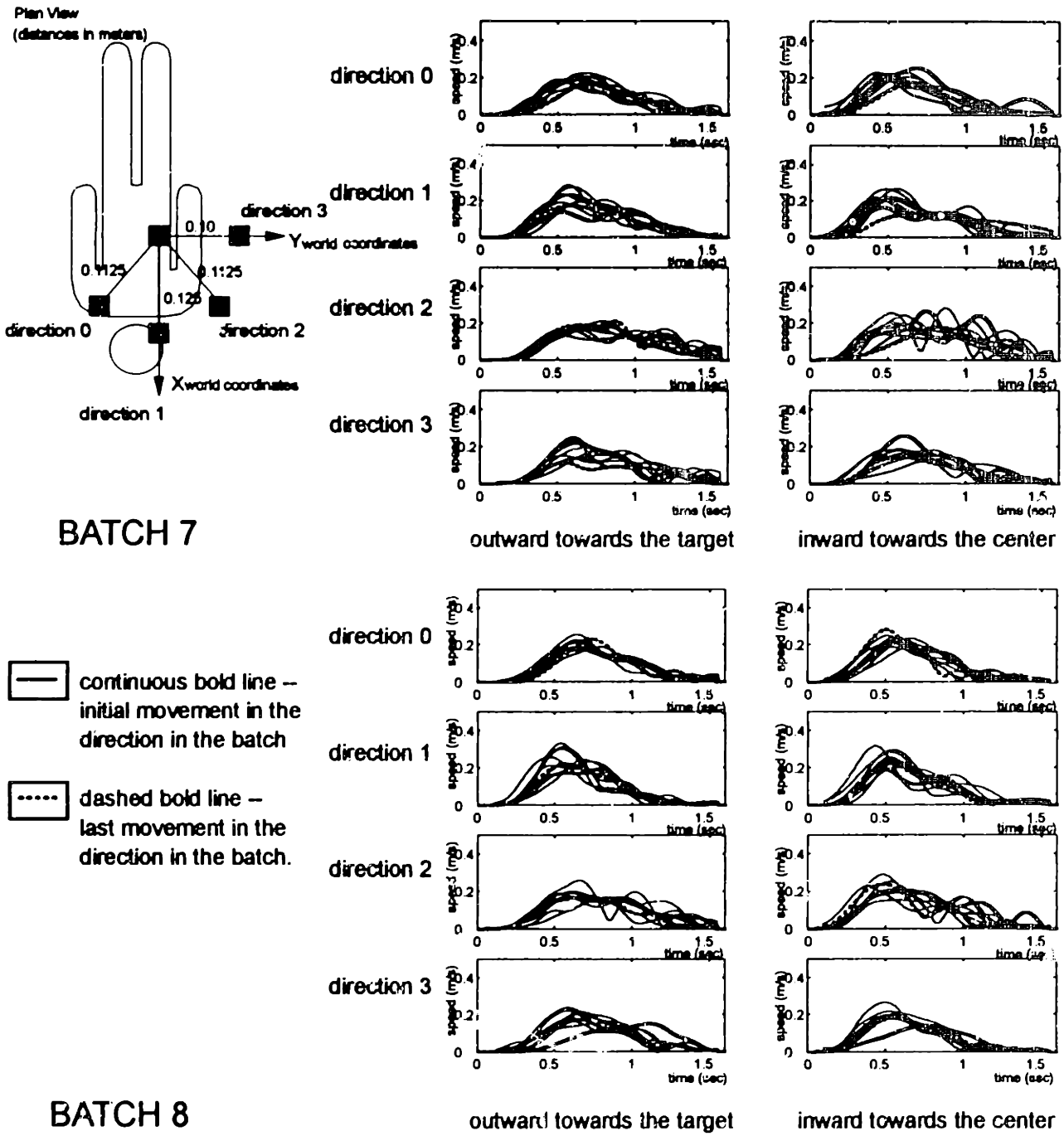

FIG.Speed.7. Speed Record for Subject MU - Batch 7 & 8
The figure shows two sets of speed records. The upper four rows correspond to batch 7 and the last four rows to batch 8. Plots on the left column contain movements from the center to randomly presented outwards targets. The right column contains movements back to the center.

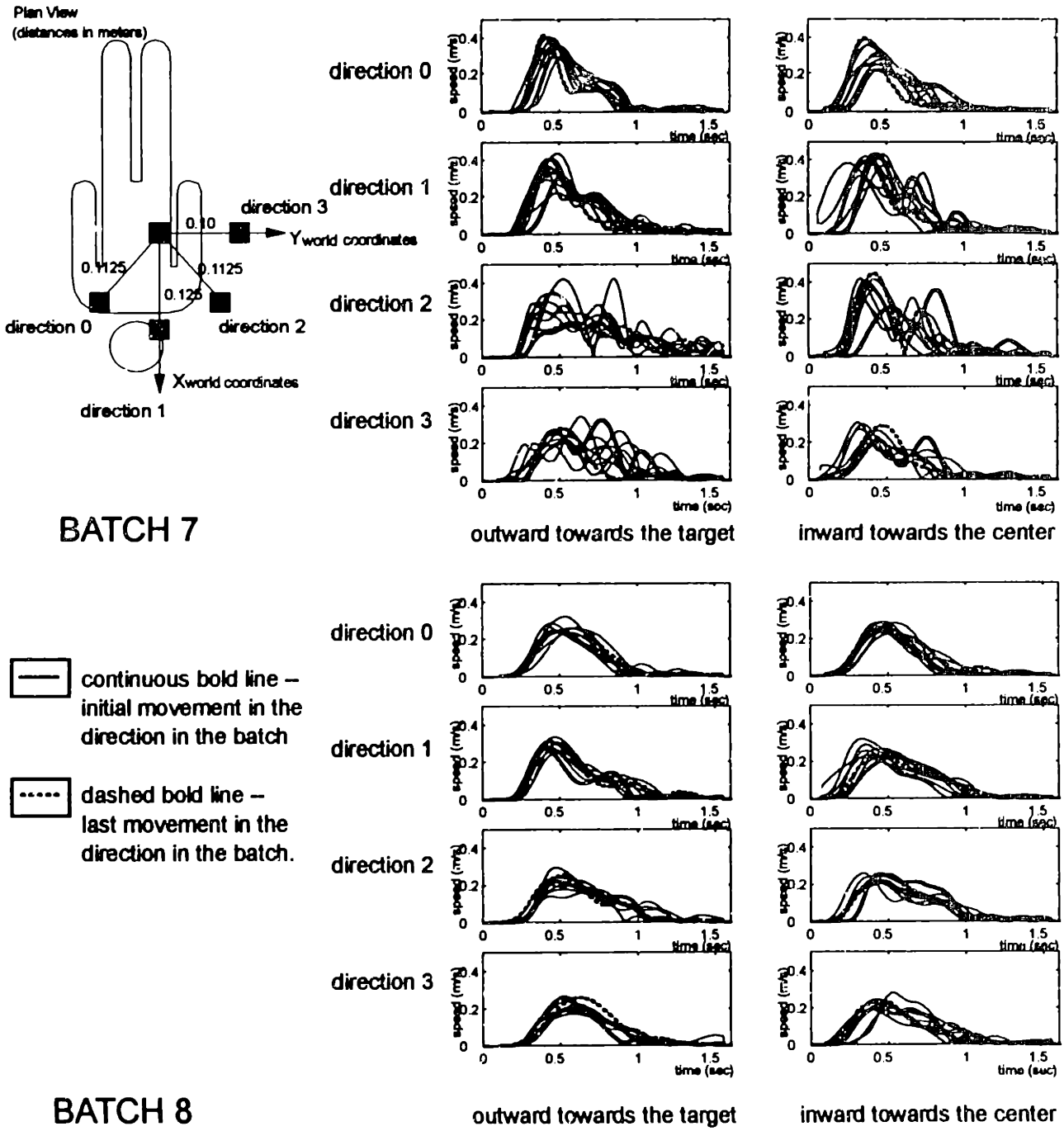

FIG.Speed.8. Speed Record for Subject TH - Batch 7 & 8
The figure shows two sets of speed records. The upper four rows correspond to batch 7 and the last four rows to batch 8. Plots on the left column contain movements from the center to randomly presented outwards targets. The right column contains movements back to the center.

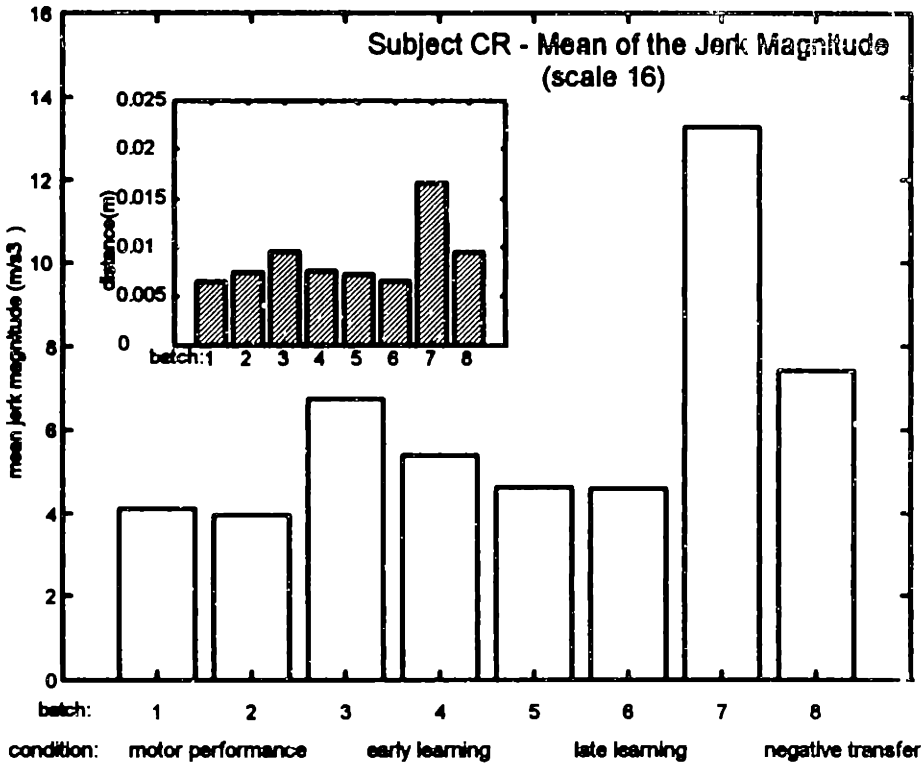

batch	1	2	3	4	5	6	7	8
1	1	1.07	0.37*	0.58*	0.79	0.80	0.10*	0.31*
2		1	0.35*	0.54*	0.74	0.75	0.09*	0.29*
3			1	1.57*	2.13*	2.16*	0.26*	0.83
4				1	1.35	1.37	0.16*	0.53*
5					1	1.01	0.12*	0.39*
6						1	0.12*	0.38*
7							1	3.19*
8								1

(*)Statistically significant [level 0.05 in 80 trials -- 0.65 < F-value < 1.53]

Jerk_Index.1. Mean Jerk Magnitude for Subject CR
The plot shows the mean jerk magnitude for each batch with the insert plot showing the mean deviation for each batch from Fig.6.10.a.

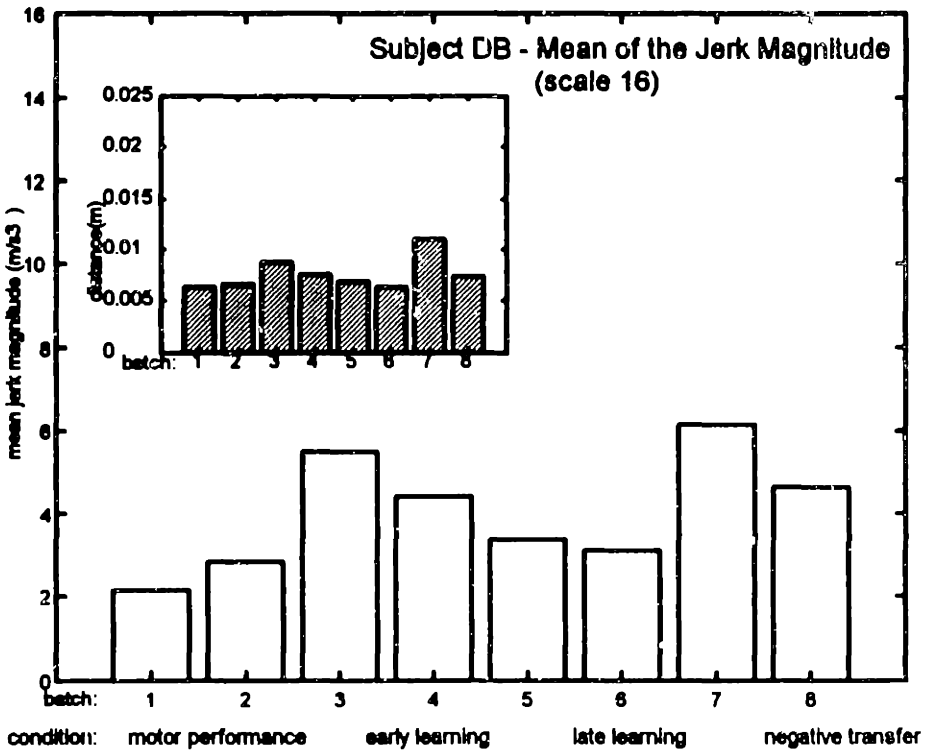

batch	1	2	3	4	5	6	7	8
1	1	0.57*	0.15*	0.23*	0.40*	0.47*	0.12*	0.21*
2		1	0.27*	0.41*	0.70	0.83	0.21*	0.37*
3			1	1.54*	2.64*	3.11*	0.80	1.40
4				1	1.71*	2.02*	0.52*	0.91
5					1	1.18	0.30*	0.53*
6						1	0.26*	0.45*
7							1	1.75*
8								1

(*)Statistically significant [level 0.05 in 80 trials – 0.65 < F-value < 1.53]

Jerk_Index.2. Mean Jerk Magnitude for Subject DB
The plot shows the mean jerk magnitude for each batch with the insert plot showing the mean deviation for each batch from Fig.6.11.a.

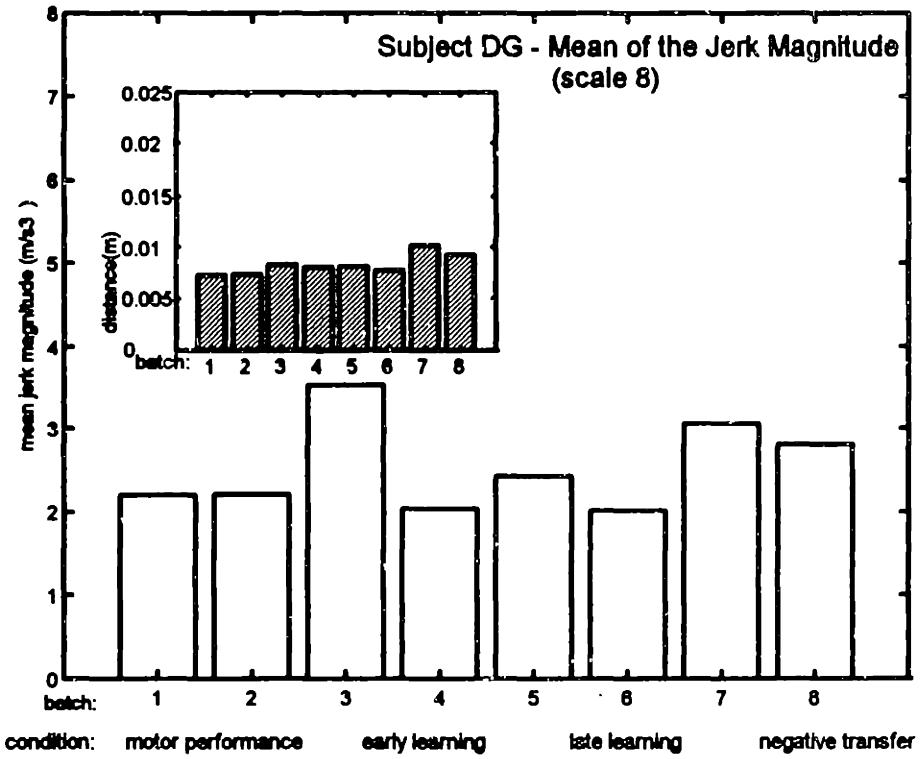

batch	1	2	3	4	5	6	7	8
1	1	0.99	0.39*	1.16	0.82	1.19	0.52*	0.62*
2		1	0.39*	1.18	0.83	1.20	0.52*	0.62*
3			1	2.99*	2.12*	3.07*	1.33	1.59*
4				1	0.71	1.03	0.45*	0.53*
5					1	1.45	0.63*	0.75
6						1	0.43*	0.52*
7							1	1.19
8								1

(*)Statistically significant [level 0.05 in 80 trials – 0.65 < F-value < 1.53]

Jerk_Index.3. Mean Jerk Magnitude for Subject DG
The plot shows the mean jerk magnitude for each batch with the insert plot showing the mean deviation for each batch from Fig.6.12.a.

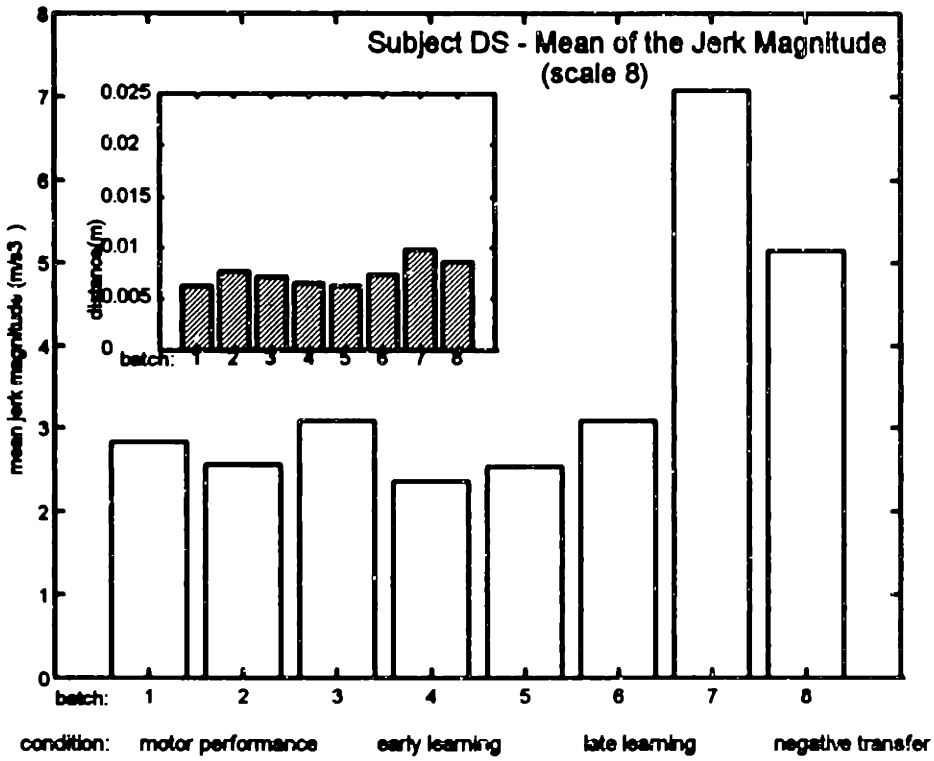

batch	1	2	3	4	5	6	7	8
1	1	1.22	0.84	1.44	1.24	0.84	0.16*	0.30*
2		1	0.69	1.18	1.02	0.69	0.13*	0.25°
3			1	1.71*	1.48	1.00	0.19*	0.36*
4				1	0.87	0.59*	0.11*	0.21*
5					1	0.68	0.13*	0.24*
6						1	0.19*	0.36*
7							1	1.89*
8								1

(*)Statistically significant [level 0.05 in 80 trials – 0.65 < F-value < 1.53]

Jerk_Index.4. Mean Jerk Magnitude for Subject DS
The plot shows the mean jerk magnitude for each batch with the insert plot showing the mean deviation for each batch from Fig.6.13.a.

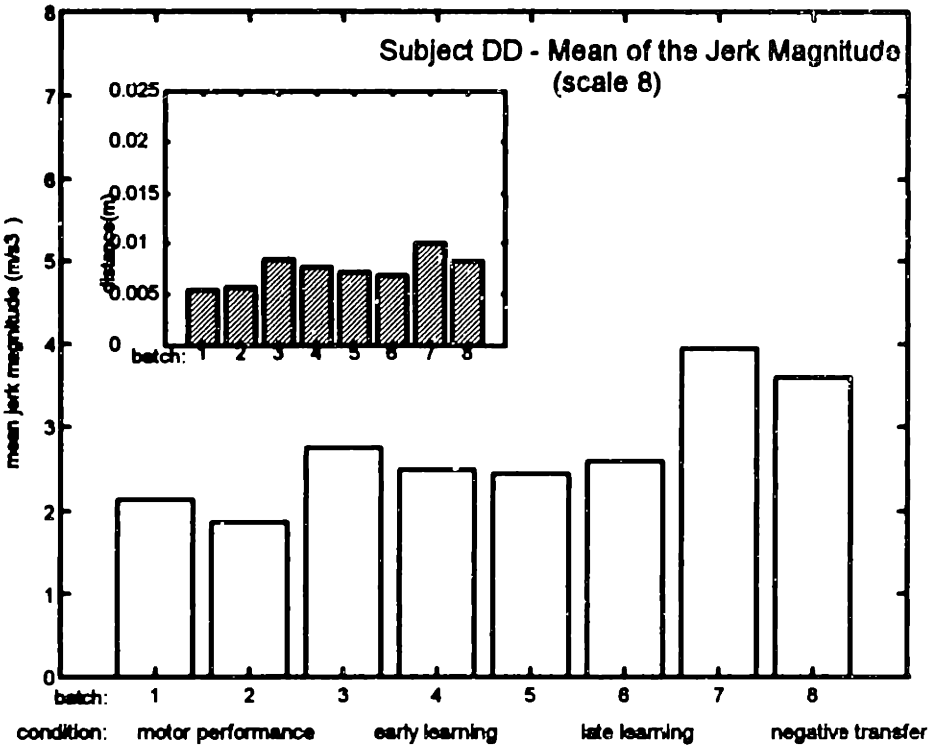

batch	1	2	3	4	5	6	7	8
1	1	1.30	0.60*	0.73	0.76	0.70	0.29*	0.35*
2		1	0.46*	0.56*	0.59*	0.52*	0.22*	0.27*
3			1	1.21	1.27	1.13	0.49*	0.59*
4				1	1.04	0.93	0.40*	0.48*
5					1	0.89	0.38*	0.46*
6						1	0.43*	0.52*
7							1	1.21
8								1

(*)Statistically significant [level 0.05 in 80 trials – 0.65 < F-value < 1.53]

Jerk_Index.5. Mean Jerk Magnitude for Subject DD
The plot shows the mean jerk magnitude for each batch with the insert plot showing the mean deviation for each batch from Fig.6.14.a.

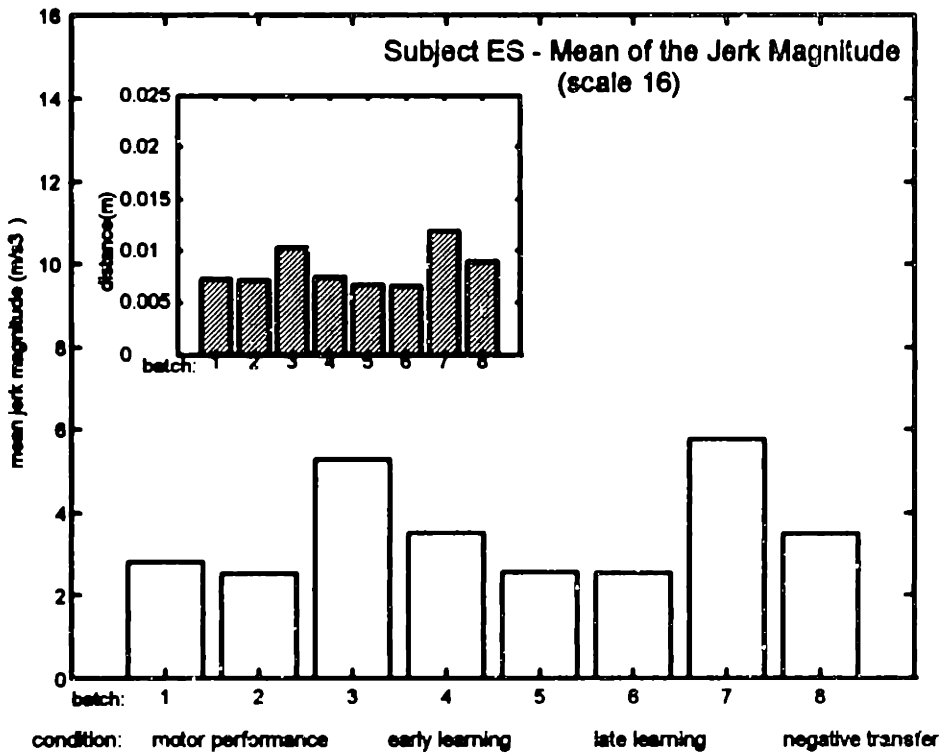

batch	1	2	3	4	5	6	7	8
1	1	1.24	0.28*	0.64*	1.21	1.23	0.24*	0.65
2		1	0.23*	0.51*	0.97	0.99	0.19*	0.52*
3			1	2.25*	4.28*	4.36*	0.83	2.28*
4				1	1.90*	1.94*	0.37*	1.01
5					1	1.02	0.19*	0.53*
6						1	0.19*	0.52*
7							1	2.74*
8								1

(*)Statistically significant [level 0.05 in 80 trials – 0.65 < F-value < 1.53]

Jerk_Index.6. Mean Jerk Magnitude for Subject ES
The plot shows the mean jerk magnitude for each batch with the insert plot showing the mean deviation for each batch from Fig.6.15.a.

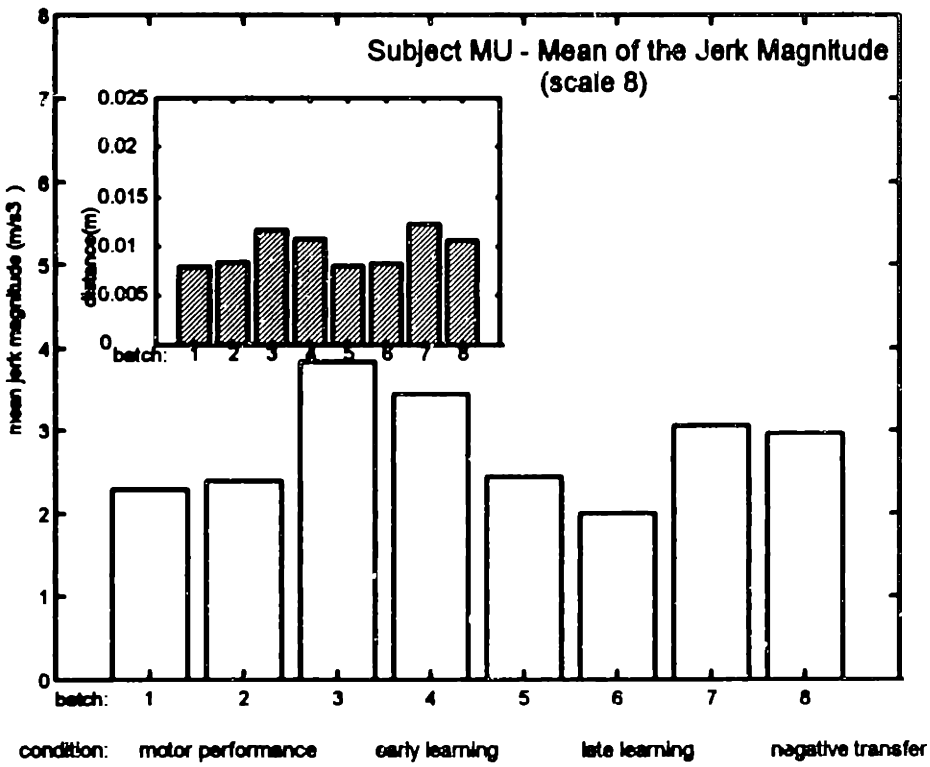

batch	1	2	3	4	5	6	7	8
1	1	0.92	0.35*	0.44*	0.88	1.30	0.56*	0.60*
2		1	0.39*	0.48*	0.96	1.42	0.61*	0.65
3			1	1.24	2.49*	3.68*	1.58*	1.69*
4				1	2.00*	2.96*	1.27	1.36
5					1	1.48	0.63*	0.68
6						1	0.43*	0.46*
7							1	1.07*
8								1

(*)Statistically significant [level 0.05 in 80 trials – 0.65 < F-value < 1.53]

Jerk_Index.7. Mean Jerk Magnitude for Subject MU
The plot shows the mean jerk magnitude for each batch with the insert plot showing the mean deviation for each batch from Fig.6.16.a.

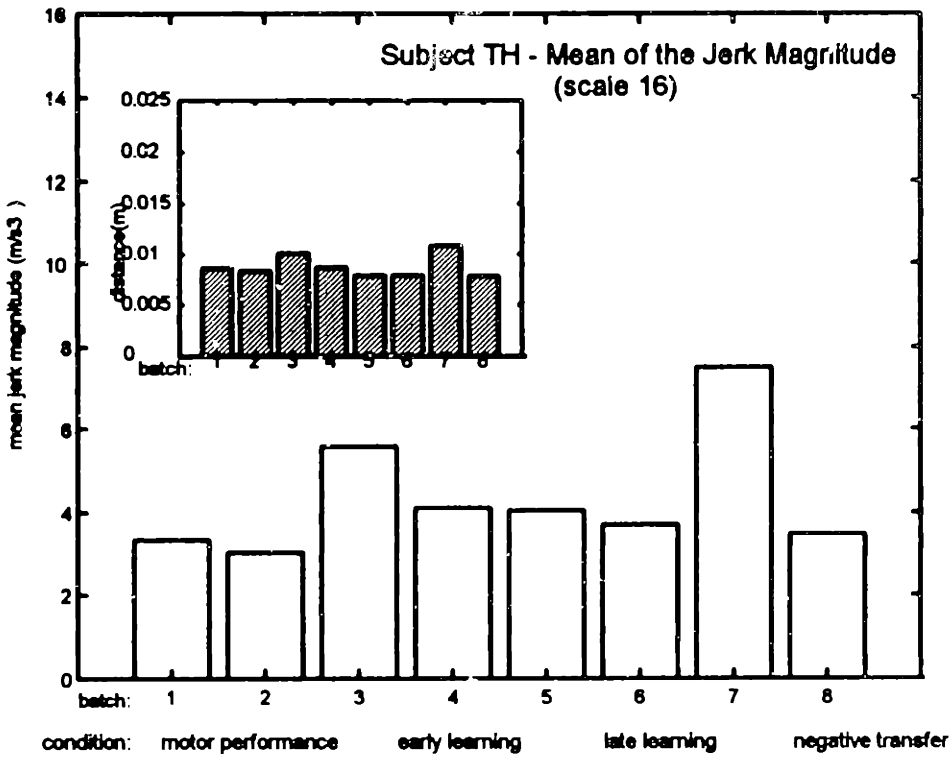

batch	1	2	3	4	5	6	7	8
1	1	1.22	0.36*	0.66	0.68	0.82	0.20*	0.93
2		1	0.29*	0.54*	0.56*	0.67	0.16*	0.76
3			1	1.84*	1.91*	2.28*	0.55*	2.59*
4				1	1.04	1.24	0.30*	1.41
5					1	1.19	0.29*	1.36
6						1	0.24*	1.14
7							1	4.67*
8								1

(*)Statistically significant [level 0.05 in 80 trials -- 0.65 < F-value < 1.53]

Jerk_Index.8. Mean Jerk Magnitude for Subject TH
The plot shows the mean jerk magnitude for each batch with the insert plot showing the mean deviation for each batch from Fig.6.17.a.

BIBLIOGRAPHY

Aisen, M.L.; Sevilla, D.; Gibson, G.; Kutt, H.; Blau, A; Edelstein, L.; Hatch, J.; Blass, J.; "3,4-Diaminopyridine as a Treatment for Amyotrophic Lateral Sclerosis;" *Journal of the Neurological Sciences*; vol.129, pp.21-24, 1995.

Alpert, N.M.; Berdichevsky, D.; Weise, S.; Tang, J.; Rauch, S.L.; "Stereotatic Transformation of PET scans by Nonlinear Least Squares;" *Quantification of Brain Function: Tracer Kinetics and Image Analysis in Brain PET. K. Uemura, N.A. Lassen, T. Jones; I. Kanno (eds.)*; Excerpta Medica; New York; 1993; 459-463.

Bahill, A.T.; Stark, L.; "The Trajectories of Saccadic Eye Movements;" *Scientific American*; vol.241., pp.108-117; 1979.

Bell, A.J. & Sejnowski, T.J.; "An Information-Maximization Approach to Blind Separation and Blind Deconvolution;" *Technical Report no. INC-9501*; Institute of Neural Computation -UCSD, San Diego, February 1995.

Brown, A.K.; Parker, M.; "Dance Notation for Beginners;" *Dance Books Ltd*; 1984.

Bizzi, E.; Accornero, N.; Chapple, W.; Hogan, N.; "Posture Control and Trajectory Formation During Arm Movement;" *Journal of Neuroscience*; vol.4., pp.2738-2744; 1984.

Bobath, B.; "Adult Hemiplegia: Evaluation and Treatment;" *William Heinemann Medical Books*; 1990.

Brashers-Krug, T.; Shadmehr, R.; Bizzi, E.; "Consolidation in Human Motor Memory;" *Nature*; vol.382, 18 July 1996.

Brunnstrom, S.; "Movement Therapy in Hemiplegia;" *Harper & Row*; 1970.

Charnnarong, J.; "The Design of an Intelligent Machine for Upper-Limb Physical Therapy;" *M.S. Thesis*; Massachusetts Institute of Technology; August, 1991.

Chollet, F.; DiPiero, V.; Wise, R.J.S.; Brooks, D.J.; Dolan, R.J.; Frackowiak, R.S.J.; "The Functional Anatomy of Motor Recovery after Stroke in Humans: A Study with Positron Emission Tomography;" *Annals of Neurology*; vol.29, no.1., January, 1991.

Colebatch, J.G.; "The Distribution of Muscular Weakness in Upper Motor Neuron Lesions Affecting the Arm;" *Brain*; vol.112, pp.749-763, 1989.

Colgate, J. E. and Hogan, N.;"Robust Control of Dynamically Interacting Systems;" *International Journal of Control*; vol. 48, no. 1, pp. 65-88, 1988.

Crossman, E.R.F.W.; Goodeve, J.; "Feedback Control of Hand-Movement and Fitts' Law;" *Quarterly Journal of Experimental Psychology*; vol.35A, 251-278; 1983.

Cybenko, G.; "Approximation by Superpositions of a Sigmoidal Function;" *Mathematics of Control, Signals, Systems*; vol.2., pp.303-314; 1989.

Davis, P.; "Interpolation & Approximation;" *Dover Publications*; 1975.

Erlandson; "U.S.Patent 4,936,299;" June, 1990.

Faye, I.C.; "An Impedance Controlled Manipulandum for Human Movement Studies;" *M.S. Thesis*; Massachusetts Institute of Technology, 1986.

Feldman, A.G.; "Functional Tuning of the Nervous System with Control of Movement or Maintenance of a Steady Posture, II: Controllable Parameters of the Muscle;" *Biophysics*; vol.11., pp. 565-578; 1966.

Feeney, D.M.; Gonzales, A.; Law, W.A.; "Amphetamine. Haloperidol, and Experience Interact to Affect Rate of Recovery After Motor Cortex Injury;" *Science*, vol.217, pp.855-857; 1982.

Fitts, P.M.; "The Information Capacity of the Human Motor System in Controlling the Amplitude of the Movement;" *Journal of Experimental Psychology*; vol.47, pp.381-391, 1954.

Flash; T.; Hogan, N.; " The Coordination of Arm Movements: An Experimentally Confirmed Mathematical Model;" *The Journal of Neuroscience*; vol.5., pp.1688-1703; 1985.

Flash, T.; Henis, E.; "Arm Trajectory Modifications During Reaching Towards Visual Targets;" *Journal of Cognitive Neuroscience*; vol.3, no.3., pp.220-230; 1994.

Frackowiak, R.S.J.; "Plasticity and the Human Brain: Insights from Functional Imaging;" *The Neuroscientist*; Williams & Wilkins; vol.2., no.6; 1996.

Fugl-Meyer, A.R.; Jaasco, L.; Leyman, L.; Olsson S.; Steglind, S.; "The Post-Stroke Hemiplegic Patient;" *Scand. Journal Rehab. Med*; vol 7, pp.13-31; 1975.

Georgopoulos, A.P.; Kalaska, J.F.; Crutcher, M.D.; Caminiti, R.; Massey, J.T.; "The Representation of Movement Direction in the Motor Cortex: Single Cell and Population Studies;" *Dynamic Aspects of Neocortical Function - John Wiley & Sons* - 1984.

Girosi, F.; Poggio, T.; "Networks and the Best Approximation Property;" AI. Memo No. 1164; Massachusetts Institute of Technology; October 1989.

Giszter, S.F.; Mussa-Ivaldi, F.A.; Bizzi, E.; "Convergent Force Fields Organized in the Frog's Spinal Cord;" *The Journal of Neuroscience*; vol.13(2), pp.467-491; February, 1993.

Grafton, S.T; Woods, R.P; Tyszka; Functional Imaging of Procedural Motor Learning: Relating Cerebral Blood Flow with Individual Subject Performance;" *Human Brain Mapping*, 1994, 1:221-234.

Hodgson, A.; "Inferring Central Motor Plans from Attractor Trajectory Measurements;" *Ph.D. Thesis*; Massachusetts Institute of Technology; 1994.

Hogan, N.; "An Organizing Principle for a Class of Voluntary Movements;" *The Journal of Neuroscience*; vol.4., no.11, pp.2745-2754; November 1984.

Hogan, N.; "Planning and Execution of Multijoint Movements;" *Canadian Journal of Physiology and Pharmacology*; vol.66., pp.508-517; 1987.

Hogan, N.; "Impedance Control: An Approach to Manipulation: Part I, Part II, Part III;" *Journal of Dynamic Systems, Measurement, and Control*; Transaction of the ASME; vol.107, pp. 1-24, 1985.

Hogan, N.;"On the Stability of Manipulators Performing Contact Tasks;" *IEEE Journal of Robotics and Automation*; vol.4, pp. 677-686, 1988.

Hollerbach, J.M.; "Computers, Brains and the Control of Movement;" *Elsevier Biomedical Press*, 1982.

Hollerbach, J.M; Atkenson, C.G.; "Inferring Limb Coordination Strategies from Trajectory Kinematics;" *Journal of Neuroscience Methods*; vol.21., pp.181-194; 1987.

Hornik, K.; Stinchcombe, M.; White, H.; "Multilayer Feedforward Networks Are Universal Approximators;" *Neural Networks*; vol.2., pp.359-366; 1989.

IEEE White Book; "Recommended Practice for Electric Systems in Health Care Facilities;" *The Institute of Electrical and Electronics Engineers*; ANSI/IEEE Std 602-1986

Jagacinski, R.J.;Hartzell, E.J.; Ward, S.; Bishop, K; "Fitts' Law as a Function of System Dynamics and Target Uncertainty;" Journal of Motor Behavior; vol.10, pp.123-131; 1978.

Jagacinski, R.J.; Repperger, D.W.; Moran, M.S.; Ward, S.L.; Glass, B.; "Fitts' Law and the Microstructure of Rapid Discrete Movements;" *Journal of Experimental Psychology: Human Perception and Performance*; vol.6., no.2., pp.309-320; 1980.

Kalaska, J.F., Cohen, D.A., Hyde, M.L. & Prud'homme, M.; "A Comparison of Movement Direction-Related Versus Load Direction-Related Activity in Primate Motor Cortex Using a Two-Dimensional Reaching Task;" *Journal of Neuroscience*; 9:2080-2102, 1989.

Kerr, R.; "Diving, Adaptation, and Fitts' Law;" *Journal of Motor Behavior*; vol.10., pp.255-260; 1978.

Lacquaniti, F.; Terzuolo, C.A.; Viviani, P.; "The Law Relating the Kinematic and Figural Aspects of Drawing Movements;" *Acta Psychology*; vol.54, pp.115-130; 1983.

Linsker, R.; "Self-Organization in a Perceptual Network;" *Computer*; pp.105-117; March 1988.

Mansfield, J.M.; "Functional Assessment of Amputee Performance;" *Ph.D. Thesis*; Massachusetts Institute of Technology; 1992.

Mesulam, M~Marsel; "Principles of Behavioral Neurology;" *F.A. Davis Company*; 1985.

Milner, T.E.; "A Model for the Generation of Movements Requiring Endpoint Precision;" *Neuroscience*; vol.49, no.2., pp.487-496; 1992.

Minekime, C.M.; "Friction Mapping in the Workspace of an Occupational Therapy Robot;" *B.S. Thesis*; Massachusetts Institute of Technology; May, 1994.

Miyai, I.; Blau, A.D.; Reding, M.J.; Volpe, B.T.; "Patients with Stroke Confined to Basal Ganglia Have Diminished Response to Rehabilitation Efforts;" *Neurology*; January, 1997 (in press).

Morasso, P.; "Spatial Control of Arm Movements;" *Experimental Brain Research*; vol.42, pp.223-227; 1981.

Morasso, P.; Mussa-Ivaldi, F.A.; "Trajectory Formation and Handwriting: A Computational Model;" *Biological Cybernetics*; vol.45., pp.131-142; 1982.

Nakayama, H.; Jorgensen, H.S.; Raaschou, H.O.; Olsen, T.S.; "Recovery of Upper Extremity Function in Stroke Patients: The Copenhagen Stroke Study;" *Arch. Phys. Med. Rehabil*; vol.75, April 1994.

Nelson, W.L.; "Physical Principles for Economies of Skilled Movements;" *Biological Cybernetics*; vol.46, pp.135-147, 1983.

Nudo, R.J.; Wise, B.M.; SiFuentes, F.; Milliken, G.W.; "Neural Substrates for the Effects of Rehabilitative Training on Motor Recovery After Ischemic Infarct;" *Science*; vol.272., pp.1791-1794; 1996.

Ojakangas, C.L.; Ebner, T.J.; "Scaling of the Metrics of Visually-Guided Arm Movements During Motor Learning in Primates;" *Experimental Brain Research*; vol.85, pp.314-323; 1991.

Oldfield, R.C.; "The assessment and analysis of handedness: the Edinburgh Inventory;" *Neuropsychologica*; 1971, 6, 97-113.

Oppenheim, A.V.; Schafer, R.W.; "Discrete-Time Signal Processing;" *Prentice-Hall*; 1989.

Papoulis, A.; "Probability, Random Variables, and Stochastic Processes;" *McGraw Hill*; 1991.

Poggio, T.; Girosi, F.; "Regularization Algorithm for Learning that are Equivalent to Multilayer Networks;" *Science*; vol.247; pp.978-982; 23 February 1990.

Polit, A.; Bizzi, E.; "Characteristics of Motor Programs Underlying Arm Movements in Monkeys;" *Journal of Neurophysiology*; vol.42, no.1, pp.183-194; January 1979.

Prablanc, C.; Echallier, J.E.; Jeannerod, M.; Komilis, E.; "Optimal Response of Eye and Hand Motor Systems in Pointing at a Visual Target;"*Biological Cybernetics*; vol.35, pp.183-187; 1979.

Pratt, J.W.; Raiffa, H.; Schlaifer, R.; "Statistical Decision Theory;" *The MIT Press*; 1995.

Rauch, S.L.; Savage, C.R.; Alpert, N.M; Miguel, E.C.; Baer, L.; Breiter, H.C.; Fischman, A.J.; Manzo, P.A.; Moretti, C.; Jenike, M.A.; "A positron emission tomographic study of simple phobic symptom provocation;" *Arch. Gen. Psychiatry*, 1995; 52:20-28.

Rauch, S.L.; Savage, C.R.; Brown, H.D.; Curran, T.; Alpert, N.M.; Kendrik, A.; Fischman, A.J.; Kosslyn, S.M.; "A PET Investigation of Implicit and Explicit Sequence Learning;" *Human Brain Mapping; Wiley-Liss*; 3:271-286; 1995.

Roy, C.S.; Sherrington, C.S.; "On the Regulation of the Blood Supply of the Brain;" *Journal of Physiology*; vol.11, pp.85-108; 1890.

Sanger, T.D.; "Optimal Unsupervised Learning in a Single-Layer Linear Feedforward Neural Network;" *Neural Networks*; vol.2., pp.459-473; 1989.

Sanner, R.M.; Slotine, J.J.E.; "Stable Recursive Identification Using Radial Basis Function Networks;" *Proc. 1992 Automatic Control Conference*; June, 1992.

Sanner, R.M.; "Stable Adaptive Control and Recursive Identification of Nonlinear Systems Using Radial Gaussian Networks;" *Ph.D. Thesis*; Massachusetts Institute of Technology; May, 1993.

Scott, D.L.; "Design and Fabrication of a Human-Machine Interface for Upper Limb Physical Therapy;" *B.S. Thesis*; Massachusetts Institute of Technology; June, 1995.

Schwartz, A.B.; "Direct Cortical Representation of Drawing;" *Science*; vol.265, pp.540-542; 22 July 1994.

Simoncelli, E.P.; Adelson, E.H.; "Nonseparable Extensions of Quadrature Mirror Filters to Multiple Dimensions;" *Proc. IEEE*; vol.78, pp.652-664; April, 1990.

Shadmehr, R.; Mussa-Ivaldi, F.A.; "Adaptive Representation of Dynamics during Learning a Motor Task;" *The Journal of Neuroscience*; vol.14(5): 3208-3224; May 1994.

Strang, G.; Truong, N.; "Waveletes and Filter Banks;" *Wellesley-Cambridge Press*, 1996.

Talairach, J.; Tournoux P.; "Co-Planar Stereotaxic Atlas of the Human Brain;" *Thieme Medical Publishers*, 1988.

Thompson, D.; "On Growth and Form;" *Cambridge University Press*; 1961.

Trombly, C.A.; "Occupational Therapy for Physical Dysfunction;" *Williams & Wilkins*; 1995.

Viviani, P.; Terzuolo, C.; "Space-Time Invariance in Learned Motor Skills;" *North-Holland Publishing Company*; Tutorials in Motor Behavior; G.E.Stelmach and J.Requin (eds); Chapter 32; 1980.

Viviani, P.; Terzuolo, C.; "Trajectory Determines Movement Dynamics;" *Neuroscience*; vol.7., pp.431-437; 1982.

Von Hofsten, C.; Lindhagen, K.; "Observations on the Development of Reaching for Moving Objects;" *Journal of Experimental Child Psychology*; vol.28, pp.158-173; 1979.

Von Hofsten, C.; "Predictive Reaching for Moving Objects by Human Infants;" *Journal of Experimental Child Psychology*; vol.30, pp.369-382; 1980.

Von Laban, R.; "Principles of Dance and Movement Notation;" 1956.

Weiner, W.J.; Lang, A.E.; "Movement Disorders: A Comprehensive Survey;" *Futura Publishing Company*; 1989.

Wolpert, D.M.; Ghahramani, Z.; Jordan, M.I.; "Are Arm Trajectories Planned in Kinematic or Dynamic Coordinates? An Adaptation Study;" *Technical Report 9308*; MIT Computational Cognitive Science; February 1994.

Woodworth, R.S.; "Accuracy of Voluntary Movement;" *Ph.D. Thesis*; Columbia University; 1899.